DIENERIAN (EARLY TRIASSIC) AMMONOIDS : TAXONOMY, BIOCHRONOLOGY AND DIVERSITY DYNAMICS

Dissertation

zur

Erlangung der naturwissenschaftlichen Doktorwürde
(Dr. sc. nat.)

vorgelegt der

Mathematisch-naturwissenschaftlichen Fakultät

der

Universität Zürich

von

David Ware

aus

Frankreich

Promotionskomitee

Prof. Dr. Hugo Bucher
(Leiter der Dissertation, Vertreter der Universität Zürich)
Dr. Jean Guex (Université de Lausanne)
Dr. Arnaud Brayard (Université de Bourgogne)

Zürich, 2015

This dissertation is dedicated to the memory of father, Colin M. Ware. He encouraged in me both a passion for paleontology and one for wine. In fact, it was during a trip with him to the vineyards of St Aubin, Burgundy, that I discovered my first ammonites. I will always miss sharing a glass of wine with him, and the discussions we shared on science and my research.

Table of Content

Abstract

The end Permian mass extinction is largely considered as the greatest crisis in the history of life, leading to the replacement of typical Palaeozoic faunas by typical modern communities. The recovery which followed is generally considered as delayed, with several groups (e.g. corals, radiolarians) or marine ecosystems (e.g. reefal communities) not reaching pre-extinction levels before the Middle Triassic. However, ammonoids or conodonts recovered much faster, reaching levels of diversity higher than in the Permian as early as the early Smithian. Ammonoids are of paramount importance for biostratigraphic analyses, but with the exception of the Smithian times, the detailed tempo of their recovery is still poorly known, and has only been analysed at the sub-stage level. It is especially the case for the Dienerian, for which very few studies based on detailed bed-rock controlled sampling have been published. More importantly, no such studies concern the Northern Indian Margin (NIM) despite the fact that most Dienerian ammonoid taxa were originally described there. The aim of this study is the revision of Dienerian ammonoids taxonomy and the construction of a high resolution biozonation in order to analyse their biodiversity dynamics.

In the first part of this dissertation, some ammonoids from the Candelaria Hills (Nevada, USA) are described. This fauna was known since the mid 20th century, but has never been described or illustrated. One new family (Mullericeratidae), one new genus (*Mullericeras*) and two new species (*Mu. fergusoni* and *Proptychites pagei*) are described.

The second and main part of this dissertation concerns ammonoids from the Salt Range (Pakistan), an iconic locality where the first Dienerian ammonoids were described. More than 2000 specimens were collected with a detailed bedrock and stratigraphic control. This vast collection enabled us to thoroughly revise their taxonomy, with a special emphasis on their intraspecific variability and ontogeny. Emended diagnoses for families, genera and species are given whenever possible, together with detailed discussions concerning their synonymy and phylogenetic relationships. 5 new genera (*Kyoktites*, *Ghazalaites*, *Pashtunites*, *Awanites* and *Subacerites*) and 18 new species (*Kyoktites hebeiseni*, *Ghazalaites roohii*, *Gyronites schwanderi*, *Ambites tenuis*, *Am. bojeseni*, *Am. subradiatus*, *Am. bjerageri*, *Awanites awani*, *Koiloceras sahibi*, *Bukkenites sakesarensis*, *Proptychites wargalensis*, *Mullericeras shigetai*, *Mul. indusense*, *Mul. niazii*, *Ussuridiscus ventriosus*, *U. ornatus*, *Pseudosageceras simplelobatum* and *Subacerites friski*) are described. A total of 12 regional zones were recognised.

The third part is a work similar to that made in the Salt Range, but in the Spiti District (Himashal Pradesh, India). It is based on more than a thousand specimens, most of them belonging to species already described in the Salt Range. Only 4 new species (*Gyronites levilatus*, *Gy. bullatus*, *Ambites nyingmai* and *Vavilovites meridialis*) are described. 10 out of the 12 regional zones identified in the Salt Range were recognised, with nearly the same faunal content.

Fourth, a few Dienerian ammonoids from two consecutive beds of a new section near Tulong (South Tibet) are described and compared with the faunas from the Salt Range. 3 regional zones are represented, two of them in a condensed horizon.

Finally, an analysis by means of the Unitary Association Method was performed, based on the data obtained from the Salt Range and Spiti. This lead to the recognition of 12 zones from the NIM and to the division of the Dienerian into three parts (early, middle and late). This unprecedented high resolution strongly contrasts with previous works, where only 3 or 4 zones were recognised, and the Dienerian being originally divided in only two parts (early and late). Analysis of ammonoid biodiversity dynamics based on this new high resolution time frame highlights (1) a first modest peak of diversity in the early Dienerian, (2) a very low diversity persisting throughout the middle Dienerian and (3) a slow increase of diversity during the late Dienerian, just before the explosive radiation of the early Smithian. Turnover rates are very high during this entire time interval, and the boundaries between early-middle and middle-late Dienerian are emphasized by complete renewals of the faunas. The low diversity values in the middle and early late Dienerian are concomitant with an anoxic event and coincide with warmer temperatures than those of the early Dienerian and early Smithian.

Keywords: Early Triassic recovery, Ammonoids, Dienerian, Salt Range, Spiti, South Tibet, Nevada.

Zusammenfassung

Das Massenaussterben am Ende des Perm wird als die grösste Krise in der Geschichte des Lebens angesehen und führte zum Austausch der typisch paläozoischen Faunen durch moderne Lebensgemeinschaften. Die Phase der Erholung welche auf die Krise folgte wird generell als verzögert angesehen und einige Gruppen (z.B. Korallen, Radiolarien) oder marine Ökosysteme (z.B. Riffgemeinschaften) haben erst in der Mitteltrias dasselbe Niveau wie vor dem Massenaussterben erreicht. Die Ammonoideen und Conodonten andererseits, haben sich viel schneller erholt und erreichten schon im unteren Smithium höhere Diversitätsniveaus als im Perm. Ammonoideen sind von höchster Bedeutung für die biostratigraphische Analyse. Allerdings ist, mit Ausnahme des Smithium, nur sehr wenig über die genaue Geschwindigkeit der Erholung bekannt und Untersuchungen wurden bisher nur auf Unterstufenniveau durchgeführt. Dies gilt insbesondere für das Dienerium, über das besonders wenige, auf detaillierter Beprobung der Gesteinsschichten beruhende Studien publiziert wurden. Zudem gibt es keine solchen Studien den Northern Indian Margin (NIM) betreffend, obwohl die meisten Ammonoideen aus dem Dienerium ursprünglich aus dieser Region beschrieben wurden. Das Ziel dieser Studie ist die Neubearbeitung der Taxonomie der Ammoideen aus dem Dienerium und die Erstellung einer hochaufgelösten Biozonierung um die Dynamik der Biodiversität zu analysieren.

Der ersteTeil dieser Dissertation beinhaltet die Beschreibung von Ammonoideen aus den Candelaria Hills (Nevada, USA). Diese Fauna ist seit der Mitte des 20. Jahrhunderts bekannt, wurde bis jetzt aber noch nicht beschrieben oder illustriert. Eine neue Familie (Mullericeratidae), eine neue Gattung (*Mullericeras*) und zwei neue Arten (*Mu. Fergusoni* und *Proptychites pagei*) werden hier beschrieben.

Der zweite Teil und Hauptteil dieser Dissertation behandelt die Ammonoideen der Salt Range (Pakistan), eine einzigartige Lokalität von der die ersten Ammonoideen aus dem Dienerium beschrieben wurden. Mehr als 2000 Exemplare wurden gesammelt, zusammen mit einer detaillierten Dokumentation der Gesteinsabfolge und der Stratigraphie. Diese ausgedehnte Sammlung erlaubte es, die Taxonomie der Ammonoideen mit einem speziellen Augenmerk auf die intraspezifische Variabilität und Ontogenie zu überarbeiten. Wann immer möglich sind revidierte Diagnosen für Familien, Gattungen und Arten zusammen mit detaillierten Diskussion zur Synonymie und zu phylogenetischen Verwandtschaftsbeziehungen angegeben. Fünf neue Gattungen (*Kyoktites*, *Ghazalaites*, *Pashtunites*, *Awanites* und *Subacerites*) und achtzehn neue Arten (*Kyoktites hebeiseni*, *Ghazalaites roohii*, *Gyronites schwanderi*, *Ambites tenuis*, *Am. bojeseni*, *Am. subradiatus*, *Am. bjerageri*, *Awanites awani*, *Koiloceras sahibi*, *Bukkenites sakesarensis*, *Proptychites wargalensis*, *Mullericeras shigetai*, *Mul. indusense*, *Mul. niazii*, *Ussuridiscus ventriosus*, *U. ornatus*, *Pseudosageceras simplelobatum* und *Subacerites friski*) werden beschrieben. Insgesamt wurden 12 neue regionale Zonen vorgeschlagen.

Der dritte Teil ist eine Arbeit die derjenigen über die Salt Range ähnelt, jedoch Fossilen aus dem Spiti-Distrikt (Himashal Pradesh, Indien) behandelt. Die Basis dieser Arbeit bilden mehr als 1000 Exemplare, von denen die meisten Arten angehören, die bereits für die Salt Range beschrieben wurden. Nur vier Arten (*Gyronites levilatus*, *Gy. bullatus*, *Ambites nyingmai* und *Vavilovites meridialis*) werden beschrieben. Zehn der zwölf regionalen Zonen, die auch in der in der Salt Range identifiziert wurden, werden auch hier erkannt und weisen fast denselben Fauneninhalt auf.

Viertens, einige Ammonoideen aus dem Dienerium aus zwei aufeinanderfolgenden Schichten eines neuen Profils in der Nähe von Tulong (Südliches Tibet) sind beschrieben und werden mit der Fauna der Salt Range verglichen. Drei regionale Zonen sind vertreten, zwei davon in einem kondensierten Horizont.

Zum Schluss wurde mit den Daten der Salt Range und von Spiti eine Analyse mit Hilfe der Unitary-Association-Methode durchgeführt. Dies führte zur Erkennung von 12 Zonen der NIM und der Aufteilung des Dieneriums in drei Teile (unteres, mittleres und oberes). Diese beispiellos hohe Auflösung kontrastiert stark mit älteren Arbeiten, bei denen nur drei oder vier Zonen erkannt und das Dienerium normalerweise in nur zwei Abschnitte (unteres und oberes) unterteilt wurde. Die Analyse der Dynamik der Biodiversität der Ammonoideen, die auf diesem neuen, hochauflösenden Zeitfenster beruht, zeigt folgendes auf: (1) Einen ersten, mässigen Diversitätshöhepunkt im unteren Dienerium, (2) eine sehr geringe Diversität während des mittleren Dieneriums und (3) einen langsamen Anstieg der Diversität während des späten Dieneriums, kurz vor der explosiven Radiation im unteren Smithium. Die Turnover-Raten sind während des gesamten Zeitintervalls hoch und die Grenzen sowohl zwischen dem unteren und mittleren, als auch zwischen dem mittleren und oberen Dienerium sind durch eine komplette Erneuerung der Faunen gekennzeichnet. Die niedrigen Diversitätswerte im mittleren und frühen oberen Dieneriums treten zusammen mit einem anoxischen Ereignisses auf und decken sich mit wärmeren Temperaturen als die des unteren Dieneriums und unteren Smithiums.

Schlagwörter: Frühtriassische Erholung, Ammonoideen, Dienerium, Salt Range, Spiti, Südliches Tibet, Nevada

INTRODUCTION

It has been estimated that about 90% of all marine species disappeared during the end-Permian mass extinction (e.g. Raup & Sepkoski, 1982). It is the biggest known biodiversity crisis in the history of life, and it lead to the replacement of typical Palaeozoic faunas by typical modern communities (Sepkoski, 1984). The recovery which followed during the Early Triassic is an intensively studied topic. This recovery is usually considered as delayed in comparison to other mass extinctions (e.g. Erwin, 1998, 2006) as several major marine clades such as corals (Stanley, 2003), foraminifers (Tong & Shi, 2000) or radiolarians (Racki, 1999) recovered only in the late Spathian or the Anisian, nearly 4.5 My after the Permian-Triassic boundary. This delay is classically interpreted as the consequence of persisting anoxic conditions (Wignall & Twitchett, 2002) and unstable environmental conditions during the entire Early Triassic (Payne *et al.*, 2004). However, several recent studies suggest a more complex scenario, with pulses of recovery interrupted by periods of additional extinctions. For example, conodonts (Orchard, 2007, Goudemand *et al.*, 2008) first underwent an important turnover at the Griesbachian-Dienerian boundary, followed by an explosive radiation in the early-middle Smithian, an extinction in the late Smithian, and another radiation during the Spathian. Ammonoids also recovered very fast compared to other groups, reaching pre-extinction levels of diversity already in the Smithian (Fig. 1, Brayard *et al.*, 2009).

This dissertation is a contribution to a multidisciplinary research project conducted under the leadership of Prof.

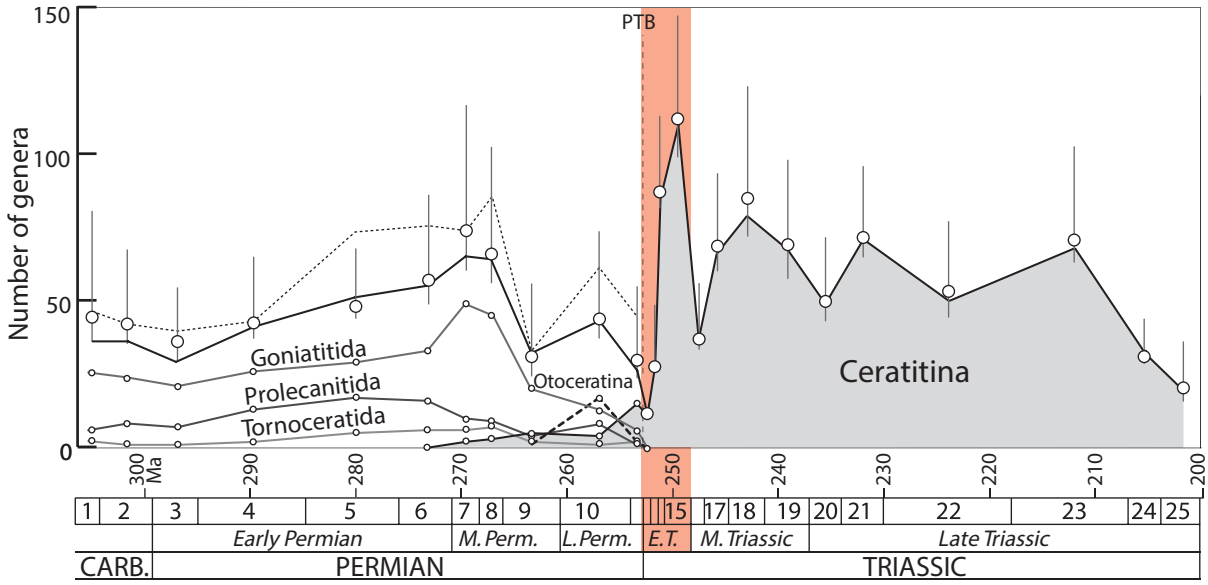

Fig. 1. Total generic richness (black bold line, all ammonoids; gray lines, major ammonoid groups) and mean Chao2 estimate of the overall generic richness with its 95% confidence interval (large circles with vertical bars). The Early Triassic is highlighted in red. PTB, Permian-Triassic boundary; 1, Kasimovian; 2, Gzhelian; 3, Asselian; 4, Sakmarian; 5, Artinskian; 6, Kungurian; 7, Roadian; 8, Wordian; 9, Capitanian; 10, Wuchiapingian; unlabeled successive intervals, Changhsingian, Griesbachian, Dienerian, Smithian; 15, Spathian; 16, Early Anisian; 17, Middle Anisian; 18, Late Anisian; 19, Ladinian; 20, Early Carnian; 21, Late Carnian; 22, Early Norian; 23, Middle Norian; 24, Late Norian; 25, Rhaetian.

Hugo Bucher at the Palaeontological Institute and Museum of the University of Zürich concerning different aspects of the Early Triassic recovery, including its timing and climatic constraints. This project includes many localities worldwide, including several localities on the Northern Indian Margin (NIM; i.e. Oman, Salt Range, Spiti and Tibet), South China, western USA, Spitsbergen, Greenland and the Italian Alps. Several studies conducted by our team contradict the scenario of a simple protracted recovery linked with harsh environmental conditions during the whole Early Triassic. Hofmann *et al.* (2014) showed that benthic ecosystems started to recover already in the Griesbachian, but this recovery has been interrupted by a return to harsh environmental conditions during the Dienerian, itself succeeded by another recovery pulse during the Smithian. Based on palynological and carbon isotopes analysis, Hermann *et al.* (2011a, 2011b, 2012a, 2012b) and Schneebeli-Hermann *et al.* (2012, 2014) contradicted the idea of persistent widespread anoxia, and showed that this anoxia was restricted to the middle-late Dienerian and late Smithian time intervals, and associated with a spore spike similar to the one observed during the end-Permian extinction interval. However, many studies addressing the recovery are based on insufficiently resolved paleontological age controls, so the construction of a detailed time scale for the Early Triassic is the cornerstone on which any study concerning this biotic recovery must be based and one of the main task of our research group. Galfetti *et al.* (2007) showed that the Early Triassic was a short time interval of ca. 4.5 My and that its substages were of very uneven duration, the Spathian representing more than half of this interval (fig. 2). Brayard & Bucher (2008) proposed a new detailed biostratigraphic scheme based on ammonoids for the Smithian of South China. Brühwiler *et al.* (2010a) constructed the most highly resolved biostratigraphic scheme for the Smithian

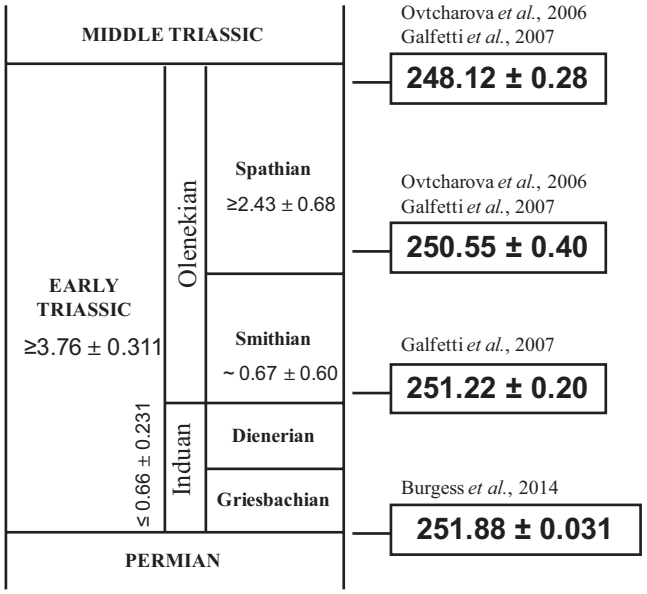

Fig. 2. Early Triassic stage and substage subdivision (Ogg, 2012) calibrated with recently published radiometric ages from South China.

based on ammonoids from the NIM. At this fine scale level, they showed that ammonoids underwent an explosive radiation in the early Smithian, a constant high diversity associated with extremely high turnover rates throughout the middle Smithian and a major extinction in the late Smithian. At the same time, conodonts did also suffer from a drastic extinction. This extinction could not be detected in Brayard *et al.* (2009) due to the broad scale of this study. The aim of this work is to perform a similar work as has been done for the Smithian, but for Dienerian times. The following other aspects of the Early Triassic biotic recovery are currently being investigated by Bucher's group:

- Late Permian and Early Triassic floras (E. Schneebeli-Hermann, P. Hochuli)
- Griesbachian ammonoids from NE Greenland and Spiti (M. Meier);
- Permian-Griesbachian palynology of NE Greenland (A. Sanson Barrera);
- Early Triassic conodonts from the NIM (M. Brosse, M. Leu);
- Smithian ammonoids from Timor (R. Jattiot)
- Late Permian foraminifers (B. Bargherpour)
- Early Triassic benthic faunas (R. Hofmann, M. Hautmann)
- Early Triassic fishes (C. Romano, W. Brinkmann)

The stage subdivisions of the Early Triassic are still a subject of debate (Fig. 2). In the latest version of the Geologic Time Scale (Ogg, 2012), the twofold subdivision of the Early Triassic introduced by Kiparisova & Popov (1956), with the Induan and Olenekian, is endorsed. The four stages defined by Tozer (1965) are then considered as substages, the Induan being subdivided into Griesbachian and Dienerian, and the Olenekian into Smithian and Spathian. This twofold scheme is however strongly criticised, mainly as it does not reflect the end Smithian crisis, the most important extinction event known for both ammonoids and conodonts within the entire Triassic. Moreover, having the Induan defined in the Tethyan realm and the Olenekian in the Boreal Realm makes the correlation of this stage boundary across such a broad palaeolatitudinal range an extremely arduous task. Tozer (1965) provided only a vague definition of the Dienerian/Smithian boundary (corresponding to the Induan/Olenekian boundary), explaining that it was probable that in Canada, the oldest Smithian fauna may be younger than typical Smithian faunas from other areas. Krystyn *et al.* (2007a, 2007b) proposed the Mud section (Spiti valley, India) as a GSSP candidate for this boundary. They based their definition of the boundary on the first occurrence of the conodont *Neospathodus waageni sensu lato*. However, Brühwiler *et al.* (2010b) demonstrated the presence in the same section of ammonoid genera typical of the Smithian below the boundary as originally placed by Krystyn *et al.* (2007a, 2007b), and thus suggested to use the first occurrence of *Flemingites bhargavai* as the index fossil for this boundary. This species is also present in the Salt Range (Pakistan; Brühwiler *et al.*, 2010a, 2012). Consequently, this definition is adopted here. Tozer (1965, 1994) originally subdivided the Dienerian of Canada into two parts (early and late), each composed of one zone (the *Proptychites candidus* zone and the *Vavilovites sverdrupi* zone), the second one being further subdivided into 3 subzones. However, this zonation is based on scattered occurrences of the faunas, often without superpositional information. Other zonations have been proposed for Northern Siberia (Dagys & Ermakova, 1996) and Primorye (Shigeta & Zakharov, 2009), but uncertainties in correlating these do persist. Based on material from Nepal, a biozonation has been proposed by Waterhouse (1994, 1996) for the northern Gondwanian margin. Unfortunately, this Nepalese material is very poorly preserved and does not allow constructing a

robust taxonomy, a pre-requisite for any attempt in constructing a biozonation.

The NIM has long been recognised as a key area for the study of Early Triassic ammonoids and the establishment of the Early Triassic time scale. During the Early Triassic, it was situated in southern Tethys, at a palaeolatitude of ca. 40°S (Fig. 3). The very first Dienerian ammonoids were discovered in the Salt Range by Andrew Fleming in the mid-19th century and this material was described by de Koninck (1863). Waagen (1895) conducted the most impressive and exhaustive study on Early Triassic ammonoids from the Salt Range. Diener (1897) and Krafft & Diener (1909) published two monographs concerning ammonoids from the Early Triassic of nowadays Indian Himalayas, many of them coming from the Spiti valley. The very first ammonoid biozonation of the Early Triassic has been published by Mojsisovics *et al.* (1895) based on these two regions. They recognised only two zones in what we consider here as Dienerian, and this biozonation hardly changed since as no other detailed work concerning Dienerian ammonoids of the Salt Range and Spiti has been published. For the Salt Range, Noetling (1905) and Spath (1934) added a few species

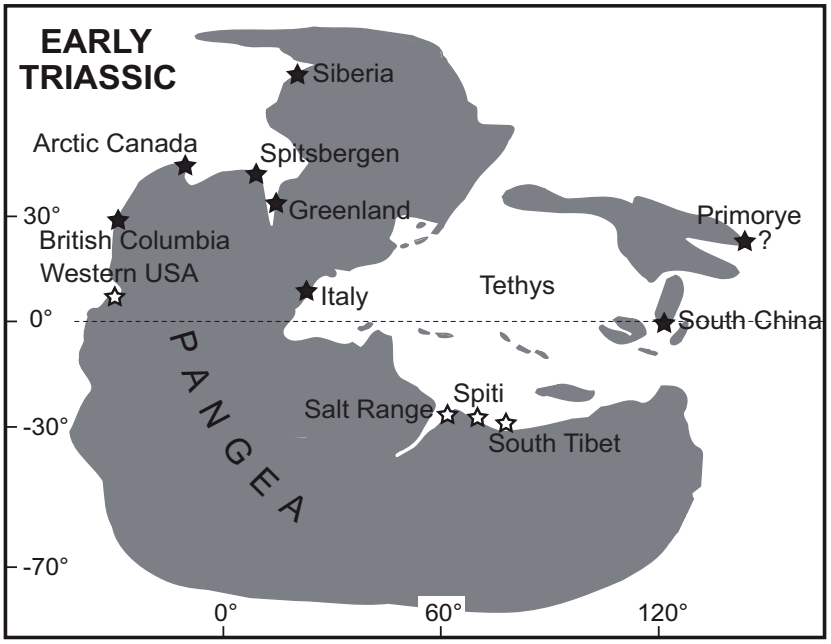

Fig. 3. Simplified palaeogeographical map of the Early Triassic with the palaeopositions of the studied localities (white stars) and of other localities mentioned in the text (black stars). Modified after Brayard *et al.* (2006).

and proposed slightly different classifications. Griesbachian ammonoids were first discovered by Schindewolf (1954) in the Salt Range. Kummel provided a detailed history of the stratigraphic and paleontological investigations on the Permian and Triassic of the Salt Range (Kummel 1966, Kummel & Teichert 1966, 1970). He also mentioned that he collected numerous Dienerian ammonoids and that he intended to publish this material later on, a task he unfortunately never completed. Since Kummel's work, only two contributions on Early Triassic ammonoids from the Salt Range were published. The works by Guex (1978) and by the Pakistani-Japanese Research Group (PJRG, 1985) only include scarce material of Griesbachian and Dienerian ages. Concerning ammonoids from the Indian Himalayas, only Bando (1981) described a few ammonoids from Kashmir, and Krystyn & Orchard (1996) and Krystyn *et al.* (2004, 2007a, 2007b) gave some details concerning ammonoid biostratigraphy of Spiti, but without any description of ammonoids. A few poorly preserved ammonoids from South Tibet were also described by Wang & He (1976), and Waterhouse (1996) published an extensive revision of Dienerian ammonoids from Nepal, but based on extremely poorly preserved material and thus of little use. Outside the NIM, only a few regions yielding well preserved Dienerian ammonoid faunas have been studied in detail: British Columbia and Arctic Canada (e.g. Tozer, 1994), the Verkhoyansk basin (Siberia, e.g. Dagys & Ermakova, 1996), Primorye (e.g. Shigeta & Zakharov 2009) and South China (e.g. Brühwiler *et al.*, 2008). Some Dienerian ammonoids from the Candelaria Hills (Nevada, USA) have been cited in several works as similar to the faunas from the NIM (Muller & Ferguson, 1936, 1939, Page, 1959, Silberling & Tozer, 1968), but never described nor illustrated.

Considering the scarcity of detailed works concerning Dienerian ammonoid taxonomy, a detailed revision based on new material with a detailed stratigraphic control was necessary. From 2007 to 2010, our research group carried out intensive field work in the Salt Range, in Spiti, in Tibet and in Nevada. A detailed bedrock controlled sampling of several sections in these regions was performed in order to revise Dienerian ammonoid taxonomy and build a new,

highly resolved biostratigraphic scheme. The results concerning Dienerian ammonoids from the Salt Range are given in chapter 2. As the Salt Range is the type locality of most Dienerian ammonoid taxa, it was the region where the most intensive field work was done, and the vast majority of the material described here comes from there. Hence, this chapter constitutes the main part of this dissertation and includes a thorough revision of Dienerian ammonoid taxonomy, including emended diagnoses of families, genera and species whenever possible. Dienerian ammonoids from Spiti are described in chapter 3. Ammonoids from two other localities are described: the Candelaria Hills (chapter 1) and a new section near Tulong (South Tibet; chapter 4). The final chapter and conclusion of this dissertation is a synthetic paper which includes the construction by means of the Unitary Association Method (Guex, 1991) of a new biozonation for the Dienerian of the NIM based on ammonoids from the Salt Range and Spiti, the analysis of their biodiversity dynamics and comparison with palaeoenvironmental proxies. This new highly resolved biozonation, together with the detailed revision of Dienerian ammonoids taxonomy, will provide a firm basis for all future works concerning the detailed study of the Early Triassic biotic recovery.

REFERENCES

Bando, Y., 1981. Lower Triassic Ammonoids from Guryul Ravine and the Spur three kilometres north of Burus. *In* Nakazawa, K. & Kapoor, H. M. (eds): *The Upper Permian and Lower Triassic faunas of Kashmir*. *Palaeontologia Indica 46*, 135-178.

Brayard, A., Bucher, H., Escarguel, G., Fluteau, F., Bourquin, S. & Galfetti, T., 2006. The Early Triassic ammonoid recovery: Paleoclimatic significance of diversity gradients. *Palaeogeography, Palaeoclimatology, Palaeoecology 239*, 374-395.

Brayard, A. & Bucher, H., 2008. Smithian (Early Triassic) ammonoid faunas from northwestern Guangxi (South China): taxonomy and biochronology. *Fossils and Strata 55*, 179 pp.

Brayard, A., Escarguel, G., Bucher, H., Monnet, C., Brühwiler, T., Goudemand, N., Galfetti T. & Guex, J., 2009. Good Genes and Good Luck: Ammonoid Diversity and the End-Permian Mass Extinction. *Science 325*, 1118-1121.

Brühwiler, T., Brayard, A., Bucher, H. & Guodun, K., 2008. Griesbachian and Dienerian (Early Triassic) Ammonoid Faunas from Northwestern Guangxi and Southern Guizhou (South China). *Palaeontology 51*, 1151-1180.

Brühwiler, T., Bucher, H., Brayard, A. & Goudemand, N., 2010a. High-resolution biochronology and diversity dynamics of the Early Triassic ammonoid recovery: The Smithian faunas of the Northern Indian Margin. *Palaeogeography, Palaeoclimatology, Palaeoecology 297*, 491-501.

Brühwiler, T., Ware, D., Bucher, H., Krystyn, L. & Goudemand, N., 2010b. New Early Triassic ammonoid faunas from the Dienerian/Smithian boundary beds at the Induan/Olenekian GSSP candidate at Mud (Spiti, Northern India). *Journal of Asian Earth Sciences 39*, 724-739.

Burgess, S.D., Bowring, S., & Shen, S.-Z., 2014. High-precision timeline for Earth's most severe extinction. *Proceedings of the National Academy of Sciences of the United States of America 111*, 3316-3321

Dagys, A. S. & Ermakova, S., 1996. Induan (Triassic) ammonoids from North-Eastern Asia. *Revue de Paléobiologie 15*, 401-447.

Diener, C., 1897. Part I: The Cephalopoda of the Lower Trias. *Palaeontologia Indica, Series 15*. *Himalayan fossils 2*, 1-181.

Erwin, D.H., 1998. The end and the beginning: recoveries from mass extinctions. *Trends in Ecology & Evolution 13*, 344-349.

Erwin, D.H., 2006. *Extinction: how life on Earth nearly ended 250 million years ago*. Princeton University Press, 296 pp.

Galfetti, T., Bucher, H., Ovtcharova, M., Schaltegger, U., Brayard, A., Brühwiler T., Goudemand, N., Weissert H., Hochuli, P., Cordey, F. & Guodon K., 2007. Timing of the Early Triassic carbon cycle perturbations inferred from new U-Pb ages and ammonoid biochronozones. *Earth and Planetary Science Letters 258*, 593-604.

Goudemand, N., Orchard, M., Bucher, H., Brayard, A., Brühwiler, T., Galfetti, T., Hochuli, P.A., Hermann, E. & Ware, D., 2008. Smithian-Spathian boundary: The biggest crisis in Triassic conodont history. *Abstracts with Program, Geological Society of America 40*, 505.

Guex, J., 1978. Le Trias inférieur des Salt Ranges (Pakistan): problèmes biochronologiques. *Eclogae Geologia Helvetica 71*, 105-141.

Guex, J., 1991. *Biochronological Correlations*, Springer, Berlin, 252 pp.

Hermann, E., Hochuli, P.A., Bucher, H., Brühwiler, T., Hautmann, M., Ware, D. & Roohi, G., 2011a. Terrestrial ecosystems on North Gondwana following the end-Permian mass extinction. *Gondwana Research 20*, 630-637.

Hermann, E., Hochuli, P.A., Méhay, S., Bucher, H., Brühwiler, T., Ware, D., Hautmann, M., Roohi, G., ur-Rehman, K. & Yaseen, A., 2011b. Organic matter and palaeoenvironmental signals during the Early Triassic biotic recovery: The Salt Range and Surghar Range records. *Sedimentary Geology 234*, 19-41.

Hermann, E., Hochuli, P.A., Bucher, H., Brühwiler, T., Hautmann, M., Ware, D., Weissert, H., Roohi, G., Yaseen, A.

& ur-Rehman, K., 2012a. Climatic oscillations at the onset of the Mesozoic inferred from palynological records from the North Indian Margin. *Journal of the Geological Society, London 169*, 227-237.

Hermann, E., Hochuli, P.A., Bucher, H. & Roohi, G., 2012b. Uppermost Permian to Middle Triassic palynology of the Salt Range and Surghar Range, Pakistan. *Review of Palaeobotany and Palynology 169*, 61-95.

Hofmann, R., Hautmann, M., Brayard, A., Nützel, A., Bylund, K.G., Jenks, J., Vennin, E., Olivier, N., Bucher, H., 2014. Recovery of benthic marine communities from the end-Permian mass extinction at the low-latitudes of Eastern Panthalassa. *Palaeontology 57*, 547-589.

Kiparisova, L.D. & Popov, Y.N., 1956. Subdivision of the lower series of the Triassic system into stages. *Doklady Academy Sciences U.S.S.R. 109*, 842-845 [In Russian].

de Koninck, L.G., 1863. Description of some fossils from India, discovered by Dr. A. Fleming, of Edinbourg. *The Quaterly Journal of the Geological Society of London 19*, 1-19.

Krafft, A.V. & Diener, C., 1909. Lower Triassic cephalopoda from Spiti, Malla Johar, and Byans. *Palaeontologia Indica 6*, 1-186.

Krystyn, L. & Orchard, M.J., 1996. Lowermost Triassic ammonoid and conodont biostratigraphy of Spiti, India. *Albertiana 17*, 10-21.

Krystyn, L., Balini, M. & Nicora, A., 2004. Lower and Middle Triassic stage and substage boundaries in Spiti. *Albertiana 30*, 40-53.

Krystyn, L., Bhargava, O.N. & Richoz, S., 2007a. A candidate GSSP for the base of the Olenekian Stage: Mud at Pin Valley; district Lahul & Spiti, Himachal Pradesh (Western Himalaya), India. *Albertiana 35*, 5-29.

Krystyn, L., Richoz, S. & Bhargava, O.N., 2007b. The Induan-Olenekian Boundary (IOB) in Mud – an update of the candidate GSSP section M04. *Albertiana 36*, 33-45.Ogg, J.G., 2012. Triassic. *In* Gradstein, F.M., Ogg, J.G., Schmitz, M.D. & Ogg, G.M. (eds): *The Geologic Time Scale 2012*, 681-730. Elsevier, Amsterdam.

Kummel, B., 1966. The Lower Triassic Formations of the Salt Range and Trans-Indus Ranges, West Pakistan. *Bulletin of the Museum of Comparative Zoology 134*, 361-429.

Kummel, B. & Teichert, C., 1966. Relations between the Permian and Triassic formations in the Salt Range and Trans-Indus ranges, West Pakistan. *Neues Jahrbuch für Geologie Paläontologie. Abhandlungen 125*, 297-333.

Kummel, B. & Teichert, C., 1970. Stratigraphy and Paleontology of the Permian-Triassic Boundary Beds, Salt Range and Trans-Indus Ranges, West Pakistan. *In* Kummel, B.& Teichert, C. (eds): *Stratigraphic Boundary Problems: Permian and Triassic of West Pakistan*, 1-110. Special Publication of the Department of Geology, Vol. 4, University of Kansas.

Mojsisovics, E. V., Waagen, W. & Diener, C., 1895. Entwurf einer Gliederung der pelagischen Sedimente des Trias-Systems. *Sitzungberichte der Akademie der Wissenschaften in Wien (I) 104*, 1271-1302.

Muller, S.W. & Ferguson, H.G., 1936. Triassic and Lower Jurassic formations of west-central Nevada. *Bulletin of the Geological Society of America 47*, 241-252.

Muller, S.W. & Ferguson, H.G., 1939. Mesozoic stratigraphy of the Hawthorne and Tonopah Quadrangles, Nevada. *Bulletin of the Geological Society of America 50*, 1573-1624.

Noetling, F., 1905. Die asiatische Trias. *In* Frech, F. (ed): *Lethaea Geognostica, Das Mesozoicum*, 107-221. verlag der E. Schweizerbart'schen Verlagsbuchhandlung (E. Nägele), Stuttgart, Germany.

Ogg, J.G., 2012. Triassic. *In* Gradstein, F.M., Ogg, J.G., Schmitz, M.D. & Ogg, G.M. (eds): *The Geologic Time Scale 2012*, 681-730. Elsevier, Amsterdam.

Orchard, M.J., 2007. Conodont diversity and evolution through the latest Permian and Early Triassic upheavals. *Palaeogeography, Palaeoclimatology, Palaeoecology 252*, 93-117.

Ovtcharova, M., Bucher, H., Schaltegger, U., Galfetti, T., Brayard, A., and Guex, J., 2006. New Early to Middle Triassic U-Pb ages from South China: Calibration with ammonoid biochronozones and implications for the timing of the Triassic biotic recovery. *Earth and Planetary Science Letters 243*, 463-475.

Page, B.M., 1959. Geology of the Candelaria mining district, Mineral County, Nevada. *Nevada Bureau of Mines, Bulletin 56*, 1-67.

Pakistani-Japanese Research Group, 1985. Permian and Triassic Systems in the Salt Range and Surghar Range, Pakistan. *In* Nakazawa, K. & Dickins, J.M. (eds): *The Tethys, her paleogeography and paleobiogeography from Paleozoic to Mesozoic*, 221-312. Tokai University Press, Tokyo.

Payne, J.L., Lehrmann, D.J., Wei, J.Y., Orchard, M.J., Schrag, D.P., Knoll, A.H., 2004. Large perturbations of the carbon cycle during recovery from the end-Permian extinction. *Science 305*, 506-509.

Racki, G., 1999. Silica-secreting biota and mass extinctions: survival patterns and processes. *Palaeogeography, Palaeoclimatology, Palaeoecology 154*, 107-132.

Raup, D.M. & Sepkoski, J.J., 1982. Mass extinctions in the marine fossil record. *Science 215*, 1501-1503.

Sepkoski, J.J., 1984. A kinetic-model of Phanerozoic Taxonomic Diversity. 3. Post-Paleozoic Families and Mass Extinctions. *Paleobiology 10*, 246-267.

Schindewolf, O.H., 1954. Über die Faunenwende vom Paläozoikum zum Mesozoikum. *Zeitschrift der Deutschen*

Geologischen Gesellschaft 105, 153-182.

Schneebeli-Hermann, E., Kürschner, W.M., Hochuli, P.A., Bucher, H., Ware, D., Goudemand, N. & Roohi, G. 2012. Palynofacies analysis of the Permian–Triassic transition in the Amb section (Salt Range, Pakistan): Implications for the anoxia on the South Tethyan Margin. *Journal of Asian Earth Sciences 60*, 225-234.

Schneebeli-Hermann, E., Kürschner, W.M., Bomfleur, B., Hochuli, P.A, Ware, D., Roohi, G. & Bucher, H., 2014. Vegetation history across the Permian-Triassic boundary in Pakistan (Amb section, Salt Range), *Gondwana Research*. DOI: 10.1016/j.gr.2013.11.007.

Shigeta, S. & Zakharov, Y.D., 2009. Cephalopods. *In* Shigeta, Y., Zakharov, Y.D., Maeda, H. & Popov, A.M. (eds). *The Lower Triassic System in the Abrek bay area, South Primorye, Russia*, 44-140. National Museum of Nature and Science Monographs 38, Tokyo.

Silberling, N.J. & Tozer, E.T., 1968. Biostratigraphic Classification of the marine Triassic in North America. *Geological Society of America, Special Paper* 110, 63pp.

Spath, L.F., 1934. *Catalogue of the Fossil Cephalopoda in the British Museum (Natural History), part IV: The Ammonoidea of the Trias*, 521 pp. The Trustees of the British Museum, London.

Stanley, G.D., 2003. The evolution of modern corals and their early history. *Earth-Science Reviews 60*, 195-225.

Tong, J., Shi, G.R., 2000. Evolution of the Permian and Triassic foraminifera in south China. *In*: H. Yin, Dickins, J.M., Shi, G.R., Tong, J. (Editor), *Permian-Triassic Evolution of Tethys and Western Circum-Pacific. Developments in Palaeontology and Stratigraphy*. Elsevier, Amsterdam, 291-307.

Tozer, E.T., 1965. Lower Triassic stages and Ammonoid zones of Arctic Canada. *Paper of the Geological Survey of Canada 65-12*, 14 pp.

Tozer, E.T., 1994. Canadian Triassic Ammonoid Faunas. *Bulletin of the Geological Survey of Canada 467*, 1-663.

Waagen, W., 1895. Salt Ranges Fossils. vol. 2: Fossils from the Ceratites formation - Part I - Pisces, Ammonoidea. *Palaeontologia Indica 13*, 1-323.

Wang, Y.G. & He, G.X., 1976. Triassic ammonoids from the Mount Jolmo Lungma region. *In*: *A report of scientific expedition in the Mount Jolmo Lungma region (1966-1968)*, 223-502. Palaeontology, fascicule 3. Science Press, Beijing [In Chinese].

Waterhouse, J.B., 1994. The Early and Middle Triassic ammonoid succession of the Himalayas in western and central Nepal. Part 1. Stratigraphy, classification and Early Scythian ammonoid systematics. *Palaeontographica A232*, 1-83.

Waterhouse, J.B., 1996. The Early and Middle Triassic ammonoid succession of the Himalayas in western and central Nepal. Part 2. Systematic studies of the Early Middle Scythian. *Palaeontographica A241*, 27-100.

Wignall, P.B., and Twitchett, R.J., 2002. Extent, duration, and nature of the Permian-Triassic superanoxic event. *Geological Society of America, Special Paper 356*, 395-413.

CHAPTER 1

Dienerian (Early Triassic) ammonoids from the Candelaria Hills (Nevada, USA) and their significance for palaeobiogeography and palaeoceanography

Swiss J Geosci (2011) 104:161–181
DOI 10.1007/s00015-011-0055-3

Dienerian (Early Triassic) ammonoids from the Candelaria Hills (Nevada, USA) and their significance for palaeobiogeography and palaeoceanography

David Ware · James F. Jenks · Michael Hautmann · Hugo Bucher

Received: 25 November 2010 / Accepted: 4 February 2011 / Published online: 16 March 2011

Abstract A well-preserved ammonoid fauna of Early Dienerian age has long been known from the lower portion of the Candelaria Formation in the old Candelaria silver mining district in Mineral and Esmeralda Counties, Nevada, but for a number of reasons, this fauna has never been studied in detail nor illustrated. Previous authors assigned this ammonoid fauna to the Early Dienerian *Proptychites candidus* Zone of Canada. In reality, it more closely resembles the Tethyan faunas than the higher palaeolatitude Canadian faunas, thus indicating the presence of some degree of equatorial faunal exchange between opposite sides of the Panthalassic Ocean during Early Dienerian time. It also indicates the onset of a provincialism, which contrasts with the cosmopolitan Griesbachian faunas. A rigorous taxonomic analysis of the Candelaria fauna allows us to differentiate the following ten species, which include two new species and one new genus (*Mullericeras* nov. gen.) belonging to the new family Mullericeratidae: *Ambites lilangensis* (Krafft, 1909), *Ambites* aff. *radiatus* (Brühwiler, Brayard, Bucher and Guodun, 2008), *Ussuridiscus* sp. indet., "*Koninckites*" aff. *kraffti* Spath, 1934, *Mullericeras spitiense* (Krafft, 1909), *Mullericeras fergusoni* nov. sp., *Mullericeras* sp. indet., *Proptychites haydeni* (Krafft, 1909), *Proptychites pagei* nov. sp., *Vavilovites* sp. indet. and *Parahedenstroemia kiparisovae* Shigeta and Zakharov, 2009. This Early Dienerian fauna correlates with the *Ambites* fauna known from the base of the Ceratite Marls in the Salt Range and from the base of the "*Meekoceras*" beds in Spiti (northern Gondwanian margin). The fauna also permits the precise dating of a shelfal anoxic episode on the equatorial North American margin. This anoxic event correlates in time with similar palaeoceanographic changes in the southern Tethys, which indicates that the Early Triassic biotic recovery was at least partly shaped by such discrete, short events rather than by pervasive and lingering adverse environmental conditions.

Keywords Ammonoidea · Ceratitida · Biotic recovery · Anoxia

Résumé Une faune d'ammonites bien préservées de la base du Dienérien a depuis longtemps été reconnue à la base de la formation Candelaria dans le district des anciennes mines d'argent de Candelaria, Mineral et Esmeralda County, Nevada, mais pour différentes raisons, celle-ci n'avait jamais été étudiée en détail ni figurée. Les précédents auteurs ont corrélé cette faune avec la Zone à *Proptychites candidus* du Dienérien inférieur du Canada. Elle est en réalité plus proche des faunes téthysiennes que des faunes canadiennes, provenant de plus hautes paléolatitudes, ce qui indique la présence, au niveau de l'équateur, d'échanges de faunes entre les deux côtés de l'Océan Panthalassique au Dienérien inférieur. Cela démontre aussi la mise en place d'un provincialisme qui contraste avec les faunes cosmopolites du Griesbachien.

Editorial handling: Daniel Marty.

Electronic supplementary material The online version of this article (doi:10.1007/s00015-011-0055-3) contains supplementary material, which is available to authorized users.

D. Ware (✉) · M. Hautmann · H. Bucher
Paläontologisches Institut und Museum, Universität Zürich,
Karl Schmid-Strasse 4, 8006 Zurich, Switzerland
e-mail: david.ware@pim.uzh.ch

J. F. Jenks
1134 Johnson Ridge Lane, West Jordan, UT 84084, USA

Une analyse taxonomique rigoureuse nous a permis de différencier dix espèces, y compris deux nouvelles espèces et un nouveau genre (*Mullericeras* nov. gen.) appartenant à la nouvelle famille Mullericeratidae: *Ambites lilangensis* (Krafft, 1909), *Ambites* aff. *radiatus* (Brühwiler, Brayard, Bucher et Guodun, 2008), *Ussuridiscus* sp. indet., "*Koninckites*" aff. *kraffti* Spath, 1934, *Mullericeras spitiense* (Krafft, 1909), *Mullericeras fergusoni* nov. sp., *Mullericeras* sp. indet., *Proptychites haydeni* (Krafft, 1909), *Proptychites pagei* nov. sp., *Vavilovites* sp. indet. et *Parahedenstroemia kiparisovae* Shigeta et Zakharov, 2009. Cette faune du Dienérien inférieur peut être corrélée avec les faunes à *Ambites* de la base des Ceratite Marls dans les Salt Range et de la base des "*Meekoceras*" beds au Spiti (marge nord Gondwanienne). Elle permet de dater précisément un épisode anoxique sur la marge nord américaine équatoriale. Cet évènement anoxique est contemporain de changements paléoocéanographiques similaires au Sud de la Téthys, ce qui démontre que la récupération biotique du Trias Inférieur était au moins en partie influencée par de tels évènements courts et discrets plutôt que par des conditions environnementales défavorables généralisées et durables.

Mots clés Ammonoidea · Ceratitida · Récupération biotique · Anoxie

Institutional abbreviations

USNM	US Geological Survey Paleontology collections, Washington, D.C., USA
PIMUZ	Paläontologisches Institut und Museum collection, University of Zürich, Switzerland
NMMNH&S	New Mexico Museum of Natural History and Science, Albuquerque, New Mexico, USA
JJ	James F. Jenks' private collection, West Jordan, Utah, USA

1 Introduction

Most of the recent studies regarding Dienerian ammonoids and their biostratigraphy have mainly concerned the boreal realm: for example, Tozer (1961, 1963, 1994) conducted a comprehensive study of faunas from Arctic Canada and British Columbia, while Popov (1961), Ermakova (1981) and Dagys and Ermakova (1996) studied faunas from Siberia. In the lower latitudes, only a few recent studies have focused on the Tethyan realm, but these were in localities where the stratigraphic record is not as refined: e.g., Shigeta and Zakharov (2009) in Primorye (Eastern Russia), and Mu et al. (2007) and Brühwiler et al. (2008) in South China. Faunas from the northern Indian Margin are currently under revision at the University of Zürich. Apart from Guex (1978), who described a few Dienerian species from the Salt Range (Pakistan), there are no recent comprehensive studies of the ammonoids from this area. The most valuable monographs for this region are those by Waagen (1895) for the Salt Range, and Diener (1897) and Krafft and Diener (1909) for the north-western Indian Himalaya.

In this context, Dienerian ammonoids from the western USA provide valuable new insight into Early Triassic palaeobiogeography. Ammonoids from the Candelaria Formation, though previously cited and discussed by several authors (Muller and Ferguson 1936, 1939; Page 1959; Silberling and Tozer 1968), have never been described in detail nor illustrated. They are, however, very important since they come from the only locality in the lower latitudes of the North American continent with well preserved specimens. To their credit, Muller and Ferguson (1939) recognized that the Candelaria fossil assemblage represented two of the earliest Triassic marine faunas then known from North America, namely an older bivalve fauna consisting largely of *Claraia stachei* and a slightly younger *Proptychites* ammonoid fauna. They also documented the close affinity of their Candelaria ammonoids with those described by Waagen (1895) from the Salt Range of Pakistan and Krafft and Diener (1909) from the NW Himalaya. Later, Silberling and Tozer (1968) assigned a late Griesbachian age to the *Claraia* bivalve assemblage and correlated the ammonoid fauna with the Early Dienerian *Proptychites candidus* Zone of Canada.

Intensive field work conducted by the authors during the last 3 years has provided new, well preserved ammonoids as well as the inadvertent discovery of complete, well preserved specimens of marine Dienerian fish (Brinkmann et al. 2010). The purpose of this study is to provide a new, revised taxonomy of the ammonoid fauna and to discuss their palaeobiogeographic and palaeoceanographic implications.

2 Palaeogeographical and geological context

During the Early Triassic, two wide oceans, the Tethys and the Panthalassa, were separated by the Pangean supercontinent and several microcontinents. At that time, the Candelaria Hills of western Nevada (Fig. 1) were located on the eastern margin of Panthalassa, just a few degrees north of the equator.

Lower Triassic sedimentary rocks of marine origin are rather common in the western USA, but they are mainly Smithian and Spathian in age. Griesbachian and Dienerian

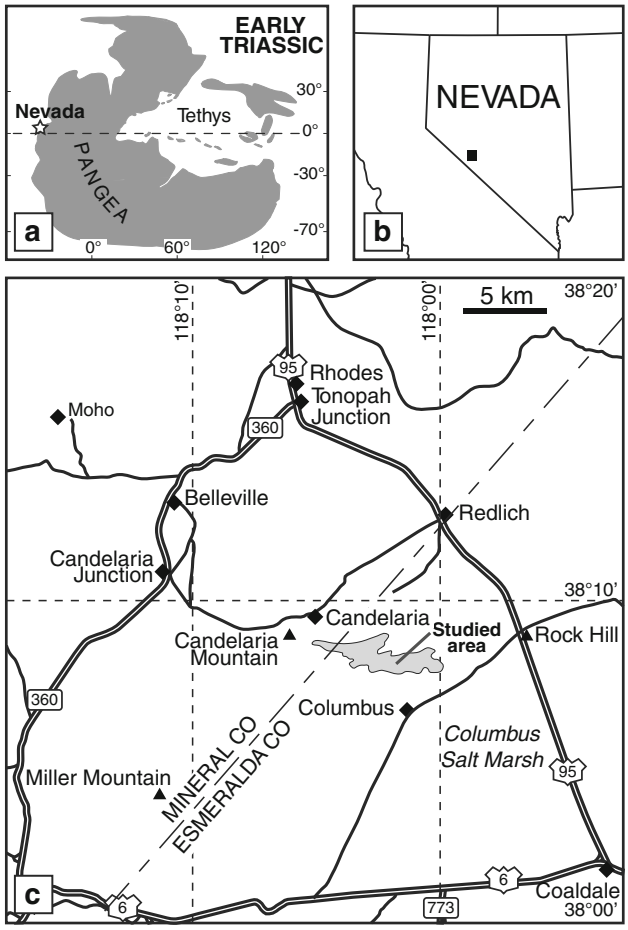

Fig. 1 **a** Simplified Early Triassic palaeogeography (modified after Brayard et al. 2006) and palaeoposition of Nevada. **b** Location of the Candelaria Hills, Nevada. **c** Location of the studied area showing areal extent of the Candelaria Formation (modified after Silberling 1984)

sediments, while not as common, are usually unfossiliferous, with the exception of the Candelaria Formation.

As discussed by Page (1959), the stratigraphic position of the Permian–Triassic boundary in the Candelaria Hills is not well defined. Muller and Ferguson (1939) regarded it as marked by an angular unconformity. The very base of the Candelaria typically contains a phosphatic nodule rich horizon named "Permian grit" by these authors, which they considered to be part of the Diablo Formation (Middle Permian). Page (1959) disagreed and considered this lower grit to actually be part of the Candelaria Formation and we fully agree with this interpretation. However, the age of the base of the Candelaria Formation remains unknown, as does the amount of time missing between the two formations. The Permian Diablo Formation is interpreted by Speed (1977) as part of the continental borderland. The lower member of the Candelaria Formation consists of ca. 100 m of quartzose and calcareous mudstones and sandstone with minor micritic limestone beds and early diagenetic nodules assigned here to an outer shelf depositional setting. With abundant breccias derived from rocks of the Golconda allochthon, the upper member of the Candelaria Formation as described by Speed (1977) records a major change in the origin of the clastic input and is considered by Saleeby and Busby-Spera (1992) to be syndeformational with the overriding plate of the Golconda. Hence, the palaeogeographic position of the low-paleolatitude Dienerian ammonoid fauna of the Candelaria Formation must be considered as plate-bound and not as belonging to an outboard terrane.

The fossiliferous interval is 20–25 m thick and approximately 45 m above the base of the Candelaria Formation. It is composed of dark bituminous shales, purplish on weathered surfaces, with a few thin beds of impure limestone and early diagenetic concretions. The lower part of this interval consists of pink weathering silty shales with a few thin silty limestone beds containing many bivalves of the genus *Claraia*, while most of the ammonoid fauna described herein is found in concretions and lenses that occur within a 10 m interval beginning about 5 m above the *Claraia* beds. However, three slightly older ammonoids were found in float concretions within the *Claraia* beds. These concretions contained fragments of *Claraia*, but their exact position within this interval will be the subject of ongoing fieldwork.

Claraia is represented by *C. stachei* Bittner, 1901 and *C.* cf. *mulleri* Newell and Kummel, 1942 (Fig. 2). The type material of *C. stachei* is from the Early Triassic of Malborgeth/Malborghetto (northern Italy), but Bittner (1901) introduced this species without giving illustrations and stratigraphic context, and he died before completing the envisaged monograph of his material. The current concept of *C. stachei* is based on material from the Griesbachian of east Greenland, which Spath (1930) identified on the basis of Bittner's (1901) short description. *C. stachei* is most abundant in the late Griesbachian (e.g., McRoberts 2010, fig. 3), but the position of the LAD of this species is uncertain. In the Western USA, *C. stachei* characterizes the "*Claraia*" zone of the Dinwoody Fm. in Wyoming and adjacent areas (Newell and Kummel 1942), which might extend into the Dienerian (Carr and Paull 1983). Ciriacks (1963, p. 80) reported an occurrence of *C. stachei* in the Thaynes formation at Hammond Creek (Idaho) in horizons "not dated in terms of ammonite zones but probably younger than the *Meekoceras* fauna, which suggests that the species ranges as high as Owenitan [=Smithian] age". However, specimens from these late occurrences have not been figured and thus their identity appears uncertain. In our samples, *C. stachei* co-occurs with ammonoids Dienerian in age (*Ambites* aff. *radiatus* and *Ussuridiscus* sp. indet.), thus confirming that it straddles the Griesbachian–Dienerian boundary. *C. mulleri* co-occurs with *C. stachei*

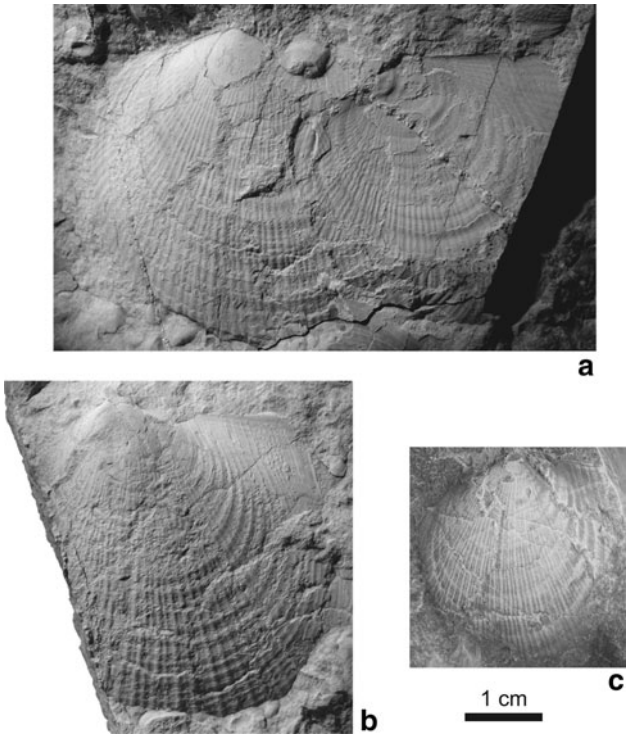

Fig. 2 *Claraia* from the Candelaria Formation, exact stratigraphic position unknown. **a** *Claraia stachei*, JJ67P, external view or left valve (*left*) and internal view or right valve (*right*). **b** *Claraia stachei*, JJ68P, external view or left valve, showing details of posterior wing. **c** *Claraia* cf. *mulleri*, JJ69P, external view of left valve

in the Dinwoody Fm. of Wyoming and differs from the latter only in having a more extended posterior auricle in the left valve and less pronounced commarginal costae (Newell and Kummel, 1942). Based on these differences, we provisionally assign one of our specimens to that species. However, analysis of larger samples might show that a consistent separation of both species is not possible.

The presence of dark, laminated bituminous shales and limestone yielding complete fishes (basal actinopterygians; Romano et al., unpublished data) is indicative of an anoxic sediment–water interface. The absence of associated benthic molluscs other than *Claraia* is an additional line of evidence diagnostic of oxygen-deficient bottom waters.

Compared to the relatively large areal extent of the Candelaria Formation (Fig. 1c), outcrops of the 25-m thick, recessive dark bituminous shale interval occur only in three areas, each of which is rather limited in size (largest is approx. 15 m × 200 m). The abundance of concretions and lenses is highly variable in these three areas. In the largest area, the slope of the hillside is fairly gentle and therefore, outcrops of concretions and lenses are very limited. Nevertheless, evidence of past collection activity is abundant as indicated by the numerous concretion fragments scattered all over the hillside. We have found only six in situ fossiliferous concretions within this area and since they were found more or less on strike, they likely represent only one concretion horizon. In contrast, the topography at one of the smaller outcrop areas is much steeper and at least three concretion horizons (Fig. 3) have been documented.

Many of our specimens lack accurate stratigraphical positioning because they were found in float concretion fragments scattered on the lower slopes of the largest outcrop area. Similarly, even though the U.S. Geological Survey-Stanford University collection contains many well preserved specimens, it also lacks precise stratigraphical information. Consequently, it is not possible to produce a precise stratigraphical log containing well documented horizons for all of the different ammonoids. Our log (Fig. 3) is based exclusively on those ammonoids occurring in the in situ concretions, with the exception of *Mullericeras spitiense*, which was found in a float concretion fragment a few meters above nodules containing *Ambites lilangensis*. Hence, we assume it co-occurs with *Parahedenstroemia kiparisovae*, but its actual source could be above or below.

3 Systematic palaeontology

Systematic descriptions are based on the classification of Waagen (1895), Tozer (1994) and Shigeta and Zakharov (2009). The quantitative morphological range of each species is expressed utilizing the four classic geometrical parameters of the ammonoid shell: diameter (D), whorl height (H), whorl width (W) and umbilical diameter (U). The three parameters (H, W and U) are plotted in absolute values as well as in relation to diameter (H/D, W/D, and U/D) provided measurements were available for at least five specimens. All measurements are given in the online resource.

Class	Cephalopoda Cuvier, 1797
Subclass	Ammonoidea Agassiz, 1847
Order	Ceratitida Hyatt, 1884
Superfamily	Meekoceratacea Waagen, 1895
Family	Gyronitidae Waagen, 1895
Genus	***Ambites* Waagen, 1895**
Type species	*Ambites discus* Waagen, 1895

***Ambites lilangensis* (Krafft, 1909)** (Figs. 4, 5, 6)

1909. *Meekoceras lilangense* Krafft, p. 23, pl. 1, figs. 2 (lectotype), 1, 3, 5, 6, 7, pl. 14 figs. 1, 2.
1934. *Prionolobus lilangensis* Spath, p. 101, pl. 4, fig. 4.
?1976. *Prionolobus lilangensis* Wang and He, p. 276, pl. 3, fig. 4, 5, text-fig. 8b.
1996. *Lilangia lilangense* Waterhouse, p. 36

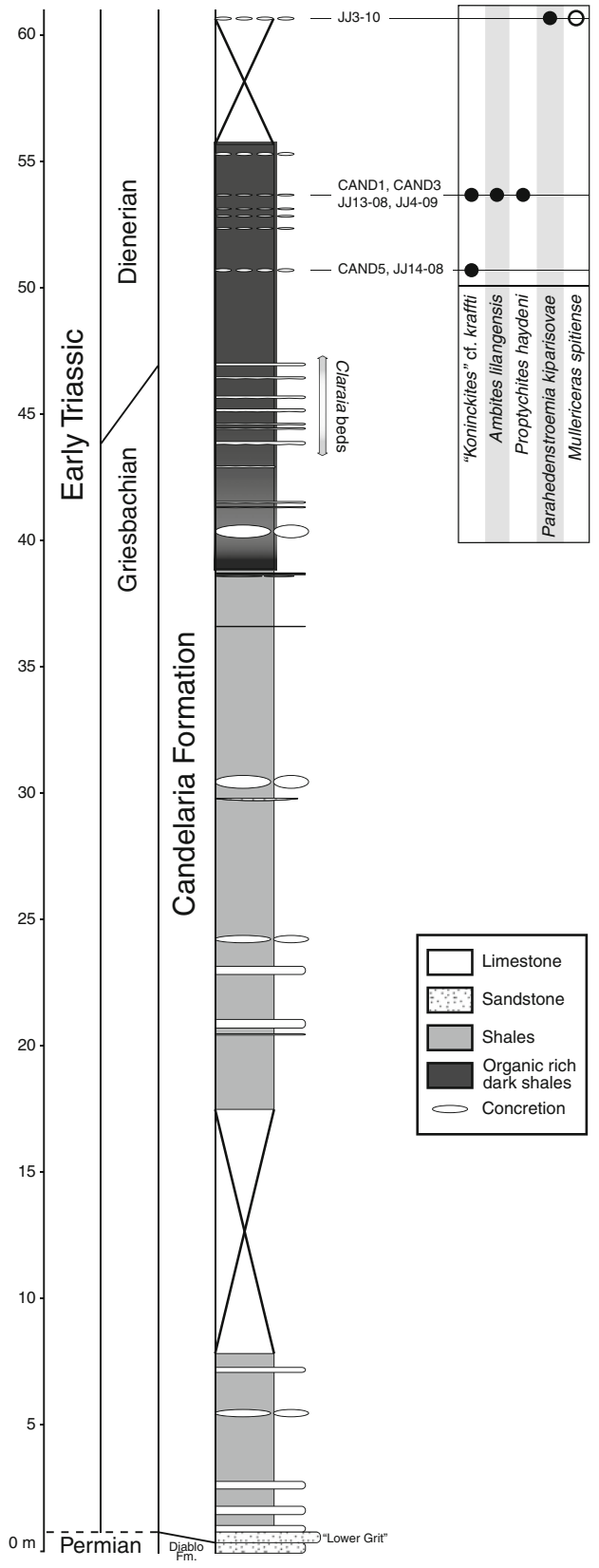

Fig. 3 Synthetic stratigraphic log with biostratigraphy of the few ammonoids found in situ (*solid circles* actual occurrence; *open circles* probable occurrence; see text for details)

Material Two specimens from the PIMUZ, 14 from the USNM, 16 from the Jenks private collection.

Description Platyconic shell with tabulate venter and angular, prominent ventrolateral shoulders protruding slightly above the flanks. Inner whorls moderately involute, generally becoming slightly more evolute during ontogeny (U/D changing from 20% to nearly 30%; some specimens, like the one shown in Fig. 4-3a, maintain the same involution during ontogeny, making them appear more involute than other specimens of similar size). Whorl cross section relatively thick (W/H varying from 40 to 60%). Flanks flat and parallel until the external third of the whorl, where they suddenly converge toward the venter. The rapidity of this change in convergence gives one the impression of a spiral line on the flank. Flanks become parallel again just before the ventrolateral shoulders, forming a slight concavity on the part of the whorl just below the ventral shoulder. Maximum whorl width occurs about mid-flank. Umbilical wall vertical and relatively high with subangular shoulder. Growth lines slightly biconcave and projected forward, accentuated on large specimens into indistinct sigmoidal folds. Faint strigation on the venter and below the ventral shoulders, which is visible only on the shell. Suture line ceratitic with three lateral rounded saddles separated by two rounded gently indentated lateral lobes, lateral lobes and saddles having approximately the same width. Auxiliary series not exposed.

Measurements See online resource and Fig. 6.

Remarks Waterhouse (1996) created a new genus, *Lilangia*, based on this species, and differentiated it from *Ambites* mainly by its denticulated lobes, whereas he considered that the type species of *Ambites* (*A. discus* Waagen, 1895) had a goniatitic suture line. He also considered *Lilangia* to have a higher, more differentiated umbilical wall. A close examination of new specimens from the type locality of *Ambites* (Amb, Salt Range, Pakistan; Ware et al., unpublished data) shows that its suture line actually has finely indentated lobes, just as *A. lilangensis* (Krafft, 1909), which is confirmed by new material collected by the first author from the type locality of this species (Lalung, Spiti Valley, Himachal Pradesh, India). The difference in shape of the umbilical wall is most probably just a consequence of the thicker whorl section of *A. lilangensis* compared to *A. discus*. We therefore consider the genus *Lilangia* to be a junior synonym of *Ambites.*

Occurrence Early Dienerian, *Proptychites* beds of Nevada, *Ambites* beds of Spiti valley (India).

***Ambites* aff. *radiatus* (Brühwiler, Brayard, Bucher and Guodun, 2008)** (Figs. 7, 8b)

2008. *Pleurambites radiatus* – Brühwiler et al., p. 1168, pl. 5, figs. 1 (holotype), 2, 3.

Material Two specimens from the Jenks private collection.

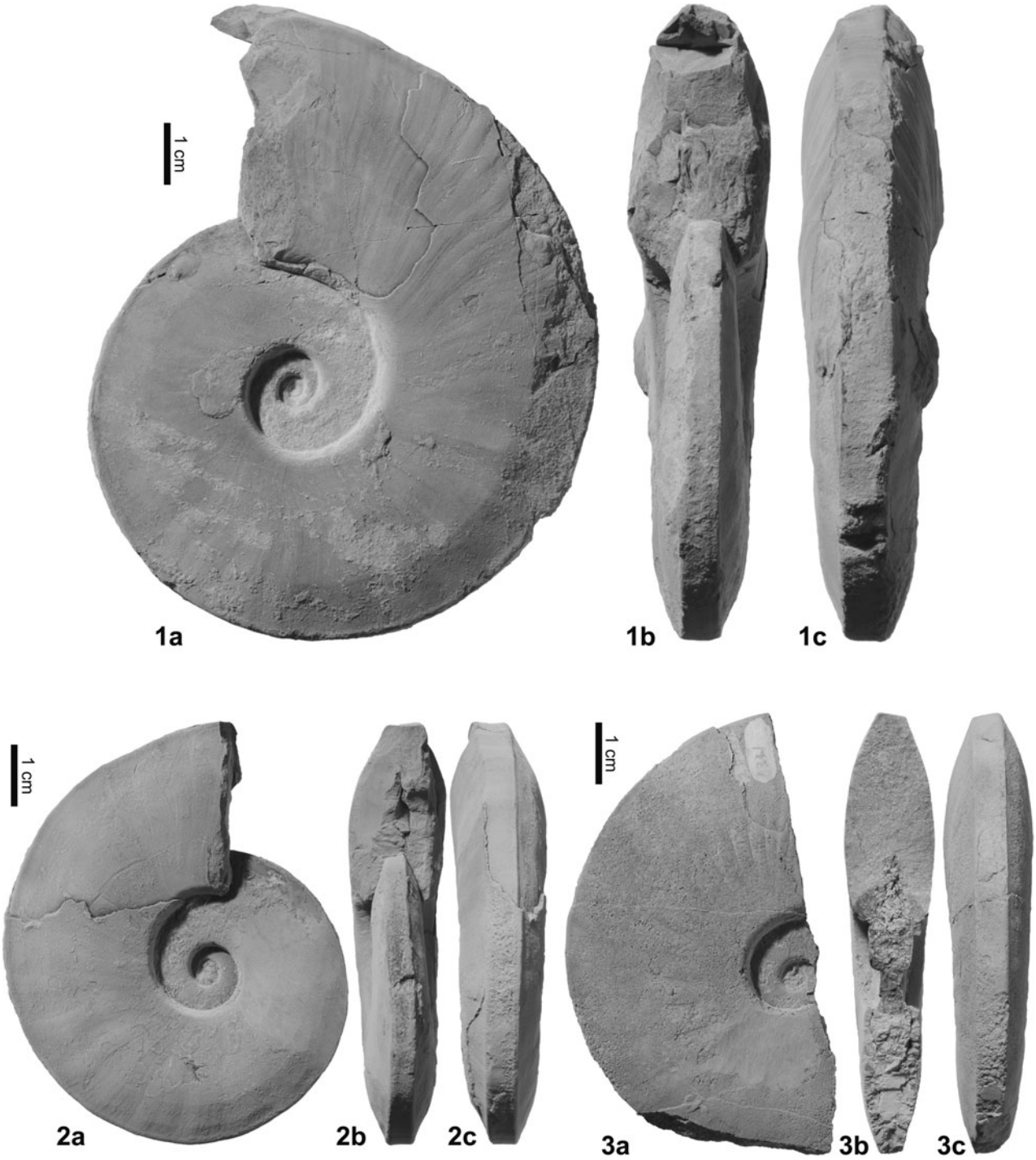

Fig. 4 *Ambites lilangensis* (Krafft, 1909). Three specimens with body chamber, but last septum not visible. **1** PIMUZ28596; **1a** lateral view; **1b** apertural view; **1c** ventral view. **2** USNM542474; **2a** lateral view; **2b** apertural view; **2c** ventral view. **3** USNM542485; **3a** lateral view; **3b** apertural view; **3c** ventral view

Description Very evolute platyconic shell with tabulate venter and angular, prominent ventrolateral shoulders protruding slightly above the flanks. Flanks slightly convex until the external quarter of the whorl, where they suddenly converge towards the venter, almost forming a spiral line as in the previously described species *A. lilangensis*. Maximum whorl width occurs about mid-flank. Umbilical wall undifferentiated, the flanks forming a gentle curve just before the umbilical seam. Slightly sigmoid radial folds, following the shape of the growth lines, become more

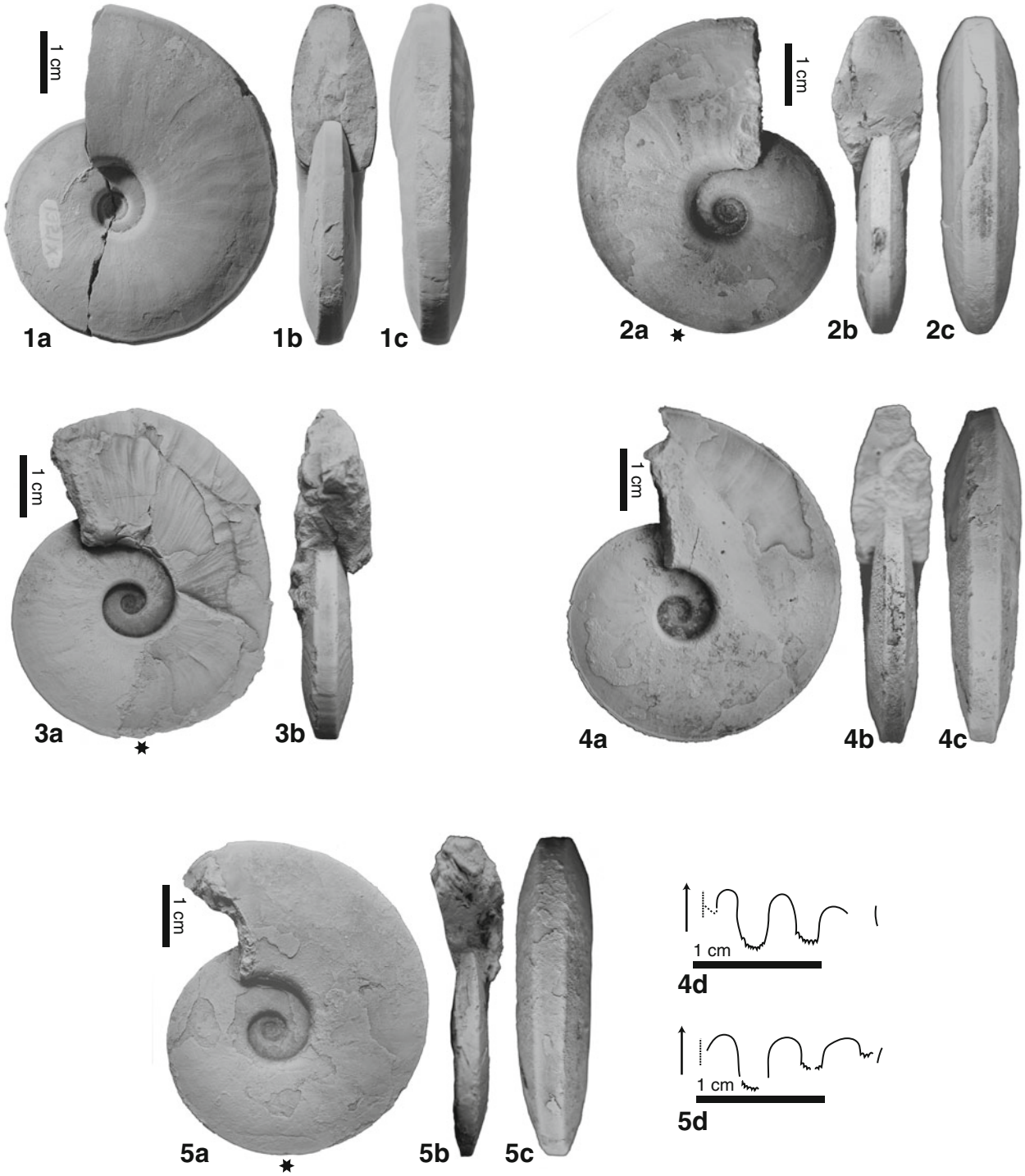

Fig. 5 *Ambites lilangensis* (KRAFFT, 1909). **1** USNM542477; **1a** lateral view; **1b** apertural view; **1c** ventral view. **2** JJ2023C; **2a** lateral view; **2b** apertural view; **2c** ventral view. **3** JJ2028C; **3a** lateral view; **3b** apertural view. **4** JJ2157C; **4a** lateral view; **4b** apertural view; **4c** ventral view; **4d** suture line at H = 16 mm. **5** JJ2154C; **5a** lateral view; **5b** apertural view; **5c** ventral view; **5d** suture line at H = 16.5 mm. *Asterisks* indicate last septum where known

abundant but less prominent on the body chamber. Suture line ceratitic with three rounded lateral saddles, the third one being much smaller than the other two. The first lateral lobe is rounded with minor indentation, and is nearly as wide as the two first lateral saddles. The second lateral lobe, also rounded, is much narrower and indentations are not visible probably because of poor preservation. Auxiliary series short.

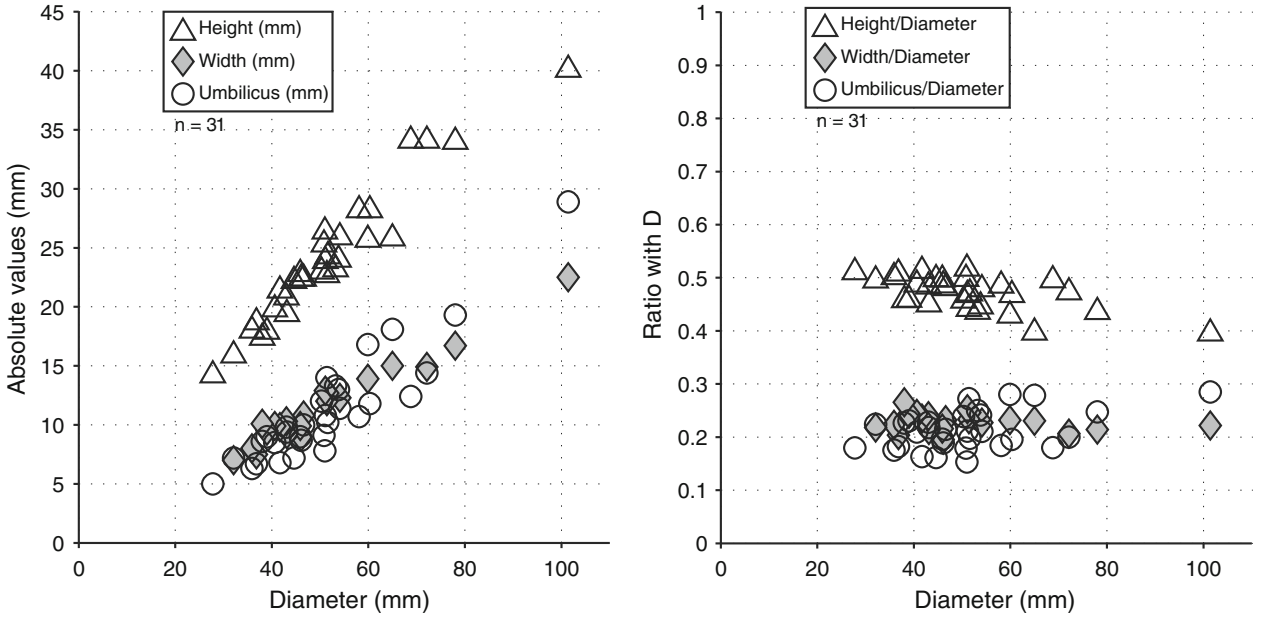

Fig. 6 Scatter diagrams of H, W, and U (*left*), and of H/D, W/D, and U/D (*right*) for *Ambites lilangensis* (Krafft, 1909). *D* diameter, *H* whorl height, *U* umbilical diameter, *W* whorl width

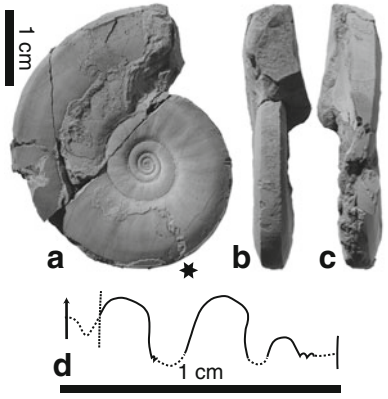

Fig. 7 *Ambites* aff. *radiatus* (Brühwiler, Brayard, Bucher and Guodun, 2008). JJ2173C, loc. JJ6-10; **a** lateral view; **b** apertural view; **c** ventral view; **d** suture line at H ≈ 8.4 mm, D ≈ 21 mm. *Asterisk* indicates last septum

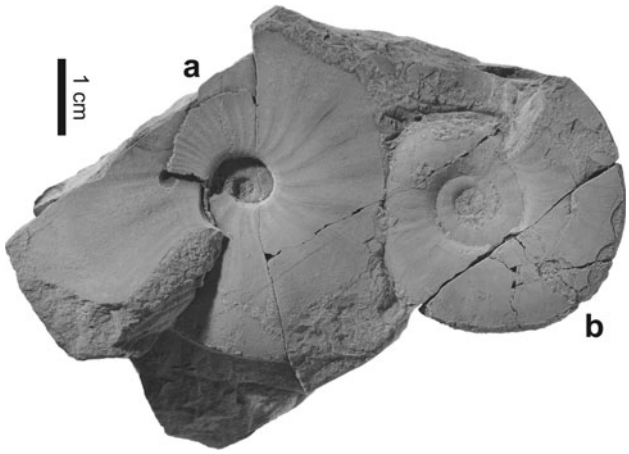

Fig. 8 JJ2175C, loc. 6-10. **a** *Ussuridiscus* sp. indet. **b** *Ambites* aff. *radiatus* (Brühwiler, Brayard, Bucher and Guodun, 2008). Both specimens retain their body chamber, but last septum is not visible

Measurements As the specimens are slightly distorted, no precise measurements were possible. However, the following proportions can be estimated. They are identical for both specimens: D ≈ 35 mm; H/D ≈ 35%; W/D ≈ 20%; U/D ≈ 35%.

Remarks These specimens differ from those described by Brühwiler et al. (2008) by their weaker ornamentation and the absence of a clearly differentiated umbilical wall. However, we have insufficient material to determine whether these differences are diagnostic or simply due to intraspecific variability. Brühwiler et al. (2008) attributed their new species to the genus *Pleurambites* Tozer, 1994. Tozer (1994) differentiated this genus from *Ambites* because of its stronger ornamentation. However, his specimens have a thicker whorl section than the type species of *Ambites*, but this difference is probably due to covariation between whorl thickness and ornamentation (first Buckman's law of covariation). Thus, we consider the genus *Pleurambites* to be a junior synonym of the genus *Ambites*. Our specimens, with their very evolute platyconic shape, are very close to the genus *Gyronites*. They, however, exhibit the following characteristics, which are typical of the genus *Ambites*: (1) the first lateral lobe is nearly as wide as the two first lateral saddle (it is much narrower in *Gyronites*), (2) the shell has a faint spiral line on the ventral

half of the flanks, (3) the ventrolateral shoulders protrude slightly above the flanks, and (4) the flank bears sigmoidal folds (some species of *Gyronites* have radial folds).

Occurrence Early Dienerian, *Claraia* beds, precise locality and horizon unknown, Candelaria Hills, Nevada, and Luolou Formation of Jinya (northwestern Guangxi, South China).

Genus *Ussuridiscus* Shigeta and Zakharov, 2009

Type species *Meekoceras* (*Kingites*) *varaha* Diener, 1895

***Ussuridiscus* sp. indet.** (Fig. 8a)

Material One specimen from the Jenks private collection.

Description Involute platyconic shell with tabulate venter and angular ventrolateral shoulders. Flanks slightly convex with maximum width at inner third of whorl height. Overhanging umbilical wall with angular shoulders. Umbilicus, which is characterized by overhanging wall with angular shoulders, suddenly becomes more open at the beginning of the last whorl. Flank exhibits faint, slightly sigmoidal folds that follow the shape of the growth lines. Suture line not visible.

Measurements Measurements not possible, specimen is slightly distorted and incomplete.

Remarks This specimen is morphologically close to those described by Shigeta and Zakharov (2009) as *Ussuridiscus varaha*, but it differs by its more convex flanks and its strong egression on the last whorl. As we have only one specimen, it is impossible to determine if these differences are due to intraspecific variability. We attributed this specimen to *Ussuridiscus* based on its overhanging umbilical wall, the main characteristic of the genus. However, this genus occurs in Primorye (where it was originally described by Shigeta and Zakharov 2009) together with the genus *Ambitoides*, which differs only by its sub-vertical umbilical wall and its stronger egression. We question the validity of the genus *Ambitoides*, since some of their very involute specimens are very close to the genus *Ussiridiscus* (differing only by their non-overhanging umbilical wall). However, other specimens become more evolute with growth and are very close to the genus *Ambites*, the genus to which the type species of *Ambitoides* (*Ambites fuliginatus* Tozer 1994) was originally ascribed.

Occurrence Early Dienerian, Candelaria Formation, *Claraia* beds, precise locality and horizon unknown, Candelaria Hills, Nevada.

Genus *Koninckites* Waagen, 1895

Type species *Koninckites vetustus* Waagen, 1895

"*Koninckites*" aff. *kraffti* Spath, 1934 (Figs. 9, 10)

1897. *Kingites varaha* Diener, p. 143, pl. 6, fig. 2, pl. 7, fig. 6.

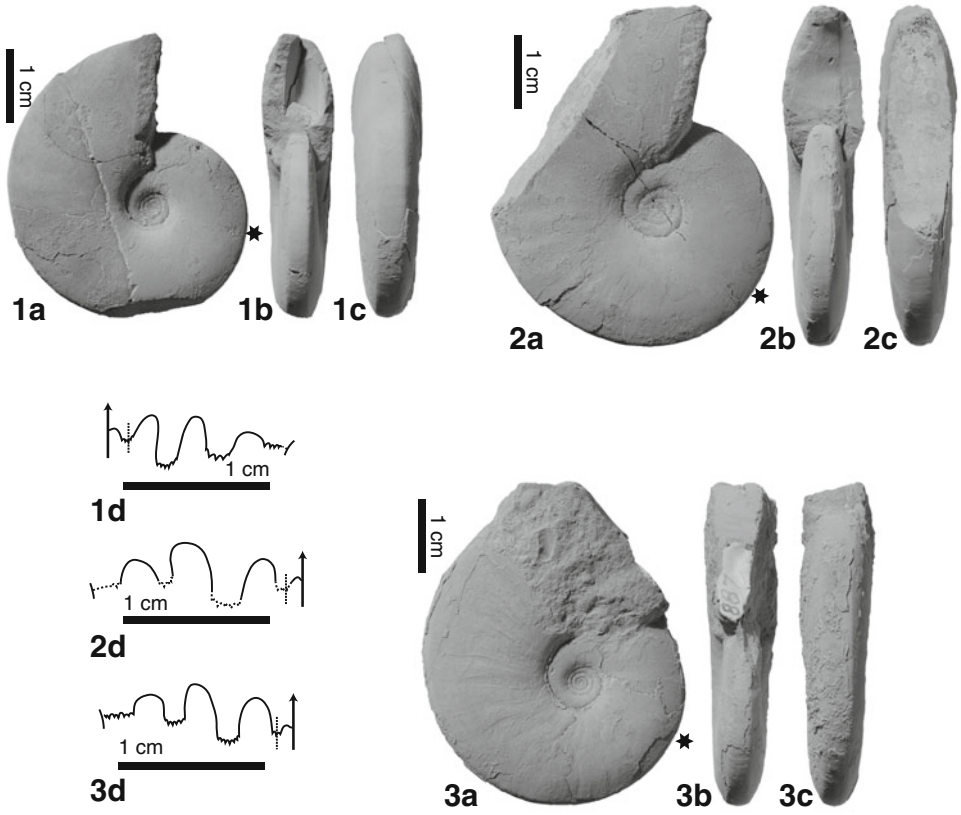

Fig. 9 "*Koninckites*" aff. *kraffti* Spath, 1934. **1** JJ2031C, loc. JJ14-08; **1a** lateral view; **1b** apertural view; **1c** ventral view; **1d** suture line at H = 10.9 mm, D ≈ 21.3 mm. **2** JJ2032C, loc. JJ14-08; **2a** lateral view; **2b** apertural view; **2c** ventral view; **2d** suture line at H = 13.2 mm, D ≈ 28.4 mm. **3** USNM542467; **3a** lateral view; **3b** apertural view; **3c** ventral view; **3d** suture line at H = 12.1 mm, D ≈ 22.1 mm. *Asterisks* indicate last septum

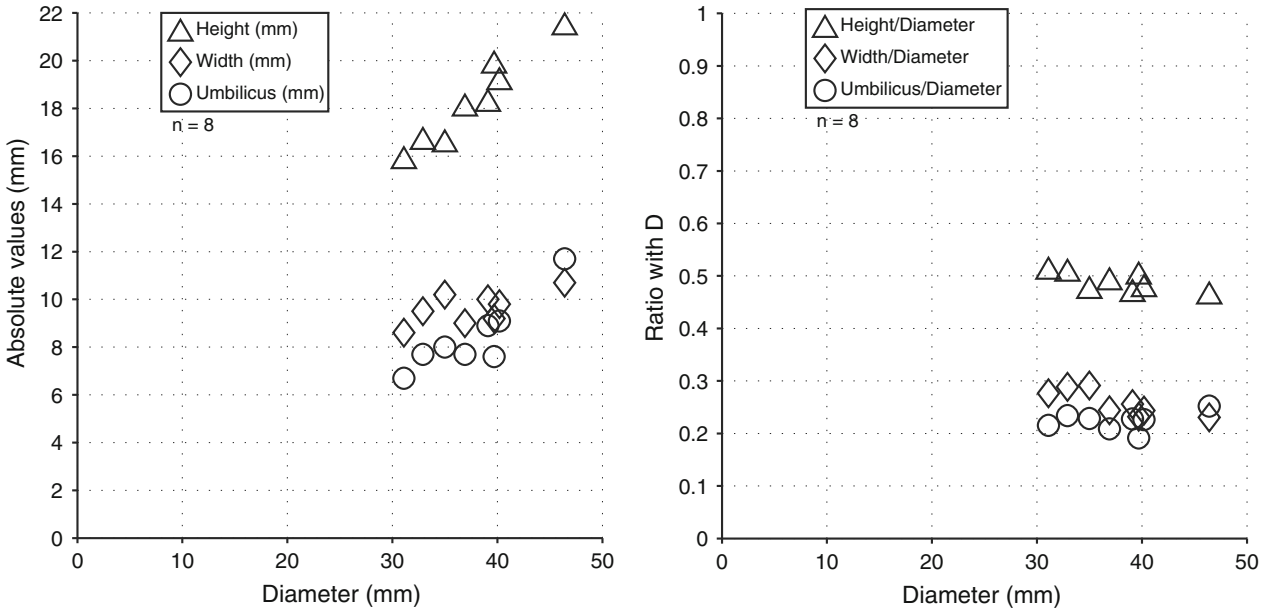

Fig. 10 Scatter diagrams of H, W, and U (*left*), and of H/D, W/D, and U/D (*right*) for "*Koninckites*" aff. *kraffti* Spath, 1934. *D* diameter, *H* whorl height, *U* umbilical diameter, *W* whorl width

1909. *Meekoceras varaha* Krafft and Diener, p. 17, pl. 2, figs. 4 (lectotype), 2, 3, 5, 6.
1915. *Meekoceras varaha* Diener, p. 195.
1930. *Meekoceras varaha* Spath, p. 28.
1934. *Koninckites kraffti* Spath, p. 155, fig. 43c.

NOT

1895. *Meekoceras* (*Kingites*) *varaha* – Diener, p. 52, pl. 1, fig. 3.

Material Two specimens from the PIMUZ, two from the USNM, six from the Jenks private collection.

Description Rather involute (U/D ≈ 20%), sub-platyconic shell with sub-tabulate venter and indistinct sub-angular ventrolateral shoulders. Flanks convex with maximum whorl width at mid-flank. Umbilical wall varying from quite high vertical wall with rounded indistinct shoulders to low indistinct wall. Shell smooth apart from slightly biconcave growth lines and a very fine strigation on the venter. Some specimens with remains of the external prismatic layer also exhibit strigation on the lower third of the flanks. Suture line ceratitic, quite similar to *Ambites lilangensis* but projected backward, with thinner lateral saddles and less rounded lateral lobes. Auxiliary series short, the largest specimen (USNM542467) showing a slightly differentiated auxiliary lobe.

Measurements See online resource and Fig. 10.

Remarks These specimens are slightly more evolute than the specimens identified by Krafft and Diener (1909) as *Meekoceras varaha* for which Spath (1934) created the species *K. kraffti*. They are otherwise very similar, and it is possible that the difference in the degree of involution is simply a result of intraspecific variability. Moreover, the genus *Koninckites* is not clearly defined; Waagen (1895) based his definition on the presence of a well-individualized auxiliary lobe, a size-dependent characteristic, which is present on most proptychitids and many other Smithan and Spathian taxa. This genus and its species requires a thorough revision. Our specimens do not exhibit a clearly individualized auxiliary lobe or saddle, but are otherwise very close to the type species of this genus. They are slightly more involute than *Ambites lilangense*, and also differ from this species by their suture line and indistinct ventrolateral shoulders.

Occurrence Early Dienerian, *Proptychites* beds of Nevada, *Ambites* beds of Spiti valley (India).

Family Mullericeratidae fam. nov.

Type genus ***Mullericeras*** gen. nov.

Etymology Named after S. W. Muller.

Diagnosis Hedenstroemiidae-like shells without adventitious lobes and saddles.

Description Compressed, very involute platyconic shell with a tabulate venter and a simple ceratitic suture line without adventitious lobes and saddles.

Remarks Species assigned to this family exhibit a morphology very similar to species belonging to Hedenstroemiidae,

such as *Clypites* or *Pseudosageceras*. They differ only by the absence of adventitious lobes and saddles, the main characteristic of the Sageceratacae, which is why we place it within the Meekoceratacae. The similarity in morphology between Mullericeratidae and Hedenstroemiidae, in addition to the fact that the former occurs in strata older than any from which hedenstroemiids with proper age constraints have thus far been described, suggests that our new family could be the ancestor of the Hedenstroemiidae. However, Waterhouse (1994) assigned a late Griesbachian specimen to the genus *Pseudosageceras*, which would contradict this hypothesis, but this specimen is extremely poorly preserved and its attribution to this genus cannot be confirmed by his illustration. It could also belong to our new family. The genus *Kymatites* Waagen, 1895 may also belong to this family, but a thorough revision of this genus is necessary to confirm it.

Genera included The type genus, *Mullericeras* nov. gen.

Occurrence Dienerian of the Candelaria Hills (Nevada, USA) and of the Spiti Valley (Himachal Pradesh, India).

Genus *Mullericeras* gen. nov.

Type species *Aspidites spitiensis* Krafft, 1909

Etymology Named after S. W. Muller.

Diagnosis. As the family Mullericeratidae fam. nov.

Description Compressed, very involute platyconic shell with a tabulate venter of variable width, sharp ventrolateral shoulders and a simple ceratitic suture line without adventitious lobes and saddles.

Remarks This genus includes species with morphologies very close to that of early hedenstroemiids such as *Clypites* or *Pseudosageceras*, but which lack adventitious lobes and saddles. Our new genus differs from *Kymatites* by its sharp ventrolateral shoulders, its narrower umbilicus and its ceratitic suture line with a well developed auxiliary series. It differs from *Koninckites* by its sharp ventrolateral shoulders, its more closed umbilicus, and by the absence of any auxiliary lobe or saddle. It differs from *Clypeoceras* (the genus to which they have been ascribed by previous authors) by its clearly tabulate venter.

Other species *Aspidites spitiensis* Krafft, 1909; *Meekoceras* (*Koninckites*) *vidharba* Diener, 1897; *Aspidites ensanus* Krafft, 1909.

Occurrence Dienerian of the Candelaria Hills (Nevada, USA) and of the Spiti Valley (Himachal Pradesh, India).

***Mullericeras spitiense* (Krafft, 1909)** (Figs. 11, 12)

1909. *Aspidites spitiensis* Krafft, p. 54, pl. 4, figs. 4 (lectotype), 5, pl. 16, figs 3, 4, 5, 6, 7, 8.
1934. *Clypeoceras spitiense* Spath, p. 160.
?1996. *Clypeoceras spitiense* Waterhouse, p. 50, text-fig. 4J, pl. 2, figs 21, 22.
?2009. *Clypeoceras spitiense* Shigeta and Zakharov, p. 125, fig. 113, 114.

Material Three specimens from the USNM, two from the Jenks private collection.

Diagnosis *Mullericeras* with a relatively thick whorl cross section (W/H ≈ 45%) and occluded umbilicus.

Description Involute and moderately compressed (W/D ≈ 25%) platyconic shell with tabulate, slightly sulcate venter of variable width and sharp ventrolateral shoulders. Venter slightly tectiform, making it appear almost tricarinate. Umbilicus occluded. Flanks slightly

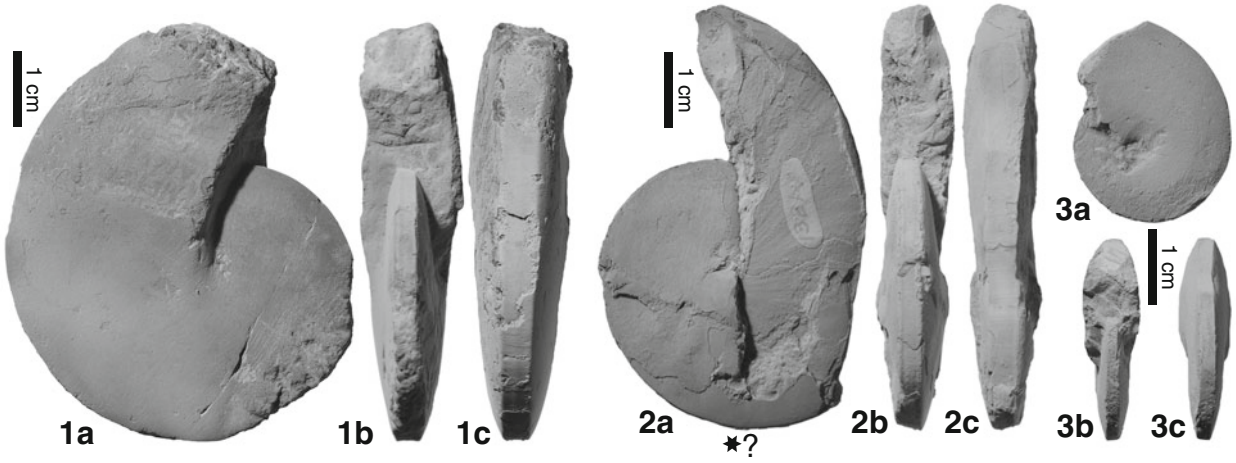

Fig. 11 *Mullericeras spitiense* (Krafft, 1909). **1** JJ2151C, loc. JJ15-08; **1a** lateral view; **1b** apertural view; **1c** ventral view. **2** USNM542471; **1a** lateral view; **1b** apertural view; **1c** ventral view. **3** USNM542470; **1a** lateral view; **1b** apertural view; **1c** ventral view. *Asterisk* with *question mark* indicates approximate position of last septum where known

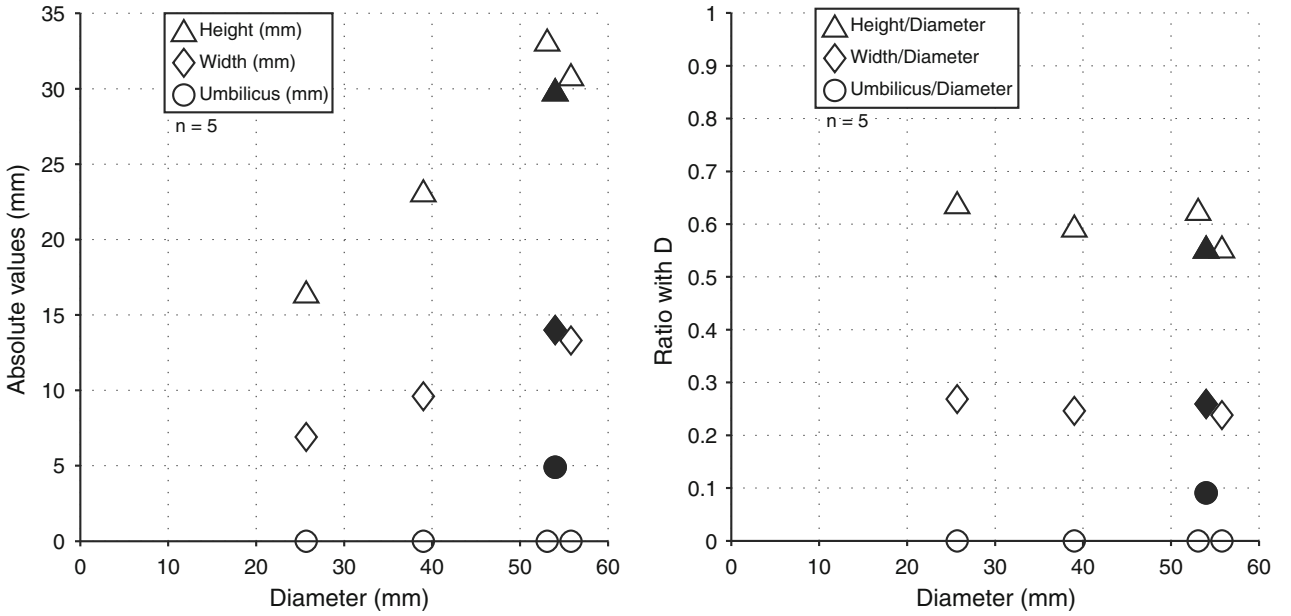

Fig. 12 Scatter diagrams of H, W, and U (*left*), and of H/D, W/D, and U/D (*right*) for *Mullericeras spitiense* (Krafft, 1909). *Solid symbols* represent the pathologic specimen figured in Fig. 21-3. *D* diameter, *H* whorl height, *U* umbilical diameter, *W* whorl width

convex, with maximum width at inner third of whorl height. Shell smooth apart from very thin, slightly biconcave growth lines. Suture line not well enough preserved to be drawn, but visible parts are coherent with drawings from Krafft and Diener (1909): ceratitic, without adventitious saddle, and with a long auxiliary series.

Measurements See online resource and Fig. 12.

Remarks Our specimens are morphologically identical to those described by Krafft and Diener (1909). The most striking point is the presence of what they referred to as "a low broad keel […] running along the siphonal area". This feature is unique among Dienerian ammonoids. Note that one of our specimens (2030C, JJ17-08) has an open umbilicus, but this opening is asymmetrical (broader on the right side than on the left side), we therefore interpret this anomaly as pathological (see discussion below). Shigeta and Zakharov (2009), following the lead of Spath (1934) and Waterhouse (1996), placed this species in the genus *Clypeoceras*, in the family Clypeoceratidae. They apparently did so because they considered that since *Clypeoceras superbus* (Waagen, 1895) (the type specimen of the type species of *Clypeoceras*) has a sub-tabulate venter, they then should include in the same genus other species with a clearly tabulate venter. In a recent study, Brühwiler et al. (in press) illustrated additional specimens from the type locality (Ceratite Sandstones of Chiddru, Salt Range, Pakistan), which clearly have a narrowly rounded venter. They actually consider this genus to be monospecific. We herein follow their classification. The specimen figured by Shigeta and Zakharov (2009) differs from the type specimen by its narrower venter, which lacks the "low broad keel […] running along the siphonal area". Moreover, its suture line is closer to that of *Clypites*: it is projected forward and exhibits narrow lateral saddles, with the second lateral saddle bent toward the umbilicus. Therefore, we question its assignment to this species. The specimen figured by Waterhouse (1996) is not well enough preserved to permit a positive identification.

Occurrence Dienerian, ?*Proptychites* beds of Nevada, ?Primorye and *Ambites* beds of Spiti valley (India).

***Mullericeras fergusoni* sp. nov**. (Fig. 13)

Holotype Specimen NMMNH P-62180, Loc. JJ17-08 (Fig. 13).

Type horizon and locality Candelaria Hills (Nevada), Candelaria Formation, precise horizon unknown. Specimen found as float.

Material Two specimens from Jenks private collection.

Etymology Species named after H. G. Ferguson.

Diagnosis Very thin *Mullericeras* with occluded umbilicus.

Description Involute and very thin (W/D not possible to measure, estimated at about 15%) oxyconic shell with narrowly sub-tabulate venter and quite indistinct ventrolateral shoulders. Umbilicus occluded. Flanks slightly convex, with maximum width at inner third of whorl

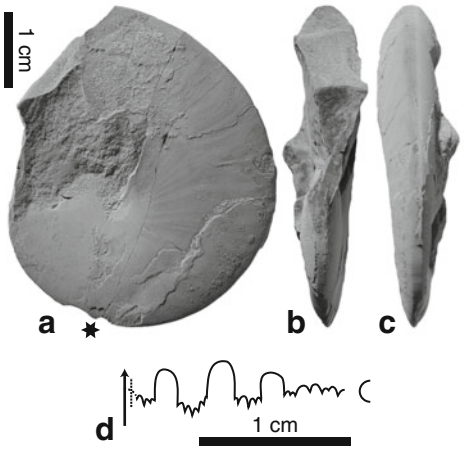

Fig. 13 *Mullericeras fergusoni* nov. sp. NMMNH P-62180, loc. JJ17-08, holotype; **a** lateral view; **b** apertural view; **c** ventral view; **d** suture line at H = 14.8 mm, D ≈ 25 mm. *Asterisk* indicates last septum

height, converging slowly towards the venter. Shell smooth apart from very thin proverse growth lines. Suture line ceratitic, with three rounded lateral saddles and two flattened lateral lobes of equal width, no adventitious saddles, and a long auxiliary series with a slightly differentiated auxiliary lobe.

Measurements See online resource.

Remarks *M. fergusoni* differs from *M. spitiensis* only by its thinner whorl section. Since specimens with a whorl width intermediate to *M. spitiense* and *M. fergusoni* have not been found, we decided to erect an additional species. Its thin whorl section makes it appear quite similar to the genus *Pseudosageceras*, but it differs by its very simple ceratitic suture line, which lacks adventitious saddles. It also differs by its whorl section, which exhibits convex flanks rather than the sub-triangular whorl section characteristic of *Pseudosageceras* with maximum width situated just above the umbilicus.

Occurrence Dienerian, Candelaria Formation, Candelaria Hills, Nevada.

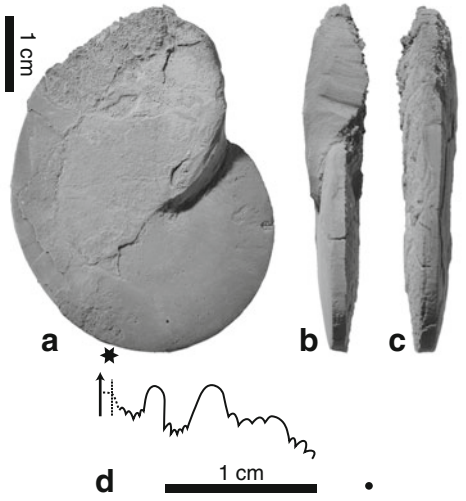

Fig. 14 *Mullericeras* sp. indet. USNM542468; **a** lateral view; **b** apertural view; **c** ventral view; **d** suture line at H ≈ 16 mm, D ≈ 27 mm. *Asterisk* indicates last septum

***Mullericeras* sp. indet.** (Fig. 14)

Material One specimen from the USNM.

Description Involute and very thin oxyconic shell with tabulate venter and sharp ventrolateral shoulders. Umbilicus occluded. Flanks sub-parallel, with maximum width just above the umbilicus. Shell smooth, growth lines not visible. Suture line ceratitic, but quite peculiar, very proverse, with narrow, elongated first lateral lobe and saddle, the second lateral saddle being wider. The second lateral lobe is very wide and shallow, the third lateral saddle is also very shallow and is almost not differentiated from the quite long but poorly preserved auxiliary series.

Measurements See online resource.

Remarks This specimen, with its very peculiar suture line, is clearly different from all of the specimens described above. However, we do not know its precise stratigraphic origin. Its matrix is somewhat different with its reddish iron oxide colour and it is slightly distorted, two points which compel us to consider that it may have come from a different part of the Candelaria Formation. Since it is the only specimen available and considering its uncertainty in age, we prefer to keep it in open nomenclature.

Occurrence Dienerian, Candelaria Formation, precise locality and horizon unknown, Candelaria Hills, Nevada.

Family Proptychitidae Waagen, 1895

Genus *Proptychites* Waagen, 1895

Type species *Ceratites lawrencianus* de Koninck, 1863

***Proptychites haydeni* (Krafft, 1909)** (Figs. 15, 16, 17)

1909. *Koninckites haydeni* – Krafft, p. 68, pl. 17, figs. 1 (lectotype), 2, 3, 4, 5, 6.

Material Four specimens from the USNM, one from the PIMUZ, and two from the Jenks private collection.

Description Involute (U/D ≈ 10%), relatively thick (W/H ≈ 50%) platyconic shell with rounded venter and indistinct ventrolateral shoulders. Inner whorls very involute (U/D ≤ 10%), becoming slightly more evolute during ontogeny (U/D = 12% for the largest specimen). Narrow, deep umbilicus with high vertical wall and rounded indistinct shoulders. Flanks convex with maximum whorl width at inner third of whorl height. Shell smooth apart from very thin

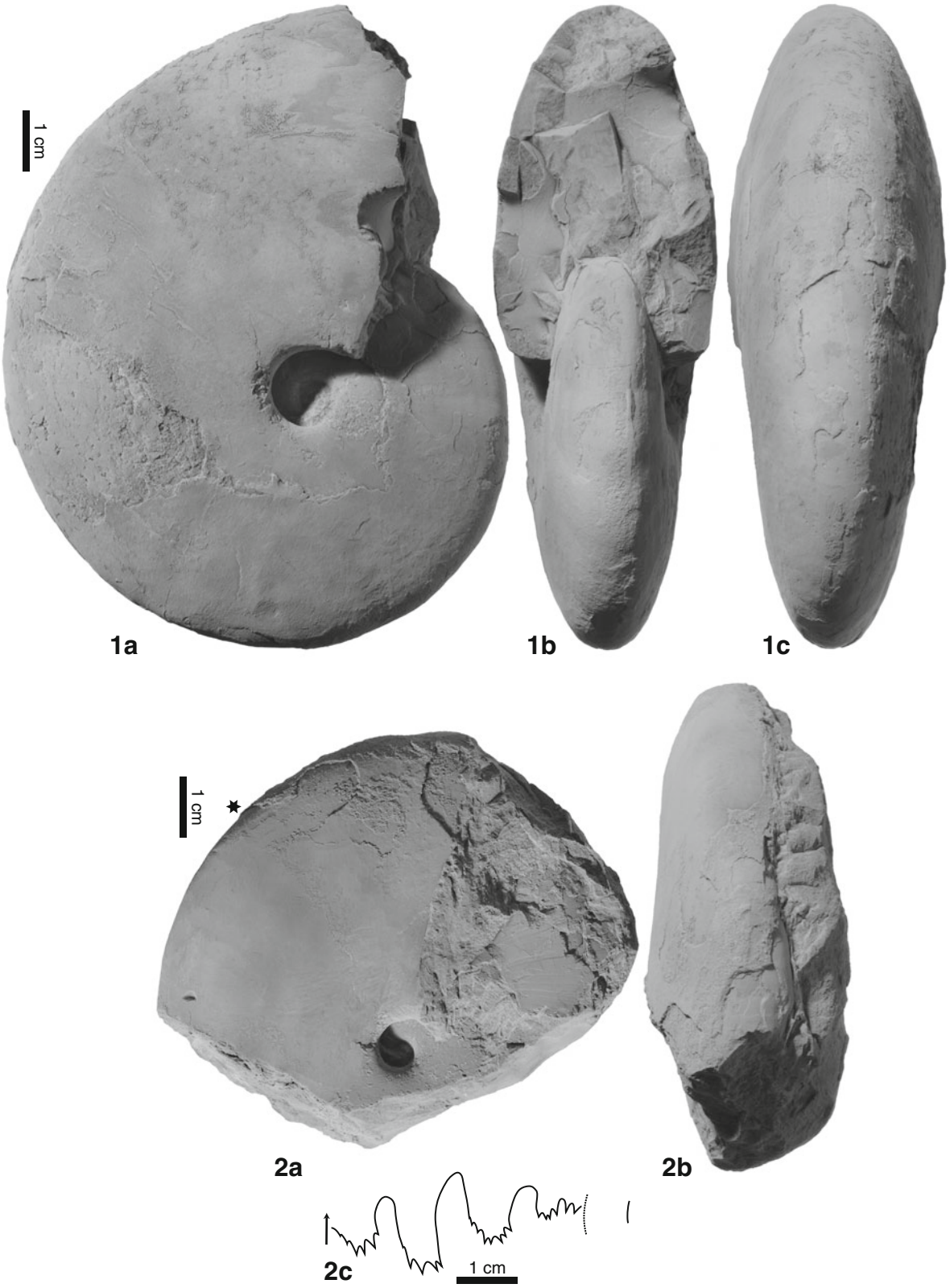

Fig. 15 *Proptychites haydeni* (Krafft, 1909). **1** USNM542461; incomplete phragmocone; **1a** lateral view; **1b** apertural view; **1c** ventral view. **2** USNM542455; **2a** lateral view; **2b** ventral view; **2c** suture line at H = 40.4 mm. *Asterisk* indicates last septum where known

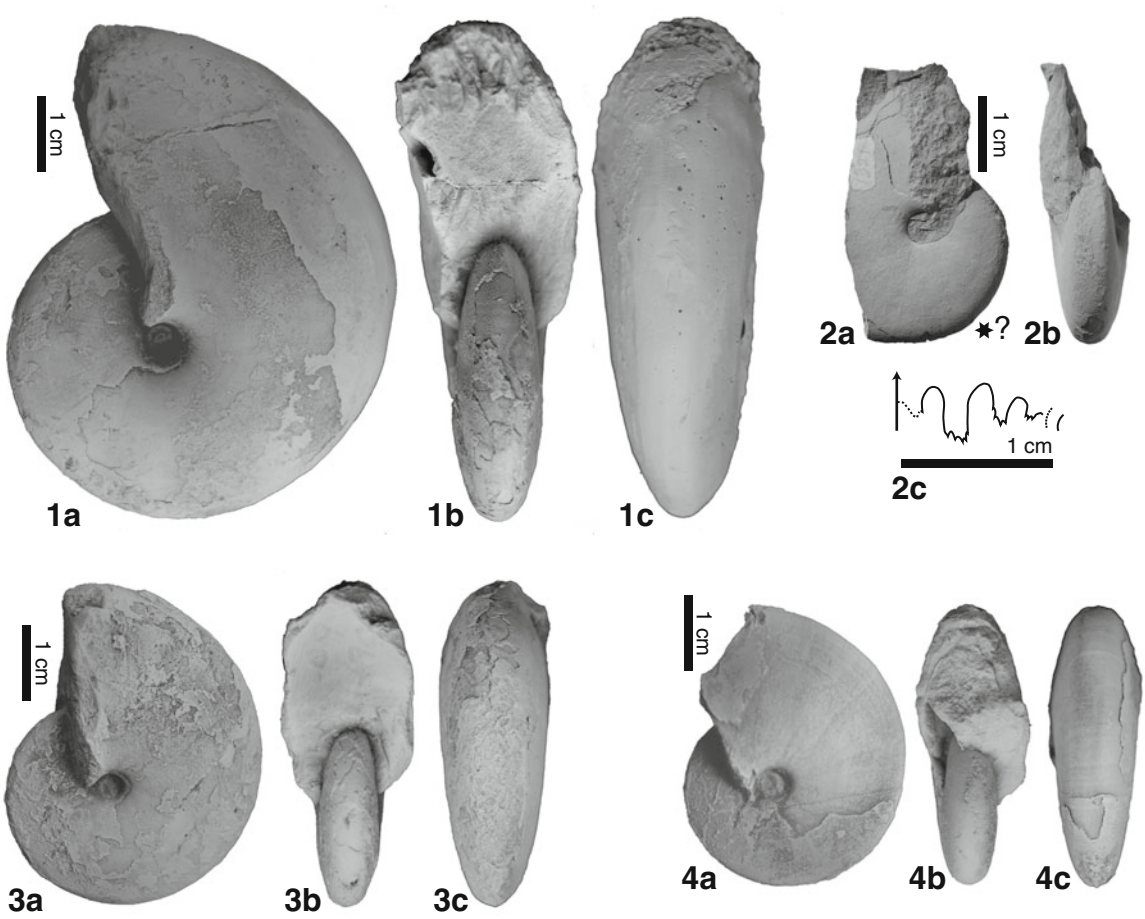

Fig. 16 *Proptychites haydeni* (Krafft, 1909). **1** JJ2148C. **1a** lateral view; **1b** apertural view; **1c** ventral view. **2** USNM542459; **2a** lateral view; **2b** apertural view; **2c** suture line at H = 9.9 mm, D ≈ 15.5 mm. **3** JJ2149C; **3a** lateral view; **3b** apertural view; **3c** ventral view. **4** JJ2150C; **4a** lateral view; **4b** apertural view; **4c** ventral view. *Asterisk* with *question mark* indicates approximate position of last septum where known

radial growth lines and, on large specimens, weak spiral ribs at the end of the phragmocone. Suture line with elongated thin saddles slightly bent towards the umbilicus, and moderately wide, heavily indentated lobes; auxiliary series with an individualized auxiliary lobe, but not completely exposed.

Measurements See online resource and Fig. 17.

Remarks This species differs from *P. ammonoides* Waagen, 1895 and *P. alterammonoides* Krafft, 1909 by its thicker whorl section, and from *P. lawrencianus* (de Koninck, 1863) by its thinner whorl section. Originally ascribed to the genus *Koninckites*, this species clearly differs from the type species of this genus (*K. vetustus* Waagen 1895) by its high, vertical umbilical wall, its broadly rounded venter and its suture line with elongated saddles bent towards the umbilicus and heavily indentated lobes. These three characteristics are typical of the genus *Proptychites*.

Occurrence Lower Dienerian, *Proptychites* beds of Candelaria Hills (Nevada), *Ambites* beds of the Salt Range (Pakistan) and of Spiti valley (India).

***Proptychites pagei* sp. nov.** (Fig. 18)

Types Holotype: specimen USNM542464 (Fig. 18-1). Paratype: specimen USNM 542465 (Fig. 18-2).

Type horizon and locality Candelaria Hills (Nevada), Candelaria Formation, precise locality and horizon unknown.

Material Two specimens from the USNM.

Etymology Species named after Ben M. Page.

Diagnosis Compressed proptychitid with occluded umbilicus.

Description Relatively thin (W/H ≈ 50%) platyconic shell with rounded venter, indistinct ventrolateral shoulders and occluded umbilicus. Flanks convex with maximum whorl width at inner third of whorl height. Shell nearly smooth with very weak radial folds. Suture line typical of proptychitids with wide, heavily indentated lateral lobes, a well differentiated auxiliary lateral lobe, and thin, elongated lateral saddles, the second one slightly bent towards

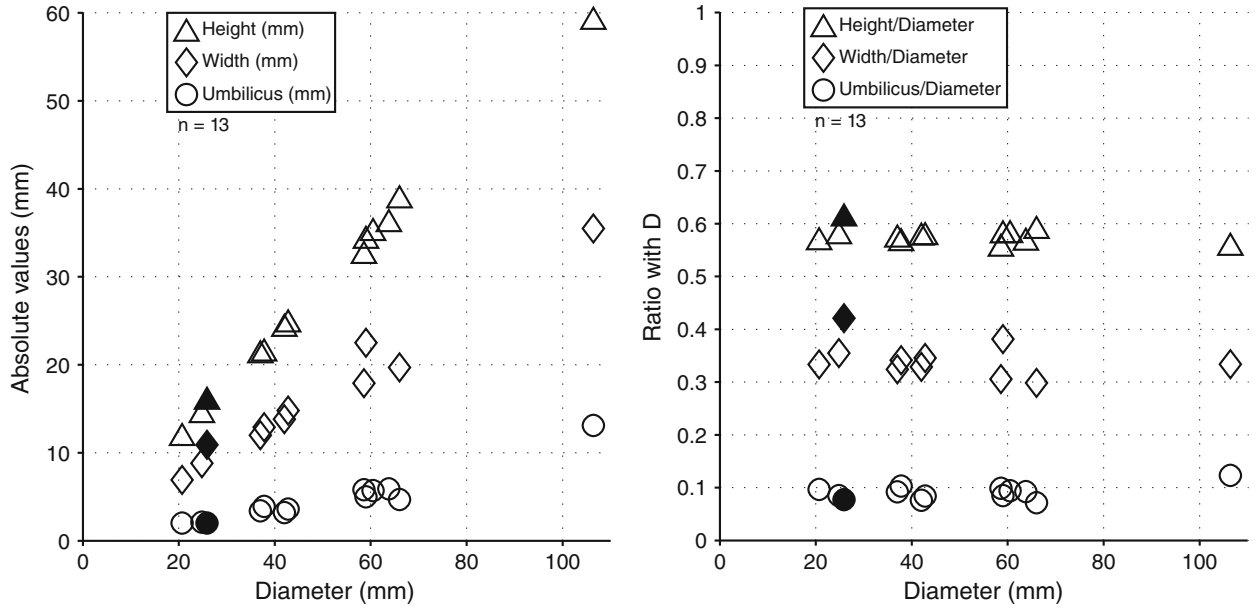

Fig. 17 Scatter diagrams of H, W, and U (*left*), and of H/D, W/D, and U/D (*right*) for *Proptychites haydeni* (Krafft, 1909). *Solid symbols* represent the pathologic specimen figured in Fig. 21-2. *D* diameter, *H* whorl height, *U* umbilical diameter, *W* whorl width

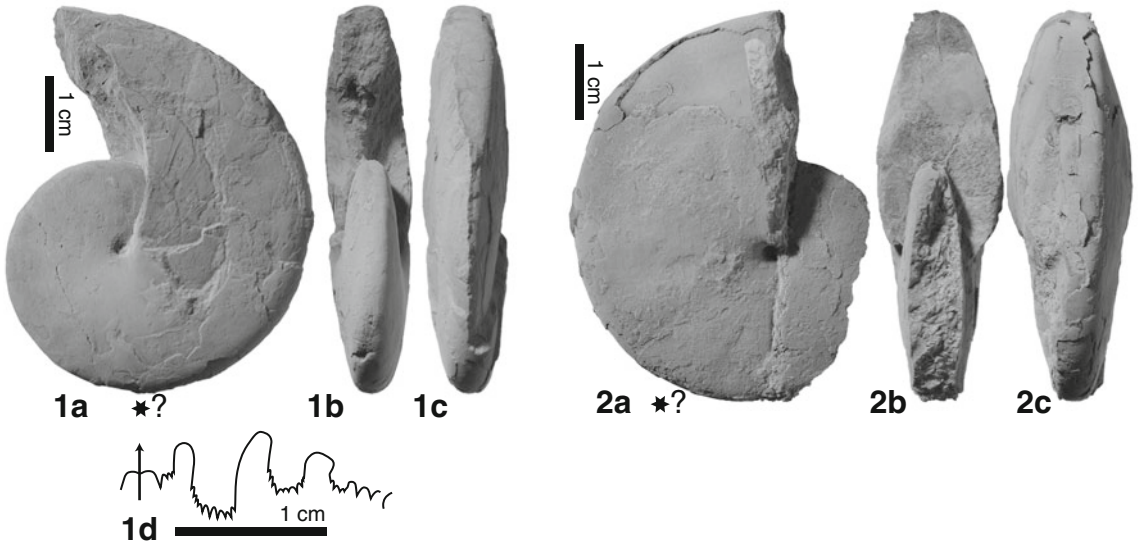

Fig. 18 *Proptychites pagei* nov. sp. **1** USNM542464, holotype; **1a** lateral view; **1b** apertural view; **1c** ventral view; **1d** suture line at H = 14.6 mm, D ≈ 23.8 mm. **2** USNM542465, paratype; **2a** lateral view; **2b** apertural view; **2c** ventral view. *Asterisks* with *question mark* indicate approximate position of last septum

the umbilicus, the third one flattened. Auxiliary series short apart from the third individualized lateral lobe.

Measurements See online resource.

Remarks This species clearly differs from any previously described species of *Proptychites* in having a relatively thin whorl section and occluded umbilicus.

Occurrence Dienerian, Candelaria Formation, Candelaria Hills, Nevada.

Genus *Vavilovites* Tozer, 1971

Type species *Paranorites sverdrupi* Tozer, 1963

***Vavilovites* sp. indet.** (Fig. 19)

Material One specimen from the PIMUZ, one specimen from the USNM.

Description Thick (W/H ≈ 65%) platyconic shell with narrow sub-tabulate, slightly arched venter delimited by distinct ventrolateral shoulders, and relatively broad

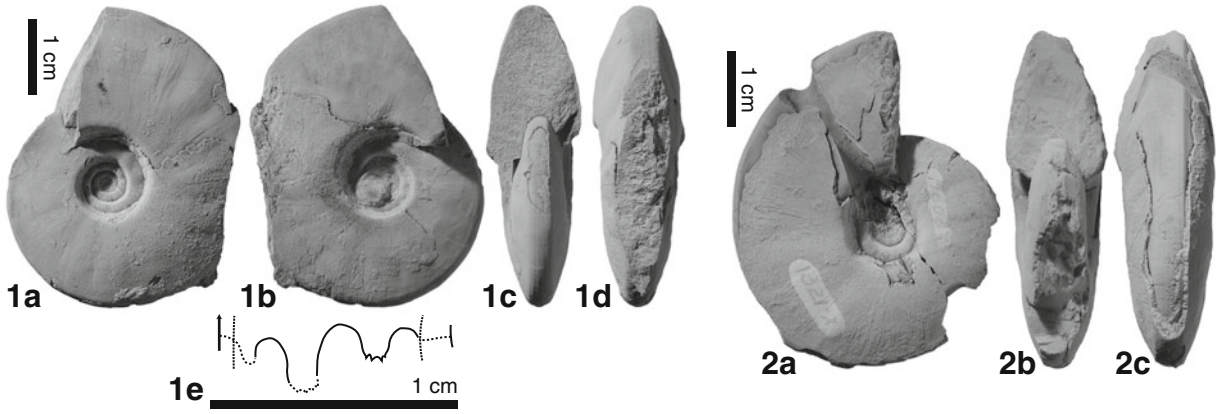

Fig. 19 *Vavilovites* sp. indet. **1** PIMUZ28850; **1a** lateral view (*right*); **1b** lateral view (*left*, with an encrusting bivalve on the umbilicus); **1c** apertural view; **1d** ventral view **1e** suture line at H = 8.7 mm. **2** USNM542472; **2a** lateral view; **2b** apertural view; **2c** ventral view. Both specimens retain their body chamber, but last septum is not visible

umbilicus (U/D ≈ 25%). Maximum whorl thickness at top of umbilical shoulder, giving the whorl section a sub-triangular shape. High, sub-vertical and slightly concave umbilical wall with distinct, rounded shoulders. Ornamentation consists of weak, but large, sinuous and slightly proverse radial folds that parallel the thin growth lines, and fine strigation on the venter. Suture line ceratitic with three rounded lateral saddles, the second one being larger than the other two and slightly bent towards the umbilicus, and a short auxiliary series starting at the umbilical shoulder.

Measurements See online resource.

Remarks A Stanford University collection card, dated 1935, that accompanied this specimen identifies it as *Ophiceras* (*Lytophiceras*) *sakuntala*. However, its degree of involution, narrow sub-tabulate venter and the presence of strigation on the venter preclude the attribution of this specimen to Ophiceratidae. Its sub-triangular whorl section and sub-tabulate venter indicate strong affinities with the genus *Vavilovites* Tozer, 1971, especially to juveniles of *V. turgidus* Dagys and Ermakova, 1996, but its suture line differs by its short auxiliary series. However, it was only possible to draw the suture line at a small diameter (at the beginning of the last preserved whorl, corresponding to an estimated diameter of about 2 cm). We have elected to retain the generic assignment of *Vavilovites* for our specimens because the variability of this taxon's juvenile suture lines has never been studied and the suture lines illustrated by Tozer (1963, 1994) represent much larger specimens of the type species of *Vavilovites*. In addition, as these specimens are small compared to other previously described species, we prefer to keep them in open nomenclature. Additional material would be necessary to determine whether they represent a new species. Note that one specimen (USNM542472, Fig. 19-2) is slightly asymmetric, its umbilicus being deeper on the left side than on the right side which could be the consequence of a growth disturbance induced by epizoans, such as in vivo encrusting bivalves on the umbilicus as described below. The other specimen (PIMUZ28850, Fig. 19-1) had bivalves attached to both sides of the umbilicus. The bivalve on the right side was removed during preparation, but that on the left side is visible in Fig. 19-1b. In this case, the bivalves have not induced any obvious growth disturbance.

Occurrence Dienerian, Candelaria Formation, precise locality and horizon unknown, Candelaria Hills, Nevada.

Superfamily Sageceratacеae Hyatt, 1884
Family Hedenstroemiidae Hyatt, 1884
Genus *Parahedenstroemia* Spath, 1934

Type species *Hedenstroemia acuta* Krafft, 1909

***Parahedenstroemia kiparisovae* Shigeta and Zakharov, 2009** (Fig. 20)

2009. *Parahedenstroemia kiparisovae* Shigeta and Zakharov, p. 137, fig. 128.

Material One specimen from the Jenks private collection.

Description Involute, thin (W/D = 27%) oxyconic shell with acute venter and occluded umbilicus. Flanks convex with maximum whorl width at about mid-flank. Shell smooth with fine, sinuous prorsiradiate growth lines. Suture line with a wide ventral lobe and a well individualized adventitious saddle. Lateral lobes relatively thin and deep with strong denticulation at their base. Auxiliary series not preserved.

Measurements See online resource.

Remarks This specimen appears to be identical in nearly every respect to the specimens considered by Shigeta and Zakharov (2009) to be juveniles. However, our specimen is

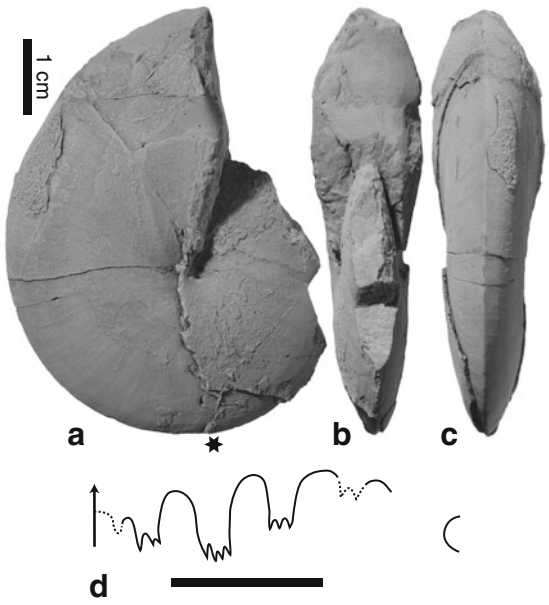

Fig. 20 *Parahedenstroemia kiparisovae* Shigeta and Zakharov, 2009. JJ2164C, loc. JJ3-10; **a** lateral view; **b** apertural view; **c** ventral view; **d** suture line at H = 20.3 mm, D ≈ 36 mm. *Asterisk* indicates last septum

intermediate in size to their juveniles and their holotype, which is quite different with its thicker whorl section and less-acute venter. Its suture line is also very different, with strongly phylloid saddles and more denticulated lobes. However, we don't have sufficient material to determine if these differences are diagnostic or simply the result of intraspecific variability. Therefore, we prefer to keep our specimen in the same species.

Occurrence Dienerian, Candelaria Formation, Candelaria Hills, Nevada, and Zhitkov Formation, South Primorye, Russia.

4 Palaeopathology: growth disturbance induced by epizoan bivalves

Many of the ammonoid specimens from the Candelaria Formation exhibit an umbilicus that has been encrusted on both sides by bivalves. On some specimens, these bivalves have induced a distortion of the umbilical wall of the ultimate whorl, thus indicating they encrusted the ammonoids in vivo. Whether or not anoxic bottom waters played a role in this high frequency of epizoans attached to living ammonoids remains to be quantitatively assessed through comparisons with the next older and younger faunas. The resulting modification of the umbilical morphology can be substantial, and it can therefore lead to the mis-identification of some specimens. This feature can best be seen on the complete specimen of "*Koninckites*" cf. *kraffti* (Fig. 21-1). On the right side of this specimen, the body chamber overlaps the completely preserved bivalve, which encrusted the preceding whorl, thus modifying the width of the umbilicus and causing the umbilical wall to overhang. Only a piece of the attached valve is preserved on the specimen's left side, but it did not induce any obvious growth disturbance on that side.

A few ammonoid specimens have bivalves encrusting other parts of the shell, but since no details of the bivalve's shell interior are visible, their taxonomic affinity remains unknown. We cannot exclude the possibility that they may represent more than one species. Some specimens remotely resemble *Placunopsis*, which is well-known for encrusting Middle Triassic ammonoids from the Germanic Basin. However, some individuals exhibit an unusually high doming of the upper valve, a trait which has not been observed in *Placunopsis*.

No remains of bivalves are preserved on the other two illustrated specimens (Fig. 21-2, 21-3), but they both exhibit an umbilicus that has been modified, most likely by the same type of bivalves. Figure 21-2 illustrates a juvenile specimen of *Proptychites haydeni*, whose right side umbilicus is normal, but on its left side, its umbilicus exhibits a very high umbilical wall with a sharp shoulder protruding over the flank. Figure 21-3 shows a fully developed specimen of *Mullericeras spitiense*, which differs from other specimens by having a slightly open umbilicus (a crucial point which could lead to misidentification), but it is asymmetrical, with the umbilicus more open on the right side than on the left side.

5 Discussion and conclusions

Although there are no common species between this fauna and the Canadian faunas described by Tozer (1961, 1994), the presence of the genus *Ambites* in each fauna permits the correlation of the Candelaria fauna with the lower Dienerian *Proptychites candidus* Zone of mid-palaeolatitude British Columbia and Arctic Canada, which was already pointed out by Silberling and Tozer (1968). The genus *Ambites* is also very common in the Northern Indian Margin. It is well documented from the base of the Ceratite Marls in the Salt Range, Pakistan (Waagen 1895) and from the base of the "*Meekoceras* beds" in Spiti and Kashmir (Diener 1897; Krafft and Diener 1909). The Candelaria fauna correlates with the base of the "*Prionolobus rotundatus, Paranorites volutus*" Zone of Guex (1978), with the base of the *Proptychites lawrencianus* Zone of Mojsisovics et al. (1895) and with the base of the *Gyronites frequens* Zone of Krystyn et al. (2004, 2007). A general low-paleolatitude correlation scheme based on residual maximal associations (Guex, 1991) translating into a

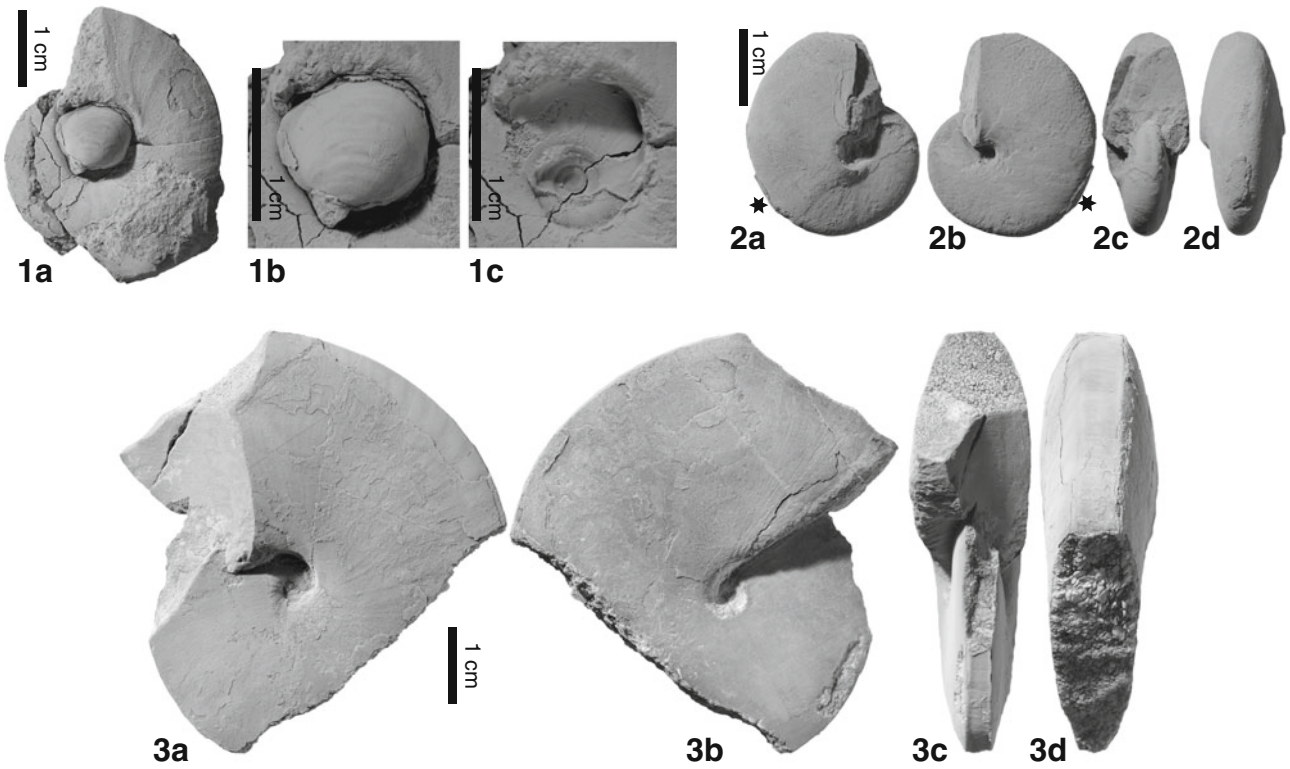

Fig. 21 Specimens with growth disturbance induced by epizoans: **1** "*Koninckites*" aff. *kraffti* Spath, 1934, PIMUZ28597. Specimen with preserved bivalve attached to the umbilicus. **1a** Lateral view; **1b** close-up view of the umbilicus with the bivalve and **1c** without the bivalve. **2** *Proptychites haydeni* (Krafft, 1909), USNM542458; **2a** lateral view (*left*); **2b** lateral view (*right*); **2c** apertural view; **2d** ventral view. **3** *Mullericeras spitiense* (Krafft, 1909), JJ2030C, loc. JJ17-08; **3a** lateral view (*right*); **3b** lateral view (*left*); **3c** apertural view; **3d** ventral view. *Asterisks* indicate last septum where know

homogenous biochronological nomenclature must await the completion of the high-resolution analyses of the Dienerian faunal successions from Spiti and from the Salt Range (Ware et al., unpublished data).

Not surprisingly, the low-palaeolatitude Candelaria ammonoid fauna tends to more closely resemble the Tethyan faunas than the higher palaeolatitude Canadian faunas. This observation is supported by the presence of *Proptychites haydeni*, *Ambites lilangensis* and *Mullericeras spitiense*, which occur in the southern Tethys but not in the boreal realm. These similarities at least demonstrate that equatorial faunal exchanges occurred across the Panthalassa during Early Dienerian times. The differences between the low palaeolatitude faunas and those from the boreal realm document the onset of provincialism, which contrasts with the cosmopolitan Griesbachian ammonoid faunas. This Dienerian provincialism likely induced a weak latitudinal diversity gradient (Brayard et al. 2006).

The Early Dienerian fauna typically occurs within a 20–25 m thick anoxic episode in the Candelaria Formation. The fauna described here allows the precise dating of this discrete anoxic episode, which occurred in the equatorial region of the North American continental margin. Coeval anoxic or dysoxic events have also been reported from several localities in the Tethys: in the Salt Range (Pakistan; Hermann et al. 2011), in Spiti (NW India; Galfetti et al. 2007) and in Guangxi (South China, Galfetti et al. 2008), as well. This discrete anoxic episode clearly recorded in the north Gondwanian shelves can now be safely extended to the equatorial North American margin. If it apparently reflects a large scale oceanographic change within the low paleolatitude shelves, the bathymetric extension of this Early Dienerian anoxic event must be assessed in order to test the commonly invoked scenario of a rise of the oxygen minimum zone coupled with transgressions. How this Dienerian event is manifested into the higher palaeolatitude records also remains to be investigated. It nevertheless already appears that the "complex" image of a pervasive anoxia popping up here and there at many different times during most of the Early Triassic (e.g., Wignall and Twitchett 2002) does not withstand the accumulation of new evidence. The new general trend that is globally emerging is that of a discrete time distribution of a few events of oxygen deficiency.

Acknowledgments Kevin McKinney, USGS Paleontology Collections Curator and Norman Silberling, both of Denver Colorado, are thanked for their respective roles in arranging for the loan of the USGS-Stanford University collection of Candelaria ammonoids. Technical support for preparation and photography was provided by Markus Hebeisen and Rosemarie Roth (Zürich). Claude Monnet (Zürich) is thanked for providing his statistical software. Spencer Lucas and Dieter Korn are thanked for their useful reviews which helped improve the final version of this work. This paper is a contribution to the Swiss National Science Foundation project 200020-127716 (to HB).

References

Bittner, A. (1901). Über *Pseudomonotis Telleri* und verwandte Arten der unteren Trias. *Jahrbuch der Kaiserlich-Königlichen Geologischen Reichsanstalt, 50*, 559–592.

Brayard, A., Bucher, H., Escarguel, G., Fluteau, F., Bourquin, S., & Galfetti, T. (2006). The Early Triassic ammonoid recovery: Paleoclimatic significance of diversity gradients. *Palaeogeography, Palaeoclimatology, Palaeoecology, 239*, 374–395.

Brinkmann, W., Romano, C., Bucher, H., Ware, D., & Jenks, J. F. (2010). Palaeobiogeography and stratigraphy of advanced gnathostomian fishes (Chondrichthyes and Osteichthyes) in the Early Triassic and from selected Anisian localities (Report 1863–2009). *Zentralblatt für Geologie und Paläontologie, II*(Heft 5/6), 765–812.

Brühwiler, T., Brayard, A., Bucher, H., & Guodun, K. (2008). Griesbachian and Dienerian (Early Triassic) ammonoid faunas from Northwestern Guangxi and Southern Guizhou (South China). *Palaeontology, 51*, 1151–1180.

Brühwiler, T., Bucher, H., Ware, D., Hermann, E., Hochuli, P. A., Roohi, G., Rehman, K., & Yaseen, A. Smithian (Early Triassic) ammonoids from the Salt Range, Pakistan. *Special papers in palaeontology* (in press).

Carr, T. R., & Paull, R. K. (1983). Early Triassic stratigraphy and palaeogeography of the Cordilleran miogeocline. In M. W. Reynolds & E. D. Dolly (Eds.), *Mesozoic paleogeography of the West-central United States* (pp. 39–55). Rocky Mountain Paleogeographic Symposium, 2, SEPM Rocky Mountain Section, Denver.

Ciriacks, K. W. (1963). Permian and Eotriassic bivalves of the Middle Rockies. *Bulletin of the American Museum of Natural History, 125*, 1–100.

Dagys, A. S., & Ermakova, S. (1996). Induan (Triassic) ammonoids from North-Eastern Asia. *Revue de Paléobiologie, 15*, 401–447.

Diener, C. (1895). Triadische Cephalopodenfaunen der ostsibirischen Küstenprovinz. *Mémoires du Comité géologique de Saint Pétersbourg, 14*, 1–59.

Diener, C. (1897). Part I. The Cephalopoda of the Lower Trias. *Palaeontologia Indica 15*, Himalayan fossils *2*(1), 1–181.

Diener, C. (1915). *Fossilium Catalogus I, Animalia. Part 8, Cephalopoda Triadica*. W. Junk, Berlin.

Ermakova, S. V. (1981). *Ammonoids and biostratigraphy of the Lower Triassic of the Verkhoyansk Range*. U.S.S.R. Academy of Sciences, Yakutsk Filial, Geological Institute, Nauka, Moscow (in Russian).

Galfetti, T., Bucher, H., Brayard, A., Hochuli, P. A., Weissert, H., Goudun, K., et al. (2007). Late Early Triassic climate change: Insights from a carbonate carbon isotopes, sedimentary evolution and ammonoid paleobiogeography. *Palaeogeography, Palaeoclimatology, Palaeoecology, 243*, 394–411.

Galfetti, T., Bucher, H., Martini, R., Hochuli, P. A., Weissert, H., Crasquin-Soleau, S., et al. (2008). Evolution of Early Triassic outer platform paleoenvironments in the Nanpanjiang Basin (South China) and their significance for the biotic recovery. *Sedimentary Geology, 204*, 36–60.

Guex, J. (1978). Le Trias inférieur des Salt Ranges (Pakistan): problèmes biochronologiques. *Eclogae Geologicae Helvetiae, 71*, 105–141.

Guex, J. (1991). *Biochronological correlations*. Berlin: Springer.

Hermann, E., Hochuli, P. A., Méhay, S., Bucher, H., Brühwiler, T., Hautmann, M., et al. (2011). Organic matter and palaeoenvironmental signals during the Early Triassic biotic recovery: The Salt Range and Surghar Range records. *Sedimentary Geology, 234*, 19–41.

Krafft, A. V., & Diener, C. (1909). Lower Triassic Cephalopoda from Spiti, Malla Johar, and Byans. *Palaeontologia Indica 15, 6*(1), 1–186.

Krystyn, L., Balini, M., & Nicora, A. (2004). Lower and Middle Triassic stage and substage boundaries in Spiti. *Albertiana, 30*, 40–53.

Krystyn, L., Bhargava, O. N., & Richoz, S. (2007). A candidate GSSP for the base of the Olenekian Stage: Mud at Pin Valley; district Lahul & Spiti, Himachal Pradesh (Western Himalaya), India. *Albertiana, 35*, 5–29.

McRoberts, C. A. (2010). Biochronology of Triassic bivalves. In S. G. Lucas (Ed.), *The Triassic timescale* (pp. 201–219). Geological Society of London, Special Publications 334.

Mojsisovics, E. V., Waagen, W., & Diener, C. (1895). Entwurf einer Gliederung der pelagischen Sedimente des Trias-Systems. *Sitzungberichte der Akademie der Wissenschaften in Wien (I), 104*, 1271–1302.

Mu, L., Zakharov, Y. D., Li, W.-Z., & Shen, S.-Z. (2007). Early Induan (Early Triassic) cephalopods from the Daye Formation at Guiding, Guizhou Province, South China. *Journal of Paleontology, 81*, 858–872.

Muller, S. W., & Ferguson, H. G. (1936). Triassic and Lower Jurassic formations of west-central Nevada. *Bulletin of the Geological Society of America, 47*, 241–252.

Muller, S. W., & Ferguson, H. G. (1939). Mesozoic stratigraphy of the Hawthorne and Tonopah Quadrangles, Nevada. *Bulletin of the Geological Society of America, 50*, 1573–1624.

Newell, N. D., & Kummel, B. (1942). Lower Eo-Triassic stratigraphy, Western Wyoming and Southeast Idaho. *Bulletin of the Geological Society of America, 53*, 937–995.

Page, B. M. (1959). Geology of the Candelaria mining district, Mineral County, Nevada. *Nevada Bureau of Mines, Bulletin, 56*, 1–67.

Popov, Y. N. (1961). Triassic ammonoids of northeast USSR. *Transactions, Scientific Research Institute for the Geology of the Arctic* (*NIIGA*), *79*, 1–179 (in Russian).

Saleeby J. B., & Busby-Spera C. (1992). Early Mesozoic tectonic evolution of the western U.S. Cordillera. In B. C. Burchfiel, P. W. Lipman, & M. L. Zoback (Eds.), *The Cordilleran orogen: Conterminous U.S., The Geology of North America* (pp. 107–168). Geological Society of America, Vol. G3.

Shigeta, Y., & Zakharov, Y. D. (2009). Systematic paleontology: cephalopods. In Y. Shigeta, Y. D. Zakharov, H. Maeda, & A. M. Popov (Eds.), *The Lower Triassic system in the Abrek Bay area, South Primorye, Russia* (pp. 44–140). Tokyo: National Museum of Nature and Science.

Silberling, N. J. (1984). Map showing localities and correlation of age-diagnostic lower Mesozoic megafossils, Walker Lake 1 degree by 2 degrees Quadrangle, Nevada and California. Miscellaneous Field Studies Map, MF-1382-O, USGS.

Silberling, N. J., & Tozer, E. T. (1968). Biostratigraphic Classification of the marine Triassic in North America. *Geological Society of America, Special Paper 110*, 1–63.

Spath, L. F. (1930). The Eotriassic invertebrate fauna of east Greenland. *Meddelelser om Grönland, 83*, 1–90.

Spath, L. F. (1934). *Catalogue of the Fossil Cephalopoda in the British Museum* (*Natural History*), *part IV: The Ammonoidea of the Trias*. The Trustees of the British Museum, London.

Speed, R. C. (1977). Island arc and other paleogeographic terranes of late Palezoic age in the western Great Basin. In J. H. Stewart, C. H. Stevens, & A. E. Fritsche (Eds.), *Paleozoic paleogeography of the western U.S., Pacific Coast Paleogeography Symposium I, April 22, 1977* (pp. 349–362). Los Angeles: Pacific Section, Society of Economic Paleontologists and Mineralogists.

Tozer, E. T. (1961). Triassic stratigraphy and faunas, Queen Elizabeth Islands, Arctic Archipelago. *Memoirs of the Geological Survey of Canada, 316*, 1–116.

Tozer, E. T. (1963). Lower Triassic ammonoids from Tuchodi Lakes and Halfway River areas, northeastern British Columbia. *Geological Survey of Canada Bulletin, 96*, 1–28.

Tozer, E. T. (1994). Canadian Triassic ammonoid faunas. *Geological Survey of Canada Bulletin, 467*, 1–663.

Waagen, W. (1895). Salt Ranges Fossils. vol. 2: Fossils from the Ceratites formation—Part I—Pisces, Ammonoidea. *Palaeontologia Indica 13*, 1–323.

Wang, Y.-K., & He, G.-X. (1976). Triassic ammonoids from Mount Jolmo Lungma Region. In: *A scientific expedition in the Mount Jolmo Lungma region* (*1966–1968*). *Paleontology, fasc. 3*, 223–502 (in Chinese).

Waterhouse, J. B. (1994). The early and middle Triassic ammonoid succession of the Himalayas in western and central Nepal, part 1, stratigraphy, classification and Early Scythian ammonoid systematics. *Paleontographica, Abteilung A, 232*, 1–83.

Waterhouse, J. B. (1996). The early and middle Triassic ammonoid succession of the Himalayas in western and central Nepal, part 2, systematic studies of the early Middle Scythian. *Paleontographica, Abteilung A, 241*, 27–100.

Wignall, P. B., & Twitchett, R. J. (2002). Extent, duration, and nature of the Permian-Triassic superanoxic event. In C. Koeberl & K. G. MacLeod (Eds.), *Catastrophic events and mass extinctions: Impacts and beyond* (pp. 395–413). Boulder: Geological Society of America Inc.

CHAPTER 2

Griesbachian and Dienerian (Early Triassic) ammonoids from the Salt Range, Pakistan

Griesbachian and Dienerian (Early Triassic) ammonoids from the Salt Range, Pakistan

by David Ware, Hugo Bucher, Thomas Brühwiler, Elke Schneebeli-Hermann, Peter A. Hochuli, Ghazala Roohi, Khalil ur-Rehman *and* Amir Yaseen

David Ware, Hugo Bucher, Thomas Brühwiler, Elke Schneebeli-Hermann and Peter A. Hochuli: Paläontologisches Institut und Museum der Universität Zürich, Karl Schmid-Strasse 4, CH-8006 Zürich, Switzerland; e-mails: david.ware@pim.uzh.ch, hugo.fr.bucher@pim.uzh.ch, bruehwiler@pim.uzh.ch, elke.schneebeli@pim.uzh.ch, peter.hochuli@pim.uzh.ch

Ghazala Roohi, Khalil ur-Rehman and Amir Yaseen: Earth Science Division, Pakistan Museum of Natural History, Garden Avenue, Shakarparian, Islamabad 44000, Pakistan; e-mails: roohighazala@yahoo.com, reman_geol@yahoo.com, geologistgeologist@yahoo.com

Abstract

The Salt Range (Pakistan) is the type locality of many Early Triassic taxa and since the pioneering work of Waagen in the late 19th century, it has always been considered a key area for the study of the biotic recovery following the end-Permian mass extinction. However, previous studies concerning Griesbachian and Dienerian ammonoid taxonomy and biostratigraphy were all based on a few and/or poorly preserved specimens, often with low stratigraphic resolution. Intensive bed-rock controlled sampling of four areas (Nammal Nala, Chiddru, Amb and Wargal) in the Salt Range has yielded abundant well-preserved Griesbachian and Dienerian ammonoids. This material allowed an extensive revision of the taxonomy and to construct a new, high-resolution biostratigraphic frame. The Griesbachian is represented by the following three distinct regional zones (in ascending order): the *Hypophiceras* cf. *gracile* beds, the *Ophiceras connectens* beds and the *Ophiceras sakuntala* beds. The much thicker series of Dienerian age comprises 12 distinct regional zones leading to a threefold subdivision into early, middle and late Dienerian. It represents by far the most complete Dienerian ammonoid succession known worldwide. The early Dienerian, based on the occurrence of the genus *Gyronites*, can be divided into three horizons: the *Gyronites dubius* beds, the *Gyronites plicosus* beds and the *Gyronites frequens* beds, in ascending order. The middle Dienerian, based on the occurrence of the genus *Ambites*, can be divided into five horizons: the *Ambites atavus* beds, the *Ambites radiatus* beds, the *Ambites discus* beds, the *Ambites superior* beds and the *Ambites bjerageri* beds. The late Dienerian, whose base is defined by the first representatives of Paranoritidae, can be divided into four horizons: the *Vavilovites* cf. *sverdrupi* beds, the *Kingites davidsonianus* beds, the *Koninckites vetustus* beds and the *Awanites awani* beds. Correlations with other localities are difficult because of the scarcity of such highly resolved studies on Dienerian ammonoids. Emended diagnoses and detailed synonymy lists are provided for most previously known taxa. In addition, 5 new genera (*Kyoktites*, *Ghazalaites*, *Pashtunites*, *Awanites* and *Subacerites*) and 18 new species (*Kyoktites hebeiseni*, *Ghazalaites roohii*, *Gyronites schwanderi*, *Ambites tenuis*, *Am. bojeseni*, *Am. subradiatus*, *Am. bjerageri*, *Awanites awani*, *Koiloceras sahibi*, *Bukkenites sakesarensis*, *Proptychites wargalensis*, *Mullericeras shigetai*, *Mul. indusense*, *Mul. niazii*, *Ussuridiscus ventriosus*, *U. ornatus*, *Pseudosageceras simplelobatum* and *Subacerites friski*) are described.

Introduction

The biotic recovery following the end Permian mass extinction is an intensively studied topic, for which high accuracy and high precision time control is of paramount importance. Nekto-pelagic clades such as ammonoids and conodonts recovered very quickly compared to other marine clades (e.g. Brayard *et al.*, 2006, 2009, Orchard, 2007) and play the leading roles in dating Early Triassic marine rocks. However, many studies addressing the recovery are based on insufficiently resolved paleontological age controls. Detailed ammonoid zonations for the Dienerian have been proposed for Arctic Canada (Tozer, 1994), Northern Siberia (Dagys & Ermakova, 1996) and Primorye (Shigeta & Zakharov, 2009), but uncertainties in correlating these do often persist. Based on material from Nepal, a biozonation has been proposed by Waterhouse (1994, 1996) for the northern Gondwanian margin. Unfortunately, this Nepalese material is very poorly preserved and does not allow constructing a robust taxonomy, a pre-requisite for any attempt in constructing a biozonation. The Salt Range has always been considered as an essential region for the study of the earliest Triassic marine faunas. The very first Dienerian ammonoids were discovered in the Salt Range by Andrew Fleming in the mid-19th century and this material was described by de Koninck (1863). Waagen (1895) conducted the most impressive and exhaustive bedrock-controlled study on Early Triassic ammonoids from the Salt Range. Noetling (1905) and Spath (1934) added a few species and proposed slightly

different classifications. Griesbachian ammonoids were first discovered by Schindewolf (1954) in the Salt Range. Kummel provided a detailed history of the stratigraphical and paleontological investigations on the Permian and Triassic of the Salt Range (Kummel, 1966, Kummel & Teichert, 1966, 1970). He also mentioned that he collected numerous Dienerian ammonoids and that he intended to publish this material later on, a task he unfortunately never completed. Since Kummel's work, only two contributions on Early Triassic ammonoids from the Salt Range were published. The works by Guex (1978) and by the Pakistani-Japanese Research Group (PJRG, 1985) only include scarce material of Griesbachian and Dienerian ages. From 2007 to 2010, our research group carried out intensive field work in the Salt Range and the Surghar Range. Palynological and carbon isotope records have been recently published by Hermann *et al.* (2011a, 2011b, 2012a, 2012b) and Schneebeli-Hermann *et al.* (2012), oxygen isotopes from biogenic phosphates by Romano *et al.* (2013), Smithian ammonoids by Brühwiler *et al.* (2012) and bivalves of Smithian and Spathian ages by Wasmer *et al.* (2012). The present work focuses on Griesbachian and Dienerian ammonoids from four different areas in the Salt Range. It is based on abundant and well preserved material sampled bed by bed. This new material provides the basis for a comprehensive revision of the taxonomy and biostratigraphy of Griesbachian and Dienerian ammonoids in the Salt Range, where all relevant section are found. Because of the unrivalled quality of the Dienerian ammonoid record of the Salt Range, this taxonomic and biostratigraphic re-investigation is an essential contribution to the early Triassic ammonoid zonation of the Northern Indian Margin (NIM) and to the understanding of the Early Triassic biotic recovery.

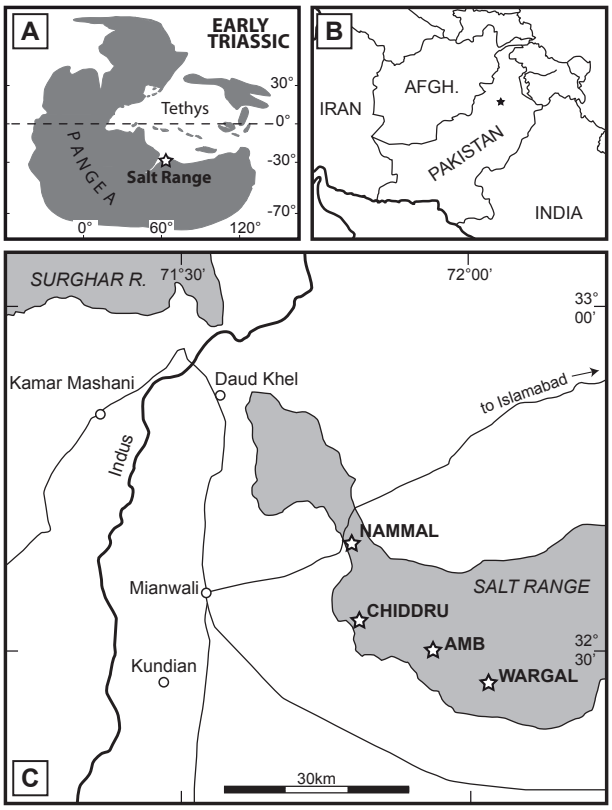

Fig. 1. A) Palaeogeographical map of the Early Triassic with the palaeoposition of the Salt Range (modified from Brayard *et al.* 2006). **B)** Map of Pakistan with position of the studied area. **C)** Location map of sampled sections in the Salt Range (modified after Brühwiler *et al.* 2012).

Geological framework

General context

The Salt Range constitutes a long and narrow mountain range, approximately 150 km SSW of Islamabad (Fig. 1B-C). The southern limit of the Salt Range defines the Himalayan main frontal thrust, which exposes a northern Gondwanian margin succession ranging from the Cambrian to the Cenozoic. It typically consists of a stack of tectonic slices with a south vergence, thus repeatedly exposing Triassic rocks of the Mianwali, Tredian and Kingriali formations. During the Early Triassic, marine rocks of the Mianwali Fm. were deposited at a palaeolatitude of ca. 30°S (Fig. 1A). The Mianwali Fm. is a ca. 120 m thick succession of limestone and siliciclastic sediments. It unconformably rests on top of the Late Permian Chiddru Fm. In the eastern part of the Salt Range, The Mianwali Fm. is truncated by post-Cretaceous erosion and directly capped by Palaeocene marine rocks. In the western part, it is overlaid by the Middle Triassic Tredian Fm. The Griesbachian and Dienerian are represented by three units of the Mianwali Fm: the Kathwai Member (KM, which is further subdivided into a dolomitic unit and a limestone unit), the Lower Ceratite Limestone (LCL) and the lower part of the Ceratite Marls (CM). The thickness of each of these units is highly variable throughout the Salt Range. Their boundaries are here demonstrated to be diachronous across the different tectonic slices, thus suggesting that at least some of these thrusts are inverted Triassic normal faults. As a typical example among many others, Brühwiler *et al.* (2012) documented that the Dienerian-Smithian boundary coincides with the LCL-CM boundary in Chiddru, whereas it is found within the lower third (ca. 7 m above the base) of the CM in Nammal. Most previous works (e.g. Mojsisovics *et al.*, 1895, Spath, 1934, Guex, 1978, PJRG, 1985) did not recognise this diachronism, and assumed that lithological boundaries are synchronous throughout the Salt Range and the Surghar Range. Independent processing of biostratigraphic data from each section in a first step and then utilizing the resulting sequences for the construction of regional correlations in a second step

requires no a priori assumption about the synchronicity of lithological boundaries.

Lithology and taphonomy

Despite differences in thicknesses and ages in the different sections, the three units studied here show remarkably uniform facies throughout the Salt Range. Detailed lithological descriptions of these units were already published in Kummel & Teichert (1970) and in Hermann *et al.* (2011b). Therefore, only a summary of the lithological succession is given here, along with additional observations pertaining to the taphonomy of ammonoids.

Kathwai Member (KM), dolomitic unit. – The dolomitic unit of the KM consists of a few massive beds of sandy dolomites. Fossils are very rare in this unit and are usually only represented by broken and unidentifiable shells. Only one ammonite (*Hypophiceras* aff. *gracile*) was found in this unit, in Nammal Nala. It occurred in a small lens full of bivalves within a massive dolomitic bed.

Kathwai Member, limestone unit. – The limestone unit of the KM consists mostly of calcareous glauconitic sandstone beds alternating with thin shale beds. Although fossils are not rare, they are generally very poorly preserved. Some beds contain accumulations of rhynconellid brachiopods and echinid spines. Ammonites are rare, and usually represented only by extremely poorly preserved specimens. Identification, even at the genus level, is impossible. Therefore, they have not been included in the present study. The only exception is in Chiddru, where a few better preserved specimens assigned to *Ophiceras connectens* were found at the base of this unit.

Lower Ceratite Limestone (LCL). – The LCL consists of thin, hard, coarse-grained coquinoid limestone beds. Glauconite and iron oxides are locally very abundant. Although very frequent, the fossils are mostly fragmented, and generally very difficult to prepare mechanically. The coarse grained sparitic matrix often crosses the shell boundaries. Ammonoids are very unevenly distributed, often imbricated and accumulated in lenses within the different layers of the LCL. The body chamber of small specimens is generally broken, while large specimens (Proptychitidae) are represented by incomplete phragmocones, the upper side of outer whorls being corroded or eroded (see Pl. 21: 13 for a good example). Phragmocones are often completely recrystallised, hence suture lines are only occasionally preserved. Considering the abundance of glauconite and the facies, the LCL may be affected by condensation. However, in the absence of similar studies in sections where the LCL is expanded, cases of paleontological condensations are impossible to pinpoint. Only one horizon in the LCL is here considered as condensed. The second bed of the LCL in Nammal Nala contains both the genera *Ophiceras* and *Gyronites*, an association which has not been documented in any other area. Moreover, the species *Gy. dubius* has also been found in Amb, without any *Ophiceras*. This association is thus interpreted herein as being the result of condensation.

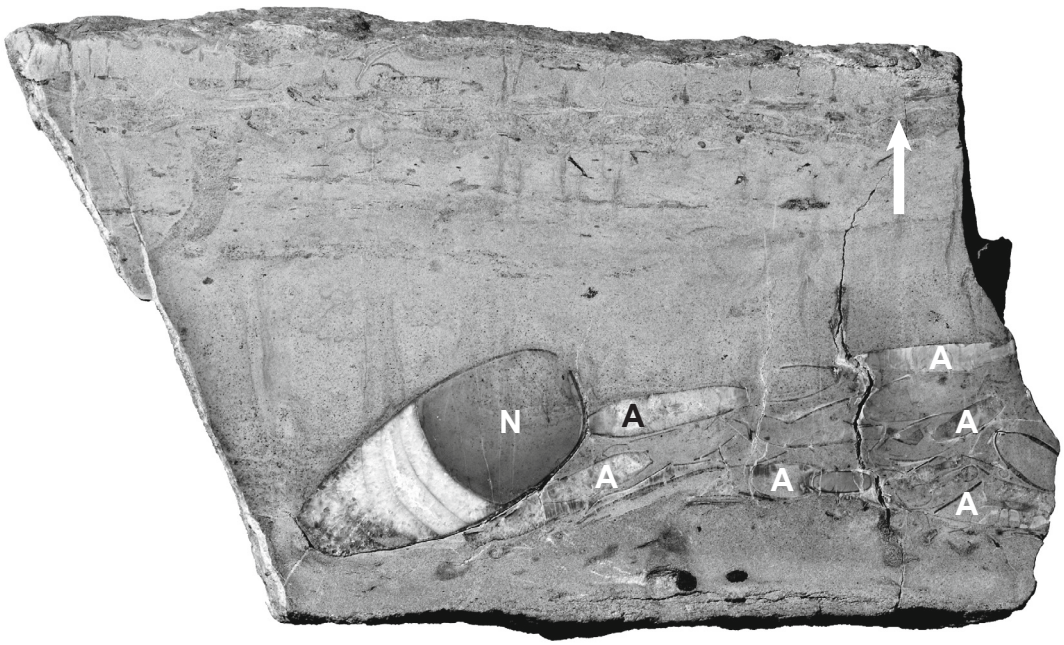

Fig. 2. Polished section of the *Ambites bleragerі* bed (Nam100 and equivalents) of Nammal Nala, showing the typical facies of limestone beds at the base of the CM, with an accumulation of imbricated shells at its base with a nautiloid (N), several imbricated complete and broken ammonoids (A). Natural size, arrow indicates top of bed and bioturbation increasing toward the top of the bed. Specimen PIMUZ30235.

In Nammal Nala, the two uppermost beds of the LCL are different, being composed of fine grained limestone. The penultimate bed is only 1 to 2 cm thick, locally absent, and contains numerous and nearly complete ammonoids, some bivalve fragments and abundant fish scales and teeth. Ammonoids are accumulated at the top of the bed, often encrusted by worm tubes and only partially covered by a very thin limestone layer (Pl. 3: 1-2). The last bed is ca. 7 cm thick and composed of fine grained limestone with locally abundant, nearly complete but strongly recrystallised ammonoids. Its surface is encrusted by centimetric iron oxide concretions, indicating a sedimentation break.

Ceratite Marls (CM). – The CM is composed of a ca. 30 m thick succession of marls with intercalated limestone and sandstone beds. Limestone beds are abundant at the base, while sandstone beds become gradually more abundant in the upper half of the CM. In the lower third, ammonoids are very abundant and well preserved in numerous limestone beds and lenses. The thickness of these beds is variable. Many of these beds show imbrication and size sorting of shells, indicative of bottom currents. A typical example of this facies is shown in figure 2, with small imbricated, both complete and broken ammonoids accumulated at the base of the bed. The body chamber is generally partially broken. Large specimens (all belonging to Proptychitidae) often have their venter abraded. For example, the specimen illustrated on Pl. 25: 4 is a complete phragmocone, the body chamber of which is missing, and whose venter has been abraded on almost the entire last preserved volution. In the Dienerian part of the CM, involute shells often have their narrow umbilicus encrusted by bivalves on both sides, similar to the ones already described in Ware *et al.* (2011). These bivalves may occasionally induce an irregular coiling of the umbilicus, thus indicating *in vivo* encrusting of epizoans. These bivalves are sometimes also present on the flanks of the whorl and, where overlapped by the body chamber, they are lined by a dorsal shell layer. Usually, only their cimentated valve is preserved. The hinge of these *in vivo* encrusting bivalves could not be observed, so their identification remains uncertain. Some specimens have a rather flattened upper valve and closely resemble the genus *Crittendenia* Newell & Boyd, 1995, while others have an unusually high doming of the upper valve and may be related to the Triassic bivalve generally referred to as "*Placunopsis*" Morris & Lycett, 1853. Todd & Palmer (2002) suggested that these Triassic domed bivalves may represent a new taxon, without further precision. It cannot be excluded that some of the intraspecific variability of the umbilical width observed on these involute shells is a consequence of the presence of these epizoans, but as no faunas without these encrusting bivalves could be found for comparison, this hypothesis cannot be tested. The presence or absence of bivalves in the umbilicus has therefore not been taken into account in the taxonomical analyses, except when they induced an obvious pathological coiling of the ammonoid shell. Such *in vivo* encrusting bivalves have so far not been observed in older or younger ammonoid faunas in the Salt Range, even in Early Smithian faunas which are found in similar facies. It is tempting to relate this unusual high frequency of epizoans to a coeval oxygen-poor water-sediment interface.

Hermann *et al.* (2011a, 2011b, 2012a, 2012b) and Schneebeli-Hermann *et al.* (2012) proposed a detailed palaeoenvironmental reconstruction based on several sections (including the ones studied here) throughout the Salt Range and Surghar Range. These studies documented that in Nammal, the middle to late Dienerian record a local peak of anoxia, unlike previous (Griesbachian to early Dienerian) and subsequent (early and middle Smithian) time intervals. Romano *et al.* (2013) showed that temperature also peaked during the middle and late Dienerian (phase Ib of Romano *et al.*, 2013).

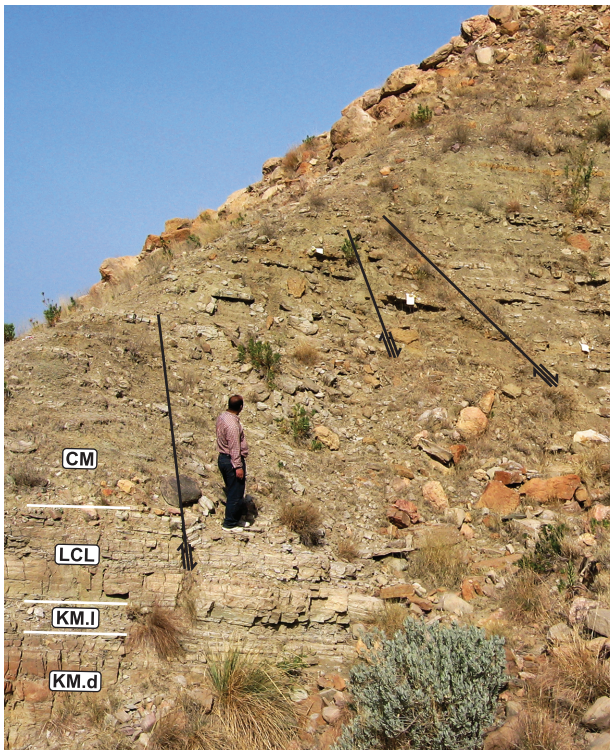

Fig. 3. Section near the entrance of Nammal Nala (N32°39'27.6", E71°47'29.2"). KM.d: Kathwai Member, dolomitic unit; KM.l: Kathwai Member, limestone unit; LCL: Lower Ceratite Limestone; CM: Ceratite Marls. Note the presence of small normal faults (black lines).

Present work

The ammonoids presented in this study were collected in four different areas (Fig. 1C): Nammal Nala, Chiddru,

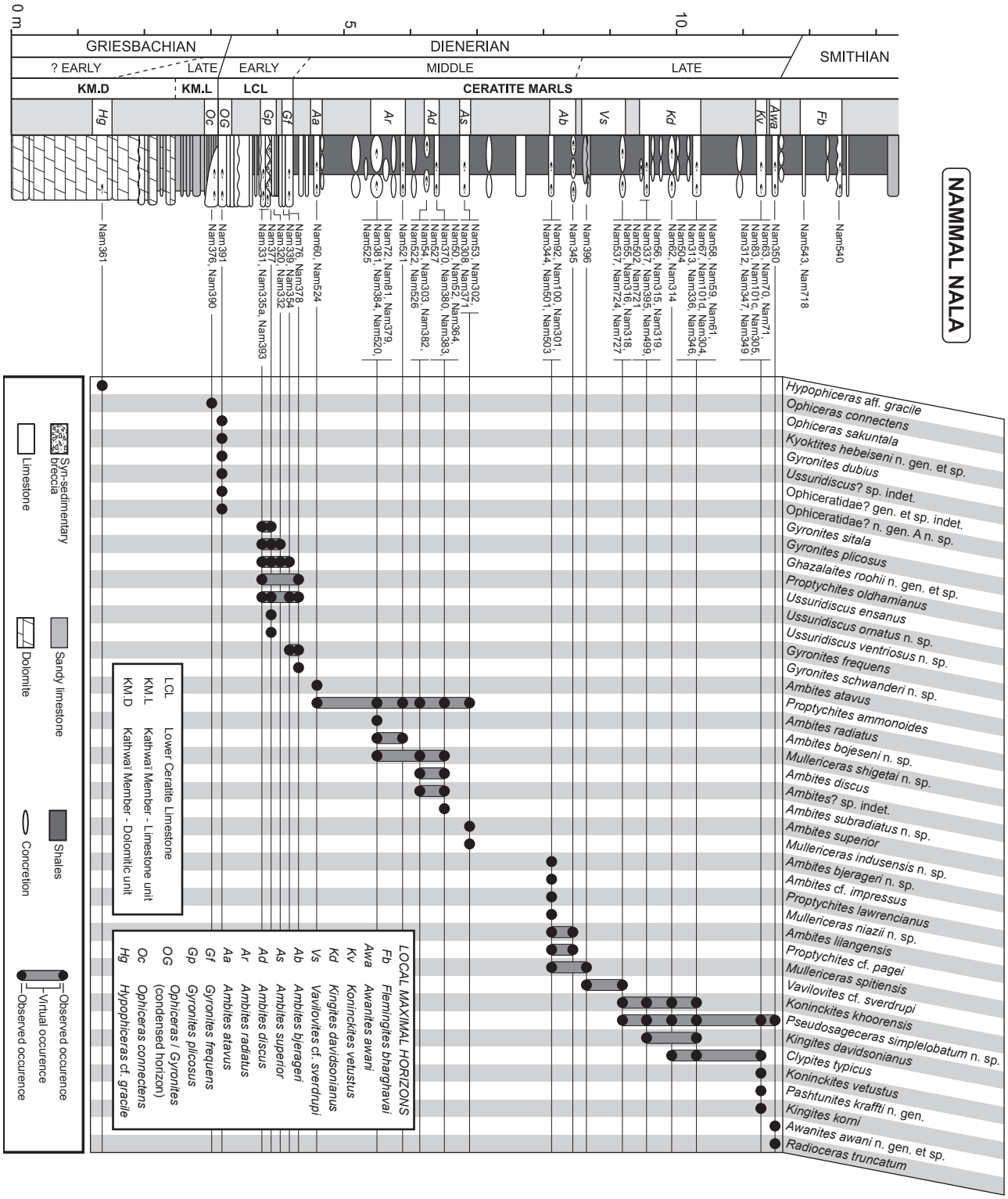

Fig. 4. Composite section and distribution of ammonoids in Nammal Nala. Faunal content of NAM543, NAM718 and NAM540: see Brühwiler *et al*. (2012).

Amb and Wargal. In each case, detailed stratigraphic logs with the exact position of the samples are given. Based on lithological correlations, composite logs were constructed for each area. Therefore, several samples (each with a distinct number) may have been obtained from the same bed.

Nammal Nala is a narrow canyon situated about 5 km east of the village of Musa Khel (ca. 25 km ENE of Mianwali). This area was previously studied by Kummel (1966), Kummel & Teichert (1966, 1970), Guex (1978) and the PJRG (1985). The Early Triassic Mianwali Fm. is beautifully exposed and repeated by faulting. All the

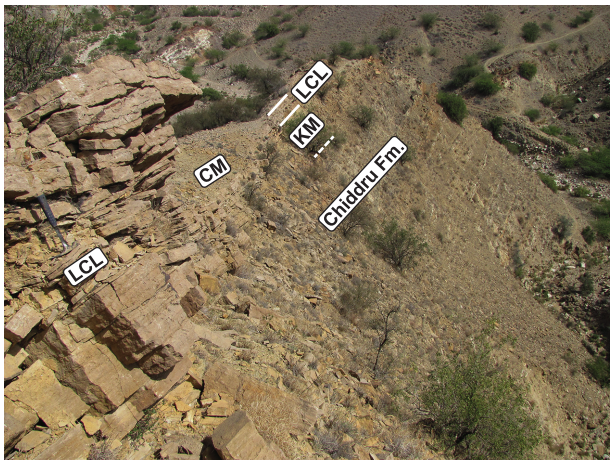

Fig. 5. Section above the village of Chiddru (N32°32'59.7", E71°47'55.9") on the West side of the gorge, previously described by Kummel and Teichert (1966, 1970) and Kummel (1966). Chiddru Fm.: Chiddru formation; KM: Kathwai Member; LCL: Lower Ceratite Limestone; CM: Ceratite Marls.

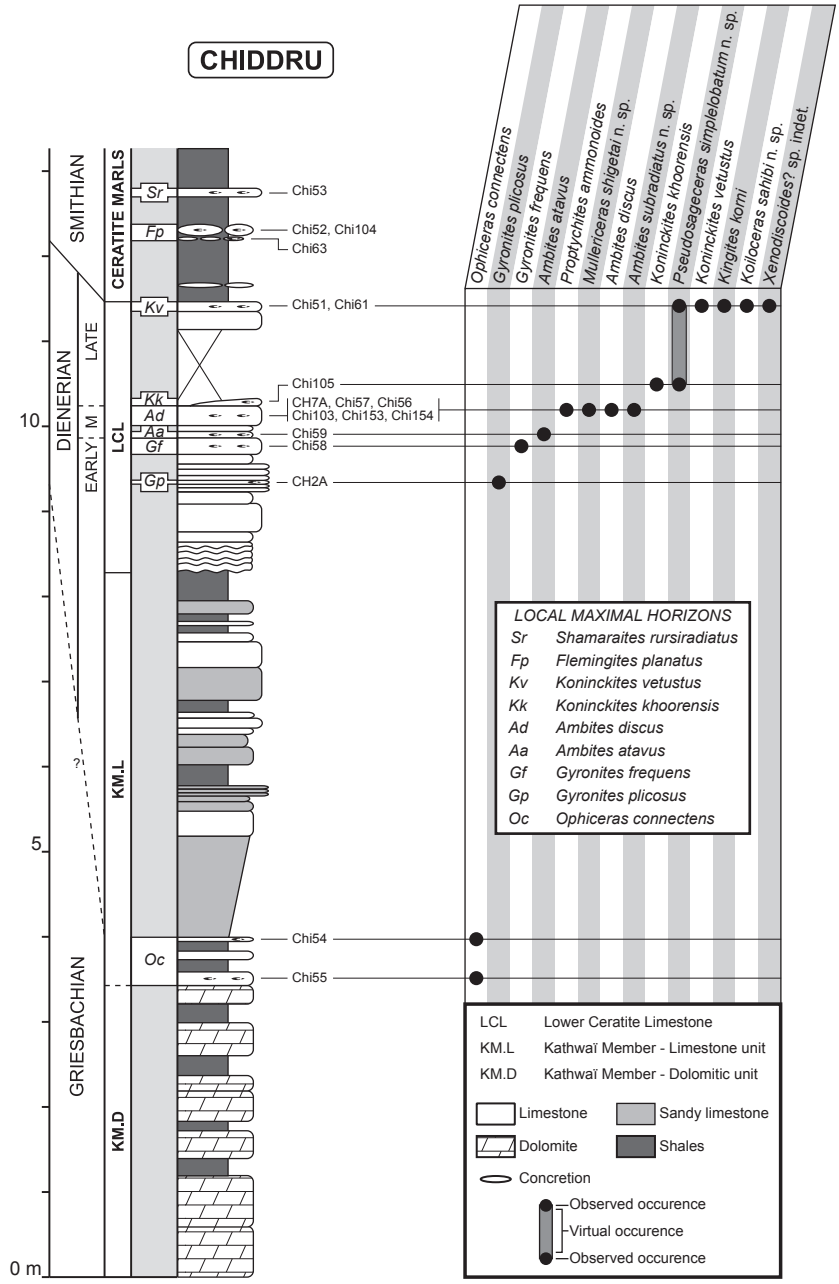

Fig. 6. Composite section and distribution of ammonoids at Chiddru. Faunal content of CHI63, CHI52, CHI104 and CHI53: see Brühwiler *et al*. (2012).

Fig. 7. Section about 1 km south-east of the village of Amb (N32°29'48.1", E71°56'20.6"). Scale indicated by a geologist (circled) in the middle of the view. KM.d: Kathwai Member, dolomitic unit; KM.l: Kathwai Member, limestone unit; LCL: Lower Ceratite Limestone; CM: Ceratite Marls.

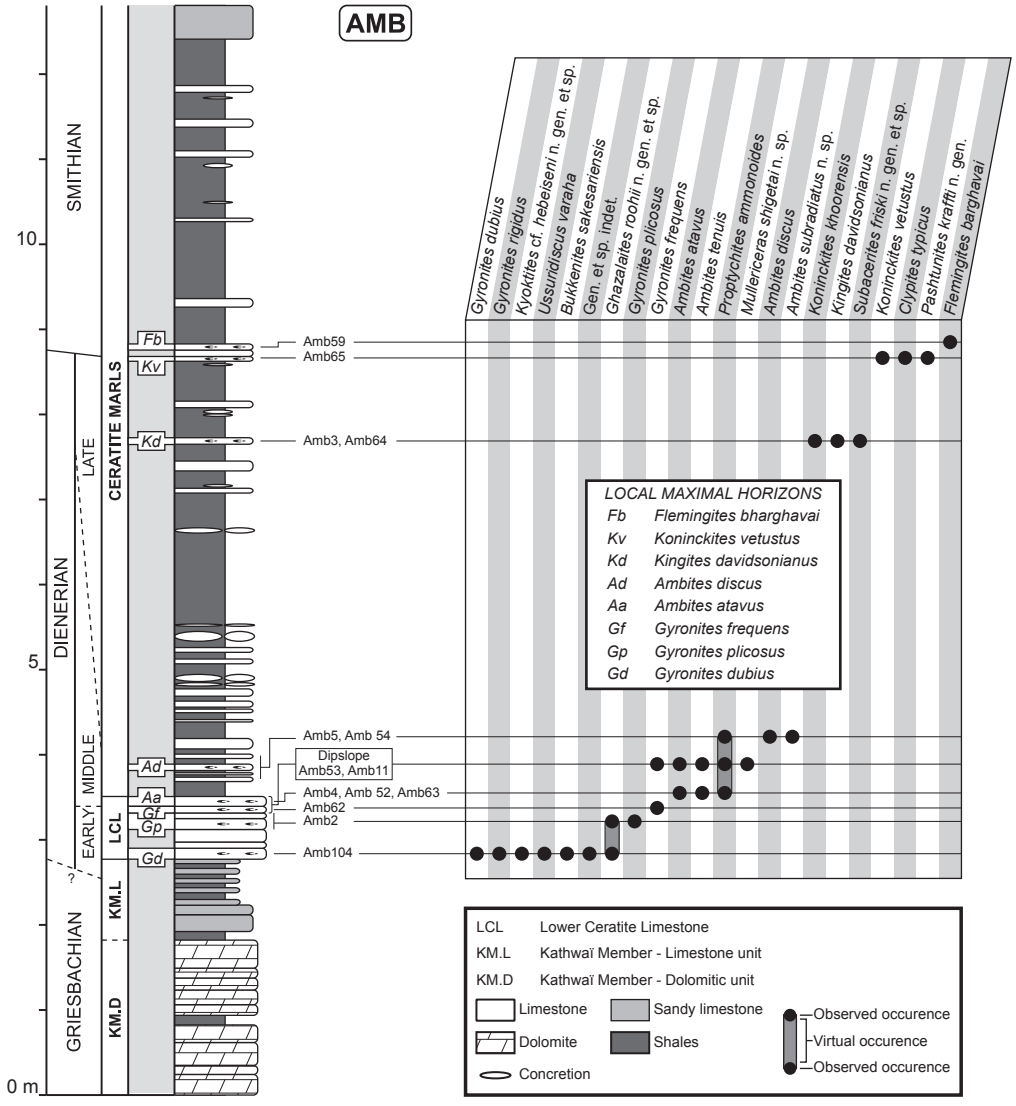

Fig. 8. Composite section and distribution of ammonoids at Amb. AMB53 and AMB11 were collected on a dipslope formed by the two uppermost beds of the LCL, without any further distinction.

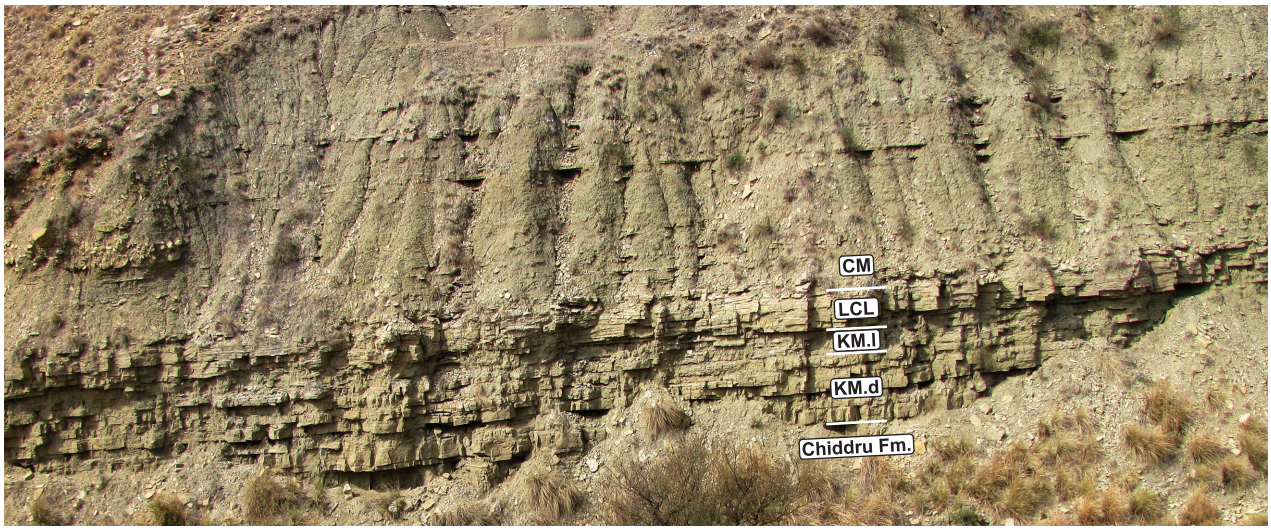

Fig. 9. Section of Munta Nala, about 2.5 km West of the village of Wargal (N32°27'07", E72°01'56.7"; Kummel and Teichert, 1966, 1970, Kummel, 1966). No scale available, thickness of KM and LCL amounts to ca. 6 m. KM.d: Kathwai Member, dolomitic unit; KM.l: Kathwai Member, limestone unit; LCL: Lower Ceratite Limestone; CM: Ceratite Marls.

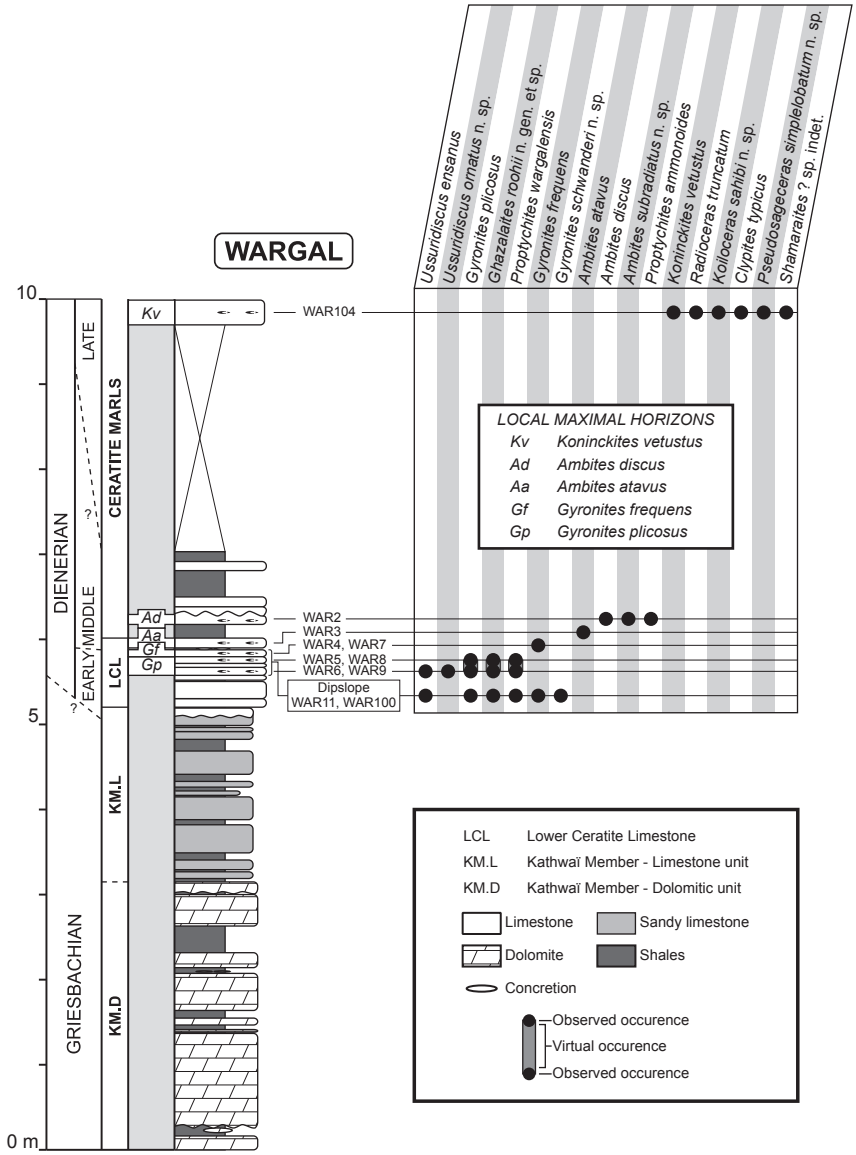

Fig. 10. Composite section and distribution of ammonoids at Wargal. WAR11 and WAR100 were collected on a dipslope formed by several beds in the middle part of the LCL, without any further precision.

exposures reported here are from the northern side of the canyon, which is in part illustrated in figure 3. A composite log with the ammonoid distribution is given in figure 4. The most complete Griesbachian and Dienerian sequence of the Salt Range was found in Nammal Nala, especially for the base of the CM, where ammonoids are very abundant and well preserved. This canyon is also of very easy access, thus allowing intensive sampling. The vast majority of the ammonoids (about 1200 specimens) described here come from Nammal Nala.

The sections studied in Chiddru are situated in a valley about 2.5 km east of the village (ca. 25 km ESE of Mianwali). Several sections were sampled in 2008 and 2010, but the best ones for the Dienerian were already described by Kummel (1966) and Kummel & Teichert (1966, 1970), especially the one on the west side of the valley (Fig. 5). A synthetic log showing ammonoid distribution is given in figure 6. In this area, the KM and LCL are much thicker than in other areas, and the Dienerian is restricted to

the LCL. The base of the CM is already early Smithian in age (Brühwiler *et al.*, 2012). In the LCL, ammonoids are abundant but generally broken and poorly preserved. Specimens well enough preserved for identification are rather rare. Despite intensive sampling, only ca. 50 specimens could be included in this study. However, this area is very important for the Dienerian, since it is the type locality of *Koninckites vetustus*, the type species of *Koninckites*. This area has been known since the beginning of the geological investigations in the Salt Range, and has been included in every study dealing with the Early Triassic of this region.

Amb is a small village situated ca. 35 km east of Mianwali. Three different outcrops were sampled during one field trip (2010) in the valley just south of the village, the best section being situated about 1 km south-east of the village (Fig. 7). A composite section showing the ammonoid distribution is given in figure 8. The KM and LCL have thicknesses similar to those of Nammal, but the Dienerian part of the CM is thinner, with less limestone beds. Although often broken, ammonoids from the LCL are very abundant and better preserved than in Nammal. In the CM ammonoids are rather rare, usually strongly recrystallised and difficult to prepare. A total of about 120 specimens from Amb could be included in this study. This locality is the type locality of the genus *Ambites*. Since the pioneer work of Waagen (1895), the Early Triassic faunas of Amb have never been studied in detail.

The sections near Wargal are situated in a syncline about 2.5 km west of the village, along Munta Nala. Although the KM and LCL are thicker than in Amb, and the CM thinner, the two sections are very similar. Only three days were spent in this locality, mostly to collect specimens of the genus *Prionolobus*, as it is the type locality of its type species *Pri. atavus* and of *Pri. rotundatus*. About 100 specimens were collected, mostly in the LCL and at the very base of the CM, easily accessible in the section previously described by Kummel (1966) and Kummel & Teichert (1966, 1970), and illustrated here in figure 9. Only the upper part of the CM was sampled in another nearby tributary, where a *Kon. vetustus* fauna (WAR104) was found. A composite section showing the ammonoid distribution is given in figure 10. As in Amb, ammonoids from the LCL are abundant and rather well preserved, but they are also abundant and well preserved in the CM. Since the work of Waagen (1895), this area has only been investigated by Kummel (1966) and Kummel & Teichert (1966, 1970).

Biostratigraphy

The extensive bed-rock-controlled sampling on which the present work is based allows the recognition of a total of 15 regional zones (RZ): 3 of Griesbachian age and 12 of Dienerian age (Figs. 11-12). The resulting provisional zonation is entirely new and remarkable, since only three of these RZ were recognised in the most

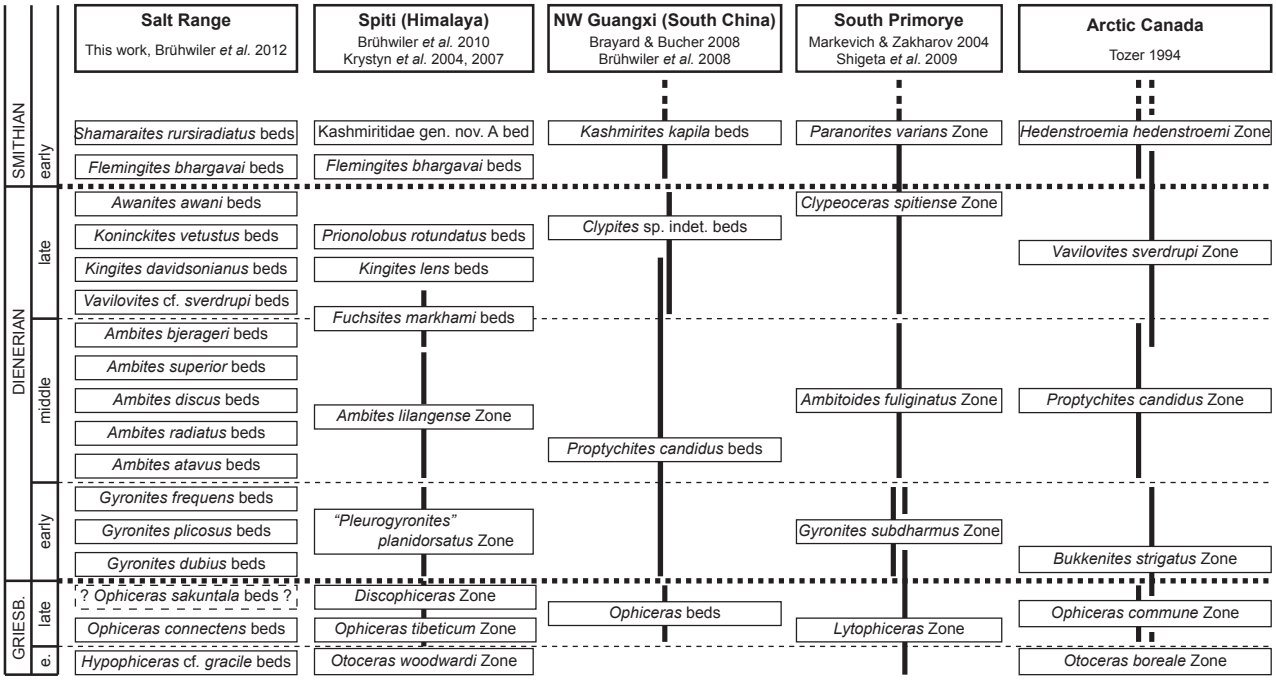

Fig. 11. Biostratigraphic subdivisions of the Griesbachian, Dienerian and earliest Smithian of the Salt Range and correlation with zonations of other regions. Thick vertical black bars indicate uncertainty intervals for correlations. The *O. sakuntala* beds, indicated with question marks and a dashed frame, correspond to a horizon identified only in the condensed horizon of Nammal Nala. See text for details.

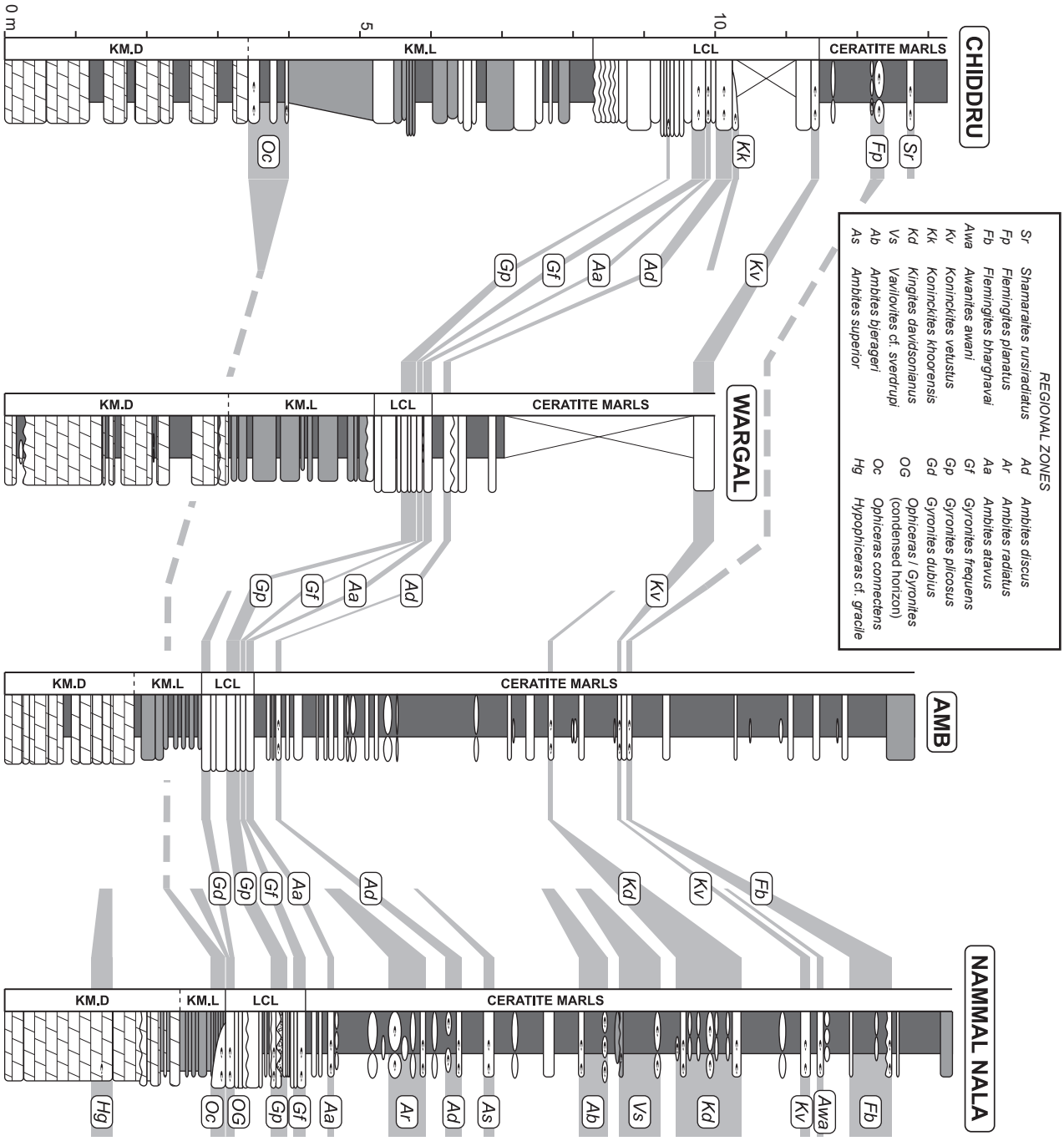

Fig. 12. Biostratigraphic correlations of Chiddru, Wargal, Amb and Nammal Nala sections. Note the diachronism of the LCL between the different sections.

recent works on the Salt Range (Guex, 1978 and PJRG, 1985), and since Tozer (1965, 1994) recognised only two zones and four subzones in the Dienerian of Canada. A preliminary version of this zonation was published in Romano *et al.* (2013). We propose here a new threefold subdivision of the Dienerian. The different RZ are described herein and their correlation with ammonoid zonations from other basins is discussed. Synthetic range charts for Griesbachian and Dienerian ammonoid species and genera from the Salt Range are given in figures 13 and 14, respectively. We here prefer the term "beds" to describe the sequence of RZ, as the usage of formal zone names would imply a well established lateral reproducibility of the faunal sequence between different basins. Technically, most of these RZ correspond directly to the definition of the local maximal horizons (LMH) of Guex (1991), except for the *Gy. plicosus* beds and the *V.* cf. *sverdrupi* beds (see below).

General subdivisions

The stage subdivisions of the Early Triassic are a subject of debate. In the latest version of the Geologic Time Scale (Ogg, 2012), the twofold subdivision of the Early

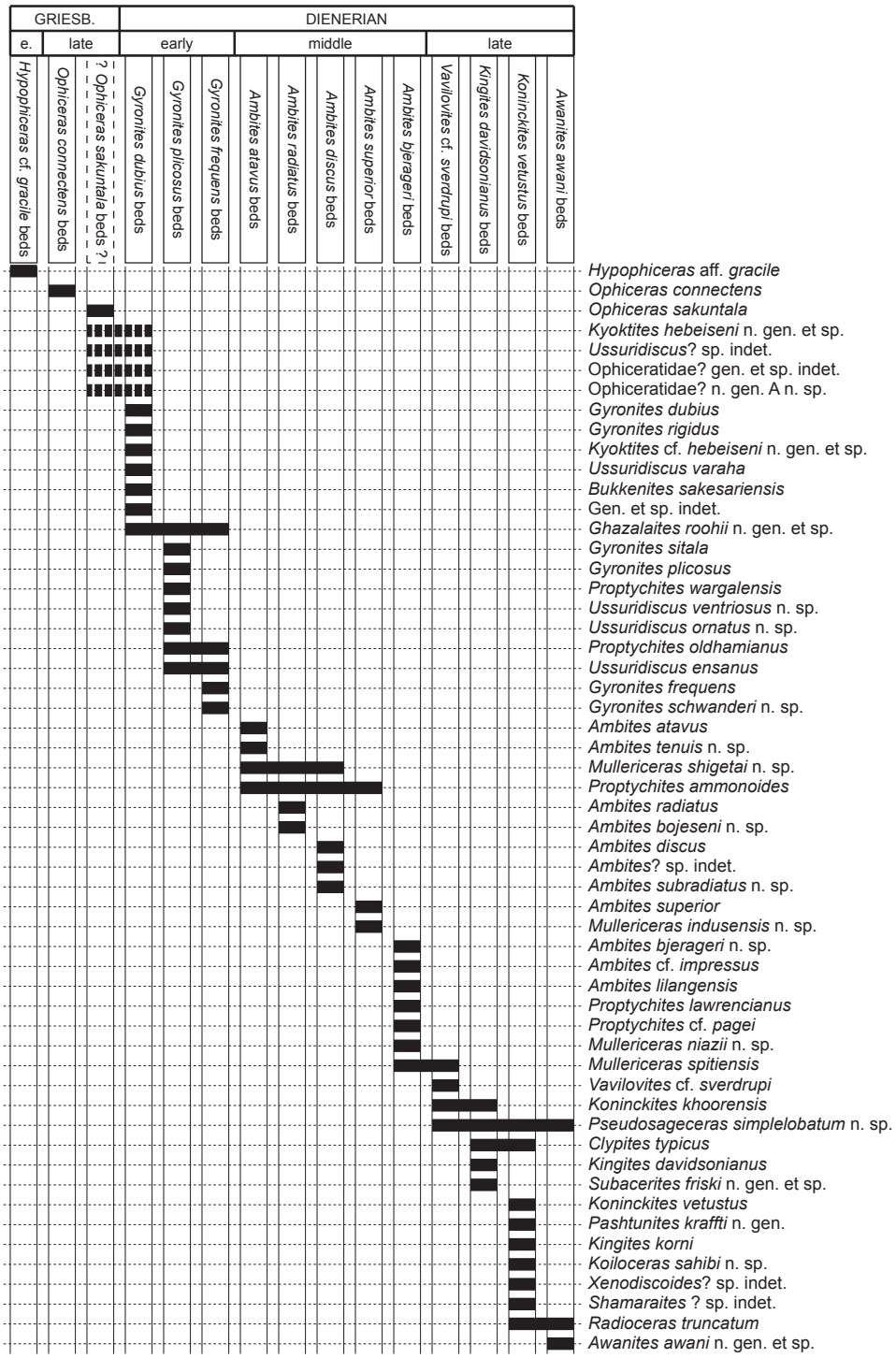

Fig. 13. Synthetic range chart showing the biostratigraphical distribution of Griesbachian and Dienerian ammonoid species in the Salt Range. Dashed thick lines correspond to species of uncertain age found in the condensed horizon of Nammal Nala.

Triassic introduced by Kiparisova & Popov (1956), with the Induan and Olenekian, is endorsed. The four stages defined by Tozer (1965) are then considered as substages, the Induan being subdivided into Griesbachian and Dienerian, and the Olenekian into Smithian and Spathian. This twofold scheme is however strongly criticised, mainly as it does not reflect the end Smithian crisis, the most important extinction event known for both ammonoids (e.g. Brayard *et al.*, 2009, Brühwiler *et al.*, 2010b) and conodonts (Orchard, 2007, Goudemand *et al.*, 2008) within the entire Triassic. Moreover, having the Induan defined in the Tethyan realm and the Olenekian in the Boreal Realm makes the correlation of this stage boundary across such a broad palaeolatitudinal range an extremely arduous task. Selective preservation resulting from the meagre amount of carbonate rocks in the Boreal Realm generates an extremely discontinuous faunal record.

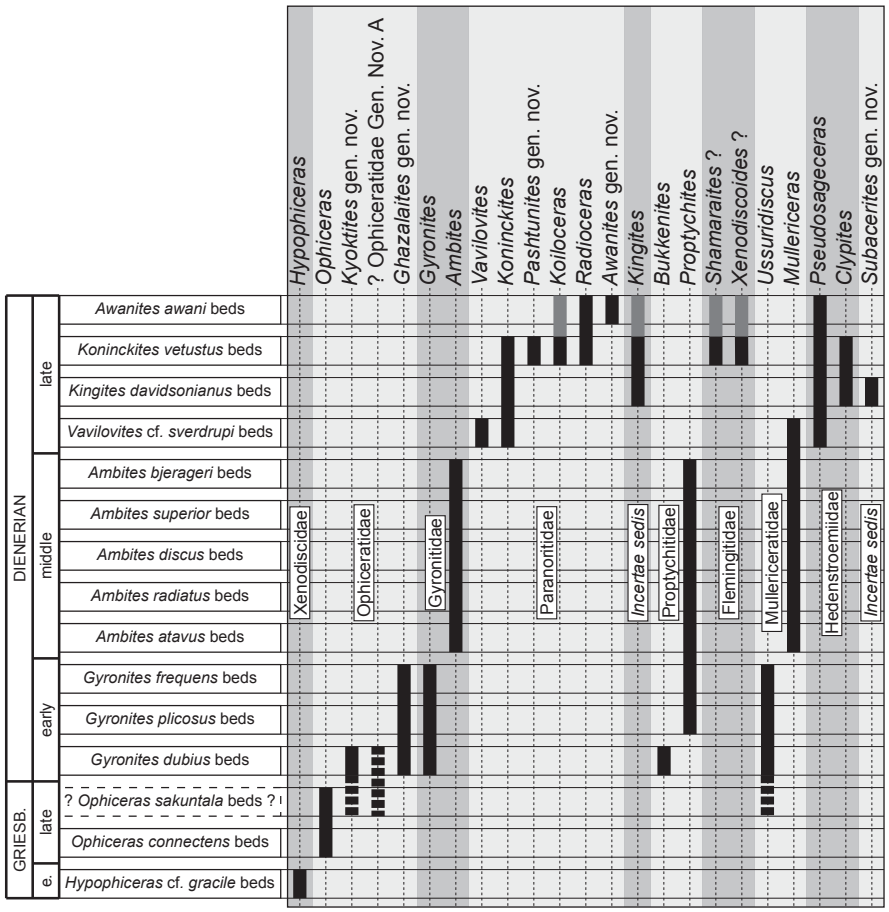

Fig. 14. Synthetic range chart showing the biostratigraphic distribution of Griesbachian and Dienerian ammonoid genera (grouped by families) in the Salt Range. Dashed thick lines correspond to genera of uncertain age occurring in the condensed horizon of Nammal Nala. Grey thick lines correspond to virtual occurrences.

The Griesbachian/Dienerian boundary was originally defined by Tozer (1965) by the first occurrence of Meekoceratidae (corresponding here to Gyronitidae), an opinion which is here supported and endorsed. However, no consensus has yet been reached for the Dienerian/Smithian boundary. Tozer (1965) provided only a vague definition of it, explaining that it was probable that in Canada, the oldest Smithian fauna may be younger than typical Smithian faunas from other areas. Krystyn *et al.* (2007a, 2007b) proposed the Mud section (Spiti valley, India) as a GSSP candidate for this boundary. They based their definition of the boundary on the first occurrence of the conodont *Neospathodus waageni sensu lato*. However, Brühwiler *et al.* (2010a) demonstrated the presence in the same section of ammonoid genera typical of the Smithian below the boundary as originally placed by Krystyn *et al.* (2007a, 2007b), and thus suggested to use the first occurrence of *Flemingites bhargavai* as the index fossil for this boundary. This species is also present in the Salt Range (Brühwiler *et al.*, 2010b, 2012). Consequently, this definition is adopted here.

Tozer (1965) divided the Griesbachian and the Dienerian into two parts (early and late) each, a scheme which has been followed by every author since. Because of the paucity of Griesbachian faunas in the Salt Range, this twofold subdivision cannot be assessed here. However, for the Dienerian, the much higher resolution subdivisions obtained in this study leads to a threefold subdivision of the Dienerian (early, middle and late). The early Dienerian is characterised by the occurrence of the genera *Gyronites* and *Ussuridiscus*, the middle Dienerian by the co-occurrence of the genera *Ambites* and *Mullericeras*, and the late Dienerian by the appearance of Paranoritidae and Sageceratacea.

Griesbachian and Dienerian Ammonoid biostratigraphy of the Salt Range

Griesbachian

Griesbachian ammonoids are very rare and generally poorly preserved in the Salt Range. Moreover, Griesbachian ammonoids from other regions of the NIM have hardly been investigated in detail since the work of Diener (1895) and Krafft & Diener (1909). A new biozonation for the Griesbachian of Spiti Valley (Indian Himalayas) has been attempted by Krystyn *et al.* (2004), but without explanation or illustration of the taxonomic definitions, thus making this scheme difficult to apply or to test in other areas. As a consequence, the three Griesbachian RZ described here cannot be correlated with confidence.

Hypophiceras *cf.* gracile *beds.* – This RZ is here based on a single specimen found in the dolomitic unit of the KM. Although species assignment remains uncertain, identification at the genus level is very robust. The genus *Hypophiceras* is known in the Arctic (Siberia, Arctic Canada and NE Greenland), where it occurs together with early Griesbachian taxa. However, Kummel (1970) reported one specimen from the KM of Kathwai, which may be conspecific with ours, and correlated this bed on the basis of lithology with the *O. connectens* beds of Chiddru of late Griesbachian age. In the absence of additional material, and considering that this correlation is exclusively based on lithology, this RZ is here kept separate from the subsequent *O. connectens* beds. Additional work on the Griesbachian of the Tethys is necessary to decipher whether the genus *Hypophiceras* is restricted to the early Griesbachian or if it ranges up into the late Griesbachian. This RZ corresponds to the horizon MH-G1 in Romano *et al.* (2013).

Ophiceras connectens *beds.* – This RZ has been identified in Nammal Nala and Chiddru and only yields poorly preserved specimens of *O. connectens*. This species was considered as a synonym of *O. tibeticum* by Waterhouse (1994), who thus treated this fauna as an equivalent of the Himalayan *O. tibeticum* zone of late Griesbachian age. Acceptance or rejection of this treatment requires revision of the taxonomy of Ophiceratidae and of the Griesbachian faunal succession of the NIM. This RZ correspond to the horizon MH-G2 in Romano *et al.* (2013).

Ophiceras sakuntala *beds*. – The species *O. sakuntala* has only been found in the condensed layer at the base of the LCL in Nammal Nala. Because this layer yields both late Griesbachian and earliest Dienerian taxa, the natural association of species belonging to this RZ is obscured. *O. sakuntala* also occurs in Shalshal Cliff in the central Himalayas where it was originally described by Diener (1897). This condensed layer corresponds to the horizon MH-G3 in Romano *et al.* (2013).

Early Dienerian

Early Dienerian ammonoids from the Salt Range are abundant and usually quite well preserved, but very difficult to prepare. They are all found in the LCL, an interval characterized by low sedimentation rates. The early Dienerian biostratigraphic record may be treated with caution with respect to potential hiatuses and condensation. The Salt Range nevertheless provides the most expanded and diverse faunal succession worldwide for the early Dienerian. A likely case of condensation is found at the base of the LCL in Nammal Nala, where *Gyronites dubius* of earliest Dienerian age occurs together with *O. sakuntala* of late Griesbachian age.

The early Dienerian is best characterised by the genus *Gyronites*. In the Salt Range, the genus *Ussuridiscus* is also restricted to the early Dienerian, but in Primorye, its type species *U. varaha* is found in four consecutive beds belonging to three different zones (Shigeta & Zakharov, 2009), ranging from the late Griesbachian to the middle Dienerian, whereas it is restricted to a single bed in the Salt Range. Its presence in the late Griesbachian is uncertain, as its occurrence in this substage is based on bed 1009 of Shigeta & Zakharov (2009, Fig. 15), which yielded a poorly preserved specimen assigned to *Lytophiceras*? sp. indet. However, the presence of *U. varaha* in the middle Dienerian is confirmed by its association in bed 1013 of Shigeta & Zakharov (2009) with "*Ambitoides*" *fuliginatus* (here re-assigned to *Mullericeras*), *Proptychites ammonoides* and "*Gyronites*" (here re-assigned to *Ambites* on the basis of the bottlenecked shape of the venter). The *Gyronites subdharmus* zone, which Shigeta & Zakharov (2009) assigned to the late Griesbachian, contains the genus *Gyronites* and therefore likely correlates with the early Dienerian as described here. However, *Gy. subdharmus* is absent in the Salt Range, so a correlation at the species level cannot be made. Krystyn *et al.* (2004) placed their "*Pleurogyronites*" beds from Spiti into the late Griesbachian. These beds also yield *Gyronites* and thus better correlates with our early Dienerian. Additional material from these layers in Spiti is currently being studied. In north-western Guangxi (South China), Brühwiler *et al.* (2008) found some specimens initially ascribed to "*Koninckites*" cf. *timorense* but which were synonymised with *Ussuridiscus varaha* by Shigeta & Zakharov (2009, an assignment which we partially confirm here), so their *Proptychites candidus* beds may partially correlate with the early Dienerian as defined here (whereas the original *Proptychites candidus* zone of Tozer is here considered as middle Dienerian; see below). The genus *Gyronites* has never been reported outside of the Tethys, but conodonts from the *Bukkenites strigatus* zone of the Canadian Arctic indicate that the topmost part of this zone may actually already be Dienerian (Orchard, 2008) and thus may correspond partially to our early Dienerian.

Gyronites dubius *beds.* – This RZ is here based on the association found at the base of the LCL in Amb. It also occurs at the base of the LCL in Nammal Nala, where it is included in a condensed layer that is useless for biostratigraphical purposes. This RZ is characterised and dominated by the species *Gy. dubius*, but *Ussuridiscus varaha*, *Bukkenites sakesarensis* sp. nov. and *Ghazalaites roohii* gen. et sp. nov. are also abundant. *Gy. rigidus* and *Kyoktites* cf. *hebeiseni* gen. et sp. nov. are each represented by a single specimen. *Gy. dubius* and *Gy. rigidus* also occur in several localities in the Indian Himalayas, where they were first described by Krafft

& Diener (1909) and Diener (1897), indicating further extension of this fauna to the NIM. This RZ corresponds partially to the condensed horizon MH-G3 in Romano *et al.* (2013).

Gyronites plicosus *beds.* – This RZ has been recognised in every investigated section, in several beds in the middle of the LCL, except in Chiddru where it occurs in the lower third of the LCL. The characteristic species *Gy. plicosus* is largely dominant, but *Gh. Roohii* and *U. ensanus* are not rare. Other species that also occur in this RZ are very rare and are represented only by very few specimens. *Gy. sitala*, *Proptychites oldhamianus*, *U. ornatus* sp. nov. and *U. ventriosus* sp. nov. were only found in Nammal, whereas *Pro. wargalensis* sp. nov. has only been found in Wargal, thus forming two distinct LMH. These two LMH are here lumped, as this distinction may be the result of the scarcity of some of their respective characteristic species. Moreover these two LMH have not been found in sequence anywhere, thus providing an additional argument to merge them. *Gy. sitala*, *U. ensanus* and some species here synonymised with *Gy. plicosus* and *Pro. oldhamianus* described by Diener (1897) and Krafft & Diener (1909) occur in several localities in the Indian Himalayas, indicating the broader extension of this fauna throughout the NIM. This RZ corresponds to the horizon MH-D1 in Romano *et al.* (2013).

Gyronites frequens *beds.* – This RZ occurs in every investigated section: in the two topmost beds of the LCL in Nammal Nala, in the penultimate bed of the LCL in Amb and Wargal, and in one bed in the middle of the LCL in Chiddru. It is characterised by very abundant specimens of *Gy. frequens*, associated with rare specimens of *Gy. schwanderi* sp. nov., *Pro. oldhamianus* and *U. ensanus*. Some species described by Krafft & Diener (1909) are here synonymised with *Gy. frequens*, thus indicating the extension of this RZ in the Indian Himalayas. Some specimens described by Wang & He (1976) and Waterhouse (1996) may also belong to *Gy. frequens*, indicating that this RZ may also expand to Nepal and Tibet. This RZ corresponds to the horizon MH-D2 in Romano *et al.* (2013).

Middle Dienerian

Depending on the areas, middle Dienerian ammonoids occur either in the LCL or at the base of the CM. The middle Dienerian is here defined by the occurrence of *Ambites*, a genus which is generally very abundant and with a worldwide distribution. The genus *Mullericeras* is mostly restricted to the middle Dienerian, except for one species (*Mu. spitiense*) which extends up into the late Dienerian. In Spiti, *Ambites* is very abundant in the lower half of the "*Ambites* beds", in the *Ambites lilangense* zone and at the base of the *Fuchsites markhami* beds (Brühwiler *et al.*, 2010a). Several species of *Ambites* were found in different sections in north-western Guangxi (Brühwiler *et al.*, 2008), which were all considered as belonging to the *Pro. candidus* beds. In this work, the authors did not provide any more precise subdivisions because of the scattered occurrence of the faunas, but a comparison with the faunas from the Salt Range should allow the refinement of the biozonation for this area. In South Primorye, *Ambites* is present in bed 1013 of Shigeta & Zakharov (2009), corresponding to their "*Ambitoides*" *fuliginatus* zone. Correlation with the Dienerian biozonation established by Tozer (1965, 1994) is not clear. The faunas from north-eastern British Columbia described by Tozer (1963, 1994) are different from those described by Tozer (1961, 1994) from Arctic Canada. Hence correlations between these two basins are uncertain. What Tozer called *Pro. candidus* in British Columbia, on which his correlation with Arctic Canada is based, is not conspecific with the species originally described by Tozer (1961) in Arctic Canada. Moreover, several species clearly belonging to the genus *Ambites* occur in British Columbia, indicating a middle Dienerian age for the Candidus Zone of this region. However, Tozer assigned only one species (*Am. ferruginus*) from Arctic Canada to *Ambites*. The latter differs from all other *Ambites* species by its involute coiling and unusually thick trapezoidal whorl section. Hence, the correlation of the Candidus Zone of Arctic Canada with our middle Dienerian cannot be confirmed here. The zonation of Tozer (1994) is based on scattered occurrences of these faunas, often without superpositional information. Additional investigations in these areas would probably allow the construction of a more detailed biozonation and more accurate correlations.

Ambites atavus *beds.* – This RZ has been documented in every studied locality: at the base of the CM in Nammal Nala, in the topmost bed of the LCL in Amb and Wargal, and in a bed in the middle of the LCL in Chiddru. It is characterised and largely dominated by *Am. atavus*. The three other species with which it is associated are extremely rare. *Am. tenuis* sp. nov. is only represented by two specimens from Amb. *Pro. ammonoides* has only been found in Nammal Nala and Amb. A single specimen of *Mu. shigetai* sp. nov. has been found in these beds in Amb. *Am. atavus* has so far only been recorded from the Salt Range. This RZ corresponds to the horizon MH-D3 in Romano *et al.* (2013).

Ambites radiatus *beds*. – This RZ has only been recognized in Nammal Nala, in a group of nodular beds about 1 m above the base of the CM. It is characterised and largely dominated by *Am. radiatus*. The co-occurring species *Am. bojeseni* sp. nov., *Mu. shigetai* sp. nov. and *Pro. ammonoides* are very rare. *Am. radiatus* also occurs in

Jinya in north-western Guangxi, where it was originally described by Brühwiler *et al.* (2008), extending this fauna to the South China block. This RZ corresponds to the horizon MH-D4 in Romano *et al.* (2013).

Ambites discus *beds.* – This RZ has been recorded from every studied locality: in a group of beds about 2 m above the base of the CM in Nammal Nala, at the base of the CM in Amb and Wargal, and in a bed in the middle of the LCL in Chiddru. It is characterised and largely dominated by *Am. discus*. The co-occurring species *Am. subradiatus* sp. nov., *Mu. shigetai* sp. nov. and *Pro. ammonoides* are rare. Some species described by Diener (1897) and Krafft & Diener (1909) from several localities in the Indian Himalayas are here synonymised with *Am. discus*, thus enlarging the distribution of this RZ to this region. Some specimens described by Wang & He (1976) and Mu *et al.* (2007) may also belong to *Am. discus*, thus further documenting this RZ in Tibet and north-western Guangxi, respectively. This RZ corresponds to the horizon MH-D5 in Romano *et al.* (2013).

Ambites superior *beds.* – This RZ has only been recognized in Nammal Nala, in a bed about 3 m above the base of the CM. It is characterised and largely dominated by *Am. superior*. The co-occurring species *Mu. indusensis* sp. nov. and *Pro. ammonoides* are rare. One specimen described by Krafft & Diener (1909) may also belong to *Am. superior*, indicating that this RZ may also expand to the Indian Himalayas. This RZ corresponds to the horizon MH-D6 in Romano *et al.* (2013).

Ambites bjerageri *beds.* – This RZ has only been identified in Nammal Nala, in a bed about 4 m above the base of the CM. It is characterised and dominated by *Am. bjerageri* sp. nov., but *Am. lilangensis*, *Pro. lawrencianus* and *Mul. niazii* sp. nov. are also common. *Pro.* cf. *pagei* and *Mul. spitiense* are very rare. One species, originally ascribed to *Gy. frequens* by Brühwiler et al. (2008) and here synonymised with *Am. bjerageri*, occurs in Shanggan in north-west Guangxi, indicating the presence of this RZ in South China. *Am. lilangensis* and its synonyms have been found in various localities worldwide: in Spiti Valley in India (Krafft & Diener, 1909), in British Columbia (Tozer, 1994), in Nepal (Waterhouse, 1996) and in Nevada (Ware *et al.*, 2011). Some specimens described by Wang & He (1976) may also belong to *Am. lilangensis*, indicating that this RZ may also be present in Tibet. This RZ corresponds to the horizon MH-D7 in Romano *et al.* (2013).

Late Dienerian

Late Dienerian ammonoids occur in the upper part of the lower third of the CM in Nammal, Amb and Wargal, and in the second half of the LCL in Chiddru. The late Dienerian is here defined by the first occurrence of Paranoritidae, as exemplified by the typically Dienerian genera *Koninckites*, *Vavilovites* and *Awanites*. Sageceratacеae also appear in this interval, and the rare genus *Clypites* has so far only been documented in this time interval. The late Dienerian, as defined here, can easily be identified in Spiti, where Paranoritidae occur in abundance in the upper part of the "*Ambites* beds" of Brühwiler *et al.* (2010a), at the top of the *Fuchsites markhami* beds, in the *Kingites lens* beds and in the *Prionolobus rotundatus* beds. A species described as *Proptychites* sp. indet. by Brühwiler *et al.* (2008) from Yuping section is here synonymised with *Kon. khoorensis*, thus indicating the presence of the base of the late Dienerian in the "*Proptychites candidus* beds" of north-western Guangxi. In the same area, the *Clypites* sp. indet. beds of Brayard & Bucher (2008) from Waili section are also most likely late Dienerian in age as this genus is so far only known in this interval. In Primorye (Shigeta & Zakharov 2009), one species originally ascribed to *Clypeoceras spitiense* is here synonymised with *Clypites typicus*, a Sageceratacеae which is so far only known from the late Dienerian. *Ambitoides orientalis*, with which it co-occurs, has a suture line typical of Paranoritidae, so the *Clypeoceras timorense* zone of Primorye is most likely late Dienerian in age. The genus *Vavilovites* is here considered as a representative of Paranoritidae, with a typical range in the late Dienerian. Therefore, the *Vavilovites sverdrupi* zone of Tozer (1994) correlates at least in part with the late Dienerian as defined here. However, the correlatives of the three subzones included in the *Vavilovites sverdrupi* zone are difficult to assess. The first subzone is based on the single occurrence of one species (*Kon. dimidiatus* Tozer, 1994) for which no equivalent is known anywhere else. The second subzone contains the type species of *Vavilovites*, and thus clearly belongs to the late Dienerian. The third one is characterised by two species belonging to genera which do not occur in the Salt Range: *Heibergites heibergensis* and *"Kingites" discoidalis*. The assignment of the latter to *Kingites* is here rejected (see taxonomic descriptions) and no correlations can be inferred from these two taxa. Tozer (1994, p. 24) also describes some species as being derived "from beds in the Toad Formation that closely follow Subzone 2", among which *Flemingites reticulatus* and *Xenodiscoides scapulatus* are undoubtedly of Smithian affinity. This fauna may thus correlate with the earliest Smithian as defined by Brühwiler *et al.* (2010b). In Eastern Verkhoyansk (Siberia; Dagys & Ermakova, 1996), the Dienerian is divided into three zones. The first one is a clear correlative of the *Vavilovites sverdrupi* zone, and is thus of late Dienerian age. The second zone is subdivided into two subzones characterised by *V. subtriangularis* and *V. umbonatus*, respectively. The assignment of these two species to the genus *Vavilovites* is uncertain because of their

different whorl sections. Other co-occuring species are also referred to as *Vavilovites* and are again restricted to this region. Therefore, no robust correlations can be inferred between the Subtriangularis Zone of Eastern Verkhoyansk and the Salt Range. The third zone is characterised by *Kingites*? *korostolevi*, a species whose assignment to *Kingites* is here rejected (see taxonomic descriptions). It also contains *Sakhaitoides allarense*, *Sa. verkhoyanicum* and *Episageceras antiquum*, three species for which no equivalent are known anywhere else, thus making its assignment to the late Dienerian uncertain.

Vavilovites *cf*. sverdrupi *beds.* – This RZ corresponds to two LMH found only in Nammal, in two consecutive beds ca. 4 m above the base of the CM. The first one contains only thirteen specimens belonging to *V.* cf. *sverdrupi* and *Mu. spitiense*. The second local maximal horizon contains fifty eight specimens, including fifty four *Kon. khoorensis*, three *V.* cf. *sverdrupi* and one *Ps. simplelobatum*. Because of the small sample size of the first horizon and the scarcity of *Mu. spitiense* (the species which distinguishes the first LMH from the second one), these two LMH are lumped together. This reunion of two LMH corresponds to the horizon MH-D8 in Romano *et al.* (2013).

Kingites davidsonianus *beds.* – This RZ occurs in 3 successive beds between 5 and 6 m above the base of the CM in Nammal. These beds yielded the most abundant material, largely dominated by *Kon. khoorensis*. *Kingites davidsonianus* is much less abundant, while *C. typicus* and *Ps. simplelobatum* are rare. This RZ has also been identified in Amb, in a bed about 4 m above the top of LCL, where the single specimen of *Subacerites friski* gen. et sp. nov. is also derived from. In Chiddru, a single isolated specimen of *Kon. khoorensis* has been found ca. 1 m below the top of the LCL, without further associated species: it may belong to this RZ or to the previous one. In Spiti valley, the *Ki. lens* beds (Brühwiler *et al.*, 2010a) are an exact correlative of this RZ. This RZ corresponds to the horizon MH-D9 in Romano *et al.* (2013).

Koninckites vetustus *beds.* – This RZ has been identified in every studied locality: in Nammal Nala ca. 7 m above the base of the CM, in Amb ca. 5 m above the base of the CM, in Wargal ca. 4 m above the base of the CM, and in Chiddru at the top of the LCL. It is characterised and largely dominated by *Kon. vetustus*, associated with the rather rare *C. typicus*, *Ps. simplelobatum*, *Ki. korni*, *Pashtunites kraffti* gen. nov. and *Radioceras truncatum*. In Spiti, the *Prionolobus rotundatus* beds (Brühwiler *et al.*, 2010a) are an exact correlative of this RZ. This RZ corresponds to the horizon MH-D10 in Romano *et al.* (2013).

Awanites awani *beds.* – This RZ has only been identified in Nammal Nala, in a bed situated just above the *Kon. vetustus* bed. It is characterised by *Awanites awani* gen. et sp. nov., which occurs together with rare *R. truncatum* and *Ps. simplelobatum*. This RZ corresponds to the horizon MH-D11 in Romano *et al.* (2013).

Conclusion

Abundant and well preserved Dienerian ammonoid faunas were sampled in detailed bed-rock controlled Early Triassic successions in Nammal Nala, Chiddru, Amb and Wargal in the Salt Range. This led to a thorough revision of the taxonomy of Dienerian ammonoids, with emphasis on their intraspecific variability and ontogeny. Most Dienerian ammonoid species were previously insufficiently known because of insufficient sample size and/or poor preservation. Griesbachian ammonoids are much rarer in the Salt Range, and will need further investigation in other areas of the Tethys to refine their taxonomy and biostratigraphy.

This new data enabled us to construct a detailed biostratigraphic scheme for the Dienerian of the Salt Range, with a total of 12 successive ammonoid assemblages. It is by far the most comprehensive Dienerian ammonoid record known worldwide, confirming that the Salt Range represents a key area for the study of the Early Triassic biotic recovery and its ammonoid zonation. Detailed studies such as this one are a necessary prerequisite for analyses of ammonoid diversity dynamics and phylogeny.

Systematic palaeontology
(By Ware, D. & Bucher, H.)

Classification

The suprageneric classification used here is mostly based on the classification established by Spath (1934), with some modifications which are discussed in the text. Our classification diverges from more recent ones (e.g. Tozer, 1994, Dagys & Ermakova, 1996, Shigeta & Zakharov, 2009), in which Gyronitidae are treated as a synonym of Meekoceratidae and Paranoritidae as a synonym of Proptychitidae, two points which are here rejected. Waterhouse (1994) provided a completely different classification which was exclusively based on the suture lines. However, his method did not take into account the intraspecific variability of the suture lines, and as a consequence, extreme variants belonging to a single species should be placed in different families according to his classification. According to the very narrow definitions of his classification and considering the asymmetry of the suture line (here illustrated by

some specimens for which the suture line could be drawn from both sides), most of our specimens would be placed in different families depending on which side of the specimen the suture line is obtained from. Hence, the classification of Waterhouse (1994) is not further considered hereafter.

Our classification is essentially based on abundant material, and as most taxa considered here were initially described by Waagen (1895) and Spath (1934) from the Salt Range, emended diagnoses are provided for both genera and species. At the family level, emended diagnoses are given only for two families (Gyronitidae and Mullericeratidae), whose respective ranges are restricted to the Dienerian. For other families, a more comprehensive study including taxa from other regions and time intervals would be necessary to establish emended diagnoses.

The population approach: intraspecific variability and convergences

As already underlined by many authors (e.g. Tozer, 1994, Brayard & Bucher, 2008, Monnet *et al.*, 2010), ammonoid species usually exhibit a wide range of intraspecific variability, so the taxonomy of ammonoids must be based on a population approach. This variability mostly follow the "Buckman's Law of Covariation" of Westerman (1966), ranging from involute, compressed shells with subdued ornamentation and a highly frilled suture line to more evolute, depressed, coarsely ornamented shells with a simpler suture line. This is particularly important for Dienerian ammonoids. They have a very low morphological disparity (Brosse *et al.*, 2013), and as already noticed by Brayard & Bucher (2008) for Smithian ammonoids and Monnet & Bucher (2005) for Anisian ammonoids, convergences of shell shapes of compressed end-member variants from different lineages are very frequent. Such convergences can only be detected by the analysis of big samples within a highly resolved time frame. As differences between compressed end-members of different taxa can be small, and intraspecific variability is generally large, it is necessary to work with large populations to decipher which characteristics are of intra- or interspecific significance. Several clear examples of convergences are here given. For example, the convergence between *Kon. khoorensis* and Proptychitidae, between some very evolute species of *Ambites* and smooth forms of *Gyronites*, or between involute tabulate Paranoritidae and Mullericeratidae. In these cases, differences between the taxa are very small, and not always visible on each specimen of the population. For example, *Ambites bjerageri* sp. nov. has a sub-serpenticonic shape and a tabulate venter, thus superficially resembling *Gyronites*, but some individuals have a clear bottleneck shaped venter and weak spiral ridges on their flanks, two characteristics which are typical of the genus *Ambites*. These two characteristics are however not present on every specimen, so the affinities of this species can only be deciphered by working at the population level. Moreover, these characteristics are not prominent, and can be detected only on well preserved specimens. Thus, good preservation is also a prerequisite to establish a reliable taxonomy, as even slight weathering, corrosion or distortion of the specimen can be sufficient to alter traits of supraspecific significance.

Ideally, the intraspecific variability should be quantified for every trait of the shell. Considering that ornamentation and whorl section are the result of a highly integrated growth module whose accurate shape is difficult to quantify (e.g. Urdy *et al.*, 2010 a & b), only the four classic geometrical parameters of the ammonoid shell are here statistically treated: the diameter (D), whorl height (H), whorl width (W) and umbilical diameter (U), and the corresponding ratios of the latter three parameters with the diameter (H/D, W/D and U/D). Providing that these parameters are available for at least five specimens within each species, H, W, U and the corresponding ratios are first plotted against the diameter to ascertain their variability and potential allometric growth. As every species shows strong allometric growth, these graphs allow the categorisation into size classes for which no or nearly no allometry occurs (i.e., usually excluding the juveniles, which are always more evolute than adults, and in some cases the largest specimens, when they show a clear umbilical egression). To test the normality of the three relative parameters within the population, the corresponding histograms should show a normal distribution within each species. Providing that at least 30 specimens (excluding juveniles and forms with an umbilical egression at maturity) were available within a species, normality was tested using the Liliefors (1967) test: the label "normal" on each histogram indicates that the test cannot reject the null hypothesis of normality at a confidence interval of 95 %. They are otherwise labelled "not normal". To compare different closely related species, boxplots (Monnet & Bucher, 2005) for each of these three relative parameters are provided. These display the 25th, 50th (median) and 75th percentiles of the range of measures covered by 99 % of the specimens from a normally distributed sample. Outliers represent specimens not falling within the normal distribution. As for histograms, these were calculated only on a certain range of size, excluding juveniles and forms with a strong umbilical egression at maturity, to avoid problems of growth allometries.

Suture lines

As a consequence of the comparatively low morphological disparity of Dienerian ammonoids, most

authors focused on the suture lines to establish their taxonomy and phylogeny. The most extreme example is Waterhouse (1994), who established a completely new taxonomy for Triassic ammonoids exclusively based on suture lines, underplaying the characters of the shell. The problem is that the morphology of the suture line is not an independent trait, as it covaries with the shape of the whorl section (as already noticed by Spath, 1919a). Within the frame of intraspecific variation, involute compressed variants have more elements exposed outside of the umbilical suture and more indentations on the lobes and auxiliary series than evolute depressed variants. This covariation is most likely the result of the morphogenesis of the septum, and has been tentatively explained by the means of viscous fingering model of Checa & García-Ruiz (1996) through a domain effect, i.e. the number of elements depends on the "distance between opposite elements of the septal suture". This can be illustrated in our material by the development of the auxiliary series. In involute and compressed forms, this distance is very small (it corresponds in this case to the distance between the flank of the whorl and the flank of the overlapped preceding whorl), so the auxiliary series will be long with differentiated elements; in similarly involute but more depressed variants, the auxiliary series is also long but with less differentiated elements; in evolute shells, the overlap with the preceding whorl is much smaller, resulting in an auxiliary series which is very short with less differentiated elements. As a consequence, the presence or absence of an auxiliary lobe is not necessarily of taxonomic significance, as it may be the result of covariation with the shell shape and thus may appear or disappear during ontogeny as a result of allometric growth. This is especially important in our case, as many authors have considered this characteristic as extremely important. For example, Tozer (1994) divided Dienerian ammonoids into two groups mostly based on this characteristic: Meekoceratidae, without auxiliary lobe, and Proptychitidae, with an auxiliary lobe. He therefore considered Paranoritidae as a synonym of Proptychitidae, and Gyronitidae as a synonym of Meekoceratidae, a view we cannot support as an auxiliary lobe can appear or disappear within a clade without having any phylogenetic significance.

Another problem with suture lines is that their variability has never been taken into account. The suture line has often been analysed in a very typological way. However, as seen previously, the pattern of the suture line covaries with the shape of the whorl section. It is of course difficult to quantify this variability, but here we tried to give an overview of it by drawing, when possible, suture lines of different variants (e.g. involute and evolute, with a vertical and with an oblique umbilical wall, etc.). This showed that the suture line is, within a single population, highly variable, especially concerning its external dorsal half (i.e. the auxiliary series and third lateral saddle). We also noticed a general asymmetry of the suture line. Here, three complete external suture lines have been drawn, and all of them are strongly asymmetrical, especially concerning the auxiliary series and the ventral lobe, two parameters which are usually considered as of primary importance for ammonoid classification. These specimens do not show any asymmetry in their shell shape, so they cannot be considered as pathologic. In *Koninckites vetustus* (Pl. 15: 6) and in *Proptychites lawrencianus* (Pl. 23: 1), an auxiliary lobe is clearly individualised on the right side, but not on the left side. As a consequence, according to Tozer's classification, their right side is typical of Proptychitidae, while their left side is typical of Meekoceratidae. Another example is given for a specimen of *Clypites typicus* (Pl. 31: 6), which has a clearly individualised adventitious saddle on the right side, not on the left side. Yacobucci and Manship (2011) noticed a similarly strong asymmetry of the suture line in Cretaceous ammonites and Carboniferous goniatites, and interpreted this as a possible consequence of soft part asymmetry. Actually, this asymmetry is better explained as being the product of a septum plane which is not exactly perpendicular to the coiling plane (i.e. a line connecting homologous elements on both sides of the shell is not perpendicular to the coiling plane). The intraspecific variability and asymmetry of suture lines were already noticed by Spath (1919b), who concluded that classification of ammonoids could not be solely based on the characteristics of the suture lines. These examples show that the shape of the suture line cannot always be directly treated as a character of higher taxonomic significance. It must be treated with the same weight, including its intraspecific variability and a certain plasticity, as all other traits of the shell.

In the present work, all species have a ceratitic suture line. To facilitate comparison between the different suture lines illustrated, those from the right side were mirrored to match the orientation of those from the left side.

Ontogeny and growth allometry

Early Triassic ammonoids generally show important growth allometries, with significant morphological changes between juvenile and adult stages. As a consequence, some authors placed juvenile specimens in different taxa (even sometimes different families) than the adult ones. Numerous juvenile specimens were found, and in order to associate these with the corresponding adults, the ontogeny of some key taxa is here studied, providing that enough specimens were available. These growth allometries were quantified by cutting some specimens perpendicularly to the coiling plane, and grinding them until the middle of the protoconch is reached. These sections allow the measurement of the four geometric parameters of ammonoids previously

mentioned every half whorl, and thus to construct the growth trajectories of these specimens and to show them on the same graphs as the rest of the population. The change in whorl section shape (appearance/ disappearance of the tabulate venter, modification of the umbilical wall or change of convexity of the flanks) could also be analysed visually on these polished sections. Ten specimens were cut, including *Ambites discus* (1), *Am. superior* (1), *Koninckites khoorensis* (3), *Kon. Vetustus* (3), *Proptychites lawrencianus* (1), *Kingites davidsonianus* (1) and *Pseudosageceras simplelobatum* (1). They all follow the same four stages of growth: 1) the neanic stage, until a diameter of 5 to 10 mm, where the shell becomes more evolute; 2) the juvenile stage, where the shell becomes more involute and compressed, until a diameter of 20 to 30mm; 3) the submature stage, where the shell almost keeps the same proportions or becomes more evolute; 4) the adult stage, where umbilical egression finally occurs. This last stage is not present in every species and could not be clearly seen on the growth trajectories as, first, the specimens cut did not have their complete body chamber, and second because this umbilical egression often occurs very rapidly, in less than half a whorl, and thus the resolution obtained from cut specimens is not sufficient to detect it clearly. In fact, it was only detected by visual examination of the complete specimens. The study of these growth allometries is very important, as the evolution of the different lineages are largely the result of developmental heterochronies on forms with a strong allometric growth, i.e. a minor change in the slope of allometry of the submature stage or of the diameter at which a specimen changes growth stage can result in major differences in adulthood. It also allows a better understanding of the intraspecific variability within each species, which is mostly the result of different allometric slopes and/or of change of growth stage. It also explains the larger intraspecific variability of juveniles compared with adult forms, already noticed by some authors (e.g. Monnet *et al.*, 2012). A good example is given here with the growth trajectories of *Kon. vetustus* (Fig. 36). In this species, the submature stage is reached at a smaller diameter in evolute variants than in involute variants. During the submature stage, shell proportions of evolute variants remain approximately the same or become slowly more involute, while involute variants become slowly more evolute. These convergences of ontogenetic trajectories lead to more homogenous morphologies toward maturity.

Systematic descriptions

Repository of figured and measured specimens is abbreviated PIMUZ (Paläontologisches Institut und Museum der Universität Zürich) and GSI (Geological Survey of India, Calcutta). Locality numbers are reported on measured sections (Figs. 3, 6, 8, 10). Synonymy lists and taxa in open nomenclature are annotated following the recommendations of Matthews (1973) and Bengtson (1988). The proportions of the shells are quantified using the four classic geometrical parameters of the ammonoid shell: diameter (D), whorl height (H), whorl width (W) and umbilical diameter (U).

Class Cephalopoda Cuvier, 1797
Subclass Ammonoidea Agassiz, 1847
Order CERATITIDA Hyatt, 1884
Superfamily Xenodiscaceae Frech, 1902
Family Xenodiscidae Frech, 1902

Genus *Hypophiceras* Trümpy, 1969
Type species. – *Glyptophiceras triviale* Spath, 1935.

***Hypophiceras* aff. *gracile* (Spath, 1930)**

Pl. 1: 1

? 1930 *Glyptophiceras gracile* nov. gen. et sp. Spath, p. 34-36, Pl. 7: 3, 4, 5 (holotype), 6, Pl. 8: 10.
? 1970 *Glyptophiceras* sp. indet. – Kummel, Pl. 1: 1.

Occurrence. – One specimen from sample Nam361 at Nammal Nala.
Description. – Very evolute sub-serpenticonic shell with weakly compressed whorl section. Flanks with maximal width at the umbilical shoulder, slightly converging towards the broadly rounded venter, without forming any ventro-lateral shoulder. Umbilical wall high, slightly oblique, delimited by a narrowly rounded umbilical shoulder. Flanks ornamented by distant thick blunt radial ribs in the inner whorls, becoming progressively thinner and denser on the last whorl. Suture line not preserved.
Measurements. – see table 1.
Discussion. – This specimen differs from the specimens originally described by Spath (1930) by its less evolute coiling. It is otherwise very close to this species. As we have only one specimen available, a definitive species assignment is not possible. Griesbachian Xenodiscidae are in need of a revision, as these forms have been splitted into different genera and species without taking intraspecific variability and covariation into account. The specimen figured by Kummel (1970), which also comes from the dolomitic unit of the Kathwai member, seems very close to ours, but is too incomplete to be firmly identified. In the Boreal Realm, the genus *Hypophiceras* occurs only in the early Griesbachian, so this single specimen and that of Kummel (1970) would suggest that this bed is equally early Griesbachian in age. However, Griesbachian Xenodiscidae are very poorly known in the Tethys, and an in-depth study of the Tethysian Griesbachian ammonoids is needed prior giving a firm conclusion about the age of this specimen.

Genus	*species*	Specimen number	Section	Age	D	H	W	U
Ambites	cf. *impressus*	PIMUZ30349	Nammal	*Ab*	36.6	14.2	9.4	11.6
Ambites	*tenuis*	PIMUZ30309	Amb	*Aa*	28.6	10.2	5.6	11.1
Ambites	*tenuis*	PIMUZ30308	Amb	*Aa*	39.9	14.1	7.2	15.9
Ambites?	sp. indet.	PIMUZ30326	Nammal	*Ad*	38.7	18.8	8.7	7.1
Ambites?	sp. indet.	PIMUZ30327	Nammal	*Ad*	37.3	20.3	8.1	5
Ambites?	sp. indet.	PIMUZ30325	Nammal	*Ad*	41	21.5	8	5.8
Ambites?	sp. indet.	PIMUZ30328	Nammal	*Ad*	24	12.6	5.6	3.6
Ambites?	sp. indet.	PIMUZ30329	Nammal	*Ad*	27	14.8	6.7	3.5
Gen. Indet.	sp. indet.	PIMUZ30511	Amb	*Gd*	13.7	8.3	3.4	1
Gyronites	*schwanderi*	PIMUZ30279	Wargal	*Gd*	41.4	15	10.8	16.3
Gyronites	*schwanderi*	PIMUZ30280	Wargal	*Gf*	49.4	18	10.7	18.4
Gyronites	*schwanderi*	PIMUZ30281	Nammal	*Gf*	66.5	19.3	13.8	31
Gyronites	*schwanderi*	PIMUZ30282	Nammal	*Gf*	70.8	25.1	15.2	29
Gyronites	*rigidus*	PIMUZ30267	Amb	*Gd*	19	6.8	4.4	7.6
Gyronites	*sitala*	PIMUZ30277	Nammal	*Gp*	33.6	10.4	8.4	14.5
Gyronites	*sitala*	PIMUZ30278	Nammal	*Gp*	41.2	11.1	9	21
Hypophiceras	aff. *gracile*	PIMUZ30236	Nammal	*Hg*	30.6	9.3	7.7	13.6
Kyoktites	cf. *hebeiseni*	PIMUZ30245	Amb	*Gd*	40	17.5	8.3	9.4
Kyoktites	*hebeiseni*	PIMUZ30244	Nammal	OG	30.5	14.6	6.8	6.2
Kyoktites	*hebeiseni*	PIMUZ30243	Nammal	OG	49.9	23.9	11.6	10.2
Mullericeras	*indusense*	PIMUZ30461	Nammal	*As*	33.4	16.7	7.3	6.1
Mullericeras	*indusense*	PIMUZ30463	Nammal	*As*	33.9	16.7	7.4	6.7
Mullericeras	*indusense*	PIMUZ30459	Nammal	*As*	35.7	17.5	7.5	7
Mullericeras	*indusense*	PIMUZ30460	Nammal	*As*	44	21.4	9.6	8.4
Mullericeras	*spitiense*	PIMUZ30452	Nammal	*Ab*	35	21.1	9.2	0
?Ophiceratidae gen. et sp. indet.		PIMUZ30242	Nammal	*OG*	18.8	10	4.8	2.5
Ophiceras	*sakuntala*	PIMUZ30241	Nammal	*OG*	41.9	16.3	9.2	12.2
Ophiceras	*sakuntala*	PIMUZ30240	Nammal	*OG*	58.1	22	13.6	16.4
Ophiceras	*connectens*	PIMUZ30237	Chiddru	*Oc*	43.9	16.1	11.1	14.2
Ophiceras	*connectens*	PIMUZ30238	Nammal	*Oc*	45.6	16.3	10.5	16.4
Ophiceras	*connectens*	PIMUZ30239	Nammal	*Oc*	63.9	22.8	15.2	24.9
Proptychites	cf. *pagei*	PIMUZ30450	Nammal	*Ab*	55.6	35.4	15	0
Proptychites	cf. *pagei*	PIMUZ30451	Nammal	*Ab*	83.2	52.9	19.9	0
Proptychites	cf. *pagei*	PIMUZ30448	Nammal	*Ab*	100.9	63.4	30.2	0
Proptychites	cf. *pagei*	PIMUZ30449	Nammal	*Ab*	90.1	57.8	26.8	0
Proptychites	*oldhamianus*	PIMUZ30440	Nammal	*Gp*	86.6	44	31	16.7
Proptychites	*oldhamianus*	PIMUZ30441	Nammal	*Gp*	39.4	19.2	14.5	7.8
Proptychites	*oldhamianus*	PIMUZ30439	Nammal	*Gf*	66.9	36.1	24	9.6
Proptychites	*wargalensis*	PIMUZ30438	Wargal	*Gp*	53.4	25.5	16.6	11.6
Shamaraites?	sp. indet.	PIMUZ30426	Wargal	*Kv*	12.5	4.7	3.3	5
Subacerites	*friski*	PIMUZ30510	Amb	*Kd*	40.4	24.8	9	0
Ussuridiscus	*ornatus*	PIMUZ30481	Nammal	*Gp*	33.8	17.1	7.2	4.4
Ussuridiscus	*ornatus*	PIMUZ30479	Wargal	*Gp*	26	13.8	5.6	2.5
Ussuridiscus	*ornatus*	PIMUZ30480	Wargal	*Gp*	40.7	21.2	9.1	4.2
Ussuridiscus	*ventriosus*	PIMUZ30482	Nammal	*Gp*	39.4	21.4	10.3	4.1
Ussuridiscus?	sp. indet.	PIMUZ30484	Nammal	*OG*	19	11.8	4.3	1.2
Ussuridiscus?	sp. indet.	PIMUZ30483	Nammal	*OG*	29.4	16.1	5.6	2.4
Vavilovites	cf. *sverdrupi*	PIMUZ30357	Nammal	*Vs*	39.5	19.8	12.1	7.1
Vavilovites	cf. *sverdrupi*	PIMUZ30359	Nammal	*Vs*	45.7	23.4	12.8	6.7
Vavilovites	cf. *sverdrupi*	PIMUZ30358	Nammal	*Vs*	60	31.8	16.3	8.4
Xenodiscoides?	sp. indet.	PIMUZ30425	Chiddru	*Kv*	22.5	8.9	5.8	7.7

Table 1. Measurements of Induan ammonoids from the Salt Range for which less than 5 specimens were measurable. D, Diameter; H, whorl height; W, whorl width; U, umbilical diameter. For the age, abbreviations as in Fig. 12.

Superfamily Meekocerataceae Waagen, 1895
Family Ophiceratidae Arthaber, 1911

Genus *Ophiceras* Griesbach, 1880

Type species. – *Ophiceras tibeticum* Griesbach, 1880.

Ophiceras connectens Schindewolf, 1954

Pl. 1: 2-4

1954 *Ophiceras connectens* nov. sp. Schindewolf, p. 178-180, abb. 4, Pl. 6: 4 (holotype).
1970 *Ophiceras connectens* – Kummel, p. 189-191, fig. 2B-2D, Pl. 1: 2 (holotype), 3-9.

Occurrence. – Samples Chi54 and Chi55 from Chiddru, Nam376 and Nam390 from Nammal Nala.
Description. – Evolute (U/D ≈ 36 %) *Ophiceras* with a slightly compressed whorl section (W/D ≈ 24 %, W/H ≈ 67 %) and a broadly rounded venter without any trace of ventro-lateral shoulders. Flanks nearly flat with maximal thickness at the umbilical shoulder, slowly converging towards the venter. Umbilical wall oblique, individualised

by a rounded shoulder. No ornamentation visible. Suture line poorly preserved, with rather elongated saddles having a rounded tip and lobes having very fine indentations at their base.
Measurements. – see table 1.
Discussion. – Our largest specimen is more evolute than the two smaller ones. It is also the case for the holotype, which is larger and more evolute than the other specimens figured by Kummel (1970). These differences are most likely the result of a growth allometry, but not enough well preserved specimens are available to demonstrate it. The suture line was visible on only one specimen. It has deeper lobes and saddles than the holotype and other specimens illustrated by Kummel (1970). However, as shown here for other species, the depth of lobes can be subject to substantial intraspecific variability, so this difference is here not considered as important. Kummel (1970) suggested that this species could be a synonym of some species from the Himalayas described by Diener (1897), but a detailed revision of the Himalayan Ophiceratidae would be first necessary. Waterhouse (1994) actually placed *O. connectens* in synonymy with *O. tibeticum*, and considered Kummel's specimens to belong to another species, *Lytophiceras chamunda* (Diener, 1897). However, his material is far too poorly preserved for a proper revision of this group. We therefore follow Kummel's approach by keeping the species name *O. connectens* for our specimens, until a revision of the faunas from the central Himalayas becomes available.

***Ophiceras sakuntala* Diener, 1897**

Pl. 1: 5-6

1897 *Ophiceras sakuntala* nov. sp. Diener, p. 114-118, Pl. 10: 1 (lectotype), 2-7, Pl. 11: 1, 2, 4.

Occurrence. – Sample Nam391 from Nammal Nala.
Description. – Rather involute (U/D ≈ 29 %) *Ophiceras* with a compressed whorl section (W/D ≈ 23 %, W/H ≈ 59 %) and a narrowly rounded venter without any trace of ventro-lateral shoulders. Flanks slightly convex with maximal thickness at the umbilical shoulder, strongly converging towards the venter. Umbilical wall very oblique, individualised by an indistinct rounded shoulder. No ornamentation visible. Suture line with relatively short and rounded saddles, lobes with very fine denticules at their base, auxiliary series short with hardly discernible indentations.
Measurements. – see table 1.
Discussion. – The two specimens described here are in perfect agreement with the specimens originally described by Diener (1897). Considering that only two specimens are here available, no detailed study of their ontogeny and intraspecific variability could be done and hence, no synonymy list is provided. An extended synonymy list for this species was given by Bando (1981), but it was partially contradicted by Tozer (1994). As for the other species of *Ophiceras* described here, a revision of Himalayan Ophiceratidae is necessary.

Genus *Kyoktites* gen. nov.

Derivation of name. – Named after the Kyokti Valley (Himashal Pradesh, India), where the holotype of *Meekoceras kyokticum* Krafft, 1909 comes from.
Type species. – *Kyoktites hebeiseni* sp. nov.
Composition of the genus. – *Kyoktites hebeiseni* sp. nov., *Meekoceras kyokticum* Krafft, 1909.
Diagnosis. – Moderately involute, compressed sub-platyconic Ophiceratidae with a narrowly rounded venter and a shallow umbilicus with a vertical umbilical wall.
Occurrence. – ?Latest Griesbachian to earliest Dienerian of Spiti valley (India) and Salt Range.
Discussion. – This genus is very close to other involute Ophiceratidae genera such as *Discophiceras* or *Ghazalaites*, but it differs by its more platyconic shape with more compressed whorl section and flatter flanks. Waterhouse (1996) created the genus *Khangsaria* in which he included the species *Meekoceras kyokyticum* Krafft, 1909. However, the type species of this genus, *Kh. galteensis* Waterhouse, 1996, is based on material which poor preservation precludes any identification at the species level. Therefore, the genus *Khangsaria* is considered here as a *nomen dubium*.

***Kyoktites hebeiseni* sp. nov.**

Pl. 2: 1

Derivation of name. – Named after Markus Hebeisen (PIMUZ).
Holotype. – Specimen PIMUZ30243 (Pl. 2: 1).
Type locality. – Nammal Nala, Salt Range, Pakistan.
Type horizon. – Sample Nam391, condensed horizon from the base of LCL with late Griesbachian and earliest Dienerian faunas.
Diagnosis. – Rather involute platyconic *Kyoktites* with sub-parallel flanks.
Occurrence. – Sample Nam391 from Nammal Nala.
Description. – Rather involute (U/D = 20 %) compressed (W/D = 23 %, W/H = 47 %) platyconic shell with a rounded venter. Flanks with maximal thickness at mid-height, the flanks being only very slightly convex or sub-parallel. Umbilical wall low and vertical, bordered by a rounded shoulder. Some very low thin sigmoidal folds occur on the inner half of flanks. Suture line simple, with a narrow and shallow ventral lobe, elongated rounded first and second lateral saddle, a deep first lateral lobe and a shallow second lateral lobe both with a few small

indentions at their bases, and a very broad but short sub-rectangular third lateral saddle. Auxiliary series short, not well enough preserved to be described.
Measurements. – see table 1.
Discussion. – This species is very close to *Kyo. kyokticum* (Krafft, 1909), from which it differs by its more parallel flanks. As the two only specimens studied here come from a condensed bed containing both typical Griesbachian and typical Dienerian faunas, its precise age cannot be defined here.

***Kyoktites* cf. *hebeiseni* sp. nov.**

Pl. 2: 2

Occurrence. – A single specimen from sample Amb104 from Amb.
Description. – Moderately involute (U/D = 23.5 %) very compressed (W/D = 21 %, W/H = 47 %) sub-platyconic shell with a narrowly rounded venter. Flanks convex with maximal thickness at inner third. Umbilical wall very low and vertical, poorly individualised by a rounded shoulder. No ornamentation visible. Suture line very simple with short rounded lateral saddles. Lateral lobes with very small indentations at their base. Third lateral saddle broader than high and broadly rounded. Auxiliary series short with numerous small indentations.
Measurements. – see table 1.
Discussion. – This specimen is very close to the holotype of *Kyo. hebeiseni*, but differs by its more evolute and compressed whorls, its more convex flanks and its suture line with shallower lobes and shorter saddles, the third lateral saddle being broadly rounded. Considering the small amount of material available for study, it cannot be excluded that these two species could represent variants of a single species.

Genus *Ghazalaites* gen. nov.

Derivation of name. – Named after Ghazala Roohi (Pakistan Museum of Natural History).
Type species. – *Ghazalaites roohii* sp. nov.
Composition of the genus. – Type species only.
Diagnosis. – Compressed shell with a narrowly rounded venter and a pronounced allometric growth. Inner whorls are very involute, the umbilicus being almost occluded, and a strong umbilical egression starts on the last whorl of the adult phragmocone. No differentiated umbilical wall. Mature ornamentation consists of broad and proverse wavy folds on flanks. Suture line characterised by an asymmetrical third lateral saddle merging with the auxiliary series without clear boundary.
Occurrence. – Early Dienerian of the Salt Range.
Discussion. – This genus is close to *Discophiceras* and *Kyoktites*, from which it differs by its more involute inner whorls followed by a stronger umbilical egression, and by its suture line with the characteristic shape of its third lateral saddle. It also differs from *Kyoktites* by its convex flanks and asymmetric third lateral saddle. The resemblance between these three genera suggests a close phylogenetic relationship.

***Ghazalaites roohii* sp. nov.**

Pl. 2: 4-8; Fig. 15

v? 1978 *Lytophiceras* sp. ind. – Guex, Pl. 1: 4.

Derivation of name. – Named after Ghazala Roohi (Pakistan Museum of Natural History).
Holotype. – Specimen PIMUZ30248 (Pl. 2: 7).
Type locality. – Nammal Nala, Salt Range, Pakistan.
Type horizon. – Sample Nam332 (middle LCL), *Gyronites plicosus* beds, early Dienerian.
Diagnosis. – As for the genus.
Occurrence. – Samples Amb2 and Amb104 from Amb, Nam320, Nam331, Nam332, Nam335a and Nam377 from Nammal Nala, War8, War9 and War100 from Wargal.
Description. – Compressed (W/D ≈ 25 %, W/H ≈ 46 %) discoidal shell with a rounded venter showing a strong umbilical egression at maturity. Inner whorls are very involute (U/D ≈ 5 %), with maximal width at inner quarter of the flanks. From the point of maximal thickness, the flanks converge towards the narrowly rounded venter, forming a slightly convex gentle slope. The flanks bend rapidly towards the umbilicus, joining the preceding whorl at a right angle but without individualising any umbilical wall. Flanks are smooth. Near maturity, at a point which varies between one whorl before the end of the phragmocone and the beginning of the body chamber, the coiling becomes more evolute. On the largest measured specimen, at a diameter of 55.5 mm, U/D = 16 %. At the same stage, the point of maximal thickness shifts towards the inner third of flanks, forming an indistinct shoulder grading into the very oblique umbilical wall. Some low, broad, prorsiradiate sigmoidal folds following the shape of the growth lines appear progressively and become stronger towards the aperture. Suture line with shallow lobes and short saddles. Ventral lobe divided by a shallow ventral saddle into two small lateral branches with three small indentations at their base. Lateral lobes shallow with a few small indentations at their base. First two lateral saddles broad and rounded. Third lateral saddle very characteristic, asymmetrical, without any individualised flank on its dorsal side. The auxiliary series is thus differentiated from the third lateral saddle only by the progressive appearance of small indentations. The auxiliary series is long, with many very small regularly spaced indentations, and becomes shorter when the egression starts.

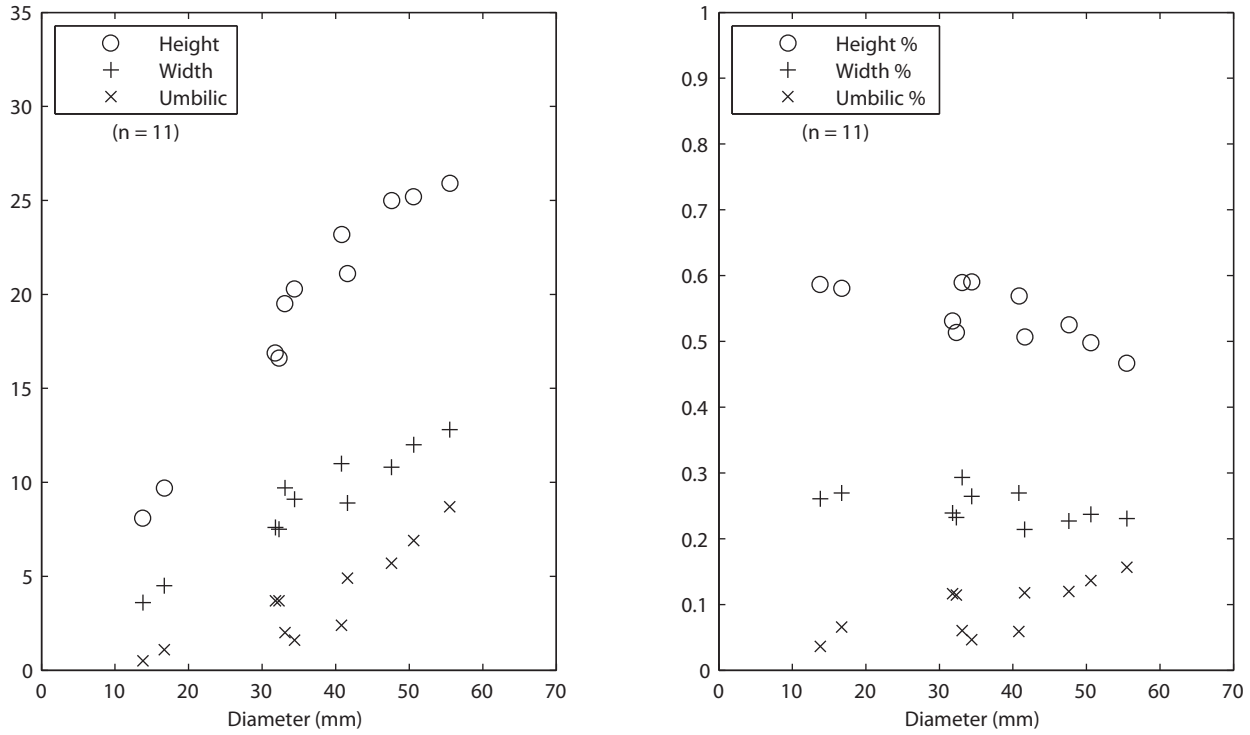

Fig. 15. Scatter diagrams of H, W, and U, and of H/D, W/D, and U/D for *Ghazalaites roohii* gen. et sp. nov.

Measurements. – see Fig. 15.
Discussion. – Guex (1978) illustrated a small poorly preserved, broken and distorted specimen coming from the same bed as the ones here studied and with which it is probably conspecific. However, its poor preservation precludes any further comparison.

Ophiceratidae? gen. nov. A sp. nov. A

Pl. 2: 3

Occurrence. – A single poorly preserved specimen from sample Nam391 from Nammal Nala.
Description. – Very involute and compressed platyconic shell with broadly rounded venter and parallel flanks. Umbilicus not clearly visible, very narrow. Maximal thickness apparently at outer third of the flanks. Suture line very simple, with extremely shallow lobes and short saddles, lobes having very few small denticules at their base. Third lateral saddle extremely broad and flat. Auxiliary series long, with numerous small indentations.
Measurements. – Specimen too distorted and poorly preserved to be measured. Maximal diameter can be estimated at about 6 cm, U/D ≈ 10 %, and W/H ≈ 45 %.
Discussion. – The simple suture line and broadly rounded venter indicate that this specimen most likely belongs to Ophiceratidae. However, its very involute platyconic shape and its peculiar suture line are very unusual, so it likely belongs to a new genus and species. This specimen is nevertheless too poorly preserved to be used as a holotype and to provide a detailed diagnosis. Therefore, it is here let in open nomenclature. A better preserved specimen would be necessary to erect a new genus and species for this form.

Ophiceratidae? gen. et sp. indet.

Pl. 1: 7

Occurrence. – A single poorly preserved specimen from sample Nam391 from Nammal Nala.
Description. – Very involute (U/D = 13 %) discoidal small shell with a narrowly rounded venter. Flanks slightly convex with maximal width at inner third. No ornamentation. Suture line only partially visible, very simple, with shallow lobes and rounded short saddles, lobes having very small denticules at their base, and the third lateral saddle being broader than high.
Measurements. – see table 1.
Discussion. – This single juvenile specimen, with its simple suture line and its rounded venter, most probably belongs to Ophiceratidae, possibly to one of the two co-occuring ophiceratid species, *O. sakuntala* or *Kyo. hebeiseni*. However, considering that only a couple of specimens belonging to these two species have been found, their intraspecific variability and ontogeny could not be studied here. Hence, the species assignment of this small specimen remains uncertain.

Family Gyronitidae Waagen, 1895

Type genus. – *Gyronites* Waagen, 1895.
Composition of the family. – *Gyronites* Waagen, 1895, *Ambites* Waagen, 1895.

Emended diagnosis. – Compressed shells of variable involution with a tabulate venter delimitated by sharp, angular shoulders which may fade out on adult body chamber. Suture line ceratitic with relatively broad lobes and saddles, lobes having small indentations at their base, saddles being well rounded. Auxiliary series short, generally with just a few small indentations and no auxiliary lobe.

Discussion. – This family, which was emended by Spath (1934), has been considered by most subsequent authors (e.g. Tozer, 1994, Shigeta & Zakharov, 2009) as a synonym of Meekoceratidae Waagen, 1895, a family which was then considered as having a very broad scope. However, Brühwiler *et al.* (2012) indicated that *Meekoceras*, the type genus of Meekoceratidae, was actually very close to Prionitidae Hyatt, 1900 and that Meekoceratidae is a largely polyphyletic taxon, the superficial and occasional similarity between Gyronitidae and some representatives of Prionitidae being the result of convergence. This opinion is here followed. After a careful analysis of our faunas, Gyronitidae are here restricted to two genera, and thus appear in the early Dienerian and disappear at the end of the middle Dienerian, and are succeeded by Paranoritidae in the late Dienerian. Actually, considering the synonymy of the different genera included by Spath (1934) in Gyronitidae, our understanding of this family and his are identical: the genus *Gyrophiceras* is based on a single, obviously pathological specimen which most probably belongs to *Gyronites*; *Gyrolecanites* is based on a species which is here considered as belonging to *Ambites*; the type species of *Prionolobus* (*Prionolobus atavus* Waagen, 1895) is considered as belonging to the genus *Ambites*. Spath also included the genus *Catalecanites* within Gyronitidae, but only with doubts, mentioning that it could also correspond to a simplified offshoot of Flemingitidae. This genus and its type species, based on a fragment illustrated by Diener (1897) has never been used by any subsequent author, and is here considered as a *nomen dubium*. One problem in Spath's concept of this family concerns the genus *Prionolobus*. Although the type species of this genus is here considered as belonging to *Ambites*, the other species included in it by Waagen, as well as the additional species of Spath, all belong to different genera, mostly *Koninckites* and *Paranorites*, which are both (in agreement with Spath) included in Paranoritidae. Hence, Gyronitidae were considered to range up to the early Smithian in previous work, a distribution which must now be shortened to the early and middle Dienerian.

Tozer (1965) based his definition of the Dienerian on the first appearance of Gyronitidae (which he synonymised in later works with Meekoceratidae). In Nammal Nala, a few specimens of *Gy. dubius* were found associated with the typical Griesbachian species *Ophiceras sakuntala*. However, this association could be the result of condensation (see biostratigraphy), so it does not contradict Tozer's definition for the base of the Dienerian. The hypothetical presence of *Gyronites* in the Griesbachian would require confirmation from a section without any sign of condensation.

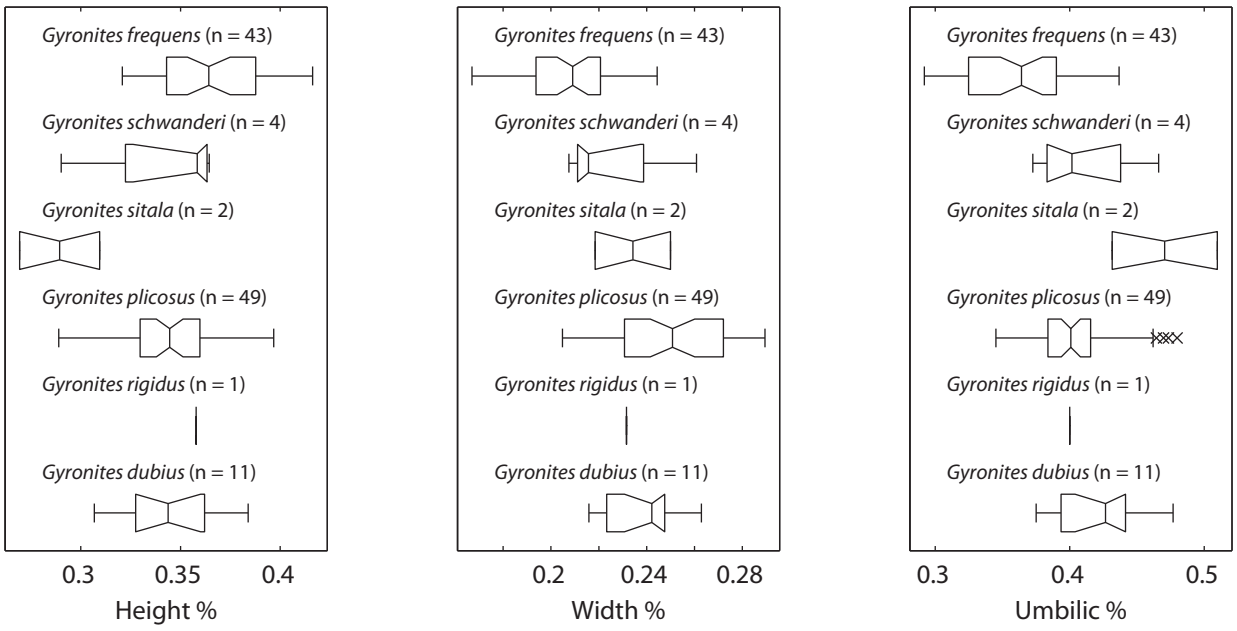

Fig. 16. Boxplots for the different species of *Gyronites* from the Salt Range. The box plot displays the 25th, 50th (median) and 75th percentiles of the range of measures covered by 99% of the specimens from a normal distribution. Outliers represent specimens not falling within the normal distribution. Because of allometric growth, these boxplots were calculated excluding specimens smaller than 20 mm in diameter, except for *G. frequens* which shows a strong allometry and for which specimens smaller than 30 mm in diameter have been excluded.

Genus *Gyronites* Waagen, 1895

Type species. – *Gyronites frequens* Waagen, 1895.
Composition of the genus. – *Gyronites frequens* Waagen, 1895, *Meekoceras dubium* Krafft, 1909, *Danubites rigidus* Diener, 1897, *Gyronites plicosus* Waagen, 1895, *Danubites sitala* Diener, 1897, *Gyronites subdharmus* Kiparisova, 1961, *Gyronites schwanderi* sp. nov.
Emended diagnosis. – Compressed, evolute, sub-platyconic to serpenticonic small sized Gyronitidae (maximal diameter of ca. 7 cm) with a tabulate venter, becoming occasionally rounded on the adult body chamber. Ornamentation varying from nearly smooth forms to variants with strong blunt radial ribs, which tend to disappear on the adult body chamber. Suture line very simple, lobes with few small indentations, second lateral saddle much larger than the others while the third one is much smaller, auxiliary series very short, sometimes nearly absent, with few and very small indentations.
Occurrence. –Early Dienerian of the Salt Range (Pakistan), Central Himalayas (India, Nepal), South Tibet (China), South Primorye (Russia).
Discussion. – The nearly smooth variants of this genus can be mistaken for evolute species of *Ambites*, from which it differs by its venter, tabulate but not bottleneck shaped, simpler suture line with fewer, smaller denticulations on the lobes and a less developed auxiliary series, and by the absence of spiral ridges on the flanks. Sub-serpenticonic ribbed variants resemble some variants of Griesbachian Xenodiscidae (*e.g. Tompophiceras, Hypophiceras*) and early Smithian Kashmiritidae, but the presence of a clearly tabulate venter in their inner whorls allows differentiating them clearly from these two families. Tozer (1994) created the new genus *Pleurogyronites* based on one specimen from the Dienerian of British Columbia. He considered this specimen as very close to *Gyronites*, differing only by the presence of ribs. According to our emended definition of the genus *Gyronites*, the presence or absence of ribs is not of generic significance, and falls within the normal range of intraspecific variability. Moreover, the type species of *Gyronites* was originally described by Waagen (1895) as perfectly smooth, but he based his diagnosis on weathered specimens. Additionally, it is shown here that *Gy. frequens* varies from nearly smooth forms to forms with strong, blunt radial ribs. It is therefore likely that *Pleurogyronites* is a synonym of *Gyronites*. Waterhouse (1996) created the genus *Wangyikangia* for the species *Gyronites nangaensis* Waagen, 1895, but this species is here shown to be a thinly ribbed variant of *Gy. frequens* (see below), hence the genus erected by Waterhouse is a junior synonym of *Gyronites*. He also erected the genus *Himoceras* for the species *Meekoceras dubium* Krafft, 1909, differing from *Gyronites* by its sub-trapezoidal whorl section and its very simple suture line which resembles the species *Ophiceras tibeticum* Griesbach, 1880. These differences are here not considered as justifying its separation from other species of *Gyronites*, hence the genus *Himoceras* is also a junior synonym of *Gyronites*. The similarities between *Gy. dubius* and *O. tibeticum* indicate that *Gyronites* most probably derives from *Ophiceras*.

***Gyronites frequens* Waagen, 1895**

Pl. 3: 1-3; Pl. 4: 1-6; Figs. 16-18

1895 *Gyronites frequens* nov. gen. et sp. Waagen, p. 292-294, Pl. 38: 1, 2 (lectotype), 3, 4, Pl. 40: 4.
1895 *Gyronites nangaensis* nov. gen. et sp. Waagen, p. 297-298, Pl. 37: 5 (holotype).
1895 *Lecanites psilogyrus* nov. sp. Waagen, p. 280-281, Pl. 39: 5 (holotype).
1895 *Lecanites undatus* nov. sp. Waagen, p. 281-282, Pl. 38: 1 (lectotype), 2.
1895 *Prionolobus compressus* nov. gen. et sp. Waagen, p. 313-315, Pl. 35: 3 (holotype).
1895 *Prionolobus plicatus* nov. gen. et sp. Waagen, p. 315-316, Pl. 35: 2 (holotype).
1895 *Prionolobus plicatilis* nov. gen. et sp. Waagen, p. 318-319, Pl. 36: 1 (holotype).
? 1909 *Xenodiscus lilangensis* nov. sp. Krafft *in* Krafft & Diener, p. 97-99, Pl. 25: 6-10.
1909 Xenodiscus khoorensis nov. sp. Krafft *in* Krafft & Diener, p. 88.
1934 *Gyronites frequens* – Spath, p. 91-92, fig. 19 [cop. Waagen 1895].
? 1976 *Gyronites psilogyrus* – Wang & He, p. 274, fig. 7a, Pl. 1: 9-10.
? 1976 *Prionolobus plicatilis* – Wang & He, p. 275, fig. 8a, Pl. 3: 13-15.
v 1978 *Gyronites frequens* – Guex, Pl. 1: 3.
v 1978 *Gyronites undatus* – Guex, Pl. 8: 3.
? 1996 *Gyronites frequens* – Waterhouse, p. 33-34, Text-fig. 4A, Pl. 1: 1-4.
? 1996 *Gyronites planissimus* – Waterhouse, p. 34-35, Text-fig. 4A, Pl. 1: 5, 8
? 1996 *Gyronites spiralis* nov. sp. Waterhouse, p. 35-36, Text-fig. 4A, Pl. 1: 6, 7, 9, 10.
non v 2008 *Gyronites frequens* – Brühwiler *et al.*, p. 1168, Pl. 5: 7, 8.

Emended diagnosis. – Compressed, moderately evolute *Gyronites* with a strong allometric growth. Flanks convex, most compressed variants being weakly ribbed and with a low, poorly differentiated oblique umbilical wall, depressed variants having sub-radial stronger ribs and a high sub-vertical umbilical wall individualised by a narrowly rounded shoulder.
Occurrence. – Samples Amb11, Amb53 and Amb62 from Amb, Chi58 from Chiddru, Nam76, Nam339 and Nam354 from Nammal Nala, War4, War7 and War100

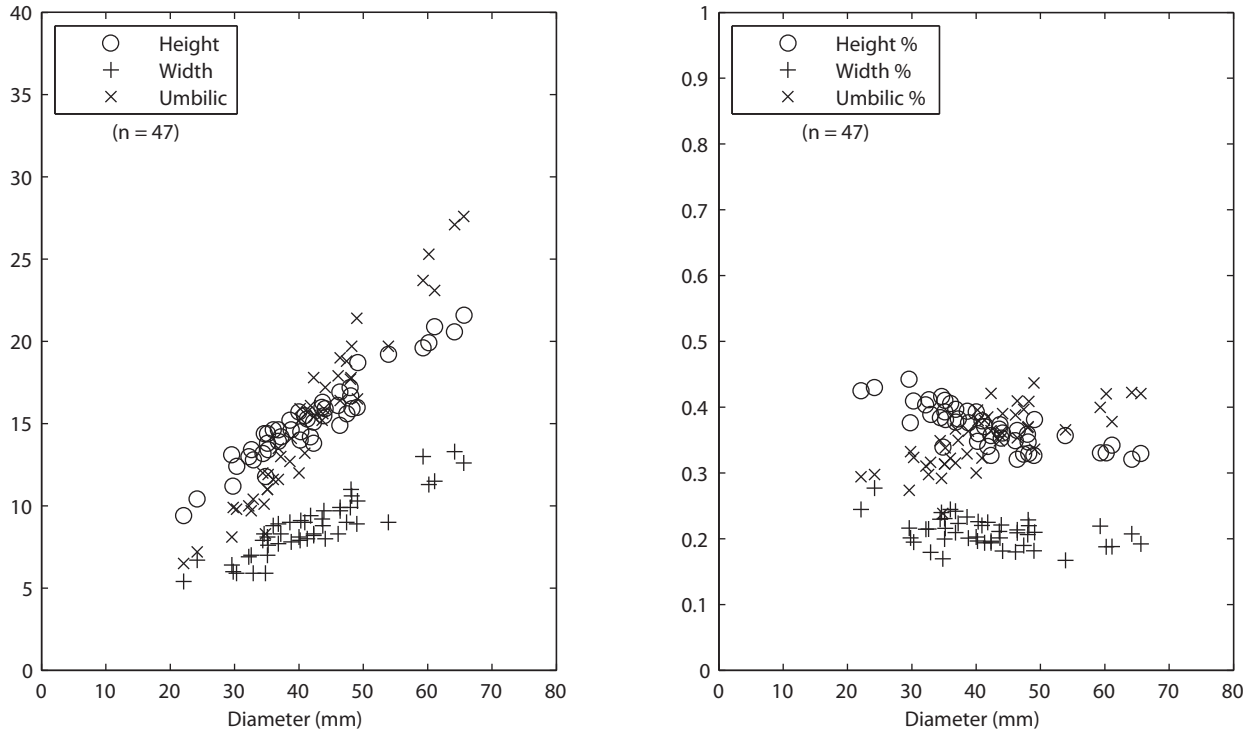

Fig. 17. Scatter diagrams of H, W, and U, and of H/D, W/D, and U/D for *Gyronites frequens* Waagen, 1895.

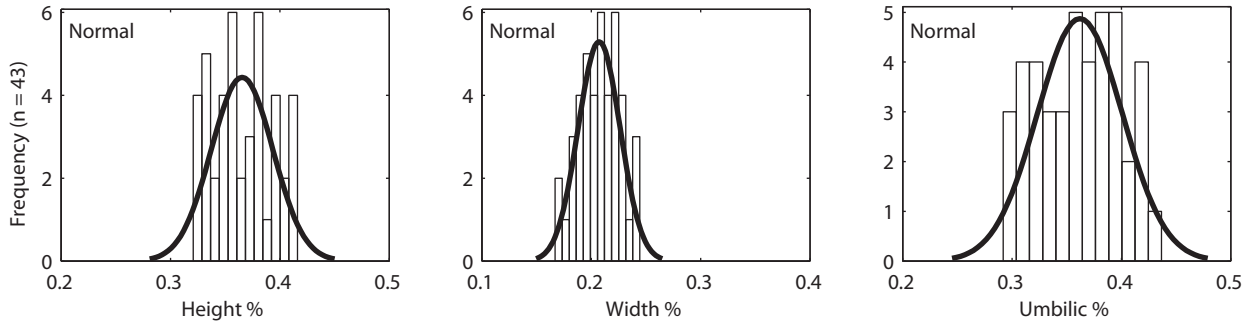

Fig. 18. Histograms of H/D, W/D, and U/D for *Gyronites frequens* Waagen, 1895. Because of allometric growth, specimens smaller than 30 mm in diameter have been excluded.

from Wargal.

Description. – Compressed (W/D ≈ 21 %, W/H ≈ 57 %) evolute sub-platyconic shells with a strong growth allometry, becoming more evolute with growth. Until a diameter of *ca*. 4 cm, the relative whorl height exceeds the relative umbilical width (*i.e.* for D < 4cm, 34.6 < H/D < 44.3 % and 27.4 < U/D < 39.1%), and above a diameter of 4 cm, the umbilical width becomes larger than the whorl height (*i.e.* for D > 4cm, 32.1 < H/D < 38.1 % and 32.3 < U/D < 43.7 %). Venter tabulate with sharp ventro-lateral shoulders at all stages of growth. Moderately to very compressed whorl section, with convex flanks and maximum width generally at inner third of the flanks, except on the most robust variants where it is situated just above the umbilical wall. Umbilical wall undifferentiated on compressed variants, the flanks sloping progressively towards the umbilicus without forming any shoulder and reaching the preceding whorl at a slightly obtuse angle. On robust variants, the umbilical wall is nearly vertical, well separated from the flanks by a narrowly rounded umbilical shoulder. Ornamentation variable, varying as a function of shell geometry. Compressed variants are nearly smooth, with faint slightly sigmoid folds following the trajectory of the growth lines, while robust variants have weak sub-radial blunt ribs which rise near the umbilical shoulder, reach their maximal strength around inner third of the flank and fade towards the venter. These ribs or folds appear at a diameter of ca. 2 cm, reach their maximal strength at a diameter of ca. 4 cm, become more numerous and thinner with growth and tend to disappear on the adult body chamber. Suture line with relatively deep lobes and elongated saddles compared with other species of *Gyronites*.

Measurements. – see Figs. 16-18.

Discussion. – The type series of *Gy. frequens*, which come

from the lowest bed of the LCL of the hills West of Khoora, are all weathered inner moulds, and Waagen (1895) stated in his report (p. 293) that although abundant, there are "only a few localities where specimens of it can be detached from the rock". Waagen considered this species as being perfectly smooth, but this is most probably the consequence of the weathering of his material, as even compressed variants actually have folds. Two characters lead Waagen to split this species into 7 species: the ornamentation and the suture line. As the ornamentation of this species is quite variable, Waagen separated smooth variants from variants with low broad folds and variants with blunt ribs. It is here shown that these variants form a continuum, and therefore all belong to the same species. Waagen also gave much importance to the indentations of the suture line, and placed specimens with a goniatitic suture line in the genus *Lecanites*, specimens with a goniatitic ventral lobe and a few, small indentations on the lateral lobes in the genus *Gyronites*, and specimens with a few indentations on the lateral branches of the ventral lobe and strong denticulations in the lateral lobes and the auxiliary series in the genus *Prionolobus*. Hence, several specimens with a nearly identical shell morphology were separated into different species belonging to different genera based on their suture line. This is especially the case, for example, of *Lecanites psilogyrus* and *Gy. frequens* for smooth variants, of *L. undatus* and *Pri. plicatus* for variants with low broad folds, and of *Gy. nangaensis* and *Pri. plicatilis* for variants with small, numerous ribs. *Pri. compressus* corresponds to a robust variant of *Gy. frequens*. Considering that, as stated by Noetling (1901) and underlined again by Kummel (1966), most of Waagen's type specimens were poorly preserved and strongly weathered, these differences of suture line are most probably the reflect of the weathering stage of the specimen rather than a genuine morphological difference. The species *Xenodiscus lilangensis* of Krafft (in Krafft & Diener, 1909) may be a synonym of *Gy. frequens*, corresponding to robust variants of this species, but the ornamentation seems to be stronger than that of all our specimens, and the type specimens are strongly distorted, making comparisons with our material difficult. Wang & He (1976) figured two specimens which they ascribe to a species here considered as synonyms of *Gy. frequens*. These are very poorly preserved and thus cannot be clearly identified. Guex (1978) collected two specimens which can both be ascribed to *Gy. frequens* without any doubt. The specimens ascribed to *Gy. frequens*, *Gy. planissimus* and *Gy. spiralis* by Waterhouse (1996) are very close to our material included in *Gy. frequens* but are too poorly preserved to be synonymised with certainty. The specimens described by Brühwiler *et al.* (2008) as *Gy. frequens* are actually placed in the genus *Ambites* (see below).

***Gyronites dubius* (Krafft, 1909)**

Pl. 4: 7-12; Figs. 16, 19

? non 1897 *Meekoceras* sp. ind. ex. aff. *plicatile* – Diener, p. 137-138, Pl. 15: 6.
1909 *Meekoceras dubium* – Krafft *in* Krafft & Diener, p. 50-51, Pl. 24: 6-10, 11 (lectotype), 12-14.

Lectotype. – Designated by Waterhouse (1996) as specimen GSI9499 illustrated by Krafft & Diener (1909), Pl. 24: 11.
Diagnosis. – *Gyronites* characterised by its sub-trapezoidal thick whorl cross-section, with high vertical umbilical wall and nearly flat flanks converging towards the tabulate venter.
Occurrence. – Samples Amb104 from Amb and Nam391 from Nammal.
Description. – Very evolute (U/D ≈ 42 %) shell with a thick whorl section (W/D ≈ 24 %, W/H ≈ 72 %). Venter tabulate with sharp ventro-lateral shoulders. Umbilical wall very high and vertical, delimited by a narrowly rounded shoulder. Flanks flat to slightly convex with maximal width at the umbilical shoulder, converging towards the venter, giving the whorl section a sub-trapezoidal outline. Ornamentation varying from very vague radial folds on the most compressed variants to relatively strong radial ribs on robust variants. Folds and ribs do not cross the venter, which is perfectly smooth. Ornamentation fades on the adult body chamber. Suture line typical of *Gyronites* with finely denticulated lobes, a very large second lateral saddle, and a small third lateral saddle. Auxiliary series poorly preserved, with or without very small indentations.
Measurements. – see Figs. 16, 19.
Discussion. – This species can easily be differentiated from all other congeneric species by its very characteristic sub-trapezoidal whorl cross-section. As already noticed by Krafft & Diener (1909) and by Waterhouse (1996), this species is very close to *Ophiceras tibeticum* Griesbach, 1880, differing only by its tabulate venter with sharp shoulders. This similarity may indicate a direct phylogenetic link between these two species. Krafft & Diener also indicated that the specimen ascribed by Diener (1897) to *Meekoceras* sp. ind. ex. aff. *plicatile* is a synonym of the present species. Actually, according to the drawing and the measurements provided by Diener, this small specimen (D = 19 mm) has a more compressed whorl section than the specimens of similar size examined here. Its whorl section is less trapezoidal than our specimens. Additional material would be necessary to analyse the intraspecific variability of the juveniles of this species in order to validate any synonymy. Waterhouse (1996) created the new genus *Himoceras* based on this species, which in

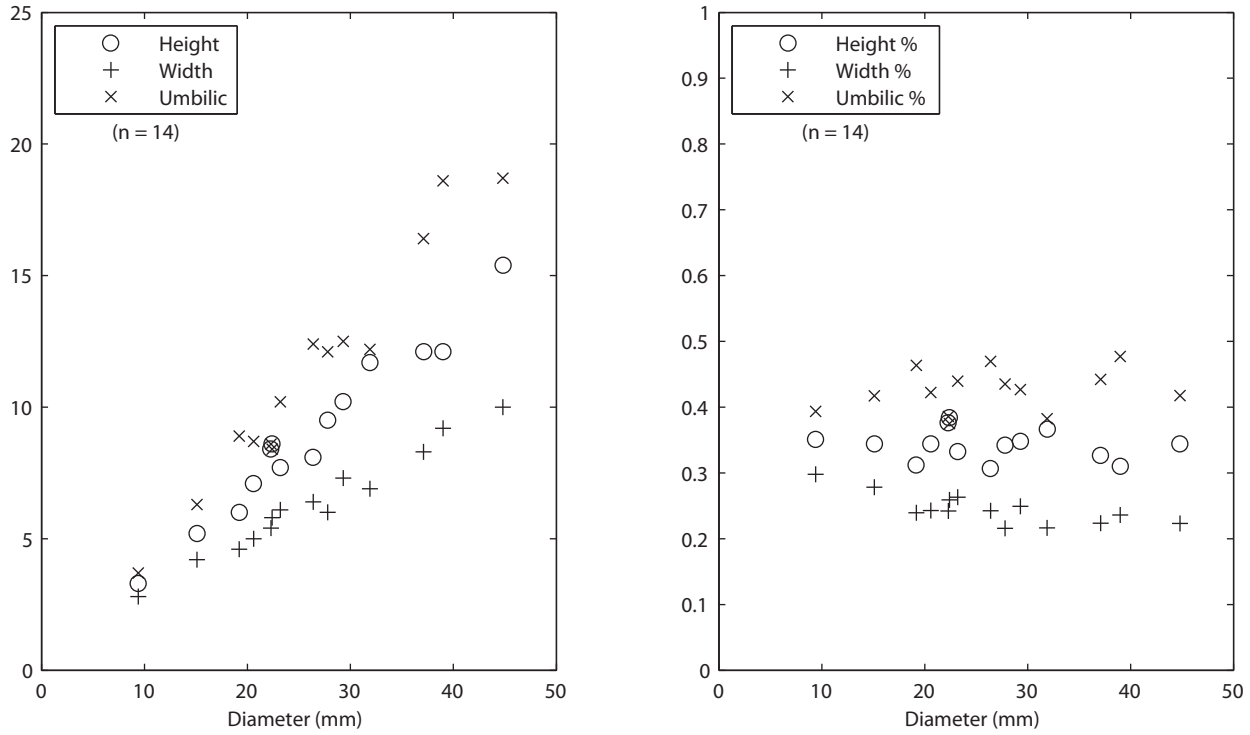

Fig. 19. Scatter diagrams of H, W, and U, and of H/D, W/D, and U/D for *Gyronites dubius* (Krafft, 1909).

our opinion is not necessary because this species shows all the characteristics of the genus *Gyronites* as revised here. When doing so, he also designated a lectotype for this species, "the specimen GSI 9499 (Krafft & Diener, 1909, pl. 24, fig. 1)". However, the figure he designated corresponds to the species *Xenodiscus nivalis* Diener, 1897, not to *Me. dubium*. This specimen corresponds actually to the one figured on Pl. 24: 11 in Krafft & Diener (1909).

***Gyronites rigidus* (Diener, 1897)**

Pl. 5: 1; Fig. 16

1897 *Danubites rigidus* sp. nov. Diener, p. 36-37, Pl. 15: 4 (lectotype), 5.
? 1909 *Xenodiscus* cf. *plicosus* – Krafft & Diener, p. 101-102, Pl. 25: 4.

Lectotype. – Here designated as the specimen GSI6023, figured in Diener (1897), Pl. 15: 4.
Diagnosis. – Evolute, moderately compressed sub-platyconic *Gyronites* of small size with a thick tabulate venter delimited by very sharp ventro-lateral shoulders. Flanks convex with thin, very slightly sigmoid ribs which disappear on the outer third of the flanks.
Occurrence. – A single specimen from sample Amb104 from Amb.
Description. –Evolute (U/D = 40 %) small shell (D = 19 mm) with a moderately compressed whorl section (W/D = 23 %, W/H = 65 %). Flanks convex with maximal width at mid-flanks, merging the thick tabulate venter almost at a right angle, thus imparting very sharp-shaped ventro-lateral shoulders. Upper flanks grading into indistinct umbilical wall. Ornamentation consisting of thin and blunt ribs following the shape of the growth lines, reaching their maximal strength at mid-flanks and fading towards the perfectly smooth venter. Suture line only partially visible and too recrystallised to be drawn and described.
Measurements. – see table 1 and Fig. 16.
Discussion. – This single specimen can be easily differentiated from the associated *Gy. dubius* by its whorl cross section and ornamentation. It can also be distinguished from all other species of *Gyronites* by its more evolute shape at similar size, the absence of individualised umbilical wall, its thin ribs and its very sharp ventro-lateral shoulders. It is nearly identical to the smallest of the two specimens of *Danubites rigidus* illustrated by Diener (1897, Pl. 15: 5), differing only by its slightly less numerous ribs (9 ribs on the last half whorl preserved for our specimen, against 12 for Diener's specimen). This small difference is here interpreted as intraspecific variability. The other specimen described by Diener, here designated as lectotype of this species, is slightly larger (D = 30 mm) and has even more numerous ribs, a probable consequence of its larger size. It has 15 ribs on its last half whorl, but only 9 (as our specimen) on its penultimate half whorl. The ribs of this specimen tend to disappear at the end of its body chamber, indicating that it is probably an adult specimen. The specimen identified as *Xenodiscus* cf. *plicosus* by Krafft

& Diener (1909) differs from the specimens described here by its thinner whorl section and more distant ribs. This difference may represent intraspecific variability, but additional material would be necessary to confirm it.

***Gyronites plicosus* Waagen, 1895**

Pl. 5: 2-10; Figs. 16, 20-21

1895 *Gyronites plicosus* nov. gen. et sp. Waagen, p. 298-300, Pl. 38: 11 (holotype).
1895 *Prionolobus buchianus* nov. gen. Waagen, p. 320-322, Pl. 35: 5.
1897 *Danubites* sp. ind. ex. aff. *planidorsato* – Diener, p. 35-36, Pl. 15: 3, 7.
? 1905 *Celtites radiosus* – Noetling, pl. 22: 1.
? 1905 *Celtites fortis* – Noetling, pl. 22: 2.
1909 *Xenodiscus rotula* – Krafft & Diener, p. 93-97, Pl. 23: 4, 5, Pl. 25: 11, Pl. 27: 4, 5.
v 1978 *Hypophiceras plicosum* – Guex, Pl. 1: 1, 2, 5.
v? 1978 *Gyronites plicatilis* – Guex, Pl. 5: 9.

Diagnosis. – Relatively thick, moderately to very evolute *Gyronites* with weak to strong ribs that fade on the mature body chamber. Compressed variants have weak ribs, a poorly differentiated oblique umbilical wall and a thick tabulate venter with sharp shoulders extending to the end of the adult body chamber. Robust variants have coarse ribs, a high sub-vertical umbilical wall individualised by a narrowly rounded shoulder, and a tabulate venter on the inner whorls, becoming rounded at maturity. Suture line with a very short, sometimes almost absent auxiliary series.
Occurrence. – Samples Amb2 from Amb, CH2A from Chiddru, Nam320, Nam331, Nam332, Nam335a, Nam377 from Nammal Nala and War5, War6, War9 and

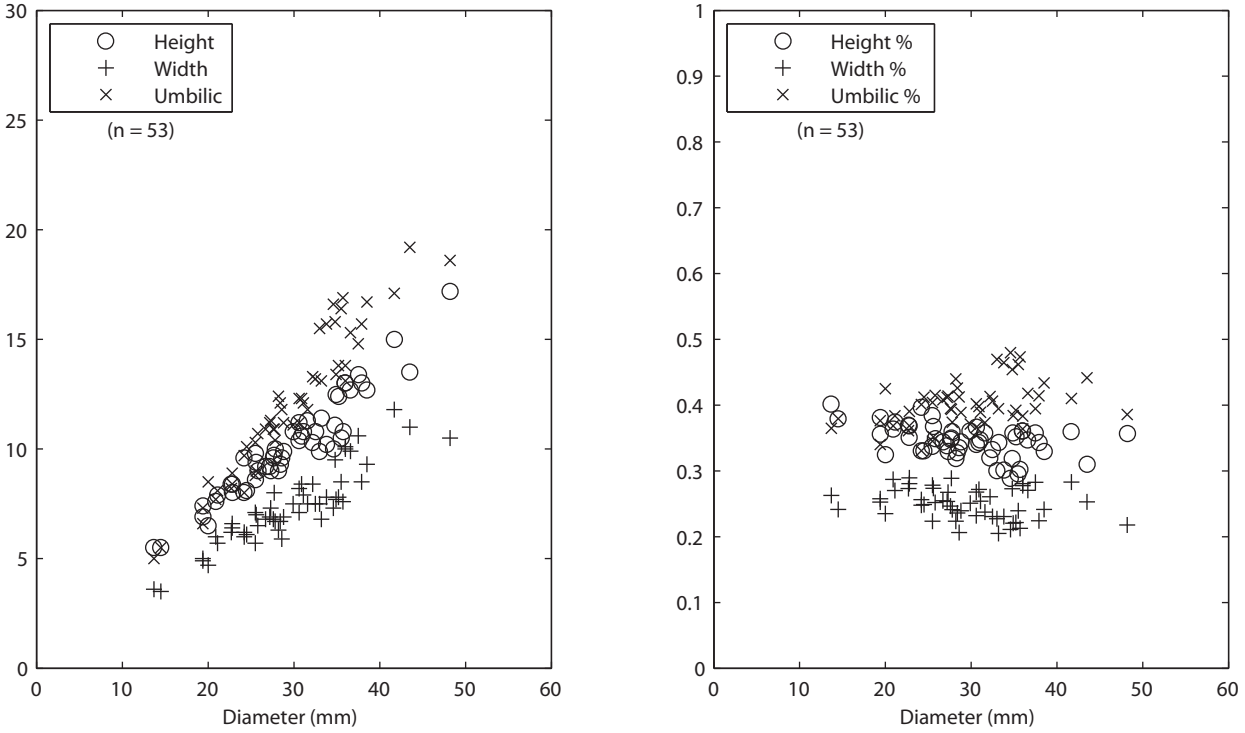

Fig. 20. Scatter diagrams of H, W, and U, and of H/D, W/D, and U/D for *Gyronites plicosus* Waagen, 1895.

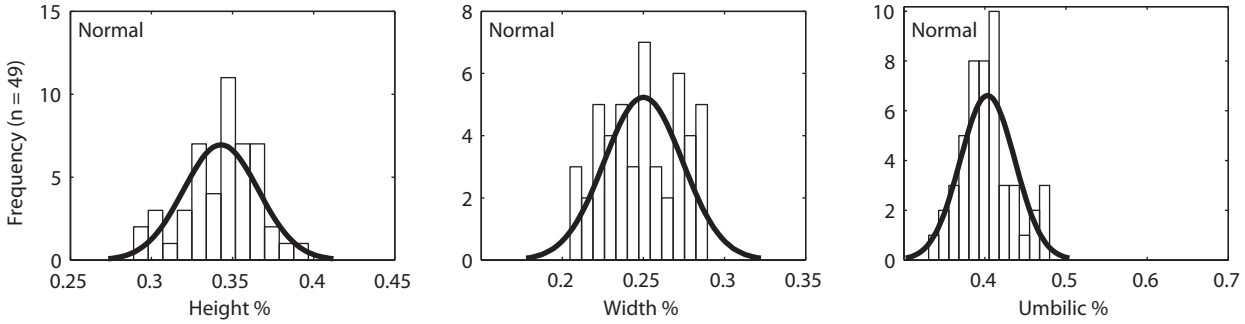

Fig. 21. Histograms of H/D, W/D, and U/D for *Gyronites plicosus* Waagen, 1895. Because of allometric growth, specimens smaller than 20 mm in diameter have been excluded from this analysis.

War100 from Wargal.
Description. – Evolute (U/D ≈ 40 %) shell with a rather thick whorl section (W/D ≈ 25 %, W/H ≈ 73 %), the shell becoming slightly more evolute with growth. The whorl section and ornamentation are highly variable. Compressed specimens have a whorl section with maximal width at inner third and convex flanks. Their venter is tabulate, delimitated by sharp ventro-lateral shoulders, even on the adult body chamber. Their oblique umbilical wall is low, poorly individualised by a broadly rounded shoulder. Their ornamentation consists of numerous thin, sigmoid and blunt ribs (up to 18 on the last half whorl of the phragmocone). On thick variants, the maximal width is situated just above the umbilical wall and the flanks are nearly flat and converging towards the venter. Their venter is tabulate on inner whorls, delimitated by narrowly rounded shoulders, and becomes broadly rounded on the last whorl. Their umbilical wall is high, almost vertical with a narrowly rounded shoulder. Their ornamentation consists of few (down to 6 on the last half whorl of the phragmocone) radial, thick and blunt ribs. In all variants, ribs become weaker towards the smooth venter, and fade on the body chamber. Suture line with a very broad and asymmetrical second lateral saddle, the first lateral lobe being much deeper than the second one. The third lateral saddle is very small with a flattened tip, and situated so close to the umbilical seam that there is no space left for the auxiliary series.
Measurements. – see Figs. 16, 20-21.
Discussion. – The illustration of the type specimen of *Gy. plicosus* in Waagen (1895) appears to be more compressed than the specimens assigned here to this species. Waagen (1895, p. 299) measured a whorl thickness of 7 mm, but mentions that "this latter measurement is only approximate as the specimen is firmly embedded in the rock". As this specimen is otherwise identical to our thick variants, this measurement is most likely underevaluated, and thus the drawing of the specimen he provides probably should have a thicker whorl section. Waagen did not illustrate the suture line, but the description he gives is also in agreement with our material. The same reasoning applies to the specimen that Waagen called *Pri. buchianus* de Koninck, 1863, which is strongly weathered. It should be noted here that the original species of de Koninck is poorly illustrated and accompanied by a vague description. It should be considered as a *nomen dubium* unless the original specimen is refigured and described. *Danubites planidorsatus* Diener, 1897 differs from our specimens by its much thinner whorl section. But the two specimens Diener (1897) refers to as *D.* sp. ind. ex. aff. *planidorsato* are very similar to our specimens, and most likely conspecific. Noetling (1905) considered two specimens from the LCL as belonging to the genus *Celtites*. These specimens most likely belong to *Gy. plicosus*, but the illustrations in Noetling's work are insufficient to confirm it. The specimens assigned to *Xenodiscus rotula* Waagen, 1895 by Krafft & Diener (1909) correspond to robust variants of *Gy. plicosus*. The original species *Gy. rotula* of Waagen (1895) comes from the Ceratite Sandstones and is thus early Smithian in age, and most probably belongs to the genus *Kashmirites*. Guex (1978) assigned this species to the genus *Hypophiceras*, probably because of its ornamentation and its rounded venter on outer whorl. A re-examination of his material showed that his specimens, like ours, do have a tabulate venter at least at the beginning of their last whorl, indicating that his specimens are clearly conspecific with ours and belong to the genus *Gyronites*. The specimen assigned to *Gy. plicatilis* by Guex (1978) is an incomplete, poorly preserved fragment of *Gyronites* which may correspond to a compressed variant of *Gy. plicosus*, but is too incomplete to allow identification at the species level. Robust variants of *Gy. plicosus* are actually very close to *Gy. sitala*, differing only from the latter by their greater involution and their more angular whorl section. They also resemble inner whorls of *Gy. schwanderi* sp. nov., from which they differ by their more rounded venter. Small and smooth variants of *Gy. plicosus* resemble *Gy. rigidus* (see above), but are more involute.

***Gyronites sitala* (Diener, 1897)**

Pl. 5: 11-12; Fig. 16

1897 *Danubites sitala* nov. sp. Diener, p. 49-50, Pl. 15: 12 (lectotype), 13.

Lectotype. – Here designated as the specimen GSI6031, figured in Diener (1897), Pl. 15: 12.
Diagnosis. – Very evolute and serpenticonic *Gyronites* with a sub-rounded whorl-section and a very narrowly tabulate venter.
Occurrence. – Samples Nam331 and Nam377 from Nammal Nala.
Description. –Very evolute (U/D ≈ 47 %) serpenticonic shell with a sub-rounded, slightly compressed whorl section (W/D ≈ 23 %, W/H ≈ 81 %). Flanks strongly convex with maximal width at mid-flanks. No differentiated umbilical wall, the flanks sloping progressively towards the umbilicus and merging the umbilical seam at a right angle. Venter tabulate and very narrow (its width represents about a third of the whorl width), the flanks joining the venter at a very obtuse angle, the ventro-lateral shoulders being thus angular but only visible with fringing light. Inner whorls with widely spaced and blunt radial ribs, becoming thinner, more numerous and sigmoid on the last whorl. Suture line not well enough preserved to be drawn and described.
Measurements. – see table 1 and Fig. 16.
Discussion. – In the original description of this species,

Diener (1897) mentioned that the venter was rounded. However, Krafft (in Krafft & Diener, 1909, p. 97) mentioned that the two specimens on which Diener based this species are "too fragmentary and weather-worn to deserve the introduction of a new specific name". He nevertheless recognised that it "is probably an independent species", a statement which is in contradiction with his previous sentence. The original specimens are probably too weathered to see the very obtuse angular ventro-lateral shoulders, but they otherwise agree perfectly with our specimens. We therefore consider this species name as valid. With their serpenticonic shape and strong ribbing, their morphology is somewhat reminiscent of that of Griesbachian Xenodiscidae such as *Hypophiceras* or *Tompophiceras* and that of Smithian Kashmiritidae. However, they differ clearly from these taxa in having a narrow tabulate venter.

***Gyronites schwanderi* sp. nov.**

Pl. 5: 13-14; Fig. 16

Derivation of name. – Named after Hans-Jörg Schwander (Faculty of Science, University of Zürich).
Holotype. – Specimen PIMUZ30281 (Pl. 5: 14).
Type locality. – Nammal Nala, Salt Range, Pakistan.
Type horizon. – Sample Nam378 (topmost LCL), *Gyronites frequens* beds, early Dienerian.
Diagnosis. – *Gyronites* with a sub-trapezoidal whorl section and strong, blunt ribs which disappear completely on the body chamber. Venter tabulate with sharp ventro-lateral shoulders. Umbilical wall steep and oblique, outlined by a narrowly rounded shoulder.
Occurrence. – Sample Nam378 from Nammal and War100 from Wargal.
Description. – Evolute (U/D ≈ 41 %) shell with a sub-trapezoidal, moderately compressed whorl section (W/D ≈ 22 %, W/H ≈ 66 %). Venter narrowly tabulate with sharp ventro-lateral shoulders becoming narrowly rounded at the end of the adult body chamber. Flanks nearly flat with maximal width at the umbilical shoulder, converging towards the venter and imparting the whorl section its sub-trapezoidal section. Umbilical wall steep and oblique, delimited by a narrowly rounded shoulder, and becoming less steep on the adult body chamber. Inner whorls with widely spaced and blunt ribs, which disappear completely on the body chamber. Suture line not well enough preserved to be drawn and described.
Measurements. – see table 1 and Fig. 16.
Discussion. –This species differs from the co-occuring species *Gy. frequens* by its more evolute coiling, its thicker whorl section, its sub-trapezoidal whorl section and its stronger ribbed inner whorls. It resembles robust variants of *Gy. plicosus* but differs from them by its larger size, its more angular whorl section with a sharper umbilical shoulder, and its narrower tabulate venter which persists until the end of the body chamber. Some specimens assigned to two species described by Krafft & Diener (1909) are quite close to *Gy. schwanderi*. The first ones, misidentified as *Xenodiscoides radians* (Waagen, 1895), differ by their more convex flanks. The original species of Waagen comes from the Ceratite Sandstones and is, as in the case of *Gy. rotula* previously discussed, a Smithian Kashmiritidae. The second species, *Ophiceras obtusoangulatum* Diener *in* Krafft & Diener, 1909, differs by its narrower venter and less angular umbilical shoulders. In both cases, the differences with our specimens are not very important and could conceivably reflect intraspecific variability. However, with only four specimens in our collections, this hypothesis cannot be tested and we therefore prefer to erect a new species.

Genus *Ambites* Waagen, 1895

Type species. – *Ambites discus* Waagen, 1895.
Composition of the genus. – *Ambites discus* Waagen, 1895, *Prionolobus atavus* Waagen, 1895, *Gyronites superior* Waagen, 1895, *Lecanites impressus* Waagen, 1895, *Meekoceras lilangense* Krafft, 1909, *Pleurambites frechi* Tozer, 1994, *Pleurambites radiatus* Brühwiler *et al*. 2008, *Ambites tenuis* sp. nov., *Ambites bojeseni* sp. nov., *Ambites subradiatus* sp. nov., *Ambites bjerageri* sp. nov.
Emended diagnosis. – Compressed, moderately involute, platyconic to serpenticonic Gyronitidae with a tabulate venter. Ventro-lateral shoulders protruding over the flanks, usually underlined by a very thin strigation and by a slight concavity on the flanks, giving the ventral part of the whorl section a bottlenecked outline. Ornamentation varying from nearly smooth forms to variants with two spiral ridges and sigmoid ribs or folds on their flanks. Suture line simple, lobes with numerous small indentations, auxiliary series short to long with small indentations and generally no differentiated auxiliary lobe.
Occurrence. – Middle Dienerian of the Salt Range (Pakistan), Central Himalayas (India, Nepal), South Tibet and Guangxi (China), South Primorye (Russia), British Columbia (Canada), Nevada (USA).
Discussion. – The most characteristic trait of this genus is its bottlenecked venter, although within each species there are always specimens which do not show it and it waxes and wanes during ontogeny. This peculiar trait is never seen among representatives of *Gyronites* or of Paranoritidae. It also differs from *Gyronites* by the occasional presence of two low spiral ridges on flanks. Its suture line has more rounded lobes and saddles, with more numerous indentations in the lobes and a longer auxiliary series with more denticulations than that of *Gyronites*. It differs from *Koninckites* by its rounder umbilical shoulder, more evolute adult shell and suture line without auxiliary lobe and with more numerous but smaller indentations. Some species have very involute

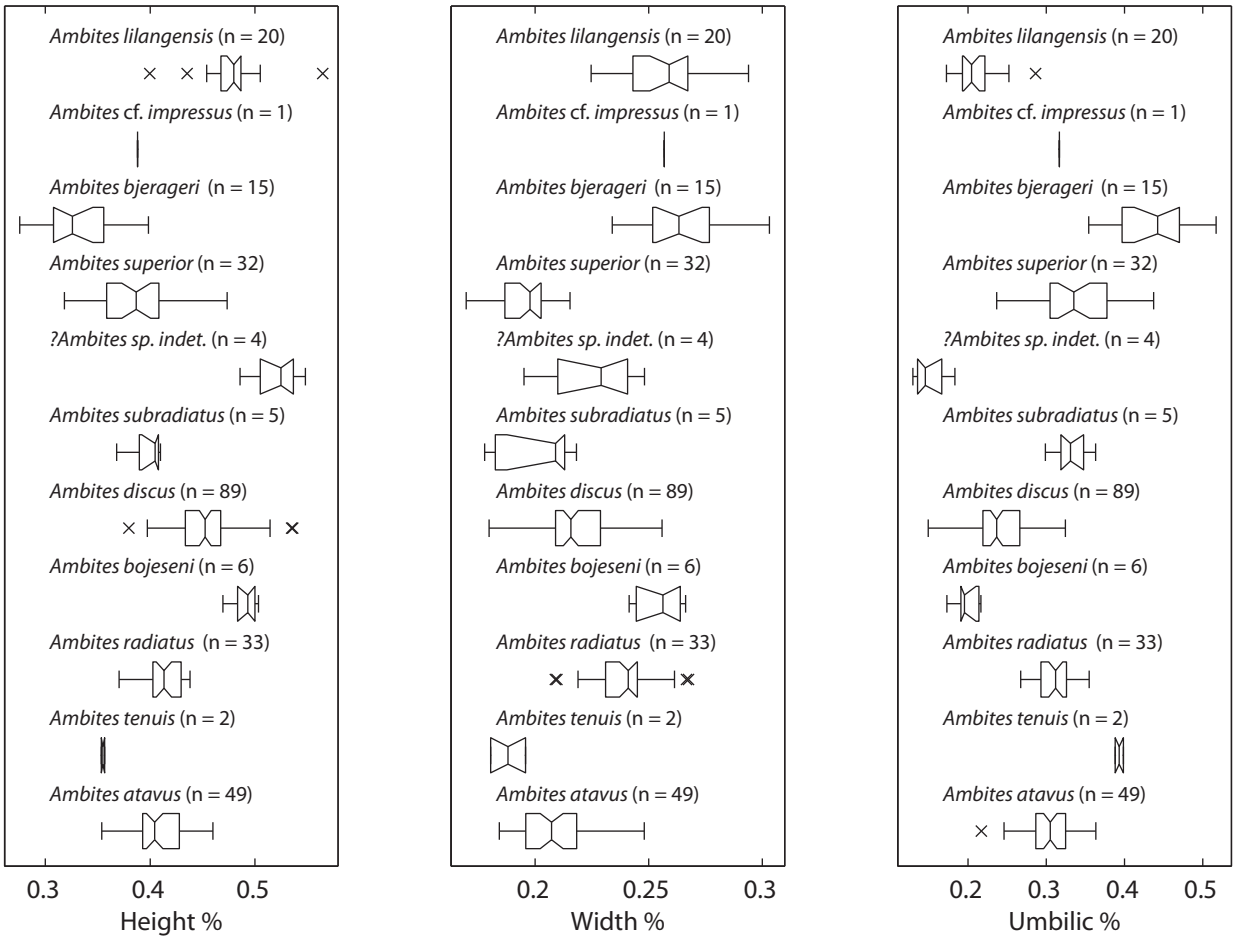

Fig. 22. Boxplots for the different species of *Ambites* from the Salt Range. The box plot displays the 25th, 50th (median) and 75th percentiles of the range of measures covered by 99% of the specimens from a normal distribution. Outliers represent specimens not falling within the normal distribution. Because of allometric growth, these boxplots were calculated excluding specimens smaller than 25 mm in diameter.

inner whorls (e.g. *Am. discus*) which can be very difficult to differentiate from co-occuring juvenile specimens of *Mullericeras*. Only some small specimens can be clearly assigned to one or the other genus. The most evolute ones and the ones which have an already clearly visible "bottlenecked venter" belong to *Ambites*, whereas the most involute ones with a very broad third lateral saddle clearly belong to *Mullericeras*. However, a few intermediate specimens cannot be clearly identified.

This genus was originally defined by Waagen (1895) as having a goniatitic suture line. Some confusion arose from this original description, leading him and other authors to create new genera for species which had clearly ceratitic suture lines. However, Krafft & Diener (1909, p. 48) noticed on the type specimen of *Am. discus* some "very delicate, indistinct denticulations on two or three succeeding principal lateral lobes". Additional specimens from the type locality (lowest bed of the CM in Amb) all do show these small denticulations, even at very small diameters (ca. 1cm). Therefore, the suture line of this genus is never goniatitic, but simply ceratitic with numerous small indentations in the lobes. As a consequence, the genus *Ambitoides* created by Shigeta & Zakharov (2009), based on a species of Tozer (1994) originally assigned to *Ambites* (*Am. fuliginatus* Tozer, 1994) and explicitly defined by Shigeta & Zakharov (2009) as being distinguished from the genus *Ambites* because of its ceratitic suture line is here considered as a synonym of *Ambites* (note that we here reject the assignment of their specimens to Tozer's species, and consider them as possibly belonging to a new species belonging to *Mullericeras*; see below). Because of their ceratitic suture line, many species belonging to *Ambites* were assigned to the genus *Prionolobus*. The latter genus is here considered as a synonym of *Ambites* (although not all species originally assigned to *Prionolobus* actually belong to *Ambites*), as its type species (*Pri. atavus* Waagen, 1895) clearly belongs to *Ambites* (see below). Spath (1934) erected the genus *Gyrolecanites* for *Lecanites impressus* Waagen (1895). According to Waagen's drawing and description, this species has a very clearly bottlenecked shaped venter, and the holotype is, according to Spath (1934), strongly weathered and still embedded in the rock. Its apparently very simple suture line is then probably a consequence of the weathering, and its bottleneck

shaped venter clearly places this species within *Ambites*, the genus *Gyrolecanites* becoming then a junior synonym of *Ambites*. Tozer (1994) introduced the name *Pleurambites* for shells with thicker whorl section and stronger ornamentation. This is a typical case of the first Buckman law of covariation, and some species described here do range from nearly smooth to rather strongly ribbed variants. The presence of ribs therefore does not indicate that it is a separate species, and the genus *Pleurambites* is consequently treated here as a synonym of *Ambites*. Finally, Waterhouse (1996) introduced the genus *Lilangia* based on the species *Meekoceras lilangense* Krafft, 1909. This species, with its strongly bottleneck shaped venter clearly belongs to *Ambites*, and the genus *Lilangia* is also a synonym of *Ambites*. Being extremely poorly preserved, new species of *Lilangia* established by Waterhouse (1996) cannot be clearly identified.

***Ambites discus* Waagen, 1895**

Pl. 6: 1-13; Pl. 7: 1-6; Figs. 22-24

1895 *Ambites discus* nov. sp. Waagen, p. 152-154, pl. 21: 4, 5 (lectotype).
1895 *Ambites magnumbilicatus* nov. sp. Waagen, p. 154-155, pl. 21: 6 (holotype).
1895 *Koninckites impressus* nov. sp. Waagen, p. 263-265, pl. 35: 6 (holotype).
1897 *Meekoceras hodgsoni* nov. sp. Diener, p. 133-135, pl. 6: 1 (holotype).
? 1897 *Koninckites vidharba* nov. sp. Diener, p. 139-150, pl. 7: 9 (holotype).
1905 *Ophiceras discus* – Noetling, pl. 13: unnumbered text-fig. in footnote 2 (holotype).
non 1905 *Ophiceras discus* – Noetling, pl. 13: 4.
p 1909 *Meekoceras lilangense* nov. sp. Krafft *in* Krafft & Diener, pl. 14: 1, 2.
p 1909 *Meekoceras hodgsoni* – Krafft *in* Krafft & Diener, p. 26-28, pl. 2: 9 (holotype).
p? 1909 *Meekoceras hodgsoni* – Krafft *in* Krafft & Diener, pl. 3: 2.
non 1909 *Meekoceras hodgsoni* – Krafft *in* Krafft & Diener, pl. 30: 1.
1909 *Meekoceras* cf. *discus* – Krafft *in* Krafft & Diener, p. 47-50, pl. 6: 2.
1934 *Prionolobus impressus* – Spath, p. 100-101, fig. 22 [cop. Waagen 1895].
1934 *Ambites discus* – Spath, p. 102-103, fig. 23 [cop. Waagen 1895].
? 1976 *Prionolobus tulungensis* nov. sp. Wang & He, p. 277, fig. 8d, pl. 2: 13-15 (holotype).
1985 *Prionolobus impressus* – Pakistani-Japanese Research group, pl. 12: 1.
? 2007 *Prionolobus impressus* – Mu *et al.*, p. 869, figs. 12.4, 13.1-13.3

Emended diagnosis. – Relatively involute (U/D ≈ 24 %) compressed (W/D ≈ 22 %, W/H ≈ 49 %) *Ambites* with very involute internal whorls and usually strongly convex flanks with two strong spiral ridges, the venter being then quite narrow and the umbilical wall very low but vertical with a narrowly rounded shoulder.
Occurrence. – Samples Amb5 and Amb54 from Amb, CH7A, Chi56, Chi57, Chi103, Chi153 and Chi154 from Chiddru, Nam50, Nam52, Nam54, Nam303, Nam364, Nam370, Nam380, Nam382, Nam383, Nam400, Nam526 and Nam527 from Nammal Nala, War2 from Wargal.
Description. – Moderately involute, compressed platyconic shell with a relatively thin tabulate venter (the venter amounts to 30-35% of the whorl width). This species shows a very strong growth allometry. The shell becomes very involute up to a diameter of about 25 mm, where U/D varies between 10 and 20%. From this diameter on, the umbilicus opens slowly, reaching between 25 and 35% of the diameter for the largest specimens found. As these largest specimens do not have their body chamber preserved, the umbilicus probably becomes even larger at maturity. The intensity of this allometry is highly variable, some specimens reaching adult size with a still strong involution and compressed whorl section, whereas others already nearly have an adult morphology at a diameter of 30 mm. The ornamentation and whorl section shape varies according to this allometry and the first Buckman law of covariation. The flanks are divided dorso-ventrally into three parts by two low spiral ridges which are absent on the most involute immature specimens and well visible on the most evolute specimens and on adults. The maximum width is situated at the inner third of the whorl on involute juveniles, and at mid-flanks, between the two spiral ridges on more evolute forms. On adults and sub-adults, the whorl section shape is very variable. The flanks of the most involute forms are sub-parallel on their inner and middle third, and bend progressively on their outer third. On other variants, the whorl section is occasionally sub-octagonal, with both inner and outer third of the flanks (clearly delineated by the two spiral ridges) forming a straight or slightly concave slope towards the umbilical wall and the venter, respectively. Some other variants have a sub-hexagonal whorl section, the inner third of the flanks being sub-parallel and the umbilical wall relatively high (see Pl. 6: 7). Some low sigmoid ridges on inner whorls of the most involute adult forms almost disappear on outer whorls, whereas they are stronger on the most evolute variant, sometimes becoming sub-angular and proverse on the inner and outer third of the flanks, and radial between the two spiral ridges. As already stated previously, the suture line is clearly ceratitic. It bears very small indentations already at small diameter (less than 1 cm), where its second lateral saddle is bent spirally and its third lateral

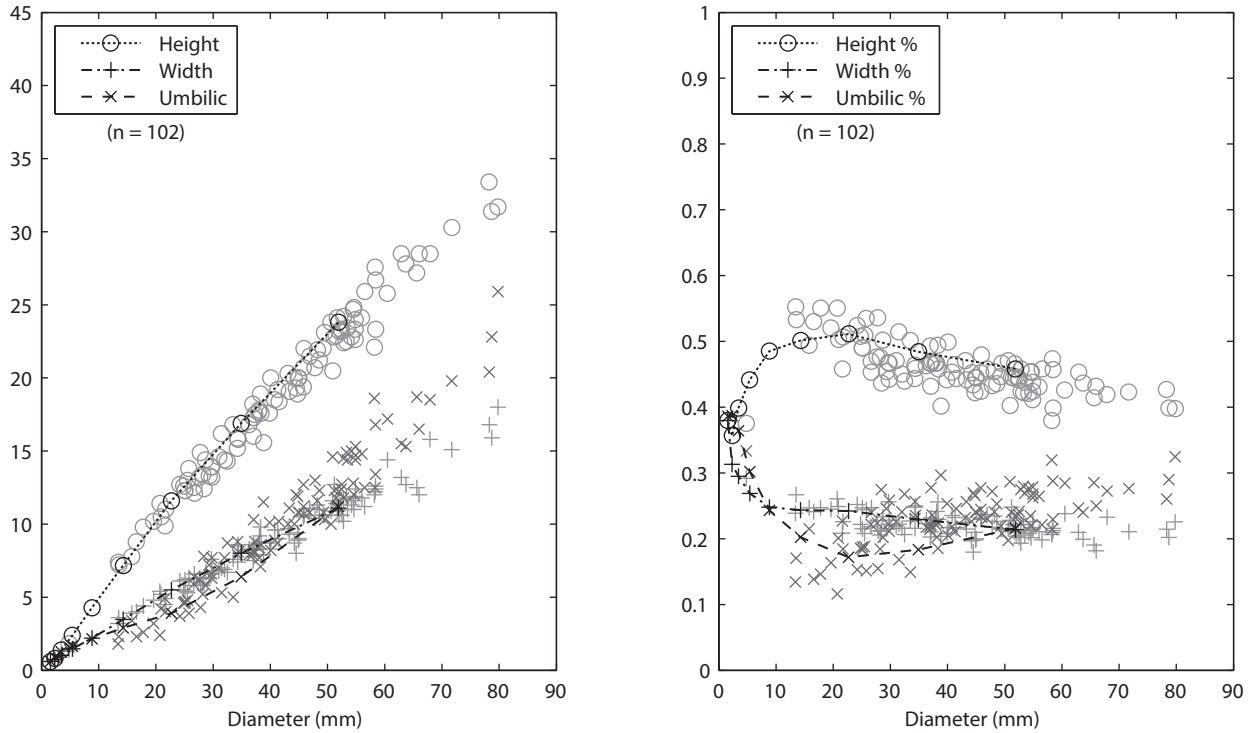

Fig. 23. Scatter diagrams of H, W, and U, and of H/D, W/D, and U/D for *Ambites discus* Waagen, 1895. Ontogenetic trajectories obtained from sectioned specimen illustrated on Pl. 6: 7 are shown in black.

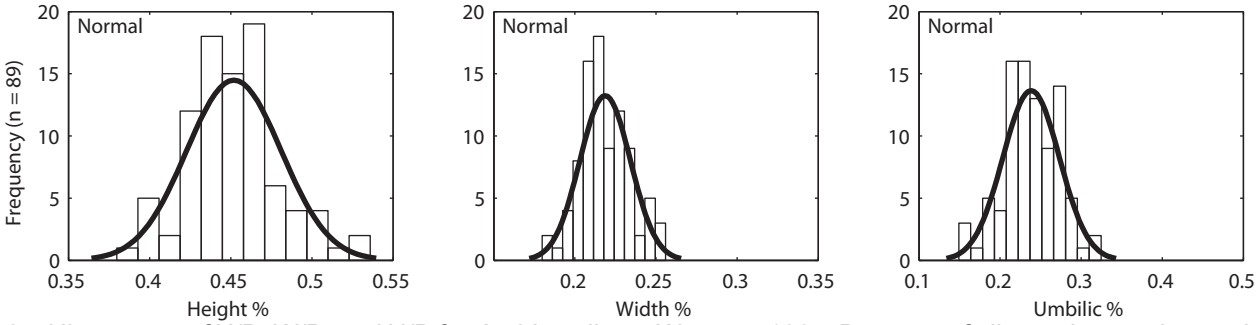

Fig. 24. Histograms of H/D, W/D, and U/D for *Ambites discus* Waagen, 1895. Because of allometric growth, specimens smaller than 25 mm in diameter have been excluded.

saddle is sub-rectangular (broader than high) and hardly differentiated from the auxiliary series which bears a few minor indentations. At larger diameters, the second lateral saddle becomes more straight, the two first lateral saddles and the two lateral lobes being well rounded and of almost even size. The length of lobes and saddles is very variable. Some specimens have lobes and saddles much longer than broad, having then a ventral lobe divided by a narrow elongated ventral saddle, a third lateral saddle quite elongated and slightly bent towards the umbilicus, and an auxiliary series with numerous indentations. Others have lobes and saddles nearly as long as broad, having then a ventral lobe divided by a short ventral saddle, a third lateral saddle broader than high with a well rounded to sub-rectangular outline, and an auxiliary series with a few minor indentations. The auxiliary series is always quite long, without any clearly differentiated auxiliary lobe.

Measurements. – see Figs. 22-24.

Discussion. – This species is clearly differentiated from other species of *Ambites* by its compressed whorl section with a relatively thin venter combined with a rather strong involution, even at adult size. Waagen (1895) already noticed the strong allometric growth of this species. The lectotype corresponds to a small involute variant, the paratype is larger and more evolute, both agreeing with our specimens. He described a second species of *Ambites*, *Am. magnumbilicatus*, which he considered as difficult to differentiate from the type species, and is here, in agreement with Krafft & Diener (1909), considered as a synonym. The species *Kon. impressus* is very similar to our specimens in every respect except for its suture line, which has a clearly differentiated auxiliary lobe. This distinction was used by Waagen (1895, p. 264) for a distinct assignment to *Koninckites*. It is otherwise very similar to the variants with a concave inner third of the whorl, and according to his original description, also has a bottleneck shaped venter. As discussed previously,

the portion of the suture line near the umbilicus (*i.e.* the third lateral saddle and the auxiliary series) can be highly variable within one species, and within a species with a simple but long auxiliary series like *Am. superior* (see below), it is possible that a few individuals do have an auxiliary lobe whereas the majority do not. This species is therefore here considered as an extreme variant (in terms of suture line) of *Am. discus*. Noetling (1905) illustrated a cast of the holotype of *Am. discus* together with an emended diagnosis of the species in a footnote of his plate 13. However, the specimen he ascribed to this species in plate 13, fig. 4 is clearly different from this species. With its very involute tabulate shell and parallel flanks, Noetling's specimen most probably belongs to Mullericeratidae. The type of *Meekoceras hodgsoni* Diener, 1897 is clearly identical to those of our specimens that exhibit a rather high, vertical umbilical wall. Among the two other specimens attributed to this species by Krafft & Diener (1909), the type of *Koninckites vidharba* Diener (1897, Pl. 7: 9, re-figured in Krafft & Diener, 1909, Pl. 3: 2) could correspond to the involute inner whorls of *Am. discus*, but identification at this diameter, especially for these compressed, involute and tabulate form is very difficult if not impossible without a clear stratigraphic control or the associated variants. The second specimen illustrated by Krafft & Diener (1909, Pl. 30: 1) is very involute, and may belong to *Ussuridiscus*. Krafft & Diener (1909) attributed two specimens to *Meekoceras lilangense* which are more compressed than the type of this species and are most probably conspecific with *Am. discus*. Specimens referred to as *Prionolobus compressus* by the Pakistani-Japanese research group (1985) clearly correspond to this species. Two specimens from China, one described by Wang & He (1976) as *Prionolobus tulungensis* and one described by Mu *et al.* (2007) as *Prionolobus impressus*, agree in proportion with *Am. discus*, but their poor state of preservation prevents further comparison.

***Ambites atavus* (Waagen, 1895)**

Pl. 8: 1-8; Pl. 9: 1; Figs. 22, 25-26

1895 *Prionolobus atavus* nov. sp. Waagen, p. 309-310, pl. 34: 4 (lectotype), Pl. 35: 4.
1895 *Gyronites evolvens* nov. sp. Waagen, p. 295-297, pl. 35: 7 (holotype).
non 1905 *Prionolobus atavus* – Noetling, pl. 22: 7.
1934 *Gyronites planissimus* nov. sp. Koken in Spath, p. 92-93, pl. 8: 4 (holotype).
non 1976 *Gyronites evolvens* – Wang & He, p. 273-274, fig. 7b-c, pl. 3: 6-12.
non 2010a *Mudiceras planissimus* gen. nov. Brühwiler *et al.*, p. 732, fig. 13.
non 2012 *Mudiceras planissimus* – Brühwiler *et al.*, p. 47-51, fig. 28Q-U.

Emended diagnosis. – Relatively evolute (U/D ≈ 30 %) compressed (W/D ≈ 21 %, W/H ≈ 51 %) *Ambites* with usually weak ornamentation. Spiral ridges very weak but always present, even at small size (for D around 3 cm). Umbilical wall poorly differentiated on evolute variants, very low and vertical on the most involute ones. Suture line with a broad third lateral saddle with a flattened tip.
Occurrence. – Samples Amb4, Amb11, Amb52, Amb53 and Amb 63 from Amb, Chi59 from Chiddru, Nam60 and Nam524 from Nammal Nala, War3 from Wargal.
Description. – Evolute, compressed, discoidal to sub-platyconic shell with a thin tabulate venter (the venter representing between 30 and 35% of the whorl width). Growth slightly allometric, juveniles tending to be slightly more involute and thicker than the adults. Flanks usually strongly convex with maximum width at the inner third of whorl height, at the level of the inner spiral ridge. In some involute, compressed variants, the segment of the flanks comprised between the two spiral ridges is sub-parallel. From the maximum width, the flanks form a nearly flat slope towards the umbilicus, where they abruptly bend before joining the preceding whorl, thus forming a low vertical umbilical wall poorly individualised by a broadly rounded edge (as described by Waagen (1895) for the type specimen). Suture line simple, with lobes generally narrower than saddles. Lateral lobes with numerous thin indentations which are either aligned in an almost straight line, or along a broadly rounded curve. The two first lateral saddles are relatively broad and rounded, the second one being larger than the first one and slightly bent towards the umbilicus. The third lateral saddle is broader than high, generally sub-rectangular but occasionally well rounded. Auxiliary series short with very small indentations and occasional weakly developed auxiliary lobe (see Pl. 8: 3d and 7d).
Measurements. – see Figs. 22, 25-26.
Discussion. – This species is very close to *Am. superior* (Waagen, 1895), from which it differs mainly by its suture line. *Am. atavus* has a very broad, sometimes sub-rectangular third lateral saddle, and has fewer indentations on the lateral lobes than *Am. superior*. Its umbilical wall is also usually less differentiated. Additionally, no variants of *Am. atavus* have an ornamentation as robust as that of *Am. superior*, and *Am. atavus* never becomes as evolute as some variants of *Am. superior* (see boxplot Fig. 22 for comparison). *Am. atavus* and *Am. tenuis*, which are the oldest representatives of the genus and share an identical stratigraphic distribution, are morphologically the nearest *Ambites* species to the youngest *Gyronites*, i.e. *Gy. frequens*. However, *Am. atavus* clearly differs from *Gy. frequens* by its bottleneck shaped venter and the presence of two spiral ridges on the flanks. Waagen (1895) erected two different species (*Pri. atavus* and

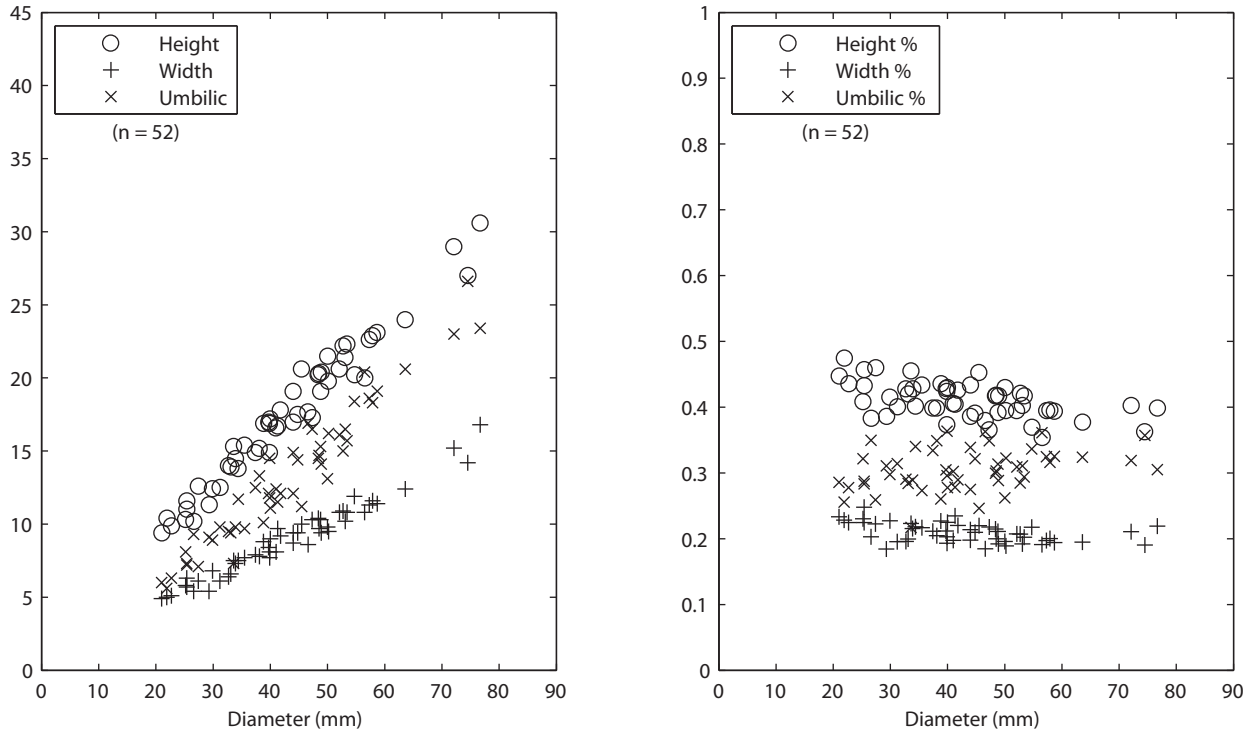

Fig. 25. Scatter diagrams of H, W, and U, and of H/D, W/D, and U/D for *Ambites atavus* (Waagen, 1895).

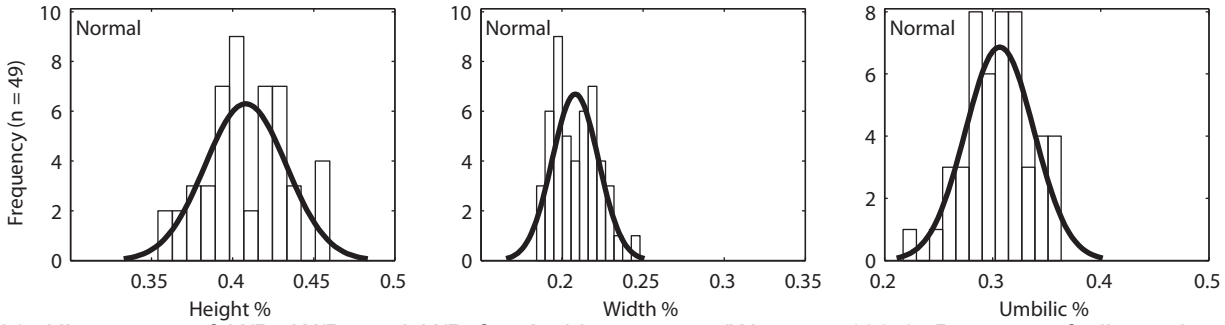

Fig. 26. Histograms of H/D, W/D, and U/D for *Ambites atavus* (Waagen, 1895). Because of allometric growth, specimens smaller than 25 mm in diameter have been excluded.

Gy. evolvens) for the material here included in *Am. atavus*. We choose the name *Am. atavus* as the valid name because the type specimen has the most typical morphology for this species. Incidentally, *Am*. *atavus* was the type species of the genus *Prionolobus* and was used as such by many previous authors, whereas *Gy. evolvens* has seldom been used. The lectotype of *Am. atavus* (designated by Spath, 1934) is a weathered phragmocone, which explains why Waagen did not notice its bottleneck shaped venter and the two spiral ridges which are barely visible on these evolute, relatively thick variants of *Am. atavus*. The second species, *Gyronites evolvens*, corresponds to a more involute variant of *Am. atavus*. The material referred to as *Gy. evolvens* by Wang & He (1976) is too poorly preserved to be clearly identified, but these specimens are more involute and thicker than any variant of *Am. atavus*. Koken (in Spath, 1934) created the species *Gy. planissimus* for a large specimen coming from the LCL of Wargal. The holotype is quite weathered and its ornamentation is not visible anymore. Although larger than any of our specimens, its morphology agrees with variants of *Am. atavus* with compressed whorl section and sub-parallel flanks, and its suture line with a relatively broad third lateral saddle is, as far as can be seen from his photo (Spath 1934, Pl. 8: 4), nearly identical to the one shown in Pl.8: 5. Brühwiler *et al.* (2010a, 2012) misidentified some early Smithian specimens as *Gy. planissimus*, and erected the new genus *Mudiceras* for these specimens. Although their overall shape is similar to the original specimen described by Spath (1934), their suture line is very different, typical of Paranoritidae, with a poorly individualised auxiliary lobe. These early Smithian specimens thus belong to an unnamed new species.

***Ambites tenuis* sp. nov.**

Pl. 9: 2-3; Fig. 22

Derivation of name. – From the Latin "tenuis", meaning thin.
Holotype. – Specimen PIMUZ30308 (Pl. 9: 2)
Type locality. – Amb, Salt Range, Pakistan.
Type horizon. – Sample Amb63 (topmost LCL), *Ambites atavus* beds, middle Dienerian.
Diagnosis. – Ambites with a very peculiar shape, very evolute (U/D ≈ 39 %) and compressed (W/D ≈ 19 %, W/H ≈ 53 %) with sub-radial thin ribs.
Occurrence. – Sample Amb63 from Amb.
Description. – Very evolute and compressed discoidal shell with a relatively broad tabulate venter (the venter amounting to 45-50% of the whorl width). Flanks convex with maximal width at mid-flanks. On the holotype, flanks are slightly concave just above the venter, and have two very indistinct spiral ridges that form a swelling at the intersections with the ribs. The flanks slope gently towards the umbilicus and bend just before reaching it, forming an undifferentiated vertical umbilical wall without shoulder. Suture line very simple, with rounded lateral saddles broader than lateral lobes, with a few very thin indentations at the bottom of the lobes. Auxiliary series short with five small indentations.
Measurements. – see table 1 and Fig. 22.
Discussion. – This species is based on only two specimens found together with *Am. atavus* in Amb. Although some specimens of similar small size of *Am. atavus* are close to these two specimens, they are still slightly less evolute and do not show the strong ornamentation of *Am. tenuis*. The very evolute platyconic shape and simple suture line of *Am. tenuis* compares well with that of some ribbed forms of *Gyronites*, but the presence of a slight concavity underlying the venter and of the two spiral ridges, although visible only on the largest specimen, allow to place them within the genus *Ambites*.

***Ambites radiatus* (Brühwiler, Brayard, Bucher & Guodun, 2008)**

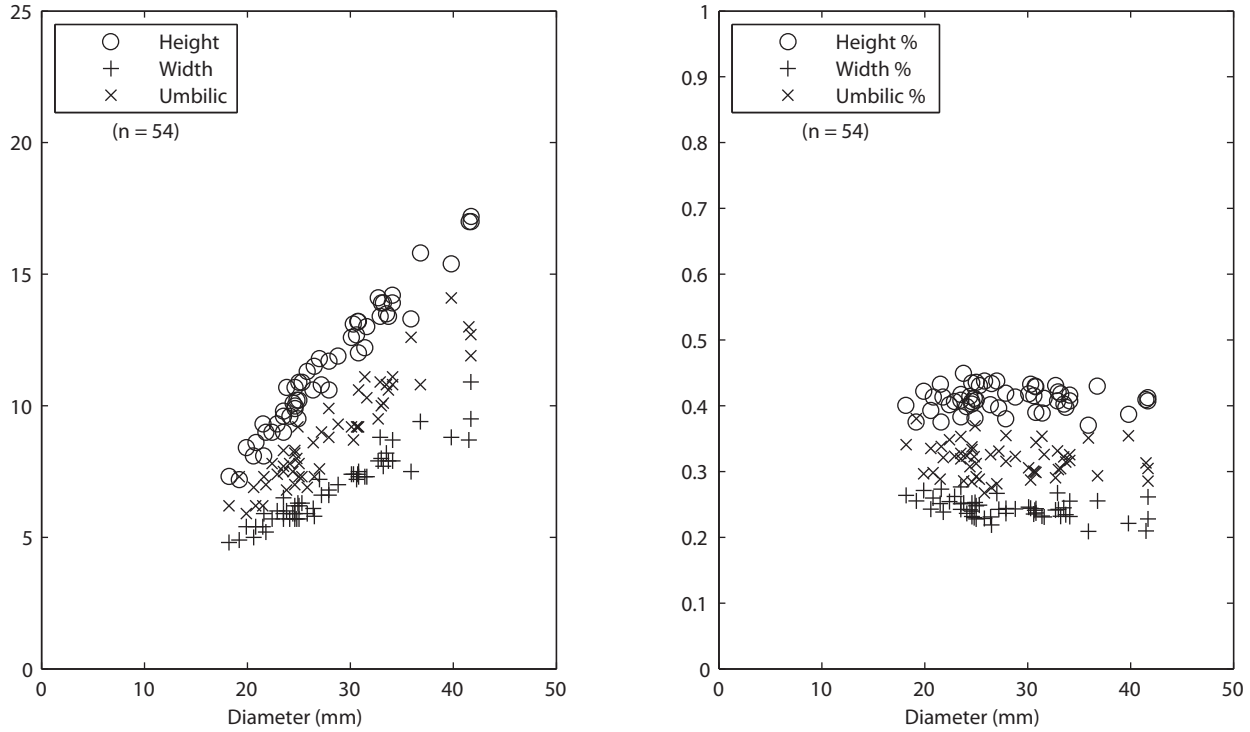

Fig. 27. Scatter diagrams of H, W, and U, and of H/D, W/D, and U/D for *Ambites radiatus* (Brühwiler, Brayard, Bucher & Guodun, 2008).

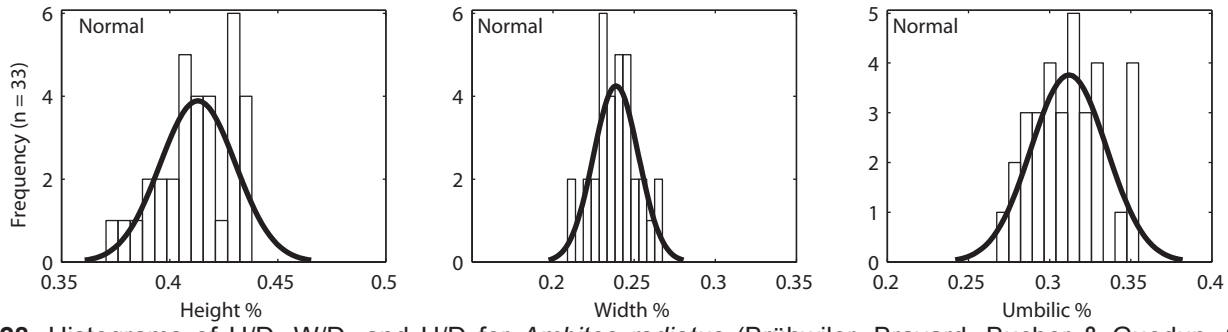

Fig. 28. Histograms of H/D, W/D, and U/D for *Ambites radiatus* (Brühwiler, Brayard, Bucher & Guodun, 2008). Because of allometric growth, specimens smaller than 25 mm in diameter have been excluded.

Pl. 9: 4-10; Figs. 22, 27-28

v 2008 *Pleurambites radiatus* nov. sp. Brühwiler *et al.*, p. 1168, pl. 5: 1 (holotype), 2-3.

Emended diagnosis. –Evolute (U/D ≈ 32%) platyconic *Ambites* of small size (maximal observed diameter of 41.7 mm on specimens with nearly complete body chamber) with relatively thick (W/H ≈ 59%, W/D ≈ 24%) sub-rectangular whorl-section and almost no or little allometric growth.
Occurrence. – Samples Nam72, Nam81, Nam379, Nam381, Nam384, Nam520 and Nam525 from Nammal Nala.
Description. – Very evolute platyconic to sub-serpenticonic shell with a relatively thick whorl section and thick tabulate venter (the venter amounting to 45-55% of the whorl width). Flanks weakly convex with maximal width at mid-flanks. Umbilical wall vertical and relatively high, with a narrowly rounded shoulder. The broad tabulate venter, the high vertical umbilical wall and the weakly convex flanks confer a sub-rectangular shape to the whorl-section. With further growth, the whorl-section tends to become slightly more compressed and the tabulate venter becomes slightly convex, but still with clear, slightly protruding ventro-lateral shoulders. Strength of ornamentation variable, ranging from smooth shells to slightly sigmoid folds or ribs and with the usual two spiral ridges. On the most heavily ornamented variants, the ribs tend to cross the venter, giving the shell a wavy outline in lateral view. Suture line quite simple, with numerous very thin indentations in the lobes. The lateral branches of the ventral lobe are very broad, with numerous small indentations at their base. Lateral lobes and saddles of nearly equivalent size, relatively elongated. The third lateral saddle is as broad as high, with its top slightly rounded. Auxiliary series with numerous regularly spaced indentations, without differentiated elements.
Measurements. – see Figs. 22, 27-28.
Discussion. – This species was originally based on only three specimens, including two very small juveniles. Our new, more abundant material allows a better understanding of its characteristics, we therefore provide here an emended diagnosis. Compared to other specimens, the holotype is a strongly ornamented variant.

***Ambites bojeseni* sp. nov.**

Pl. 9: 11; Pl. 10: 1-3; Figs. 22, 29

Derivation of name. – Named after Dr. Jørgen Bojesen-Koefoed (Geological Survey of Denmark and Greenland).
Holotype. – Specimen PIMUZ30318 (Pl. 10: 1).
Type locality. – Nammal Nala, Salt Range, Pakistan.
Type horizon – Sample Nam384 (lower CM, ca. 1,5 m above base), *Ambites radiatus* beds, middle Dienerian.
Diagnosis. – Rather involute (U/D ≈ 20% for D > 25 mm) and thick (W/H ≈ 52%, W/D ≈ 25% for D > 25 mm) *Ambites*, becoming more evolute with size (U/D estimated at 25% on the holotype), with very weak ornamentation and a simple suture line with deep, nearly symmetrical lateral lobes and saddles, the lobes bearing numerous very

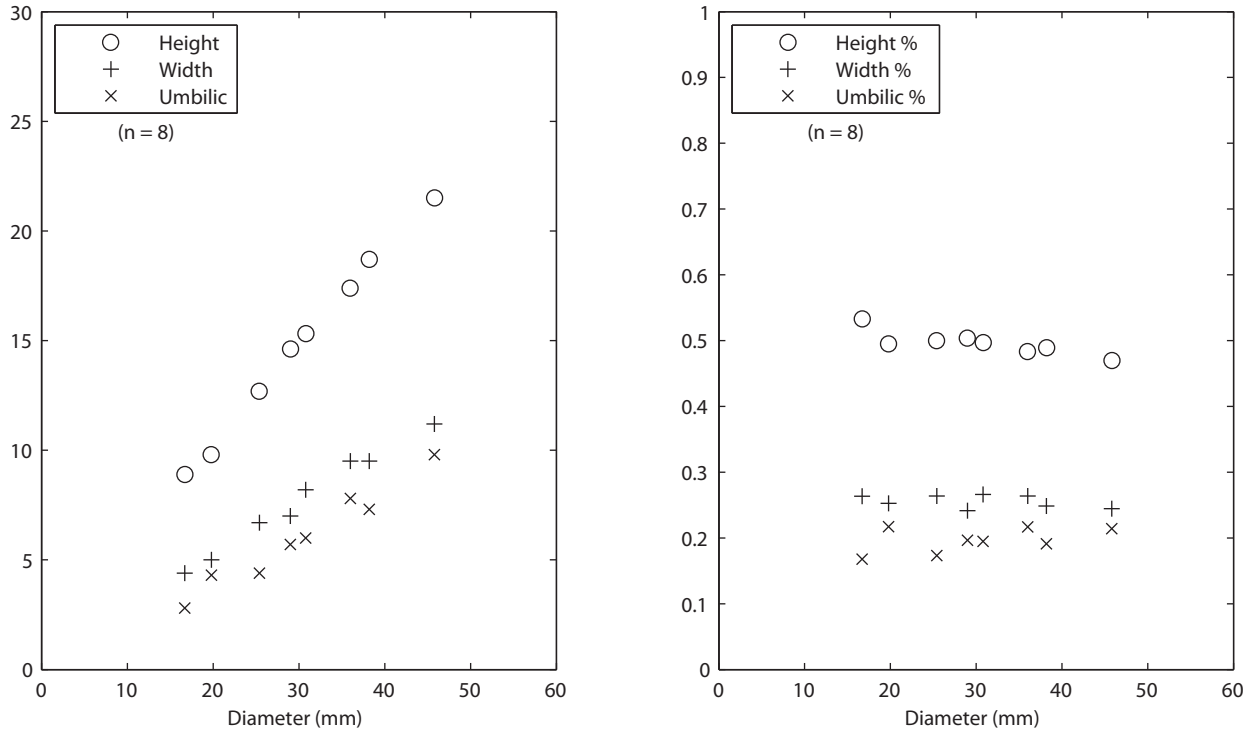

Fig. 29. Scatter diagrams of H, W, and U, and of H/D, W/D, and U/D for *Ambites bojeseni* sp. nov.

small indentations at their base.
Occurrence. – Samples Nam72, Nam381, Nam384, Nam520, Nam521 and Nam525 from Nammal Nala.
Description. – Involute and thick platyconic shell with a broad tabulate venter, the venter amounting to ca. 50% of the whorl thickness. Despite the small number of specimens, a slight allometry could be detected, the shell becoming more evolute with growth. Flanks reaching their maximum thickness at mid-flanks, sub-parallel between the umbilical shoulder and the point of maximum width from where they gently slope towards the venter, thus forming a faint spiral ridge. Umbilical wall vertical and high, poorly differentiated in small specimens but well delineated by a sharp shoulder on larger specimens. Ornamentation nearly absent apart from very low and slightly sigmoid folds. Suture line simple, with narrow and deep lateral lobes. Lobes with numerous small indentations at their base. Ventral lobe large, divided by a deep ventral saddle into two large branches. The two first lateral saddles are elongated with rounded top and are approximately of equal size. The third lateral saddle has a flattened top and is thus sub-rectangular, as broad as high on juveniles, broader than high on larger specimens. Auxiliary series short, with numerous regularly spaced small indentations.
Measurements. – see Figs. 22, 29.
Discussion. – This species is very close to *Am. lilangensis*, with which it shares similar proportions. It mainly differs by its suture line, with deeper, narrower lobes and more elongated saddles, a broader ventral lobe, lobes with more numerous indentations at their base, a more simple auxiliary series without any tendency to have a differentiated auxiliary lobe, and an almost symmetrical third lateral saddle with a sub-rectangular outline. It also tends to have less convex flanks, with less ornamentation, and its venter is always clearly tabulate and flat, whereas some specimens of *Am. lilangensis* have a slightly convex venter. It is clearly differentiated from all other species of *Ambites* by its more involute coiling and thicker whorl thickness.

***Ambites subradiatus* sp. nov.**

Pl. 10: 4-7; Figs. 22, 30

v 2011 *Ambites* aff. *radiatus* – Ware *et al.*, p. 165-168, fig.7, 8b.

Derivation of name. – Refers to the species name of *Am. radiatus*, with the prefix "sub", in reference to its close affinity with this species.
Holotype. – Specimen PIMUZ30321 (Pl. 10. 4).
Type locality. – Amb, Salt Range, Pakistan.
Type horizon – Sample Amb54 (lowermost bed of the CM), *Ambites discus* beds, middle Dienerian.
Diagnosis. – Very evolute (U/D ≈ 32 %) platyconic *Ambites* with rather compressed whorl-section (W/H ≈ 52 %, W/D ≈ 21 %) and almost no detectable growth allometry.
Occurrence. – Samples Amb 54 from Amb, Chi56 from Chiddru, Nam50, Nam52 and Nam380 from Nammal Nala, War2 from Wargal.
Description. – Very evolute thin sub-platyconic shell with a pronounced bottleneck shaped venter. Flanks

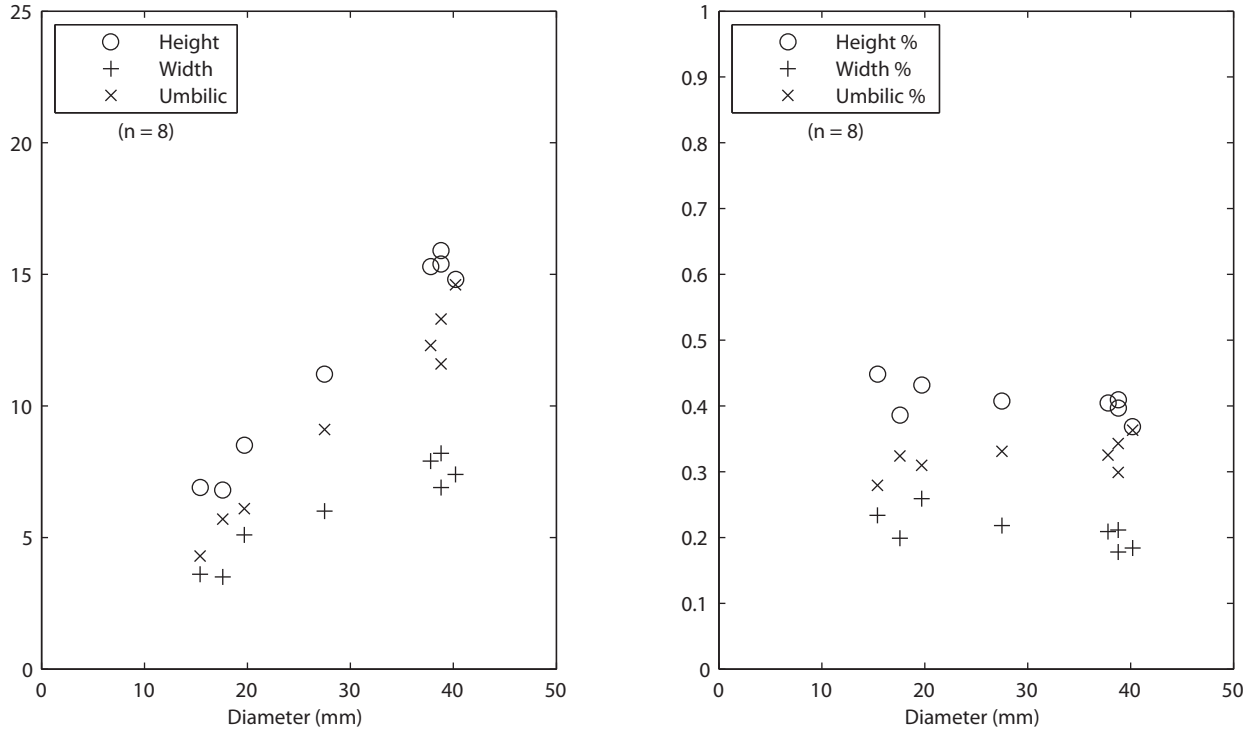

Fig. 30. Scatter diagrams of H, W, and U, and of H/D, W/D, and U/D for *Ambites subradiatus* sp. nov.

convex with a low and variable umbilical wall, ranging from variants without umbilical wall, the flanks joining the preceding whorl at an obtuse angle, to variants with a low umbilical wall delineated by a rounded shoulder. Flanks almost smooth, with very weak slightly sigmoid folds and two weak spiral ridges. Suture line simple, with numerous small indentations in lateral lobes. The lateral branches of the ventral lobe are very thin, with only three indentations at their base. The first two lateral saddles are of similar size, moderately elongated, with well rounded tips. The first lateral lobe is almost twice deeper than second lateral lobe, but has a comparable width. The third lateral saddle is much smaller than the two first ones and also rounded. Auxiliary series with a few, irregularly spaced indentations.
Measurements. – see Figs. 22, 30.
Discussion. – This species is very close to *Am. radiatus*, from which it differs mainly by its thinner whorl section, lower umbilical wall, more convex flanks and its more strongly marked bottleneck shaped venter. Its suture line differs from that of *Am. radiatus* by its smaller third lateral saddle and its ventral lobe with thinner lateral branches. No robust variant such as the holotype of *Am. radiatus* has been found. However, only very few specimens are available and it cannot be completely excluded that this difference is due to the small number of specimens available. On the other hand, specimens from Nevada described by Ware *et al.* (2011) are strictly identical to those described here, thus supporting a distinction at the species level.

***Ambites*? sp. indet.**

Pl. 10: 8-9; Fig. 22

Occurrence. – Four specimens from samples Nam380, Nam382 and Nam526 from Nammal Nala.
Description. – Very involute (U/D ≈ 15%) compressed (W/H ≈ 43%) platyconic shell with a relatively thin tabulate venter. Flanks slightly convex with maximal width at inner third. Umbilical wall vertical, individualised by a narrowly rounded shoulder. Flanks nearly smooth with weak and slightly sigmoid folds. Suture line simple with lobes bearing only few very small denticulations. Ventral lobe divided into two branches by a very shallow ventral saddle, the branches being short with only two or three small indentations at their base. The third lateral saddle is sub-rectangular (wider than deep), much smaller than the two others. Auxiliary series long, with numerous regularly spaced small indentations, without auxiliary lobe.
Measurements. – see table 1 and Fig. 22.
Discussion. – These four specimens closely resemble juveniles (i.e. at a diameter of ca. 2 cm) of the co-occurring species *Am. discus*, and could therefore represent extreme variants of this species which keep a juvenile morphology up to 3 or even 4 cm in diameter. However, they plot separately from *Am. discus* of similar size (not illustrated in figures). Moreover, if we include them in the histograms of *Am. discus*, the histogram (Fig. 24) corresponding to the relative whorl height (H/D) does not show anymore a normal distribution, these four specimens forming a small peak at the extreme right end of the distribution (for H/D between 53 and 55 %). We therefore decided to keep them separate, but their identification at the species level remains difficult because of the small number of available specimens. They closely resemble juveniles of *Am. discus*, but they lack the typical bottleneck shaped venter of this genus. They also closely resemble *Mullericeras niazii* sp. nov. (see below), but their suture line is much more simple than this species, and they lack the large ventral lobe with large branches with many indentations typical of *Mullericeras*. They most probably belong to Gyronitidae, but additional material would be necessary to decide whether they belong to a distinct species or genus.

***Ambites superior* (Waagen, 1895)**

Pl. 10: 10-12; Pl. 11: 1-9; Pl. 12: 1; Figs. 22, 31-32

1895 *Gyronites superior* nov. sp. Waagen, p. 294-295, pl. 37: 6 (holotype).
? 1895 *Prionolobus ovalis* nov. gen. et sp. Waagen, p. 316-317, pl. 35: 1 (holotype).
p? 1909 *Meekoceras disciforme* nov. sp. Krafft *in* Krafft & Diener, p. 45-47, pl. 3: 5-6.

Emended diagnosis. – Very evolute (U/D ≈ 34 %) compressed (W/H ≈ 51 %, W/D ≈ 20 %) *Ambites* with a suture line with very deep lobes and elongated saddles , the third lateral saddle being much smaller than the others.
Occurrence. – Samples Nam53, Nam302, Nam308 and Nam371 from Nammal Nala.
Description. – Very evolute compressed sub-platyconic shell with usually a pronounced bottleneck shaped venter. Evolute variants with convex flanks and maximum width at inner third of the whorl. Involute variants with more parallel flanks, the part of the flanks situated between the two lateral spiral ridges being parallel, with maximal width at mid-flanks. Umbilical wall varying from vertical with a very narrowly rounded umbilical shoulder to gently curved and sloping gradually toward the umbilical seam without any clear shoulder. Flanks with two relatively strong spiral ridges and slightly sigmoid folds whose strength is very variable. Some specimens are almost smooth, while others bear strong ribs. Growth slightly allometric, juveniles being more involute and less compressed than larger specimens. The ornamentation tends to disappear on very large specimens. Suture line with deep, well indented lobes.

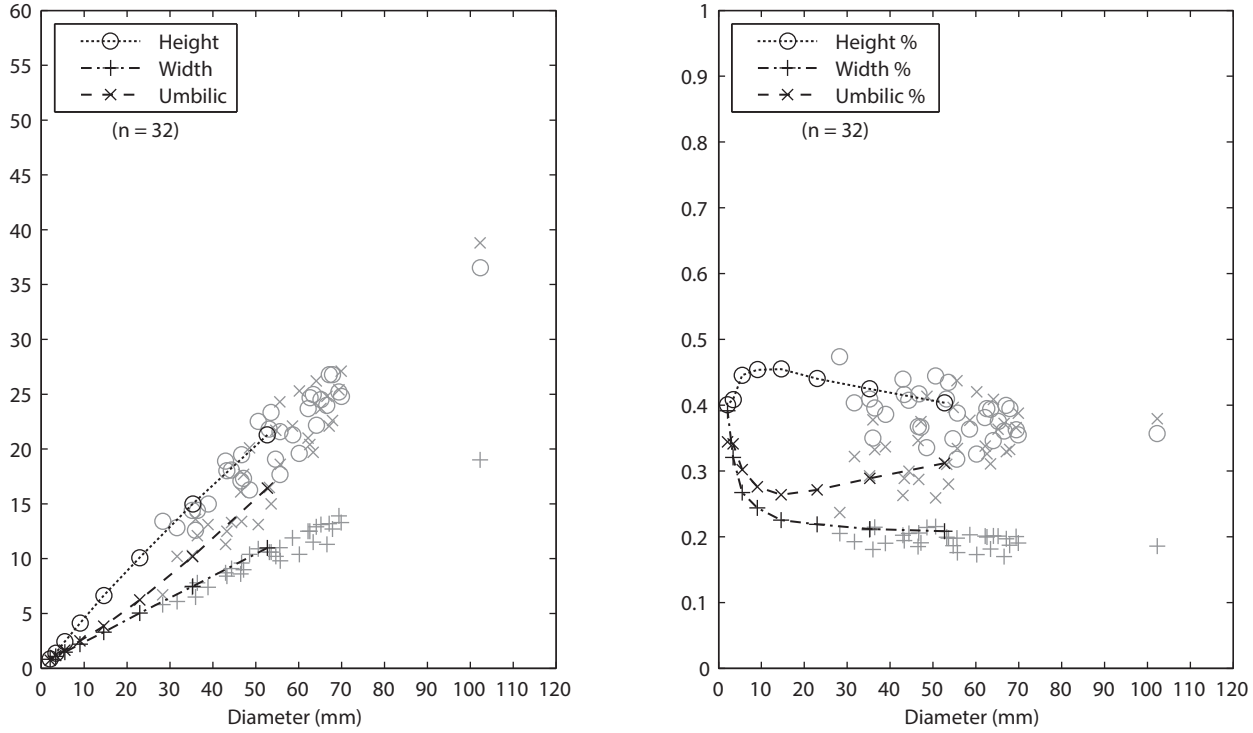

Fig. 31. Scatter diagrams of H, W, and U, and of H/D, W/D, and U/D for *Ambites superior* (Waagen, 1895). Ontogenetic trajectories obtained from sectioned specimen illustrated on Pl. 10: 12 are shown in black.

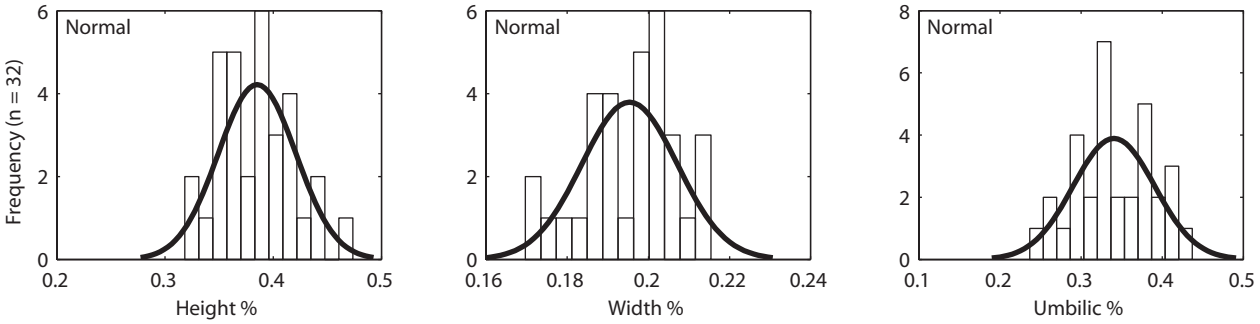

Fig. 32. Histograms of H/D, W/D, and U/D for *Ambites superior* (Waagen, 1895). Because of allometric growth, specimens smaller than 25 mm in diameter have been excluded.

The lateral branches of the ventral lobe are usually broad with many indentations. The three lateral saddles are very elongated with well rounded tips, the second one being the largest, the third one being very small. Auxiliary series varying from a few regularly spaced small indentations to a clearly individualised auxiliary lobe followed by a few deep indentations.

Measurements. – see Figs. 22, 31-32.

Discussion. – This species is clearly differentiated from other representatives of *Ambites* by its very evolute, compressed shell and its suture line with very deep lobes. The holotype corresponds to a moderately evolute variant, with slightly convex flanks. *Prionolobus ovalis* Waagen, 1895, which is based on one single specimen from the same bed as the holotype of *Am. superior* (topmost LCL of Khoora) differs from the latter by its venter, described by Waagen as "indistinctly flattened", a characteristic which does not apply to any specimens of *Am. superior*. It is otherwise very similar and it cannot be excluded that this difference in the ventral shape is the result of a shell repair. Some specimens of *Am. discus* in our samples clearly display this type of shell repair, where the bottleneck shaped venter is replaced by a sub-rounded venter in the subsequent part of the whorl. This assumption can only been confirmed by a close examination of the type specimen, which leaves the synonymy of this species uncertain. Waterhouse (1996) based his new genus *Ovaliconchia* on *Pri. ovalis*, which opens the possibility that the genus erected by Waterhouse may ultimately become a junior synonym of *Ambites*. Two specimens illustrated by Krafft & Diener (1909) and assigned to his new species *Meekoceras disciforme* are quite close to our specimens. However, they do not have a clearly visible bottlenecked venter and their suture line does not have the characteristic deep lobes and elongated saddles, but these specimens

are, as stated by the author, strongly weathered, which may explain these differences. However, their much more compressed whorl section distinguishes them from the two other illustrated specimens which were designated by Krafft as the types of this species. It should be noted here that Spath (1934, p. 103) designated the specimen figured by Krafft (1909) on plate 3, figure 6, as the lectotype of *Meekoceras disciforme*, whereas Krafft (1909) designated two other specimens as types of this species. This conflicts with the code of zoological nomenclature, which clearly indicates (article 74.2) that a lectotype must be chosen among the syntypes. The designation of Spath is therefore not valid.

***Ambites lilangensis* (Krafft, 1909)**

Pl. 12: 2-5; Pl. 13: 1-2; Figs. 22, 33

1909 *Meekoceras lilangense* nov. sp. Krafft *in* Krafft & Diener, p. 23-25, pl. 1: 1, 2 (lectotype), 3, 5-7.
non 1909 *Meekoceras lilangense* nov. sp. Krafft *in* Krafft & Diener, pl.14: 1-2.
1909 *Meekoceras lingtiense* nov. sp. Krafft *in* Krafft & Diener, p. 25-26, pl. 2: 1 (holotype).
1934 *Prionolobus lilangensis* – Spath, p. 101-102, pl. 4: 4.
1967 Prionolobus sp. cf. *P. lilangense* – Tozer, p. 18, 73.
1970 *Prionolobus lilangense* – Tozer, pl. 16: 6.
? 1976 *Prionolobus lilangensis* – Wang & He, p. 276, text-fig. 8b, pl. 3: 4-5.
p? 1976 *Gyronites evolvens* – Wang & He, p. 273-274, text-fig. 7c, pl. 3: 11-12.
p 1994 *Ambites fuliginatus* nov. sp. Tozer, p. 67, fig. 15a, pl. 13: 5, 7, pl. 14: 8 (holotype).
non p 1994 *Ambites fuliginatus* – Tozer, pl. 13: 4.
1996 *Lilangia lilangensis* – Waterhouse, p. 36, 60-61, text-fig. 7G, pl. 5: 2-7,9-10, pl. 6:1.
2011 *Ambites lilangensis* – Ware *et al.*, p. 164-165, figs. 4-5.

Occurrence. – Samples Nam100, Nam344, Nam345, Nam501 and Nam503 from Nammal Nala.
Description. –Involute (U/D ≈ 21%) and thick (W/H ≈ 54%, W/D ≈ 26%) discoidal to sub-platyconic shell with a broad tabulate venter, the venter representing about 50% of the whorl width. Coiling becoming more evolute with growth. Venter tabulate to slightly convex with strong bottleneck shaped edges. Flanks with maximum thickness at inner third of the whorl height on juvenile stage and at mid-flanks on sub-adult stage. Flanks slightly to strongly convex, showing occasionally two marked spiral ridges which impart the whorl section a compressed sub-octagonal shape. Umbilical wall vertical and high, with a sharp shoulder. Ornamentation varying from nearly absent to rather strong sigmoid folds following the trajectory of the growth lines and crossing the venter. Suture line with generally asymmetrical, broad and short lateral saddles bent towards the umbilicus. Ventral lobe narrow, with narrow lateral branches bearing a few (3 or 4) deep indentation at their base. Lateral lobes with a low rounded base bearing few rather strong indentations. Auxiliary series with irregularly spaced, relatively deep indentations, occasionally with a small and clearly individualised

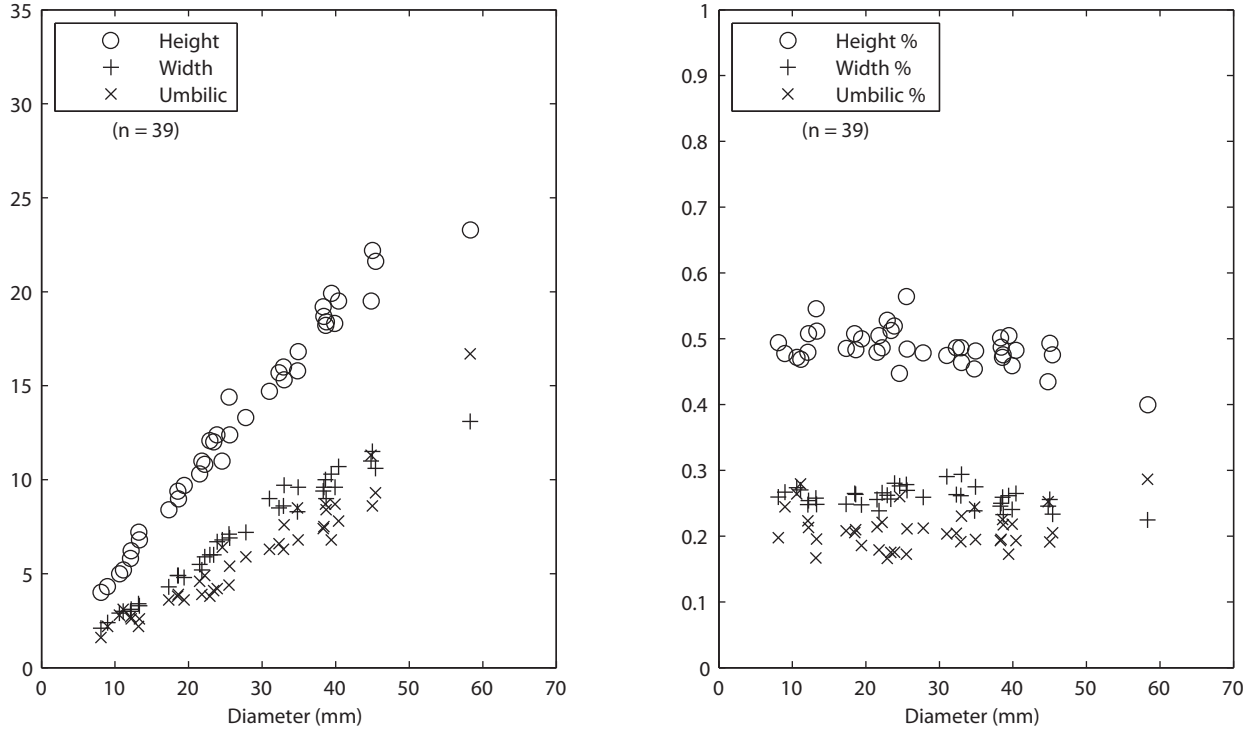

Fig. 33. Scatter diagrams of H, W, and U, and of H/D, W/D, and U/D for *Ambites lilangensis* (Krafft, 1909).

auxiliary lobe.
Measurements. – see Figs. 22, 33.
Discussion. – Because no large specimens of this species were found in the Salt Range, and because its type locality is in the Spiti Valley, no emended diagnosis is provided here. As discussed previously, this species closely resembles *Am. bojeseni*, from which it differs mainly by its suture line. Among the syntypes of *Am. lilangensis*, Krafft (in Krafft & Diener 1909) figured two specimens which do not match with our sample, both having a much thinner whorl section and one being much more evolute. These two specimens are here assigned to *Am. discus* (see above). As a consequence of this revised identification, their assumption that this species was found in five different layers within the "*Meekoceras* beds" of Lalung can be questioned. This species has been documented in a single RZ by us in the Salt Range. Krafft (in Krafft & Diener, 1909) distinguished *Me. lingtiense* from this species on the basis of its "delicate striæ, which cross the external part", which are "directly opposed to the concentric external striæ […] of *Me. lilangense*". The presence of these very delicate "concentric external striæ" is strongly influenced by the preservation. It is visible only when the shell is exceptionally well preserved, and has not been observed in our specimens, but this feature is most probably present in every species of *Ambites* and can therefore not be considered as diagnostic. The specimen figured by Wang & He (1976) is too poorly preserved to validate its identification. As previously mentioned, one of their specimens assigned to *Gy. evolvens* agrees in proportions with *Am. lilangensis*, but is also too poorly preserved for a reliable identification. Tozer (1967, 1970, 1994) initially ascribed some specimens from British Columbia to this species, but finally decided to erect a distinct species for these (*Am. fuliginatus*) on the basis of their "appreciably more conspicuous ribs and striae on the body chamber". It is shown here that this is part of the intraspecific variability of this species, and actually some specimens he did not illustrate (Ware, pers. obs., 2011) are strictly identical to ours. One of the specimens he ascribed to this new species (in Tozer 1994, pl. 13: 4) is distinctly more involute and thus may belong to the genus *Mullericeras* (see below). The specimens described by Waterhouse (1996) are reasonably well preserved and we agree with their assignment to *Am. lilangensis*. However, as already discussed, erecting the new genus *Lilangia* for this species is not justified in our view.

***Ambites bjerageri* sp. nov.**

Pl. 13: 4-9; Figs. 22, 34

v 2008 *Gyronites frequens* – Brühwiler *et al.*, p. 1168, pl. 5: 7-8.

Derivation of name. – Named after Dr. Morten Bjerager (Geological Survey of Denmark).
Holotype. – Specimen PIMUZ30351 (Pl. 13: 5).
Type locality. – Nammal, Salt Range, Pakistan.
Type horizon – Sample Nam100 (4 m above base of CM), *Ambites bjerageri* beds, middle Dienerian.
Diagnosis. – Small-sized sub-serpenticonic to

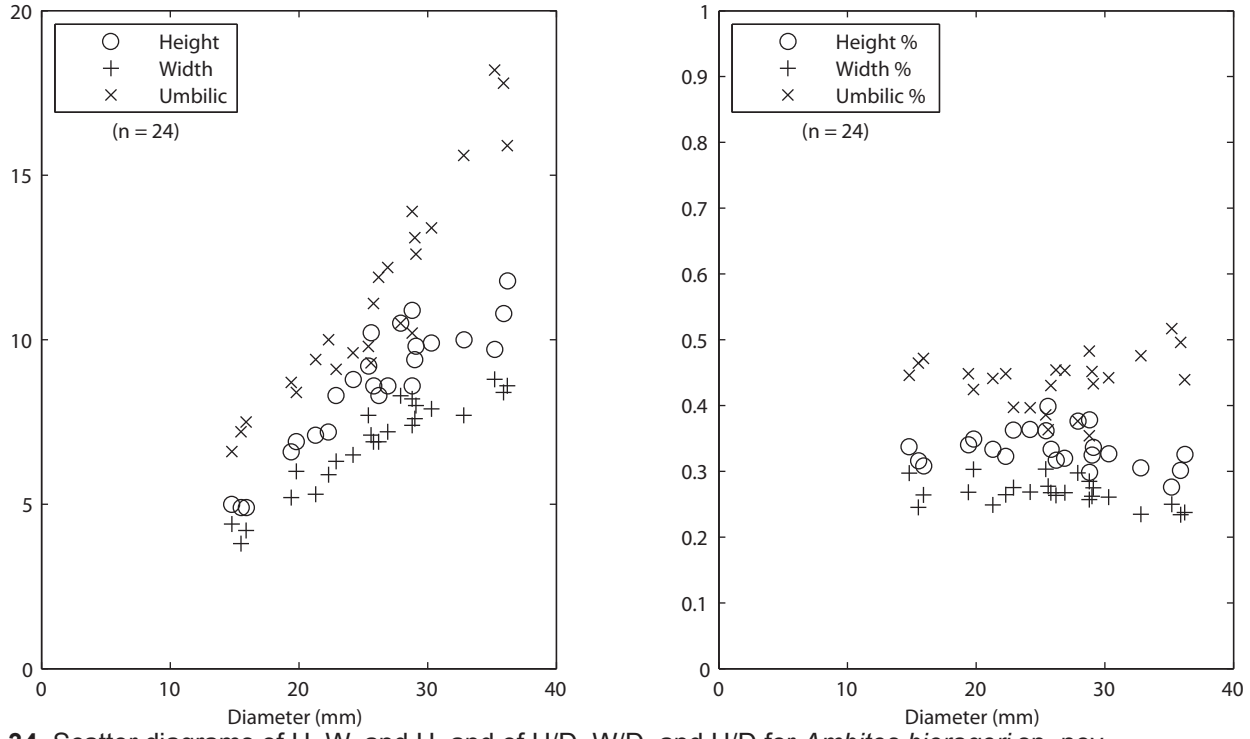

Fig. 34. Scatter diagrams of H, W, and U, and of H/D, W/D, and U/D for *Ambites bjerageri* sp. nov.

serpenticonic *Ambites* (maximal diameter estimated at ca. 45 mm).
Occurrence. – Samples Nam92, Nam100, Nam300, Nam344, Nam 501 and Nam503 from Nammal Nala.
Description. – Very evolute (U/D ≈ 44 %) sub-serpenticonic to serpenticonic shell with an almost isometric whorl section (W/H ≈ 80%, varying between 70 and 90%). Flanks very convex with maximum width at mid-flanks. The tabulate venter sometimes tends to disappear on adult specimens, and every intermediate exist between forms with a thick tabulate, bottleneck shaped venter, giving the whorl section a sub-rectangular shape, and forms without any clearly differentiated venter and a sub-rounded whorl-section. Umbilical wall undifferentiated on forms with a sub-rounded whorl-section, oblique to sub-vertical on forms with a sub-rectangular whorl-section, vaguely differentiated by a broadly rounded shoulder. Ornamentation almost absent, consisting of very weak, slightly sigmoid folds following the trajectory of the growth lines and two occasional very weak spiral ridges. Suture line simple with rounded lateral saddles. The branches of the ventral lobe are very thin, with two or three small indentations at their base. The two lateral lobes are of nearly equal size, with numerous small indentations at their base. The second lateral saddle is much larger than the others, the third lateral saddle is very small. Auxiliary series very short, with a few regularly spaced indentations.
Measurements. – see Figs. 22, 34.
Discussion. – With its sub-serpenticonic shape, this species clearly differs from all other species of *Ambites*. The presence of variants with a clear *Ambites* like whorl section (sub-rectangular with a clearly marked bottleneck shaped venter) indicates a clear affinity with *Ambites*. The specimens identified by Brühwiler *et al.* (2008) as *Gy. frequens* are clearly identical to our specimens with a broad tabulate bottleneck shaped venter. Shigeta & Zakharov (2009) synonymised these specimens with *Gy. subdharmus* Kiparisova (1961), an assignment we do not endorse because *Gy. subdharmus* lacks the characteristic bottleneck shaped venter, includes variants with a strong ornamentation and has a simpler suture line with fewer indentations at the base of the lobes.

***Ambites* cf. *impressus* (Waagen, 1895)**

Pl. 13: 3; Fig. 22

? 1895 *Lecanites impressus* nov. sp. Waagen, p. 286-287, pl. 37: 7 (lectotype, here designated), 8.
? 1934 *Gyrolecanites impressus* – Spath, p.85-86, fig. 21 [cop. Waagen 1895].

Occurrence. – A single specimen from sample Nam344 from Nammal Nala.
Description. – Moderately evolute (U/D = 31.7 %) relatively thick (W/H = 66.2 %, W/D = 25.7%) discoidal shell. Strongly convex flanks with maximum whorl width at inner third. Umbilical wall high, sub-vertical, poorly individualised by a broadly rounded umbilical shoulder. Flanks nearly smooth, with very weak and slightly sigmoid folds. Suture line not visible.
Measurements. – see table 1 and Fig. 22.
Discussion. – This specimen has proportions which are exactly intermediate between the two co-occurring species of *Ambites* (*Am. bjerageri* and *Am. lilangensis*). It cannot be excluded that it represents an extreme variant of one of these two species. It closely resembles the two specimens ascribed to *Lecanites impressus* by Waagen (1895), whose intraspecific variability cannot be assessed. Waagen also indicated that the type specimens were heavily weathered, and still mostly embedded in the matrix, but that their goniatitic suture line was probably not entirely due to this weathering. However, Waagen clearly described its bottleneck shaped venter, which is clearly visible on his illustrations. This species therefore clearly belongs to the genus *Ambites*, and its supposed very simple goniatitic suture line without auxiliary series is most likely a preservation artefact.

Family Paranoritidae Spath, 1930

Type genus. – *Paranorites* Waagen, 1895.
Composition of the family. – *Paranorites* Waagen, 1895, *Koninckites* Waagen, 1895, *Vavilovites* Tozer, 1971, *Radioceras* Waterhouse, 1996, *Nanningites* Brayard & Bucher 2008, *Wailiceras* Brayard & Bucher 2008, *Urdyceras* Brayard & Bucher 2008, *Vercherites* Brühwiler *et al.*, 2010a, *Koiloceras* Brühwiler *et al.*, 2012, *Pashtunites* gen. nov., *Awanites* gen. nov.
Discussion. – Since its introduction and discussion by Spath (1930, 1934), this family has been considered as a synonym of Proptychitidae (e.g. Arkell *et al.*, 1957, Tozer, 1961, 1994, Brühwiler *et al.*, 2012). However, typical representative of the Proptychitidae, such as the genera *Proptychites*, *Pseudoproptychites*, *Bukkenites* or *Pseudaspidites* all have a broadly rounded venter without any distinct shoulder, inflated inner whorls, no spiral ridges on the flanks and a suture line with usually very deep lobes and elongated saddles, the saddles tending to be slightly phylloid and the lobes having numerous and deep denticulations extending on their lateral sides. In the Salt Range, a group of species which were previously assigned to this family do not show any of these characteristics of the suture line. They all have a tabulate or sub-tabulate venter at least in the inner whorls, compressed inner whorls, and the most robust specimens within each species have two or more spiral ridges on the flanks. They also all have a very similar suture line with moderately to very deep lobes and elongated saddles, the lobes having a few rather deep indentations restricted to their base, the

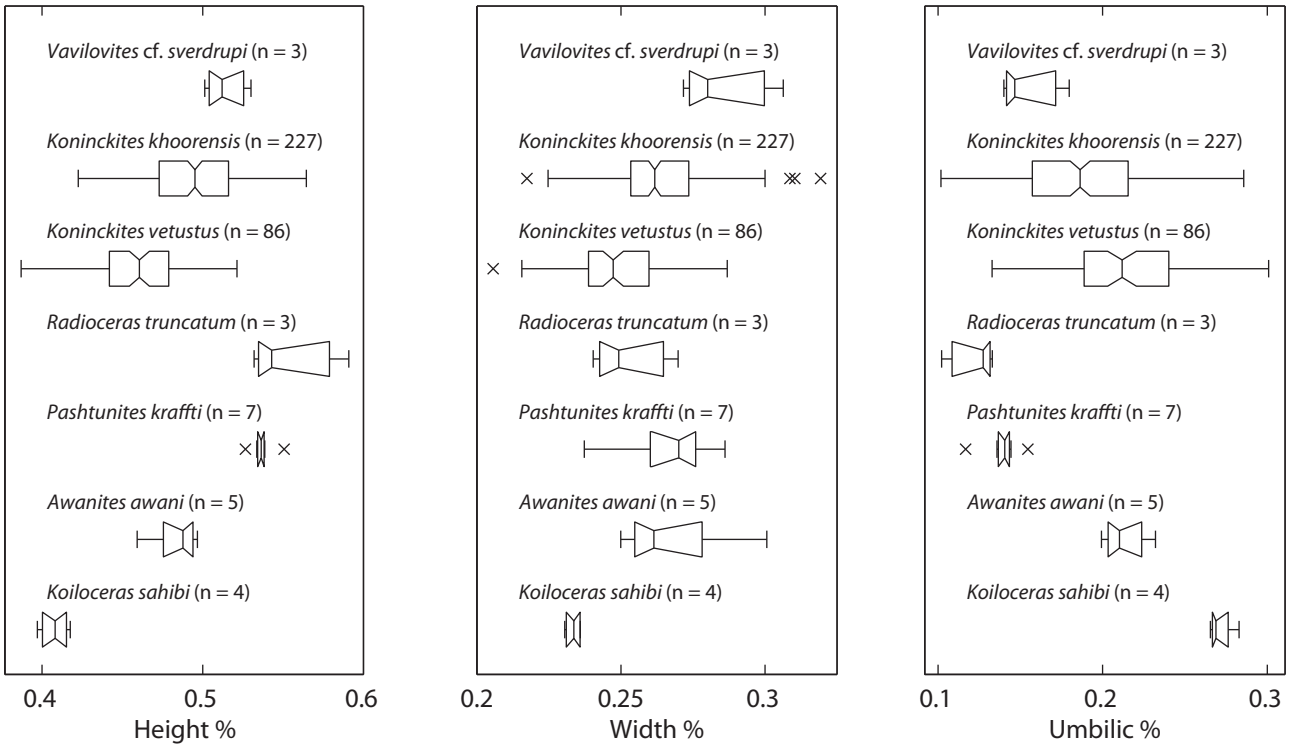

Fig. 35. Boxplots for the different species of Paranoritidae from the Dienerian of the Salt Range. The box plot displays the 25th, 50th (median) and 75th percentiles of the range of measures covered by 99% of the specimens from a normal distribution. Outliers represent specimens not falling within the normal distribution. Because of allometric growth, these were calculated only for specimens of 30 to 70 mm in diameter.

third lateral saddle being elongated, and a long auxiliary series with a poorly differentiated auxiliary lobe. These forms can therefore clearly be differentiated from Proptychitidae, as already noticed by Spath (1934) who created the family Paranoritidae to group them. Spath also suggested that these two families were closely related. This opinion was followed by the subsequent authors, who even considered them as synonyms. Spath (1934) based his opinion on the similarity between the suture lines of *Paranorites gigas* Waagen, 1895 and that of one specimen assigned to *Meekoceras markhami* (Diener, 1897) by Krafft *in* Krafft & Diener (1909). This last species is of uncertain affinity, so this similarity of suture line is not sufficient to demonstrate a phylogenetic link between the two families. On the other hand, some characteristics of Paranoritidae can also be found in Gyronitidae, such as the tabulate venter, spiral ridges on the flanks, a strigation on the ventro-lateral shoulders, and the compressed inner whorls. Moreover, the youngest species of *Ambites*, *Am. lilangensis*, has a more differentiated suture line than that of other members of the genus *Ambites*, with less numerous, deeper indentations on the lobes and sometimes an auxiliary lobe. Some specimens of *Am. lilangensis* lose their bottle-neck venter, their venter becoming then sub-tabulate, low arched with sharp ventro-lateral shoulders, as embodied by *Vavilovites*. Paranoritidae are therefore more likely to root within Gyronitidae, as suggested by *Vavilovites* which is an intermediate form between *Ambites* and *Koninckites*.

Genus *Vavilovites* Tozer, 1971

Type species. – *Paranorites sverdrupi* Tozer 1963.
Discussion. – The type species of this genus was originally placed in the genus *Paranorites*, within the family Paranoritidae. When Tozer erected *Vavilovites*, he also synonymised Paranoritidae with Proptychitidae. We already justified above that the two families should be kept separate, and that Paranoritidae is a derivative of Gyronitidae (a family which Tozer considered as a synonym of Meekoceratidae). We therefore here re-assign this genus to Paranoritidae and exclude it from Proptychitidae.

***Vavilovites* cf. *sverdrupi* (Tozer, 1963)**

Pl. 13: 10-13; Fig. 35

? 1963 *Paranorites sverdrupi* nov. sp. Tozer, p. 12-15, Pl: 4: 1, 2 (holotype), 3-6.
? 1967 *Paranorites sverdrupi* – Tozer, Pl: 4: 2.
? 1970 *Paranorites sverdrupi* – Tozer, Pl: 16: 7 (holotype).
? 1994 *Vavilovites sverdrupi* nov. gen. Tozer, p. 63, fig. 16A, Pl: 15: 1, 2 (holotype), 3; Pl. 20: 2.
? 1996 *Vavilovites tabulatus* nov. sp. Waterhouse, p. 74-75, Text-fig. 10C, pl. 8: 13-16, pl. 9: 1-3 (holotype), 4-6.
v 2011 *Vavilovites* sp. indet. – Ware *et al.*, p. 176-177,

fig. 19.

Occurrence. – Samples Nam316, Nam318 and Nam396 from Nammal Nala.
Description. –Involute (U/D ≈ 15.5 %) relatively thick (W/H ≈ 55.7 %, W/D ≈ 28.6%) discoidal shell with broad tabulate venter. Flanks nearly flat with maximum whorl width just before the umbilical wall, giving the whorl section a sub-trapezoidal outline. Umbilical wall high, vertical, individualised by a narrowly rounded umbilical shoulder. Flanks nearly smooth, with very weak sigmoid folds. Growth lines not visible. Suture line typical of Paranoritidae, with a clearly individualised auxiliary lobe, and a relatively large third lateral saddle.
Measurements. – see table 1 and Fig. 35.
Discussion. – Only four poorly preserved specimens belonging to this species have been found. The smallest (Pl. 13: 11) is slightly more evolute and has a thicker whorl section than the three other specimens. It has exactly the same morphology as the specimens described by Ware *et al.* (2011) as *Vavilovites* sp. indet. from Nevada. The difference between this specimen and the other three is here interpreted as intraspecific variability. Although Tozer (1994) based his species on a total of 63 specimens, he did not provide measurements for all of them nor any biometrical analyses concerning intraspecific variability and growth allometry. Moreover, the specimens for which he provides measurements are generally much larger (between 8 and 20 cm) than our specimens. It is therefore very difficult to estimate whether our specimens are conspecific with those of Tozer or not. The two smallest specimens measured by Tozer (1963) agree in proportions with our material.

Genus *Koninckites* Waagen, 1895

Type species. **–** *Koninckites vetustus* Waagen, 1895.
Composition of the genus. – *Koninckites vetustus* Waagen, 1895, *Proptychites khoorensis* Waagen, 1895.
Emended diagnosis. – Compressed platyconic to discoidal shells whose involution shows an important intraspecific variability, from moderately to very involute shells. Maximum diameter of ca. 15 cm, with a strong allometric growth. The innermost whorls (up to D ≈ 15 mm) are moderately to very evolute, with a moderately compressed whorl section, sometimes sub-serpenticonic. With further growth, the shell becomes more involute and compressed, reaching its maximal whorl compression at a diameter of ca. 15 mm and its maximal involution at a diameter of ca. 30 mm. Venter tabulate to well rounded, the innermost whorls of forms with a rounded venter being sub-tabulate. Umbilical wall varying from very oblique and concave to vertical, always well individualised by a clear angular umbilical shoulder. Ornamentation always weak, consisting of low sigmoid folds parallel to the growth lines and of two low spiral ridges on the flanks, nearly absent on the most involute forms. Sculpture fading away on adult body chamber. The juvenile ornamentation of the more evolute variants is more pronounced (following the first Buckman law of covariation) and variable, consisting usually of deep constrictions, more rarely of ribs and sometimes of a strigation on the flanks. Suture line typical of Paranoritidae with a poorly to well individualised auxiliary lobe, the auxiliary series being long on involute forms, short on evolute ones.
Occurrence. – Late Dienerian of the Salt Range (Pakistan), Central Himalayas (India, Nepal), Guangxi (China).
Discussion. – This genus has been used by many authors as a wastebasket taxon for every compressed, involute and tabulate species with a simple suture line with one individualised auxiliary lobe. We here redefine this genus on the basis of its type species and give it a more restricted and precise scope.

***Koninckites vetustus* Waagen, 1895**

Pl. 14: 1-13; Pl. 15: 1-6; Pl. 16: 1-5; Pl. 17: 1; Figs. 35-37

1895 *Koninckites vetustus* nov. gen. et sp. Waagen, p. 261-262, pl. 27: 4 (lectotype), ?5.
1895 *Prionolobus rotundatus* nov. gen. et sp. Waagen, p. 310, pl. 34: 1 (lectotype), 2, 3.
1905 *Prionolobus rotundatus* – Noetling, pl. 23: 1.
1909 Meekoceras waageni nov. sp. Diener *in* Krafft & Diener , p. 16.
1909 *Meekoceras smithii* nov. sp. Krafft *in* Krafft & Diener, p. 39, pl. 4: 1 (holotype).
1934 *Koninckites apertus* nov. sp. Koken *in* Spath, p. 154, pl. 11: 1 (holotype).
? 1996 *Koninckites apertus* – Waterhouse, p. 46-48, Text-fig. 4H, pl. 2: 9, 11, 13-15, pl. 9: 7-12.
v 2010a *Prionolobus rotundatus* – Brühwiler *et al.*, p. 728, fig. 6,7.

Emended diagnosis. – Moderately to very involute and discoidal *Koninckites* with a tabulate venter persisting until transition to mature body chamber. Flanks strongly convex, umbilical wall oblique, sometimes slightly concave.
Occurrence. – Samples Amb65 from Amb, Chi51 and Chi61 from Chiddru, Nam63, Nam71, Nam83, Nam101c, Nam305, Nam312, Nam347 and Nam349 from Nammal Nala, and WAR104 from Wargal.
Description. – Moderately to very involute compressed discoidal shells with a marked, although highly variable allometry. Following the evolute neanic stage (where U/D varies between 30 and 35%), the most involute variants show the same allometry as *Kon. khoorensis* (see below), becoming very involute and compressed up to a diameter of ca. 30 mm, reaching a relative umbilical width of ca. 15%, and then becoming gradually more

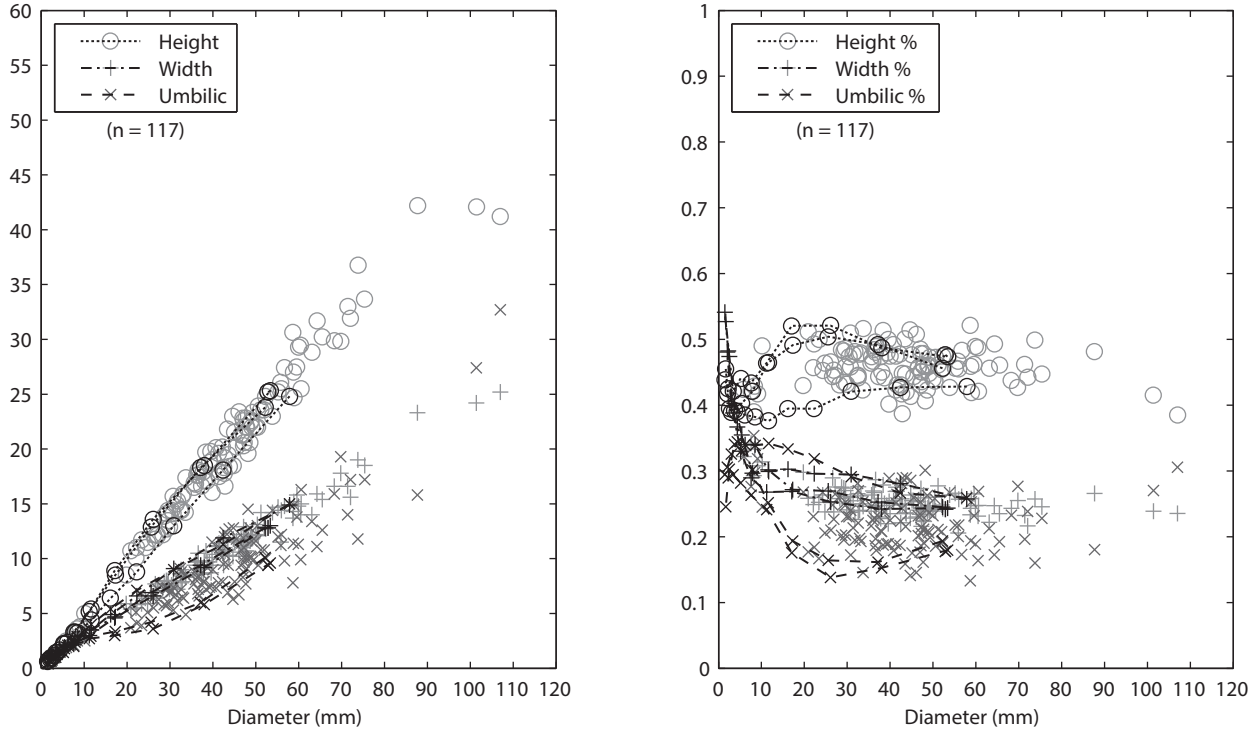

Fig. 36. Scatter diagrams of H, W, and U, and of H/D, W/D, and U/D for *Koninckites vetustus* Waagen, 1895. Ontogenetic trajectories obtained from sectioned specimen illustrated on Pl. 14: 11-13 are shown in black.

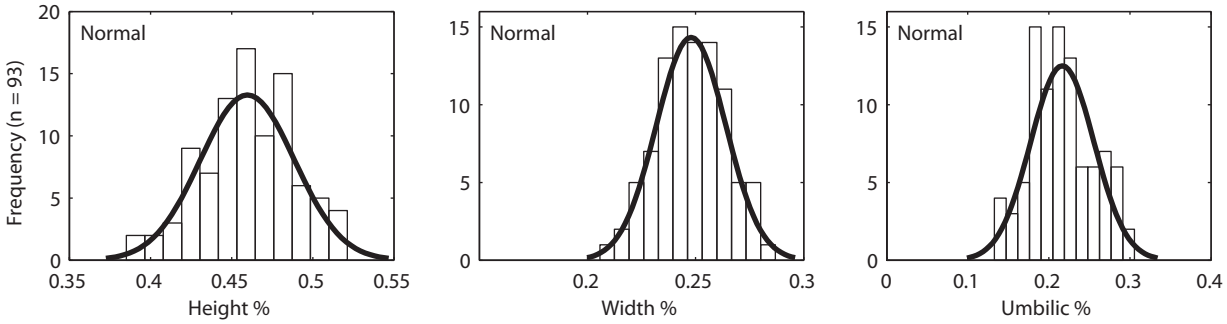

Fig. 37. Histograms of H/D, W/D, and U/D for *Koninckites vetustus* Waagen, 1895. Because of allometric growth, specimens smaller than 30 mm in diameter have been excluded.

evolute. Some involute variants show a strong egression of the mature body chamber. The involution of the most evolute variants increases slowly and steadily until maturity, where the relative umbilical width still amounts to as much as 25%. Both extremes have an equivalent whorl width (W/D between 25 and 30%) which they reach very early, at a diameter of ca. 20 mm. The venter becomes clearly tabulate with almost sharp ventro-lateral shoulders after the neanic stage (at a diameter of ca. 5 mm), and stays so until the beginning of the mature body chamber where the ventro-lateral shoulders become more rounded or even indistinct, the venter becoming then narrowly rounded. The flanks are strongly convex, with maximum width between inner third and mid-flanks. Umbilical wall oblique, sometimes slightly concave. It forms a very obtuse angle with the flanks, the umbilical shoulder being narrowly rounded on the outer shell, absent or nearly absent on the inner mould. It tends to disappear on the body chamber. On involute variants, the umbilical seam follows the umbilical shoulder of the preceding whorl, thus imparting the umbilicus a funnel shape. Innermost whorls with marked prorsiradiate constrictions which disappear at a diameter of ca. 10 mm. The ornamentation becomes then very weak, generally consisting of very low, thin sigmoid folds following the growth lines and one low spiral ridge at external third of the whorl height, more rarely a second spiral ridge at inner third of the whorl height. These two ridges then bracket the second lateral saddle as observed in the genus *Ambites*. Some very evolute specimens have low broad folds on their flanks. Suture line simple, with moderately deep lobes. Saddles with well rounded tips, sometimes slightly phylloid, the second lateral saddle being occasionally bent towards the umbilicus. Auxiliary series well developed, although shorter on evolute variants than on involute ones.

Auxiliary lobe usually well individualised, but sometimes differentiated from the rest of the auxiliary series only by its smaller and denser indentations.
Measurements. – see Figs. 35-37.
Discussion. – This species shows a very strong intraspecific variability, especially concerning its umbilical width, a pattern also shared with *Kon. khoorensis*. This strong variability led previous authors to assign them to different species, genera and even families. The type species of *Koninckites*, *Kon. vetustus*, is mostly based on one, rather poorly preserved specimen from Chiddru, of which a photography is here included (Pl. 15: 1). The original drawing of Waagen is thus a reconstitution of this specimen. Waagen originally described it as having a well rounded venter. However, the photography shows that the venter is actually sub-tabulate near the beginning of the body chamber, a trait that Waagen apparently did not notice. The phragmocone is too damaged for its ventral shape to be clearly seen, but it can be expected to be tabulate. Waagen also did not notice an umbilical shoulder, but the umbilicus of the holotype is poorly preserved and only visible as an internal mould near the end of the body chamber, where this shoulder generally fades away. This specimen corresponds to an extreme, very involute and thick variant of *Kon. vetustus*. A nearly identical but well preserved specimen inclusive of the suture line is figured in Pl. 15: 3. The other specimen which Waagen assigned to this species is too fragmentary to be identified with certainty. The species *Prionolobus rotundatus* corresponds to the more typical variants of the species, rather involute and compressed with a funnel shaped umbilicus. This species was renamed *Meekoceras waageni* by Diener (*in* Krafft & Diener, 1909). *Kon. apertus* also corresponds to these typical variants. *Meekoceras smithii* corresponds to the most evolute variants. The specimens described by Waterhouse (1996) as *Kon. apertus* seem also to correspond to this species, but they are too poorly preserved for unambiguous identification. With its strongly oblique umbilical wall, very convex flanks and tabulate venter, *Kon. vetustus* can easily be distinguished from all other Paranoritidae.

***Koninckites khoorensis* (Waagen, 1895)**

Pl. 17: 2-13; Pl. 18: 1-18; Pl. 19: 1-5; Pl. 20: 1-5; Figs. 35, 38-40

1895 *Proptychites khoorensis* nov. gen. et sp. Waagen, p. 176-178, pl. 20: 4 (holotype).
1895 *Dinarites minutus* nov. sp. Waagen, p. 31-32, pl. 7a: 1 (lectotype), 2.
1895 *Proptychites undatus* nov. gen. et sp. Waagen, p. 180-182, pl. 24: 4 (holotype).
1895 *Meekoceras koninckianum* nov. gen. et sp. Waagen, p. 245-245, pl. 26: 6 (holotype).
1895 *Koninckites ovalis* nov. gen. et sp. Waagen, p. 262-263, pl. 28: 3 (lectotype), 4.
1905 *Aspidites declivis* – Noetling, pl. 22: 8.
non 1905 *Prionolobus undatus* – Noetling, pl. 25: 2.
1909 *Meekoceras tenuistriatum* nov. sp. Krafft *in* Krafft & Diener, p. 34, pl. 4: 3 (holotype).
?p 1909 *Meekoceras varaha* – Diener *in* Krafft & Diener,

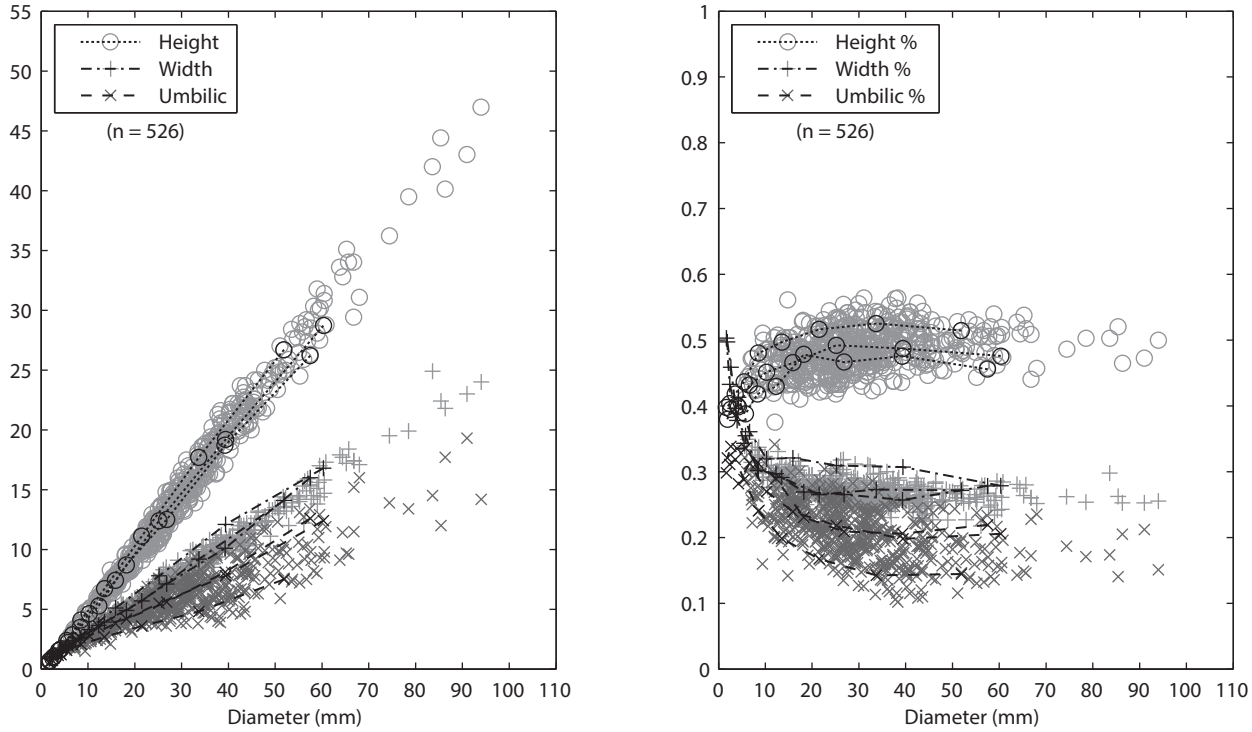

Fig. 38. Scatter diagrams of H, W, and U, and of H/D, W/D, and U/D for *Koninckites khoorensis* (Waagen, 1895). Ontogenetic trajectories obtained from sectioned specimen illustrated on Pl. 18: 10-12 are shown in black.

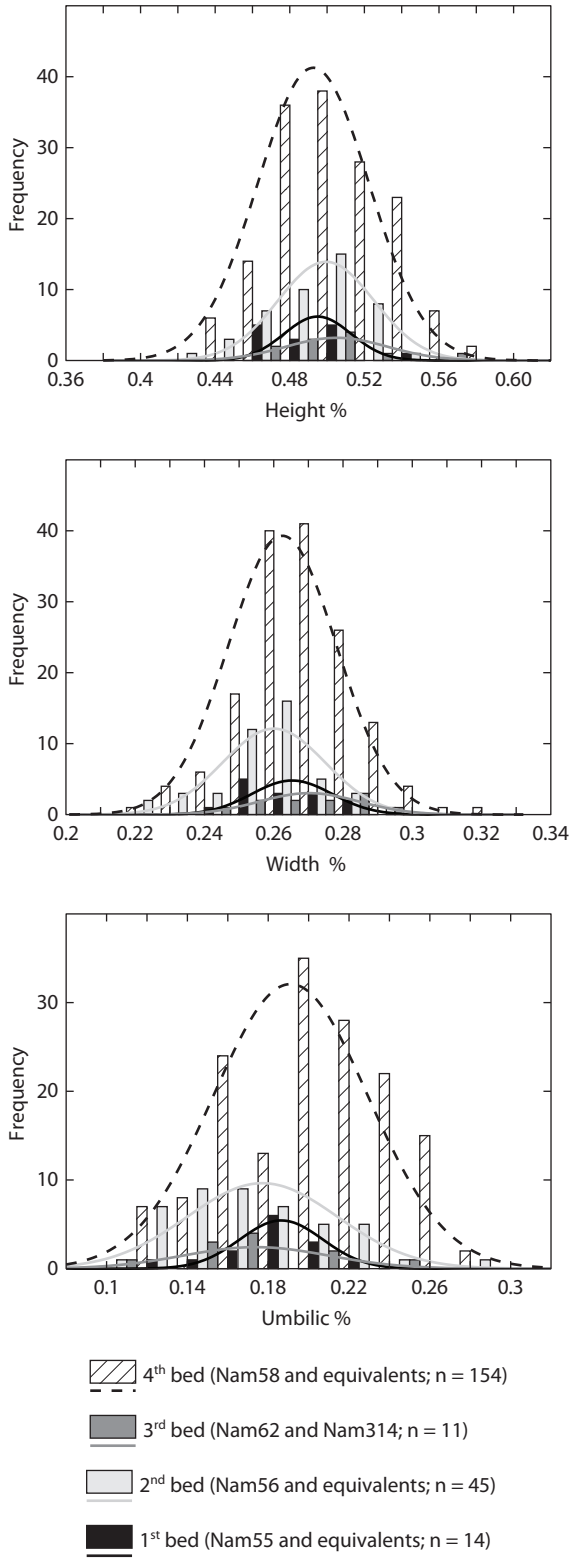

Fig. 39. Comparison between the histograms of H/D, W/D, and U/D for four samples of *Koninckites khoorensis* (Waagen, 1895) occurring in four successive beds at Nammal Nala. Because of allometric growth, only specimens of 30 to 70 mm in diameter were taken into account.

p. 17, Pl. 2: 2.
v 1978 *Proptychites khoorensis* – Guex, pl. 2: 3, 4, 6.
1996 *Prejuvenites angdawai* nov. gen. et sp. Waterhouse, p. 55-56, Text-fig. 7A, pl. 3: 5-9, 10 (holotype), 11-13.
1996 *Proptychites chuluensis* nov. sp. Waterhouse, p. 68-70, Text-fig. 11E, pl. 7: 7, 8 (holotype).
v 2008 *Proptychites* sp. indet. – Brühwiler *et al.*, p. 1164, pl.2: 3-5

Emended diagnosis. – *Koninckites* whose venter becomes well rounded early in ontogeny (at a diameter of ca. 30 mm). Umbilical wall oblique and concave to vertical. Thin, slightly sinuous to radial lirae appear at a diameter of ca. 20 mm.
Occurrence. – Samples Amb3 and Amb64 from Amb, Chi105 from Chiddru, Nam55, Nam56, Nam58, Nam59, Nam61, Nam62, Nam67, Nam101d, Nam130, Nam304, Nam313, Nam314, Nam315, Nam318, Nam319, Nam336, Nam337, Nam346, Nam395, Nam499, Nam502, Nam504, Nam537, Nam721, Nam724 and Nam727 from Nammal Nala.
Description. – Moderately to very involute, discoidal to platyconic shell with a strong allometry and a broadly rounded venter. At the end of the neanic stage (i.e. at D ≈ 5 mm), shells are evolute discoidal (U/D ≈ 35 %), with a rounded whorl section (W/H ≈ 100 %) and prorsiradiate deep constrictions (4 or 5 per whorl) which generally cross the venter. Between 5 and ca. 25 mm, the involution and compression of the shell increase rapidly, the venter becomes sub-tabulate with narrowly rounded ventro-lateral shoulders, the umbilical wall starts to differentiate, the constrictions become more abundant and shallower, and strigation appears. The strength of this allometric growth and change in morphology is very variable, so the intraspecific variability is maximal in these juvenile forms: U/D varies from 15 to 30 % and W/H from 50 to 70 %. The ornamentation is also very variable and follows Buckman's first law of covariation. The most evolute variants usually have a slightly compressed oval whorl section and numerous deep constrictions crossing the venter. The majority have a moderately compressed (W/H ≈ 60 %) sub-trapezoidal whorl section, the constrictions becoming shallower and fading on the venter. The most involute variants have a compressed whorl section with sub-parallel flanks and no constriction. The strigation varies independently of the whorl section shape. It can be very weak, visible only on the shell and restricted to the venter, or very strong, visible both on the shell and the inner mould, and present also on the flanks. At a diameter of ca. 20 mm, sigmoid lirae appear, and on specimens with a strong strigation it gives the outer shell a reticulated aspect. For diameters larger than ca. 25mm, the proportions of the shell stay nearly constant, the umbilicus sometimes becomes a little broader, and the ornamentation changes. The broad folds disappear, a spiral ridge situated at the

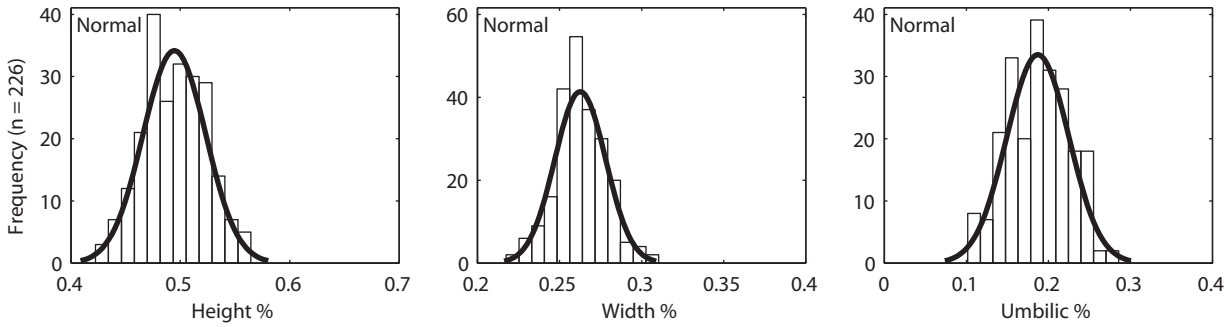

Fig. 40. Histograms of H/D, W/D, and U/D for *Koninckites khoorensis* (Waagen, 1895). Because of allometric growth, only specimens of 30 to 70 mm in diameter were taken into account.

external third of flank appears, along with an occasional second one emerging at the inner third of flank. These two ridges then bracket the second lateral saddle. The venter usually changes into a rounded outline. However, a few specimens show very weak ventro-lateral shoulders that may persist with further growth. The umbilical wall becomes clearly individualised by a sharp shoulder, and varies from oblique and slightly concave to vertical, independently of the shell proportions. The strigation tends to disappear on the flanks, but 2 to 4 spiral lines remain at a position homologous to that of the ventro-lateral shoulders. On some specimens, the constrictions are replaced by faint sigmoid folds, emphasised by stronger lirae. The lirae become straight on the involute, sub-platyconic variants. At the sub-adult or adult stage, the general morphology of the shells varies from moderately involute (U/D ≈ 25%) with convex flanks and a maximum width at the inner third of the flank, to very involute (U/D ≈ 15%). On very involute forms, the flanks can be convex with maximal width at inner third, or sub-parallel with maximal width at the umbilical shoulder. The inner third of the flank is generally very flat, sometimes even very slightly concave. Suture line typical of the genus, the auxiliary lobe being clearly individualised even at small size (for D ≈ 15 mm), with deep lobes. Lobes deeper and auxiliary series longer on involute specimens than on evolute ones.

Measurements. – see tables 2, 3 and Figs. 35, 38-40.

Discussion. – More than 500 specimens of this species have been measured for biometrical analyses, the vast majority coming from four consecutive beds in Nammal. The very important intraspecific variability of this species, and especially of its umbilicus size, may actually be increased by the presence of *in vivo* encrusting bivalves in the umbilicus. A vast majority of involute specimens larger than 3 cm in diameter are carrying such epibionts. Hence, measurements of U may be influenced by such noise and absence of unaffected specimens prevents quantifying this effect. The first step of this study is to check if the samples display a normal distribution for the measured characters. To avoid biases linked with allometry, only specimens between 30 and 70 mm of diameter were taken into account. A Lilliefors test was performed. The results of this univariate study are summarised on table 2. The corresponding histograms are shown in Fig. 39. The null hypothesis (the population is normally distributed) could be rejected only in one case. For the third bed, the relative whorl width does not follow a normal distribution ($p = 0.039$). However, only 11 specimens with a diameter comprised between 30 and 70 mm from this bed could be measured, making this result a not very robust one. It is likely that a larger sample from this bed would modify this result. The second step is to compare the different beds. The results of the One-way ANOVA and Kruskal-Wallis tests (PAST, Hammer *et al.*, 2001; see table 3) show that for all three parameters, the specimens from the four different beds come from a uniform population. Pairwise comparisons show that all beds have the same mean and median, with only one exception, the population from the second bed. These specimens have a median relative umbilicus width which is significantly different from those of the fourth bed (Mann-Whitney $p = 0.024$). As these two beds are the ones with the maximum number of specimens, this result is *a priori* robust, with a median of U/D of 17 % for the second bed, and of 19.2 % for the fourth bed. However, the range of variation of the two samples is nearly the same, and a difference of 2.2 % in the umbilicus relative width is not very significant from a taxonomical point of view. The interpretation is that both populations represent the same species (i.e. every variant of this species can be found in both beds), but involute forms are more abundant in the second bed than in the fourth bed. A visual examination showed that all the variability of the ornamentation, of the whorl section and of the suture line can be found in the four samples. As a consequence, all these populations are interpreted to represent a single species. Histograms for the pooled samples (between 30 and 70 mm of diameter), including the few specimens from Amb and Chiddru (Fig. 40), show that the resulting distributions are normal.

Inclusion of this species in the genus *Koninckites* may seem odd at first sight. The well rounded venter of adult forms led previous authors to include it in the genus *Proptychites*. However, this species shows all the

	bed	N	Mean	Median	Minimum	Maximum	Standard deviation	Lilliefors test (p)
H/D	1st bed	14	0.495	0.495	0.472	0.543	0.019	0.429
	2nd bed	45	0.499	0.506	0.422	0.543	0.026	0.058
	3rd bed	11	0.505	0.508	0.465	0.563	0.029	0.860
	4th bed	154	0.493	0.491	0.429	0.565	0.030	0.276
W/D	1st bed	14	0.265	0.266	0.249	0.285	0.012	0.086
	2nd bed	45	0.260	0.260	0.227	0.298	0.015	0.156
	3rd bed	11	0.270	0.279	0.243	0.291	0.015	0.039
	4th bed	154	0.262	0.262	0.217	0.310	0.016	0.675
U/D	1st bed	14	0.186	0.191	0.139	0.220	0.021	0.238
	2nd bed	45	0.177	0.170	0.115	0.286	0.038	0.193
	3rd bed	11	0.174	0.163	0.106	0.247	0.038	0.187
	4th bed	154	0.191	0.192	0.102	0.278	0.038	0.157

Table 2. Univariate statistics of H/D, W/D and U/D for each population of *Koninckites khoorensis* (Waagen, 1895) occurring in four successive beds at Nammal Nala. Due to problems of growth allometries, only specimens of 30 to 70 mm in diameter were taken into account for this analysis. D, Diameter; H, whorl height; W, whorl width; U, umbilical diameter.

	Comparison between beds	One-way ANOVA		Kruskal-Wallis	
		(p)	Tukey (p)	(p)	Mann-Whitney (p)
H/D	1st bed vs 2nd bed	0.322	0.957	0.223	0.269
	1st bed vs 3rd bed		0.654		0.366
	1st bed vs 4th bed		0.994		0.701
	2nd bed vs 3rd bed		0.916		0.821
	2nd bed vs 4th bed		0.869		0.084
	3rd bed vs 4th bed		0.488		0.200
W/D	1st bed vs 2nd bed	0.224	0.690	0.235	0.350
	1st bed vs 3rd bed		0.720		0.366
	1st bed vs 4th bed		0.938		0.537
	2nd bed vs 3rd bed		0.138		0.058
	2nd bed vs 4th bed		0.955		0.423
	3rd bed vs 4th bed		0.360		0.089
U/D	1st bed vs 2nd bed	0.101	0.851	0.079	0.243
	1st bed vs 3rd bed		0.698		0.218
	1st bed vs 4th bed		0.979		0.489
	2nd bed vs 3rd bed		0.993		0.984
	2nd bed vs 4th bed		0.623		0.024
	3rd bed vs 4th bed		0.447		0.163

Table 3. Comparison with statistical tests of H/D, W/D and U/D between the four populations of *Koninckites khoorensis* (Waagen, 1895) occurring in four successive beds at Nammal Nala. Due to problems of growth allometries, only specimens of 30 to 70 mm in diameter were taken into account for this analysis. D, Diameter; H, whorl height; W, whorl width; U, umbilical diameter.

diagnostic traits listed above as typical for *Koninckites*. The most important similarity between this species and the type species of *Koninckites* (*Kon. vetustus*) are the ontogenetic trajectories of the two species, which are strictly identical until the adult stage, where *Kon. vetustus* shows a greater umbilical egression than *Kon. khoorensis*. Moreover, evolute variants of *Kon. khoorensis* with an oblique umbilical wall are nearly identical to evolute thick variants of *Kon. vetustus*. They differ only by their venter (rounded on *Kon. khoorensis*) and the presence of radial lirae on *Kon. khoorensis*. Both show a similarly wide range of variation, this range and the median being slightly shifted towards more evolute, more compressed forms in *Kon. vetustus* than in *Kon. khoorensis* (see Fig. 35). The innermost whorls (from 5 to 20 mm in diameter) of the two species are nearly identical, the only difference being the venter, which is clearly tabulate in *Kon. vetustus*, whereas it is sub-tabulate in *Kon. khoorensis*. The suture lines of the two species are nearly identical. Considering the similarities

of ontogeny, suture line and intraspecific variability, we decided to assign the two species to the same genus. The rounded venter of adults and sub-adults *Kon. khoorensis* is here interpreted as a convergence towards the genus *Proptychites*, from which they differ by their simpler suture line, their ontogeny, their ornamentation and their clearly differentiated umbilical wall. This species also resembles the co-occuring *Ki. davidsonianus*, from which it differs by its more complex suture line, its ontogeny, its wider umbilicus and, when present, its stronger ornamentation.

The very different morphology of the juveniles compared with that of the adults of this species confused several authors who assigned the juveniles to different families or even superfamilies than the adults. This is the case for *Dinarites minutus* Waagen, 1895 and *Prejuvenites angdawai* Waterhouse, 1996. As a consequence, the genus *Prejuvenites* Waterhouse, 1996, based on these specimens, is here synonymised with *Koninckites*. Waagen (1895) described five species which can be synonymised. As he was the first to describe these forms, we have to choose one of these five names. We here choose to keep the species name *Kon. khoorensis* because this name corresponds to the first described adult or sub-adult specimen in Waagen's work and because it is the only name which has been used by subsequent authors. *Proptychites khoorensis* Waagen, 1895 (both in the original paper and in Guex, 1978), *Aspidites declivis* (in Noetling, 1905) and *Meekoceras tenuistriatum* Krafft, 1909 correspond to involute variants of this species. *Proptychites undatus* Waagen, 1895, *Meekoceras koninckianum* Waagen, 1895 and *Koninckites ovalis* Waagen, 1895 correspond to evolute variants. *Proptychites chuluensis* Waterhouse, 1996 corresponds to an intermediate variant. *Proptychites* sp. indet. (in Brühwiler *et al.*, 2008) corresponds to small, sub-adult specimens of this species. One specimen identified by Diener (*in* Krafft & Diener, 1909, Pl: 2: 2) as *Meekoceras varaha*, which is clearly pathologic with an irregularly shaped umbilicus and outline, seems to have lirae as in the specimens here described. It may correspond to an involute, pathologic variant of *Kon. khoorensis*, but no lateral view is illustrated, thus preventing any firm assignment of this specimen.

Genus *Radioceras* Waterhouse, 1996

Type species. – *Meekoceras radiosum* Waagen 1895.

Emended diagnosis. – Compressed and involute shell with tabulate venter, showing a strong allometry during growth. Inner whorls (up to ca. 5 cm) very involute, with nearly flat flanks and angular ventro-lateral and umbilical shoulders imparting the whorl section a compressed trapezoidal outline, with umbilical wall vertical to overhanging. Subsequent whorls more evolute, with more convex flanks and less angular whorl section. Suture line typical of Paranoritidae with one slightly differentiated auxiliary lobe.

Discussion. – Waterhouse (1996) created this genus for several small involute, compressed tabulate forms with a vertical umbilical wall and a suture line with a differentiated auxiliary series. The suture line of this genus is actually diagnostic of Paranoritidae. As already been shown by Brühwiler *et al.* (2010a, 2012), it can actually reach a large size (more than 15 cm) with a strong allometric growth. The diagnosis provided by Waterhouse is therefore incomplete. This genus is closely related to the genus *Koninckites*, from which it differs by its more involute shape in sub-adult specimens, and its more angular whorl section. The species *Meekoceras timorense* Wanner, 1911, which was included in the genus *Koninckites* by Spath (1934) and in the genus *Clypeoceras* by Shigeta & Zakharov (2009), most probably belongs to this genus.

***Radioceras truncatum* (Spath, 1934)**

Pl. 21: 1-2; Figs. 35, 41

1895 *Koninckites davidsonianus* nov. gen. Waagen, p. 272-273, pl. 33: 4.
? 1897 *Meekoceras (Kingites) varaha* – Diener, p. 143-144, Pl. 6: 2, Pl. 7: 6.
1934 *Koninckites truncatus* nov. sp. Spath, p. 152-153, figs. 43c, 44 (holotype) [cop. *Koninckites davidsonianus* in Waagen 1895].
? 1996 *Radioceras truncatum* nov. gen. Waterhouse, p. 41, Text-fig. 4C, pl. 2: 1, 2.
v 2010a *?Radioceras* cf. *kraffti* – Brühwiler *et al.*, p. 728-729, fig. 8-9.
v 2012 *Radioceras* cf. *kraffti* – Brühwiler *et al.*, p. 53, figs 31Q-T, 33A-U, 34A-Z.

Emended Diagnosis. –Involute shell becoming more evolute at maturity. Whorl section sub-trapezoidal. Venter tabulate, with sharp shoulders on inner whorls becoming rounded on outer whorls. High vertical to overhanging umbilical wall with sharp shoulders on inner whorls, becoming less steep and less differentiated on outer whorls.

Occurrence. – Samples Nam350 from Nammal and War104 from Wargal.

Description. – Only a few small immature specimens of this species have been found in the late Dienerian. Innermost whorls (up to 2 cm in diameter) are very close to those of *Koninckites vetustus*, slightly more involute (U/D ≈ 24 %), with a tabulate venter, weakly convex convergent flanks and weak, slightly sinuous prorsiradiate constrictions. They rapidly become more involute (U/D ≈ 12 % for diameter between 3 and 4 cm), and compressed (W/D ≈ 25 %, W/H ≈ 46 %), and the flanks become nearly flat with maximal width at or slightly

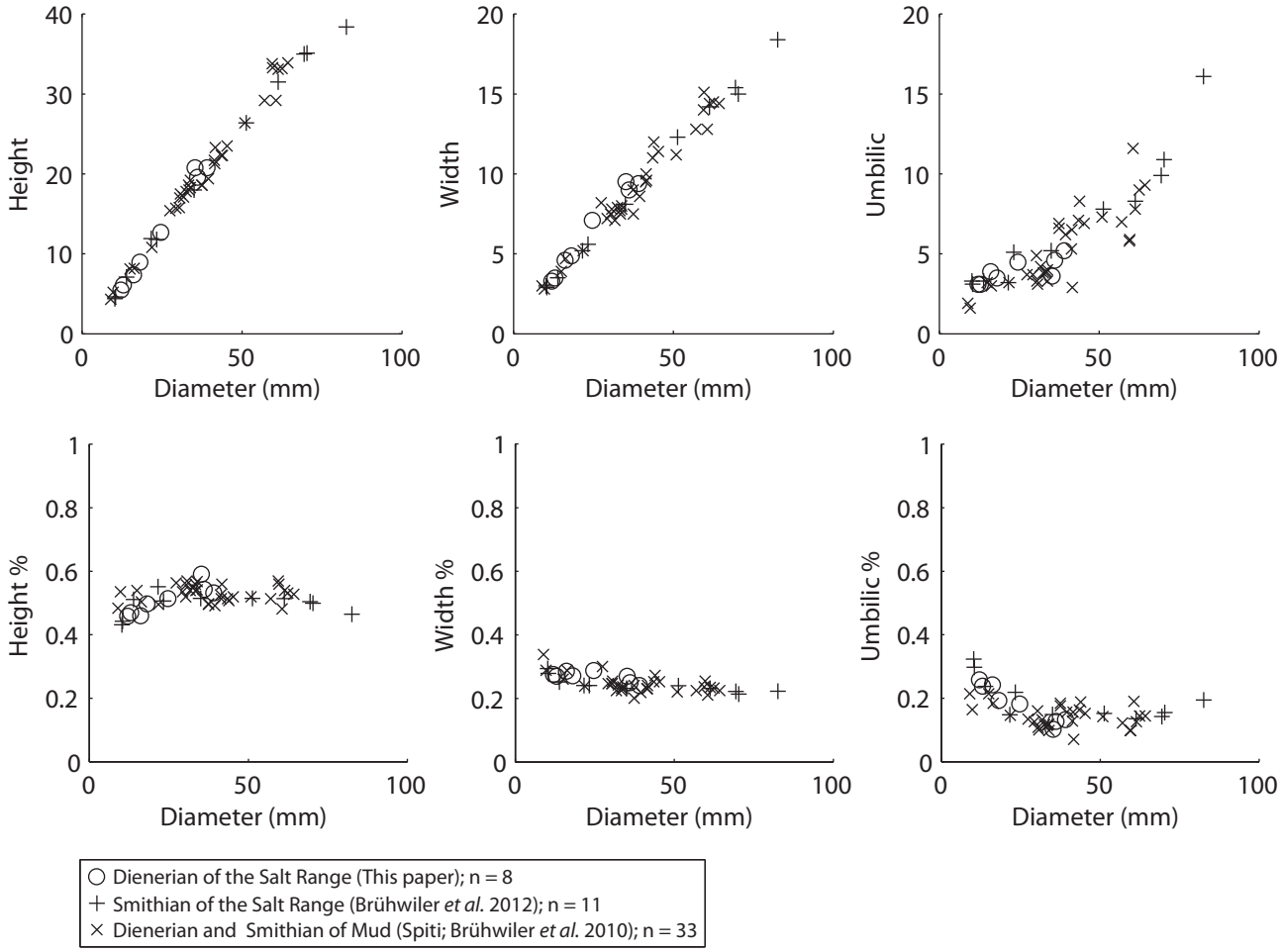

Fig. 41. Scatter diagrams of H, W, and U, and of H/D, W/D, and U/D for *Radioceras truncatum* (Spath, 1934) from the Dienerian of the Salt Range, with comparison with faunas from the Smithian of the Salt Range (data from Brühwiler *et al.*, 2012) and from the Dienerian and Smithian of Mud (Spiti Valley, India; data from Brühwiler *et al.*, 2010a).

above the umbilical shoulder, giving the whorl section a very elongated sub-trapezoidal shape. The umbilical wall is vertical to slightly overhanging, individualised by a sharp shoulder. Some specimens have very weak, slightly sinuous prorsiradiate folds, following the trajectory of the growth lines, which sometimes cross the venter. The only suture line which could be drawn here has slightly deeper lobes than the ones illustrated by Waagen (1895) and by Brühwiler *et al.* (2010a, 2012), which were in both case from larger specimens, but is otherwise very similar with a long auxiliary series and a weakly differentiated auxiliary lobe. According to the specimens described in Brühwiler *et al.* (2010a, 2012), adult specimens become more evolute, and the overall whorl section becomes less angular (ventro-lateral and umbilical shoulders become more rounded while the flanks become more convex, with a maximal width around inner third of whorl height), while the umbilical wall changes from vertical to slightly oblique.

Measurements. – see Figs. 35, 41.

Discussion. – Spath (1934) created this species for a specimen misidentified by Waagen (1895) as *Koninckites davidsonianus* (de Koninck, 1863). We agree with Waterhouse (1996) who placed this species in a new genus together with *R. radiosum* (Waagen 1895), a species from which it differs by its less differentiated suture line, its smaller adult size and the more angular whorl section of immature stages. However, the specimen assigned by Waterhouse to this species is too poorly preserved to be identified with certainty. The two specimens referred to as *Meekoceras (Kingites) varaha* by Diener (1897) agree in their proportions and suture line with the specimens described here. They seem to have a less angular whorl section, but are described by the author as having sharp shoulders, as in the present species. Their assignment to *R. truncatum* cannot be confirmed without examination of Diener's type material. The specimens from the Smithian of the Salt Range and from the Dienerian/Smithian boundary of Mud (Spiti valley, India) were previously ascribed to *Kon.* cf. *kraffti* (Spath, 1934). It is here shown that this latter species differs from *R. truncatum* by a smaller adult size, absence of umbilical egression, less angular whorl section with narrowly rounded ventro-lateral and umbilical shoulders, vertical to slightly oblique umbilical wall and more convex flanks, even at small size. These involute

tabulate Paranoritidae closely resemble some species included below in *Mullericeras*, especially *Mu. shigetai* sp. nov. and *Mu. indusense* sp. nov. The main difference between these two species and *R. truncatum* concerns the suture line. Species belonging to *Mullericeras* have a very wide ventral lobe, numerous small indentations at the base of the lobes and in the auxiliary series, generally without well differentiated auxiliary lobe. *R. truncatum* does not have the very wide lateral branches of the ventral lobe characteristic of *Mullericeras*, has fewer and larger indentations at the base of the lobes and in the auxiliary series, and a differentiated auxiliary lobe. *R. truncatum* also tends to have a thinner whorl section than *Mu. shigetai* and a smaller umbilicus than *Mu. indusense* for specimens smaller than 6 cm in diameter. This close resemblance is here interpreted as another example of convergence of two phylogenetically distant taxa towards the "meekoceratoid" morphology.

Genus *Pashtunites* gen. nov.

Derivation of name. – Named after the Pashtun people, a major ethnic group in Mianwali District.
Type species. – *Koninckites kraffti* Spath 1934.
Composition of the genus. – Type species only.
Diagnosis. – Involute, compressed tabulate paranoritid of small size with convex flanks, vertical umbilical wall and narrowly rounded ventro-lateral and umbilical shoulders.
Occurrence. – Late Dienerian of the Salt Range and of Spiti (India).
Discussion. – This genus is very close to *Radioceras*, but no specimens of large size have been found (the largest specimen found has a maximum estimated diameter of ca. 7 cm). Its umbilical wall is slightly oblique to vertical (never overhanging).Between 3 and 7 cm, the shell is slightly more evolute, has a slightly more inflated whorl section, more convex flanks and less angular whorl cross section (i.e. with narrowly rounded ventro-lateral and umbilical shoulders) than *Radioceras*.

***Pashtunites kraffti* (Spath, 1934)**

Pl. 21: 3-4; Figs. 35, 42

p 1909 *Meekoceras varaha* – Diener *in* Krafft & Diener, p. 17, Pl. 2: 4 (holotype of *Pa. kraffti* designated by Spath 1934).
non p *Meekoceras varaha* – Diener *in* Krafft & Diener, p. 17, Pl. 2: 2, 3, 5, 6.
1934 *Koninckites kraffti* nov. sp. Spath, p. 155-156, fig. 43c (holotype).
non v 2010a *?Radioceras* cf. *kraffti* – Brühwiler *et al.*, p. 728-729, fig. 8-9.
non v 2012 *Radioceras* cf. *kraffti* – Brühwiler *et al.*, p. 53, figs 31Q-T, 33A-U, 34A-Z.

Emended diagnosis. – As for the genus.
Occurrence. – Samples Amb65 from Amb and Nam63, Nam83 and Nam305 from Nammal.
Description. – Involute (U/D ≈ 15 %), moderately compressed (W/D ≈ 27 %, W/H ≈ 51 %), tabulate, small sized shell (maximum diameter estimated at ca. 7 cm) whose flanks are slightly convex with maximum width at

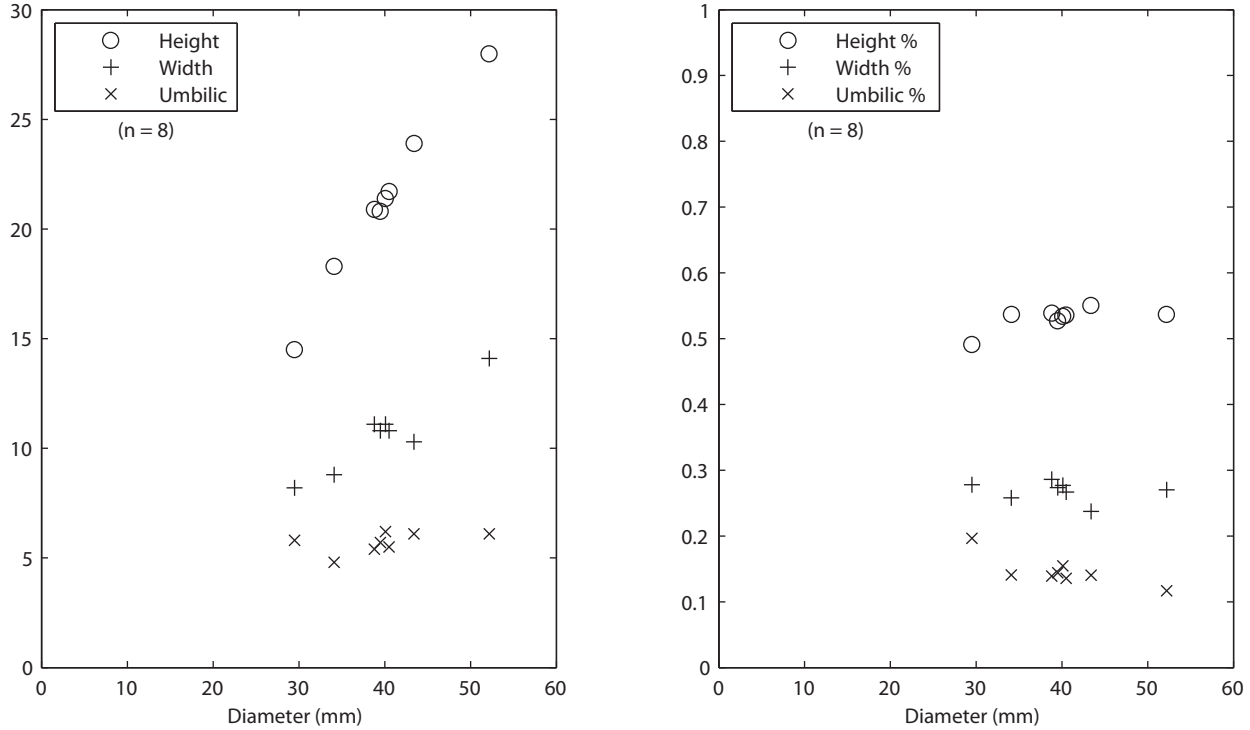

Fig. 42. Scatter diagrams of H, W, and U, and of H/D, W/D, and U/D for *Pashtunites kraffti* (Spath, 1934) gen. nov.

inner third. Venter tabulate, becoming slightly convex on the adult body chamber, with narrowly rounded ventro-lateral shoulders. Umbilical wall slightly oblique to vertical with rounded umbilical shoulder. Ornamentation absent except for weak folds on the inner third of the whorl, following the shape of the growth lines. Suture line typical of involute Paranoritidae with deep lobes having few deep indentations at their base, and a long auxiliary series with a poorly differentiated auxiliary lobe.

Measurements. – see Figs. 35, 42.

Discussion. – This species was created by Spath (1934) based on a series of specimens considered by Diener (*in* Krafft & Diener, 1909) as being conspecific and belonging to *Meekoceras varaha*. However, these specimens most probably belong to different species of different ages. The assignment of our specimens to this species is here only based on their comparison with the specimen figured by Krafft & Diener (1909, Pl. 2: 4) and designated by Spath as the holotype. As Spath (1934) agreed with Krafft & Diener (1909) that all the specimens they figured were conspecific, he based his diagnosis on all of them, not only on the holotype. His diagnosis is thus not valid and we provide here a more restrictive emended diagnosis.

Genus *Awanites* gen. nov.

Derivation of name. – Named after the Awan tribe, a tribe of the Salt Range in the Mianwali District.

Type species. – *Awanites awani* sp. nov.

Composition of the genus. – Type species only.

Diagnosis. – Moderately involute (U/D ≈ 21 %) and moderately compressed (W/D ≈ 27 %, W/H ≈ 55 %) paranoritid of small size (maximal diameter of ca. 55 mm) with a very angular sub-trapezoidal whorl cross section (i.e. with very sharp ventro-lateral and umbilical shoulders), thick tabulate venter and slightly overhanging umbilical wall. Suture line with a wide third lateral saddle and a short auxiliary series with a very small and poorly differentiated auxiliary lobe.

Occurrence. – Latest Dienerian of Nammal Nala, Salt Range.

Discussion. – The umbilical part of the suture line of this new genus is slightly different from that of other paranoritids, so its assignment to this family is arguable. However, it has a poorly differentiated auxiliary lobe (although small), and the lateral and ventral part of the suture line agree with the other genera belonging to this family. Moreover, the suture line could only be drawn from one specimen, so intraspecific variability could not be assessed. As previously discussed, the umbilical portion of the suture line is likely to show more variability than its lateral and ventral portion. The tabulate venter, the sharp umbilical shoulder and the occasional presence of low spiral ridges on the flanks agree with other representatives of Paranoritidae. With its very angular whorl section, it is similar to inner whorls of the genus *Radioceras*, but it is distinguished from these by its more evolute and inflated shape. Some robust variants have radial ribs identical with those of the younger and larger *Paranorites*.

***Awanites awani* gen. et sp. nov.**

Pl. 21: 5-7; Figs. 35, 43

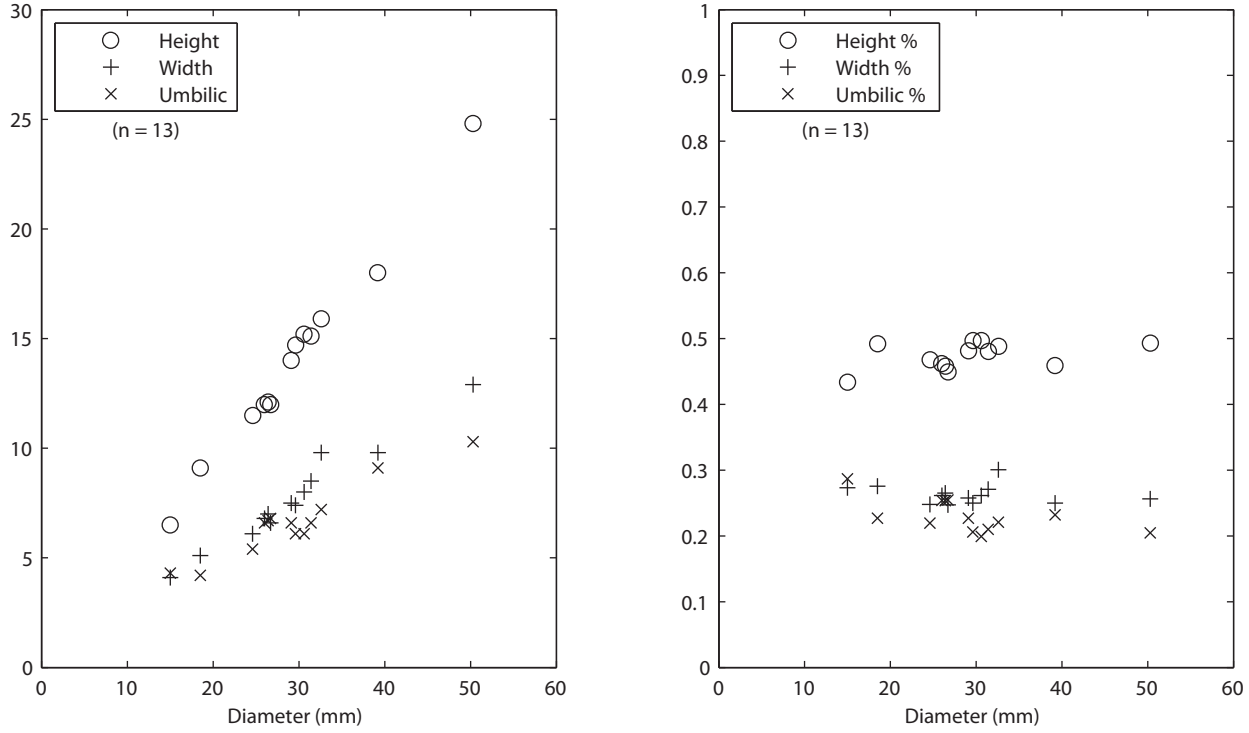

Fig. 43. Scatter diagrams of H, W, and U, and of H/D, W/D, and U/D for *Awanites awani* gen. et sp. nov.

Derivation of name. – As for the genus.
Holotype. – Specimen PIMUZ30422 (Pl. 21: 7).
Type locality. – Nammal Nala, Salt Range, Pakistan.
Type horizon. – Sample Nam350 (lower CM, ca. 4.5 m above base), *Awanites awani* beds, late Dienerian.
Diagnosis. – As for the genus.
Occurrence. – Sample Nam350 from Nammal.
Description. – Moderately involute (U/D ≈ 21 %) and moderately compressed (W/D ≈ 27 %, W/H ≈ 55 %) shell with broad tabulate venter bordered by sharp ventro-lateral shoulders. On inner whorls, flanks slightly convex with maximal width at inner third of whorl height. On the single large specimen available (the holotype, PIMUZ30422, Pl. 21: 7), a very shallow concavity appears on the body chamber between the umbilical shoulder and the point of maximal width. Umbilical wall slightly overhanging, joining the flank with an acute angle, thus forming a sharp umbilical shoulder. Flanks usually nearly smooth, with vague sigmoid folds following the shape of the growth lines and fading on the body chamber. Two weak spiral ridges are sometimes visible on the phragmocone around mid-flanks. One robust variant (specimen PIMUZ30420, Pl. 21: 5) has relatively strong radial ribs which do not cross the venter. Suture line with deep lateral lobes and few small indentations at their base, first lateral saddle elongated and slightly phylloid, second lateral saddle elongated and dorsally bent, third lateral saddle relatively broad, arched, and somewhat asymmetrical. Auxiliary series with three very small and closely spaced indentations, corresponding to the auxiliary lobe, followed by two larger and more distant indentations.
Measurements. – see Figs. 35, 43.
Discussion. – As for the genus.

Genus *Koiloceras* Brühwiler & Bucher, 2012

Type species. – *Koiloceras romanoi* Brühwiler *et al.*, 2012.
Discussion. – This genus was originally included in Gyronitidae. With our emended definition of this family, the suture line of this genus does not agree with that of gyronitids. The type species has a slightly differentiated auxiliary lobe, agreeing with our definition of Paranoritidae. Lobes are broader and saddles shallower than those of other members of Paranoritidae. Moreover, the specimens identified by Brühwiler *et al.* (2010a) as Gyronitidae gen. et sp. indet. A are probably conspecific with *Koi. romanoi*, and have a suture line which agrees with that of paranoritids. *Koiloceras* also shares with other paranoritids the mature egression of the umbilical suture and the transition from tabulate to rounded venter on adult body chamber. Therefore, assignment of this genus to Paranoritidae is more appropriate.

***Koiloceras sahibi* sp. nov.**

Pl. 21: 8-9; Figs. 35, 44

Derivation of name. – Named after Syed Mian Ali Sahib, founder of Mianwali.
Holotype. – Specimen PIMUZ30423 (Pl. 21: 8).
Type locality. – Chiddru, Salt Range, Pakistan.
Type horizon. – Sample Chi51 (topmost LCL), *Koninckites vetustus* beds, late Dienerian.

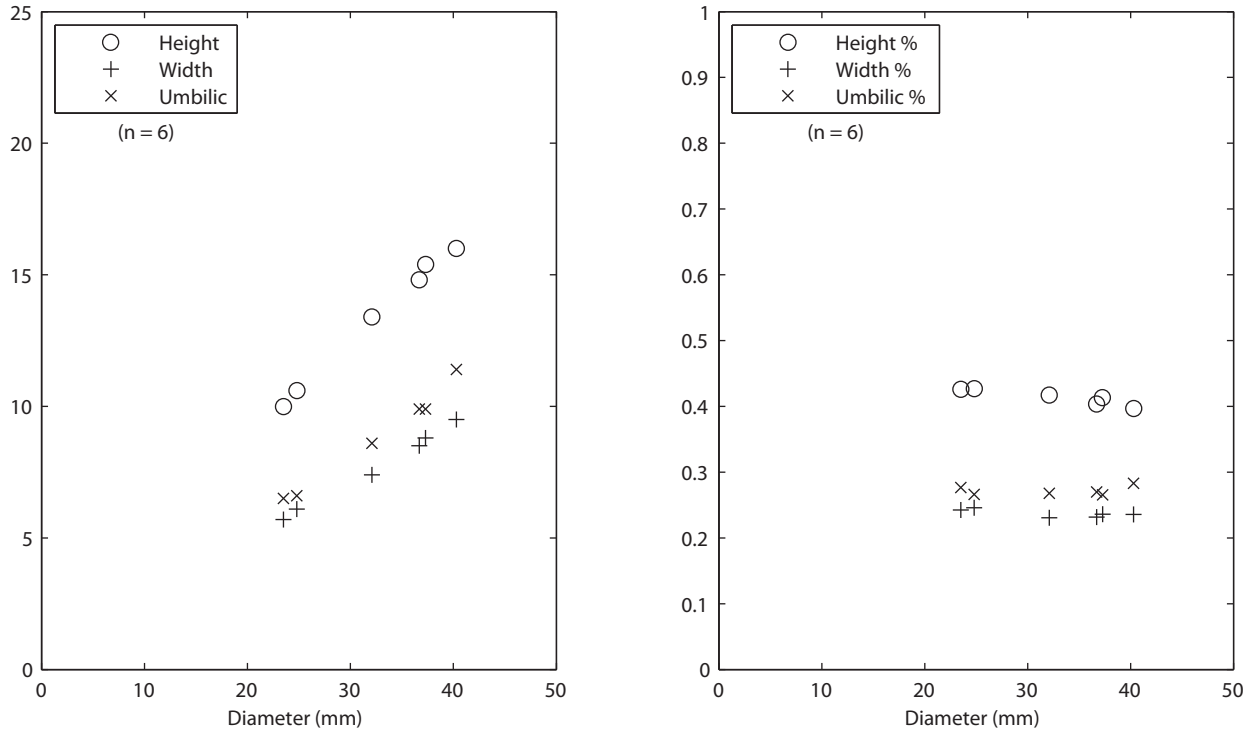

Fig. 44. Scatter diagrams of H, W, and U, and of H/D, W/D, and U/D for *Koiloceras sahibi* sp. nov.

Diagnosis. – *Koiloceras* with a relatively thick whorl section.
Occurrence. – Samples Chi51 from Chiddru and War104 from Wargal.
Description. – Moderately evolute (U/D ≈ 24 %) platyconic shell with a relatively thick whorl section (W/D ≈ 24 %, W/H ≈ 57 %). Venter tabulate with sharp ventro-lateral shoulders on inner whorls, becoming slightly arched with narrowly rounded shoulders on the last whorl. Maximum width at mid-flanks, the inner half of the flanks being slightly concave while its external half is convex. Umbilical wall not well differentiated, the flanks bending abruptly before the umbilical seam without forming any distinct shoulder. Flanks nearly smooth, with occasional vague broad folds following the shape of the growth lines and reaching their maximal strength at mid-flanks. Suture line too poorly preserved to be drawn or described in detail.
Measurements. – see Figs. 35, 44.
Discussion. – This new species differs from the type species by its slightly thicker whorl section (in *Koi. romanoi*, W/D ≈ 21 %, W/H ≈ 54 %). However, our specimens are smaller than the ones illustrated by Brühwiler *et al.* (2012), so this difference of only 3 % of the whorl width can well be the result of ontogenetic change and/or of intraspecific variability. However, we have too few specimens of this rare genus to test if this difference is significative and do not exclude that this new species may ultimately turn out as a junior synonym of the type species.

Family Flemingitidae Hyatt, 1900

Genus *Xenodiscoides* Spath, 1930

Type species. – *Xenodiscus perplicatus* Noetling, 1905.

***Xenodiscoides*? sp. indet.**

Pl. 21: 10

Occurrence. – A single specimen from sample Chi51 from Chiddru, topmost LCL, *Koninckites vetustus* beds.
Description. – Moderately evolute (U/D = 32 %) and compressed (W/D = 26 %, W/H = 65 %) sub-platyconic shell. Venter tabulate with sharp ventro-lateral shoulders. Flanks slightly convex with strong and slightly rursiradiate blunt ribs which fade before reaching the venter. Umbilical wall indistinct, the flanks bending abruptly before the umbilical seam without forming any clear shoulder. Suture line too poorly preserved for description.
Measurements. – see table 1.
Discussion. – This small specimen, with its coarse rursiradiate ribs and its tabulate venter, resembles the genus *Xenodiscoides*. Its rather compressed shape is quite close to *X. variocostatus* Brühwiler *et al.*, 2010a, but the very small size of this specimen precludes any further comparison with the much larger specimens of the type series. It is therefore placed here in open nomenclature.

Genus *Shamaraites* Shigeta & Zakharov, 2009

Type species. – *Anakashmirites shamarensis* Zakharov, 1968.

***Shamaraites*? sp. indet.**

Pl. 21: 11

Occurrence. – A single specimen from sample War104 from Wargal, lower third of CM, *Koninckites vetustus* beds.
Description. –Evolute (U/D = 40 %) sub-serpenticonic shell with a slightly compressed whorl section (W/D = 26 %, W/H = 70 %). Venter tabulate with sharp ventro-lateral shoulders. Flanks convex, with very vague broad radial folds. Umbilical wall not well differentiated, the flanks bending abruptly before the umbilical seam without forming any clear shoulder. Suture line too poorly preserved for description.
Measurements. – see table 1.
Discussion. – This very small specimen differs from coeval juvenile of *Kon. vetustus* by its more evolute coiling and the absence of any constriction. Its general shape is reminiscent of the Early Smithian genus *Shamaraites*, but its very small size precludes any direct comparison with the much larger specimens previously illustrated. It is therefore placed in open nomenclature.

Family Proptychitidae Waagen, 1895

Discussion. – According to Tozer (1994), Proptychitidae range from the late Griesbachian to the end of the Spathian. However, this family is in need of revision. Tozer had a very broad definition of this family, considering Paranoritidae as a synonym of Proptychitidae based on the presence of an auxiliary lobe. Proptychitidae have a highly discontinuous record in the Tethys, and many species and genera are based on single specimens whose stratigraphic position is not known precisely. They are more abundant in the Boreal Realm, where Tozer defined two zones with Proptychitidae: the *Bukkenites strigatus* zone in the Late Griesbachian and the *Proptychites candidus* zone in the Early Dienerian. Tozer (1994) also included the genus *Vavilovites* in this family, but we provide here new evidence that this genus belongs to Paranoritidae (see above). The different species from northern Siberia assigned to *Vavilovites* by Dagys &

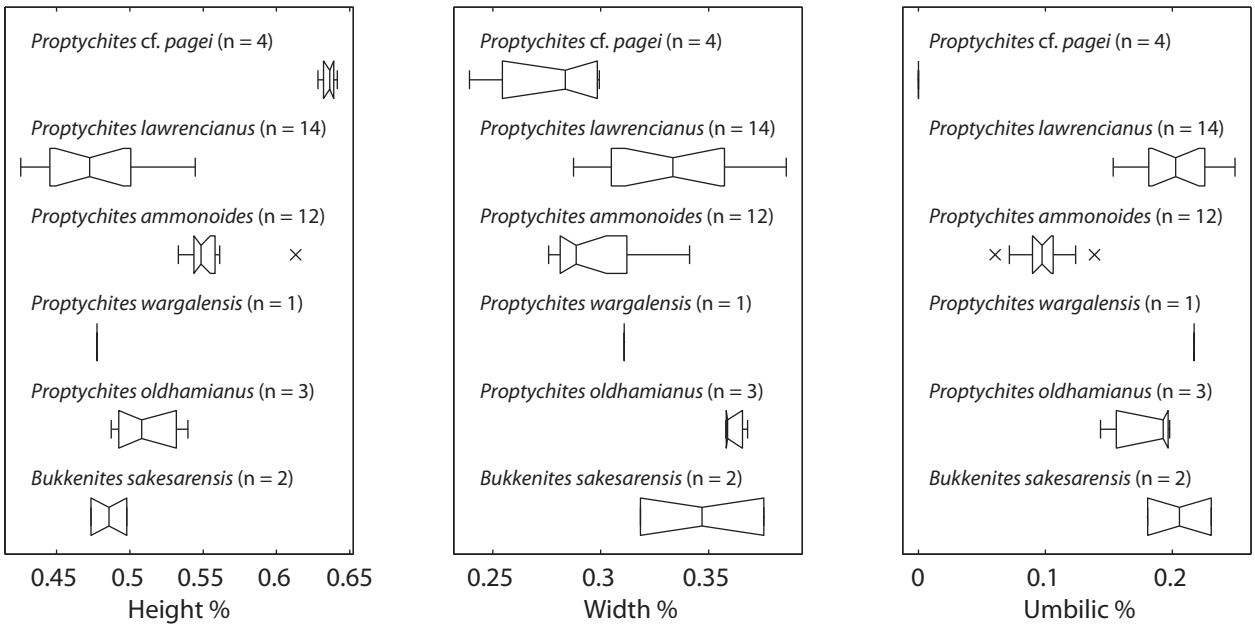

Fig. 45. Boxplots for the different species of Proptychitidae from the Dienerian of the Salt Range. The box plot displays the 25th, 50th (median) and 75th percentiles of the range of measures covered by 99% of the specimens from a normal distribution. Outliers represent specimens not falling within the normal distribution. Because of allometric growth, these boxplots were calculated without the specimens smaller than 30 mm in diameter.

Ermakova (1996) may, at least partially, represent a new genus, the affinity of which needs to be established. To provide a proper emended definition of this family, a broader view is necessary, including the Smithian and Spathian Proptychitidae. This is beyond the scope of the present paper, and although an emended diagnosis of its type genus *Proptychites* is provided, no emended diagnosis is proposed here for this family. Considering that Paranoritidae are not anymore considered as a synonym of this family, and are shown here to be not directly related to Proptychitidae, this family now exclusively comprises forms having a rounded venter. The origin and classification of this family also need to be re-investigated in detail. It is generally considered to be derived from involute Ophiceratidae (e.g. Arkell, 1957). However, the complex suture line of some Dienerian *Proptychites* is very close to that of *Otoceras*, differing only by the absence of a lobe dividing the third lateral saddle in two parts. These two genera also have inflated juvenile whorls, thus differing from the typically compressed juvenile whorls of Meekoceratacеae. These similarities suggest that Otoceratidae and Proptychitidae are closely related, and that Proptychitidae should thus be placed in the superfamily Otocarataceae and not in Meekoceratacеae. Such a change of classification would result in a very different picture for the Early Triassic recovery. Otoceratacеae would then no longer be short-term survivors, and Triassic ammonoids would then derive from two different Permian groups, not exclusively from Xenodiscidae. Considering the importance of such a change, this hypothesis would need further investigation to be properly tested, especially concerning the latest Otoceratidae and Griesbachian Proptychitidae, which are both absent in our sections. Hence, we provisionally follow the traditional classification, placing Proptychitidae in Meekoceratacеae. In the sections studied here, Proptychitidae are present only in the early and middle Dienerian, not in the late Dienerian, unless the genus *Kingites*, whose affinities remain unclear, belongs to Proptychitidae. Proptychitidae "reappear" in strata of early Smithian age (Brühwiler *et al.*, 2012). As a consequence, the morphological similarity between Dienerian and Smithian Proptychitidae cannot be excluded to be the result of a convergence, a hypothesis which cannot be tested here owing to the rarity of this family in the Salt Range, especially in the early Smithian.

Genus *Bukkenites* Tozer, 1994

Type species. – *Proptychites strigatus* Tozer 1961.

Discussion. – Tozer (1994) defined this genus mostly on its suture line, differing "from true *Proptychites* […] by lacking an auxiliary lobe". Although most of the species he included in this genus have a subtrigonal whorl section, Tozer did not regard this trait as being of generic significance, an opinion which is here followed. The shape of the ventral lobe is here also regarded as an important additional character. *Bukkenites* has a ventral lobe with narrow lateral branches that exhibit only a few small indentations at their base, whereas *Proptychites* has a ventral lobe with wide lateral branches with deep indentations at their base.

***Bukkenites sakesarensis* sp. nov.**

Pl. 21: 12-13; Pl. 22: 1-4; Figs. 45, 46

Derivation of name. – Named after the Sakesar Mountain near Amb, the highest point of the Salt Range.
Holotype. – Specimen PIMUZ30429 (Pl. 22: 1).
Type locality. – Amb, Salt Range, Pakistan.
Type horizon. – Sample Amb104 (lowermost LCL), *Gyronites dubius* beds, early Dienerian.
Diagnosis. – *Bukkenites* with evolute inner whorls, a sub-rounded whorl section and distant thick radial folds, becoming more involute with growth, with sub-parallel and smooth flanks.
Occurrence. – Sample Amb104 from Amb.
Description. – Involute shell with a broadly rounded venter and a pronounced allometric growth. Juveniles are relatively evolute (for D < 30 mm, U/D ≈ 29 %) with a thick whorl section (for D < 30 mm, W/D ≈ 41 %, W/H ≈ 96 %), most specimens having low broad radial folds on the inner half of the whorl, while some robust variants have a few distant strong blunt ribs fading just above the venter. With growth, the shell becomes smooth, more involute and compressed. For the holotype, which is the largest available specimen, U/D = 18 %, W/D = 32 % and W/H = 64 % at a diameter of 98 mm. Umbilical wall vertical to slightly overhanging, delineated by a very narrowly rounded umbilical shoulder. Flanks with maximal width at the umbilical shoulder in juveniles, at inner third of the whorl section on the holotype. Suture line with a narrow ventral lobe, lateral lobes with a few small indentations at their base, and short auxiliary series with irregular indentations which do not form any clear auxiliary lobe.
Measurements. – see Figs. 45, 46.
Discussion. – This species differs from the species assigned to *Bukkenites* by Tozer (1994) mainly by its sub-oval instead of trigonal whorl section, and by the presence of folds or ribs in the inner whorls. However, its suture line is similar to those illustrated by Tozer. Its marked allometry of the shell proportions, ornamentation on inner whorls, sub-oval whorl section and simple suture line allow to distinguish it from all other proptychitids.

Genus *Proptychites* Waagen, 1895

Type species. – *Ceratites lawrencianus* de Koninck, 1863.
Composition of the genus. – *Ceratites lawrencianus* de Koninck 1863, *Proptychites oldhamianus* Waagen 1895, *Proptychites ammonoides* Waagen 1895, *Proptychites candidus* Tozer 1961, *Proptychites subgrandis* Guex, 1978, *Proptychites pagei* Ware, Jenks, Hautmann & Bucher, 2011, *Proptychites wargalensis* sp. nov.
Emended diagnosis. – Involute, moderately compressed to thick discoidal shell with a broadly rounded venter. Suture line complex, with deep lobes. Ventral lobe very broad, divided by a deep ventral saddle into two wide lateral branches with numerous and deep indentations at their base. Lateral lobes very deep, with deep indentations at their base and simpler indentations on their flanks, occasionally reaching up to half of the height of the adjacent saddles in some species. Lateral saddles very elongated, slightly phylloid. Auxiliary series

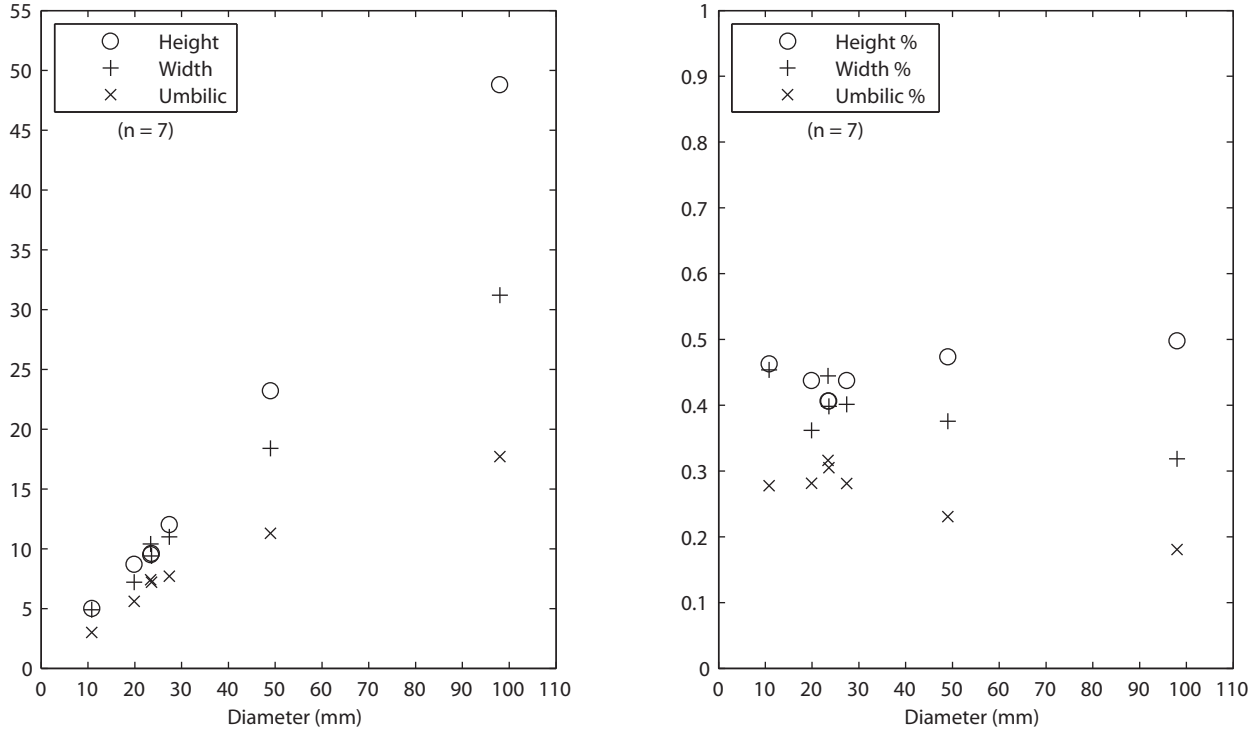

Fig. 46. Scatter diagrams of H, W, and U, and of H/D, W/D, and U/D for *Bukkenites sakesarensis* sp. nov.

short to long depending on involution. Evolute variants with a short auxiliary series and an auxiliary lobe clearly individualised at least on one side of the shell, involute variants with a very long auxiliary series, a clearly individualised auxiliary lobe and sometimes also an auxiliary saddle. At large sizes, the indentation of the lobes tend to become digitate (e.g. Pl. 23: 1d).

Occurrence. – Early to middle Dienerian of the Salt Range (Pakistan), Spiti valley (India), Nepal, Primorye (Russia), Queen Elizabeth Islands and British Columbia (Canada), Nevada (USA).

Discussion. – This genus is here restricted to early and middle Dienerian Proptychitidae, and differs from other members of this family mostly by its suture line. Griesbachian representatives of Proptychitidae (*Bukkenites*, *Pachyproptychites* Diener, 1916) differ in having a simpler suture line. Early Smithian representatives of Proptychitidae (such as *Clypeoceras* Smith, 1932, *Paraspidites* Spath, 1934, *Pseudaspidites* Spath, 1934, *Proptychitoides* Spath, 1930, *Eoptychites* Spath, 1930) tend to have more phylloid saddles and more indentations on the lobes. The juvenile suture line of the holotype of *Proptychites candidus* is simpler than that of our specimens, especially the ventral lobe. However, this suture line was drawn from the inner whorls of the holotype and other larger specimens of this species illustrated by Tozer (1994) have a suture line which does agree with that of our definition of *Proptychites.* Hence, in the absence of additional information, *P. candidus* is here kept into this genus. On the other hand, the specimens assigned to *Proptychites candidus* by Brühwiler *et al.* (2008), as well as the previously published specimens from China they synonymised with this species, have a much simpler suture line and thus belong to another species and genus. Waterhouse (1996) described several new species of *Proptychites*, but they are all based on too poorly preserved material to allow any identification at the species level. This author also erected the genus *Aspitella* with *Aspidites crassus* Krafft, 1909 as a type species, which we consider here as being a synonym of *Prop. Ammonoides*. Hence, the genus *Aspitella* is here considered as a junior synonym of *Proptychites*.

***Proptychites lawrencianus* (de Koninck, 1863) *sensu* Waagen, 1895**

Pl. 22: 5; Pl. 23: 1-4; Figs. 45, 47

? 1863 *Ceratites lawrencianus* nov. sp. de Koninck, p. 14, pl. 6: 3 (holotype).
1895 *Proptychites lawrencianus* nov. gen. Waagen, p. 168-170, Pl. 18: 1, Pl. 17: 2.
v 1978 *Proptychites ammonoides* – Guex, Pl. 8: 8.

Occurrence. – Samples Nam100, Nam300, Nam301, Nam344, Nam501 and Nam503 from Nammal Nala.

Description. – Moderately involute, relatively thick shell with a broadly rounded venter and a marked allometric growth. Starting from the neanic stage, the shell rapidly becomes very involute, reaching its maximal involution

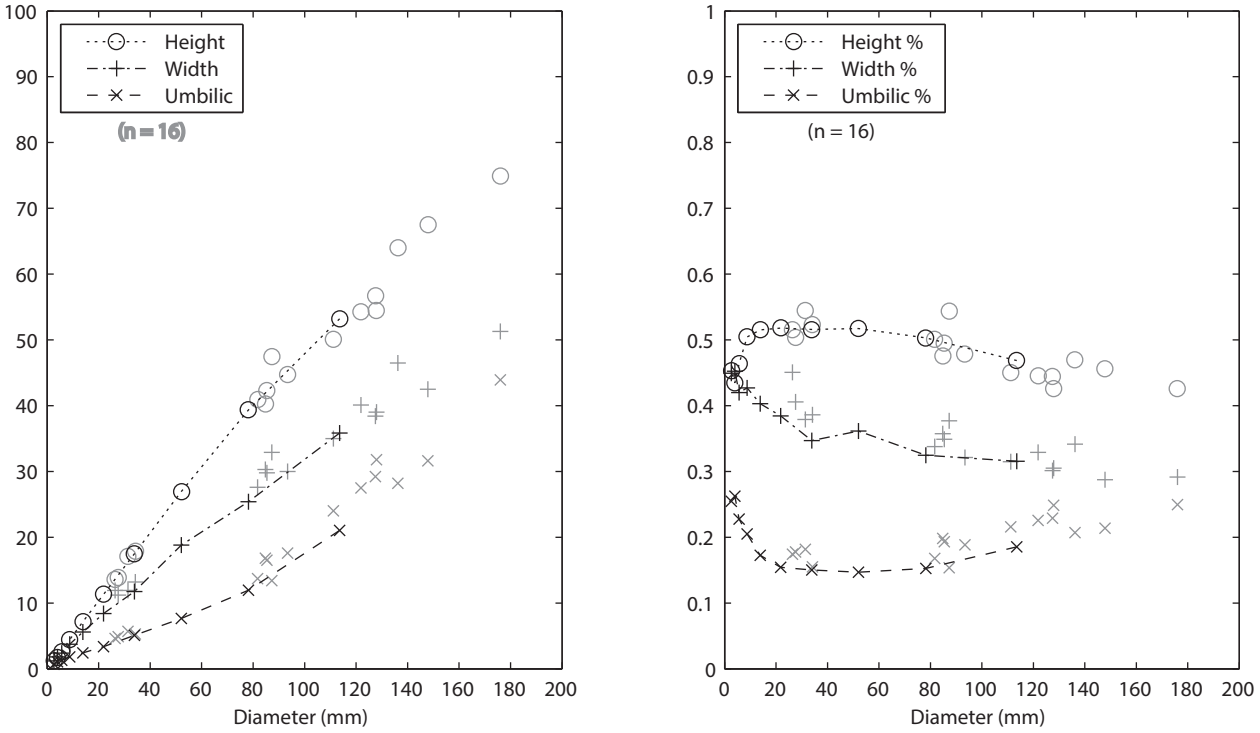

Fig. 47. Scatter diagrams of H, W, and U, and of H/D, W/D, and U/D for *Proptychites lawrencianus* (de Koninck, 1863) *sensu* Waagen, 1895. Ontogenetic trajectories obtained from sectioned specimen illustrated on Pl. 22: 5 are shown in black.

at a diameter of ca. 3 cm, where U/D reaches about 15 %. From this point, the shell becomes slowly and progressively more evolute, U/D reaching 25 % on the largest specimen measured at a diameter of 17.6 cm. The whorl thickness decreases rather slowly and steadily during growth. As measured on a prepared section, W/D = 45 % and W/H = 104 % at the end of the neanic stage (D = 4 mm) and decrease to reach 32 % and 67 % at a diameter of 114 mm, respectively. The maximal whorl thickness is situated at or just above the umbilical shoulder in the inner whorls, and shifts progressively towards the middle part of the flank with growth, the whorl section becoming more and more oval. The umbilical wall is vertical to slightly overhanging on the inner whorls. It becomes progressively slightly oblique with growth, permanently delineated by a broadly rounded umbilical shoulder. The shell is generally smooth, but some specimens have broad radial folds which appear at a minimum diameter of ca. 7 cm. The suture line could only be clearly seen on two specimens, a small and a large one. In both cases, lobes are very deep and saddles are very elongated. Lobes are deeply indentated, and the auxiliary series is short. The small specimen, which is very involute, has phylloid saddles, and a very well individualised auxiliary lobe. On the larger, more evolute specimen, the saddles are not phylloid, and the suture line is strongly asymmetric, especially the auxiliary series, which has a clearly differentiated auxiliary lobe on the right side, whereas it is poorly differentiated on the other (see Pl. 23:1d).
Measurements. – see Figs. 45, 47.
Discussion. – The illustration of the holotype of this species given by de Koninck (1863) is not very informative, lacks ventral or apertural view, and is accompanied by a very brief description. Waagen's interpretation of this species is only a guess based on what is visible of the suture line on de Koninck's drawing. However, it is the interpretation of Waagen which has been used by subsequent authors (from Spath, 1934 to Waterhouse, 1996), and which is also adopted here. It should be noted here that the specimen of de Koninck comes from the collections of Dr. A. Fleming, and the author does not indicate where this collection is curated. It is therefore possible that the holotype is lost, so a neotype could be chosen in the collections of Waagen. This, however, would need a careful investigation and the establishment of a neotype requires a formal request to the ICZN. According to the measurements provided by de Koninck, his holotype is much less inflated (W/D = 30 %, W/H = 55 %) than our specimens and than those of Waagen, all of which are similar to our material. The holotype is thus closer in proportions to the species here referred to as *Proptychites ammonoides*. Until the holotype can be adequately re-described, the definition of Waagen is here kept by default, but no emended diagnosis is provided. Guex (1978) figured a specimen which he assigned to *Prop. ammonoides*. The thickness of this specimen is actually more in agreement with that of *Prop. lawrencianus* than with that of *Prop. ammonoides*.

***Proptychites oldhamianus* Waagen, 1895**

Pl. 24: 2-4; Fig. 45

1895 *Proptychites oldhamianus* nov. gen. et sp. Waagen, p. 166-167, Pl. 19: 3 (holotype).
1909 *Proptychites typicus* nov. sp. Krafft *in* Krafft & Diener, p. 77-79, pl. 19: 4,5, Pl. 20: 6, Pl. 21: 2, 3 (lectotype), 4.

Emended diagnosis. – Involute, thick *Proptychites* with nearly flat flanks in inner whorls, strongly converging towards the rounded venter, imparting a sub-trigonal shape to the whorl section. Inner whorls bear weak radial folds just above the umbilical wall. The flanks become more convex and the ornamentation disappears with growth. Suture line simple compared to that of other *Proptychites*, with non phylloid saddles and few rather shallow indentations in the lobes.
Occurrence. – Samples Nam335a and Nam378 from Nammal.
Description. – Moderately involute (U/D ≈ 18 %), relatively thick (W/D ≈ 36 %, W/H ≈ 51 %) shell with a narrowly rounded venter. Inner whorls have their maximal width at the umbilical shoulder, the flanks being only very slightly convex and strongly converging towards the venter, thus giving the whorl section a sub-trigonal shape. With growth, the flanks become progressively more convex, and the maximal whorl width shifts progressively towards the inner third of the flanks. Umbilical wall vertical at every stage of growth, delimited by a narrowly rounded umbilical shoulder. On inner whorls, some weak radial folds occur on the dorsal half of the flanks. They disappear completely with growth. Suture line fairly simple for *Proptychites*, but with the characteristic ventral lobe having broad lateral branches and a clearly individualised auxiliary lobe, even at small size. Lateral saddles not phylloid, the third one being strongly bent towards the umbilicus. Lobes with few and rather small indentations.
Measurements. – see table 1 and Fig. 45.
Discussion. – Only three specimens of this species have been documented. They occur in massive limestone beds from the LCL of Nammal Nala, and are very difficult to prepare. The suture line is visible only on the last preserved whorl of the smallest specimen, but despite its small size, it shows already the characteristic ventral and auxiliary lobes of the genus *Proptychites*. Our specimens agree very closely with the holotype of Waagen, except for the low radial folds on the inner whorls. Incidentally, Waagen's specimen is a weathered inner mould, hence this difference is most probably a preservation bias.

The strongly bent third lateral saddle of the suture line is somewhat peculiar compared to that of other representatives of *Proptychites*, but considering the large intraspecific variability of this portion of the suture line in other species, this trait is here not considered as being relevant. *Prop. typicus* as illustrated by Krafft & Diener (1909) also agrees perfectly with our material. These authors mentioned that "the periphery of the inner volutions is of indistinctly polygonal outlines", a characteristic which is shared by our smallest specimen. All the specimens of *Prop. oldhamianus* described so far are of smaller size than the younger representatives of *Proptychites*. However, this small size may well be the result of a taphonomical bias, as they all come from shallower, higher energy environment. Our largest specimen being too recrystallised to see any suture lines, it is not possible to conclude if its body chamber is preserved or not.

***Proptychites wargalensis* sp. nov.**

Pl. 24: 1; Fig. 45

Derivation of name. – Named after the locality of Wargal.
Holotype. – Specimen PIMUZ30438 (Pl. 24: 1).
Type locality. – Wargal, Salt Range, Pakistan.
Type horizon. – Sample War5 (middle LCL), *Gyronites plicosus* beds, early Dienerian.
Diagnosis. – Relatively evolute and thick whorled *Proptychites* with a sub-oval whorl section and a simple suture line with a poorly differentiated auxiliary lobe.
Occurrence. – Samples War5, War6, War11 and War100 from Wargal.
Description. – Relatively evolute (U/D = 22 %) and thick (W/D = 31 %, W/H = 65 %) shell with a broadly rounded venter. Flanks convex with maximal width at the inner third of the whorl. Umbilical wall vertical, grading into a rounded shoulder. No visible ornamentation. Suture line relatively simple, with moderately elongated and non phylloid saddles, a ventral lobe with broad lateral branches, lateral lobes with numerous small indentations at their base, and a very shallow auxiliary lobe individualised by having thinner indentations than the rest of the auxiliary series.
Measurements. – see table 1 and Fig. 45.
Discussion. – This species is based on five poorly preserved specimens of which only one could be measured. It is very close to *Prop. oldhamianus*, from which it differs by its more evolute coiling, thinner and more oval whorl section, and its simpler suture line. However, these two species are based on only a few specimens from correlative beds from two localities. Hence, it cannot be excluded that they are conspecific, but sufficient material is not available to demonstrate it. We thus provisionally assign the specimens from Wargal to a different species than those from Nammal Nala. The fairly simple suture line of *Prop. wargalensis*, with its poorly individualised auxiliary lobe, may possibly lead to exclude this species from the genus *Proptychites*. However, on the other specimens here studied, the suture line is well enough preserved to see that its auxiliary lobe is better individualised than that of the holotype. In the absence of more abundant and better preserved material, we decided to keep this species within *Proptychites,* of which it represents the oldest known representative along with *Prop. oldhamianus*.

***Proptychites ammonoides* Waagen, 1895**

Pl. 24: 5; Pl. 25: 1-4; Pl. 26: 1; Figs. 45, 48

1895 *Proptychites ammonoides* nov. gen. et sp. Waagen, p. 171-173, Pl. 17: 1 (lectotype), Pl. 19: 2.
1909 *Aspidites crassus* nov. sp. Krafft *in* Krafft & Diener, p. 58-59, Pl. 6: 4, Pl. 7: 1, Pl. 8: 1.
1909 *Koninckites haydeni* nov. sp. Krafft *in* Krafft & Diener, p. 68-70, Pl. 17: 1, 2, 3 (lectotype), 4- 6.
1909 *Koninckites alterammonoides* nov. sp. Krafft *in* Krafft & Diener, p. 70-72, Pl. 16: 1 (lectotype), 2.
? 1996 *Aspitella crassa* nov. gen. Waterhouse, p. 51, Text-fig. 41, Pl. 3: 2-4.
2009 *Proptychites alterammonoides* – Shigeta & Zakharov, p. 110-112, figs 98, 99.
v 2011 *Proptychites haydeni* – Ware *et al.*, p. 173-175, figs. 15-17.

Emended diagnosis. – Very involute and compressed *Proptychites* with a highly denticulated suture line.
Occurrence. – Samples Amb4, Amb5 and Amb53 from Amb, Chi 56 from Chiddru, Nam50, Nam53, Nam364, Nam380, Nam384, Nam400, Nam521 and Nam522 from Nammal and War2 from Wargal.
Description. – Very involute (U/D ≈ 10 %) and compressed (W/D ≈ 30 %, W/H ≈ 54 %) discoidal shell with nearly flat, sub-parallel to slightly convex flanks. Position of maximal whorl width variable, between inner fourth of the flanks and mid-flanks. The flanks tend to be more convex in juvenile specimens and to become nearly flat with further growth, but convex flanks may persist to larger size in some specimens. Umbilical wall vertical, grading into a rounded shoulder. No clear allometric growth could be detected on our material, but one specimen (PIMUZ30443, Pl. 25: 1), a complete phragmocone showing the trace of the umbilical seam of the body chamber, displays a pronounced umbilical egression of the body chamber. This species can reach very large size, the largest specimen being a complete phragmocone of about 17 cm in diameter (PIMUZ30446, Pl. 25: 4). Adding extra minimum of half a whorl for the body chamber, it may have reached a diameter of at least 26 cm. Some specimens have very vague folds following the shape of the growth lines on the inner half of the

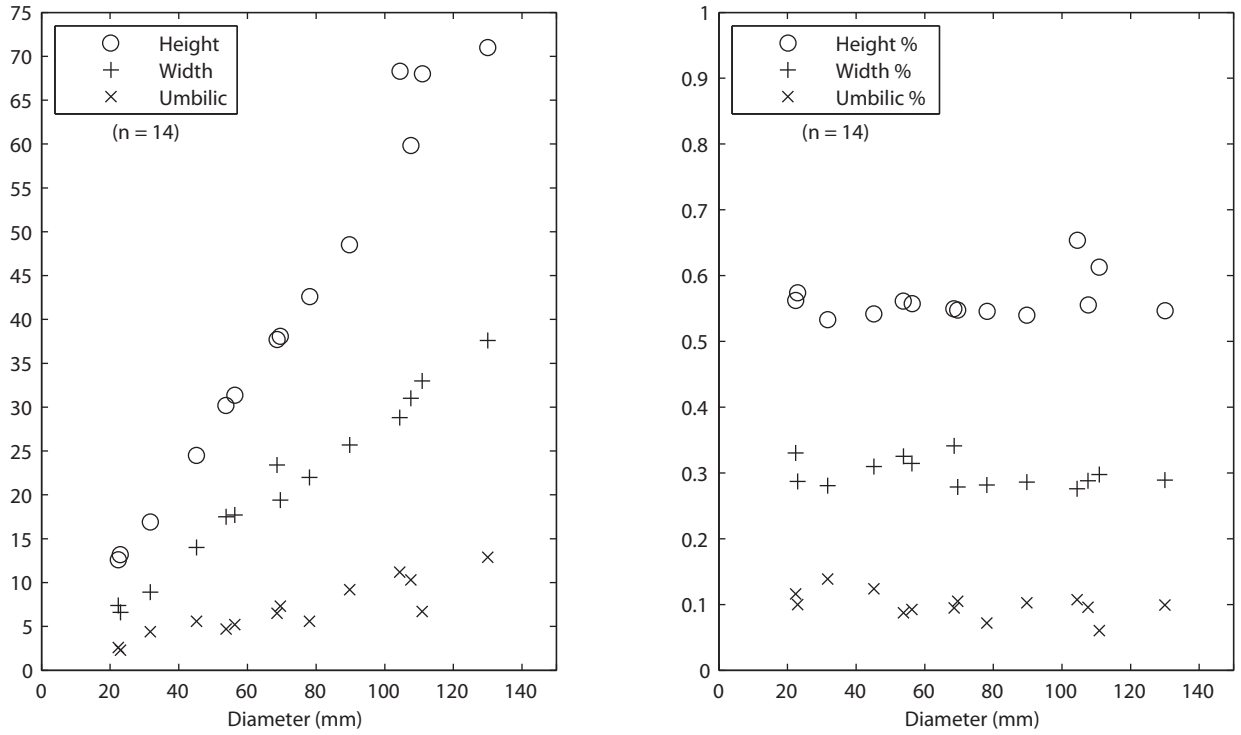

Fig. 48. Scatter diagrams of H, W, and U, and of H/D, W/D, and U/D for *Proptychites ammonoides* Waagen, 1895.

flanks. Suture line complex at maturity. Ventral lobe very wide, divided by a deep ventral saddle into two broad branches with numerous very deep indentations at their base. First lateral saddle slightly phylloid. Second lateral saddle bent dorsally and with a subtriangular outline at maturity. Third lateral saddle varying from large and rounded to narrow with a flattened tip. Lateral lobes deep, with many very deep indentations at their base and progressively shallowing on the lateral sides of the lobes. At maturity, lateral denticulations may expand on two thirds of the sides. On large specimens, the very deep indentations at the bottom of the lobes are further subdivided into smaller indentations. Auxiliary series very long, complex, and variable, with a clearly individualised auxiliary lobe even at small diameter, generally followed by an irregular series of small lobes or deep indentations, and sometimes with a clearly differentiated large auxiliary saddle.

Measurements. – see Figs. 45, 48.

Discussion. – The suture line of the lectotype of this species has a peculiar flattened top of the third lateral saddle with two small incisions, a feature which has not been observed in our material. It is otherwise similar to our specimens. Krafft & Diener (1909) erected three new species (*Aspidites crassus*, *Koninckites haydeni* and *Koninckites alterammonoides*) which can be included in the intraspecific variability of *Prop. ammonoides*. These three species have been assigned to different genera based on a wrong interpretation of *Proptychites*, which Krafft & Diener *op. cit.* defined mainly by the presence of "globose inner whorls", whereas the two genera in which they included these three species were mainly defined by their suture line. The differences between these three species concern mainly the umbilical portion of the suture line (the third lateral saddle and the auxiliary series), which is shown here to be highly variable and not necessarily diagnostic. Waterhouse (1996) created the new genus *Aspitella* based on Krafft's species *Aspidites crassus*, and as this species is here considered as a synonym of *Prop. ammonoides*, the genus *Aspitella* becomes a junior synonym of *Proptychites*. The specimens assigned by Waterhouse to this species are too poorly preserved for any identification.

Proptychites cf. *pagei* Ware, Jenks, Hautmann & Bucher, 2011

Pl. 26: 2-3; Fig. 45

v? 2011 *Proptychites pagei* – Ware *et al.*, p. 175-176, fig. 18.

Occurrence. – Samples Nam344, Nam345 and Nam501 from Nammal Nala.

Description. – Compressed (W/D ≈ 28 %, W/H ≈ 44 %) discoidal shell with occluded umbilicus. Flanks slightly convex with maximal width at inner third of whorl height. Shell smooth except for very weak broad folds following the trajectory of the growth lines on the inner half of the flanks. Suture line very complex with elongated and narrow saddles. First lateral saddle occasionally slightly phylloid. Lobes with large, deep indentations at their base and small indentations on their flanks. Auxiliary series very long with a clearly differentiated auxiliary

lobe followed by numerous irregular large indentations, occasionally with a poorly differentiated auxiliary saddle.
Measurements. – see table 1 and Fig. 45.
Discussion. – With their characteristic occluded umbilicus, these specimens differ from the type material described by Ware *et al.* (2011) by their larger size only. The smallest specimen found in the Salt Range is 55.6 mm in diameter, the largest is 10 cm in diameter, both being incomplete phragmocones, whereas the largest specimen from the Candelaria Hills (Nevada) is 51.3 mm in diameter and has a part of its body chamber preserved. The specimens from the Candelaria Hills also have a simpler suture line, but this is most likely a consequence of their smaller size. Specimens of intermediate size with preserved body chamber are needed to confirm that the Nevada and the Salt Range material belong to the same species.

Family Mullericeratidae Ware, Jenks, Hautmann & Bucher, 2011

Type genus. – *Mullericeras* Ware, Jenks, Hautmann & Bucher, 2011.

Composition of the family. – *Mullericeras*, *Ussuridiscus* Shigeta & Zakharov, 2009.
Emended diagnosis. – Involute, tabulate platyconic shell with a suture line composed of a long auxiliary series and no adventitious element in the ventral lobe.
Discussion. – This family was first erected for a single genus (*Mullericeras*). The more abundant and better preserved specimens presented in this study allow providing a more precise emended diagnosis, and shows that with its involute, tabulate platyconic shell, *Ussuridiscus* is clearly the stem group of *Mullericeras* and should be assigned to Mullericeratidae (cf. infra). Following Tozer's (1994) broad definition of Meekoceratidae, *Ussuridiscus* was originally placed in this family by Shigeta & Zakharov (2009). As discussed previously (cf. p. 21, discussion on Gyronitidae), the validity of Meekoceratidae as a monophyletic group is questionable. The superficial resemblance between *Meekoceras,* the type genus of Meekoceratidae, and evolute species of *Mullericeras* is another example of convergence. On the other hand, our new material provides further evidence that Sageceratacea root into mullericeratids , as demonstrated by the close resemblance between *Mu. spitiense* and *Clypites typicus*,

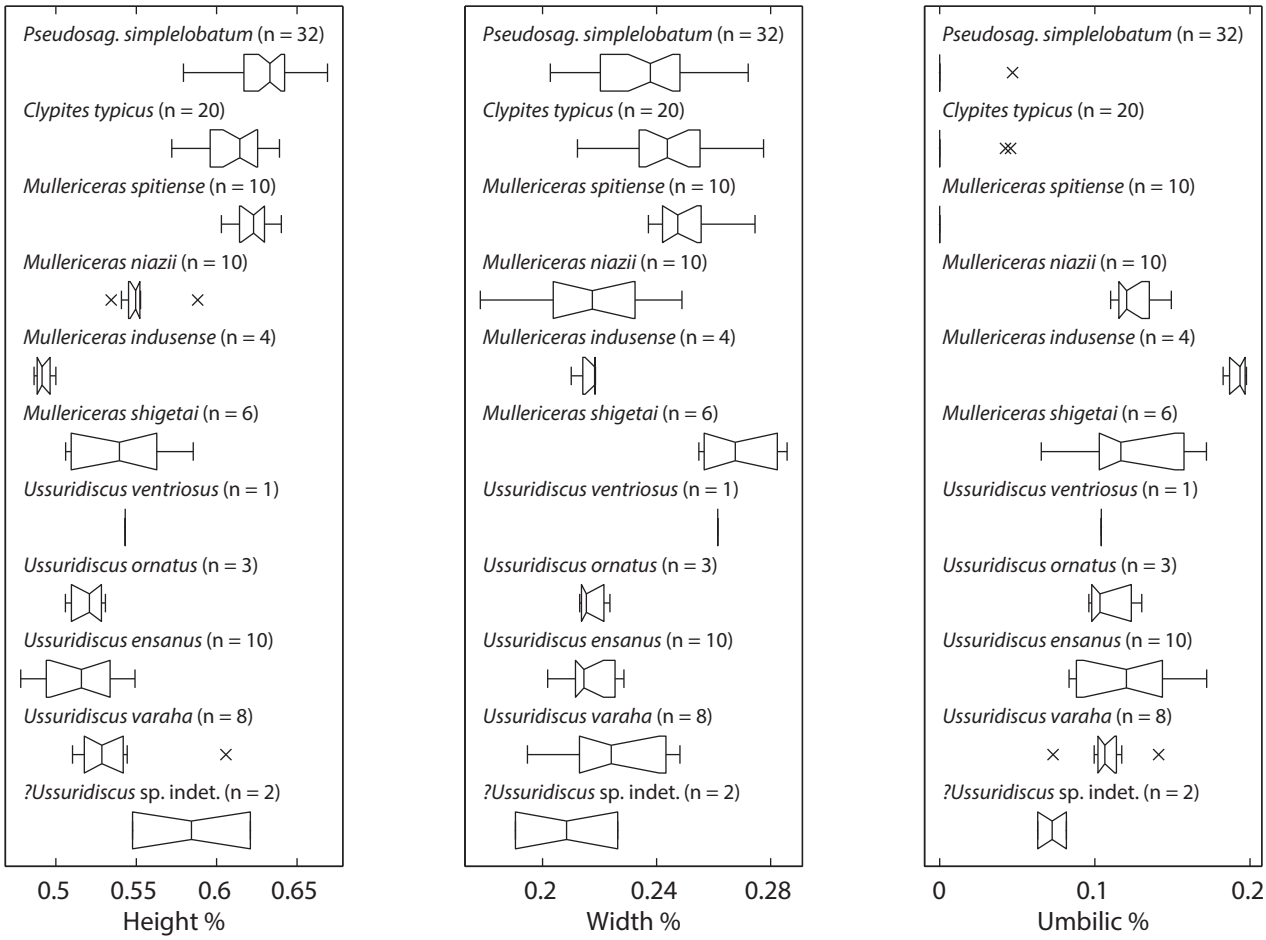

Fig. 49. Boxplots for the different species of Mullericeratidae and Hedenstroemiidae from the Dienerian of the Salt Range. The box plot displays the 25th, 50th (median) and 75th percentiles of the range of measures covered by 99% of the specimens from a normal distribution. Outliers represent specimens not falling within the normal distribution.

which can only be differentiated by their ventral lobe, without adventitious series in *Mu. spitiense*.

Genus *Mullericeras* Ware, Jenks, Hautmann & Bucher, 2011

Type species. – *Aspidites spitiensis* Krafft *in* Krafft & Diener, 1909.
Discussion. – This genus was originally described as including three species: *Mu. spitiense* (Krafft, 1909), *Meekoceras (Koninckites) vidharba* Diener, 1897 and *Aspidites ensanus* Krafft, 1909. The more detailed study presented here indicates that *Meekoceras (Koninckites) vidharba* and *Aspidites ensanus* should be assigned to *Ussuridiscus*. Two other new species are here included in the genus *Mullericeras*. It is here defined as including smooth, very involute, compressed and tabulate platyconic to sub-oxyconic shells with a very broad ventral lobe bearing numerous small indentations but without adventive series.

***Mullericeras spitiense* (Krafft, 1909)**

Pl. 27: 1-3; Fig. 49, 50

1909 *Aspidites spitiensis* nov. sp. Krafft *in* Krafft & Diener, p. 54, pl. 4: 4 (lectotype), 5, Pl. 16: 3- 8.
? 1996 *Clypeoceras spitiense* – Waterhouse, p. 50, text-fig. 4J, pl. 2: 21-22.
non 2009 *Clypeoceras spitiense* – Shigeta & Zakharov, p. 125-126, fig. 113-114.
v 2010 *Mullericeras spitiense* gen. nov. Ware *et al.*, p. 171-172, figs. 11-12.

Occurrence. – Samples Nam100, Nam344 and Nam396 from Nammal Nala.
Description. –As this species has already been re-described recently (Ware *et al.* 2011), no detailed description of the general shell morphology is given here as our specimens are strictly identical to the ones already figured. However, additional details of the suture line can be given here. Its lobes and saddles are elongated. The ventral lobe is very broad, with many indentations (9 indentations on the suture line drawn, Pl. 27: 2d). First lateral saddle elongated and straight, second and third lateral saddles broad and slightly bent towards the umbilicus, the third one being almost rectangular. Lobes with up to six deep indentations. Auxiliary series with one poorly differentiated lobe followed by a series of deep indentations.
Measurements. – see Figs. 49, 50.
Discussion. – This species is almost homeomorphic with *Clypites typicus*, from which it differs by the absence of adventive series during the whole ontogeny, its smaller maximum size, broader, less elongated lateral saddles and a slightly simpler auxiliary series. This similarity suggests that *Clypites* and other Hedenstroemiidae originated from this species, but further, more detailed study of these groups, particularly concerning their ontogeny, would be necessary to demonstrate it. The synonym list has already been discussed by Ware *et al.* (2011). However, the specimen illustrated as *Clypeoceras*

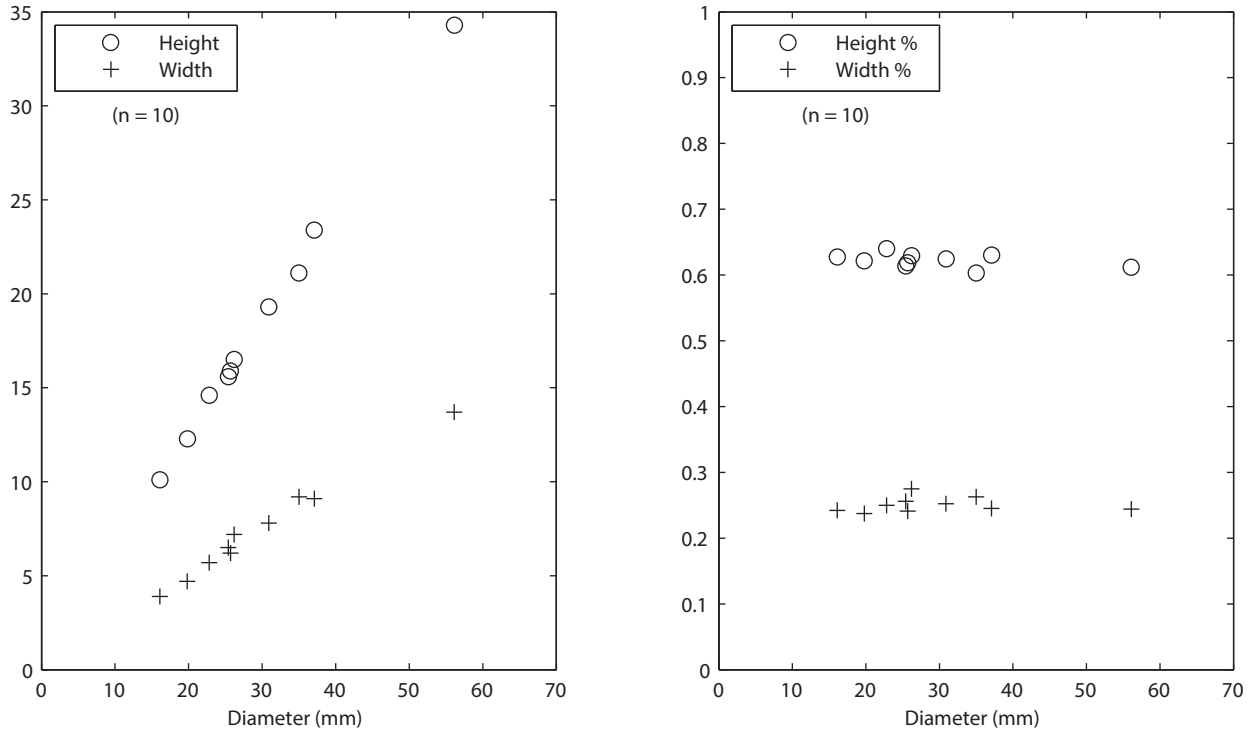

Fig. 50. Scatter diagrams of H and W, and of H/D and W/D for *Mullericeras spitiense* (Krafft, 1909).

spitiense by Shigeta & Zakharov (2009) is here assigned to *Clypites typicus* (see below).

***Mullericeras shigetai* sp. nov.**

Pl. 27: 4-9; Figs. 49, 51

?p 1994 *Ambites fuliginatus* – Tozer, pl. 13: 4.
?p 1994 *Ambites ferruginus* – Tozer, pl. 14: 1, 2, 5, 6.
? 2009 *Ambitoides fuliginatus* – Shigeta & Zakharov, p. 77-79, figs 63-64.
?v 2011 *Ussuridiscus* sp. indet. – Ware *et al.*, p. 169, fig. 8a.

Derivation of name. – Named after Dr. Yasunari Shigeta (National Museum of Nature and Science, Tokyo, Japan).
Holotype. – Specimen PIMUZ30453 (Pl. 27: 2).
Type locality. – Nammal Nala, Salt Range, Pakistan.
Type horizon. – Sample Nam381 (lower CM, ca. 1.5 m above base), *Ambites radiatus* beds, middle Dienerian.
Diagnosis. – Involute, moderately compressed (W/H ≈ 50 %) *Mullericeras* with a very high vertical to overhanging umbilical wall, a narrow but open umbilicus (U/D ≈ 12 %) and a simple suture line without clearly individualised auxiliary lobe or saddle.
Occurrence. – Samples Amb53 from Amb, Chi56 from Chiddru and Nam364, Nam381, Nam382, Nam383, Nam384, Nam527 from Nammal.
Description. – Involute, moderately compressed shell with a broad tabulate venter (on the adult holotype, the width of the venter represents 38 % of the whorl width) and sharp ventro-lateral shoulders. Flanks slightly convex with maximum whorl width just below the umbilical wall. Umbilical wall short and sub-vertical in juvenile stages and becoming slightly overhanging at later stages. Umbilical shoulder narrowly rounded. On the holotype, which is the largest and only mature specimen with a partly preserved body chamber, the umbilical wall becomes again vertical on the body chamber, where the umbilical shoulder is underlined by a slight concavity of the upper flanks. Its umbilical shoulders, like its ventro-lateral shoulders, become less angular at larger size. One specimen (PIMUZ30456, Pl. 27: 9) had remains of an *in vivo* encrusting bivalve on each side of its umbilicus, which explains its strongly overhanging umbilical wall with an extremely sharp umbilical shoulder. Egressive coiling starts from a diameter of ca. 4 cm onward. Flanks smooth, except for occasional very weak folds following the shape of the slightly sigmoid growth lines. Suture line relatively simple, without clearly individualised auxiliary lobe. Lobes and saddles broad, saddles moderately elongated. Ventral lobe divided by a broad saddle into two large rounded branches with numerous and regularly spaced small indentations at their base. Lateral lobes broadly rounded also with numerous and regularly spaced small indentations at their base. The two first lateral saddles are always moderately elongated, the second one being slightly bent towards the umbilicus. The third lateral saddle is broad, short and sub-rectangular (i.e. about twice broader than high) on the smallest and the largest specimen, as high as broad and sub-rounded on the others. The previously

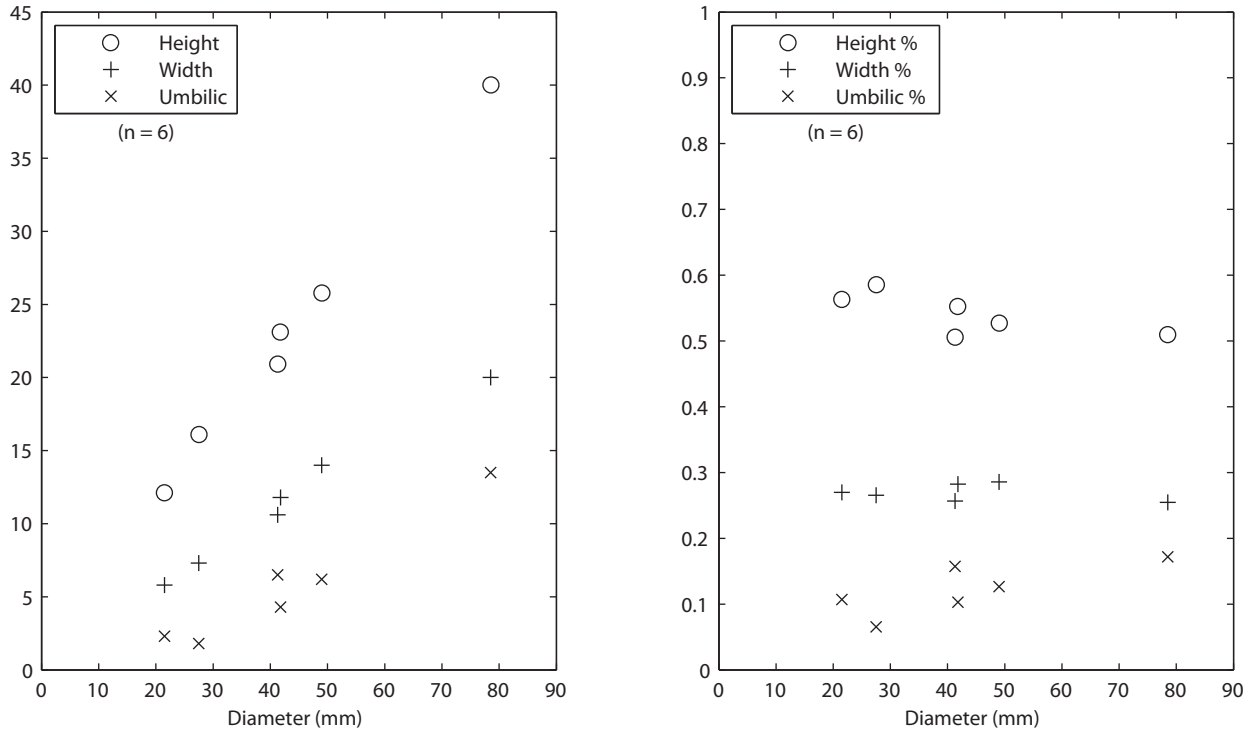

Fig. 51. Scatter diagrams of H, W, and U, and of H/D, W/D, and U/D for *Mullericeras shigetai* sp. nov.

mentioned specimen with a growth disturbance induced by an encrusting bivalve (Pl. 27: 9) has a slightly different suture line than the others. Its auxiliary series has a slightly individualised auxiliary lobe followed by a series of irregular deep indentations, less numerous than in other normal specimens. Considering the covariation between the shape of the whorl section and the pattern of the suture line, this difference is most probably the consequence of the modified dorsal part of the whorl section.
Measurements. – see Figs. 49, 51.
Discussion. – Tozer (1994; Pl.13: 4; Pl. 14: 1, 2, 5, 6) figured some involute specimens he assigned to *Ambites fuliginatus* and *Am. ferruginus*. The holotypes of these two species clearly belong to the genus *Ambites*, but these involute specimens are too involute and lack the bottleneck shaped venter characteristic of this genus. Therefore, they most probably belong to the genus *Mullericeras*. They agree in proportions with our specimens, but the exact morphology of their umbilical wall and suture line is not visible. Hence, we refer them only with caution to our species. The specimens assigned to *Am. fuliginatus* by Shigeta & Zakharov (2009) on which they base their new genus *Ambitoides* are very close to the involute specimens of Tozer (1994) previously discussed and to ours. They differ from our specimens by their more parallel flanks, their non overhanging umbilical wall and a narrower ventral lobe of the suture line. The small number of specimens of *Mu. shigetai* does not allow assessing intraspecific variability. Hence, it is not possible to establish whether these small differences can be included into the variability of *Mu. shigetai* or if they are characteristic of another new species. Hence, the specimens of Shigeta & Zakharov (2009) are referred with doubts to our species. The specimen described by Ware *et al.* (2011) as *Ussuridiscus* sp. indet. was ascribed to this genus based on its overhanging umbilical wall. This characteristic is also found in the genus *Mullericeras*, and the Nevadan specimen found together with *Ambites* most likely belongs to the genus *Mullericeras*. The morphology of its flanks and umbilicus agrees with that of *Mu. shigetai*, but its poor preservation prevents a clear species identification.

***Mullericeras indusense* sp. nov.**

Pl. 28: 1-4; Fig. 49

Derivation of name. – Named after the Indus River.
Holotype. – Specimen PIMUZ30460 (Pl. 28: 2).
Type locality. – Nammal Nala, Salt Range, Pakistan.
Type horizon. – Sample Nam302 (lower CM, ca. 2.5 m above base), *Ambites superior* beds, middle Dienerian.
Diagnosis. – *Mullericeras* with a broad umbilicus (U/D ≈ 19 %), compressed whorl section (W/H ≈ 44 %) and occasional auxiliary lobe on suture line.
Occurrence. – Samples Nam53 and Nam302 from Nammal.
Description. – Involute, moderately compressed shell with a broad tabulate venter and sharp ventro-lateral shoulders. Flanks slightly convex with maximum width around mid-flanks. Umbilical wall moderately high, vertical to slightly overhanging with narrowly rounded umbilical shoulder. No ornamentation visible except for very weak folds following the shape of the slightly sigmoid growth lines. Suture line with deep lobes and elongated saddles. Ventral lobe broad, with triangular shaped branches with many denticulations at their base. Auxiliary series long and variable, sometimes without auxiliary lobe and composed of a series of rather regular deep indentations, occasionally with a clearly individualised auxiliary lobe and saddle.
Measurements. – see Table 1 and Fig. 49.
Discussion. – This species is very close to *Mu. shigetai*, from which it differs by its larger umbilicus, more compressed whorl section and its suture line. More specifically, its ventral lobe branches are intermediate between the large rounded branches of *Mu. shigetai* and the triangular branches of *Mu. niazii*. With its relatively large umbilicus, it superficially resembles involute variants of *Ambites*, but it differs by the absence of a bottleneck shaped venter, of spiral ridges and its more complex suture line.

***Mullericeras niazii* sp. nov.**

Pl. 28: 5-7; Figs. 49, 52

Derivation of name. – Named after the Niazi tribe from Mianwali District.
Holotype. – Specimen PIMUZ30464 (Pl. 28: 5).
Type locality. – Nammal Nala, Salt Range, Pakistan.
Type horizon. – Sample Nam100 (lower CM, ca. 4 m above base), *Ambites bjerageri* beds, middle Dienerian.
Diagnosis. – Involute, very compressed (W/H ≈ 39 %) *Mullericeras* with a very short vertical umbilical wall, open but narrow umbilicus (U/D ≈ 13 %) and a clearly individualised auxiliary lobe on the suture line.
Occurrence. – Samples Nam100, Nam344, Nam501, Nam503 from Nammal.
Description. – Involute, very compressed shell with a relatively broad, very slightly concave tabulate venter (on the holotype, the venter width represents 36 % of the whorl width) and sharp ventro-lateral shoulders. Flanks slightly convex with maximum width around mid-flanks on sub-adult specimens, on inner third of flanks in juveniles. Umbilical wall short and vertical on sub-adults, individualised by narrowly rounded umbilical shoulders. In juveniles, the low umbilical wall is convex, coalescing the preceding whorl with a very acute angle. Flanks smooth except for very weak folds following the shape of the slightly sigmoid growth lines. Ventral

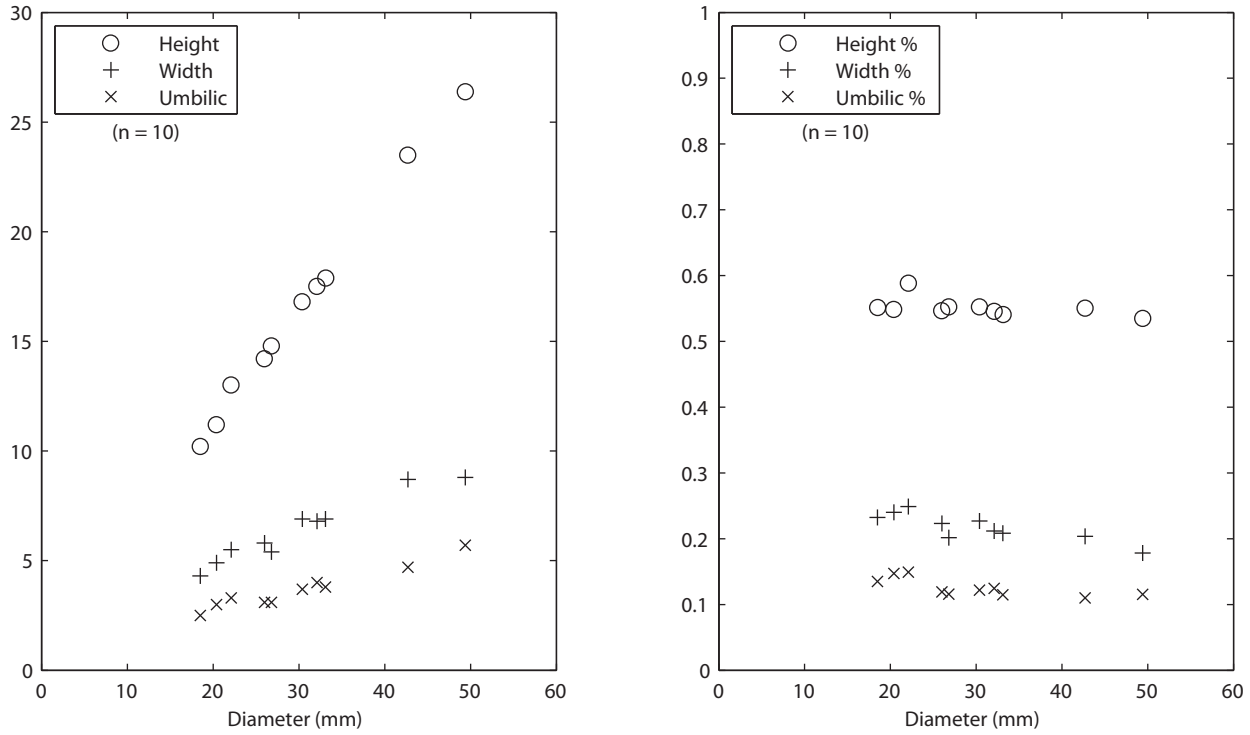

Fig. 52. Scatter diagrams of H, W, and U, and of H/D, W/D, and U/D for *Mullericeras niazii* sp. nov.

lobe broad, divided by the ventral saddle into two large triangular branches with numerous, regularly spaced small indentations at their base and ventral flank. Lateral lobes with nearly straight base, bearing a few deep denticulations. The two first lateral saddles have a narrowly rounded tip, the third one has a flattened tip. Auxiliary series very long, with a clearly individualised auxiliary lobe, sometimes also an auxiliary saddle, followed by a series of irregularly spaced denticules.

Measurements. – see Figs. 49, 52.

Discussion. – This species, with its very compressed whorl section, narrow umbilicus and peculiar ventral lobe differs clearly from other species of *Mullericeras*. It differs from the compressed forms of *Ussuridiscus* by its thicker venter, its absence of ornamentation and its wide ventral lobe. At small size (*i.e.* D < 2 cm.), some *Ambites* have almost the same morphology and can be confused with it, but the juveniles of *Ambites* are usually thicker, have a slightly bottleneck shaped venter and, more importantly, a simpler suture line with thinner ventral lobe branches and without differentiated auxiliary lobe.

Genus *Ussuridiscus* Shigeta & Zakharov, 2009

Type species. – *Meekoceras (Kingites) varaha* Diener, 1895.

Composition of the genus. – *Meekoceras (Kingites) varaha* Diener, 1895, *Aspidites ensanus* Krafft, 1909, *Ussuridiscus ventriosus* sp. nov., *Ussuridiscus ornatus* sp. nov.

Emended diagnosis. – Very involute, compressed tabulate shell. Suture line with a narrow ventral lobe bearing few small indentations.

Occurrence. –Early Dienerian of the Salt Range (Pakistan), Central Himalayas (India, Nepal), Dienerian of Guangxi (China), late Griesbachian and early Dienerian of South Primorye (Russia).

Discussion. – Shigeta & Zakharov (2009) erected this genus for a single species, and considered its overhanging umbilical wall as being its main characteristic. Our new abundant material shows that beside the type species, three other species from correlative strata in the Salt Range can be grouped within this genus, leading to an emendation of the original diagnosis. One species (*U. ventriosus*) does not have this overhanging umbilical. We however decided to group it with the others as it is otherwise very similar, and this distinction is not significant enough to create a new genus. We therefore consider this genus as including very involute, compressed platyconic to sub-oxyconic shells with a tabulate venter, a vertical to overhanging umbilical wall and a suture line with narrow ventral lobe with only a few little indentations at its base. With its involute, compressed, tabulate shell, it is very close to the genus *Mullericeras*, from which it differs by its simpler suture line with narrower ventral lobe and less numerous indentations in its lateral lobes, and by its more convex flanks. The similarity between these two genera and the occurrence of *Ussuridiscus* in older strata than *Mullericeras* suggests that the latter derives directly from the former through a complexification of the suture line. The two genera should thus be grouped within the same family (Mullericeratidae). Following the broad definition of this family by Tozer (1994), *Ussuridiscus* was originally

placed in Meekoceratidae, an interpretation which is not followed here.

***Ussuridiscus varaha* (Diener, 1895)**

Pl. 28: 8-11; Figs. 49, 53

1895 *Meekoceras (Kingites) varaha* nov. sp. Diener, p. 52, pl. 1: 2 (lectotype).
non 1897 *Kingites varaha* – Diener, p. 143-144, Pl. 6: 2, pl. 7: 6.
1905 *Meekoceras (Kingites) varaha* Noetling, pl. 32: 5 [cop. Diener 1895].
non 1909 *Meekoceras varaha* – Krafft *in* Krafft & Diener, p. 17-20, pl. 2: 2-6, pl. 14: 7-8.
1968 *Koninckites varaha* – Zakharov, p. 91, text-fig. 20b, pl. 17: 4-5.
2007 *Hubeitoceras* (?) *wangi* – Zakharov & Mu in Mu *et al.*, p. 871, figs 13.17-13.19, 15.2-15.5.
vp 2008 *"Koninckites"* cf. *timorense* – Brühwiler *et al.*, p. 1165-1166, Pl. 3. 1-4, Pl. 4: 1.
non vp 2008 *"Koninckites"* cf. *timorense* – Brühwiler *et al.*, Pl. 4: 2.
2009 *Ussuridiscus varaha* – Shigeta & Zakharov, p. 69-73, figs 50.5, 50.6, 55-57.

Occurrence. – Sample Amb104 from the lowermost bed of LCL, Amb.
Measurements. – see Figs. 49, 53.
Discussion. – Our material only differs from that described by Shigeta & Zakharov (2009) in the suture line, which shows sub-phylloid saddles and finer crenulated lobes. These small differences may express intraspecific variability, which seems important according to the illustrations of Shigeta & Zakharov (2009). Note that this species is here restricted to a single bed of earliest Dienerian age, whereas in Primorye it occurs in five beds, in the equivalent of what we consider here to be the early and middle Dienerian. The synonymy list was also already discussed by Shigeta & Zakharov (2009). We confirm here that the specimens described by Brühwiler *et al.* (2008) under the name *"Koninckites"* cf. *timorense* correspond to this species, except one specimen which has a strigation on the venter and an unclear bottleneck shaped venter. *U. varaha* superficially resembles *U. ensanus* with which it shares the same shell proportions, but it clearly differs from this species by the shape of its whorl section, which has a thicker venter and nearly flat flanks unlike the typically sub-lanceolate whorl section of *U. ensanus*.

***Ussuridiscus ensanus* (Krafft, 1909)**

Pl. 3: 1; Pl. 28: 12-14; Pl. 29: 1-5; Figs. 49, 54

1909 *Aspidites ensanus* nov. sp. Krafft *in* Krafft & Diener, p. 56-57, pl. 5: 3-4, 5(lectotype), 6-7, pl. 6: 1, pl. 14: 6.
p? 1909 *Meekoceras varaha* – Diener *in* Krafft & Diener, p. 17, Pl. 2: 3.
p? 1909 *Meekoceras hodgsoni* – Krafft *in* Krafft & Diener, p. 26-28, pl. 30: 1.
1934 *Clypeoceras ensanum* – Spath, p. 160-161, pl. 12: 3 [cop. Krafft 1909].
? 1996 *Clypeoceras ensanum* – Waterhouse, p. 49-50, pl. 2: 16-20, pl. 3:1.

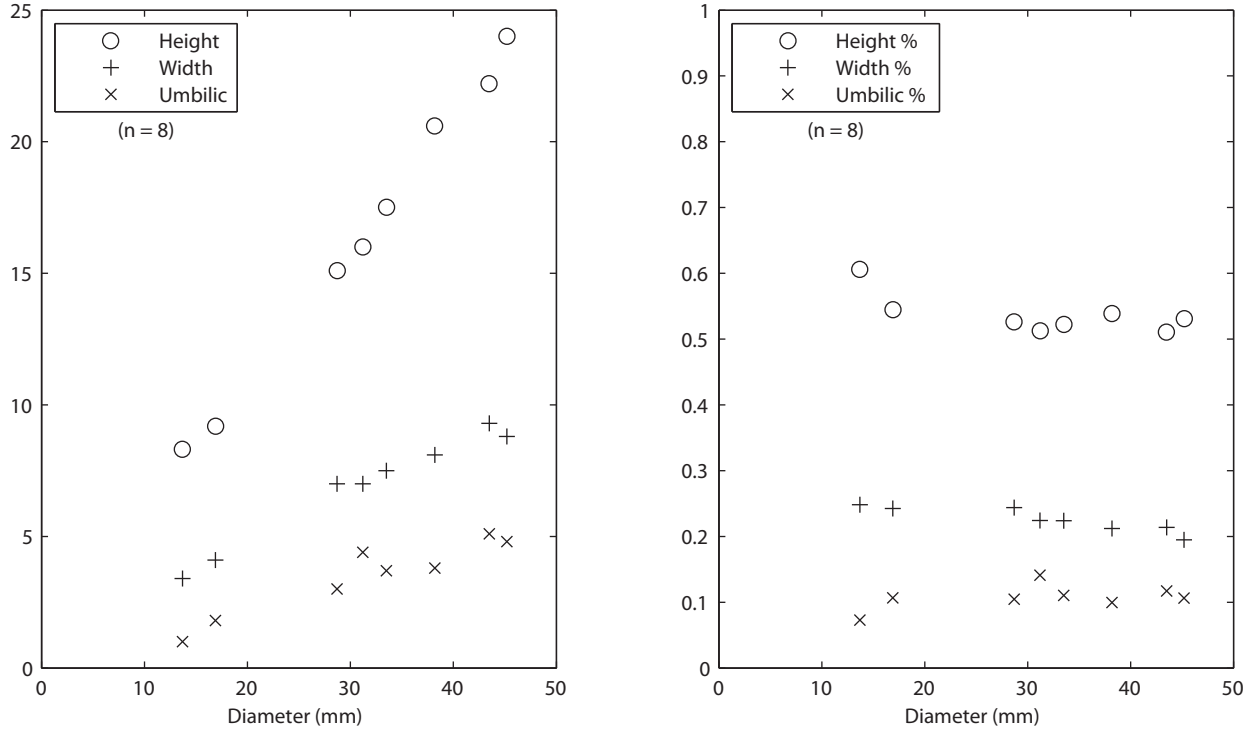

Fig. 53. Scatter diagrams of H, W, and U, and of H/D, W/D, and U/D for *Ussuridiscus varaha* (Diener, 1895).

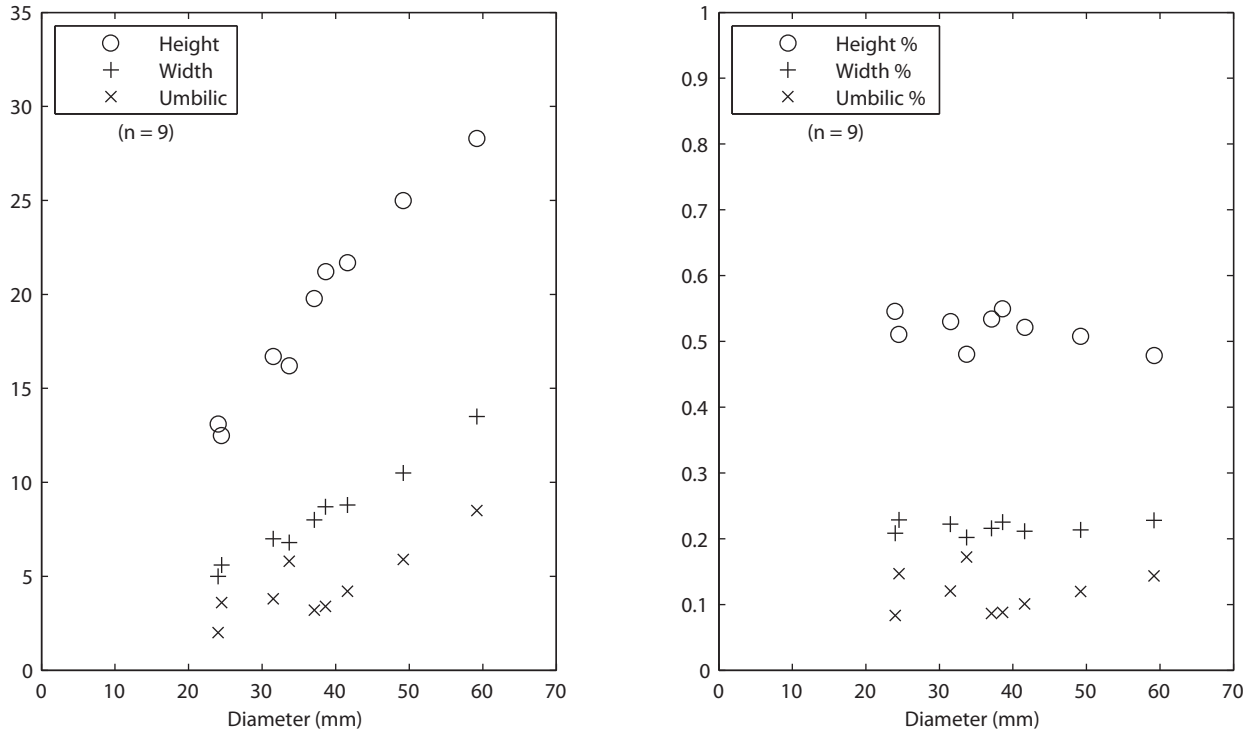

Fig. 54. Scatter diagrams of H, W, and U, and of H/D, W/D, and U/D for *Ussuridiscus ensanus* (Krafft, 1909).

Emended diagnosis. – Compressed (W/D ≈ 22%) *Ussuridiscus* with a narrowly tabulate venter, maximum whorl width at inner third of the whorl, the flanks being strongly convex on the inner half of the whorl and flat, converging towards the venter on the outer half, imparting the whorl section a very compressed sub-lanceolate shape. Suture line with a narrow and simple ventral lobe whose branches are very thin and pointed.

Occurrence. – Samples Nam339, Nam377, Nam378 and Nam393 from Nammal Nala, War9 and War100 from Wargal.

Description. – Involute (U/D ≈ 12 %), compressed (W/D ≈ 22 %, W/H ≈ 42 %) sub-oxyconic shell with a narrowly tabulate venter delimited by sharp ventro-lateral shoulders. Maximum whorl width at inner third of the whorl. The flanks are strongly convex in the inner half of the whorl section, while they become flat and finally converging towards the venter on the outer half, giving the whorl section a very compressed sub-lanceolate shape. Umbilical wall very short, overhanging with narrowly rounded umbilical shoulder. Umbilicus very narrow at small size, becoming slightly egressive from a diameter of ca. 4 cm onward. Sigmoid ribs following the trajectory of growth lines on the flanks, reaching their maximal strength on inner flank, fading towards the venter. Suture line with elongated lateral saddles, the two first ones being rounded or slightly tapered, the third one being flattened. Ventral lobe divided by a low ventral saddle. Its branches are very thin and simple, forming a small spike with occasional few very small indentations on the sides. Auxiliary series long, with a well differentiated auxiliary lobe followed by a series of irregular indentations.

Measurements. – see Figs. 49, 54.

Discussion. – The shell shape of our specimens is strictly identical to that of the holotype and other specimens figured by Krafft & Diener (1909). The only difference is found in the suture line. Their drawing shows that the lateral branches of the ventral lobe are bifid, whereas they are clearly pointed in our specimens. This small difference does not justify the erection of a new species. One specimen ascribed to *Meekoceras varaha* by Diener in Krafft & Diener (1909, Pl. 2: 3) may also belong to this species, but no firm assignment can be made as no ventral view is provided. One specimen assigned to *Meekoceras hodgsoni* by Diener in Krafft & Diener (1909, Pl. 30: 1) is here tentatively included in *U. ensanus* as it shares the same general shell outline, but it lacks the weak ornamentation and seems to have a clearly defined vertical umbilical wall with a sharp umbilical shoulder. The specimens ascribed by Waterhouse (1996) to this species are very poorly preserved for any tentative identification.

***Ussuridiscus ventriosus* sp. nov.**

Pl. 29: 10; Fig. 49

Derivation of name. – From the Latin *ventriosus*, meaning "potbellied", in reference to its thick venter.

Holotype. – Specimen PIMUZ30482 (Pl. 29: 8).

Type locality. – Nammal Nala, Salt Range, Pakistan.

Type horizon. – Sample Nam377 (middle LCL), *Gyronites plicosus* beds, early Dienerian.

Diagnosis. – *Ussuridiscus* with a thick venter and whorl section, without ornamentation.
Occurrence. – A single specimen from sample Nam377 from Nammal.
Description. –Very involute compressed sub-platyconic shell with broad tabulate venter and sharp ventro-lateral shoulders. Flanks slightly convex, with maximal whorl width at mid-flanks. The tabulate venter amounts to ca. 65% of the whorl width. Umbilicus narrow (U/D = 13 %), with a vertical umbilical wall and rounded umbilical shoulders. Shell smooth except for growth lines visible only near the umbilicus of the body chamber. Suture line with broad lateral lobes and saddles. Ventral lobe relatively broad, asymmetrical, with narrow branches having just two deep indentations on the right side and four small indentations on the other. Auxiliary series short, with a poorly individualised auxiliary lobe followed by a few regular indentations.
Measurements. – see table 1 and Fig. 49.
Discussion. – This specimen differs from all other species included here in *Ussuridiscus* by its thicker venter, its vertical umbilical wall, its absence of ornamentation and its suture line with a shorter auxiliary series. Its general outline is close to that of *Mu. shigetai*, but it differs clearly from this species by its less sharp ventro-lateral shoulders, its maximum width situated at mid-flanks, its rounded umbilical shoulder and, most importantly, its simpler suture line with less indentations and a ventral lobe with narrow branches. This last characteristic excludes its assignment to the genus *Mullericeras* and allows placing it within the genus *Ussuridiscus* despite the fact that it lacks the overhanging umbilical wall.

***Ussuridiscus ornatus* sp. nov.**

Pl. 29: 6-7; Fig. 49

p 1897 *Koninckites vidharba* nov. sp. Diener, p. 139-141, pl. 7: 8.
non 1897 *Koninckites vidharba* nov. sp. Diener, p. 139-141, pl. 7: 9 (holotype).
1909 *Aspidites vidharba* – Krafft *in* Krafft & Diener, p. 63-64, pl. 5: 1-2, pl. 14: 14.

Derivation of name. – Species name refers to the ornamentation of this species.
Holotype. – Specimen PIMUZ30481 (Pl. 29: 7).
Type locality. – Nammal Nala, Salt Range, Pakistan.
Type horizon. – Sample Nam377 (middle LCL), *Gyronites plicosus* beds, early Dienerian.
Diagnosis. – *Ussuridiscus* with a thin whorl section and thick, wavy convex ribs.
Occurrence. – Samples Nam377 from Nammal, War6 and War9 from Wargal.
Description. – Involute (U/D ≈ 12 %) compressed (W/D ≈ 22 %, W/H ≈ 43 %) sub-oxyconic shell with a tabulate venter and sharp ventro-lateral shoulders. Flanks convex with maximum width at or just below mid-flanks. Umbilical wall very short and overhanging, with a broadly rounded umbilical shoulder. Blunt convex ribs on mid-flanks, fading both on the outer half of the flanks and near the umbilical margin. Suture line with an arched outline and shallow lobes and short saddles. Lobes with very few small indentations. Auxiliary series long, with numerous irregular indentations and no auxiliary lobe. The holotype shows low and almost rectangular first two lateral saddles, the third one having a low dome outline. On the other specimen, the lateral saddles are more elongated, the two first ones being rounded and the third one being rectangular.
Measurements. – see table 1 and Fig. 49.
Discussion. – This species clearly differs from other species of *Ussuridiscus* by its strong ribbing. The specimens ascribed by Krafft & Diener (1909) to *Aspidites vidharba* are nearly identical with our specimens. They differ slightly by the position of their maximal whorl width, situated lower on the flanks, but this can possibly be interpreted as intraspecific variability. They related their specimens with one of the two specimens figured by Diener (1897, Pl. 7: 8) named *Koninckites vidharba*, and therefore kept this species name. However, Diener (1897) explicitly designated the specimen figured on Pl. 7: 9 as being the type of this species, and Krafft & Diener (1909) synonymised it with *Meekoceras hodgsoni*. Therefore, this species needed to be renamed. The illustration given by Diener (1897, Pl. 7: 8) does not really agree with our specimens, nor those of Krafft & Diener (1909) because of their nearly straight instead of convex ribs. However, Diener's (1897) description is perfectly in agreement with ours; therefore, we keep it provisionally in our synonymy list. It should be noted here that the type specimen of *Kon. vidharba* is a small and immature specimen, and that the illustration given by Diener (1897) is quite different from the illustration of the same specimen shown by Krafft & Diener (1909). It chiefly differs from our specimens by its larger umbilicus. As the type is such a small specimen, the species name *vidharba* is here considered as a *nomen dubium*.

***Ussuridiscus*? sp. indet.**

Pl. 29: 8-9; Fig. 49

Occurrence. – Sample Nam391 from Nammal.
Description. – Very involute (U/D ≈ 7 %), very compressed (W/D ≈ 20 %, W/H ≈ 36 %) platyconic shell with tabulate venter individualised by narrowly rounded ventro-lateral shoulders. Flanks nearly flat and sub-parallel with very weak sigmoid folds. Umbilicus very narrow, with an overhanging umbilical wall individualised by a sharp shoulder. Suture line simple, slightly different on the two specimens. The first one (Pl. 29: 8) has relatively

short and well rounded lateral saddles, while the second one (Pl. 29: 9) has more elongated saddles, the first one being rounded, the second one slightly bent towards the umbilicus. Its third lateral saddle is very small with a flattened top. Both specimens have a rather shallow ventral lobe, the branches of which are narrow and pointed, and a long auxiliary series with numerous irregularly spaced denticulations.
Measurements. – see table 1 and Fig. 49.
Discussion. – Since both specimens are incomplete, slightly distorted phragmocones, it is not possible to identify them with certainty. Their general shape, very involute with a tabulate venter and a narrow ventral lobe is in agreement with our definition of *Ussuridiscus*, which entails that these specimens are the oldest representatives of this genus in the Salt Range.

Family *incertae sedis*

Genus *Kingites* Waagen, 1895

Type species. – *Kingites lens* Waagen, 1895.
Composition of the genus. – *Kingites davidsonianus* (de Koninck, 1863), *Ki. korni* Brühwiler *et al.* 2010a.
Emended diagnosis. – Very involute, moderately compressed and discoidal shell with arched venter. Suture line with moderately deep lobes, a second saddle somewhat dorsally bent, a broad third lateral saddle with a rectangular outline. Lobes with numerous denticulations restricted to their base, and a rather long auxiliary series with an occasional poorly individualised auxiliary lobe.
Occurrence. – Late Dienerian and early Smithian of the Salt Range (Pakistan), Spiti valley (India) and Nepal.
Discussion. – This genus, originally ascribed to Meekoceratidae by Waagen (1895), has been placed in Paranoritidae by Spath (1934) and in Proptychitidae by Tozer (1994) who considered the two families as being synonyms. Here, we have brought evidence that Paranoritidae are not related to Proptychitidae but to Gyronitidae (see discussion on Paranoritidae above). There is no direct link between Paranoritidae and Proptychitidae. The genus *Kingites* should therefore belong to one of these two families. It is however very difficult to decide which one. Its general shape, with its broadly rounded venter, its absence of strigation and its ontogeny with very involute juvenile stages suggest affinity with compressed species of *Proptychites* such as *Pro. ammonoides*. On the other hand, its simple suture line without denticulation on the side of the lobes, its differentiated oblique umbilical wall and the presence of radial lirae suggest a connection with *Kon. khoorensis*, and thus to Paranoritidae, especially since some variants of the type species have a suture line very similar to Paranoritidae, with an auxiliary lobe (see below). In both case, it would imply a simplification of the suture line, although much stronger if considered as related to Proptychitidae rather than to Paranoritidae. Here, we decided to keep this genus in open classification. The type species of this genus is here synonymised with the species of de Koninck (1863), i.e. *Ceratites davidsonianus*. The species ascribed to this genus by Tozer (1994), *Ki. discoidalis* and *Ki. thulensis*, as well as *Ki. korostolevi* described by Zakharov (1978) and Dagys & Ermakova (1996) have a very narrowly rounded, almost acute venter, and a more complex suture line than the species here considered. Therefore, they must represent a distinct and probably new genus.

Kingites davidsonianus (de Koninck, 1863)

Pl. 30: 1-7; Pl. 31: 1-2; Fig. 55

1863 *Ceratites davidsonianus* nov. sp. de Koninck, p. 13, pl. 6: 2 (holotype).
1895 *Kingites lens* nov. gen. et sp. Waagen, p. 232-233, pl. 26: 4 (holotype).
1895 *Kingites declivis* nov. gen. et sp. Waagen, p. 233-235, pl. 26: 2 (holotype).
1934 *Koninckites davidsonianus* – Spath, p. 151-152, text-fig. 43a, pl. 5: 2 (holotype).
1934 *Koninckites occlusus* nov. sp. Spath, p. 154-155, pl. 5: 1 (holotype).
1934 *Kingites lens* – Spath, p. 157-158, fig. 45 [cop. Waagen 1895].
? 1996 *Kingites lens* – Waterhouse, p. 43, text-fig. 4E, pl. 2: 3.
1996 *Ceratites davidsonianus* – Waterhouse, p. 46, text-fig. 5 (holotype).
? 1996 *Aspitella crassa* – Waterhouse, p. 51, text-fig. 4I, pl. 3: 2-4.
1996 *Kingites elegans* nov. sp. Waterhouse, p. 73-74, text-fig. 10D, pl. 8: 4, 5, 9 (holotype), 6, 8, 10, 11.

Emended diagnosis. – *Kingites* with a narrow, generally funnel-shaped umbilicus and a suture line with occasional differentiated auxiliary lobe.
Occurrence. – Samples Amb64 from Amb, Nam58, Nam59, Nam61, Nam101d, Nam130 Nam313, Nam315, Nam336, Nam346 and Nam504 from Nammal Nala.
Description. – Very involute (U/D ≈ 9 %), moderately compressed (W/D ≈ 28 %, W/H ≈ 50 %) discoidal shell with broadly arched venter. Flanks slightly convex with maximal width between inner third and mid-flanks. Umbilical wall generally oblique, the umbilical seam being situated just above the umbilical shoulder of the preceding whorl, imparting the umbilicus a funnel shape. Umbilical shoulder sub-angular on the shell, more rounded on the inner mould. Some specimens have a sub-vertical umbilical wall. Just after the neanic stage, the juveniles become rapidly very involute to

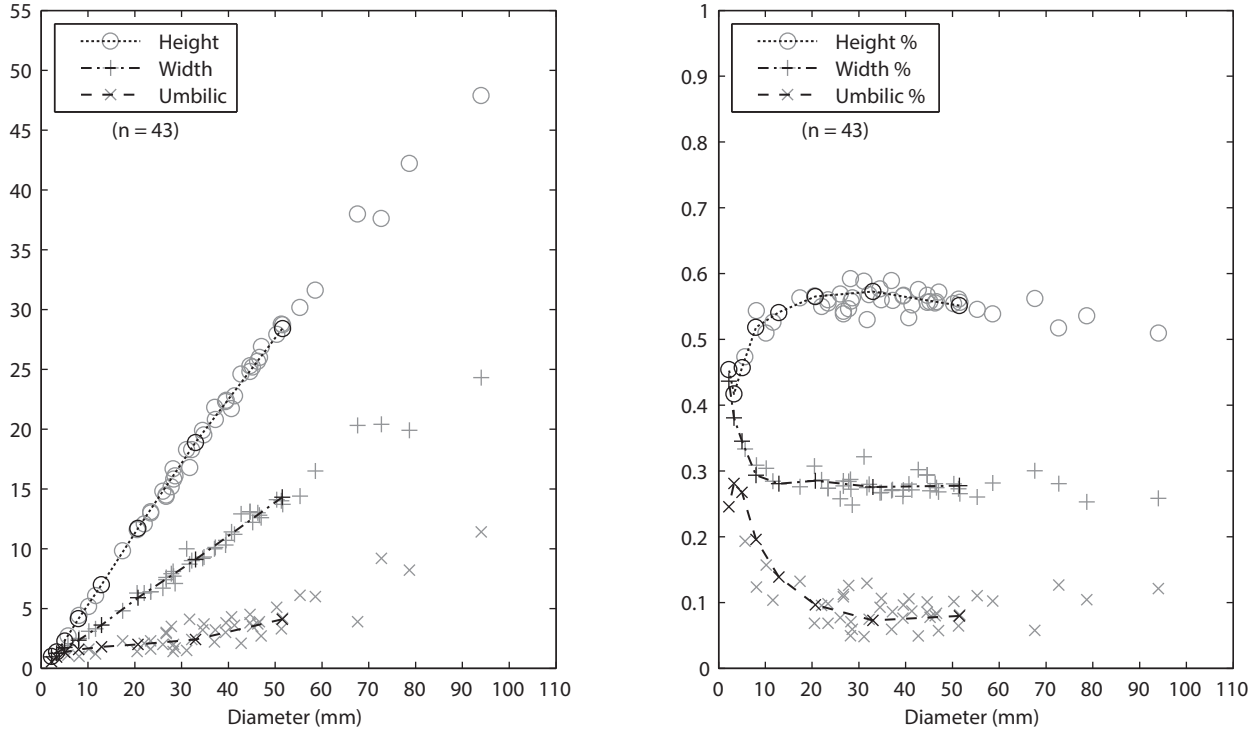

Fig. 55. Scatter diagrams of H, W, and U, and of H/D, W/D, and U/D for *Kingites davidsonianus* (de Koninck, 1863). Ontogenetic trajectories obtained from sectioned specimen illustrated on Pl. 30: 8 are shown in black.

reach sub-mature proportions at a diameter of ca. 20 mm. Some large specimens have a slight egression of the adult body chamber. Ornamentation nearly absent, with slightly sigmoid very thin radial lirae and sometimes very vague folds following the trajectory of the lirae. Suture line with moderately deep lobes and elongated saddles, lobes having small indentations at their base. Second lateral saddle slightly bent dorsally, third lateral saddle sub-rectangular, as broad as or broader than high. Auxiliary series long, with small irregular indentations. Poorly individualised auxiliary lobe only occasional.

Measurements. – see Fig. 55.

Discussion. – The type species of *Kingites*, *Ki. lens*, was originally based on one single, relatively well preserved specimen which is here re-illustrated (Pl. 30: 2). Waagen did not have access to the types of de Koninck, and thus could not notice the similarity of his specimen with *Ceratites davidsonianus* as established by de Koninck (1863). The drawing of de Koninck is merely a sketch and the suture line is not reliably drawn, especially the third lateral saddle which has been re-illustrated by Spath (1934) and Waterhouse (1996). This specimen was considered by Spath (1934) as a representative of *Koninckites*, an erroneous assignment first pointed out by Waterhouse (1996). The different species here synonymised with *Ki. davidsonianus* differ merely by small differences in their auxiliary series and their more or less oblique umbilical wall. These differences are here shown to be part of intraspecific variability. The specimens ascribed to *Ki. lens* and *Aspitella crassa* by Waterhouse (1996) are too poorly preserved to be clearly assigned to the present species. *Ki. davidsonianus* looks superficially similar to *Pro. ammonoides*, but can easily be differentiated by its much more simple suture line and its individualised umbilical wall. It also resembles closely to involute variants of the co-occurring *Kon. khoorensis*, especially variants with a differentiated auxiliary lobe, but can be distinguished by its stronger involution and the absence of strigation on its venter. One specimen (Pl. 31: 1) has its lower jaw preserved almost *in situ* at the beginning of its body chamber.

Kingites korni Brühwiler, Ware, Bucher, Krystyn & Goudemand, 2010a

Pl. 31: 3; Fig. 56

v 2010a *Kingites korni* nov. sp. Brühwiler *et al.*, p. 734, fig. 15 (holotype).
v 2010a *Kingites parkashi* nov. sp. Brühwiler *et al.*, p. 734, fig. 16 (holotype).
v 2012 ?*Kingites parkashi* – Brühwiler *et al.*, p. 53, fig. 36E-I.

Occurrence. – Samples Chi51 from Chiddru, Nam70 and Nam305 from Nammal Nala.

Description. – Extremely involute, discoidal to sub-oxyconic shell with occluded umbilicus and rounded venter. Flanks slightly convex, with maximal width at inner third or mid-flank. Surface smooth apart for very vague sigmoid folds following the trajectory of the growth lines. Suture line with relatively shallow lobes

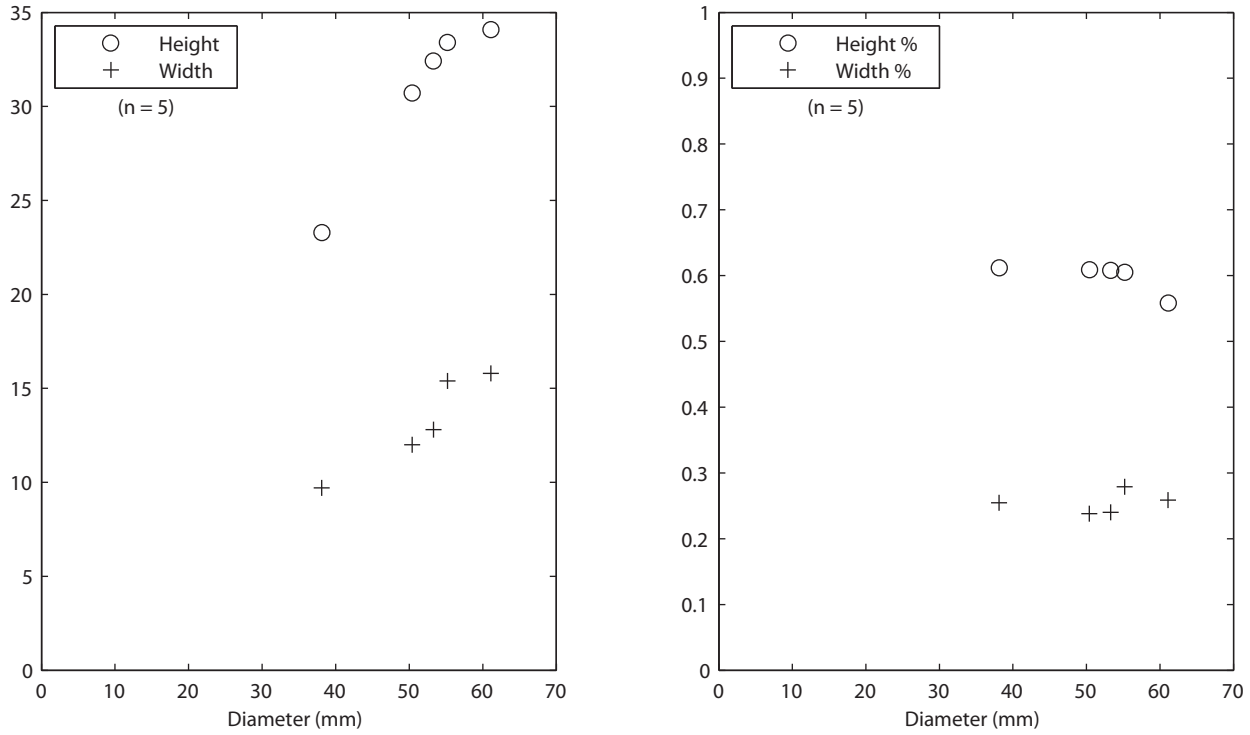

Fig. 56. Scatter diagrams of H and W, and of H/D and W/D for *Kingites korni* Brühwiler, Ware, Bucher, Krystyn & Goudemand, 2010a.

and short saddles, the third lateral saddle being low and sub-rectangular. Lateral and ventral lobes with few indentations at their base. Auxiliary series long, with numerous irregular indentations, but no clearly differentiated auxiliary lobe.
Measurements. – see Fig. 56.
Discussion. – The two new species originally described by Brühwiler *et al.* (2010a) were based on very few specimens. They were considered as different on the basis of their whorl section, with more convergent flanks and a more narrowly rounded venter in *Ki. parkashi* than in *Ki. korni*. The specimens from the Salt Range show all intermediate shapes between these two species. Therefore, they should be treated as synonyms. The specimen here figured is an inner mould, its umbilicus appears thus to be open, but it is in reality closed by a thickening of the shell on the umbilical wall. *K. korni* superficially resembles *Pro. pagei*, from which it differs by its much more simple suture line with fewer indentations and shorter lobes and saddles.

Superfamily Sageceratacеae Hyatt, 1884
Family Hedenstroemiidae Hyatt, 1884
Genus *Clypites* Waagen, 1895

Type species. – *Clypites typicus* Waagen, 1895.
Composition of the genus. – Type species only.
Emended diagnosis. – Very involute, moderately compressed, sub-oxyconic shell with occluded umbilicus. Venter tabulate, with sharp ventro-lateral shoulders at small size, becoming rounded on the body chamber of large specimens (i.e. at D ≥ 7 cm). Suture line with a poorly developed adventive series visible only on small sized specimens, disappearing at a diameter of ca. 5 cm and composed of only one adventive lobe and no adventive saddles.
Occurrence. – Late Dienerian of the Salt Range (Pakistan), Dienerian of South Primorye (Russia) and Guangxi (China).
Discussion. – This genus clearly differs from *Pseudosageceras* by its broader venter and simpler suture line. The suture line is close to that of involute forms of Meekoceratacеae such as Mullericeratidae but differs by the presence of an adventive lobe in small specimens. This similarity suggests that Hedenstroemiidae root into Mullericeratidae, *Clypites* being the link between the two families. A derivation from Prolecanitida or Otoceratacеae as suggested by other authors (e.g. Spath, 1934, Arkell *et al.*, 1957, Tozer, 1981) is consequently rejected.

Clypites typicus Waagen, 1895

Pl. 31: 4-7; Pl. 32: 1-2; Figs. 49, 57

1895 *Clypites typicus* nov. gen. et sp. Waagen, p. 143-144, pl. 21: 7 (lectotype).
1895 *Clypites kingianus* nov. gen. et sp. Waagen, p. 144-146, pl. 21: 8 (lectotype), Pl. 22: 3.
1895 *Clypites evolvens* nov. gen. et sp. Waagen, p. 146-148, pl. 22: 2(lectotype).

non 1905 *Clypites evolvens* – Noetling, pl. 23:3.
1934 *Clypites typicus* – Spath, p. 220, fig. 69 [cop. Waagen 1895].
? 2008 *Clypites* sp. indet. – Brayard & Bucher, p. 72, pl. 38: 1-4.
2009 *Clypeoceras spitiense* – Shigeta & Zakharov, p. 125-126, fig. 113-114.
non 2010a *Clypites typicus* – Brühwiler *et al.*, p. 736-737, fig. 21.

Emended diagnosis. – As for the genus.
Occurrence. – Samples Amb65 from Amb, Nam61, Nam62, Nam70, Nam83, Nam130, Nam305, Nam312, Nam319 and Nam349 from Nammal Nala and War104 from Wargal.
Description. – Very involute, moderately compressed (W/D ≈ 25%) sub-oxyconic shell with a broad tabulate venter and slightly convex flanks giving the whorl section an elongated and sub-trapezoidal shape with maximal width at the inner third of the flanks. Some specimens have a very low, broad keel as in *Mu. spitiense*, their venter being then close to tectiform. Ventro-lateral shoulders very sharp in small specimens, becoming rounded on the body chamber of large specimens. Umbilicus occluded, with a strong thickening of the shell similar to that observed in *Pseudosageceras simplelobatum* (see below). Umbilical wall vertical and well differentiated, visible only on inner moulds. Surface nearly smooth, with only low sigmoid folds following the trajectory of the growth lines. Some specimens have one to three very faint spiral folds on the outer half of the flanks (e.g. Pl. 32: 1). Suture line with deep lobes and elongated saddles and a poorly developed adventive series with only one adventive lobe which disappears at large size (D ≥ 5cm, but the diameter at which it disappears is most probably subject to intraspecific variability). One specimen (Pl. 31: 6) with a very asymmetric suture line also has an adventive saddle on its right side. Lobes have three to six deep indentations. Lateral saddles narrow and elongated, the second and third being bent dorsally. Long auxiliary series with one individualised auxiliary lobe followed by a long, rather regular series of indentations.
Measurements. – see Figs. 49, 57.
Discussion. – Due to the disappearance of the adventive series, large specimens are nearly identical to *Mu. spitiense*, from which they then differ only by their larger size, more elongated saddles and slightly more developed auxiliary series. Waagen (1895) initially erected three different species which are here considered as synonyms. *C. kingianus* is nearly identical to the holotype of *C. typicus*, the small differences noted by Waagen being just the result of its larger size. *C. evolvens* looks different at first sight, but its open umbilicus is probably a preservation bias, as its outer whorl is an internal mould (unlike the specimens of the two other species he describes), the umbilical lid being not preserved and therefore revealing an open umbilicus. The specimens assigned by Brayard & Bucher (2008) to *C.* sp. indet. are close to this species, but as mentioned by the authors, they are too poorly preserved to be identified with confidence. The specimen ascribed

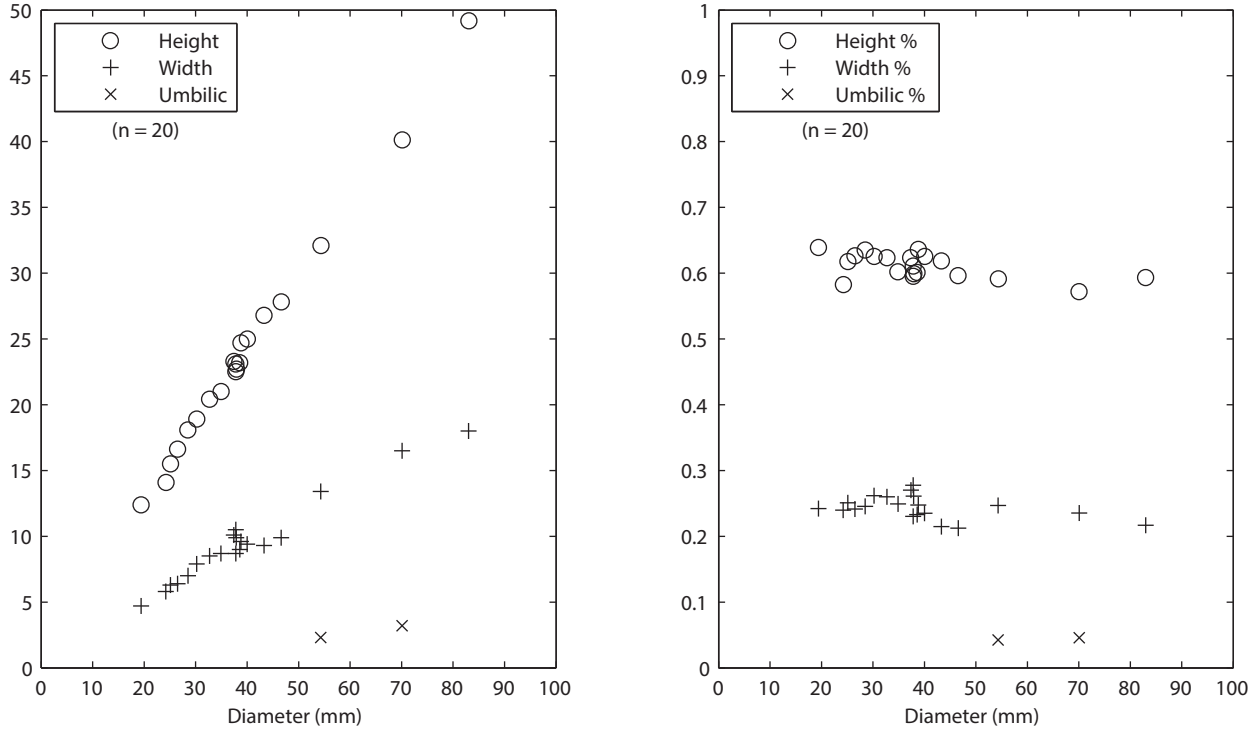

Fig. 57. Scatter diagrams of H, W, and U, and of H/D, W/D, and U/D for *Clypites typicus* Waagen, 1895. The two values for the umbilicus width were measured on internal moulds, the umbilicus being otherwise closed by an umbilical lid.

by Shigeta & Zakharov (2009) to *Clypeoceras spitiense* is here assigned to *C. typicus* as its suture line has a very long and well developed auxiliary series and more importantly, a slightly differentiated adventive lobe.

Genus *Pseudosageceras* Diener, 1895

Type species. – *Pseudosageceras* sp. indet. Diener, 1895.

***Pseudosageceras simplelobatum* sp. nov.**

Pl. 32: 3-6; Pl. 33: 1-4; Figs. 49, 58-59

1909 *Hedenstroemia lilangense* nov. sp. Krafft *in* Krafft & Diener, p. 151-152, pl. 9: 1.
? 1985 *Pseudosageceras mulilobatum* – Pakistani-Japanese Research Group, pl. 12: 5-7, pl. 14: 3, 6.
? 1994 *Tellerites* sp. indet. – Tozer, p. 84, pl. 20: 10.
1996 *Lilastroemia lilangensis* gen. et sp. nov. Waterhouse, p. 76-77.
non 1996 *Lilastroemia lilangensis* gen. et sp. nov. Waterhouse, Text-fig. 10E, pl.9: 13, 16, 17.
2010a *Clypites typicus* – Brühwiler *et al.*, p. 736-737, fig. 21.

Derivation of name. – from the Latin *simplex* and *lobatum*, meaning "simple" and "lobe", in reference to its suture line which is simpler than that of other species of *Pseudosageceras*.
Holotype. – Specimen PIMUZ30506 (Pl. 33: 1).
Type locality. – Nammal Nala, Salt Range, Pakistan.
Type horizon. – Sample Nam346 (lower CM, ca. 6 m above base), top of *Kingites davidsonianus* beds, late Dienerian.
Diagnosis. – *Pseudosageceras* characterised by a relatively simple suture line, with only two adventitious saddles and one auxiliary lobe at maturity. Lobes and saddles relatively wide and not very elongated.
Occurrence. – Samples Chi51, Chi61, Chi105 from Chiddru, Nam61, Nam62, Nam63, Nam67, Nam83, Nam101d, Nam130, Nam319, Nam336, Nam337, Nam349, Nam350, Nam502, Nam724 from Nammal and War104 from Wargal.
Description. – Very involute, compressed oxyconic shell with a narrow concave, bicarinate venter and weakly convex flanks conferring the whorl section an elongated sub-trapezoidal shape with maximal width close to the umbilical wall. Umbilicus occluded by an umbilical lid visible on the specimen which has been cut to study its ontogeny (Pl. 33: 2). Its shell thickens towards the umbilicus and forms an extension which almost closes the umbilicus. On the internal mould, the umbilical shoulder is rounded and grades into a vertical umbilical wall. The shell reaches its typical oxyconic shape at a diameter of about 1 cm. From there on, its morphology barely changes, the umbilicus relative width (here measured below the umbilical lid) increasing slightly, from 2.9% at a diameter of 15.4 mm to 6% at D = 83.3 mm. Surface almost smooth, with very weak and broad folds following the trajectory of the sigmoid growth lines. One

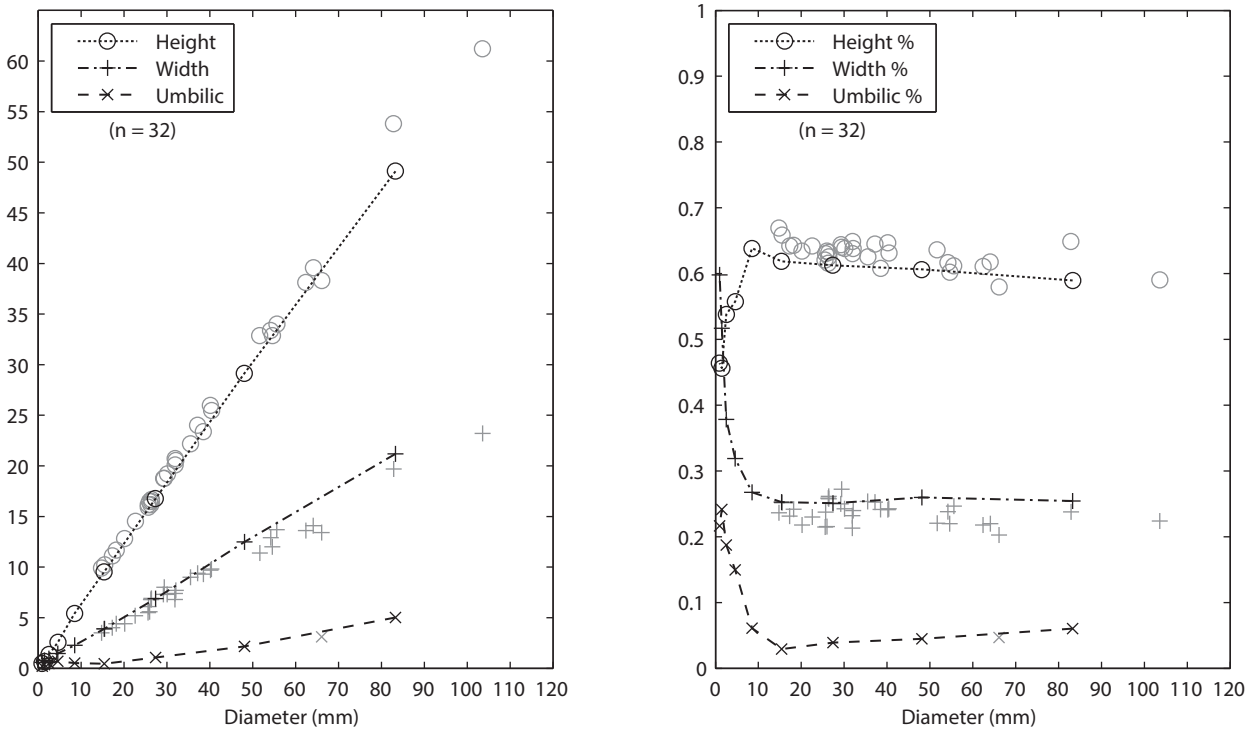

Fig. 58. Scatter diagrams of H, W, and U, and of H/D, W/D, and U/D for *Pseudosageceras simplelobatum* sp. nov.. Ontogenetic trajectories obtained from sectioned specimen illustrated on Pl. 33: 2 are shown in black. In addition to the ontogenetic trajectory of the sectioned specimen, a single additional value for the umbilicus width was measured on an internal mould, the umbilicus being otherwise occluded.

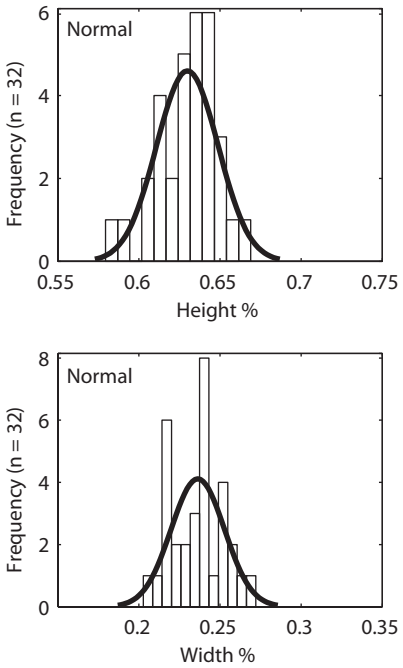

Fig. 59. Histograms of H/D and W/D for *Pseudosageceras simplelobatum* sp. nov.

specimen (Pl. 33: 4) shows a very faint strigation on the inner mould of its body chamber. Suture line typical of the genus, with a trifid first lateral lobe and a well developed adventive series including two adventive saddles. The second lateral lobe becomes bifid in large specimens, the adventive and auxiliary lobes bear only simple indentations. Lateral lobes and saddles broad, the lateral saddles being elongated and bent towards the umbilicus. Auxiliary series very well developed with only one weakly discernible auxiliary lobe followed by a long, rather regular series of indentations.

Measurements. – see Fig. 49, 58-59.

Discussion. – As the name given by Krafft (1909) to this species is preoccupied by *Ambites lilangensis* (Krafft 1909), we decided here to give it a new name to avoid confusion with this species which can also be found in the Dienerian. This species differs from all other known species of *Pseudosageceras* by its simpler suture line with only two adventive saddles and one auxiliary lobe, the auxiliary lobes and saddles being not bifid, with broader and less elongated lateral saddles. The overall shape of the suture line is closer to that of involute representatives of Meekoceratacеae (e.g. Mullericeratidae) than to that of other species of the same lineage (e.g. other species of *Pseudosageceras* or *Cordillerites*). It also differs by its ornamentation, which is very weak, all other species referred to the genus being smooth. This ornamentation is also reminiscent of the weak ornamentation of involute forms of Meekoceratacеae, which brings additional support to a derivation of *Pseudosageceras* from Meekoceratacеae via Mullericeratidae. The presence of an umbilical lid is here reported for the first time among hedenstroemiids, but as only one specimen has been sectioned, it is not possible to decide whether this is a characteristic trait of the species, genus or even family or if it is present in only some specimens. The specimens described as *H. lilangense* by Krafft (1909; for which Waterhouse created the new genus *Lilastroemia*) and as *Clypites typicus* by Brühwiler *et al.* (2010a) both show a clear trifid first lateral lobe and therefore must be assigned to *Pseudosageceras*. Their suture lines show some small differences compared to the ones figured here, with a less developed adventive series and an auxiliary series with slightly more differentiated lobes and saddles. These small differences are here interpreted as intraspecific variability. The specimens assigned to *L. lilangensis* by Waterhouse (1996) do not show any adventive lobes and saddles, and are therefore closer to Mullericeratidae than to *H. lilangense*. The specimens referred to as *Pseudosageceras multilobatum* by the Pakistani-Japanese Research Group, which come from the LCL of Chiddru and are therefore Dienerian in age, most probably belong to our new species. Because their suture line is not illustrated, a definitive assignment must be left open. The specimen described by Tozer 1994 as *Tellerites* sp. indet., which is also of late Dienerian age, could belong to this species as suggested by its apparently simple suture line. However, it is too poorly preserved for any further comparison. This species is the oldest representative of this genus described so far, with the possible exception of one extremely poorly preserved specimen described by Waterhouse (1994, p. 49, Pl. 2 fig. 16). Waterhouse's specimen is too much weathered to be assigned to any taxon. The vague trace of suture line on which this identification was based could well be the imprint of the dorsal part of suture of the missing subsequent whorl.

Superfamily *incertae sedis*
Family *incertae sedis*

Genus *Subacerites* gen. nov.

Derivation of name. – from the Latin prefix *sub-*, meaning "almost", and the Latin word *acer*, meaning "sharp", in reference to its almost acute venter.

Type species. – *Subacerites friski* sp. nov.

Composition of the genus. – Type species only.

Diagnosis. – Very involute compressed oxyconic shell with occluded umbilicus, characterised by its extremely narrowly tabulate, almost acute venter. Suture line without adventive series and with a long auxiliary series comprising one auxiliary lobe.

Occurrence. – Late Dienerian of Amb, *Kingites davidsonianus* beds.

Discussion. – This new genus is based on only a single specimen found in Amb. Its morphology is very close to

the genus *Parahedenstroemia* Spath, 1934, but it differs from the latter by its narrowly tabulate venter and, more importantly, by the absence of adventive lobes and saddles. This last trait excludes it from Hedenstroemiidae. It differs from Mullericeratidae also by its peculiar ventral lobe, by its very narrowly elongated ventral saddle, and by the absence of differentiated umbilical wall. As this genus is defined on a single specimen, we prefer here to keep its systematic position open. More material would be necessary to assess its intraspecific variability and eventually unravel its affinity.

***Subacerites friski* sp. nov.**

Pl. 33: 5

Derivation of name. – named after Dr. Åsa Marianne Frisk.
Holotype. – Specimen PIMUZ30510 (Pl. 33: 5).
Type locality. – Amb, Salt Range, Pakistan.
Type horizon. – Sample Amb3 (lower CM, ca. 4 m above base), *Kingites davidsonianus* beds, late Dienerian.
Diagnosis. – As for the genus.
Occurrence. – One single specimen from sample Amb3 from Amb.
Description. – Very involute compressed oxyconic shell with occluded umbilicus. Venter extremely narrow and tabulate, almost acute, delimited by sharp ventro-lateral shoulders which become narrowly rounded on the body chamber. Flanks convex, with maximum width at mid-flanks. Umbilicus occluded by a thickening of the shell. On the internal mould, flanks slope gently towards the umbilicus, without forming a distinct umbilical wall. Very weak ornamentation on the flanks, consisting of very low sinuous radial folds parallel to growth lines. An extremely faint strigation is visible only on the inner mould of the body chamber, on the outer and inner third of the flanks. Growth lines prorsiradiate and sinuous, being slightly offset on the outer flanks. Suture line with a peculiar ventral lobe, divided by a very narrow and elongated ventral saddle, and with broad and shallow branches having numerous, regular and small indentations. These indentations are aligned almost perpendicularly to the ventral edge. Lateral saddles short with rounded tips, lateral lobes with a small number of large indentations. Auxiliary series long, with one poorly individualised auxiliary lobe followed by a long series of irregular indentations.
Measurements. – see table 1.
Discussion. – As for the genus.

Gen. et sp. indet.

Pl. 33: 6

Occurrence. – One single specimen from sample Amb104 from Amb.
Description. – Very involute, sub-oxyconic internal mould with tabulate venter. Its umbilicus is very narrow, most likely occluded by a thickened outer shell. Flanks flat, converging towards the venter, imparting the whorl section a trapezoidal shape. No ornamentation visible on the internal mould. Its suture line is peculiar, very complex for such a small sized individual. Its ventral lobe is divided by a wide ventral saddle and a deep indentation occurs between the ventral saddle and the long, narrow and bifid branch of the ventral lobe, thus individualizing an adventive saddle. The lateral saddles are very narrow and elongated. The first one is straight, subphylloid and asymmetric, almost pointed. The second one is very long and strongly bent dorsally. The third one is also elongated, bent towards the umbilicus with a flattened tip. The first lateral lobe is thin, deep and bifid. The second one has a broad base, and lateral indentations on both sides individualize an elongated deep and bifid indentation. The auxiliary series is also very unusual, with a poorly individualised auxiliary lobe. Instead of the usual pointed indentations, a series of smooth undulations confers the auxiliary series a goniatitic pattern.
Discussion. – The outline of this shell is very close to that of *Pseudosageceras*, but its suture line prevents assignment to this genus, as it lacks the diagnostic trifid second lateral lobe of *Pseudosageceras*. The presence of an adventive saddle may indicate that it belongs to Hedenstroemiidae, but its peculiar second lateral lobe and goniatitic auxiliary series is very different from any species belonging to this group or from any other Dienerian ammonoid group. Considering that we have only one, small and fully septate specimen, we prefer to keep it here in open nomenclature. Additional larger specimens would be necessary to know if it is really a Hedenstroemiidae, if it is a new group converging towards Hedenstroemiidae, or if its peculiar suture line is induced by a pathology of some sort.

Acknowledgements

James M. Neenan (Zürich) improved the English text of an earlier version. Claude Monnet (Lille) is thanked for providing his statistical analyses software. Nicolas Goudemand (Zürich) and Séverine Urdy (Zürich) are thanked for their help with Matlab. Mike Orchard (Geological Survey of Canada, Vancouver) is thanked for providing access to the collections and archives of E.T. Tozer. Technical support for preparation and photography was provided by Markus Hebeisen and Rosemarie Roth (Zürich). This work is a contribution to the Swiss National Science Foundation project 200021-135446 to H.B. Publication costs were covered by the Swiss National Science Foundation.

References

Agassiz, L. 1847: Lettres sur quelques points d'organisation des animaux rayonnés. *Comptes Rendus de l'Académie des Sciences*, *25*, 677-682.

Arkell, W.J., Kummel, B. & Wright, C.W. 1957: Mesozoic Ammonoidea,. *In* Arkell, W.J., Furnish, W.M., Kummel, B., Miller, A.K., Moore, R.C., Schindewolf, O.H., Sylvester-Bradley, P.C. & Wright, C.W. (eds): *Treatise on Invertebrate Paleontology, Part L, Mollusca 4: Cephalopoda, Ammonoidea,* 80-436. Geological Society of America and the University of Kansas Press, Lawrence.

Arthaber, G.V. 1911: Die Trias von Albanien. *Beiträge zur Paläontologie und Geologie Österreich-Ungarns und des Orients 24*, 169-276.

Bando, Y. 1981: Lower Triassic Ammonoids from Guryul Ravine and the Spur three kilometres north of Burus. *In* Nakazawa, K. & Kapoor, H. M. (eds): *The Upper Permian and Lower Triassic faunas of Kashmir*. *Palaeontologia Indica 46*, 135-178.

Bengtson, P. 1988: Open nomenclature. *Palaeontology 31*, 223-227.

Brayard, A. & Bucher, H. 2008: Smithian (Early Triassic) ammonoid faunas from northwestern Guangxi (South China): taxonomy and biochronology. *Fossils and Strata 55*, 179 pp.

Brayard, A., Bucher, H., Escarguel, G., Fluteau, F., Bourquin, S. & Galfetti, T. 2006: The Early Triassic ammonoid recovery: Paleoclimatic significance of diversity gradients. *Palaeogeography, Palaeoclimatology, Palaeoecology 239*, 374-395.

Brayard, A., Escarguel, G., Bucher, H., Monnet, C., Brühwiler, T., Goudemand, N., Galfetti T. & Guex, J. 2009: Good Genes and Good Luck: Ammonoid Diversity and the End-Permian Mass Extinction. *Science 325*, 1118-1121.

Brosse, M., Brayard, A., Fara, E. & Neige, P., 2013. Ammonoid recovery after the Permian-Triassic mass extinction: a re-exploration of morphological and phylogenetical diversity patterns. *Journal of the Geological Society, London 170*, 225-236.

Brühwiler, T., Brayard, A., Bucher, H. & Guodun, K. 2008: Griesbachian and Dienerian (Early Triassic) Ammonoid Faunas from Northwestern Guangxi and Southern Guizhou (South China). *Palaeontology 51*, 1151-1180.

Brühwiler, T., Ware, D., Bucher, H., Krystyn, L. & Goudemand, N. 2010a: New Early Triassic ammonoid faunas from the Dienerian/Smithian boundary beds at the Induan/Olenekian GSSP candidate at Mud (Spiti, Northern India). *Journal of Asian Earth Sciences 39*, 724-739.

Brühwiler, T., Bucher, H., Brayard, A. & Goudemand, N. 2010b: High-resolution biochronology and diversity dynamics of the Early Triassic ammonoid recovery: The Smithian faunas of the Northern Indian Margin. *Palaeogeography, Palaeoclimatology, Palaeoecology 297*, 491-501.

Brühwiler, T., Bucher, H., Ware, D., Schneebeli-Hermann, E., Hochuli, P.A., Roohi, G., Rehman, K. & Yaseen, A. 2012: Smithian (Early Triassic) ammonoids from the Salt Range, Pakistan. *Special Papers in Palaeontology 88*, 1-114.

Checa, A.G. & Garcia-Ruiz, J.M. 1996: Morphogenesis of the Septum in Ammonoids. *In* Landman, N.H., Tanabe, K. & davis, R.A. (eds): *Ammonoid Paleobiology*, 253-296. Plenum Press, New York and London.

Cuvier, G.L.C.F.D. An 6 [1797]: *Tableau élémentaire de l'histoire naturelle des animaux*, *14*, 710 pp. Baudouin, Paris.

Dagys, A. S. & Ermakova, S. 1996: Induan (Triassic) ammonoids from North-Eastern Asia. *Revue de Paléobiologie 15*, 401-447.

Diener, C. 1895: Triadische Cephalopodenfaunen der Ostsibirischen Küstenprovinz. *Mémoires du Comité Géologique St. Pétersbourg 14*, 1-59.

Diener, C. 1897: Part I: The Cephalopoda of the Lower Trias. *Palaeontologia Indica, Series 15*. *Himalayan fossils 2*, 1-181.

Diener, C. 1916: Einige Bemerkungen zur Nomenklatur der Triascephalopoden. *Centralblatt für Mineralogie, Geologie und Palaeontologie*, 97-105.

Frech, F. 1902: Die Dyas: Lethaea geognostica. Theil 1. *Lethaea Palaeozoica 2*, 579-788.

Goudemand, N., Orchard, M., Bucher, H., Brayard, A., Brühwiler, T., Galfetti, T., Hochuli, P.A., Hermann, E. & Ware, D. 2008: Smithian-Spathian boundary: The biggest crisis in Triassic conodont history. *Abstracts with Program, Geological Society of America 40*, 505.

Griesbach, C.L. 1880: Palaeontological notes on the Lower Trias of the Himalayas. *Records of the Geological Survey of India 13*, 94-113.

Guex, J. 1978: Le Trias inférieur des Salt Ranges (Pakistan): problèmes biochronologiques. *Eclogae Geologia Helvetica 71*, 105-141.

Guex, J. 1991: *Biochronological Correlations*, Springer, Berlin, 252 pp.

Hammer, Ø., Harper, D.A.T. & Ryan, P.D. 2001: PAST: Paleontological statistics software package for education and data analysis. *Palaeontologia Electronica 4 (1)*: 9pp.

Hermann, E., Hochuli, P.A., Bucher, H., Brühwiler, T., Hautmann, M., Ware, D. & Roohi, G. 2011a: Terrestrial ecosystems on North Gondwana following the end-Permian mass extinction. *Gondwana Research 20*, 630-637.

Hermann, E., Hochuli, P.A., Méhay, S., Bucher, H., Brühwiler, T., Ware, D., Hautmann, M., Roohi, G., ur-Rehman, K. & Yaseen, A. 2011b: Organic matter and palaeoenvironmental signals during the Early Triassic biotic recovery: The Salt Range and Surghar Range

records. *Sedimentary Geology 234*, 19-41.

Hermann, E., Hochuli, P.A., Bucher, H., Brühwiler, T., Hautmann, M., Ware, D., Weissert, H., Roohi, G., Yaseen, A. & ur-Rehman, K. 2012a: Climatic oscillations at the onset of the Mesozoic inferred from palynological records from the North Indian Margin. *Journal of the Geological Society, London 169*, 227-237.

Hermann, E., Hochuli, P.A., Bucher, H. & Roohi, G. 2012b: Uppermost Permian to Middle Triassic palynology of the Salt Range and Surghar Range, Pakistan. *Review of Palaeobotany and Palynology 169*, 61-95.

Hyatt, A. 1884: Genera of fossil cephalopods. *Proceedings of the Boston Society of Natural History 22*, 253-338.

Hyatt, A. 1900: Cephalopoda. *In* Zittle, K.A.V. (ed): *Textbook of palaeontology vol. 1*, 502-604. C.R. Eastman, London.

Kiparisova, L.D. & Popov, Y.N. 1956: Subdivision of the lower series of the Triassic system into stages. *Doklady Academy Sciences U.S.S.R. 109*, 842-845 [In Russian].

Kiparisova, L.D. 1961: Paleontological fundamentals for the stratigraphy of Triassic deposits of Primorye region. 1. Cephalopod Mollusca. *Trudy Vsyesoyuzhogo Nauchno-isslyedovatyel'skogo Geologichyeskogo Instityta (VSEGEI). Novaya seriya 48*, 1-278 [In Russian].

de Koninck, L.G. 1863: Description of some fossils from India, discovered by Dr. A. Fleming, of Edinbourg. *The Quaterly Journal of the Geological Society of London 19*, 1-19.

Krafft, A.V. & Diener, C. 1909: Lower Triassic cephalopoda from Spiti, Malla Johar, and Byans. *Palaeontologia Indica 6*, 1-186.

Krystyn, L., Balini, M. & Nicora, A. 2004: Lower and Middle Triassic stage and substage boundaries in Spiti. *Albertiana 30*, 40-53.

Krystyn, L., Bhargava, O.N. & Richoz, S. 2007a: A candidate GSSP for the base of the Olenekian Stage: Mud at Pin Valley; district Lahul & Spiti, Himachal Pradesh (Western Himalaya), India. *Albertiana 35*, 5-29.

Krystyn, L., Richoz, S. & Bhargava, O.N. 2007b: The Induan-Olenekian Boundary (IOB) in Mud – an update of the candidate GSSP section M04. *Albertiana 36*, 33-45.

Kummel, B. 1966: The Lower Triassic Formations of the Salt Range and Trans-Indus Ranges, West Pakistan. *Bulletin of the Museum of Comparative Zoology 134*, 361-429.

Kummel, B. 1970: Ammonoids from the Kathwai Member, Mianwali Formation, Salt Range, West Pakistan. *In* Kummel, B. & Teichert, C. (eds): *Stratigraphic Boundary Problems: Permian and Triassic of West Pakistan*, 177-192. Special Publication of the Department of Geology, Vol. 4, University of Kansas.

Kummel, B. & Teichert, C. 1966: Relations between the Permian and Triassic formations in the Salt Range and Trans-Indus ranges, West Pakistan. *Neues Jahrbuch für Geologie Paläontologie. Abhandlungen 125*, 297-333.

Kummel, B. & Teichert, C. 1970: Stratigraphy and Paleontology of the Permian-Triassic Boundary Beds, Salt Range and Trans-Indus Ranges, West Pakistan. *In* Kummel, B.& Teichert, C. (eds): *Stratigraphic Boundary Problems: Permian and Triassic of West Pakistan*, 1-110. Special Publication of the Department of Geology, Vol. 4, University of Kansas.

Lilliefors, H.W. 1967: On the Kolmogorov-Smirnov test for normality with mean and variance unknown. *American Statistical Association Journal 62*, 399-402.

Matthews, S.C. 1973: Notes on open nomenclature and synonymy lists. *Palaeontology 16*, 713-719.

Mojsisovics, E. V., Waagen, W. & Diener, C. 1895: Entwurf einer Gliederung der pelagischen Sedimente des Trias-Systems. *Sitzungberichte der Akademie der Wissenschaften in Wien (I) 104*, 1271-1302.

Monnet, C. & Bucher, H. 2005: New Middle and Late Anisian (Middle Triassic) ammonoid faunas from northwestern Nevada (USA): taxonomy and biochronology. *Fossil and Strata 52*, 121 pp.

Monnet, C., Bucher, H., Wasmer, M. & Guex, J. 2010: Revision of the genus *Acrochordiceras* Hyatt, 1877 (Ammonoidea, Middle Triassic): morphology, biometry, biostratigraphy and intra-specific variability. *Palaeontology 53*, 961-996.

Monnet, C., Bucher, H., Guex, J. & Wasmer, M. 2012: Large scale evolutionary trends of Acrochordiceratidae Arthaber, 1911 (Ammonoidea, Middle Triassic) and Copes'rule. *Palaeontology 55*, 87-108.

Morris, J. & Lycett, J. 1853: *A monograph of the Mollusca from the Great Oolite, chiefly from Minchinhampton and the coast of Yorkshire. Part II. Bivalves*, 80 pp. Palaeontographical Society, London.

Mu, L., Zakharov, Y.D., Li, W.-Z. & Shen, S.-Z. 2007: Early Induan (Early Triassic) cephalopods from the Daye Formation at Guiding, Guizhou Province, South China. *Journal of Paleontology 81*, 858-872.

Newell, N.D. & Boyd, D.W. 1995: Pectinoid bivalves of the Permian-Triassic crisis. *Bulletin of the American Museum of Natural History 227*, 95 pp.

Noetling, F. 1901: Beiträge zur Geologie der Salt Range, insbesondere der permischen und Triassischen Ablagerungen. *Neues Jahrbuch für Mineralogie, Geologie und Paläontologie, Beilage-band 14*, 369-471.

Noetling, F. 1905: Die asiatische Trias. *In* Frech, F. (ed): *Lethaea Geognostica, Das Mesozoicum*, 107-221. verlag der E. Schweizerbart'schen Verlagsbuchhandlung (E. Nägele), Stuttgart, Germany.

Ogg, J.G. 2012. Triassic. *In* Gradstein, F.M., Ogg, J.G., Schmitz, M.D. & Ogg, G.M. (eds): *The Geologic Time Scale 2012*, 681-730. Elsevier, Amsterdam.

Orchard, M.J. 2007: Conodont diversity and evolution through the latest Permian and Early Triassic upheavals.

Palaeogeography, Palaeoclimatology, Palaeoecology 252, 93-117.

Orchard, M.J. 2008: Lower Triassic conodonts from the Canadian Arctic, their intercalibration with ammonoid-based stages and a comparison with other North American Olenekian faunas. *Polar Reasearch 27*, 393-412.

Pakistani-Japanese Research Group 1985: Permian and Triassic Systems in the Salt Range and Surghar Range, Pakistan. *In* Nakazawa, K. & Dickins, J.M. (eds): *The Tethys, her paleogeography and paleobiogeography from Paleozoic to Mesozoic*, 221-312. Tokai University Press, Tokyo.

Romano, C., Goudemand, N., Vennemann, T.W., Ware, D., Schneebeli-Hermann, E., Hochuli, P.A., Brühwiler, T., Brinkmann, W. & Bucher, H. 2013: Climatic and biotic upheavals following the end-Permian mass extinction. *Nature geoscience 6*, 57-60.

Schindewolf, O.H. 1954: Über die Faunenwende vom Paläozoikum zum Mesozoikum. *Zeitschrift der Deutschen Geologischen Gesellschaft 105*, 153-182.

Shigeta, S. & Zakharov, Y.D. 2009: Cephalopods. *In* Shigeta, Y., Zakharov, Y.D., Maeda, H. & Popov, A.M. (eds). *The Lower Triassic System in the Abrek bay area, South Primorye, Russia*, 44-140. National Museum of Nature and Science Monographs 38, Tokyo.

Schneebeli-Hermann, E., Kürschner, W.M., Hochuli, P.A., Bucher, H., Ware, D., Goudemand, N. & Roohi, G. 2012: Palynofacies analysis of the Permian–Triassic transition in the Amb section (Salt Range, Pakistan): Implications for the anoxia on the South Tethyan Margin. *Journal of Asian Earth Sciences 60*, 225-234.

Smith, J.P. 1932: Lower Triassic ammonoids of North America. *United States Geological Survey, Professional Paper 167*, 1-199.

Spath, L.F. 1919a: V. Notes on Ammonites. *Geological Magazine 6*, 27-35.

Spath, L.F. 1919b: IV. Notes on Ammonites. *Geological Magazine 6*, 115-122.

Spath, L.F. 1930: The Eotriassic Invertebrate Fauna of East Greenland. *Meddelelser om Grönland 83*, 1-90.

Spath, L.F. 1934: *Catalogue of the Fossil Cephalopoda in the British Museum (Natural History), part IV: The Ammonoidea of the Trias*, 521 pp. The Trustees of the British Museum, London.

Spath, L.F. 1935: Additions to the Eotriassic Invertebrate Fauna of East Greenland. *Meddelelser om Grönland 98*, 1-115.

Todd, J.A. & Palmer, T.J. 2002: The Jurassic bivalve genus *Placunopsis*: new evidence on anatomy and affinities. *Palaeontology 45*, 487-510.

Tozer, E.T. 1961: Triassic Stratigraphy and faunas, Queen Elizabeth Islands, Arctic Archipelago. *Memoir of the Geological Survey of Canada 316*, 1-116.

Tozer, E.T. 1963: Lower Triassic ammonoids from Tuchodi Lakes and Halfway River areas, northeastern British Columbia. *Bulletin of the Geological Survey of Canada 96*, 1-28.

Tozer, E.T. 1965: Lower Triassic stages and Ammonoid zones of Arctic Canada. *Paper of the Geological Survey of Canada 65-12*, 14 pp.

Tozer, E.T. 1967: A Standard for Triassic time. *Bulletin of the Geological Survey of Canada 156*, 1-103.

Tozer, E.T. 1970: Marine Triassic Faunas. *In* R. J. W. Douglas (ed): *Geology and Economic Minerals of Canada, 5 ed.*, 633-640. Geological Survey of Canada, Vancouver.

Tozer, E.T. 1981: Triassic Ammonoidea: classification, evolution and relationship with Permian and Jurassic forms. *In* M. R. HOUSE & J. R. SENIOR (eds): *The Ammonoidea: the Evolution, Classification, Mode of Life and Geological usefulness of a Major Fossil Group*, 65-100. The Systematics Association, Special Volume 18, Academic Press, London.

Tozer, E.T. 1994: Canadian Triassic Ammonoid Faunas. *Bulletin of the Geological Survey of Canada 467*, 1-663.

Trümpy, R. 1969: Lower Triassic Ammonites from Jameson Land (East Greenland). *Meddelelser om Grönland 168*, 79-121.

Urdy, S., Goudemand, N., Bucher, H. & Chirat, R. 2010a: Allometries and the morphogenesis of the molluscan shell: a quantitative and theoretical model. *Journal of Experimental Zoology 314B*, 280-302.

Urdy, S., Goudemand, N., Bucher, H. & Chirat, R. 2010b: Growth dependent phenotypic variation of molluscan shell shape: a theoretical and empirical comparison using gastropods. *Journal of Experimental Zoology 314B*, 303-326.

Waagen, W. 1895: Salt Ranges Fossils. vol. 2: Fossils from the Ceratites formation - Part I - Pisces, Ammonoidea. *Palaeontologia Indica 13*, 1-323.

Wang, Y.G. & He, G.X. 1976: Triassic ammonoids from the Mount Jolmo Lungma region. *In*: *A report of scientific expedition in the Mount Jolmo Lungma region (1966-1968)*, 223-502. Palaeontology, fascicule 3. Science Press, Beijing [In Chinese].

Wanner, J. 1911: Triascephalopoden von Timor und Rotti. *Neues Jahrbuch für Mineralogie, Geologie und Paläontologie 32*, 177-196.

Ware, D., Jenks, J.F., Hautmann, M. & Bucher, H. 2011: Dienerian (Early Triassic) ammonoids from the Candelaria Hills (Nevada, USA) and their significance for palaeobiogeography and palaeoceanography. *Swiss Journal of Geoscience 104*, 161-181.

Wasmer, M., Hautmann, M., Hermann, E., Ware, D., Roohi, G., ur-Rehman, K., Yaseen, A. & Bucher, H. 2012: Olenekian (Early Triassic) Bivalves From The Salt Range And Surghar Range, Pakistan. *Palaeontology 55*, 1043-1073.

Waterhouse, J.B. 1994: The Early and Middle Triassic

ammonoid succession of the Himalayas in western and central Nepal. Part 1. Stratigraphy, classification and Early Scythian ammonoid systematics. *Palaeontographica A232*, 1-83.

Waterhouse, J.B. 1996: The Early and Middle Triassic ammonoid succession of the Himalayas in western and central Nepal. Part 2. Systematic studies of the Early Middle Scythian. *Palaeontographica A241*, 27-100.

Westerman, G.E.G. 1966: Covariation and taxonomy of the Jurassic ammonite *Sonninia adicra* (Waagen). *Neues Jahrbuch für Mineralogie, Geologie und Paläontologie, Abhandlungen 124*, 289-312.

Zakharov, Y.D. 1968: *Biostratigraphiya i Amonoidei Nizhnego Triasa Yuzhnogo Primorya (Lower Triassic biostratigraphy and Ammonoids of South Primorye)*, 175 pp. Nauka, Moskva [In Russian].

Zakharov, Y.D. 1978: *Lower Triassic Ammonoids of East USSR*, 224 pp. Nauka, Moskva [In Russian].

Plates

Plate 1

(All figures natural size unless otherwise indicated; asterisks indicate the position of the last septum)

1a-c: *Hypophiceras* aff. *gracile* (Spath, 1930). PIMUZ30236.
Loc. Nam361, dolomitic unit of the Kathwai Member, Nammal Nala, ?early Griesbachian.

2a-c: *Ophiceras connectens* Schindewolf, 1954. PIMUZ30239.
Loc. Nam376, base LCL, Nammal Nala, *Ophiceras connectens* beds (late Griesbachian).

3a-d: *Ophiceras connectens* Schindewolf, 1954. PIMUZ30237.
Loc. Chi54, limestone unit of the Kathwai Member, Chiddru, *Ophiceras connectens* beds (late Griesbachian). a-c) lateral, apertural and ventral views. d) Suture line at H = 16.6 mm; × 1.5.

4a-c: *Ophiceras connectens* Schindewolf, 1954. PIMUZ30238.
Loc. Nam390, base LCL, Nammal Nala, *Ophiceras connectens* beds (late Griesbachian).

5a-b: *Ophiceras sakuntala* Diener, 1897. PIMUZ30240.
Loc. Nam391, base LCL, Nammal Nala, ? latest Griesbachian/earliest Dienerian.

6a-c: *Ophiceras sakuntala* Diener, 1897. PIMUZ30241.
Loc. Nam391, base LCL, Nammal Nala, ? latest Griesbachian/earliest Dienerian. a-b) lateral and ventral views. c) Suture line at H = 15.5 mm; × 1.5.

7a-b: ?Ophiceratidae gen. et sp. indet. PIMUZ30242.
Loc. Nam391, base LCL, Nammal Nala, ? latest Griesbachian/earliest Dienerian.

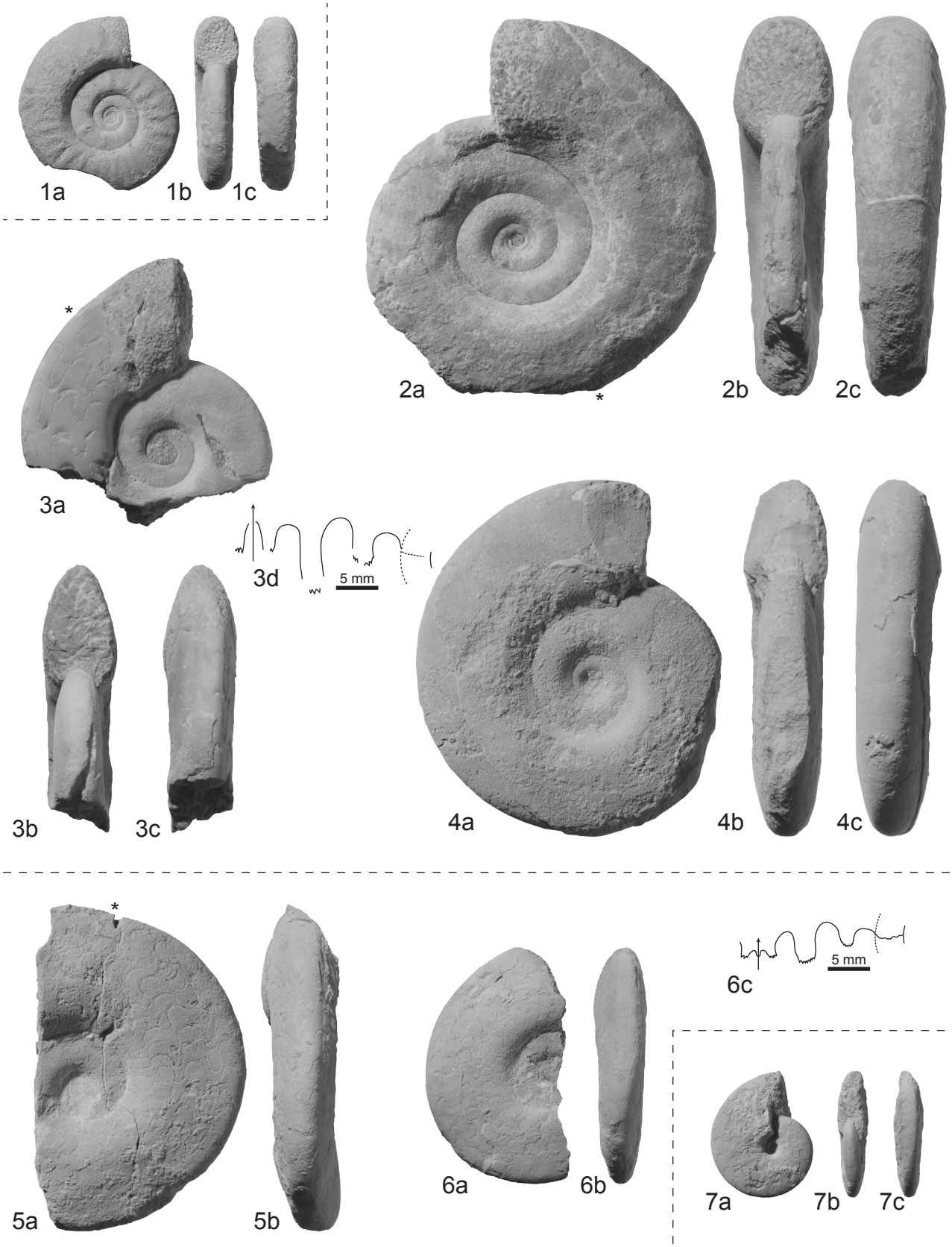
1a
1b
1c
2a
2b
2c
3a
3b
3c
3d
5 mm
4a
4b
4c
5a
5b
6a
6b
6c
5 mm
7a
7b
7c

Plate 2

(All figures natural size unless otherwise indicated; asterisks indicate the position of the last septum)

1a-c: *Kyoktites hebeiseni* n. gen., n. sp. PIMUZ30243. Holotype.
Loc. Nam391, base LCL, Nammal Nala, ? latest Griesbachian/earliest Dienerian. a-c) lateral, apertural and ventral views. d) Suture line at H = 17.5 mm; × 1.5.

2a-c: *Kyoktites* cf. *hebeiseni* n. gen., n. sp. PIMUZ30245.
Loc. Amb104, base LCL, Amb, *Gyronites dubius* beds (early Dienerian). a-c) lateral, apertural and ventral views. d) Suture line at H = 14.8 mm; × 1.5.

3a-c: ?Ophiceratidae Gen. Nov. A sp. nov. A PIMUZ30246.
Loc. Nam391, base LCL, Nammal Nala, late Griesbachian. a-b) lateral and ventral views. c) Suture line at H = 23.4 mm.

4a-c: *Ghazalaites roohii* n. gen., n. sp. PIMUZ30247. Paratype.
Loc. War8, middle LCL, Wargal, *Gyronites plicosus* beds (early Dienerian).

5a-c: *Ghazalaites roohii* n. gen., n. sp. PIMUZ30248. Holotype.
Loc. Nam332, middle LCL, Nammal Nala, *Gyronites plicosus* beds (early Dienerian).

6a-c: *Ghazalaites roohii* n. gen., n. sp. PIMUZ30249. Paratype.
Loc. Nam377, middle LCL, Nammal Nala, *Gyronites plicosus* beds (early Dienerian).

7: *Ghazalaites roohii* n. gen., n. sp. PIMUZ30250. Paratype.
Loc. Nam377, middle LCL, Nammal Nala, *Gyronites plicosus* beds (early Dienerian). Suture line at H = 18.2 mm; × 1.5.

8a-c: *Ghazalaites roohii* n. gen., n. sp. PIMUZ30251. Paratype.
Loc. Amb104, base LCL, Amb, *Gyronites dubius* beds (early Dienerian).

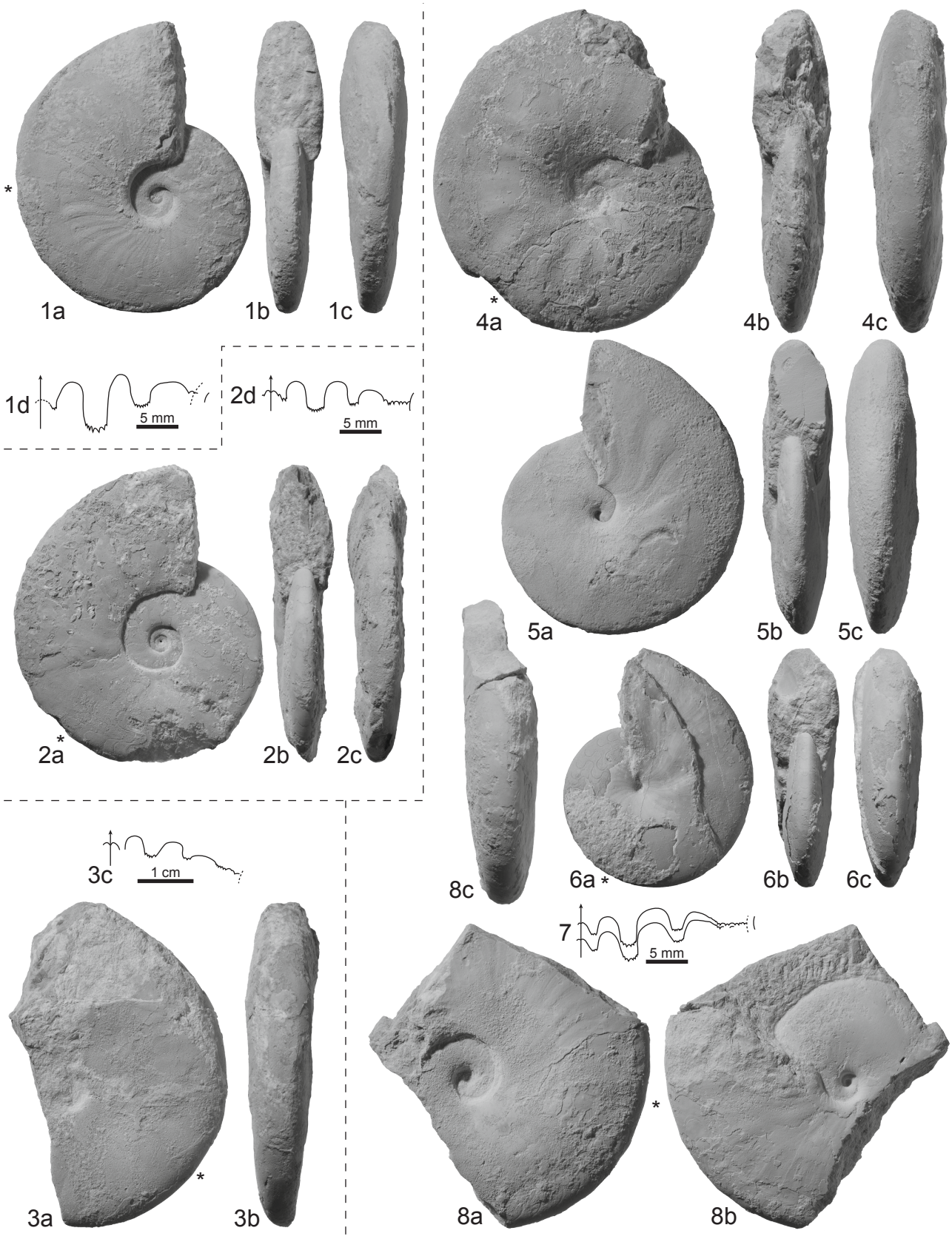
*
1a
1b
1c
1d
5 mm
2d
5 mm
2a*
2b
2c
3c
1 cm
3a*
3b
*
4a
4b
4c
5a
5b
5c
8c
6a*
6b
6c
7
5 mm
8a
*
8b

Plate 3

(All figures natural size unless otherwise indicated; asterisks indicate the position of the last septum)

1: Bedding plane with *Gyronites frequens* Waagen, 1895 and one specimen of *Ussuridiscus ensanus* (Krafft, 1909) (marked "U"). PIMUZ30252.
Loc. Nam339, top LCL, Nammal Nala, *Gyronites frequens* beds (early Dienerian); × 0.5.

2: Upperside of a specimen of *Gyronites frequens* Waagen, 1895 encrusted by worm tubes. PIMUZ30253.
Loc. Nam354, top LCL, Nammal Nala, *Gyronites frequens* beds (early Dienerian).

3a-c: *Gyronites frequens* Waagen, 1895. PIMUZ30255.
Specimen encrusted by worm tubes Loc. Nam354, top LCL, Nammal Nala, *Gyronites frequens* beds (early Dienerian).


5 cm
U
1


2
*

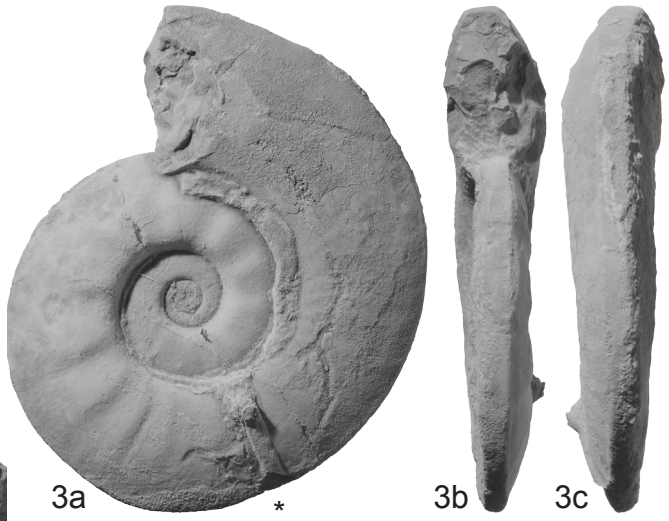
3a
*
3b
3c

Plate 4

(All figures natural size unless otherwise indicated asterisks indicate the position of the last septum)

1a-c: *Gyronites frequens* Waagen, 1895. PIMUZ30254.
Loc. Nam354, top LCL, Nammal Nala, *Gyronites frequens* beds (early Dienerian).

2a-c: *Gyronites frequens* Waagen, 1895. PIMUZ30256.
Loc. Nam76, top LCL, Nammal Nala, *Gyronites frequens* beds (early Dienerian).

3a-c: *Gyronites frequens* Waagen, 1895. PIMUZ30257.
Loc. War7, top LCL, Wargal, *Gyronites frequens* beds (early Dienerian).

4a-b: *Gyronites frequens* Waagen, 1895. PIMUZ30258.
Loc. Nam76, top LCL, Nammal Nala, *Gyronites frequens* beds (early Dienerian).

5a-b: *Gyronites frequens* Waagen, 1895. PIMUZ30259.
Loc. Nam76, top LCL, Nammal Nala, *Gyronites frequens* beds (early Dienerian).

6a-d: *Gyronites frequens* Waagen, 1895. PIMUZ30260.
Loc. War7, top LCL, Wargal, *Gyronites frequens* beds (early Dienerian). a-c) lateral, apertural and ventral views. d) Suture line at H = 15.4 mm; × 1.5.

7a-d: *Gyronites dubius* (Krafft, 1909). PIMUZ30261.
Loc. Amb104, base LCL, Amb, *Gyronites dubius* beds (early Dienerian). a-c) lateral, apertural and ventral views. d) Suture line at H = 12.7 mm; × 2 (mirrored image).

8a-c: *Gyronites dubius* (Krafft, 1909). PIMUZ30262.
Loc. Amb104, base LCL, Amb, *Gyronites dubius* beds (early Dienerian).

9a-c: *Gyronites dubius* (Krafft, 1909). PIMUZ30263.
Loc. Amb104, base LCL, Amb, *Gyronites dubius* beds (early Dienerian).

10a-c: *Gyronites dubius* (Krafft, 1909). PIMUZ30264.
Loc. Amb104, base LCL, Amb, *Gyronites dubius* beds (early Dienerian).

11a-b: *Gyronites dubius* (Krafft, 1909). PIMUZ30265.
Loc. Nam391, base LCL, Nammal Nala, ? latest Griesbachian/earliest Dienerian.

12a-c: *Gyronites dubius* (Krafft, 1909). PIMUZ30266.
Loc. Nam391, base LCL, Nammal Nala, ? latest Griesbachian/earliest Dienerian.

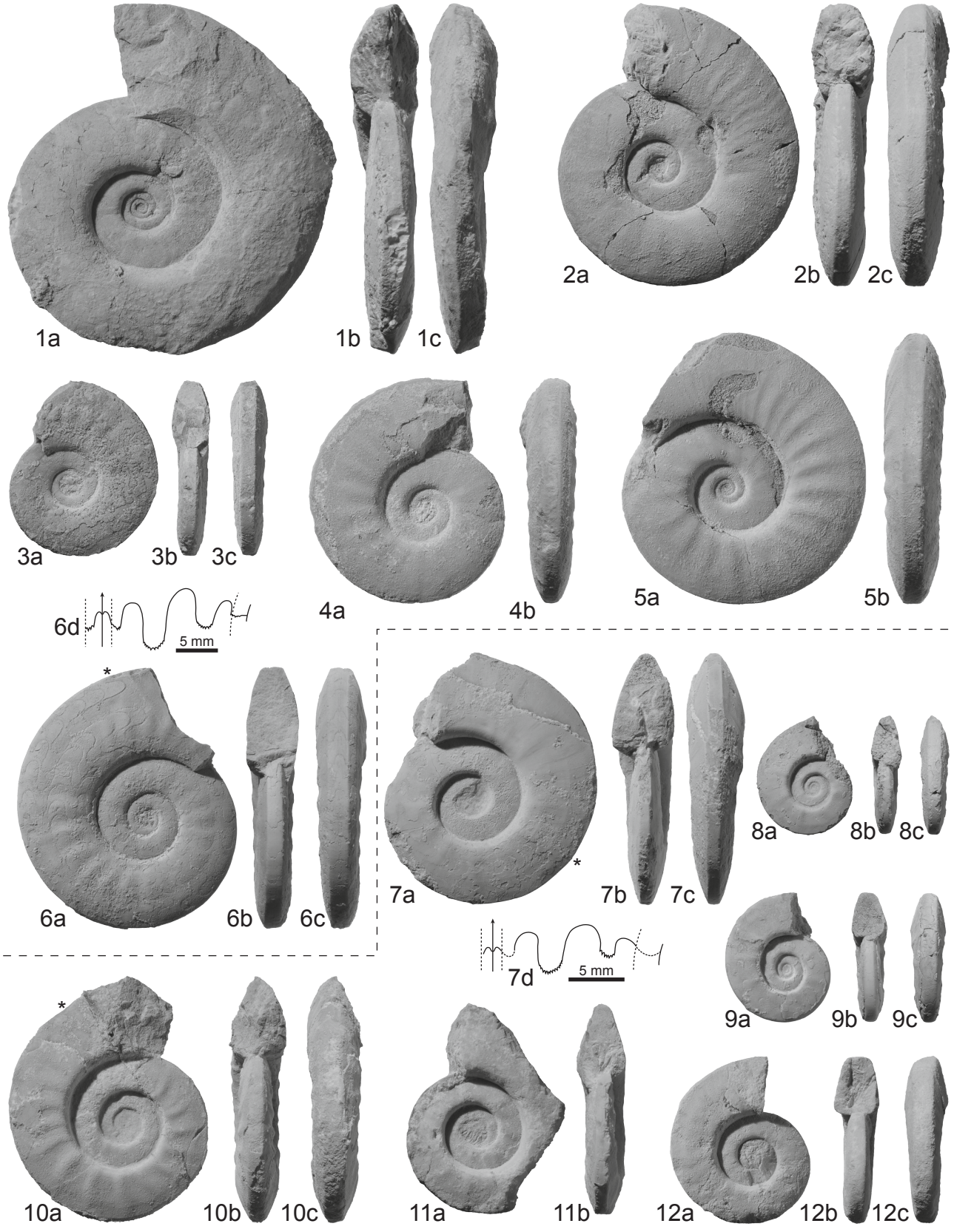
1a
1b
1c
2a
2b
2c
3a
3b
3c
4a
4b
5a
5b
6d
5 mm
*
6a
6b
6c
7a
*
7b
7c
8a
8b
8c
7d
5 mm
9a
9b
9c
*
10a
10b
10c
11a
11b
12a
12b
12c

Plate 5

(All figures natural size unless otherwise indicated; asterisks indicate the position of the last septum)

1a-c: *Gyronites rigidus* (Diener, 1897). PIMUZ30267.
Loc. Amb104, base LCL, Amb, *Gyronites dubius* beds (early Dienerian).

2a-c: *Gyronites plicosus* Waagen, 1895. PIMUZ30268.
Loc. Nam377, middle LCL, Nammal Nala, *Gyronites plicosus* beds (early Dienerian).

3a-d: *Gyronites plicosus* Waagen, 1895. PIMUZ30269.
Loc. Nam377, middle LCL, Nammal Nala, *Gyronites plicosus* beds (early Dienerian). a-c) lateral, apertural and ventral views. d) Suture line at H = 9.3 mm; × 2.

4a-c: *Gyronites plicosus* Waagen, 1895. PIMUZ30270.
Loc. Nam331, middle LCL, Nammal Nala, *Gyronites plicosus* beds (early Dienerian).

5a-b: *Gyronites plicosus* Waagen, 1895. PIMUZ30271.
Loc. Nam335, middle LCL, Nammal Nala, *Gyronites plicosus* beds (early Dienerian).

6a-c: *Gyronites plicosus* Waagen, 1895. PIMUZ30272.
Loc. Amb2, middle LCL, Amb, *Gyronites plicosus* beds (early Dienerian).

7a-c: *Gyronites plicosus* Waagen, 1895 PIMUZ30273.
Loc Nam377, middle LCL, Nammal Nala, *Gyronites plicosus* beds (early Dienerian).

8a-b: *Gyronites plicosus* Waagen, 1895. PIMUZ30274.
Loc. Amb2, middle LCL, Amb, *Gyronites plicosus* beds (early Dienerian).

9a-c: *Gyronites plicosus* Waagen, 1895. PIMUZ30275.
Loc. Nam377, middle LCL, Nammal Nala, *Gyronites plicosus* beds (early Dienerian).

10a-b: *Gyronites plicosus* Waagen, 1895. PIMUZ30276.
Loc. Nam377, middle LCL, Nammal Nala, *Gyronites plicosus* beds (early Dienerian).

11a-c: *Gyronites sitala* (Diener, 1897). PIMUZ30277.
Loc. Nam331, middle LCL, Nammal Nala, *Gyronites plicosus* beds (early Dienerian).

12a-b: *Gyronites sitala* (Diener, 1897). PIMUZ30278.
Loc. Nam377, middle LCL, Nammal Nala, *Gyronites plicosus* beds (early Dienerian).

13a-b: *Gyronites schwanderi* n. sp. PIMUZ30279. Paratype.
Loc. War100, from dipslope near top LCL, Wargal, precise age unknown (*Gyronites plicosus* or *Gyronites frequens* beds, early Dienerian).

14a-b: *Gyronites schwanderi* n. sp. PIMUZ30281. Holotype.
Loc. Nam378, top LCL, Nammal Nala, *Gyronites frequens* beds (early Dienerian).

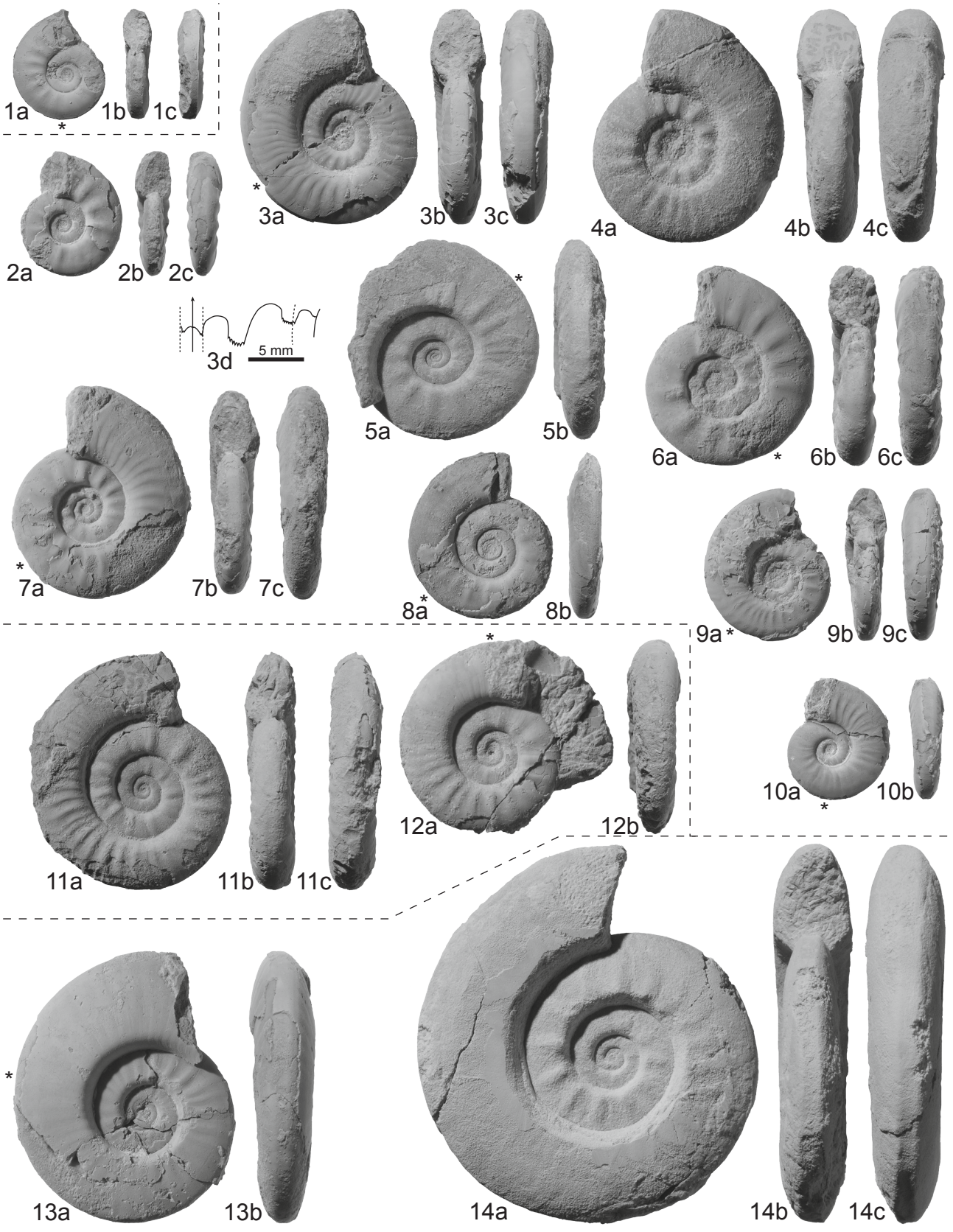
1a
1b
1c
*
2a
2b
2c
3a
3b
3c
4a
4b
4c
3d
5 mm
5a
5b
6a
6b
6c
7a
7b
7c
8a
8b
9a
9b
9c
10a
10b
11a
11b
11c
12a
12b
13a
13b
14a
14b
14c

Plate 6

(All figures natural size unless otherwise indicated; asterisks indicate the position of the last septum)

1a-b: *Ambites discus* Waagen, 1895. GSI7138. Lectotype. (Photo by B. Kummel)
Base CM, Amb, bed and locality unknown.

2a-b: *Ambites discus* Waagen, 1895. PIMUZ30283.
Loc. War2, base CM, Wargal, *Ambites discus* beds (middle Dienerian).

3a-c: *Ambites discus* Waagen, 1895. PIMUZ30284.
Loc. Nam527, base CM, Nammal Nala, *Ambites discus* beds (middle Dienerian).

4a-d: *Ambites discus* Waagen, 1895. PIMUZ30285.
Loc. Nam50, base CM, Nammal Nala, *Ambites discus* beds (middle Dienerian). a-c) lateral, apertural and ventral views. d) Suture line at H = 16.6 mm; × 1.5 (mirrored image).

5a-c: *Ambites discus* Waagen, 1895. PIMUZ30286.
Loc. Nam52, base CM, Nammal Nala, *Ambites discus* beds (middle Dienerian).

6a-b: *Ambites discus* Waagen, 1895. PIMUZ30287.
Loc. Nam50, base CM, Nammal Nala, *Ambites discus* beds (middle Dienerian).

7a-b: *Ambites discus* Waagen, 1895. PIMUZ30288.
Loc. Nam50, base CM, Nammal Nala, *Ambites discus* beds (middle Dienerian). a) Polished cross section. b) Cross section.

8a-c: *Ambites discus* Waagen, 1895. PIMUZ30289.
Loc. Nam364, base CM, Nammal Nala, *Ambites discus* beds (middle Dienerian).

9a-c: *Ambites discus* Waagen, 1895. PIMUZ30290.
Loc. Nam50, base CM, Nammal Nala, *Ambites discus* beds (middle Dienerian).

10a-d: *Ambites discus* Waagen, 1895. PIMUZ30291.
Loc. Nam50, base CM, Nammal Nala, *Ambites discus* beds (middle Dienerian). a-c) lateral, apertural and ventral views. d) Suture line at H = 29.6 mm.

11: *Ambites discus* Waagen, 1895. PIMUZ30292.
Loc. Nam52, base CM, Nammal Nala, *Ambites discus* beds (middle Dienerian). Suture line at H = 31 mm.

12: *Ambites discus* Waagen, 1895. PIMUZ30293.
Loc. Nam50, base CM, Nammal Nala, *Ambites discus* beds (middle Dienerian). Suture line at H = 26.2 mm (see also Pl.7: 6).

13: *Ambites discus* Waagen, 1895. PIMUZ30294.
Loc. Nam364, base CM, Nammal Nala, *Ambites discus* beds (middle Dienerian). Suture line at H = 10.9 mm; × 2.

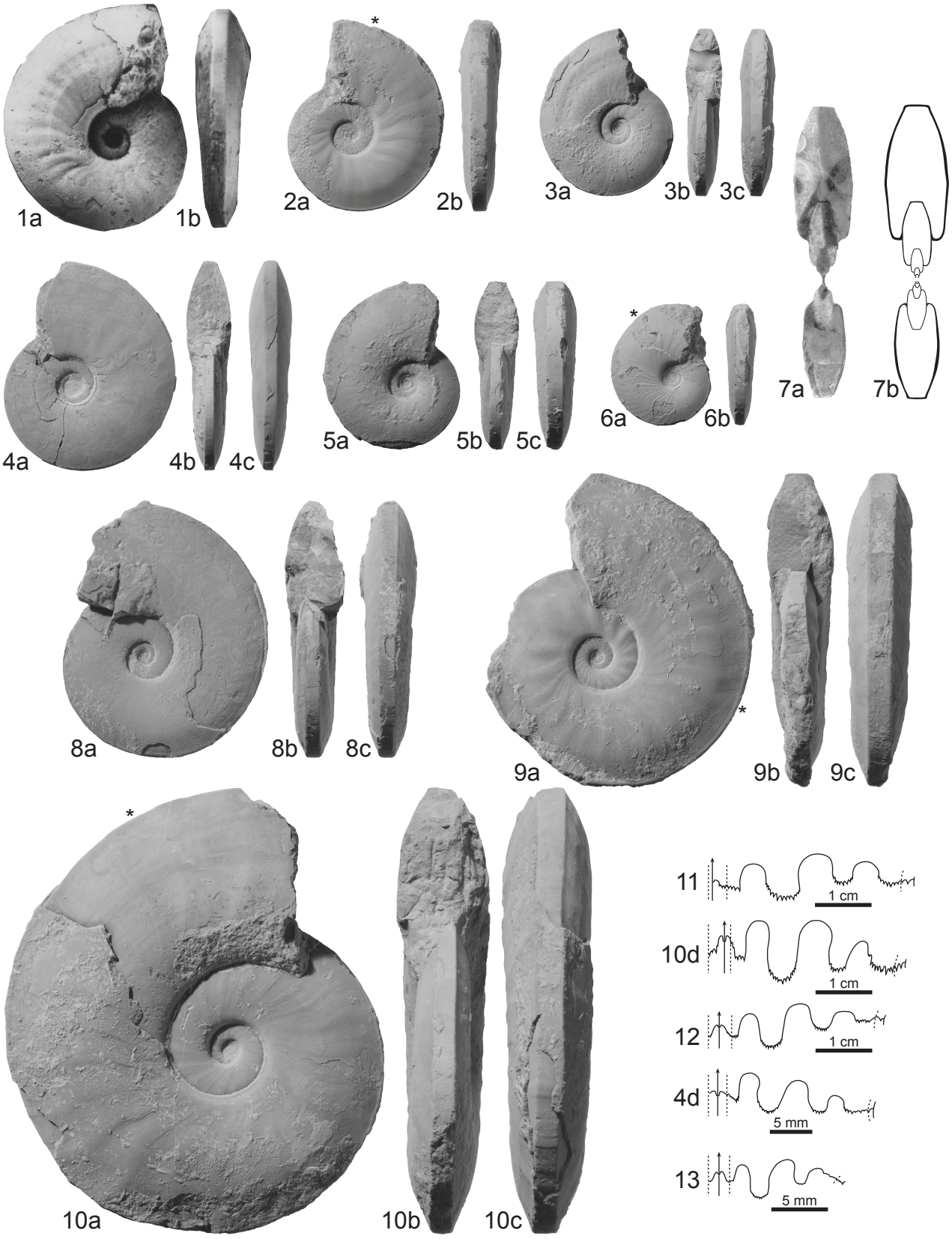
1a
1b
2a
*
2b
3a
3b
3c
7a
7b
4a
4b
4c
5a
5b
5c
*
6a
6b
8a
8b
8c
9a
*
9b
9c
*
10a
10b
10c
11
1 cm
10d
1 cm
12
1 cm
4d
5 mm
13
5 mm

Plate 7

(All figures natural size unless otherwise indicated; asterisks indicate the position of the last septum)

1a-c: *Ambites discus* Waagen, 1895. PIMUZ30295.
Loc. Nam50, base CM, Nammal Nala, *Ambites discus* beds (middle Dienerian).

2a-c: *Ambites discus* Waagen, 1895. PIMUZ30296.
Loc. Nam52, base CM, Nammal Nala, *Ambites discus* beds (middle Dienerian).

3a-c: *Ambites discus* Waagen, 1895. PIMUZ30297.
Loc. Nam50, base CM, Nammal Nala, *Ambites discus* beds (middle Dienerian).

4a-b: *Ambites discus* Waagen, 1895. PIMUZ30298.
Loc. Amb54, base CM, Amb, *Ambites discus* beds (middle Dienerian).

5a-c: *Ambites discus* Waagen, 1895. PIMUZ30299.
Loc. Ch7A, middle LCL, Chiddru, *Ambites discus* beds (middle Dienerian).

6a-c: *Ambites discus* Waagen, 1895. PIMUZ30293.
Loc. Nam50, base CM, Nammal Nala, *Ambites discus* beds (middle Dienerian; see also Pl.6: 12).

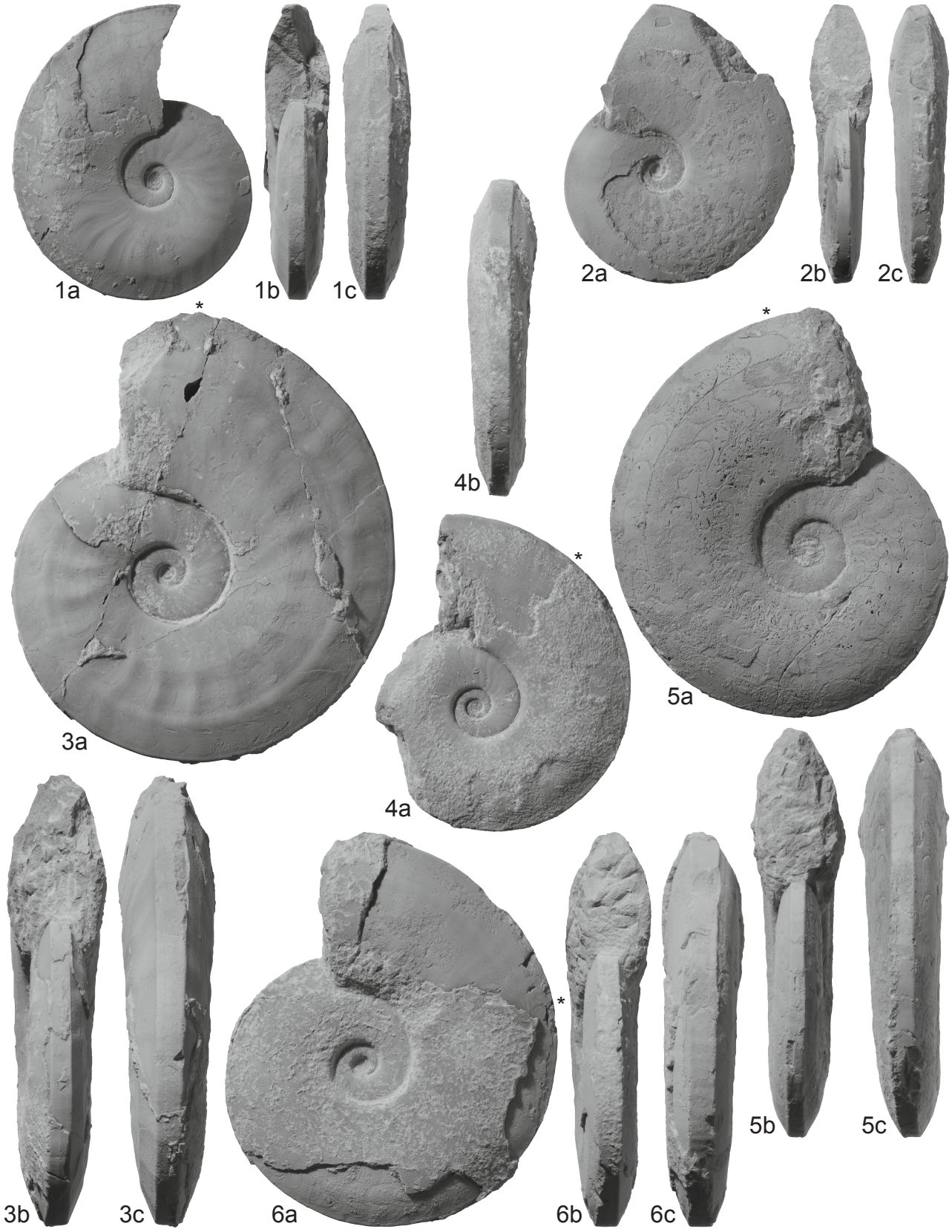
1a
1b
1c
2a
2b
2c
4b
3a
*
4a
*
5a
*
3b
3c
6a
*
6b
6c
5b
5c

Plate 8

(All figures natural size unless otherwise indicated; asterisks indicate the position of the last septum)

1a-b: *Ambites atavus* (Waagen, 1895). GSI7187. Holotype. (Photo by B. Kummel)
LCL, Wargal, bed and locality unknown.

2a-d: *Ambites atavus* (Waagen, 1895). PIMUZ30300.
Loc. Amb52, top LCL, Amb, *Ambites atavus* beds (middle Dienerian). a-c) lateral, apertural and ventral views. d) Suture line at H = 20 mm; × 1.5.

3a-d: *Ambites atavus* (Waagen, 1895). PIMUZ30301.
Loc. Amb52, top LCL, Amb, *Ambites atavus* beds (middle Dienerian). a-c) lateral, apertural and ventral views. d) Suture line at H = 18.6 mm; × 1.5.

4a-c: *Ambites atavus* (Waagen, 1895). PIMUZ30302.
Loc. Amb63, top LCL, Amb, *Ambites atavus* beds (middle Dienerian).

5a-d: *Ambites atavus* (Waagen, 1895). PIMUZ30303.
Loc. Amb11, top LCL, Amb, *Ambites atavus* beds (middle Dienerian). a-c) lateral, apertural and ventral views. d) Suture line at H = 16.7 mm; × 1.5.

6a-c: *Ambites atavus* (Waagen, 1895). PIMUZ30304.
Loc. Amb63, top LCL, Amb, *Ambites atavus* beds (middle Dienerian).

7a-d: *Ambites atavus* (Waagen, 1895). PIMUZ30305.
Loc. Nam60, base CM, Nammal Nala, *Ambites atavus* beds (middle Dienerian). a-c) lateral, apertural and ventral views. d) Suture line at H = 22.9 mm; × 1.5.

8a-c: *Ambites atavus* (Waagen, 1895). PIMUZ30306.
Loc. Amb52, top LCL, Amb, *Ambites atavus* beds (middle Dienerian).

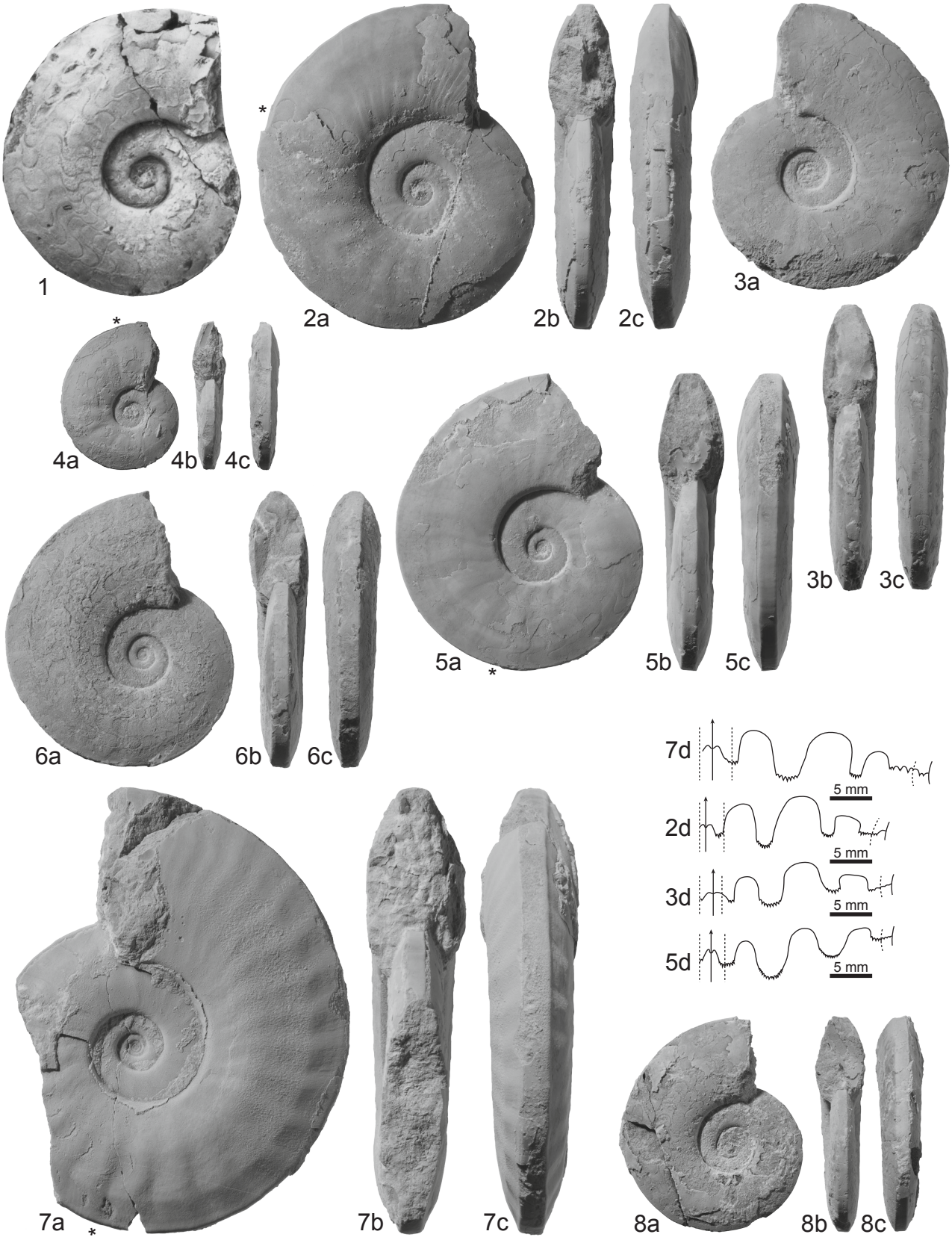
1
2a
2b
2c
3a
4a
4b
4c
5a
5b
5c
3b
3c
6a
6b
6c
7d
5 mm
2d
5 mm
3d
5 mm
5d
5 mm
7a
7b
7c
8a
8b
8c

Plate 9

(All figures natural size unless otherwise indicated; asterisks indicate the position of the last septum)

1a-b: *Ambites atavus* (Waagen, 1895). PIMUZ30307.
Loc. Amb63, top LCL, Amb, *Ambites atavus* beds (middle Dienerian).

2a-e: *Ambites tenuis* n. sp. PIMUZ30308. Holotype.
Loc. Amb63, top LCL, Amb, *Ambites atavus* beds (middle Dienerian). a-d) lateral, apertural and ventral views. e) Suture line at H = 12.8 mm; × 2.

3a-c: *Ambites tenuis* n. sp. PIMUZ30309. Paratype.
Loc. Amb63, top LCL, Amb, *Ambites atavus* beds (middle Dienerian).

4a-d: *Ambites radiatus* (Brühwiler *et al.*, 2008). PIMUZ30310.
Loc. Nam381, base CM, Nammal Nala, *Ambites radiatus* beds (middle Dienerian).

5a-b: *Ambites radiatus* (Brühwiler *et al.*, 2008). PIMUZ30311.
Loc. Nam520, base CM, Nammal Nala, *Ambites radiatus* beds (middle Dienerian).

6a-c: *Ambites radiatus* (Brühwiler *et al.*, 2008). PIMUZ30312.
Loc. Nam72, base CM, Nammal Nala, *Ambites radiatus* beds (middle Dienerian).

7a-b: *Ambites radiatus* (Brühwiler *et al.*, 2008). PIMUZ30313.
Loc. Nam381, base CM, Nammal Nala, *Ambites radiatus* beds (middle Dienerian). Specimen with partially preserved body chamber, but position of the last septum unknown.

8: *Ambites radiatus* (Brühwiler *et al.*, 2008). PIMUZ30314.
Loc. Nam381, base CM, Nammal Nala, *Ambites radiatus* beds (middle Dienerian). Suture line at H = 10 mm; × 2.

9a-c: *Ambites radiatus* (Brühwiler *et al.*, 2008). PIMUZ30315.
Loc. Nam381, base CM, Nammal Nala, *Ambites radiatus* beds (middle Dienerian).

10a-c: *Ambites radiatus* (Brühwiler *et al.*, 2008). PIMUZ30316.
Loc. Nam72, base CM, Nammal Nala, *Ambites radiatus* beds (middle Dienerian).

11a-c: *Ambites bojeseni* n. sp. PIMUZ30317. Paratype.
Loc. Nam521, base CM, Nammal Nala, *Ambites radiatus* beds (middle Dienerian).

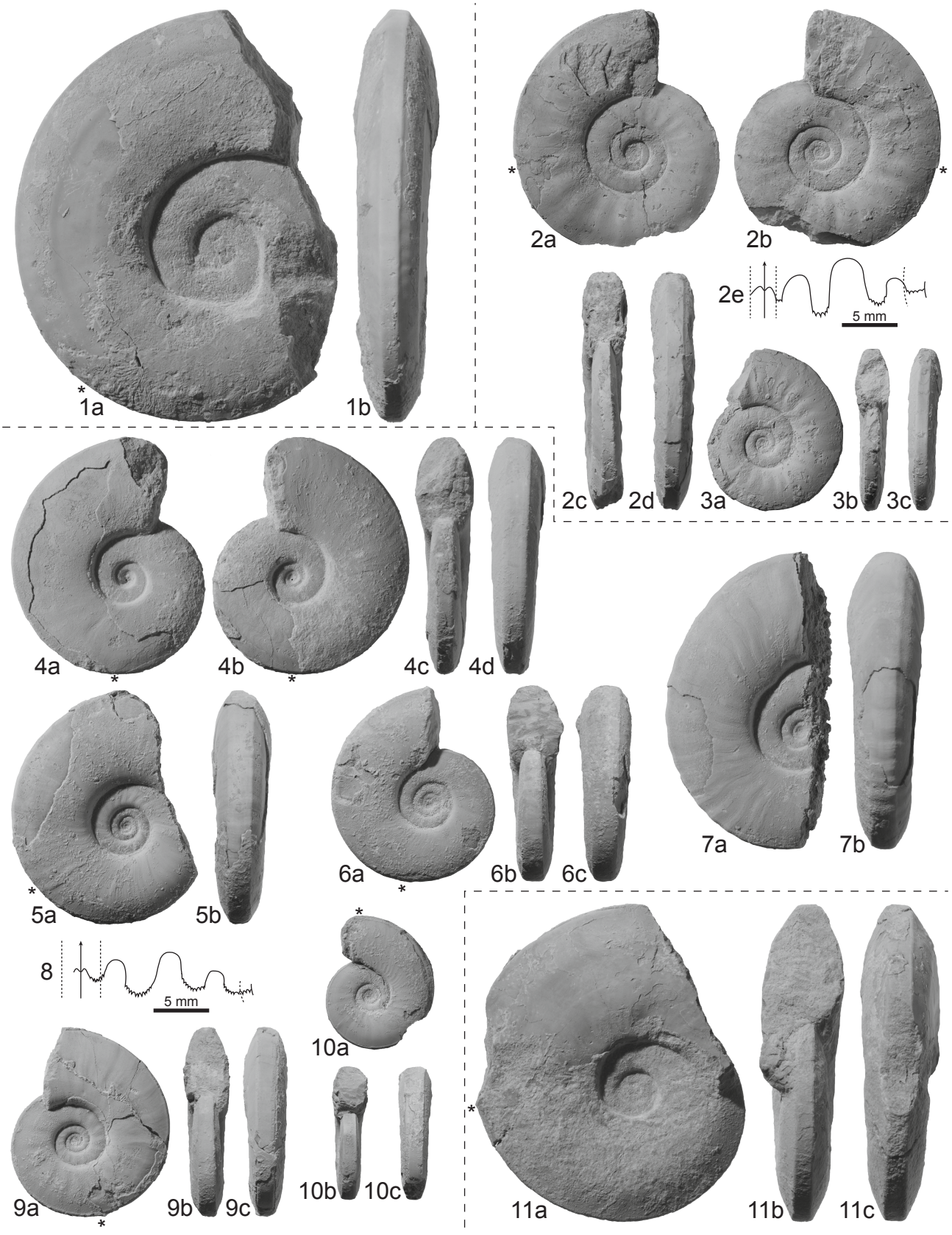
1a
1b
2a
2b
2e
5 mm
2c
2d
3a
3b
3c
4a
4b
4c
4d
5a
5b
6a
6b
6c
7a
7b
8
5 mm
9a
9b
9c
10a
10b
10c
11a
11b
11c

Plate 10

(All figures natural size unless otherwise indicated; asterisks indicate the position of the last septum)

1a-c: *Ambites bojeseni* n. sp. PIMUZ30318. Holotype.
Loc. Nam384, base CM, Nammal Nala, *Ambites radiatus* beds (middle Dienerian).

2a-d: *Ambites bojeseni* n. sp. PIMUZ30319. Paratype.
Loc. Nam72, base CM, Nammal Nala, *Ambites radiatus* beds (middle Dienerian). a-c) lateral, apertural and ventral views. d) Suture line at H = 16.6 mm; × 2.

3a-d: *Ambites bojeseni* n. sp. PIMUZ30320. Paratype.
Loc. Nam72, base CM, Nammal Nala, *Ambites radiatus* beds (middle Dienerian). a-c) lateral, apertural and ventral views. d) Suture line at H = 14.3 mm; × 2.

4a-c: *Ambites subradiatus* n. sp. PIMUZ30321. Holotype.
Loc. Amb54, base CM, Amb, *Ambites discus* beds (middle Dienerian).

5a-b: *Ambites subradiatus* n. sp. PIMUZ30322. Paratype.
Loc. Nam50, base CM, Nammal Nala, *Ambites discus* beds (middle Dienerian).

6: *Ambites subradiatus* n. sp. PIMUZ30323. Paratype.
Loc. Amb54, base CM, Amb, *Ambites discus* beds (middle Dienerian). Suture line at H = 11.1 mm; × 2.

7a-b: *Ambites subradiatus* n. sp. PIMUZ30324. Paratype.
Loc. Nam52, base CM, Nammal Nala, *Ambites discus* beds (middle Dienerian).

8a-d: *Ambites*? sp. indet. PIMUZ30325.
Loc. Nam382, base CM, Nammal Nala, *Ambites discus* beds (middle Dienerian). a-c) lateral, apertural and ventral views. d) Suture line at H = 13.4 mm; × 2.

9a-b: *Ambites*? sp. indet. PIMUZ30326.
Loc. Nam380, base CM, Nammal Nala, *Ambites discus* beds (middle Dienerian).

10a-c: *Ambites superior* (Waagen, 1895). PIMUZ30330.
Loc. Nam53, base CM, Nammal Nala, *Ambites superior* beds (middle Dienerian).

11a-c: *Ambites superior* (Waagen, 1895). PIMUZ30331.
Loc. Nam371, base CM, Nammal Nala, *Ambites superior* beds (middle Dienerian).

12a-b: *Ambites superior* (Waagen, 1895). PIMUZ30332.
Loc. Nam302, base CM, Nammal Nala, *Ambites superior* beds (middle Dienerian). a) Polished cross section. b) Cross section.

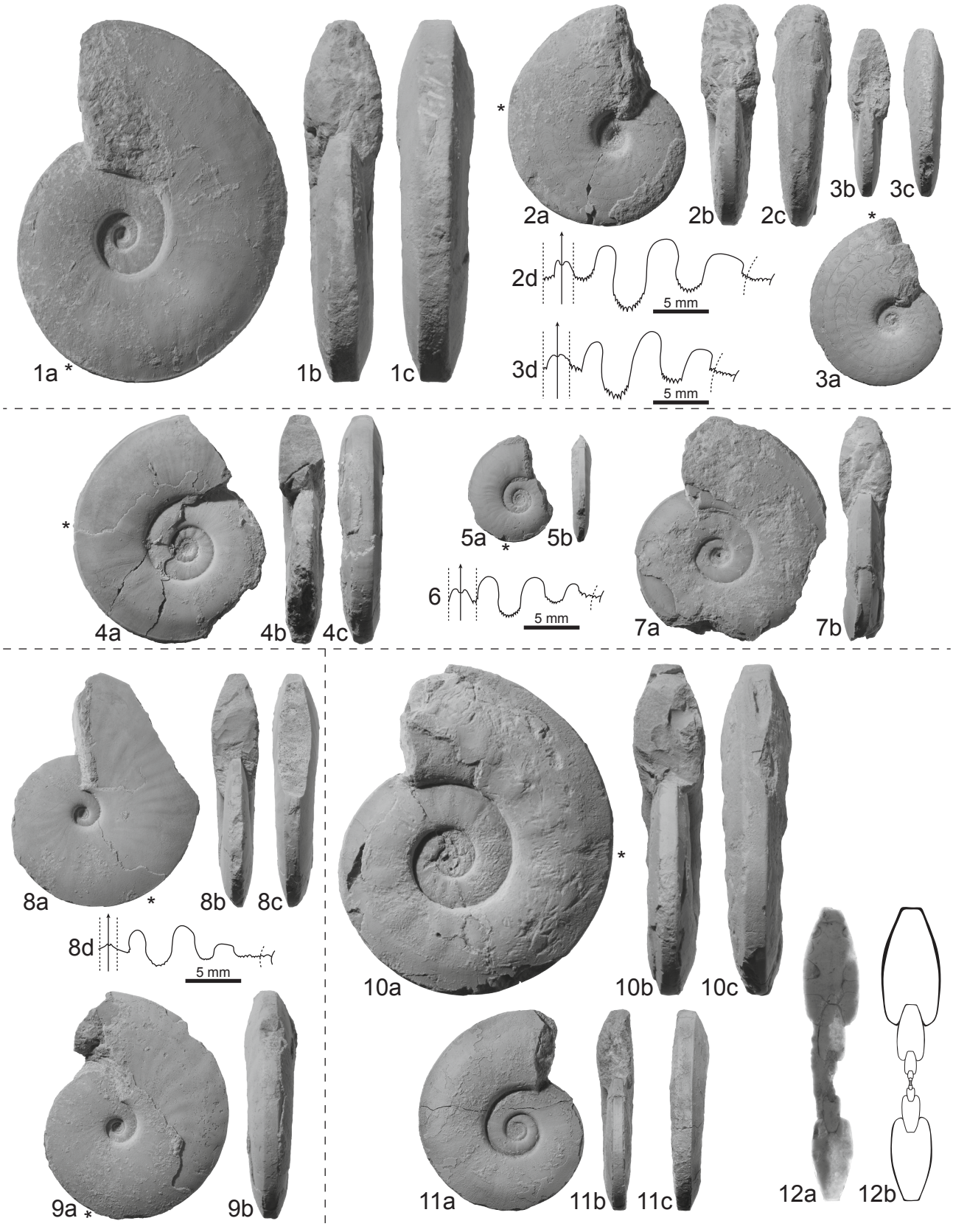
1a *
1b
1c
*
2a
2b
2c
3b
3c
2d
5 mm
3d
5 mm
*
3a
*
4a
4b
4c
5a
*
5b
6
5 mm
7a
7b
8a
*
8b
8c
8d
5 mm
9a *
9b
10a
*
10b
10c
11a
11b
11c
12a
12b

Plate 11

(All figures natural size unless otherwise indicated; asterisks indicate the position of the last septum)

1a-c: *Ambites superior* (Waagen, 1895). PIMUZ30333.
Loc. Nam302, base CM, Nammal Nala, *Ambites superior* beds (middle Dienerian).

2a-c: *Ambites superior* (Waagen, 1895). PIMUZ30334.
Loc. Nam53, base CM, Nammal Nala, *Ambites superior* beds (middle Dienerian).

3a-b: *Ambites superior* (Waagen, 1895). PIMUZ30335.
Loc. Nam53, base CM, Nammal Nala, *Ambites superior* beds (middle Dienerian).

4: *Ambites superior* (Waagen, 1895). PIMUZ30336.
Loc. Nam53, base CM, Nammal Nala, *Ambites superior* beds (middle Dienerian). Suture line at H = 20.7 mm; × 1.5 (mirrored image).

5: *Ambites superior* (Waagen, 1895). PIMUZ30337.
Loc. Nam53, base CM, Nammal Nala, *Ambites superior* beds (middle Dienerian). Suture line at H = 18.5 mm; × 1.5.

6: *Ambites superior* (Waagen, 1895). PIMUZ30338.
Loc. Nam53, base CM, Nammal Nala, *Ambites superior* beds (middle Dienerian). Suture line at H = 18.3 mm; × 1.5 (mirrored image).

7: *Ambites superior* (Waagen, 1895). PIMUZ30339.
Loc. Nam53, base CM, Nammal Nala, *Ambites superior* beds (middle Dienerian). Suture line at H = 13.9 mm; × 1.5 (mirrored image).

8a-b: *Ambites superior* (Waagen, 1895). PIMUZ30340.
Loc. Nam53, base CM, Nammal Nala, *Ambites superior* beds (middle Dienerian).

9a-b: *Ambites superior* (Waagen, 1895). PIMUZ30341.
Loc. Nam371, base CM, Nammal Nala, *Ambites superior* beds (middle Dienerian).

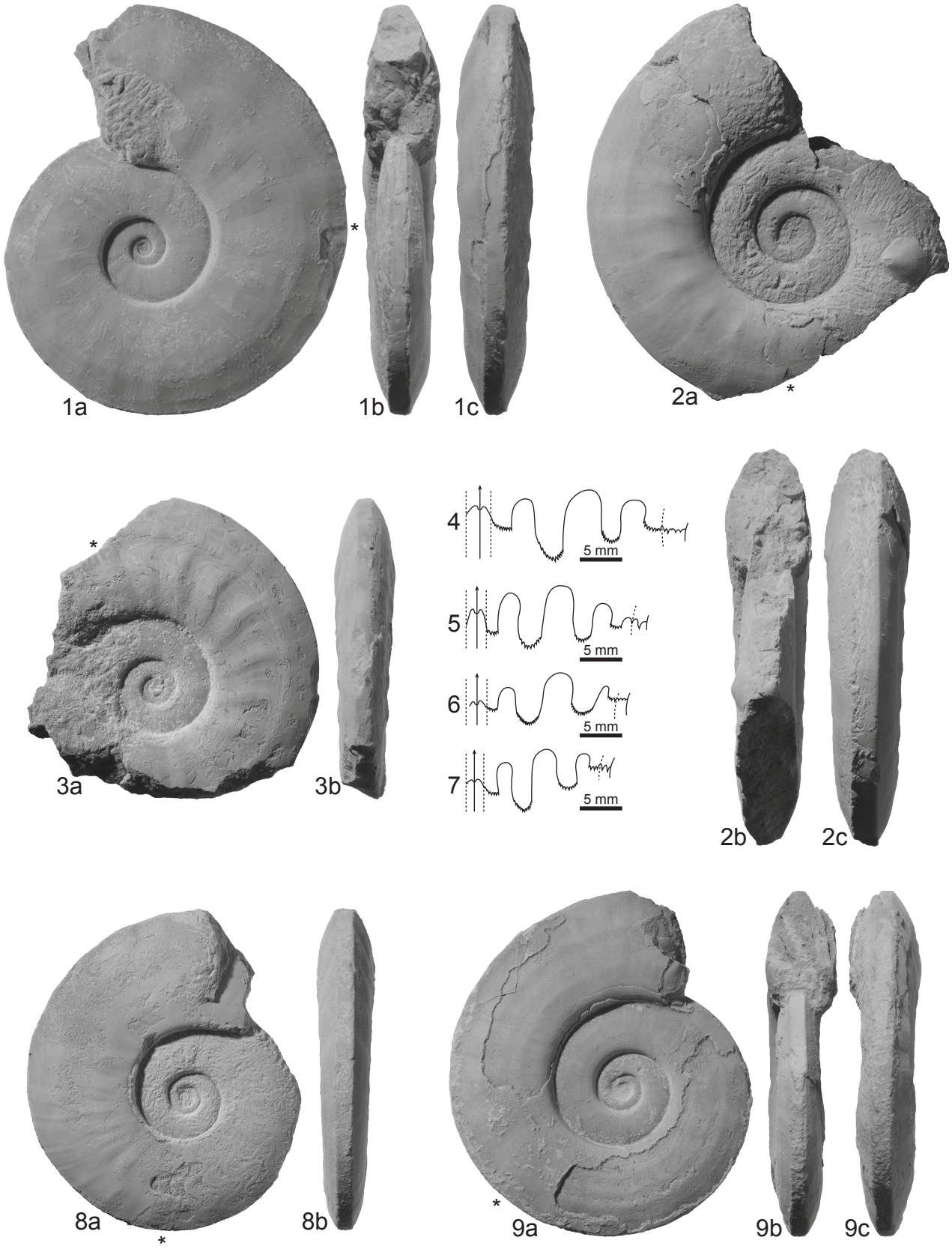
1a
1b
1c
2a
2b
2c
3a
3b
4
5
6
7
5 mm
8a
8b
9a
9b
9c

Plate 12

(All figures natural size unless otherwise indicated; asterisks indicate the position of the last septum)

1a-c: *Ambites superior* (Waagen, 1895). PIMUZ30342.
Loc. Nam308, base CM, Nammal Nala, *Ambites superior* beds (middle Dienerian).

2a-d: *Ambites lilangensis* (Krafft, 1909). PIMUZ30343.
Loc. Nam100, base CM, Nammal Nala, *Ambites lilangensis* beds (middle Dienerian). a-c) lateral, apertural and ventral views. d) Suture line at H = 19.7 mm; × 1.5.

3a-d: *Ambites lilangensis* (Krafft, 1909). PIMUZ30344.
Loc. Nam344, base CM, Nammal Nala, *Ambites lilangensis* beds (middle Dienerian). a-c) lateral, apertural and ventral views. d) Suture line at H = 13.5 mm; × 1.5.

4a-d: *Ambites lilangensis* (Krafft, 1909). PIMUZ30345.
Loc. Nam100, base CM, Nammal Nala, *Ambites lilangensis* beds (middle Dienerian). a-c) lateral, apertural and ventral views. d) Suture line at H = 22.4 mm; × 1.5.

5a-d: *Ambites lilangensis* (Krafft, 1909). PIMUZ30346.
Loc. Nam344, base CM, Nammal Nala, *Ambites lilangensis* beds (middle Dienerian). a-c) lateral, apertural and ventral views. d) Suture line at H = 17.4 mm; × 1.5.

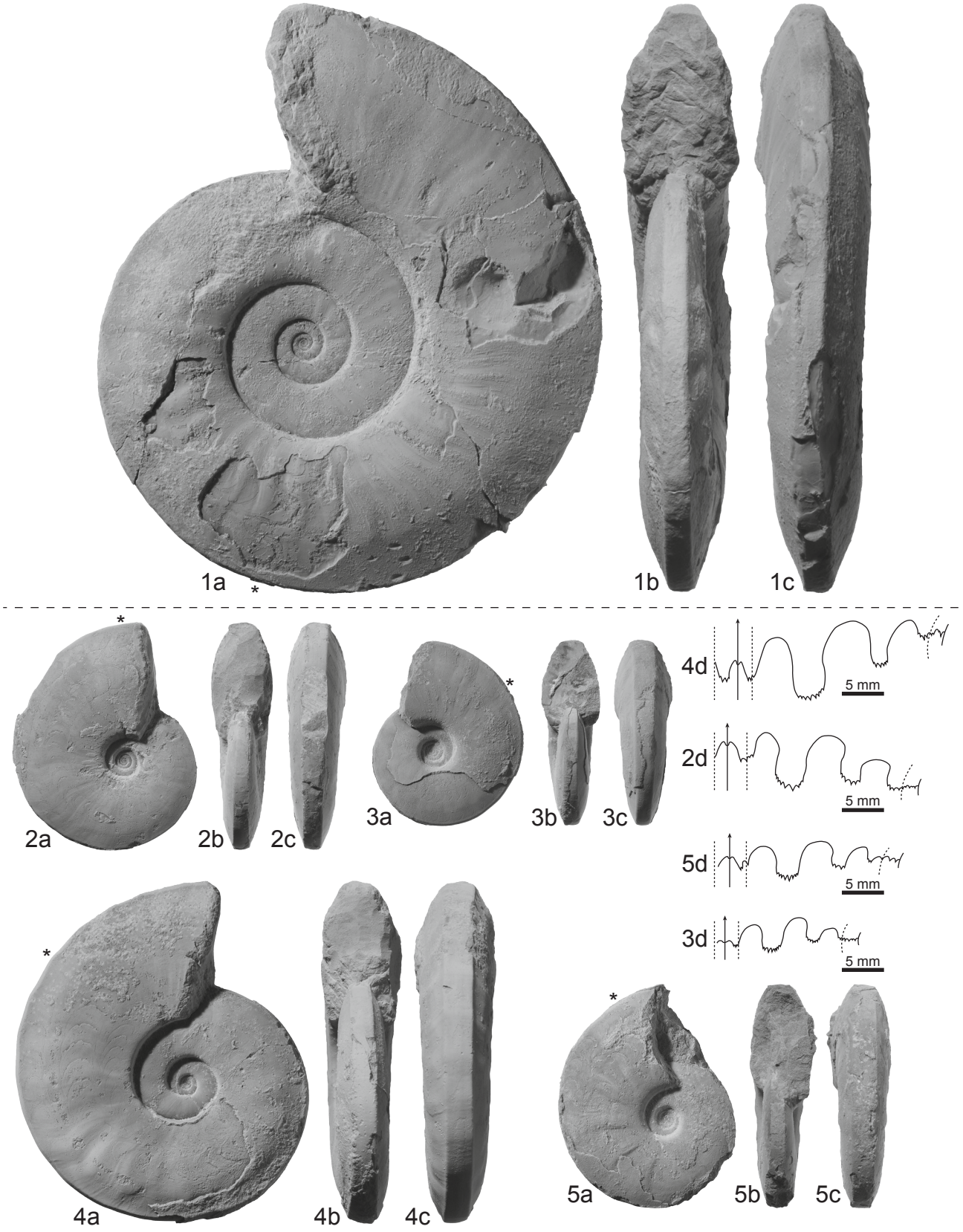
1a
*
1b
1c
*
2a
2b
2c
*
3a
3b
3c
4d
5 mm
2d
5 mm
5d
5 mm
3d
5 mm
*
4a
4b
4c
*
5a
5b
5c

Plate 13

(All figures natural size unless otherwise indicated; asterisks indicate the position of the last septum)

1a-c: *Ambites lilangensis* (Krafft, 1909). PIMUZ30347.
Loc. Nam100, base CM, Nammal Nala, *Ambites lilangensis* beds (middle Dienerian).

2a-c: *Ambites lilangensis* (Krafft, 1909). PIMUZ30348.
Loc. Nam100, base CM, Nammal Nala, *Ambites lilangensis* beds (middle Dienerian).

3a-c: *Ambites* cf. *impressus* (Waagen, 1895). PIMUZ30349.
Loc. Nam344, base CM, Nammal Nala, *Ambites lilangensis* beds (middle Dienerian).

4a-b: *Ambites bjerageri* n. sp. PIMUZ30350. Paratype
Loc. Nam503, base CM, Nammal Nala, *Ambites lilangensis* beds (middle Dienerian).

5a-d: *Ambites bjerageri* n. sp. PIMUZ30351. Holotype
Loc. Nam100, base CM, Nammal Nala, *Ambites lilangensis* beds (middle Dienerian). a-c) lateral, apertural and ventral views. d) Suture line at H = 7.7 mm; × 3.

6a-c: *Ambites bjerageri* n. sp. PIMUZ30352. Paratype
Loc. Nam92, base CM, Nammal Nala, *Ambites lilangensis* beds (middle Dienerian).

7a-c: *Ambites bjerageri* n. sp. PIMUZ30353. Paratype
Loc. Nam501, base CM, Nammal Nala, *Ambites lilangensis* beds (middle Dienerian).

8a-c: *Ambites bjerageri* n. sp. PIMUZ30354. Paratype
Loc. Nam501, base CM, Nammal Nala, *Ambites lilangensis* beds (middle Dienerian).

9a-b: *Ambites bjerageri* n. sp. PIMUZ30355. Paratype
Loc. Nam344, base CM, Nammal Nala, *Ambites lilangensis* beds (middle Dienerian).

10a-b: *Vavilovites* cf. *sverdrupi* (Tozer, 1963). PIMUZ30356.
Loc. Nam396, base CM, Nammal Nala, *Vavilovites* cf. *sverdrupi* beds (late Dienerian). a-b) lateral and ventral views. d) Suture line at H = 23.2 mm.

11a-b: *Vavilovites* cf. *sverdrupi* (Tozer, 1963). PIMUZ30357.
Loc. Nam396, base CM, Nammal Nala, *Vavilovites* cf. *sverdrupi* beds (late Dienerian).

12a-b: *Vavilovites* cf. *sverdrupi* (Tozer, 1963). PIMUZ30358.
Loc. Nam316, base CM, Nammal Nala, *Vavilovites* cf. *sverdrupi* beds (late Dienerian).

13a-b: *Vavilovites* cf. *sverdrupi* (Tozer, 1963). PIMUZ30359.
Loc. Nam318, base CM, Nammal Nala, *Vavilovites* cf. *sverdrupi* beds (late Dienerian).

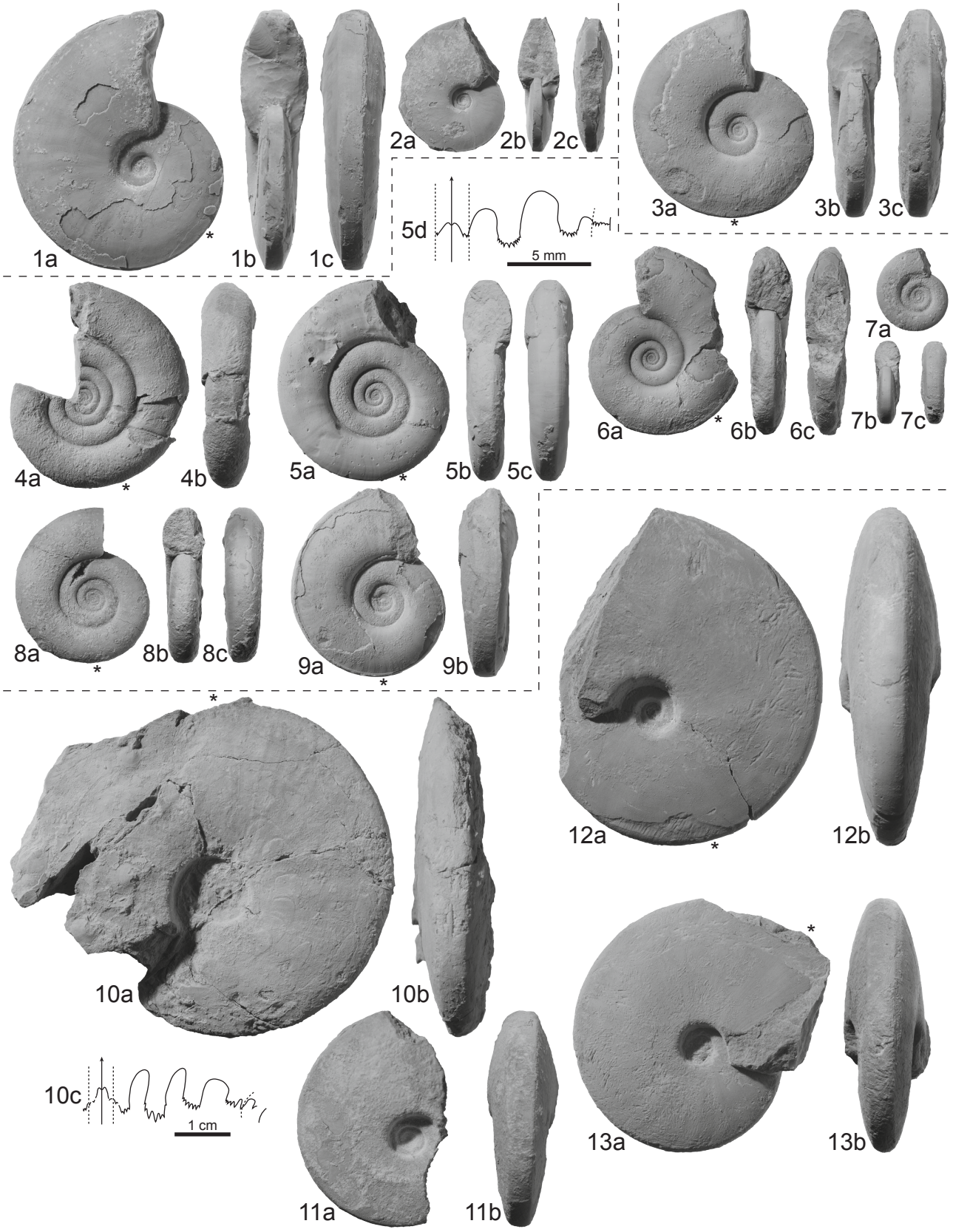
1a
1b
1c
2a
2b
2c
5d
5 mm
3a
3b
3c
4a
4b
5a
5b
5c
6a
6b
6c
7a
7b
7c
8a
8b
8c
9a
9b
12a
12b
10a
10b
10c
1 cm
11a
11b
13a
13b

Plate 14

(All figures natural size unless otherwise indicated; asterisks indicate the position of the last septum)

1a-d: *Koninckites vetustus* Waagen, 1895. PIMUZ30360.
Loc. Nam71, base CM, Nammal Nala, *Koninckites vetustus* beds (late Dienerian). Specimen with partially preserved body chamber, but position of the last septum unknown.

2a-c: *Koninckites vetustus* Waagen, 1895. PIMUZ30361.
Loc. Nam347, base CM, Nammal Nala, *Koninckites vetustus* beds (late Dienerian).

3a-b: *Koninckites vetustus* Waagen, 1895. PIMUZ30362.
Loc. War104, base CM, Wargal, *Koninckites vetustus* beds (late Dienerian). × 2.

4a-b: *Koninckites vetustus* Waagen, 1895. PIMUZ30363.
Loc. Nam305, base CM, Nammal Nala, *Koninckites vetustus* beds (late Dienerian). × 2.

5a-c: *Koninckites vetustus* Waagen, 1895. PIMUZ30364.
Loc. Nam305, base CM, Nammal Nala, *Koninckites vetustus* beds (late Dienerian).

6a-c: *Koninckites vetustus* Waagen, 1895. PIMUZ30365.
Loc. Nam349, base CM, Nammal Nala, *Koninckites vetustus* beds (late Dienerian).

7a-d: *Koninckites vetustus* Waagen, 1895. PIMUZ30366.
Loc. Nam312, base CM, Nammal Nala, *Koninckites vetustus* beds (late Dienerian).

8a-c: *Koninckites vetustus* Waagen, 1895. PIMUZ30367.
Loc. War104, base CM, Wargal, *Koninckites vetustus* beds (late Dienerian).

9a-c: *Koninckites vetustus* Waagen, 1895. PIMUZ30368.
Loc. War104, base CM, Wargal, *Koninckites vetustus* beds (late Dienerian).

10a-c: *Koninckites vetustus* Waagen, 1895. PIMUZ30369.
Loc. War104, base CM, Wargal, *Koninckites vetustus* beds (late Dienerian).

11a-b: *Koninckites vetustus* Waagen, 1895. PIMUZ30370.
Loc. Nam305, base CM, Nammal Nala, *Koninckites vetustus* beds (late Dienerian). a) Polished cross section. b) Cross section.

12a-b: *Koninckites vetustus* Waagen, 1895. PIMUZ30371.
Loc. Nam305, base CM, Nammal Nala, *Koninckites vetustus* beds (late Dienerian). a) Polished cross section. b) Cross section.

13a-b: *Koninckites vetustus* Waagen, 1895 PIMUZ30372.
Loc. Nam305, base CM, Nammal Nala, *Koninckites vetustus* beds (late Dienerian). a) Polished cross section. b) Cross section.

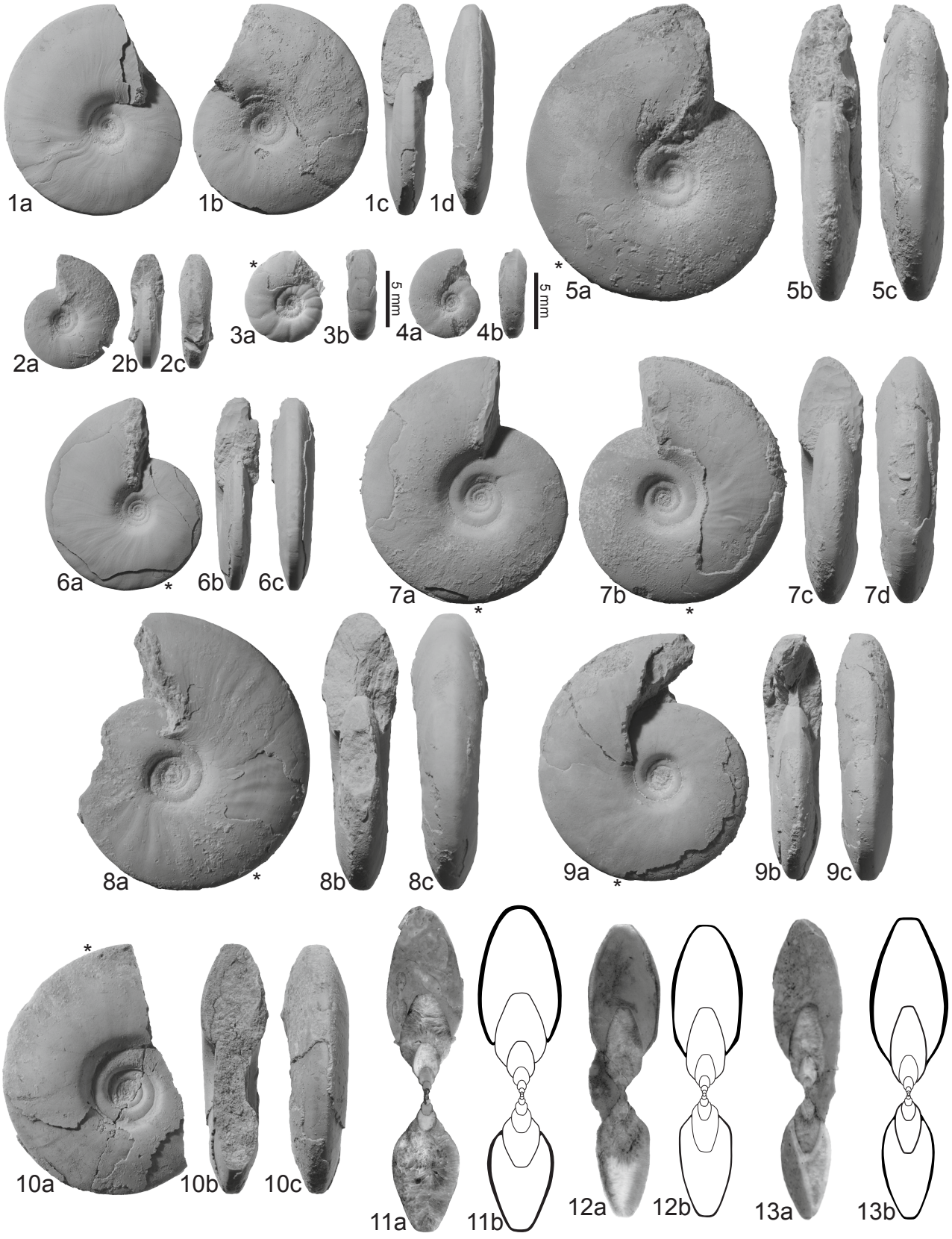
1a
1b
1c
1d
5a
5b
5c
2a
2b
2c
3a
3b
4a
4b
5 mm
5 mm
6a
6b
6c
7a
7b
7c
7d
8a
8b
8c
9a
9b
9c
10a
10b
10c
11a
11b
12a
12b
13a
13b

Plate 15

(All figures natural size unless otherwise indicated; asterisks indicate the position of the last septum)

1a-d: *Koninckites vetustus* Waagen, 1895. GSI7161. Lectotype. (Photo by B. Kummel)
LCL, Chiddru, precise bed and locality unknown.

2a-d: *Koninckites vetustus* Waagen, 1895. PIMUZ30373.
Loc. Nam63, base CM, Nammal Nala, *Koninckites vetustus* beds (late Dienerian). a-c) lateral, apertural and ventral views. d) Suture line at H = 18.5 mm; × 1.5 (mirrored image).

3a-d: *Koninckites vetustus* Waagen, 1895. PIMUZ30374.
Loc. Nam305, base CM, Nammal Nala, *Koninckites vetustus* beds (late Dienerian). a-c) lateral, apertural and ventral views. d) Suture line at H = 16.6 mm; × 1.5.

4a-d: *Koninckites vetustus* Waagen, 1895. PIMUZ30375.
Loc. Nam83, base CM, Nammal Nala, *Koninckites vetustus* beds (late Dienerian). a-c) lateral, apertural and ventral views. d) Suture line at H = 17 mm; × 1.5 (mirrored image).

5: *Koninckites vetustus* Waagen, 1895. PIMUZ30376.
Loc. Nam305, base CM, Nammal Nala, *Koninckites vetustus* beds (late Dienerian). Suture line at H = 18.7 mm; × 1.5 (mirrored image).

6a-d: *Koninckites vetustus* Waagen, 1895. PIMUZ30377.
Loc. Nam305, base CM, Nammal Nala, *Koninckites vetustus* beds (late Dienerian). a-c) lateral, apertural and ventral views; × 0.7. d) Suture line at H = 30.3 mm.

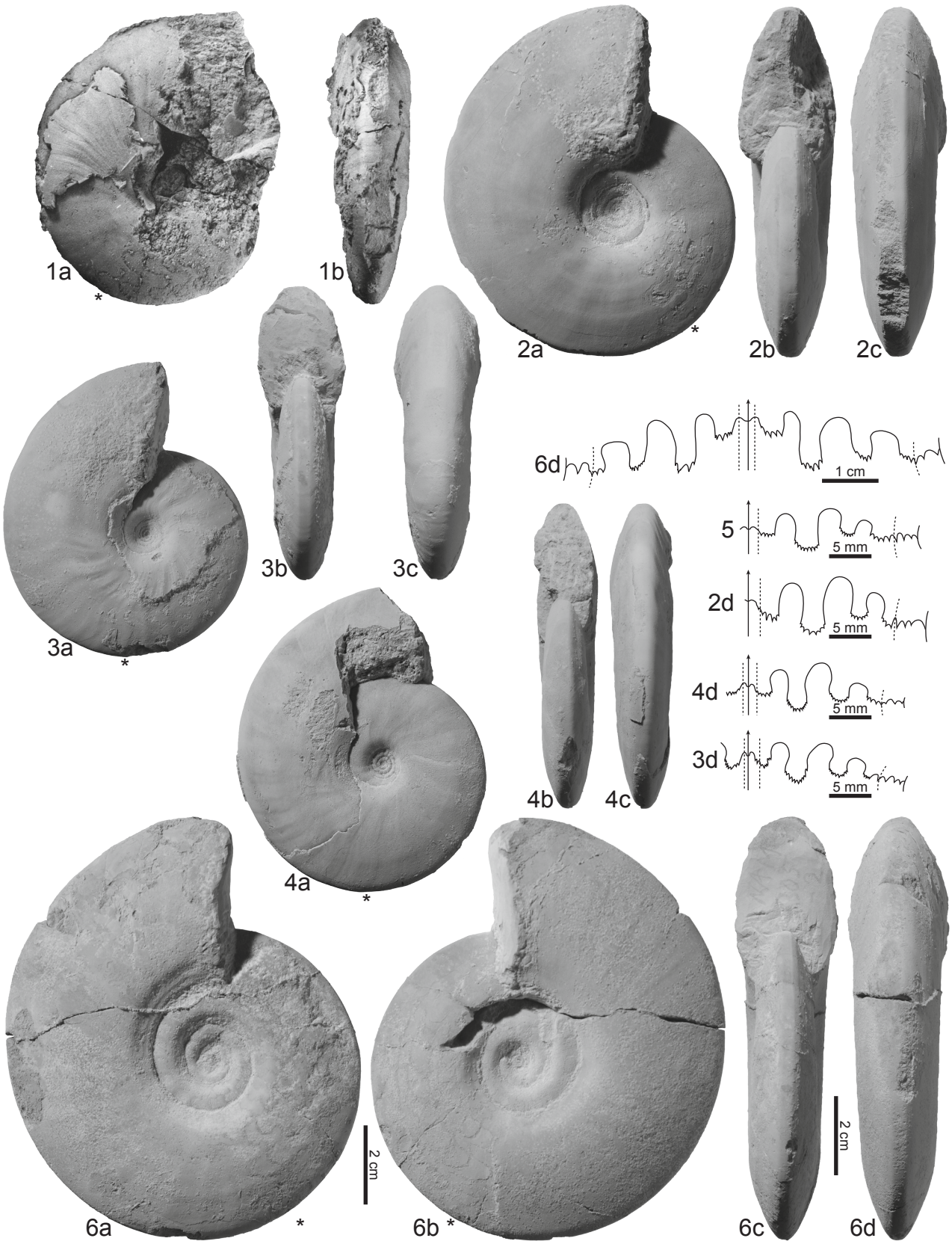
1a
*
1b
2a
*
2b
2c
6d
1 cm
3a
*
3b
3c
5
5 mm
2d
5 mm
4d
5 mm
3d
5 mm
4b
4c
4a
*
2 cm
6a
*
6b *
2 cm
6c
6d

Plate 16

(All figures natural size; asterisks indicate the position of the last septum)

1a-c: *Koninckites vetustus* Waagen, 1895. PIMUZ30378.
Loc. War104, base CM, Wargal, *Koninckites vetustus* beds (late Dienerian).

2a-c: *Koninckites vetustus* Waagen, 1895. PIMUZ30379.
Loc. Nam312, base CM, Nammal Nala, *Koninckites vetustus* beds (late Dienerian).

3a-c: *Koninckites vetustus* Waagen, 1895. PIMUZ30380.
Loc. Chi51, top LCL, Chiddru, *Koninckites vetustus* beds (late Dienerian).

4a-c: *Koninckites vetustus* Waagen, 1895. PIMUZ30381.
Loc. Nam71, base CM, Nammal Nala, *Koninckites vetustus* beds (late Dienerian).

5a-c: *Koninckites vetustus* Waagen, 1895. PIMUZ30382.
Loc. Nam312, base CM, Nammal Nala, *Koninckites vetustus* beds (late Dienerian).

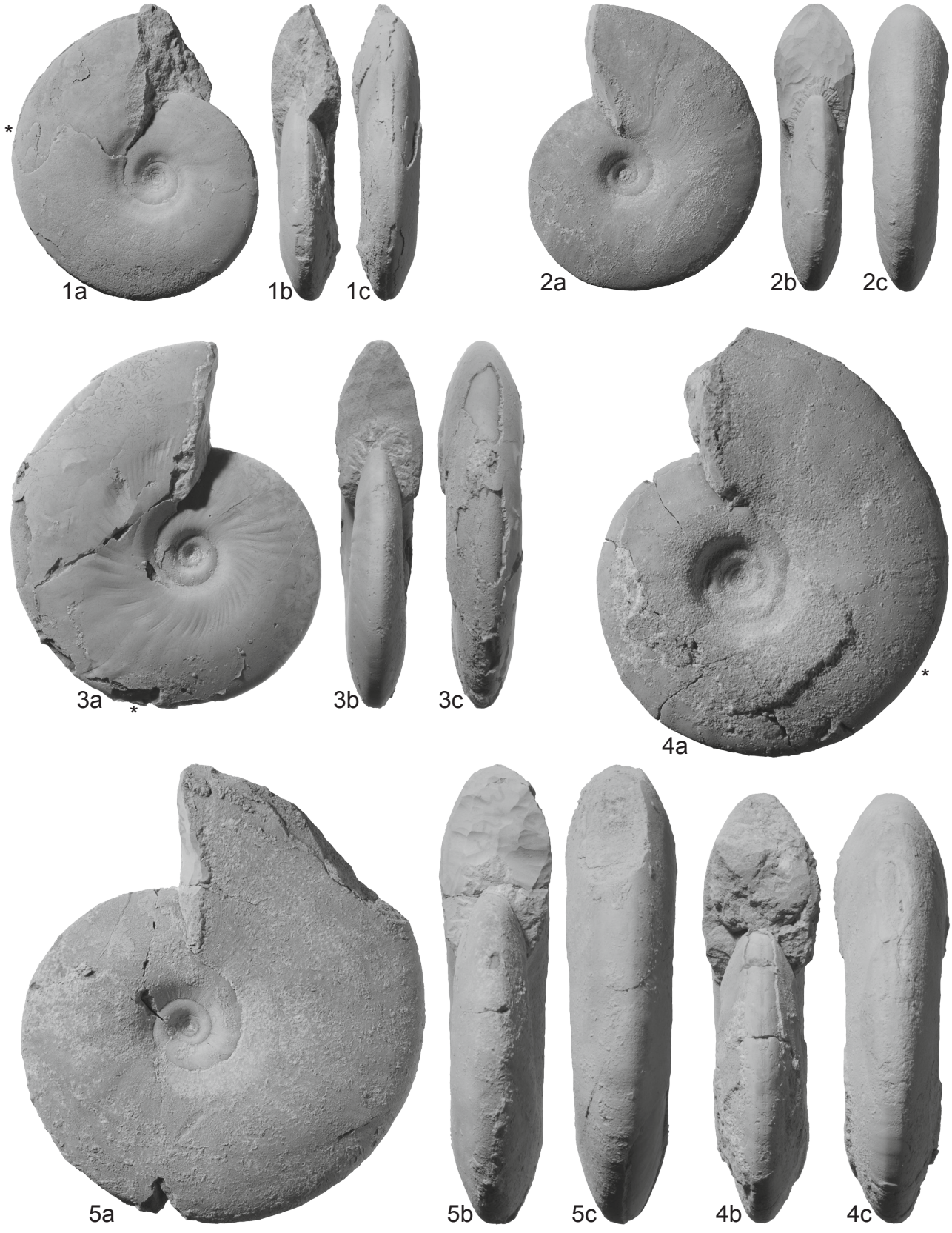
*
1a
1b
1c
2a
2b
2c
3a
*
3b
3c
4a
*
5a
5b
5c
4b
4c

Plate 17

(All figures natural size unless otherwise indicated; asterisks indicate the position of the last septum)

1a-d: *Koninckites vetustus* Waagen, 1895. PIMUZ30383.
Loc. Nam83, base CM, Nammal Nala, *Kingites davidsonianus* beds (late Dienerian).

2a-b: *Koninckites khoorensis* (Waagen, 1895). PIMUZ30384.
Loc. Nam101d, base CM, Nammal Nala, *Kingites davidsonianus* beds (late Dienerian); × 1.5.

3a-c: *Koninckites khoorensis* (Waagen, 1895). PIMUZ30385.
Loc. Nam61, base CM, Nammal Nala, *Kingites davidsonianus* beds (late Dienerian; see also Pl. 18: 9); × 1.5.

4a-c: *Koninckites khoorensis* (Waagen, 1895). PIMUZ30386.
Loc. Nam101d, base CM, Nammal Nala, *Kingites davidsonianus* beds (late Dienerian; see also Pl 18: 7).

5a-b: *Koninckites khoorensis* (Waagen, 1895). PIMUZ30387.
Loc. Nam101d, base CM, Nammal Nala, *Kingites davidsonianus* beds (late Dienerian); × 1.5.

6a-c: *Koninckites khoorensis* (Waagen, 1895). PIMUZ30388.
Loc. Nam67, base CM, Nammal Nala, *Kingites davidsonianus* beds (late Dienerian); × 1.5.

7a-c: *Koninckites khoorensis* (Waagen, 1895). PIMUZ30389.
Loc. Nam67, base CM, Nammal Nala, *Kingites davidsonianus* beds (late Dienerian).

8a-b: *Koninckites khoorensis* (Waagen, 1895). PIMUZ30390.
Loc. Nam59, base CM, Nammal Nala, *Kingites davidsonianus* beds (late Dienerian).

9a-c: *Koninckites khoorensis* (Waagen, 1895). PIMUZ30391.
Loc. Nam61, base CM, Nammal Nala, *Kingites davidsonianus* beds (late Dienerian; see also Pl. 18: 8).

10a-c: *Koninckites khoorensis* (Waagen, 1895). PIMUZ30392.
Loc. Nam61, base CM, Nammal Nala, *Kingites davidsonianus* beds (late Dienerian).

11a-c: *Koninckites khoorensis* (Waagen, 1895). PIMUZ30393.
Loc. Nam101d, base CM, Nammal Nala, *Kingites davidsonianus* beds (late Dienerian; see also Pl. 18: 6).

12a-c: *Koninckites khoorensis* (Waagen, 1895). PIMUZ30394.
Loc. Nam101d, base CM, Nammal Nala, *Kingites davidsonianus* beds (late Dienerian).

13a-c: *Koninckites khoorensis* (Waagen, 1895). PIMUZ30395.
Loc. Nam61, base CM, Nammal Nala, *Kingites davidsonianus* beds (late Dienerian).

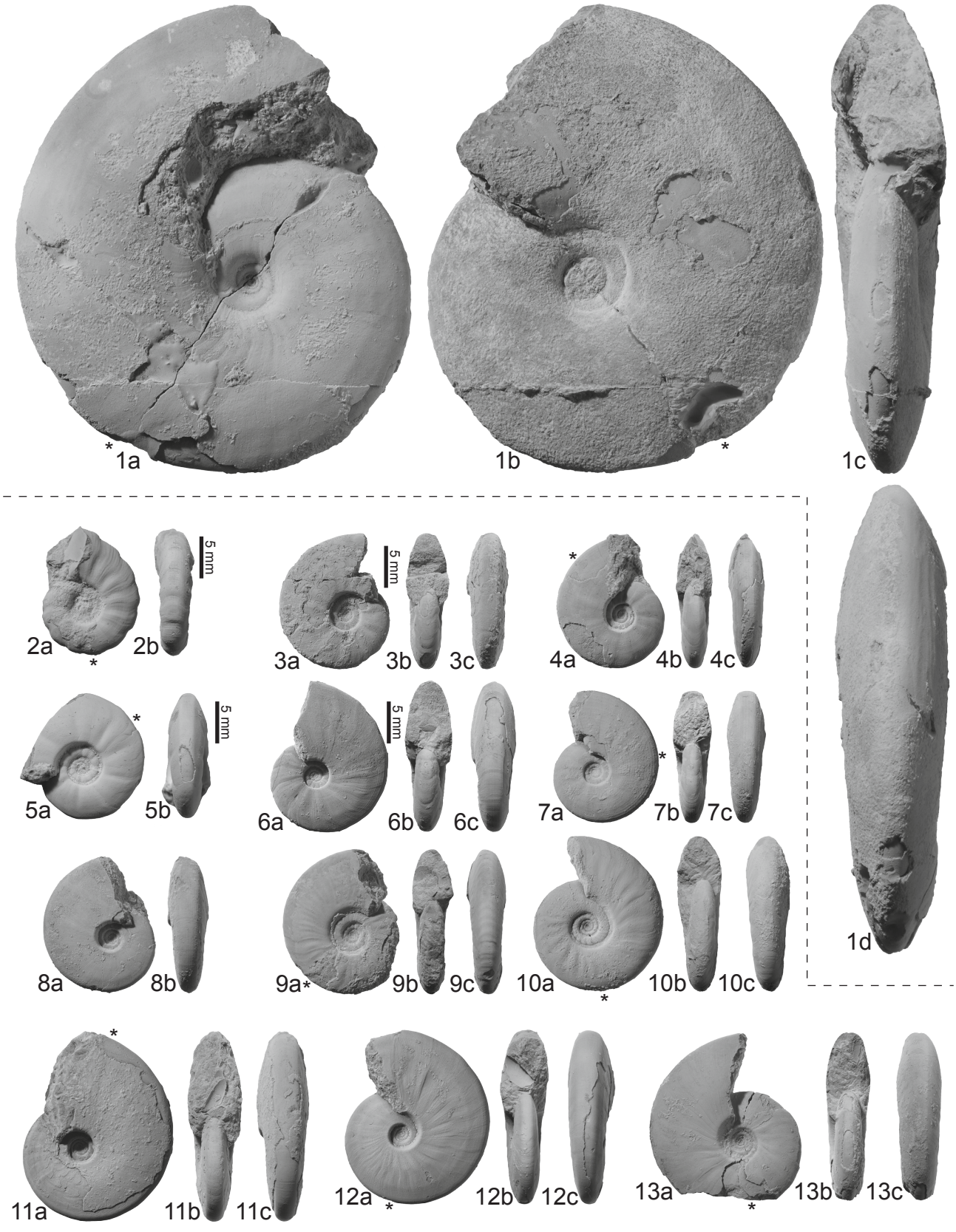
1a
1b
1c
1d
2a
2b
3a
3b
3c
4a
4b
4c
5a
5b
6a
6b
6c
7a
7b
7c
8a
8b
9a
9b
9c
10a
10b
10c
11a
11b
11c
12a
12b
12c
13a
13b
13c
5 mm

Plate 18

(All figures natural size unless otherwise indicated; asterisks indicate the position of the last septum)

1: *Koninckites khoorensis* (Waagen, 1895). PIMUZ30396.
Loc. Nam61, base CM, Nammal Nala, *Kingites davidsonianus* beds (late Dienerian). Suture line at H = 28.7 mm.
2: *Koninckites khoorensis* (Waagen, 1895). PIMUZ30397.
Loc. Nam59, base CM, Nammal Nala, *Kingites davidsonianus* beds (late Dienerian). Suture line at H = 24.3 mm (mirrored image; see also Pl. 20: 2).
3: *Koninckites khoorensis* (Waagen, 1895). PIMUZ30398.
Loc. Nam724, base CM, Nammal Nala, *Kingites davidsonianus* beds (late Dienerian). Suture line at H = 22.4 mm; × 1.2 (mirrored image; see also Pl. 20: 1).
4: *Koninckites khoorensis* (Waagen, 1895). PIMUZ30399.
Loc. Nam59, base CM, Nammal Nala, *Vavilovites* cf. *sverdrupi* beds (late Dienerian). Suture line at H = 18.9 mm; × 1.5 (mirrored image; see also Pl. 20: 3).
5: *Koninckites khoorensis* (Waagen, 1895). PIMUZ30400.
Loc. Nam59, base CM, Nammal Nala, *Kingites davidsonianus* beds (late Dienerian). Suture line at H = 17.8 mm; × 1.5 (see also Pl. 19: 4).
6: *Koninckites khoorensis* (Waagen, 1895). PIMUZ30393.
Loc. Nam101d, base CM, Nammal Nala, *Kingites davidsonianus* beds (late Dienerian). Suture line at H = 17.7 mm; × 1.5 (see also Pl. 17: 11).
7: *Koninckites khoorensis* (Waagen, 1895). PIMUZ30386.
Loc. Nam101d, base CM, Nammal Nala, *Kingites davidsonianus* beds (late Dienerian). Suture line at H = 9.9 mm; × 2 (mirrored image; see also Pl. 17: 4).
8: *Koninckites khoorensis* (Waagen, 1895). PIMUZ30391.
Loc. Nam61, base CM, Nammal Nala, *Kingites davidsonianus* beds (late Dienerian). Suture line at H = 7.5 mm; × 2 (mirrored image; see also Pl. 17: 9).
9: *Koninckites khoorensis* (Waagen, 1895). PIMUZ30385.
Loc. Nam61, base CM, Nammal Nala, *Kingites davidsonianus* beds (late Dienerian). Suture line at H = 7.3 mm; × 2 (see also Pl. 17: 3).
10a-b: *Koninckites khoorensis* (Waagen, 1895). PIMUZ30401.
Loc. Nam61, base CM, Nammal Nala, *Kingites davidsonianus* beds (late Dienerian). a) Polished cross section. b) Cross section.
11a-b: *Koninckites khoorensis* (Waagen, 1895). PIMUZ30402.
Loc. Nam61, base CM, Nammal Nala, *Kingites davidsonianus* beds (late Dienerian). a) Polished cross section. b) Cross section.
12a-b: *Koninckites khoorensis* (Waagen, 1895). PIMUZ30403.
Loc. Nam336, base CM, Nammal Nala, *Kingites davidsonianus* beds (late Dienerian). a) Polished cross section. b) Cross section.
13a-c: *Koninckites khoorensis* (Waagen, 1895). PIMUZ30404.
Loc. Nam502, base CM, Nammal Nala, *Kingites davidsonianus* beds (late Dienerian). Asymmetric specimen with a strong ornamentation on the left side.
14a-c: *Koninckites khoorensis* (Waagen, 1895). PIMUZ30405.
Loc. Nam101d, base CM, Nammal Nala, *Kingites davidsonianus* beds (late Dienerian).
15a-b: *Koninckites khoorensis* (Waagen, 1895). PIMUZ30406.
Loc. Nam304, base CM, Nammal Nala, *Kingites davidsonianus* beds (late Dienerian).
16a-c: *Koninckites khoorensis* (Waagen, 1895). PIMUZ30407.
Loc. Nam61, base CM, Nammal Nala, *Kingites davidsonianus* beds (late Dienerian).
17a-b: *Koninckites khoorensis* (Waagen, 1895). PIMUZ30408.
Loc. Nam101d, base CM, Nammal Nala, *Kingites davidsonianus* beds (late Dienerian).
18a-c: *Koninckites khoorensis* (Waagen, 1895). PIMUZ30409.
Loc. Nam59, base CM, Nammal Nala, *Kingites davidsonianus* beds (late Dienerian). a-b) lateral and ventral views. c) Suture line at H = 13.3 mm; × 2.

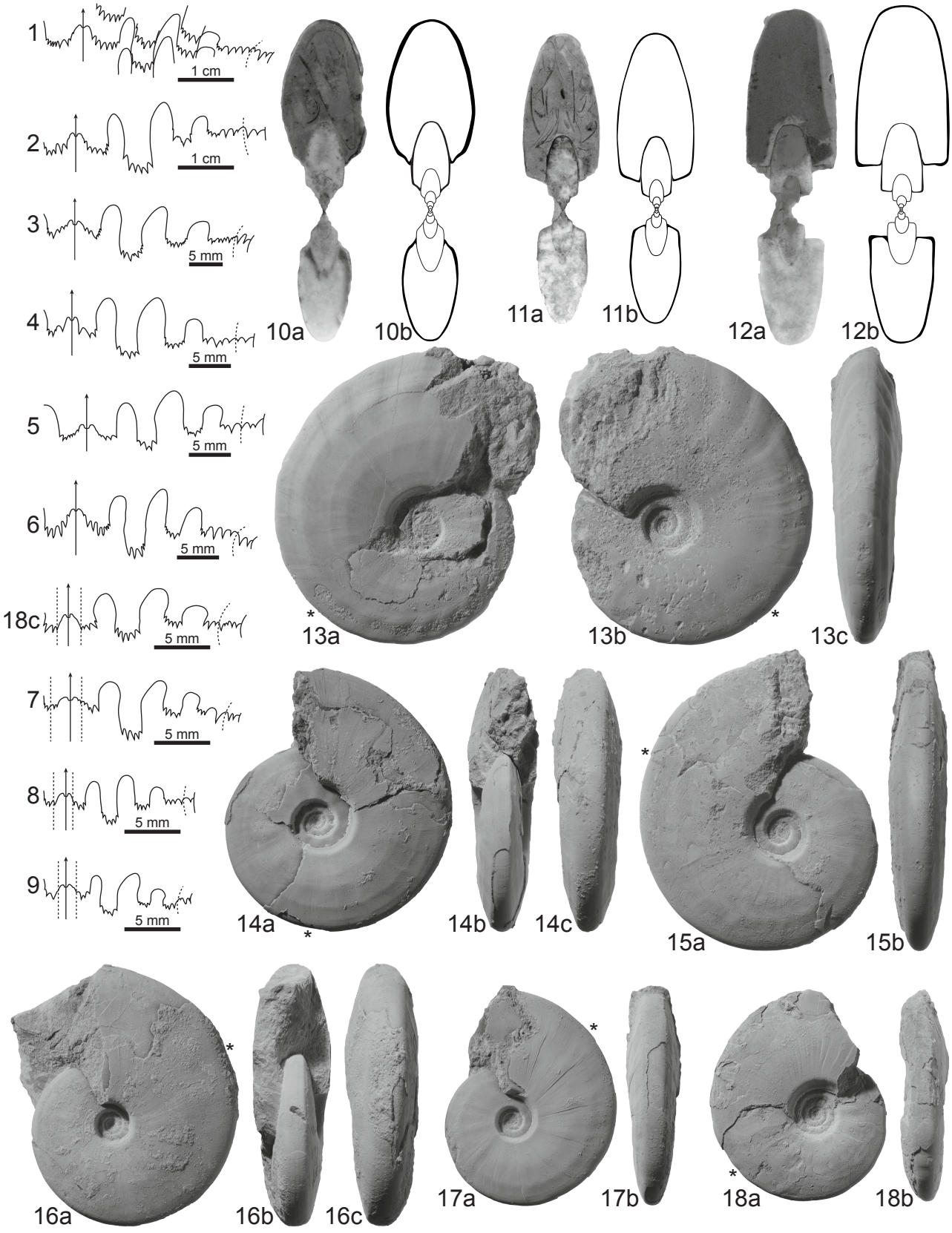
1
1 cm
2
1 cm
3
5 mm
4
5 mm
5
5 mm
6
5 mm
18c
5 mm
7
5 mm
8
5 mm
9
5 mm
10a
10b
11a
11b
12a
12b
13a
13b
13c
14a
14b
14c
15a
15b
16a
16b
16c
17a
17b
18a
18b

Plate 19

(All figures natural size; asterisks indicate the position of the last septum)

1a-b: *Koninckites khoorensis* (Waagen, 1895). PIMUZ30410.
Loc. Nam130, base CM, Nammal Nala, *Kingites davidsonianus* beds (late Dienerian).

2a-b: *Koninckites khoorensis* (Waagen, 1895). PIMUZ30411.
Loc. Nam337, base CM, Nammal Nala, *Kingites davidsonianus* beds (late Dienerian).

3a-c: *Koninckites khoorensis* (Waagen, 1895). PIMUZ30412.
Loc. Nam59, base CM, Nammal Nala, *Kingites davidsonianus* beds (late Dienerian).

4a-b: *Koninckites khoorensis* (Waagen, 1895). PIMUZ30400.
Loc. Nam59, base CM, Nammal Nala, *Kingites davidsonianus* beds (late Dienerian; see also Pl 18: 5).

5a-c: *Koninckites khoorensis* (Waagen, 1895). PIMUZ30413.
Loc. Nam61, base CM, Nammal Nala, *Kingites davidsonianus* beds (late Dienerian).


1a
1b
3b
3c
2a
2b
*
3a
*
4a
*
4b
5a
*
5b
5c

Plate 20

(All figures natural size; asterisks indicate the position of the last septum)

1a-c: *Koninckites khoorensis* (Waagen, 1895). PIMUZ30398.
Loc. Nam724, base CM, Nammal Nala, *Vavilovites* cf. *sverdrupi* beds (late Dienerian; see also Pl 18: 3).

2a-c: *Koninckites khoorensis* (Waagen, 1895). PIMUZ30397.
Loc. Nam59, base CM, Nammal Nala, *Kingites davidsonianus* beds (late Dienerian; see also Pl 18: 2).

3a-b: *Koninckites khoorensis* (Waagen, 1895). PIMUZ30399.
Loc. Nam59, base CM, Nammal Nala, *Kingites davidsonianus* beds (late Dienerian; see also Pl 18: 4).

4a-b: *Koninckites khoorensis* (Waagen, 1895). PIMUZ30414.
Loc. Nam346, base CM, Nammal Nala, *Kingites davidsonianus* beds (late Dienerian).

5a-c: *Koninckites khoorensis* (Waagen, 1895). PIMUZ30415.
Loc. Nam502, base CM, Nammal Nala, *Kingites davidsonianus* beds (late Dienerian).

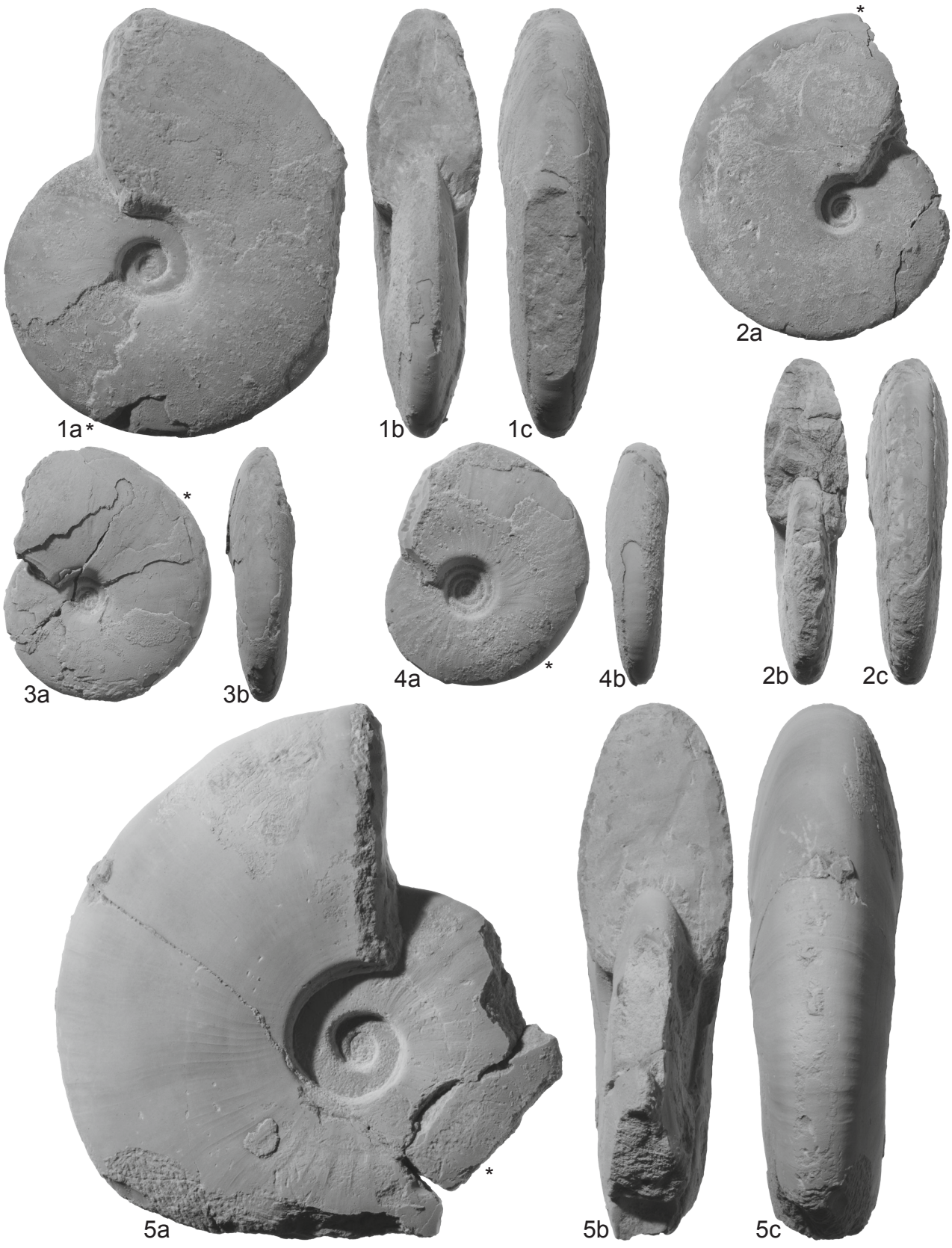
1a*
1b
1c
2a*
2b
2c
3a*
3b
4a*
4b
5a*
5b
5c

Plate 21

(All figures natural size unless otherwise indicated; asterisks indicate the position of the last septum)

1a-d: *Radioceras truncatum* (Spath, 1934). PIMUZ30416.
Loc. Nam350, base CM, Nammal Nala, *Awanites awani* beds (late Dienerian). a-c) lateral, apertural and ventral views. d) Suture line at H = 15.5 mm; × 1.5 (mirrored image).

2a-b: *Radioceras truncatum* (Spath, 1934). PIMUZ30417.
Loc. War104, base CM, Wargal, *Koninckites vetustus* beds (late Dienerian).

3a-c: *Pashtunites kraffti* (Spath, 1934) n. gen. PIMUZ30418.
Loc. Nam83, base CM, Nammal Nala, *Koninckites vetustus* beds (late Dienerian).

4a-d: *Pashtunites kraffti* (Spath, 1934) n. gen. PIMUZ30419.
Loc. Nam83, base CM, Nammal Nala, *Koninckites vetustus* beds (late Dienerian). a-c) lateral, apertural and ventral views. d) Suture line at H = 21.3 mm.

5a-c: *Awanites awani* n. gen., n. sp. PIMUZ30420. Paratype.
Loc. Nam350, base CM, Nammal Nala, *Awanites awani* beds (late Dienerian).

6a-c: *Awanites awani* n. gen., n. sp. PIMUZ30421. Paratype.
Loc. Nam350, base CM, Nammal Nala, *Awanites awani* beds (late Dienerian).

7a-c: *Awanites awani* n. gen., n. sp. PIMUZ30422. Holotype.
Loc. Nam350, base CM, Nammal Nala, *Awanites awani* beds (late Dienerian).). a-c) lateral, apertural and ventral views. d) Suture line at H = 15.8 mm; × 1.5 (mirrored image).

8a-c: *Koiloceras sahibi* n. sp. PIMUZ30423. Holotype.
Loc. Chi51, top LCL, Chiddru, *Koninckites vetustus* beds (late Dienerian).

9a-c: *Koiloceras sahibi* n. sp. PIMUZ30424. Paratype.
Loc. War104, base CM, Wargal, *Koninckites vetustus* beds (late Dienerian).

10a-c: *Xenodiscoides*? sp. indet. PIMUZ30425.
Loc. Chi51, top LCL, Chiddru, *Koninckites vetustus* beds (late Dienerian).

11a-c: *Shamaraites*? sp. indet. PIMUZ30426.
Loc. War104, base CM, Wargal, *Koninckites vetustus* beds (late Dienerian); × 2.

12a-b: *Bukkenites sakesarensis* n. sp. PIMUZ30427. Paratype.
Loc. Amb104, base LCL, Amb, *Gyronites dubius* beds (early Dienerian).

13a-b: *Bukkenites sakesarensis* n. sp. PIMUZ30428. Paratype.
Loc. Amb104, base LCL, Amb, *Gyronites dubius* beds (early Dienerian).

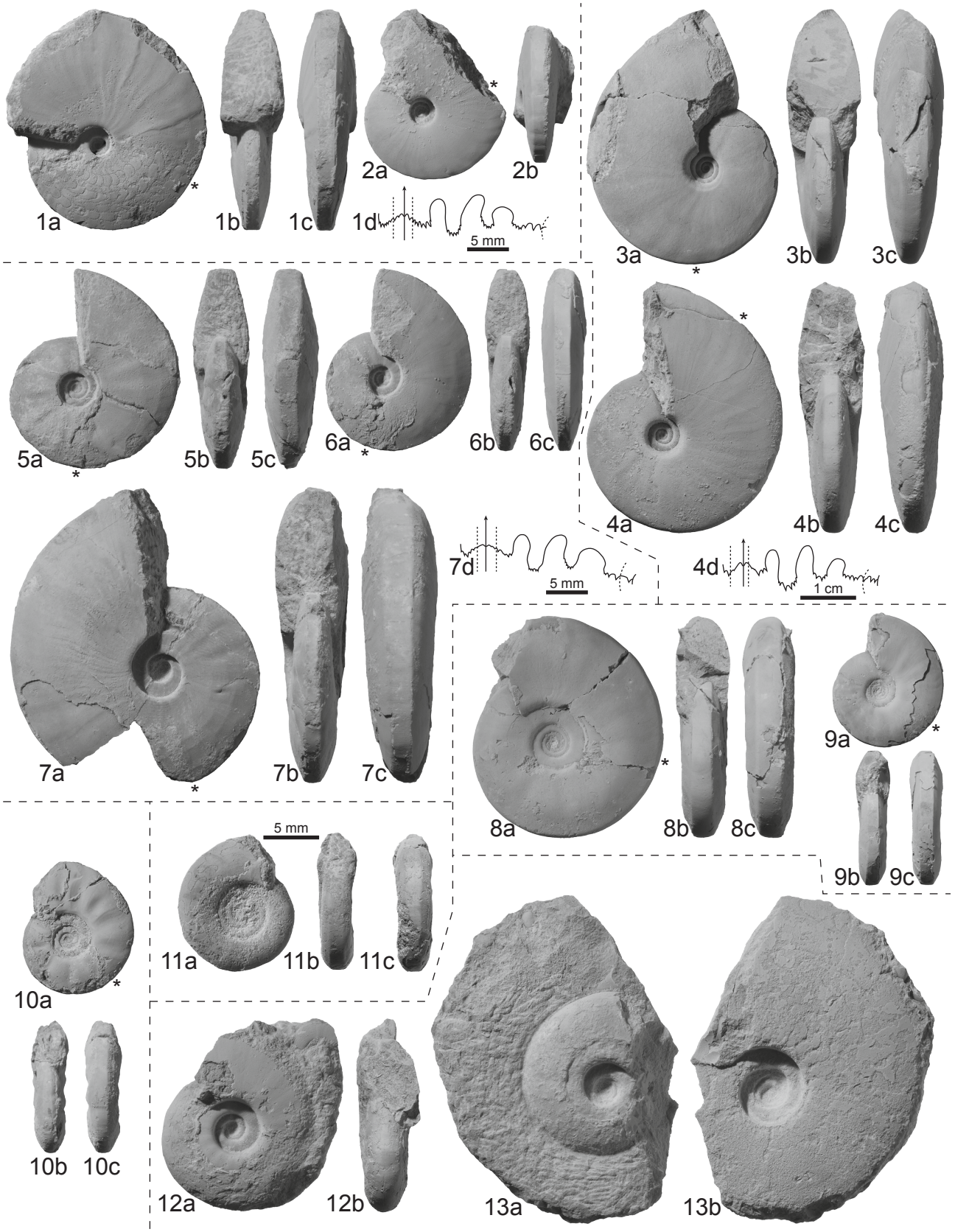
1a
1b
1c
1d
5 mm
2a
2b
3a
3b
3c
4a
4b
4c
1 cm
4d
5a
5b
5c
6a
6b
6c
7a
7b
7c
7d
5 mm
8a
8b
8c
9a
9b
9c
10a
10b
10c
11a
11b
11c
5 mm
12a
12b
13a
13b

Plate 22

(All figures natural size; asterisks indicate the position of the last septum)

1a-c: *Bukkenites sakesarensis* n. sp. PIMUZ30429. Holotype.
Loc. Amb104, base LCL, Amb, *Gyronites dubius* beds (early Dienerian).

2a-c: *Bukkenites sakesarensis* n. sp. PIMUZ30430. Paratype.
Loc. Amb104, base LCL, Amb, *Gyronites dubius* beds (early Dienerian).

3a-c: *Bukkenites sakesarensis* n. sp. PIMUZ30431. Paratype.
Loc. Amb104, base LCL, Amb, *Gyronites dubius* beds (early Dienerian). Robust variant.

4a-d: *Bukkenites sakesarensis* n. sp. PIMUZ30432. Paratype.
Loc. Amb104, base LCL, Amb, *Gyronites dubius* beds (early Dienerian). a-b) lateral and apertural views. c) Suture line at H = 21.8 mm. d) Dorsal part of the external suture line 120° further than the one drawn in 4c (H not measurable).

5a-b: *Proptychites lawrencianus* (de Konninck, 1863) *sensu* Waagen, 1895. PIMUZ30433.
Loc. Nam301, base CM, Nammal Nala, *Ambites lilangensis* beds (middle Dienerian). a) Polished cross section. b) Cross section.

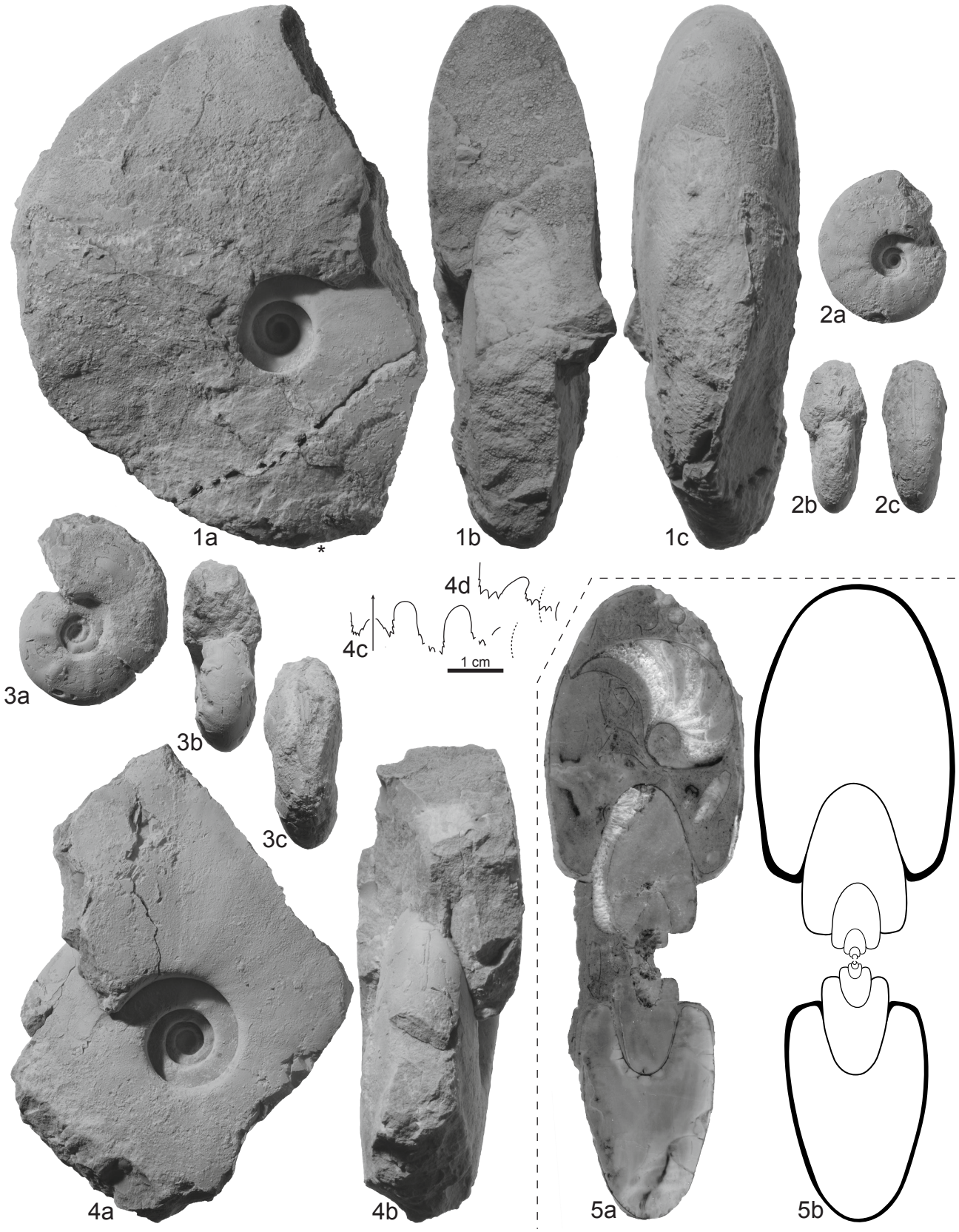
1a
*
1b
1c
2a
2b
2c
3a
3b
3c
4a
4b
4c
4d
1 cm
5a
5b

Plate 23

(All figures natural size unless otherwise indicated; asterisks indicate the position of the last septum)

1a-d: *Proptychites lawrencianus* (de Konninck, 1863) *sensu* Waagen, 1895. PIMUZ30434.
Loc. Nam300, floated block from base CM, Nammal Nala, *Ambites lilangensis* beds (middle Dienerian). a-c) lateral, apertural and ventral views; × 0.5. d) Suture line at H = 56 mm.

2a-c: *Proptychites lawrencianus* (de Konninck, 1863) *sensu* Waagen, 1895. PIMUZ30435.
Loc. Nam100, base CM, Nammal Nala, *Ambites lilangensis* beds (middle Dienerian). Inner whorls of a larger broken specimen.

3: *Proptychites lawrencianus* (de Konninck, 1863) *sensu* Waagen, 1895. PIMUZ30436.
Loc. Nam503, base CM, Nammal Nala, *Ambites lilangensis* beds (middle Dienerian). Suture line at H = 16.1 mm; × 1.5. From the inner whorls of a large broken specimen.

4a-c: *Proptychites lawrencianus* (de Konninck, 1863) *sensu* Waagen, 1895. PIMUZ30437.
Loc. Nam100, base CM, Nammal Nala, *Ambites lilangensis* beds (middle Dienerian); × 0.7.

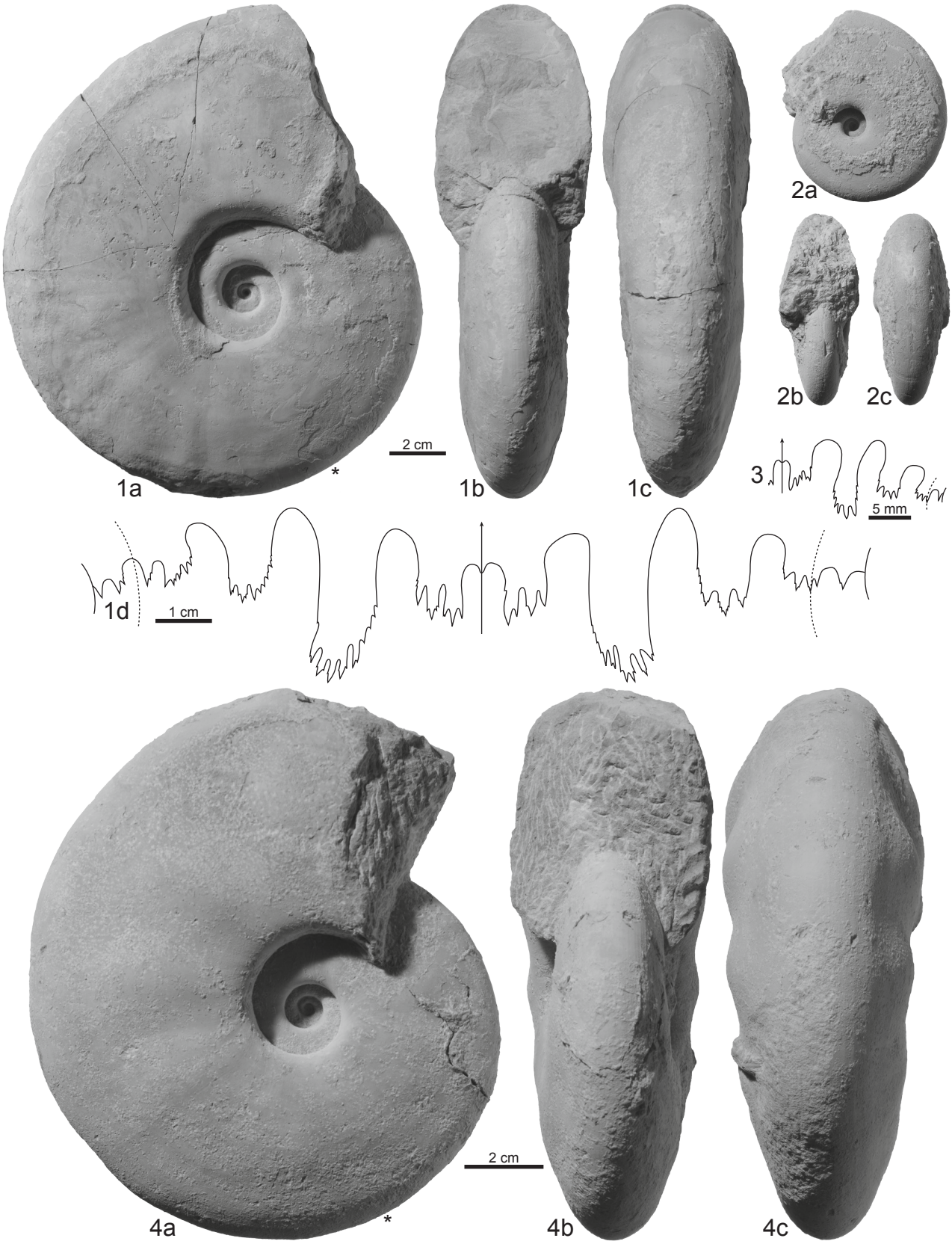
1a
*
2 cm
1b
1c
2a
2b
2c
3
5 mm
1d
1 cm
4a
*
2 cm
4b
4c

Plate 24

(All figures natural size unless otherwise indicated; all specimens are incomplete phragmocones)

1a-d: *Proptychites wargalensis* sp. nov. PIMUZ30438. Holotype.
Loc. War5, middle LCL, Wargal, *Gyronites plicosus* beds (early Dienerian). a-c) lateral, apertural and ventral views. d) Suture line at H = 25.6 mm (mirrored image).

2a-c: *Proptychites oldhamianus* Waagen, 1895. PIMUZ30439.
Loc. Nam378, top LCL, Nammal Nala, *Gyronites frequens* beds (early Dienerian).

3a-c: *Proptychites oldhamianus* Waagen, 1895. PIMUZ30440.
Loc. Nam335, middle LCL, Nammal Nala, *Gyronites plicosus* beds (early Dienerian).

4a-d: *Proptychites oldhamianus* Waagen, 1895. PIMUZ30441.
Loc. Nam335, middle LCL, Nammal Nala, *Gyronites plicosus* beds (early Dienerian). a-c) lateral, apertural and ventral views. d) Suture line at H = 10.8 mm; × 2.

5a-c: *Proptychites ammonoides* Waagen, 1895. PIMUZ30442.
Loc. Nam384, base CM, Nammal Nala, *Ambites radiatus* beds (middle Dienerian).

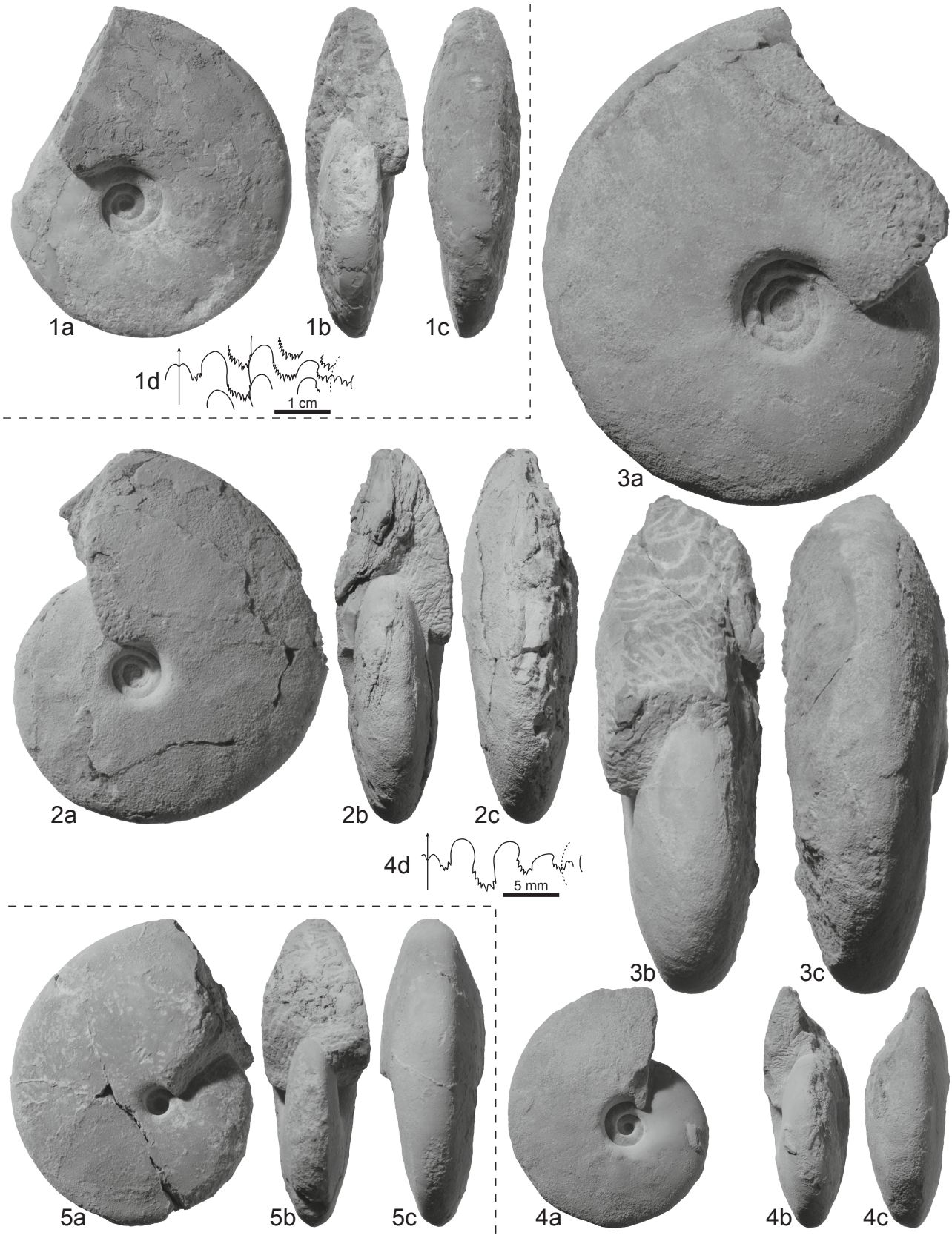
1a
1b
1c
1d
1 cm
3a
2a
2b
2c
4d
5 mm
3b
3c
5a
5b
5c
4a
4b
4c

Plate 25

(All figures natural size unless otherwise indicated; asterisks indicate the position of the last septum)

1a-e: *Proptychites ammonoides* Waagen, 1895. PIMUZ30443.
Loc. Nam380, base CM, Nammal Nala, *Ambites discus* beds (middle Dienerian). a-d) lateral, apertural and ventral views; × 0.6. e) Suture line at H = 62.7 mm (mirrored image).

2: *Proptychites ammonoides* Waagen, 1895. PIMUZ30444.
Loc. Nam53, base CM, Nammal Nala, *Ambites superior* beds (middle Dienerian). Suture line at H = 42.7 mm.

3a-c: *Proptychites ammonoides* Waagen, 1895. PIMUZ30445.
Loc. Nam50, base CM, Nammal Nala, *Ambites discus* beds (middle Dienerian). a-b) lateral and ventral views. c) Suture line at H = 15.1 mm; × 1.5.

4a-e: *Proptychites ammonoides* Waagen, 1895. PIMUZ30446.
Loc. Nam400, floated block from base CM, Nammal Nala, *Ambites discus* beds (middle Dienerian). a-d) lateral, apertural and ventral views; × 0.5. e) Suture line at H = 85 mm. Specimen with two encrusting bivalves (b) with both valves preserved.

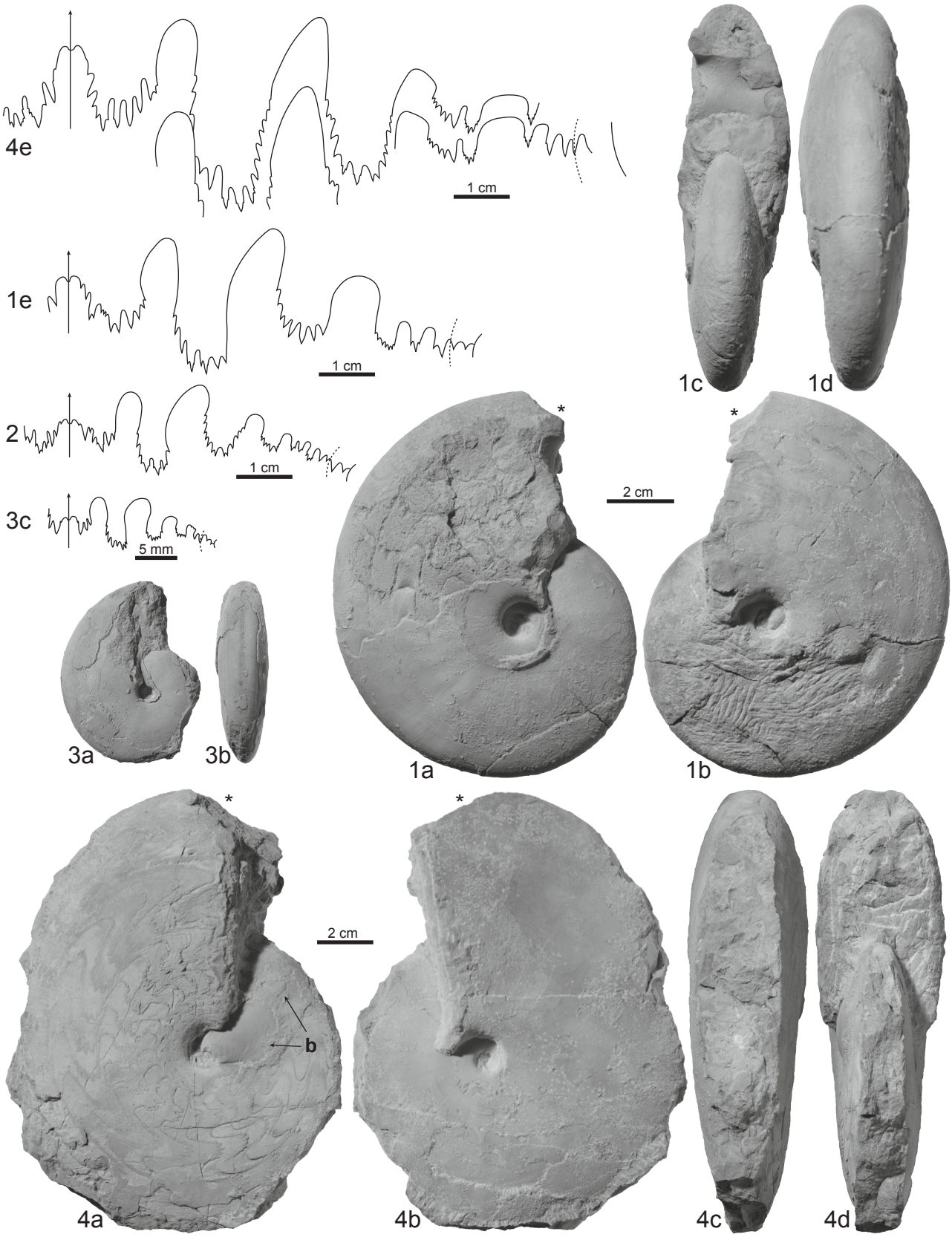
4e
1 cm
1e
1 cm
2
1 cm
3c
5 mm
1c
1d
*
2 cm
*
3a
3b
1a
1b
*
*
2 cm
b
4a
4b
4c
4d

Plate 26

(All figures natural size unless otherwise indicated)

1a-b: *Proptychites ammonoides* Waagen, 1895. PIMUZ30447.
Loc. Nam53, base CM, Nammal Nala, *Ambites superior* beds (middle Dienerian); × 0.6.

2a-e: *Proptychites* cf. *pagei* Ware *et al.*, 2011. PIMUZ30448.
Loc. Nam501, base CM, Nammal Nala, *Ambites lilangensis* beds (middle Dienerian). a-d) lateral, apertural and ventral views; left side (a) without shell, showing the umbilicus, right side (b) with shell, umbilicus occluded. e) Suture line at H = 53 mm.

3: *Proptychites* cf. *pagei* Ware *et al.*, 2011. PIMUZ30451.
Loc. Nam345, base CM, Nammal Nala, *Ambites lilangensis* beds (middle Dienerian). Slightly weathered suture line at H = 48.1 mm.

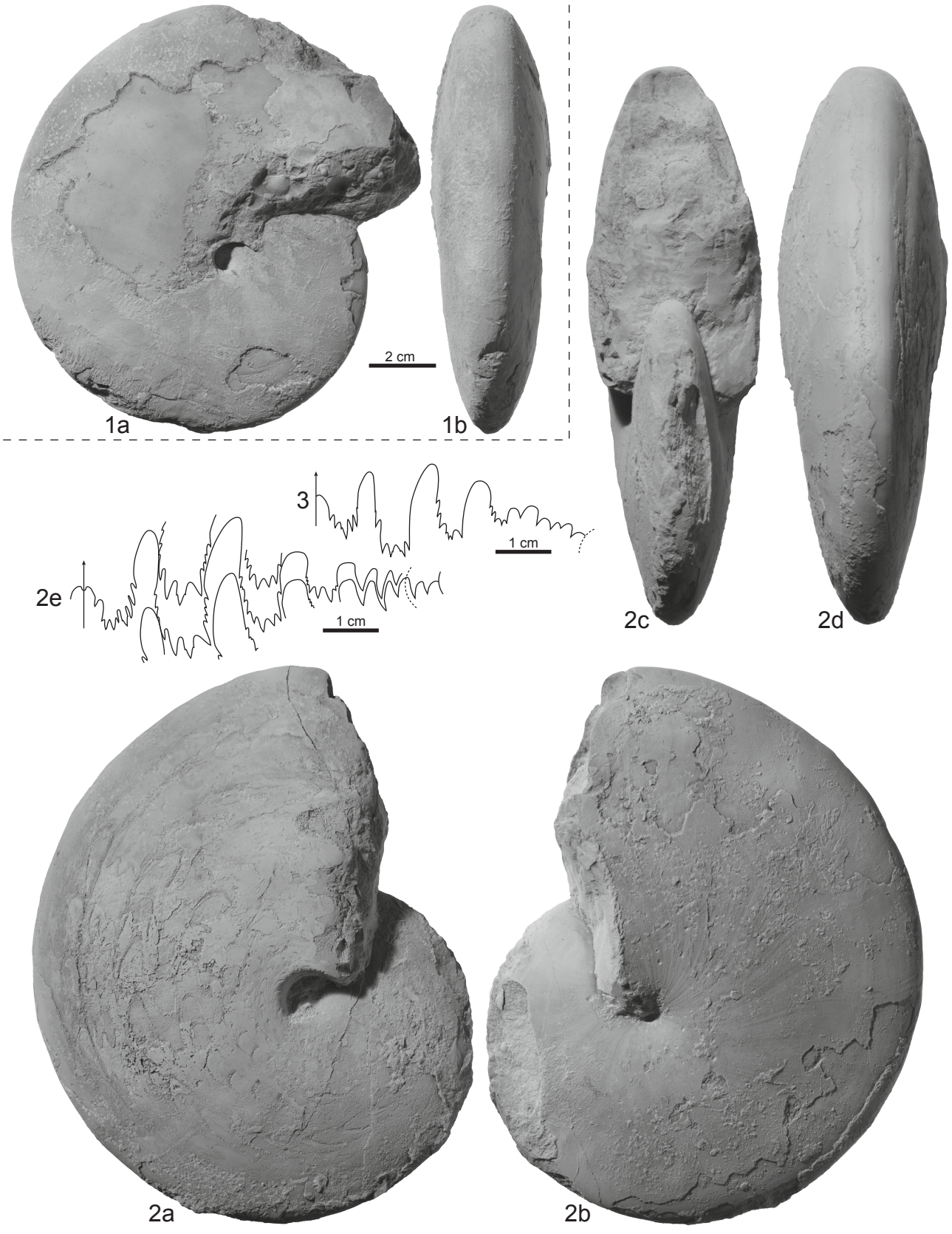
1a
1b
2 cm
2c
2d
3
1 cm
2e
1 cm
2a
2b

Plate 27

(All figures natural size unless otherwise indicated; asterisks indicate the position of the last septum)

1a-c: *Mullericeras spitiense* (Krafft, 1909). PIMUZ30500.
Loc. Nam396, base CM, Nammal Nala, *Vavilovites* cf. *sverdrupi* beds (late Dienerian).

2a-d: *Mullericeras spitiense* (Krafft, 1909). PIMUZ30452.
Loc. Nam344, base CM, Nammal Nala, *Ambites lilangensis* beds (middle Dienerian). a-c) lateral, apertural and ventral views. d) Suture line at H = 21 mm; × 1.5.

3a-b: *Mullericeras spitiense* (Krafft, 1909). PIMUZ30496.
Loc. Nam396, base CM, Nammal Nala, *Vavilovites* cf. *sverdrupi* beds (late Dienerian).

4a-d: *Mullericeras shigetai* n. sp. PIMUZ30453. Holotype.
Loc. Nam381, base CM, Nammal Nala, *Ambites radiatus* beds (middle Dienerian). a-c) lateral, apertural and ventral views. d) Suture line at H = 29 mm; × 1.5 (mirrored image).

5: *Mullericeras shigetai* n. sp. PIMUZ30454. Paratype.
Loc. Nam382, base CM, Nammal Nala, *Ambites discus* beds (middle Dienerian). Suture line at H = 20.6 mm; × 1.5.

6a-c: *Mullericeras shigetai* n. sp. PIMUZ30457. Paratype.
Loc. Nam364, base CM, Nammal Nala, *Ambites discus* beds (middle Dienerian). a-b) lateral and ventral views. c) Suture line at H = 15.3 mm; × 3 (mirrored image).

7a-c: *Mullericeras shigetai* n. sp. PIMUZ30455. Paratype.
Loc. Nam381, base CM, Nammal Nala, *Ambites radiatus* beds (middle Dienerian).

8a-d: *Mullericeras shigetai* n. sp. PIMUZ30458. Paratype.
Loc. Amb53, top LCL, Amb, *Ambites atavus* beds (middle Dienerian). a-c) lateral, apertural and ventral views. d) Suture line at H = 22.1 mm; × 1.5 (mirrored image).

9a-d: *Mullericeras shigetai* n. sp. PIMUZ30456. Paratype.
Loc. Nam527, base CM, Nammal Nala, *Ambites discus* beds (middle Dienerian). a-c) lateral, apertural and ventral views. d) Suture line at H = 20.2 mm; × 1.5.

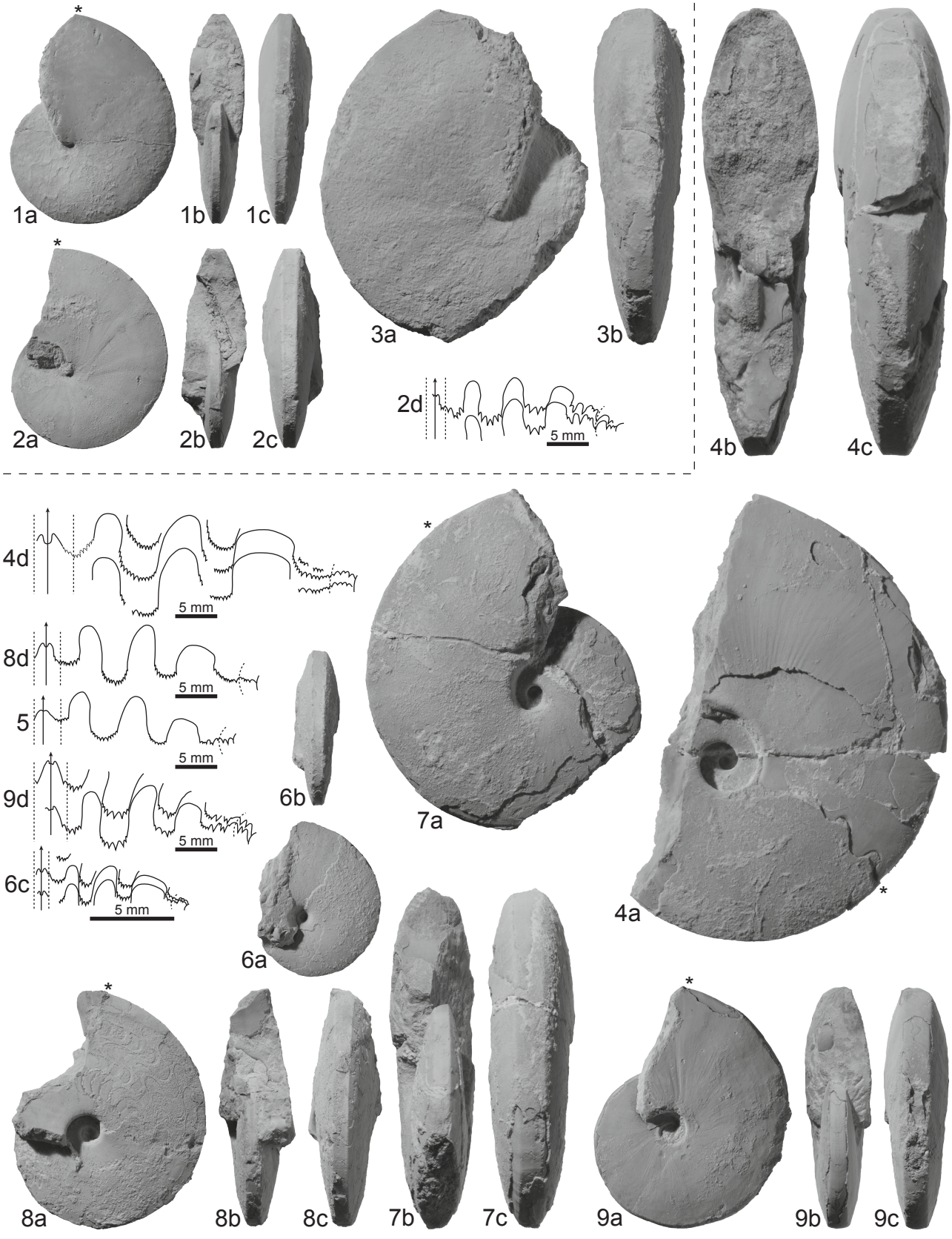
1a
1b
1c
2a
2b
2c
3a
3b
2d
5 mm
4b
4c
4d
5 mm
8d
5 mm
5
5 mm
9d
5 mm
6c
5 mm
6b
7a
4a
6a
8a
8b
8c
7b
7c
9a
9b
9c

Plate 28

(All figures natural size unless otherwise indicated; asterisks indicate the position of the last septum)

1: *Mullericeras indusense* n. sp. PIMUZ30459. Paratype.
Loc. Nam53, base CM, Nammal Nala, *Ambites superior* beds (middle Dienerian). Suture line at H = 17.3 mm; × 1.5.

2a-c: *Mullericeras indusense* n. sp. PIMUZ30460. Holotype.
Loc. Nam302, base CM, Nammal Nala, *Ambites superior* beds (middle Dienerian). a-b) lateral and ventral views. d) Suture line at H = 20.6 mm; × 1.5.

3a-c: *Mullericeras indusense* n. sp. PIMUZ30461. Paratype.
Loc. Nam302, base CM, Nammal Nala, *Ambites superior* beds (middle Dienerian).

4a-b: *Mullericeras indusense* n. sp. PIMUZ30462. Paratype.
Loc. Nam53, base CM, Nammal Nala, *Ambites superior* beds (middle Dienerian). a) lateral view; d) Suture line at H = 22.6 mm. × 1.5 (mirrored image).

5a-d: *Mullericeras niazii* n. sp. PIMUZ30464. Holotype.
Loc. Nam100, base CM, Nammal Nala, *Ambites lilangensis* beds (middle Dienerian). a-c) lateral, apertural and ventral views. d) Suture line at H = 22.4 mm; × 1.5 (mirrored image).

6a-c: *Mullericeras niazii* n. sp. PIMUZ30465. Paratype.
Loc. Nam100, base CM, Nammal Nala, *Ambites lilangensis* beds (middle Dienerian).

7a-b: *Mullericeras niazii* n. sp. PIMUZ30466. Paratype.
Loc. Nam100, base CM, Nammal Nala, *Ambites lilangensis* beds (middle Dienerian).

8a-c: *Ussuridiscus varaha* (Diener, 1895). PIMUZ30470.
Loc. Amb104, base LCL, Amb, *Gyronites dubius* beds (early Dienerian).

9a-c: *Ussuridiscus varaha* (Diener, 1895). PIMUZ30468.
Loc. Amb104, base LCL, Amb, *Gyronites dubius* beds (early Dienerian).

10a-c: *Ussuridiscus varaha* (Diener, 1895). PIMUZ30467.
Loc. Amb104, base LCL, Amb, *Gyronites dubius* beds (early Dienerian).

11a-d: *Ussuridiscus varaha* (Diener, 1895). PIMUZ30469.
Loc. Amb104, base LCL, Amb, *Gyronites dubius* beds (early Dienerian).). a-c) lateral, apertural and ventral views. d) Suture line at H = 19.8 mm; × 1.5 (mirrored image).

12a-d: *Ussuridiscus ensanus* (Krafft, 1909). PIMUZ30474.
Loc. War100, from dipslope near top LCL, Wargal, precise age unknown (*Gyronites plicosus* or *Gyronites frequens* beds, early Dienerian).

13a-c: *Ussuridiscus ensanus* (Krafft, 1909). PIMUZ30472.
Loc. Nam377, middle LCL, Nammal Nala, *Gyronites plicosus* beds (early Dienerian).

14a-c: *Ussuridiscus ensanus* (Krafft, 1909). PIMUZ30471.
Loc. Nam393, middle LCL, Nammal Nala, *Gyronites plicosus* beds (early Dienerian).

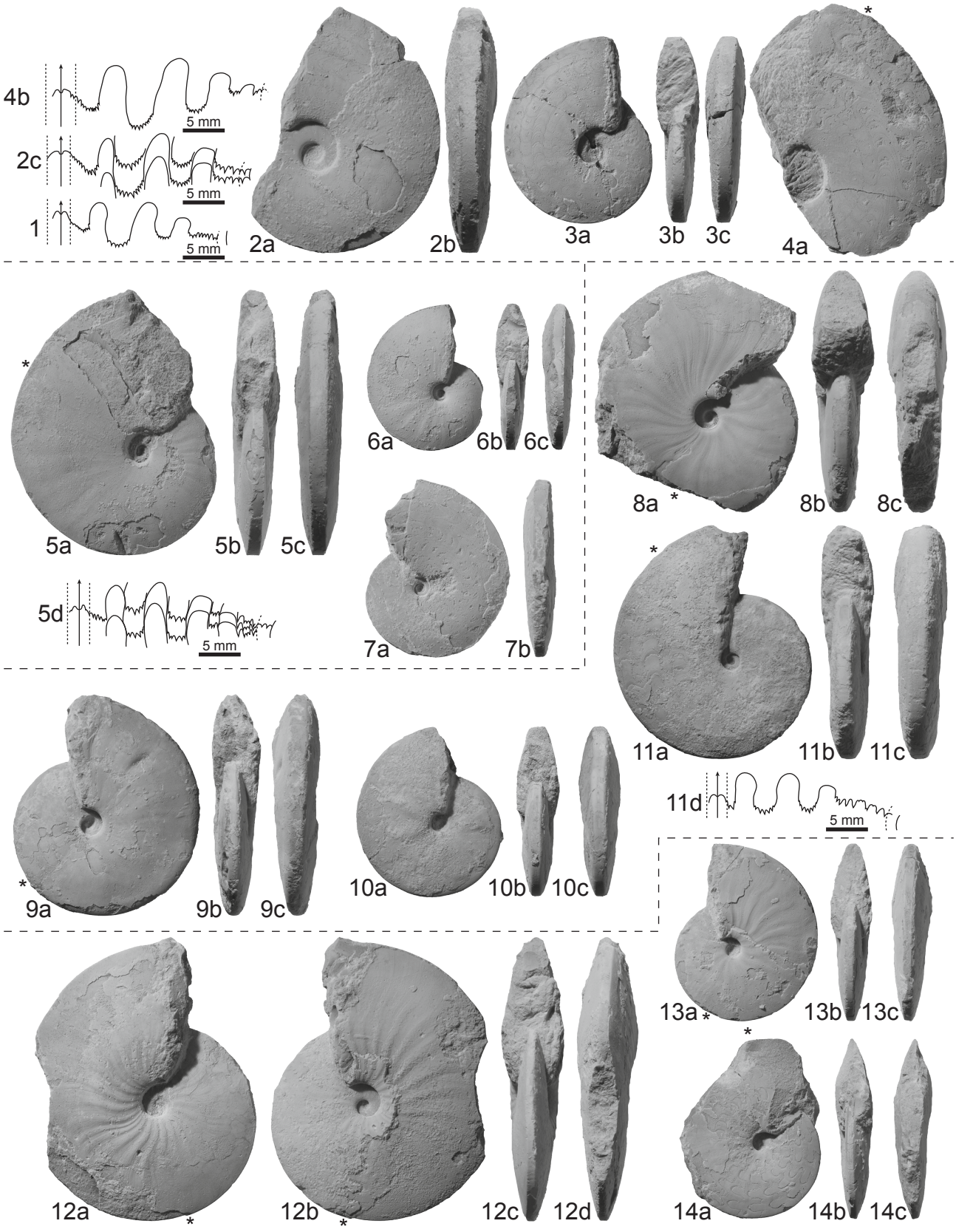
4b
5 mm
2c
5 mm
1
5 mm
2a
2b
3a
3b
3c
4a
*
5a
*
5b
5c
6a
6b
6c
5d
5 mm
7a
7b
8a
*
8b
8c
11a
*
11b
11c
11d
5 mm
9a
*
9b
9c
10a
10b
10c
13a
*
13b
13c
*
12a
*
12b
*
12c
12d
14a
14b
14c

Plate 29

(All figures natural size unless otherwise indicated; asterisks indicate the position of the last septum)

1a-c: *Ussuridiscus ensanus* (Krafft, 1909). PIMUZ30473.
Loc. Nam378, top LCL, Nammal Nala, *Gyronites frequens* beds (early Dienerian).

2a-d: *Ussuridiscus ensanus* (Krafft, 1909). PIMUZ30475.
Loc. Nam377, middle LCL, Nammal Nala, *Gyronites plicosus* beds (early Dienerian). a-c) lateral, apertural and ventral views. d) Suture line at H = 20.8 mm; × 1.5.

3: *Ussuridiscus ensanus* (Krafft, 1909). PIMUZ30476.
Loc. War100, from dipslope near top LCL, Wargal, precise age unknown (*Gyronites plicosus* or *Gyronites frequens* beds, early Dienerian). Suture line at H = 17 mm; × 1.5 (mirrored image).

4: *Ussuridiscus ensanus* (Krafft, 1909). PIMUZ30477.
Loc. War100, from dipslope near top LCL, Wargal, precise age unknown (*Gyronites plicosus* or *Gyronites frequens* beds, early Dienerian). Suture line at H = 16.3 mm; × 1.5 (mirrored image).

5a-e: *Ussuridiscus ensanus* (Krafft, 1909). PIMUZ30478.
Loc. War100, from dipslope near top LCL, Wargal, precise age unknown (*Gyronites plicosus* or *Gyronites frequens* beds, early Dienerian). a-d) lateral, apertural and ventral views. e) Suture line at H = 16 mm; × 1.5.

6a-c: *Ussuridiscus ornatus* n. sp. PIMUZ30479. Paratype.
Loc. War6, middle LCL, Wargal, *Gyronites plicosus* beds (early Dienerian).

7a-d: *Ussuridiscus ornatus* n. sp. PIMUZ30481. Holotype.
Loc. Nam377, middle LCL, Nammal Nala, *Gyronites plicosus* beds (early Dienerian). a-c) lateral, apertural and ventral views. d) Suture line at H = 14.1 mm; × 2 (mirrored image).

8a-c: *Ussuridiscus*? sp. indet. PIMUZ30483.
Loc. Nam391, base LCL, Nammal Nala, ? latest Griesbachian/earliest Dienerian. a-b) lateral and ventral views. c) Suture line at H = 16.9 mm; × 1.5 (mirrored image).

9a-c: *Ussuridiscus*? sp. indet. PIMUZ30484.
Loc. Nam391, base LCL, Nammal Nala, ? latest Griesbachian/earliest Dienerian. a-b) lateral and apertural views. c) Suture line at H = 11.5 mm; × 2 (mirrored image).

10a-d: *Ussuridiscus ventriosus* n. sp. PIMUZ30482. Holotype.
Loc. Nam377, middle LCL, Nammal Nala, *Gyronites plicosus* beds (early Dienerian). a-c) lateral, apertural and ventral views. d) Suture line at H = 14.9 mm; × 1.5.

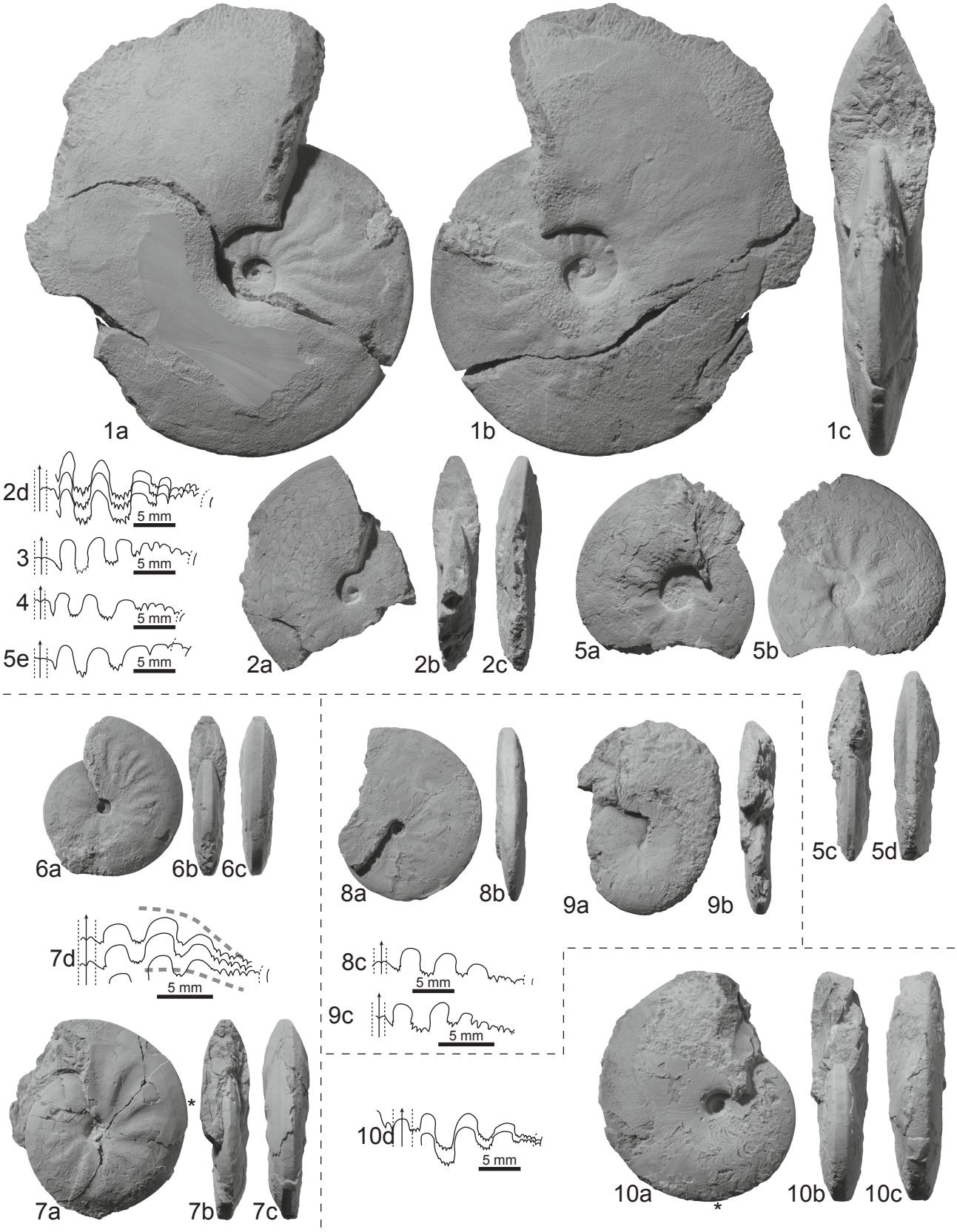
1a
1b
1c
2d
5 mm
3
5 mm
4
5 mm
5e
5 mm
2a
2b
2c
5a
5b
6a
6b
6c
8a
8b
9a
9b
5c
5d
7d
5 mm
8c
5 mm
9c
5 mm
10d
5 mm
7a
*
7b
7c
10a
*
10b
10c

Plate 30

(All figures natural size unless otherwise indicated; asterisks indicate the position of the last septum)

1a-c: *Kingites davidsonianus* (de Koninck, 1863). PIMUZ30486.
Loc. Nam346, base CM, Nammal Nala, *Kingites davidsonianus* beds (late Dienerian).

2a-b: *Kingites davidsonianus* (de Koninck, 1863). GSI7155. Holotype of *Kingites lens* Waagen, 1895. (Photo by B. Kummel)
CM, Wargal, bed and locality unknown.

3a-d: *Kingites davidsonianus* (de Koninck, 1863). PIMUZ30485.
Loc. Nam61, base CM, Nammal Nala, *Kingites davidsonianus* beds (late Dienerian). a-c) lateral, apertural and ventral views. d) Suture line at H = 25 mm (mirrored image).

4a-c: *Kingites davidsonianus* (de Koninck, 1863). PIMUZ30492.
Loc. Nam61, base CM, Nammal Nala, *Kingites davidsonianus* beds (late Dienerian). a-b) lateral and ventral views. c) Suture line at H = 21.6 mm (mirrored image). Specimen with two juvenile specimens of *Kon. khoorensis* (k) in its body chamber.

5: *Kingites davidsonianus* (de Koninck, 1863). PIMUZ30487.
Loc. Nam61, base CM, Nammal Nala, *Kingites davidsonianus* beds (late Dienerian). Suture line at H = 27.2 mm (mirrored image).

6: *Kingites davidsonianus* (de Koninck, 1863). PIMUZ30488.
Loc. Nam315, base CM, Nammal Nala, *Kingites davidsonianus* beds (late Dienerian). Suture line at H = 21.2 mm (mirrored image).

7a-d: *Kingites davidsonianus* (de Koninck, 1863). PIMUZ30489.
Loc. Nam61, base CM, Nammal Nala, *Kingites davidsonianus* beds (late Dienerian). a-c) lateral, apertural and ventral views. d) Suture line at H = 14.3 mm; × 1.5 (mirrored image).

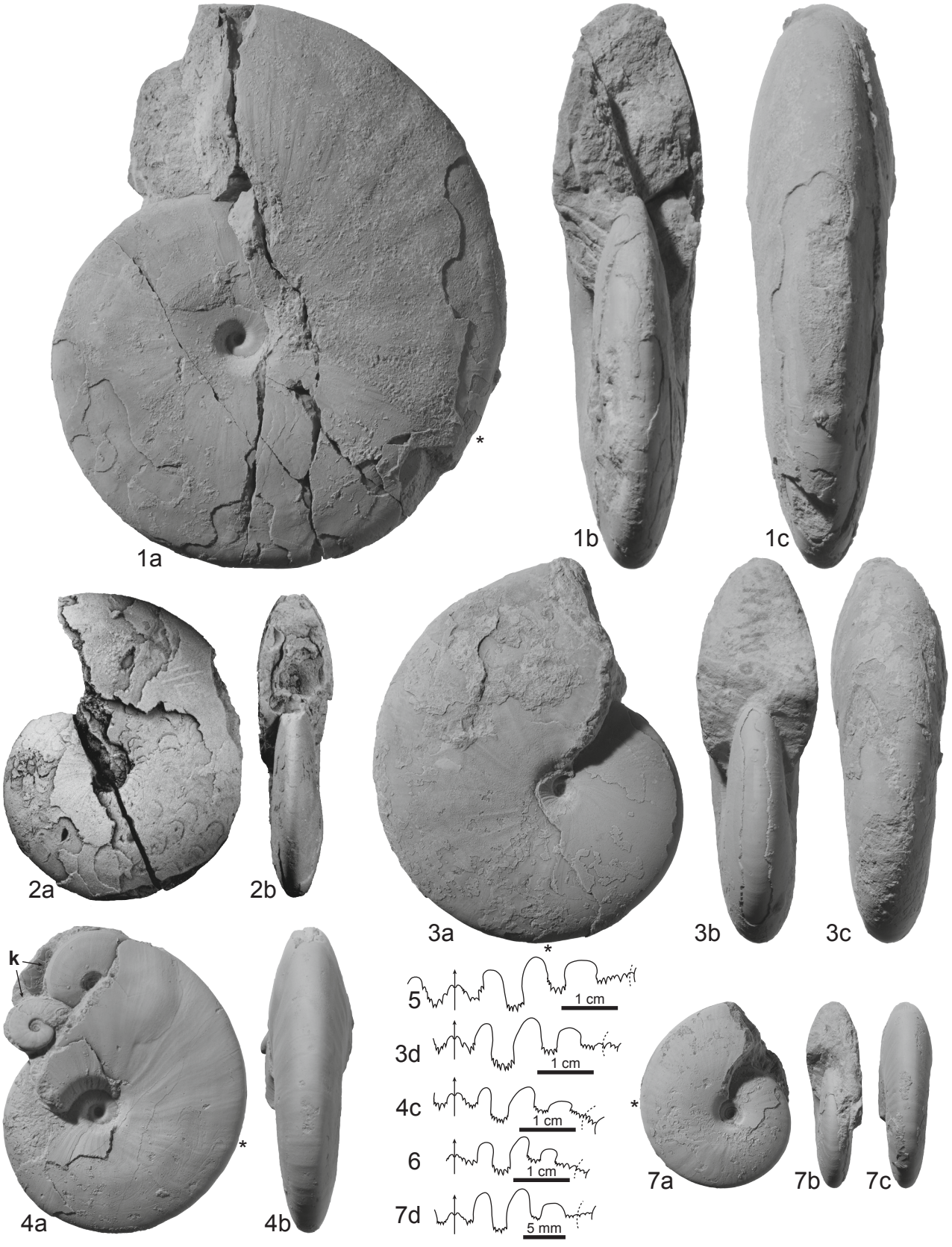
1a
1b
1c
2a
2b
3a
3b
3c
k
4a
4b
5
3d
4c
6
7d
1 cm
1 cm
1 cm
1 cm
5 mm
7a
7b
7c

Plate 31

(All figures natural size unless otherwise indicated; asterisks indicate the position of the last septum)

1a-b: *Kingites davidsonianus* (de Koninck, 1863). PIMUZ30490.
Loc. Nam101d, base CM, Nammal Nala, *Kingites davidsonianus* beds (late Dienerian). With its lower jaw (j) preserved at the beginning of its body chamber.

2a-b: *Kingites davidsonianus* (de Koninck, 1863). PIMUZ30491.
Loc. Nam313, base CM, Nammal Nala, *Kingites davidsonianus* beds (late Dienerian). a) Polished cross section. b) Cross section.

3a-e: *Kingites korni* Brühwiler *et al.*, 2010. PIMUZ30493.
Loc. Nam70, base CM, Nammal Nala, *Koninckites vetustus* beds (late Dienerian). a-d) lateral, apertural and ventral views. e) Suture line at H = 25 mm. Inner mould of a complete specimen.

4a-d: *Clypites typicus* Waagen, 1895. PIMUZ30494.
Loc. Nam130, base CM, Nammal Nala, *Kingites davidsonianus* beds (late Dienerian). a-c) lateral, apertural and ventral views. d) Suture line at H = 38 mm; × 1 (mirrored image).

5a-d: *Clypites typicus* Waagen, 1895. PIMUZ30495.
Loc. Nam61, base CM, Nammal Nala, *Kingites davidsonianus* beds (late Dienerian). a-c) lateral, apertural and ventral views. d) Suture line at H = 21.2 mm; × 1.5 (mirrored image).

6: *Clypites typicus* Waagen, 1895. PIMUZ30498.
Loc. Nam319, base CM, Nammal Nala, *Kingites davidsonianus* beds (late Dienerian). Suture line at H = 26.3 mm; × 1.5 (mirrored image).

7: *Clypites typicus* Waagen, 1895. PIMUZ30499.
Loc. Nam61, base CM, Nammal Nala, *Kingites davidsonianus* beds (late Dienerian). Suture line at H = 26.4 mm; × 1.5.

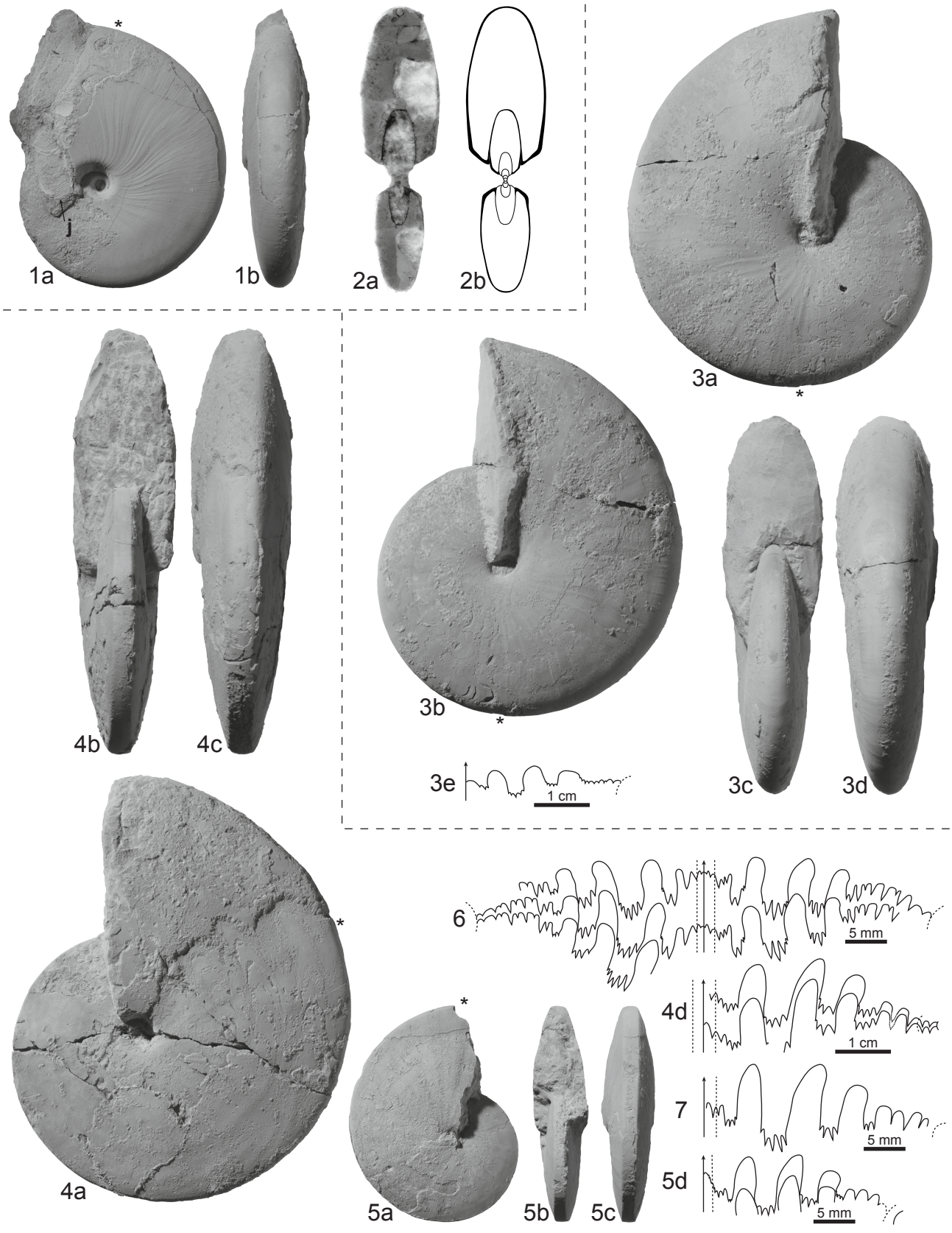
*
j
1a
1b
2a
2b
3a
*
4b
4c
3b
*
3c
3d
3e
1 cm
*
4a
6
5 mm
*
4d
1 cm
5a
5b
5c
7
5 mm
5d
5 mm

Plate 32

(All figures natural size unless otherwise indicated; asterisks indicate the position of the last septum)

1a-b: *Clypites typicus* Waagen, 1895. PIMUZ30497.
Loc. Nam130, base CM, Nammal Nala, *Kingites davidsonianus* beds (late Dienerian).

2a-b: *Clypites typicus* Waagen, 1895. PIMUZ30501.
Loc. Nam83, base CM, Nammal Nala, *Koninckites vetustus* beds (late Dienerian).

3a-d: *Pseudosageceras simplelobatum* n. sp. PIMUZ30502. Paratype.
Loc. Nam63, base CM, Nammal Nala, *Koninckites vetustus* beds (late Dienerian). a-c) lateral, apertural and ventral views. d) Suture line at H = 27.4 mm; × 1.5 (mirrored image).

4: *Pseudosageceras simplelobatum* n. sp. PIMUZ30503. Paratype.
Loc. Nam61, base CM, Nammal Nala, *Kingites davidsonianus* beds (late Dienerian). Suture line at H = 40.8 mm (mirrored image).

5a-d: *Pseudosageceras simplelobatum* n. sp. PIMUZ30504. Paratype.
Loc. Nam67, base CM, Nammal Nala, *Kingites davidsonianus* beds (late Dienerian). a-c) lateral, apertural and ventral views; × 2. d) Suture line at H = 9 mm; × 3 (mirrored image).

6a-c: *Pseudosageceras simplelobatum* n. sp. PIMUZ30505. Paratype.
Loc. Chi51, top LCL, Chiddru, *Koninckites vetustus* beds (late Dienerian).

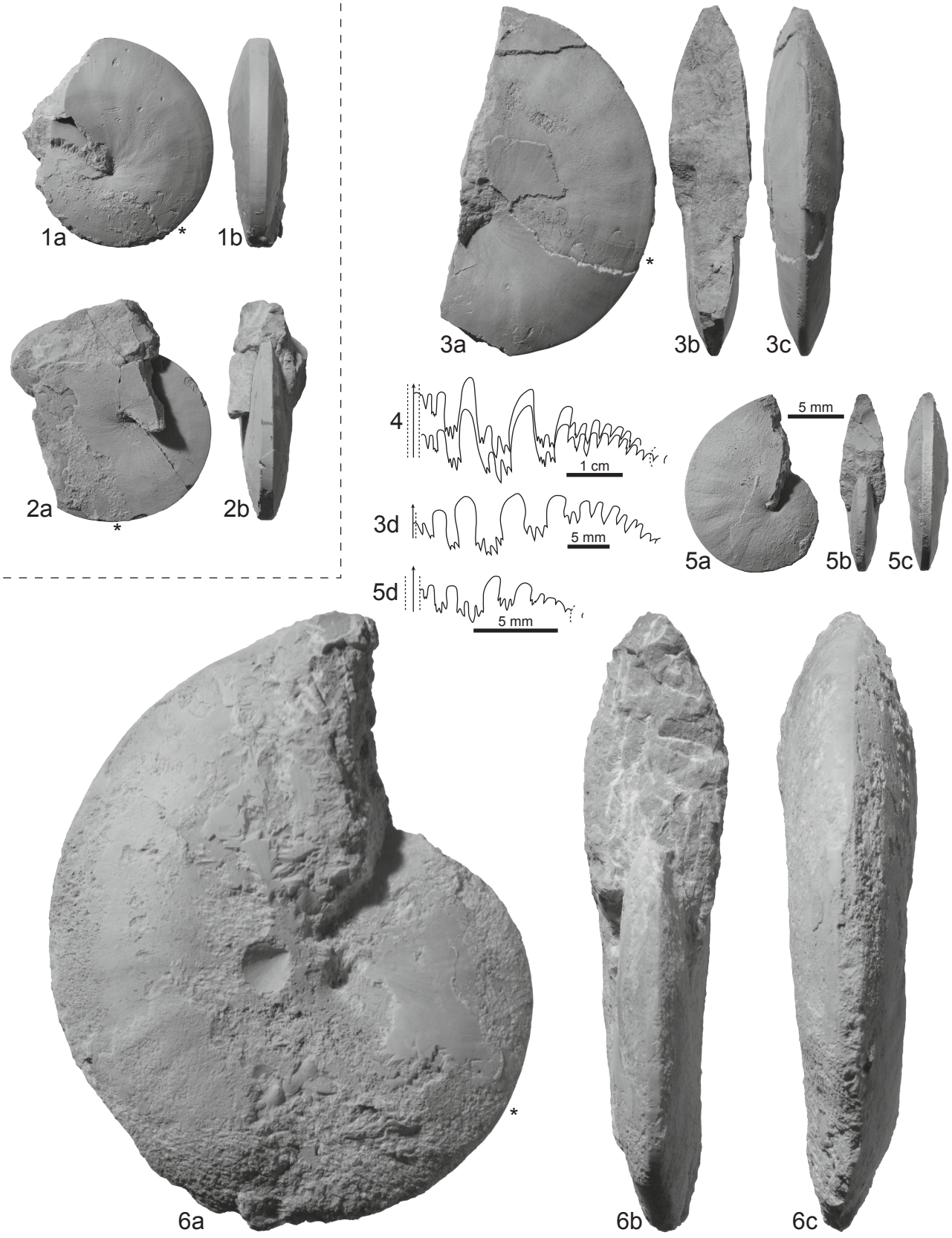
1a
*
1b
2a
*
2b
3a
*
3b
3c
4
1 cm
3d
5 mm
5d
5 mm
5 mm
5a
5b
5c
6a
*
6b
6c

Plate 33

(All figures natural size unless otherwise indicated asterisks indicate the position of the last septum)

1a-c: *Pseudosageceras simplelobatum* n. sp. PIMUZ30506. Holotype.
Loc. Nam346, base CM, Nammal Nala, *Kingites davidsonianus* beds (late Dienerian).

2a-b: *Pseudosageceras simplelobatum* n. sp. PIMUZ30507. Paratype.
Loc. Nam336, base CM, Nammal Nala, *Kingites davidsonianus* beds (late Dienerian). a) Polished cross section. b) Cross section.

3a-b: *Pseudosageceras simplelobatum* n. sp. PIMUZ30508. Paratype.
Loc. Nam346, base CM, Nammal Nala, *Kingites davidsonianus* beds (late Dienerian).

4a-c: *Pseudosageceras simplelobatum* n. sp. PIMUZ30509. Paratype.
Loc. Nam350, base CM, Nammal Nala, *Awanites awani* beds (late Dienerian).

5a-e: *Subacerites friski* n. Gen., n. sp. PIMUZ30510. Holotype.
Loc. Amb3, base CM, Amb, *Kingites davidsonianus* beds (late Dienerian). a-d) lateral, apertural and ventral views. e) Suture line at H = 19.1 mm; × 1.5 (mirrored image).

6a-d: Gen. et sp. indet. PIMUZ30511.
Loc. Amb104, base LCL, Amb, *Gyronites dubius* beds (early Dienerian). a-c) lateral, apertural and ventral views; × 2. d) Suture line at H = 8.5 mm; × 3.

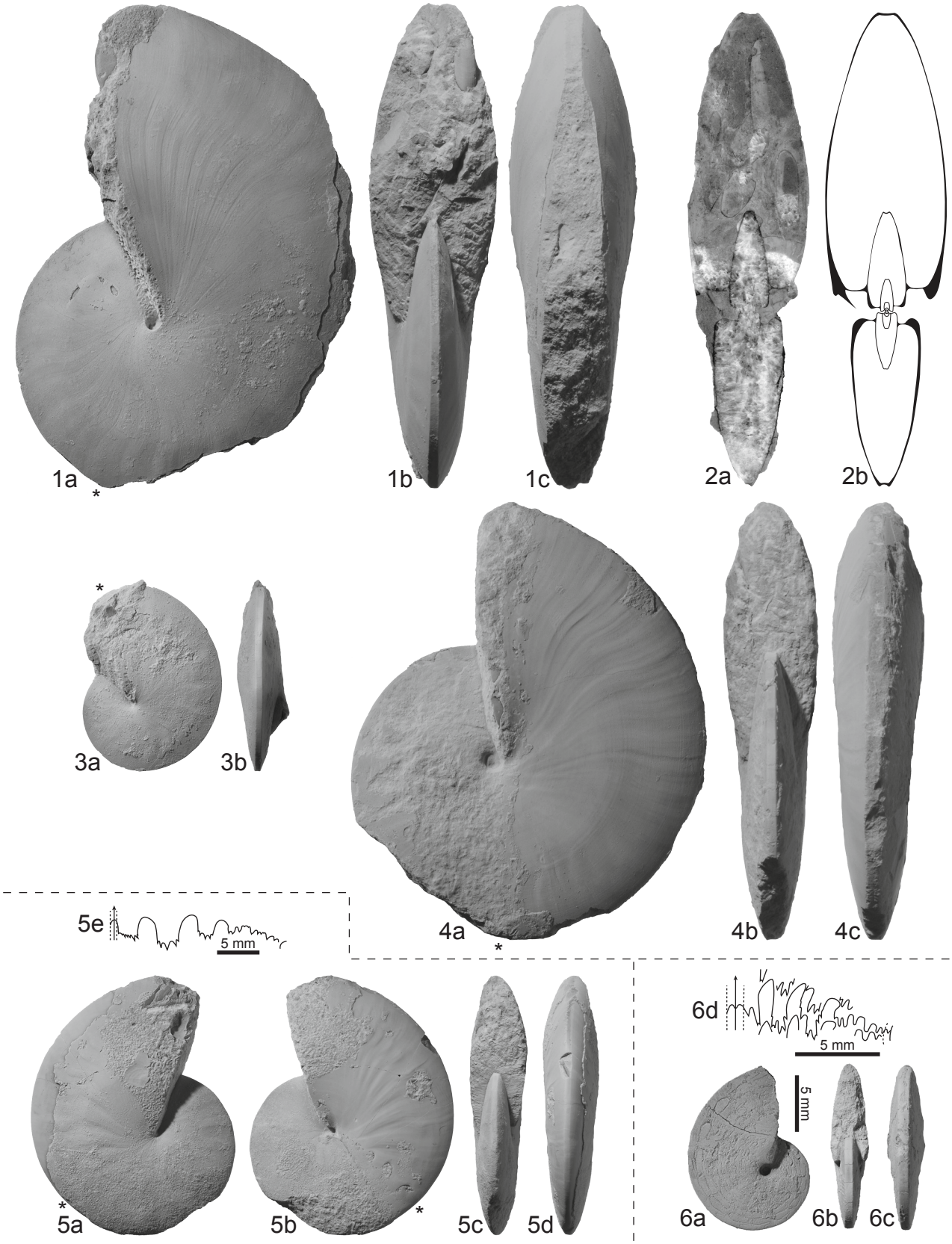
1a
*
1b
1c
2a
2b
*
3a
3b
4a
*
4b
4c
5e
5 mm
*
5a
*
5b
5c
5d
6d
5 mm
5 mm
6a
6b
6c

CHAPTER 3

Dienerian (Early Triassic) ammonoids from Spiti (Himashal Pradesh, India)

Dienerian (Early Triassic) ammonoids from Spiti (Himashal Pradesh, India)

by David Ware, Hugo Bucher, Thomas Brühwiler, *and* Leopold Krystyn

David Ware, Hugo Bucher and Thomas Brühwiler: Paläontologisches Institut und Museum der Universität Zürich, Karl Schmid-Strasse 4, CH-8006 Zürich, Switzerland; e-mails: david.ware@pim.uzh.ch, hugo.fr.bucher@pim.uzh.ch, bruehwiler@pim.uzh.ch

Leopold Krystyn: Institut für Paläontologie, Althanstraße 14, 1090 Wien, Austria; e-mail: leopold.krystyn@univie.ac.at

Abstract

Many new Early Triassic ammonoid taxa were first described from the Spiti District (Himashal Pradesh, India) in the late 19th century, but without detailed stratigraphic information. Recently, the Spiti area has gained a renewed interest with the recent proposition of a section near Mud for the GSSP of the Dienerian/Smithian (i.e. Induan/Olenekian) boundary. However, the Dienerian part of the Spiti succession was still in need of a thorough revision. Here we present the results of a high resolution bed-rock controlled sampling of three different areas (Mud, Guling and Lalung) in the Spiti District. These areas yielded abundant and rather well preserved Dienerian ammonoids, which compare very well with the revised successions from the Salt Range (Pakistan). The Dienerian ammonoid faunas from both regions are remarkably similar and the new threefold subdivision of the Dienerian (early, middle and late) proposed in the Salt Range also applies to Spiti. Moreover, 10 out of the 12 Dienerian regional zones defined in the Salt Range are recognised in Spiti, with the same associations of characteristic species. Thus the initial biostratigraphical scheme established in the Salt Range can be reproduced laterally and is most likely valid throughout most of the Northern Indian Margin. Four new species (*Gyronites levilatus*, *Gy. bullatus*, *Ambites nyingmai* and *Vavilovites meridialis*) are also introduced.

Introduction

The end Permian mass extinction and the following Early Triassic recovery constitute a key period in the history of life. The study of this recovery is the subject of ongoing and intense debate, especially concerning its timing. Among the most important key problems is the absence of any clear consensus on the definition of Early Triassic stages and sub-stages and the persistence of large portions of the record that still lack a high resolution and reliable biostratigraphical scheme. As a consequence, many studies on the Early Triassic use rather poorly resolved and/or diachronous (e.g. interval zones of conodonts) biozonations, and they do not always use consistent boundary definitions (e.g. the Induan-Olenekian boundary). In this context, the establishment of a clear and detailed biozonation based on the principle of a sound taxonomy and maximal associations (i.e. Concurrent Range Zones, Unitary Associations) is of primary importance. Previous attempts at subdividing the Early Triassic by means of Interval Zones of conodonts will always remain biased because of the diachronous first occurrences of index species, not to mention the *a priori* largely unwarranted phylogenetic assumption of utilizing index species from anagenetic lineages.

The Northern Indian Margin (NIM) is known since the end of the 19th century as a classical region for the study of Early Triassic ammonoid faunas. In a companion work (Ware *et al.*, this volume), Dienerian ammonoids of the Salt Range (Pakistan) were thoroughly revised. An entirely new high resolution biostratigraphical scheme was proposed for the Salt Range and its correlation with other recently established biozonations (such as Tozer 1994 for Arctic Canada, Dagys & Ermakova 1996 for northern Siberia, and Shigeta & Zakharov 2009 for Primorye) was discussed. However, in order to establish a formal biozonation, the lateral reproducibility of this new biostratigraphical scheme must be tested in other areas. The Spiti region (Himashal Pradesh, India) is another classical locality for Early Triassic ammonoids of the NIM. They were first described in two monographs by Diener (1897) and Krafft & Diener (1909). These two pioneering works unfortunately lack a detailed stratigraphic context, and many new species are only indicated as coming from the "lower division of the lower Trias", a very vague indication which does not meet the need for an accurate and precise biozonation. Until very recently, no other papers concerning Early Triassic ammonoids from Spiti have been published. Starting in the mid 1990s, Leopold Krystyn started the revision of different sections in Spiti which led him to propose a section near Mud as a GSSP for the Induan/Olenekian boundary (equivalent to the Dienerian/Smithian boundary –DSB–; Krystyn *et al.*, 2007a, b). Only a few ammonoids were illustrated and described in these studies which only focused on a short time interval. Following his lead, our research group in the University of Zürich conducted two intensive seasons of field work in 2008 and 2009. This lead to the discovery of typical Smithian ammonoids below the boundary proposed by Krystyn *et al.* (2007a, b; Brühwiler *et al.*,

2010), thus questioning the definition of this boundary. Middle and late Smithian ammonoids from Spiti were revised by Brühwiler *et al.* (2012b). The present work focuses on the abundant and well preserved ammonoid faunas with a detailed bed-rock controlled sampling from three locales (Mud, Guling and Lalung) in the Spiti District. The very good comparison with the faunas from the Salt Range allows us to establish a detailed and laterally reproducible biozonation for the Dienerian of the NIM.

Geological framework

General context

The Spiti District is situated in the central Himalayas in Himashal Pradesh, northern India, about 400 km North of New Delhi (Fig. 1). It includes the valley formed by the Spiti River and its tributaries. During the Early Triassic, it was situated in the southern Tethys on the northern Gondwana margin, at a latitude of ca. 30°S (Fig. 1A). In this region, the Early Triassic and Anisian are represented by the Mikin Formation (Bhargava *et al.*, 2004). It disconformably overlies the Upper Permian

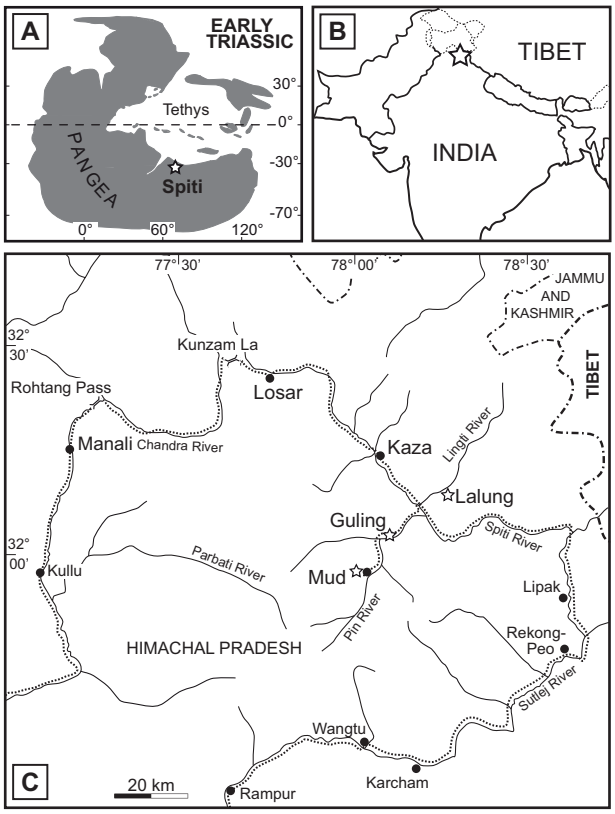

Fig. 1. A) Palaeogeographical map of the Early Triassic with the palaeoposition of Spiti (modified after Brayard *et al.* 2006). **B)** Map of India showing the location of Spiti. **C)** Location map of the three studied areas in Spiti District (modified after Brühwiler *et al.* 2012b).

Kuling Shales and is overlain by the Upper Ladinian Kaza Formation. The Mikin Formation can be divided into four members: the Lower Limestone Member (LLM), the Limestone and Shale Member (LSM), the Niti Limestone and the Himalayan Muschelkalk. The Dienerian is represented by the upper part of the LLM and the shale interval at the base of the LSM. Based on their ammonoid content, the LLM and LSM were further subdivided into a certain number of units, the names and number of which vary depending on the author (such as "*Otoceras* beds", "*Meekoceras* beds", etc.). These names have also changed depending on the stratigraphic resolution and taxonomy used by different authors. For example, the Dienerian shale interval at the base of the LSM was included into the "*Otoceras* beds" by Diener (1897), then individualised into the "*Meekoceras* beds" by Krafft & Diener (1909), which were renamed "*Gyronites* beds" by Bhargava *et al*. (2004), and finally renamed "*Ambites* beds" by Brühwiler *et al*. (2010). To avoid any confusion with previous works, and considering that lithological units should be named independently from their faunal content to avoid problems linked with possible diachronism of the lithological units, these names are not used here.

As already discussed in Ware *et al.* (this volume), the stage subdivision of the Early Triassic (Induan and Olenekian) and the correspondence of their mutual boundary with the Dienerian-Smithian boundary are still in debate. Here the fourfold robust scheme of Tozer (1965) is followed but at the substage level. The Griesbachian/Dienerian boundary (GDB) was originally defined by Tozer (1965) with the first occurrence of "Meekoceratidae" (*i.e.* Gyronitidae). In Spiti, Krystyn & Orchard (1996) placed this boundary within the LLM, considering the fauna from the upper part of this interval (their "*Pleurogyronites* beds") as typically Dienerian, based on the presence of abundant Gyronitidae, the absence of the typically Griesbachian *Ophiceras*, and the occurrence of the conodont *Sweetospathodus waageni*. This definition of the boundary coincides also generally with a minor facies change, with the appearance of thin shale intervals and less massive, finer grained limestones. This definition of the GDB was questioned by Krystyn *et al.* (2004), who considered these beds as late Griesbachian but proposed to use instead the Gangetian substage for the whole LLM. Krystyn *et al.* (2004) also reported some rare Gyronitidae (listed under the genus name "*Pleurogyronites*") associated with typical Griesbachian *Ophiceras* in the bed just below the GDB as defined by Krystyn & Orchard (1996). The same association has been found in the Salt Range (Ware *et al.*, this volume) where it has been interpreted as a result of condensation. However, both Krystyn & Orchard (1996) and Krystyn *et al.* (2004) reported exclusively Griesbachian conodonts in this bed, thus questioning the condensed nature of this association.

The definition of the GDB is thus still problematic, and more expanded sections spanning this boundary are necessary to solve this question. Here, we decided to place the GDB in agreement with Krystyn & Orchard (1996). It also corresponds to a lithological boundary which is generally easily recognisable in the field and it agrees with the definition of Ware *et al.* (this volume), in which the *Gyronites dubius* beds represent the first Dienerian faunal association.

The Dienerian/Smithian boundary (DSB), which coincides with the Induan/Olenekian boundary, is also not yet formerly defined. Krystyn *et al.* (2007a, b) proposed a section of Mud as a GSSP for this boundary, and based their definition of the Smithian on the first appearance of the conodont *Novispathodus waageni* s.l. However, ammonoids with a Smithian affinity (particularly of the genus *Flemingites*) were recently found about 1 m below this boundary (Brühwiler *et al.*, 2010). This led to a revised definition of the base of the Smithian with the occurrence of *Flemingites bhargavai*. Another typically Smithian genus, *Kashmirites*, also appears in the same horizon (Ware, unpublished data). *Flemingites bhargavai* has also been found in the Salt Range (Brühwiler *et al.* 2012a), establishing the lateral reproducibility of this definition at least at a regional scale. It is this definition of the DSB that is followed here.

Lithology and taphonomy

Dienerian ammonoids of Spiti are found in three different types of facies, one being typical of the LLM while the other two are from the shale interval at the

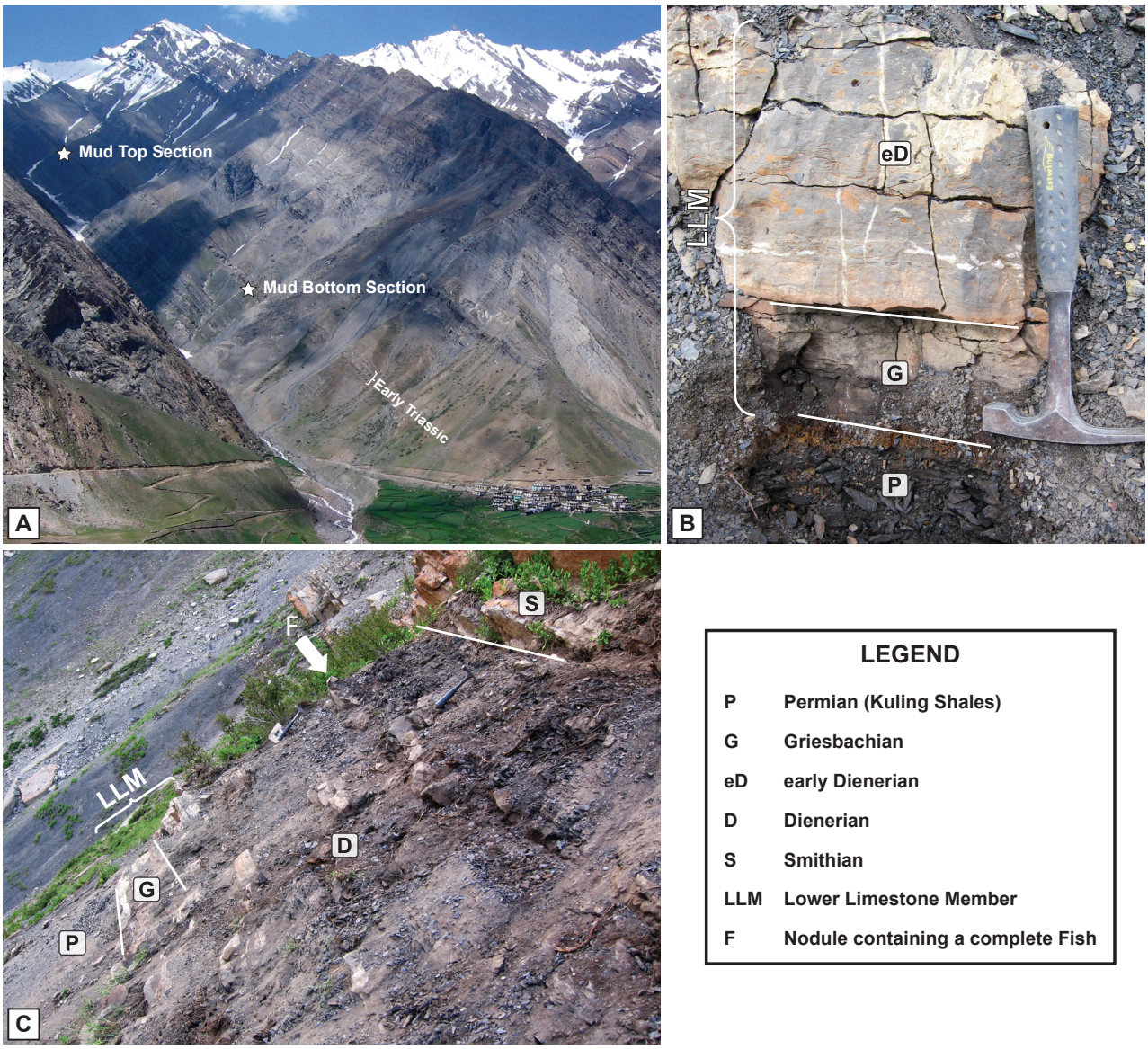

Fig. 2. A) General view of the exposures near Mud, with location of the two studied sections. **B)** Close-up view of the Permian-Triassic boundary and of the Lower Limestone Member of Mud Top Secttion. **C)** Photo of Mud Bottom Section (section M05 of Krystyn *et al.*, 2007a). Note the thickness difference of the LLM compared with the Top Section.

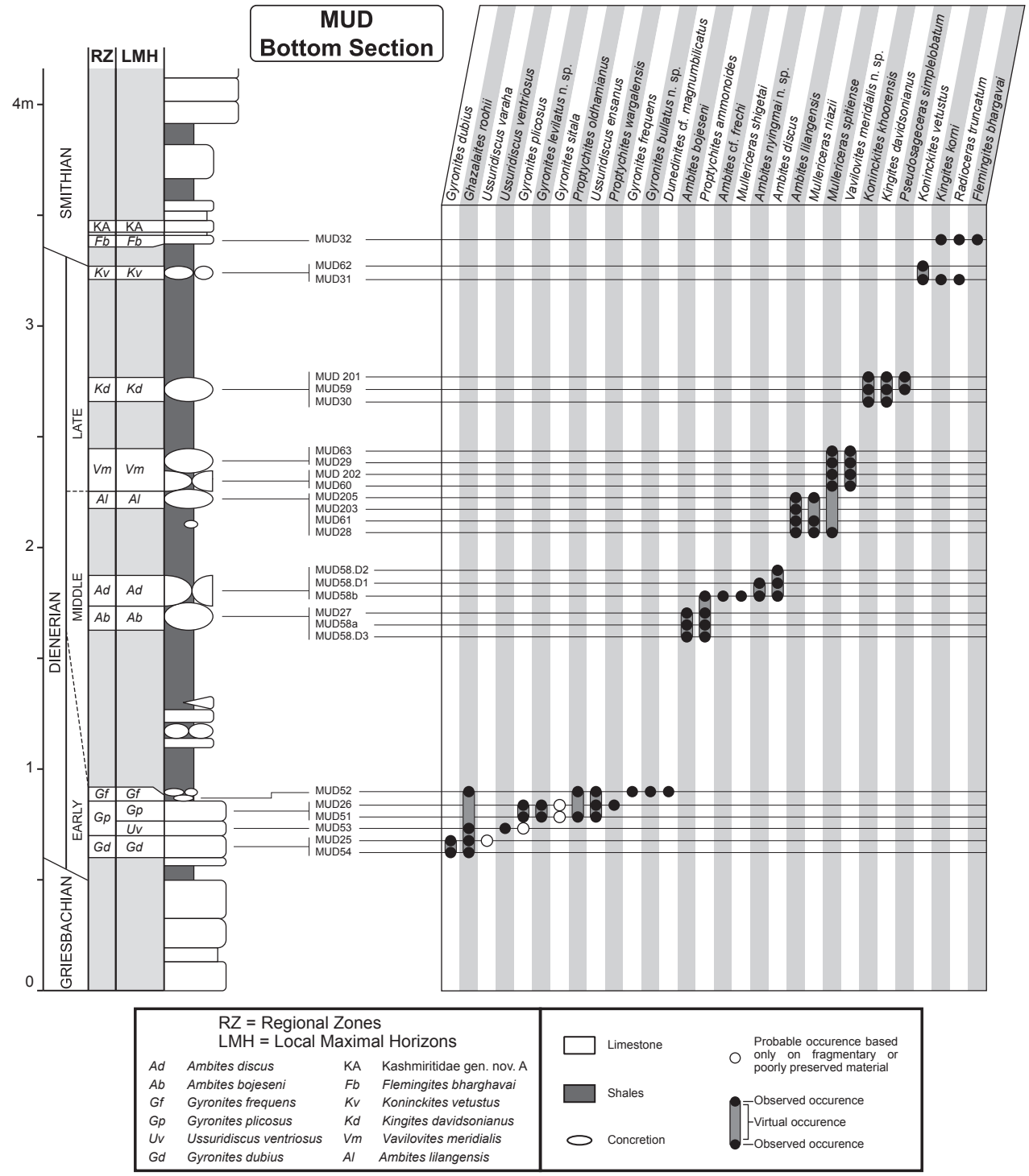

Fig. 3. Stratigraphic log and distribution of ammonoids of the section Mud Bottom.

base of the LSM.

Strata of Dienerian age in the upper part of the LLM consists of thin, hard coarse-grained coquinoid limestone beds very rich in ammonoids, bivalves and unidentifiable shell fragments. The ammonoids are often poorly preserved and broken, with only a preserved portion of the body chamber, and are frequently distorted. They are occasionally phosphatised, with fillings of iron oxides where the shell material has been dissolved. In the LLM, all specimens are usually small sized, inclusive of nuclei of larger individuals, thus suggesting some mechanical sorting. These layers were deposited in a rather shallow environment with low sedimentation rates, so the stratigraphic record is occasionally affected by condensation. In two sections, Lalung ridge 1 and Guling Village, the upper bed of the LCL contains both the genus *Gyronites*, with species typical of the *Gyronites frequens* beds (latest early Dienerian), and the genus *Ambites*, with species typical of the *Ambites atavus* beds (earliest middle Dienerian). Such condensed occurrences are

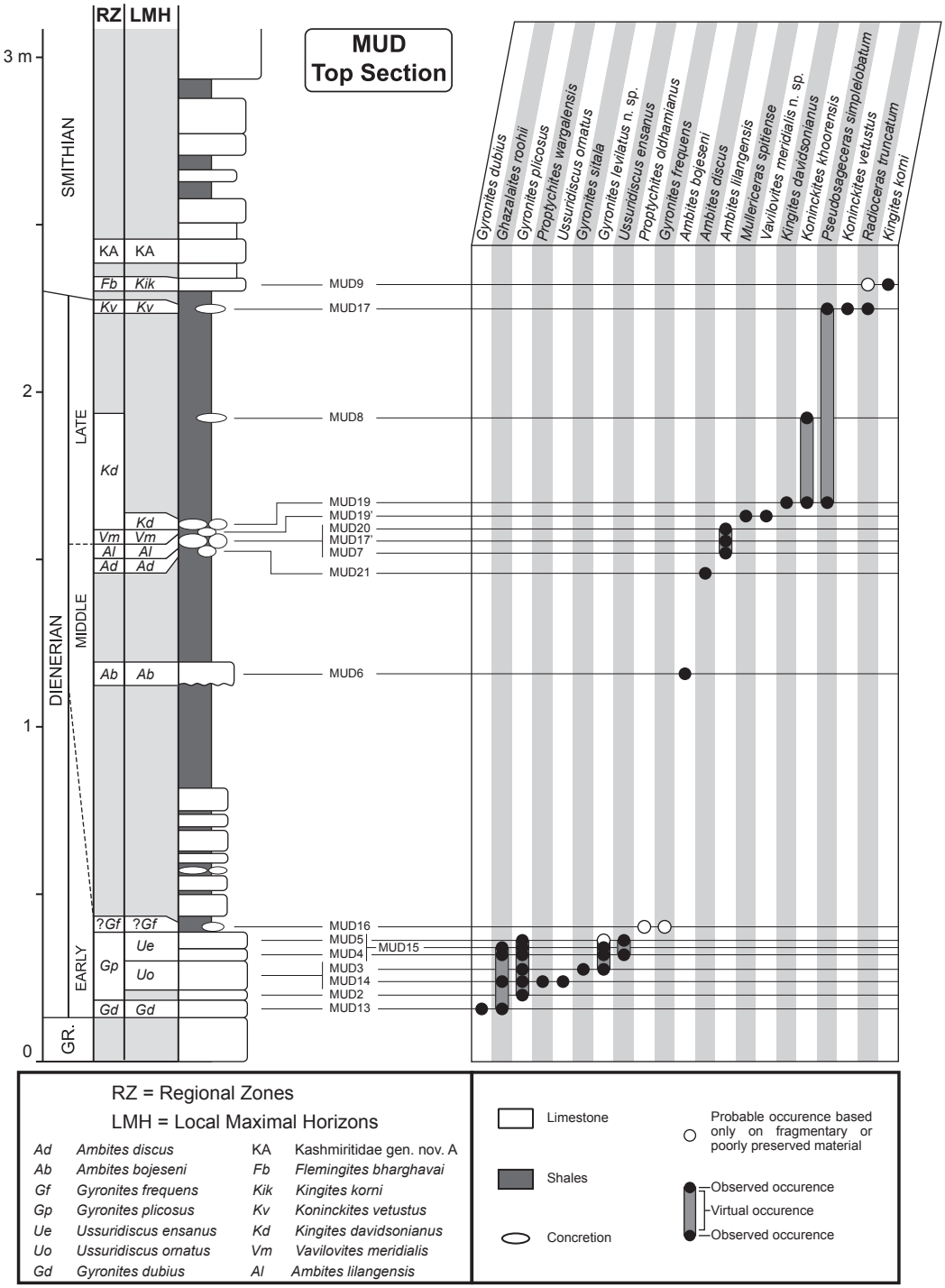

Fig. 4. Stratigraphic log and distribution of ammonoids of the section Mud Top.

excluded from the construction of the biochronological scheme. In the Mud Bottom section, the uppermost bed of the LLM shows a different, finer grained facies with well preserved and undistorted ammonoids.

The lower part of the LSM consists of a black shale interval rich in organic matter and pyrite. It contains only a few limestone beds in Mud and Guling, whereas in Lalung limestone beds are much more abundant. Ammonoids in the shales are crushed, heavily distorted and their shell is partially dissolved, usually too poorly preserved to be identified even at the family level. The limestone beds display two different types of facies. A first facies mostly consists of tempestites in which the fossils are very unevenly distributed. These beds are often discontinuous and show some grain size sorting. Ammonoids generally have their body chamber partially broken and are often imbricated and distorted. A second facies yielding ammonoids consists of large (up to ca. 50 cm in diameter) early diagenetic limestone concretions. In this case, the specimens are generally complete, undistorted, and with their peristome preserved. Their upper side of the phragmocone is often flattened, an indication of high sedimentation rates. Body chambers show geopetal structures, their upper half being filled with sparitic calcite and bitumen. These early diagenetic concretions may also yield complete, still articulated fish

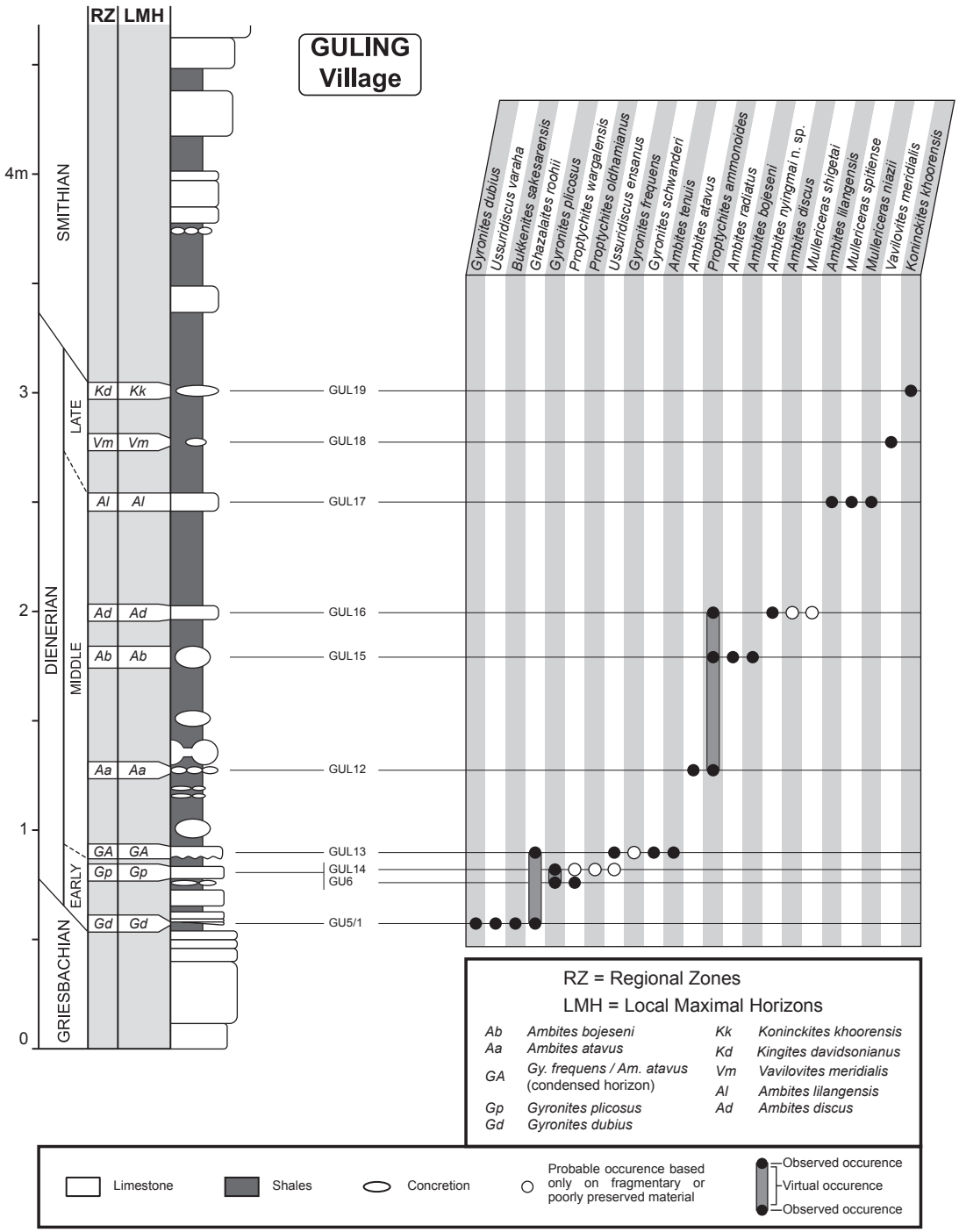

Fig. 5. Stratigraphic log and distribution of ammonoids of the section Guling Village.

skeletons. Such complete fishes, associated with the abundance of pyrite and organic matter, indicates that these layers were deposited under anoxic conditions at the sediment–sea water interface. Throughout this interval, ammonoids are very frequently encrusted by bivalves similar to the ones previously described in Ware *et al.* (2011, this volume), especially the involute forms, independently of their taxonomic affinities. These bivalves are generally encrusting the umbilicus on both sides of the shell (see for example Pl. 5: 1, Pl. 6: 6, Pl. 7: 3, 6, 7, Pl. 8: 1, 4, 6, 7, Pl. 10: 8), sometimes inducing a departure from normal umbilical coiling. Bivalves encrusting the whorl flanks of ammonoids are not unusual (see for example Pl. 6: 1). Some large ammonoid specimens are completely encrusted by hundreds of these bivalves (see for example Pl. 7: 1, Pl. 11: 1), except on the last portion of the body chamber, an additional clue that these were encrusting the shell *in vivo*. As in the Salt Range, these *in vivo* encrusting bivalves have not been found in older or younger strata and are restricted to this anoxic interval.

Present work

Most of the specimens presented herein were collected during two field work seasons in 2008 and 2009. To complete this study, a few specimens collected

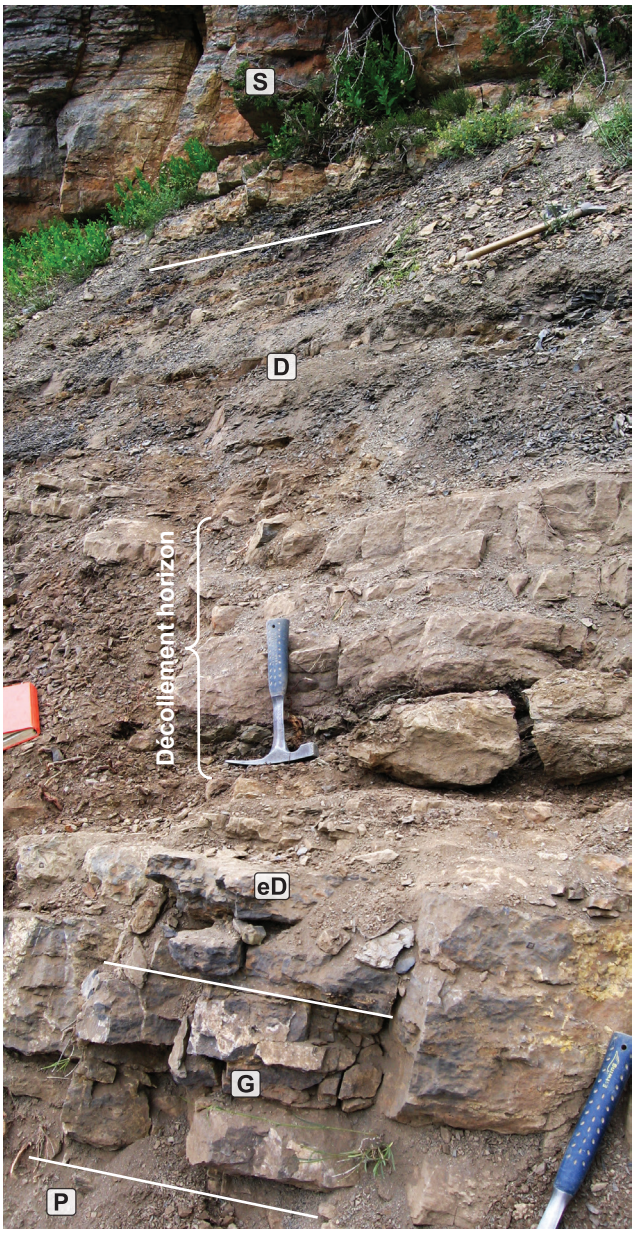

LEGEND			
P	Permian	D	middle and late Dienerian
G	Griesbachian	S	Smithian
eD	early Dienerian		

Fig. 6. Photo of the section Guling Village. Note the fault breccia, with a thick layer of irregular limestone beds replaced laterally by shales.

previously by Leopold Krystyn in Lalung and Guling were also included. Finally, following the discovery of complete fishes in 2009, further field investigations were carried out in 2010 by Winand Brinkmann (PIMUZ) to find additional fishes in the Dienerian shale interval, and supplementary ammonoids were collected in order to adequately date the fish material. Three areas were investigated, from South to North: Mud, Guling and Lalung (Fig. 1C). Mud and Guling are situated along the Pin River, a southern tributary of the Spiti River, while Lalung is situated along the Lingti River, a northern tributary of the Spiti River. These three classic locales are known since the late 19th century, thanks to the exploration of this region by the Geological Survey of India under the direction of Karl Griesbach. Several sections were sampled in detail in each of these locales. Although strata of Early Triassic age are extensively exposed throughout the Spiti region, they are very often difficult to reach, thus limiting the number of sections studied here.

Near the village of Mud, Early Triassic strata can easily be reached on the northern flank of a wide side valley NW of Mud. This area is of primary importance for Early Triassic stratigraphy as it has been proposed as a candidate GSSP for the DSB by Krystyn *et al*. (2007a, b). Two sections have been sampled (Fig. 2A). The first one corresponds to the section M05 of Krystyn *et al*. (2007a; Fig. 2C). It is situated slightly above the candidate GSSP (section M04), at ca. 4130 m of altitude, at the following coordinates: N31°57'58.4" / E78°01'21.4". This section is much better exposed than the GSSP candidate. It is here referred to as the "Mud Bottom Section", and the corresponding stratigraphic log and ammonoid distribution are given in figure 3. The second one corresponds to three partial sections spread over 100 m of continuous exposures. These sections can easily be correlated on the exclusive basis of lithology, thus allowing the construction of a single composite log as presented here. They are situated much higher, at ca. 4750 m elevation, around the following coordinates: N31°58'36.2" / E78°00'23.3". These sections are much thinner than the Mud Bottom section, especially in the case of the LLM (Fig. 2B), where the Griesbachian is represented only by a ca. 15 cm thick bed, whereas it corresponds to a 1 m thick interval which can be subdivided into 4 beds in the lower section. It is here referred to as the "Mud Top Section", and the corresponding stratigraphic log and ammonoid distribution are given in figure 4. Despite the modest distance separating these two sections, they differ in their lithological details, the upper one being thinner than the lower one.

Around Guling, Early Triassic strata form a syncline with easily accessible sections. Three sections were sampled. The first one is located about 100 m North of Guling, at ca. 3650 m elevation, at the coordinates: N32°02'44.3" / E78°05'26.2". This section is here designated "Guling Village", and the corresponding stratigraphic log and ammonoid distribution are given in figure 5. Here the shale interval was covered by scree, so a trench was dug to sample it. Consequently, the lateral continuity of the layers could not be assessed. The upper part of the LLM contains more shales than in other sections, so the boundary between the LLM and LSM does not appear clearly on the logs. It is however marked by a change in facies, and the topmost bed of the LLM corresponds to a condensed horizon containing a mixture of the *Gy.*

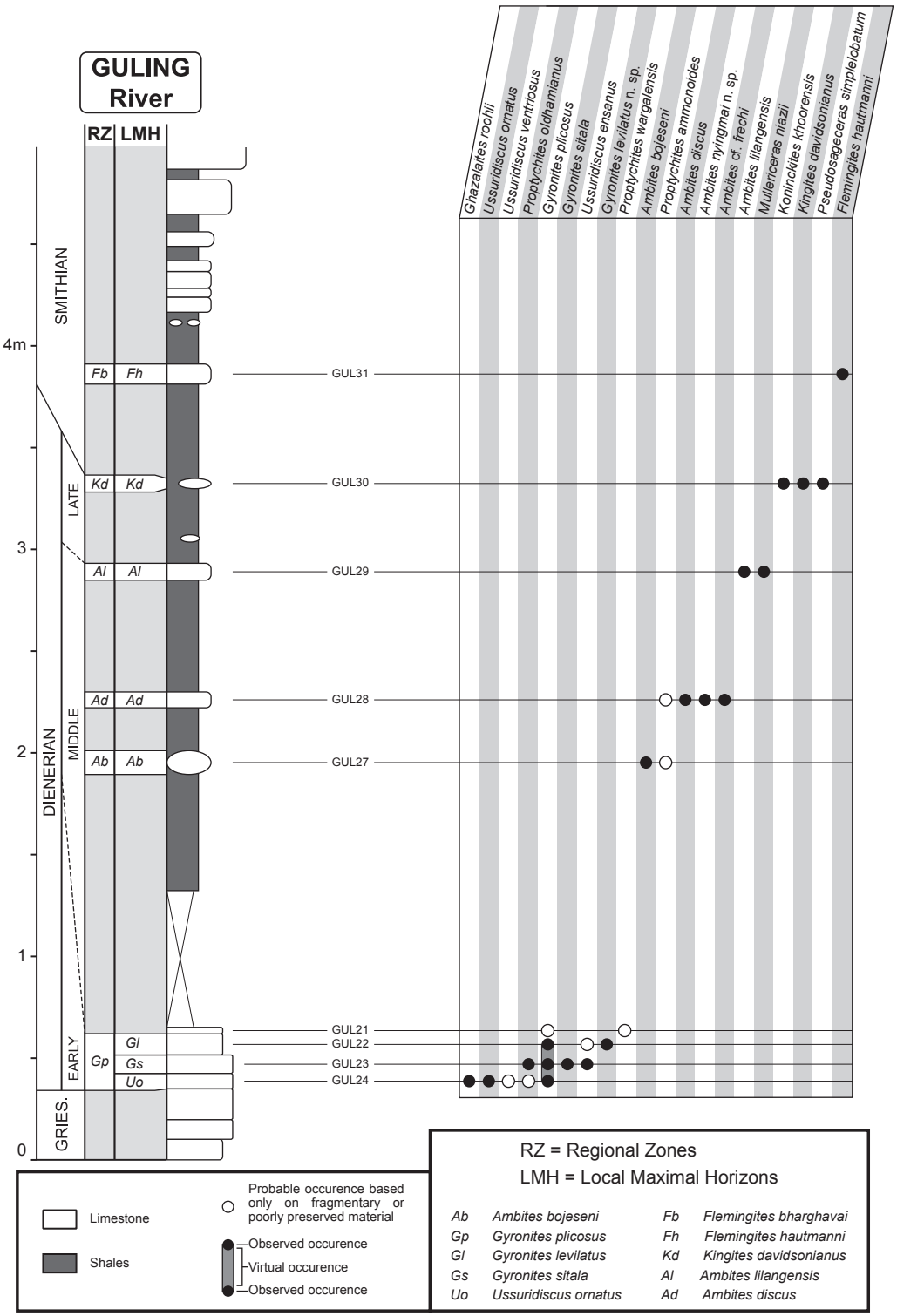

Fig. 7. Stratigraphic log and distribution of ammonoids of the section Guling River.

frequens and the *A. atavus* faunal associations. Another easily accessible section (Fig. 6) was sampled on the other side of the river, south of Guling at ca. 3740 m elevation, at coordinates: N32°02'7.1" / E78°05'10.9". It is the only section where the two parts of the LLM (Griesbachian and Early Dienerian) do not show any facies difference. The limestone beds at the base of the LSM (visible on the photo, Fig. 6) are not continuous, and have obviously been interrupted by a décollement horizon or low angle small scale faults. This section is here designated "Guling River", and the corresponding stratigraphic log and ammonoid distribution are given in figure 7. These two sections are very similar in thickness. However, the comparison of their respective bases is obscured by small scale faulting parallel to bedding in the river section. The upper parts of the sections are otherwise nearly identical. Another section, situated further South in the continuity of the Guling River section, has been briefly sampled during a field work session conducted in 2010 with the aim of collecting fishes. Only a few ammonoids

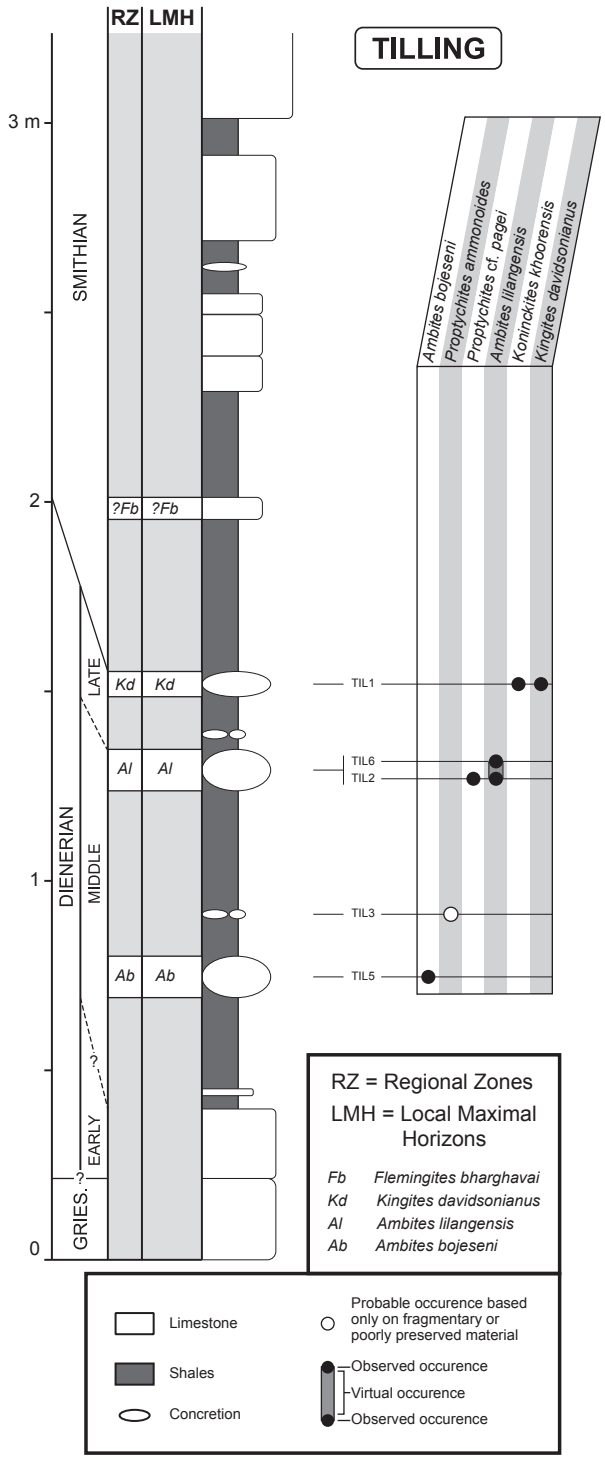

Fig. 8. Stratigraphic log and distribution of ammonoids of the section Tilling.

Fig. 9. Photo of the section Lalung Cliff. Note the abundance of limestone beds compared with the other sections. The Griesbachian-Dienerian Boundary is here not well defined as no Griesbachian or early Dienerian faunas were found. Hence, it is based on the lithological change only.

were collected in order to date the shale interval where the fishes were found. The base of this section has not been sampled. It is situated north of the village of Tilling, at ca. 4030 m elevation, at the following coordinates: N32°00'46.2" / E78°05'04.5". It is here referred to as the "Tilling" section, and the corresponding stratigraphic log and ammonoid distribution are given in figure 8. This section is much thinner than the other two sections of this area, but the sequence of beds of the interval which has been sampled is identical.

Near the Village of Lalung, extensive exposures of Early Triassic strata can be seen, but most of these are inaccessible. As a consequence, only three sections, all situated in a small gulley north of Lalung, could be investigated. The most complete section (Fig. 9) is situated on the southern side of this gulley, below a small cliff formed by the Niti Limestone. It is here referred to as the "Lalung Cliff" section, and is situated at ca. 3860 m elevation, at the following coordinates: N32°08'57.8" / E78°14'36.5". The corresponding stratigraphic log and ammonoid distribution are given in figure 10. Two other small sections situated only ca. 20 m apart on a ridge on the northern side of the same gulley were also investigated. Here, only the LLM and a few beds at the very base of the LSM are exposed, the rest of the

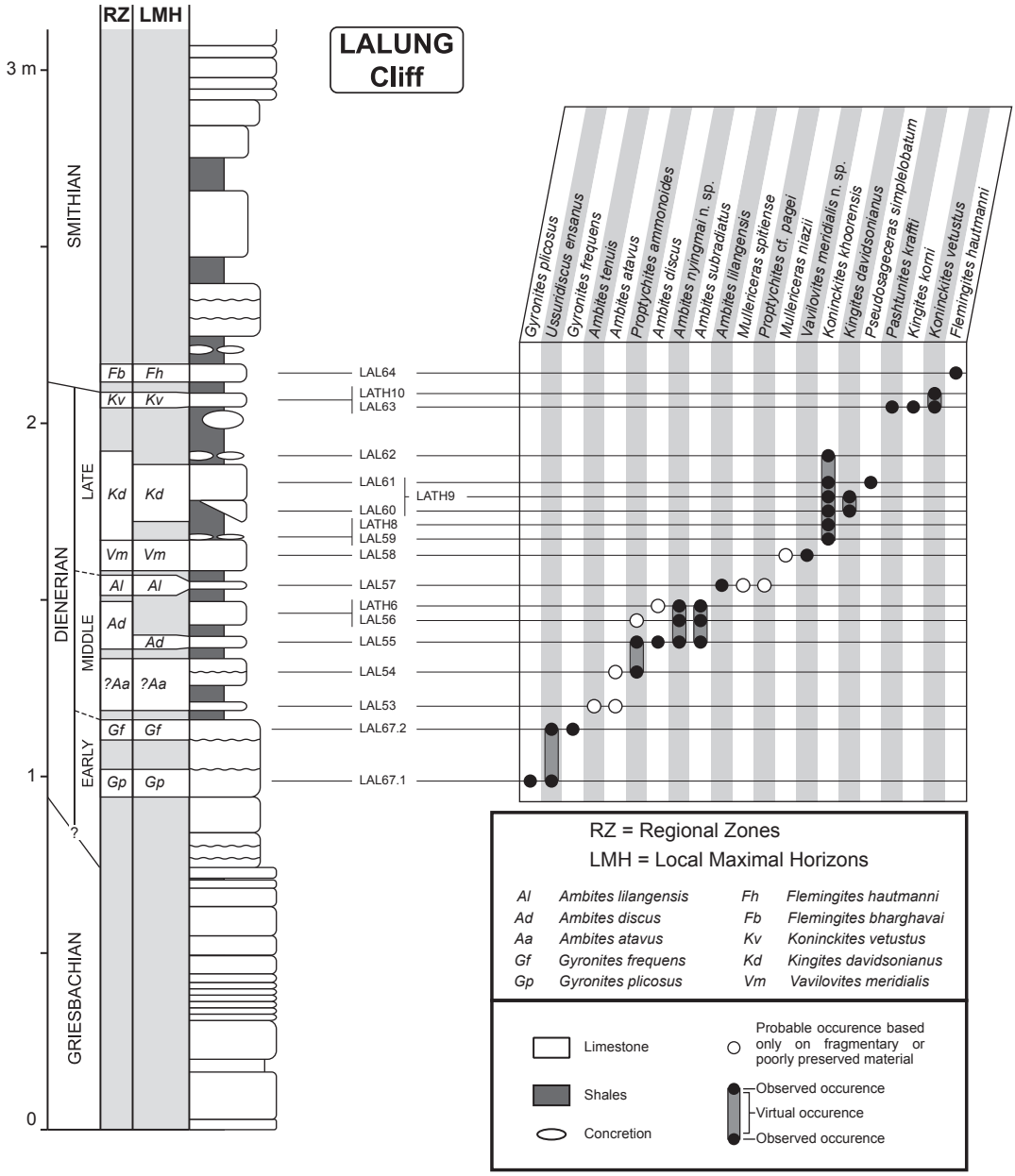

Fig. 10. Stratigraphic log and distribution of ammonoids of the section Lalung Cliff.

section being covered by scree. These two sections are intensively weathered, and even the bedding plane cannot be seen easily. As a consequence, these two sections could not be directly correlated on the basis of lithology, thus preventing the construction of a synthetic log. These two sections are here referred to as "Lalung Ridge 1" and "Lalung Ridge 2", and are situated at ca. 3840 m elevation, at the following coordinates: N32°09'05.1" / E78°14'37.4" and N32°09'04.8" / E78°14'38.1", respectively. The corresponding stratigraphic log and ammonoid distribution are given in figures 11 and 12. In this locality, the LLM is much thicker than in Mud or Guling, while the basal shale interval of the LSM is much thinner and more calcareous than in the two other localities. In the Ridge 1 section, the topmost bed of the LLM is a condensed horizon, containing a mixed assemblage of the *Gy. frequens* and *A. atavus* associations.

Biostratigraphy

The very detailed bed-rock-controlled sampling on which this study is based allowed us establishing a sequence of 10 different regional zones (RZ) for the Spiti District (Figs. 13, 14). These RZ are in very good agreement with those described in the Salt Range (Ware *et al.*, this volume). Only two RZ first identified in the Salt Range have not been subsequently recognised in Spiti. The correlation of the RZ of the Salt Range with those of Spiti is straightforward. Accordingly, the threefold subdivision (early, middle and late) of the Dienerian established for the Salt Range also applies to Spiti. This new biostratigraphical scheme considerably improves the biostratigraphic resolution of the Dienerian of Spiti, which was so far divided only into 5 zones (Krystyn *et al.*, 2004, 2007a, Brühwiler *et al.*, 2010). Most of the RZ described here directly correspond to local

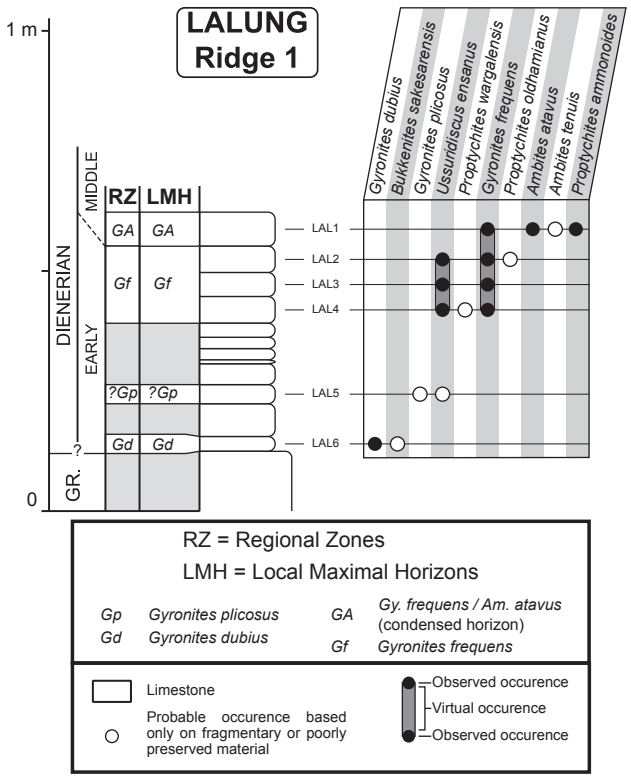

Fig. 11. Stratigraphic log and distribution of ammonoids of the section Lalung Ridge 1.

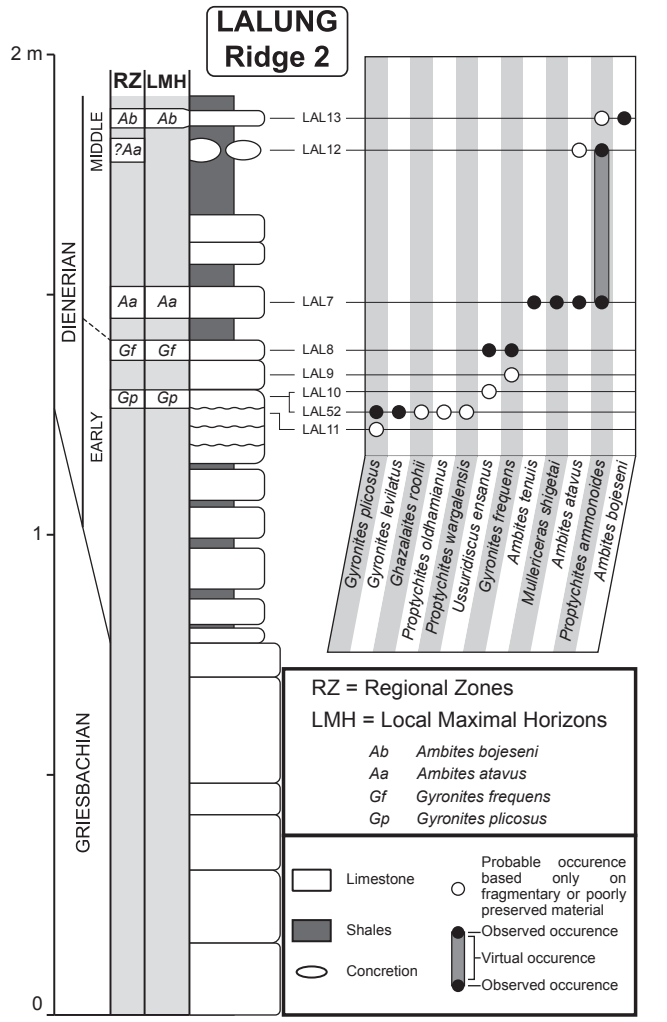

Fig. 12. Stratigraphic log and distribution of ammonoids of the section Lalung Ridge 2.

maximal horizons (LMH) of Guex (1991), with only one exception: the *Gyronites plicosus* beds (see below). The comparison of this biostratigraphical scheme with those of other regions has already been given in our revision of the Dienerian of Salt Range and is not repeated here. The synthetic range charts for Dienerian ammonoid species and genera from Spiti are given in figures 15 and 16, respectively. The RZ described here are referred to as "beds" for short, as the use of the term "zone" would imply a well established lateral reproducibility of the faunal sequence across more distant basins outside of the NIM.

Early Dienerian ammonoid faunas

Early Dienerian faunas are restricted to the upper part of the LLM. Each RZ is characterised and largely dominated by a different species of *Gyronites*. In this interval, the sedimentation rate is very low, so the stratigraphic record is occasionally affected by hiatuses and condensation. Indeed, the *Gyronites dubius* beds are missing in the section Guling River, where the *Gyronites plicosus* beds rest directly onto beds of Griesbachian age. Also, in two sections (Guling River and Lalung Ridge 1), the topmost bed of the LLM is condensed, including a mixture of species

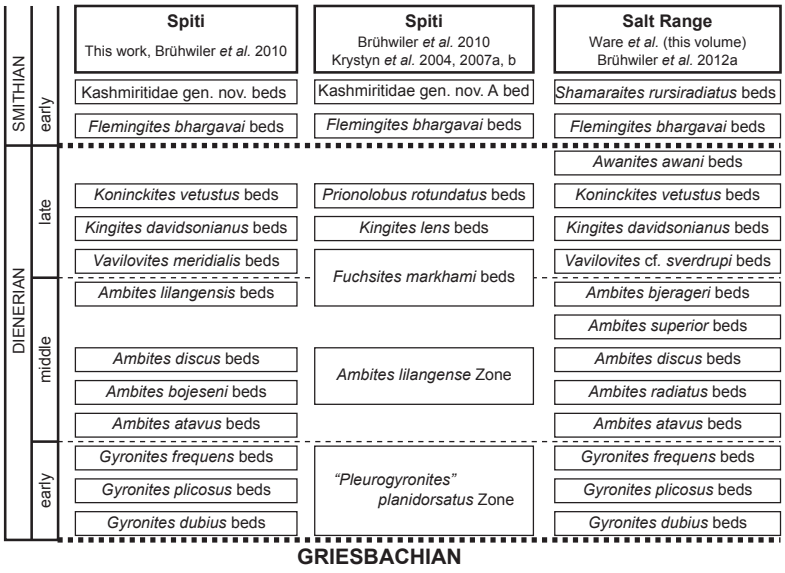

Fig. 13. Biostratigraphic subdivisions of the Dienerian and earliest Smithian of Spiti and correlation with the previously established zonation for this area and the zonation established for the Salt Range.

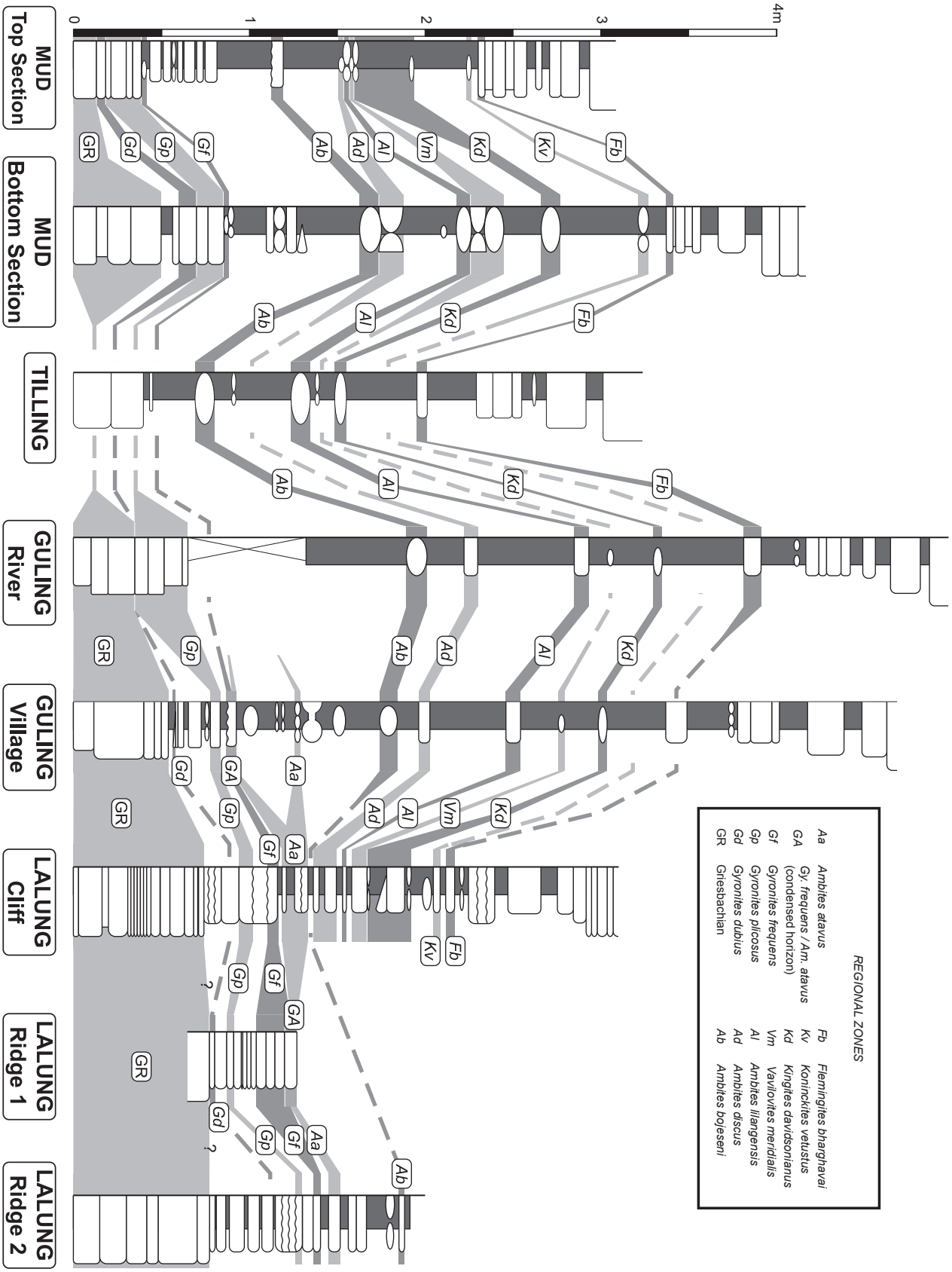

Fig. 14. Biostratigraphic correlation of the different studied sections, ordered from South to North.

characteristic of the latest early Dienerian *Gyronites frequens* beds and of the earliest middle Dienerian *Ambites atavus* beds.

Gyronites dubius *beds.* – This RZ has been recognised in all sections but three. In Guling River, it is altogether missing as previously mentioned. In Lalung Cliff

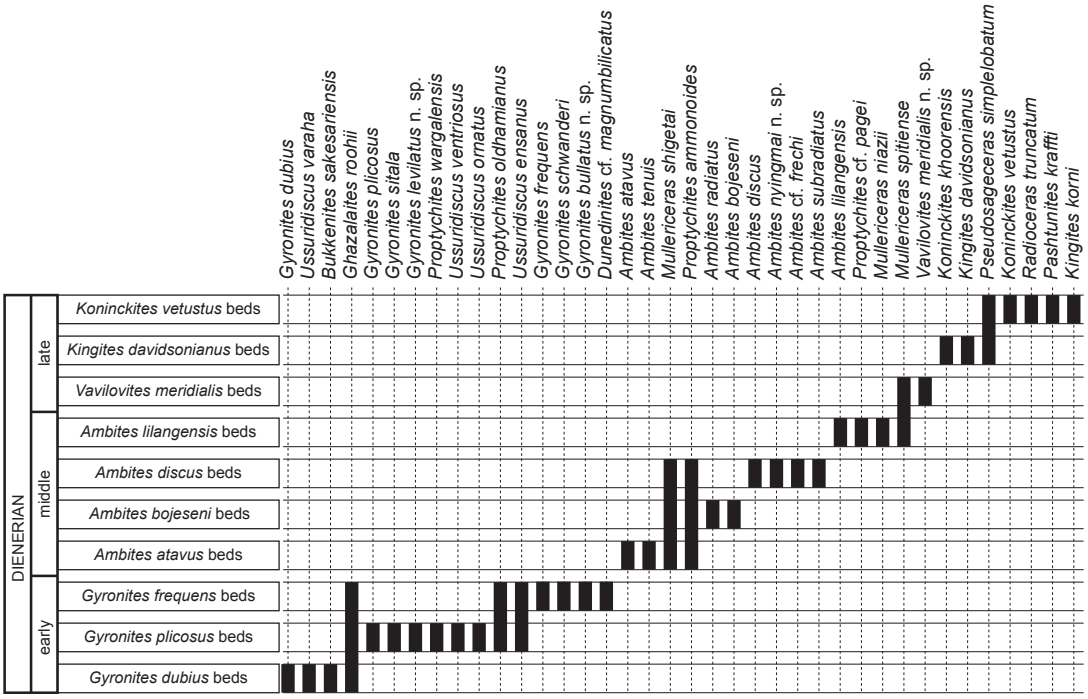

Fig. 15. Synthetic range chart showing the biostratigraphical distribution of Dienerian ammonoid species in Spiti.

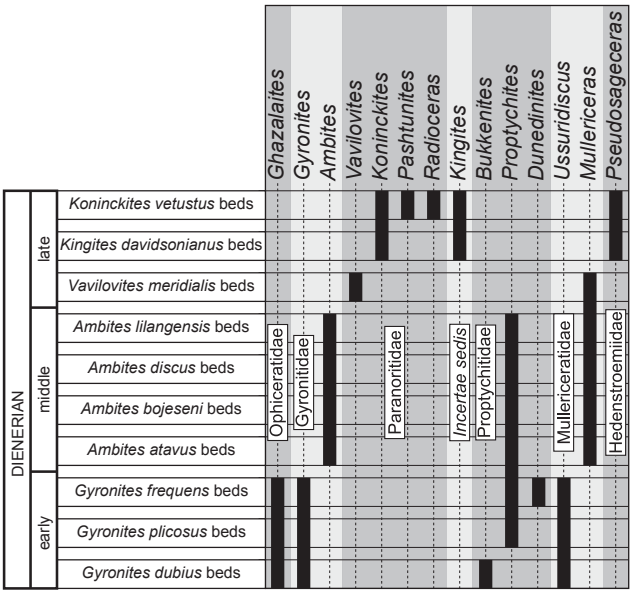

Fig. 16. Synthetic range chart showing the biostratigraphical distribution of Dienerian ammonoid genera (grouped by families) in Spiti.

and Lalung Ridge 2, the beds that may correspond stratigraphically to this zone contained only ammonoids which were too poorly preserved to be identified even at the family level, and were thus not included in this study. This RZ includes four species: *Gy. dubius*, the most abundant species, *Ussuridiscus varaha*, *Bukkenites sakesarensis* and *Ghazalaites roohii*. The very same association has been found in Amb in the Salt Range (Ware *et al.*, this volume).

Gyronites plicosus *beds.* – This RZ has been recognised in every section investigated here. With nine species, it is the most diverse fauna of Dienerian age in Spiti. It is largely dominated by *Gy. plicosus*, but *Gy. levilatus*, *U. ensanus*, *Gh. roohii* and *Proptychites oldhamianus* are not rare. *Gy. sitala*, *U. ornatus*, *U. ventriosus* and *Pro. wargalensis* are rare, being represented by a few specimens only. This association corresponds to two or three LMH in the Mud Top, Mud Bottom and Guling River sections. However, these LMH are only differentiated by rare species represented in the collections only by a few specimens. Hence, these differences are probably induced by a sampling bias and are consequently lumped into one RZ. The same RZ has been recognised in the Salt Range, except for *Gy. levilatus* which has so far only been found in Spiti.

Gyronites frequens *beds.* – This RZ corresponds in every section to the topmost bed(s) of the LLM, except in Guling River where the section is interrupted by a fault breccia. In Guling Village and Lalung Ridge 1, it is condensed and mixed with the earliest middle Dienerian fauna. It is largely dominated by *Gy. frequens*, but *U. ensanus*, *Gh. roohii* and *Proptychites oldhamianus* are not rare. *Gy. schwanderi* is rarer, while *Gy. bullatus* is represented only by two specimens and *Dunedinites* cf. *magnumbilicatus* only by one, in both cases coming from a lens with very well preserved ammonoids at the top of the LLM in the Mud Bottom section. This RZ is an obvious correlative of the *Gy. frequens* beds of the Salt Range, irrespective of the two rare species mentioned above.

Middle Dienerian ammonoid faunas

Faunas of middle Dienerian age occur in the lower half of the shale interval at the base of the LSM. Each zone is exclusively characterised by a different species of *Ambites*, each of these being very abundant. Many very well preserved and complete specimens were found in the early diagenetic limestone concretions of this interval. Specimens derived from tempestitic layers are not as well preserved as they are often broken and distorted. As previously indicated, the base of this interval is occasionally condensed and may locally include the uppermost part of the early Dienerian.

Ambites atavus *beds.* – This RZ has only been recognised in Lalung and in Guling Village sections. The corresponding interval in Mud is represented by shales and limestone beds in which only unidentifiable ammonoids were found. In Guling Village and Lalung Ridge 1, it is condensed with the *Gyronites frequens* beds. The fauna is characterised and dominated by *Ambites atavus*. The three other species of this RZ (*Am. tenuis*, *Pro. ammonoides* and *Mullericeras shigetai*) are very rare. This RZ is exactly the same as that recognised in the Salt Range.

Ambites bojeseni *beds*. – This RZ has been recognised in all sections except Lalung Cliff. It is characterised and largely dominated by *Am. bojeseni*, but *Pro. ammonoides* is not rare. *Am. radiatus* is extremely rare. No specimen of *Mu. shigetai* could be recovered from these beds, so this species is only virtually present (*i.e.* present in the underlying and overlying beds) in this RZ. Sharing exactly the same association of species, it obviously correlates with the *Ambites radiatus* beds in the Salt Range. The only difference is that *Am. radiatus* is the most abundant species in the Salt Range.

Ambites discus *beds.* – This RZ has been recognised in all sections except Tilling. It is characterised and largely dominated by *Am. discus*. *Am. nyingmai* is also frequent. *Mu. shigetai*, *Pro. ammonoides* and *Am. subradiatus* are rare. *Am.* cf. *frechi* is only documented by two immature specimens, making the occurrence of this species still somewhat uncertain. It corresponds exactly to the *Am. discus* beds in the Salt Range, with the same association of characteristic species, plus one additional new species (*Am. nyingmai*).

Ambites lilangensis *beds.* – This RZ has been recognised in all investigated sections. It is characterised and dominated by *Am. lilangensis*. *Mu. niazii* comes next in term of frequency. *Mu. spitiense* and *Pro.* cf. *pagei* are scarce. It is the correlative of the *Am. bjerageri* beds in the Salt Range. *Pro. lawrencianus*, which is quite abundant in the Salt Range, is here represented only by one specimen from a float block in Lalung which is probably derived from these beds.

Late Dienerian ammonoid faunas

The late Dienerian faunas are distributed throughout the upper half of the shale interval at the base of the LSM. Each RZ is characterized by a different paranoritid. Large numbers of very well preserved and complete specimens were found in the concretions of this interval. Faunas from tempestitic layers are not as well preserved as they are often broken and distorted. The youngest fauna of the Dienerian has been only partly described in Brühwiler *et al.* (2010).

Vavilovites meridialis *beds.* – This RZ has been recognised in every section except Tilling and Guling River. It is characterised by only two species: *V. meridialis* (the dominant species) and *Mu. spitiense.* It corresponds to the same association as that of the *V.* cf. *sverdrupi* beds of Ware *et al.* (this volume) in the Salt Range, which are here renamed *V. meridialis* beds for the sake of consistency. In the Salt Range, the species *Koninckites khoorensis* and *Pseudosageceras simplelobatum* co-occur with the two mentioned species, but have not been yet documented from this RZ in Spiti.

Kingites davidsonianus *beds.* – This RZ has been recognised in all investigated section. It is largely dominated by *Kon. khoorensis* and *Ki. davidsonianus. Ps. simplelobatum* rarely occurs in these beds. The same RZ has been found in the Salt Range, where it also contains *Clypites typicus* and *Subacerites friski*.

Koninckites vetustus *beds.* – This RZ has been recognised in the sections near Mud and Lalung, but has not been recovered from Guling. It is largely dominated by *Kon. vetustus* and *Radioceras truncatum*. The other three co-occurring species (*Ps. simplelobatum*, *Ki. korni* and *Pashtunites kraffti*) are very rare. The same association has been found in the Salt Range, with the two additional taxa *Clypites typicus* and *Koiloceras sahibi*.

Conclusion

The high-resolution bed-rock controlled sampling of different sections near Mud, Guling and Lalung yielded abundant and well preserved Dienerian ammonoids. Their comparison with the newly established taxonomy and biostratigraphic scheme of the Salt Range (Ware *et al.*, this volume) enabled us to recognise 10 out of the 12 different ammonoid RZ defined in the Salt Range, each with almost identical species contents. The only differences concern a few rare taxa and relative abundance of the different species. The similarity of faunas of the Salt Range and Spiti is very remarkable, and shows that the succession of faunal associations established in the Salt Range is laterally reproducible. It constitutes one important step towards the definition of a new formal high resolution biozonation for the Dienerian, a crucial timing for a better understanding of

the Early Triassic biotic recovery.

Systematic palaeontology
(By Ware, D. & Bucher, H.)

Systematic descriptions follow the principles and classification established for Dienerian ammonoids of the Salt Range in Ware *et al.* (this volume). Many species were described in detail in this work and their description is not repeated here. Only some remarks are made when the material from Spiti allows us to give some more details concerning the morphology. Intraspecific variability of the shell proportions is quantified by the four classic geometrical parameters of the ammonoid shell: diameter (D), whorl height (H), whorl width (W) and umbilical diameter (U). For new species, provided that at least 4 specimens were measurable, the three last parameters (H, W and U) are plotted against the diameter in absolute values as well as relative to the diameter (H/D, W/D and U/D). For all the species already described in Ware *et al.* (this volume), only the relative values are plotted and compared with the populations from the Salt Range. Measurements of species for which less than 4 measurable specimens are available are given in Table 1. All figured specimens are curated in the collections of the Paläontologisches Institut und Museum der Universität Zürich (abbreviated PIMUZ). Sample numbers are reported on the stratigraphic sections (Figs. 3-5, 7-8, 10-12). Synonymy lists and taxa in open nomenclature are annotated following the recommendations of Matthews (1973) and Bengtson (1988).

Class Cephalopoda Cuvier, 1797
Subclass Ammonoidea Agassiz, 1847
Order CERATITIDA Hyatt, 1884
Superfamily Meekocerataceae Waagen, 1895
Family Ophiceratidae Arthaber, 1911

Genus *Ghazalaites* Ware & Bucher (this volume)

Type species. – *Ghazalaites roohii* Ware & Bucher (this volume)**.**

***Ghazalaites roohii* Ware & Bucher (this volume)**

Pl. 1: 1-3; Fig. 17

v? 1978 *Lytophiceras* sp. ind. – Guex, Pl. 1: 4.
v (this volume) *Ghazalaites roohii* gen. et sp. nov. Ware *et al.*, p. xxx, Pl. 2: 4-8.

Occurrence. – Samples Mud4, Mud13, Mud14 and Mud15 from Mud Top Section, Mud25, Mud52, Mud53 and Mud54 from Mud Bottom Section, Gul24 from Guling River, GU5/1 and Gul13 from Guling Village. Poorly preserved specimens from sample Lal52 from Lalung Ridge 2 are tentatively assigned to this species.
Measurements. – see Fig. 17.

Genus	*species*	Specimen number	Level	Section	Age	D	H	W	U
Gyronites	*dubius*	PIMUZ30835	MUD25	Mud Bottom	*Gd*	26.5	8.9	6.4	11.5
Gyronites	*plicosus*	PIMUZ30836	MUD51	Mud Bottom	*Gp*	28.5	9.2	6.2	12.4
Gyronites	*plicosus*	PIMUZ30837	MUD51	Mud Bottom	*Gp*	26	7.7	5.4	12.8
Gyronites	*plicosus*	PIMUZ30838	MUD51	Mud Bottom	*Gp*	31.1	9.9	7	13.4
Gyronites	*levilatus*	PIMUZ30842	MUD5	Mud Top	*Gp*	28.8	12.6	7.2	8.4
Gyronites	*levilatus*	PIMUZ30845	MUD51	Mud Bottom	*Gp*	41.1	16.7	7.6	12.2
Gyronites	*bullatus*	PIMUZ30847	MUD52	Mud Bottom	*Gf*	10.6	3.7	2.8	4.4
Ambites	*radiatus*	PIMUZ30865	GUL15	Guling Village	*Ab*	27.4	11.9	6.7	7.3
Ambites	cf.*frechi*	PIMUZ30872	MUD58B	Mud Bottom	*Ad*	25.6	10.8	6	7.8
Proptychites	*oldhamianus*	PIMUZ30904	MUD52	Mud Bottom	*Gf*	32.8	15.1	12.9	7.2
Proptychites	*oldhamianus*	PIMUZ30903	MUD52	Mud Bottom	*Gf*	56.8	28.9	18.9	8.9
Dunedinites	cf. *magnumbilicatus*	PIMUZ30913	MUD52	Mud Bottom	*Gf*	17.3	7.3	11.1	5.8
Mullericeras	*spitiense*	PIMUZ30917	MUD28	Mud Bottom	*Al*	33.9	20.3	8.6	0
Mullericeras	*spitiense*	PIMUZ30916	MUD29	Mud Bottom	*Vm*	56.8	33.9	14.3	0
Mullericeras	*spitiense*	PIMUZ30918	MUD60	Mud Bottom	*Vm*	53.8	32.9	15	0
Mullericeras	*shigetai*	PIMUZ30919	MUD58B	Mud Bottom	*Ad*	25.9	13.8	6.8	3.8
Mullericeras	*shigetai*	PIMUZ30920	MUD58B	Mud Bottom	*Ad*	31.1	17	7.3	3.3
Kingites	*korni*	PIMUZ27863	MUD31	Mud Bottom	*Kv*	58.3	35.1	15.3	0
Kingites	*korni*	PIMUZ27864	MUD31	Mud Bottom	*Kv*	32.9	20.6	7.7	0

Table 1. Measurements of Dienerian ammonoids from Spiti for which less than 4 specimens were measurable. D, Diameter; H, whorl height; W, whorl width; U, umbilical diameter. For the age, abbreviations as in Fig. 14.

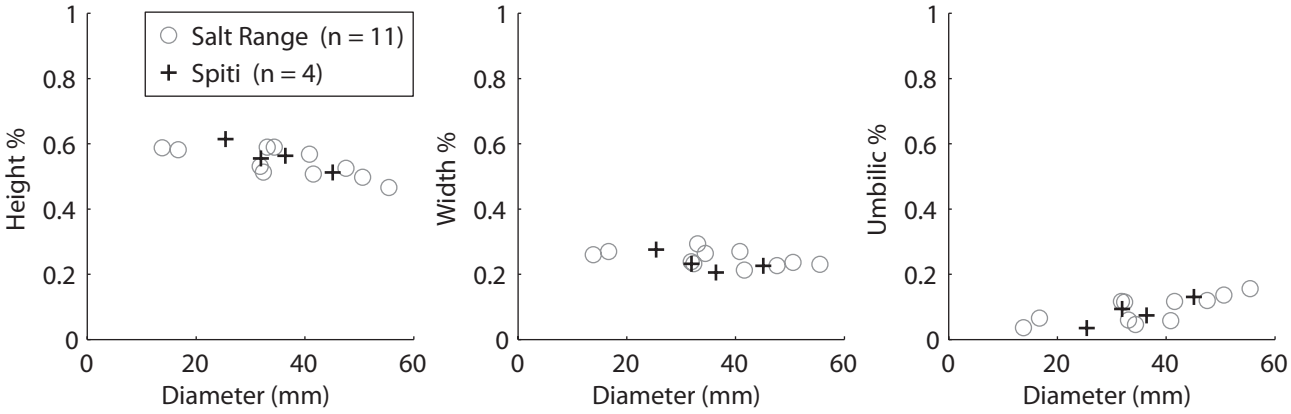

Fig. 17. Scatter diagrams of H/D, W/D, and U/D for *Ghazalaites roohii* Ware & Bucher (this volume).

Family Gyronitidae Waagen, 1895

Genus *Gyronites* Waagen, 1895

Type species. – *Gyronites frequens* Waagen, 1895.

Gyronites frequens Waagen, 1895

Pl. 1: 4-6; Fig. 18

1895 *Gyronites frequens* nov. gen. et sp. Waagen, p. 292-294, Pl. 38: 1, 2 (lectotype), 3, 4, Pl. 40: 4.
1895 *Gyronites nangaensis* nov. gen. et sp. Waagen, p. 297-298, Pl. 37: 5 (holotype).
1895 *Lecanites psilogyrus* nov. sp. Waagen, p. 280-281, Pl. 39: 5 (holotype).
1895 *Lecanites undatus* nov. sp. Waagen, p. 281-282, Pl. 38: 1 (lectotype), 2.
1895 *Prionolobus compressus* nov. gen. et sp. Waagen, p. 313-315, Pl. 35: 3 (holotype).
1895 *Prionolobus plicatus* nov. gen. et sp. Waagen, p. 315-316, Pl. 35: 2 (holotype).
1895 *Prionolobus plicatilis* nov. gen. et sp. Waagen, p. 318-319, Pl. 36: 1 (holotype).
? 1909 *Xenodiscus lilangensis* nov. sp. Krafft *in* Krafft & Diener, p. 97-99, Pl. 25: 6-10.
1909 Xenodiscus khoorensis nov. sp. Krafft *in* Krafft & Diener, p. 88.
1934 *Gyronites frequens* – Spath, p. 91-92, fig. 19 [cop. Waagen 1895].
? 1976 *Gyronites psilogyrus* – Wang & He, p. 274, fig. 7a, Pl. 1: 9-10.
? 1976 *Prionolobus plicatilis* – Wang & He, p. 275, fig. 8a, Pl. 3: 13-15.
v 1978 *Gyronites frequens* – Guex, Pl. 1: 3.
v 1978 *Gyronites undatus* – Guex, Pl. 8: 3.
? 1996 *Gyronites frequens* – Waterhouse, p. 33-34, Text-fig. 4A, Pl. 1: 1-4.
? 1996 *Gyronites planissimus* – Waterhouse, p. 34-35, Text-fig. 4A, Pl. 1: 5, 8
? 1996 *Gyronites spiralis* nov. sp. Waterhouse, p. 35-36, Text-fig. 4A, Pl. 1: 6, 7, 9, 10.
non v 2008 *Gyronites frequens* – Brühwiler *et al.*, p. 1168, Pl. 5: 7, 8.
v (this volume) *Gyronites frequens* – Ware *et al.*, p. xxx, Pl. 3: 1-3, Pl. 4: 1-6.

Occurrence. – Samples Mud52 from Mud Bottom Section, Gul24 from Guling River, Lal67.2 from Lalung Cliff, Lal1, Lal2, Lal3 and Lal4 from Lalung Ridge 1, Lal8 from Lalung Ridge 2. Poorly preserved specimens from samples Mud16 from Mud Top Section, Gul13 from Guling Village

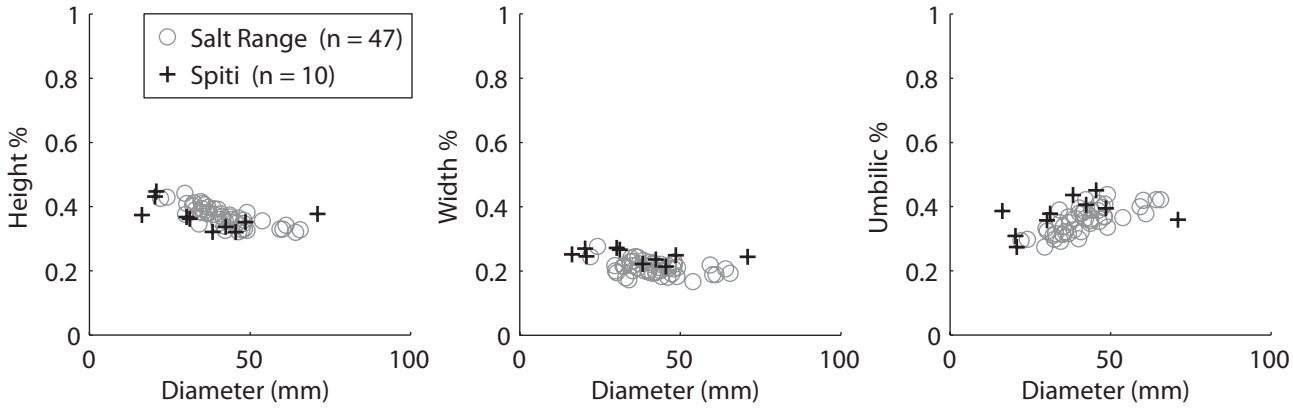

Fig. 18. Scatter diagrams of H/D, W/D, and U/D for *Gyronites frequens* Waagen, 1895.

and Lal9 from Lalung Ridge 2 are tentatively assigned to this species.
Measurements. – see Fig. 18.

***Gyronites dubius* (Krafft, 1909)**

Pl. 1: 7

? non 1897 *Meekoceras* sp. ind. ex. aff. *plicatile* – Diener, p. 137-138, Pl. 15: 6.
1909 *Meekoceras dubium* – Krafft *in* Krafft & Diener, p. 50-51, Pl. 24: 6-10, 11 (lectotype), 12-14.
v (this volume) *Gyronites dubius* – Ware *et al.*, p. xxx, Pl. 4: 7-12.

Occurrence. – Samples Mud13 from Mud Top Section, Mud25, and Mud54 from Mud Bottom Section, GU5/1 from Guling Village, and Lal6 from Lalung Ridge 1.
Measurements. – see Table 1.

***Gyronites plicosus* Waagen, 1895**

Pl. 2: 1-3

1895 *Gyronites plicosus* nov. gen. et sp. Waagen, p. 298-300, Pl. 38: 11 (holotype).
1895 *Prionolobus buchianus* nov. gen. Waagen, p. 320-322, Pl. 35: 5.
1897 *Danubites* sp. ind. ex. aff. *planidorsato* – Diener, p. 35-36, Pl. 15: 3, 7.
? 1905 *Celtites radiosus* – Noetling, Pl. 22: 1.
? 1905 *Celtites fortis* – Noetling, Pl. 22: 2.
1909 *Xenodiscus rotula* – Krafft & Diener, p. 93-97, Pl. 23: 4, 5, Pl. 25: 11, Pl. 27: 4, 5.
v 1978 *Hypophiceras plicosum* – Guex, Pl. 1: 1, 2, 5.
v? 1978 *Gyronites plicatilis* – Guex, Pl. 5: 9.
v (this volume) *Gyronites plicosus* – Ware *et al.*, p. xxx, Pl. 5: 2-10.

Occurrence. – Samples Mud2, Mud3, Mud4, Mud5, Mud14 and Mud15 from Mud Top Section, Mud26, and Mud51 from Mud Bottom Section, Gul22, Gul23 and Gul24 from Guling River, GU6 and Gul14 from Guling Village, Lal67.1 from Lalung Cliff, and Lal52 from Lalung Ridge2. Poorly preserved specimens from sample Mud53 from Mud Bottom Section, Gul21 from Guling River, Lal5 from Lalung Ridge 1 and Lal11 from Lalung Ridge 2 are tentatively assigned to this species.
Measurements. – see Table 1.

***Gyronites sitala* (Diener, 1897)**

Pl. 2: 4

1897 *Danubites sitala* nov. sp. Diener, p. 49-50, Pl. 15: 12 (lectotype), 13.
v (this volume) *Gyronites sitala* – Ware *et al.*, p. xxx, Pl. 5: 11-12.

Occurrence. – Samples Mud3 from Mud Top Section, Gul23 from Guling River. Poorly preserved specimens from sample Mud26 and Mud51 from Mud Bottom Section are tentatively assigned to this species.
Measurements. – No measurable specimen available.

***Gyronites levilatus* sp. nov.**

Pl. 2: 5-7

Derivation of name. – From the Latin *levis*, meaning smooth, and *latus*, meaning flanks.
Holotype. – Specimen PIMUZ30844 (Pl. 2: 7).
Type locality. – Mud Top Section, Himashal Pradesh, India.
Type horizon. – Sample Mud3, ca. 20 cm above base of the LLM, *Gyronites plicosus* beds.
Diagnosis. – Compressed *Gyronites* with very shallow umbilicus and smooth flanks.
Occurrence. – Samples Mud3, Mud4, Mud15 from Mud Top Section, Mud26 and Mud51 from Mud Bottom Section, Gul22 from Guling River, Lal52 from Lalung Ridge 2. Poorly preserved specimens from sample Mud5 of Mud Top Section are tentatively assigned to this species.
Description. – Moderately evolute (U/D ≈ 29 %) and compressed (W/D ≈ 22 %, W/H ≈ 51 %) platyconic shell with a broad tabulate venter. Flanks slightly convex, with maximum width at mid-flanks. The flanks bend suddenly just before the umbilical seam, joining the previous whorl with an obtuse angle, and without forming any differentiated umbilical wall. The flanks are perfectly smooth. Suture line typical of *Gyronites*, with a narrow ventral lobe, broad lateral lobes and saddles, the lobes having few small indentations at their base and a very short auxiliary series.
Measurements. – see Table 1.
Discussion. – This species is very similar to *Gy. frequens*, which was originally diagnosed as not ornamented. However, *Gy. frequens* has been documented by Ware *et al.* (this volume) to be ribbed, sometimes even rather strongly. The original material of *Gy. frequens* described by Waagen appears to be smooth because of strong weathering. *Gy. levilatus* is also more involute than *Gy. frequens*, and its indistinct umbilical wall is a unique trait among all representative of this genus. Some species of *Ambites* look superficially close to the species here described, but they differ clearly by their bottleneck shaped venter, the presence of ornamentation on the flanks, and their suture line which has a broader ventral lobe and a longer auxiliary series.

***Gyronites bullatus* sp. nov.**

Pl. 2: 8-9

Derivation of name. – Refers to the umbilical bullae on inner whorls.
Holotype. – Specimen PIMUZ30846 (Pl. 2: 8).
Type locality. – Mud Bottom Section (section M05 of Krystyn *et al.* 2007a), Himashal Pradesh, India.
Type horizon. – Sample Mud 52, top of the LLM, *Gyronites frequens* beds.
Diagnosis. – *Gyronites* with very evolute inner whorls bearing distant umbilical bullae which are replaced by weak sub-radial ribs on the more compressed adult body chamber.
Occurrence. – Sample Mud52 from Mud Bottom Section.
Description. – Evolute sub-platyconic shell characterised by a pronounced change of morphology at maturity. Inner whorls very evolute (U/D = 42 %) with a slightly compressed whorl section (W/H = 76 %). Flanks flat and slightly convergent towards the tabulate venter, imparting the whorl section a sub-trapezoidal shape. Umbilical wall rather high and vertical, grading into a narrowly rounded umbilical shoulder. Flanks with distant umbilical bullae. On the body chamber, the whorl section becomes slightly more compressed (W/H = 70 %) with slightly convex sub-parallel flanks and a slightly oblique umbilical wall. The umbilical bullae are replaced by more closely spaced, slightly sigmoid, weak, blunt ribs. Due to the incompleteness of the holotype, the transition between the juvenile and adult stage could not be observed. The suture line could only be observed on the juvenile part of the shell. It is typical of *Gyronites* with a second lateral saddle larger than the others, lobes with few small indentations at their base and no auxiliary series.
Measurements. – see Table 1.
Discussion. – This species is characterised by the presence of umbilical bullae in its inner whorls. The absence of auxiliary series is due to the small size at which the suture line could be observed. At larger size, it is probable that a short auxiliary series with a few small indentations should appear. The inner whorls resemble robust variants of *Gy. dubius*, but the latter differs by its more trapezoidal whorl section with a higher, better individualised umbilical wall. The body chamber resembles those of *Gy. frequens* and of smooth variants of *Gy. plicosus*, but the inner whorls clearly differ from those of these two species.

***Gyronites schwanderi* Ware & Bucher (this volume)**

Pl. 2: 10

v (this volume) *Gyronites schwanderi* nov. sp. Ware *et al.*, p. xxx, Pl. 5: 13-14.

Occurrence. – Sample Gul13 from Guling Village.
Measurements. – No measurable specimen available.

Genus *Ambites* Waagen, 1895

Type species. – *Ambites discus* Waagen, 1895.
Discussion. –This genus has been revised in detail in Ware *et al.* (this volume), but the very fine preservation of the shell on some specimens from Spiti allows to add the two following observations: 1) very thin sinuous lirae following the trajectory of the growth lines occur on the flanks; 2) the protruding ventro-lateral shoulders are underlined by a very fine strigation. Additionally, when some bivalves encrust the flanks of individuals belonging to this genus, they cast a fine strigation which is generally not preserved on the shell (for example, see Pl. 4: 2a and Pl. 6: 1b). This feature has not been observed in other genera, even when the specimens have encrusting bivalves on their flank.

***Ambites discus* Waagen, 1895**

Pl. 3: 1-3; Fig. 19

1895 *Ambites discus* nov. sp. Waagen, p. 152-154, Pl. 21: 4, 5 (lectotype).
1895 *Ambites magnumbilicatus* nov. sp. Waagen, p. 154-155, Pl. 21: 6 (holotype).
1895 *Koninckites impressus* nov. sp. Waagen, p. 263-265, Pl. 35: 6 (holotype).
1897 *Meekoceras hodgsoni* nov. sp. Diener, p. 133-135, Pl. 6: 1 (holotype).
? 1897 *Koninckites vidharba* nov. sp. Diener, p. 139-150, Pl. 7: 9 (holotype).
1905 *Ophiceras discus* – Noetling, Pl. 13: unnumbered text-fig. in footnote 2 (holotype).
non 1905 *Ophiceras discus* – Noetling, Pl. 13: 4.
p 1909 *Meekoceras lilangense* nov. sp. Krafft *in* Krafft & Diener, Pl. 14: 1, 2.
p 1909 *Meekoceras hodgsoni* – Krafft *in* Krafft & Diener, p. 26-28, Pl. 2: 9 (holotype).
p? 1909 *Meekoceras hodgsoni* – Krafft *in* Krafft & Diener, Pl. 3: 2.
non 1909 *Meekoceras hodgsoni* – Krafft *in* Krafft & Diener, Pl. 30: 1.
1909 *Meekoceras* cf. *discus* – Krafft *in* Krafft & Diener, p. 47-50, Pl. 6: 2.
1934 *Prionolobus impressus* – Spath, p. 100-101, fig. 22 [cop. Waagen 1895].
1934 *Ambites discus* – Spath, p. 102-103, fig. 23 [cop. Waagen 1895].
? 1976 *Prionolobus tulungensis* nov. sp. Wang & He, p. 277, fig. 8d, Pl. 2: 13-15 (holotype).
1985 *Prionolobus impressus* – Pakistani-Japanese Research group, Pl. 12: 1.
? 2007 *Prionolobus impressus* – Mu *et al.*, p. 869, figs.

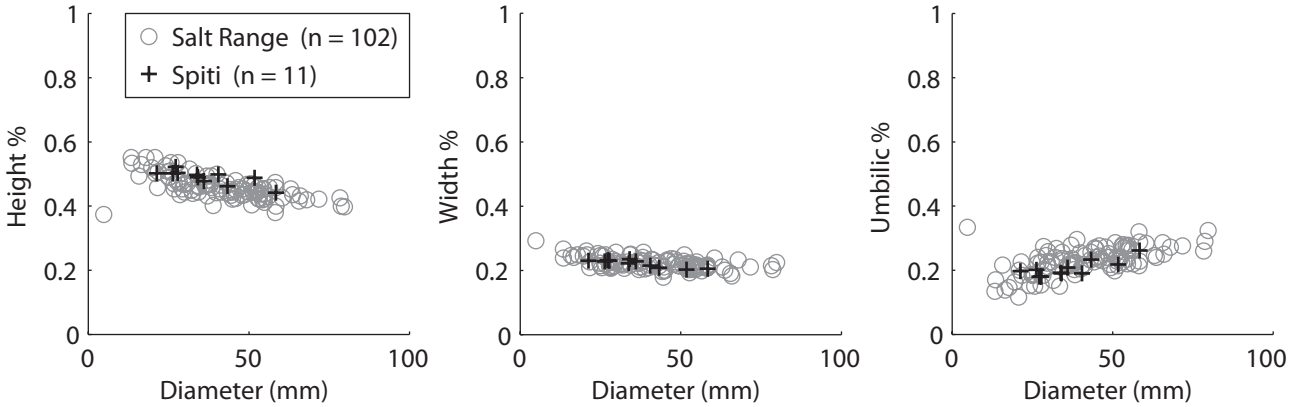

Fig. 19. Scatter diagrams of H/D, W/D, and U/D for *Ambites discus* Waagen, 1895.

12.4, 13.1-13.3
v (this volume) *Ambites discus* – Ware *et al.*, p. xxx, Pl. 6: 1-13, Pl. 7: 1-6.

Occurrence. – Samples Mud21 from Mud Top Section, Mud58b, Mud58.D1 and Mud58.D2 from Mud Bottom Section, Gul28 from Guling River and Lal55 from Lalung Cliff. Poorly preserved specimens from sample Gul16 from Guling Village and Lath6 from Lalung Cliff are tentatively assigned to this species.
Measurements. – see Fig. 19.

***Ambites atavus* (Waagen, 1895)**

Pl. 3: 4-6

1895 *Prionolobus atavus* nov. sp. Waagen, p. 309-310, Pl. 34: 4 (lectotype), Pl. 35: 4.
1895 *Gyronites evolvens* nov. sp. Waagen, p. 295-297, Pl. 35: 7 (holotype).
non 1905 *Prionolobus atavus* – Noetling, Pl. 22: 7.
1934 *Gyronites planissimus* nov. sp. Koken in Spath, p. 92-93, Pl. 8: 4 (holotype).
non 1976 *Gyronites evolvens* – Wang & He, p. 273-274, fig. 7b-c, Pl. 3: 6-12.
non 2010 *Mudiceras planissimus* nov. gen. Brühwiler *et al.*, p. 732, fig. 13.
non 2012a *Mudiceras planissimus* – Brühwiler *et al.*, p. 47-51, fig. 28Q-U.
v (this volume) *Ambites atavus* – Ware *et al.*, p. xxx, Pl. 8: 1-8, Pl. 9: 1.

Occurrence. – Samples Gul12 from Guling Village, Lal1 from Lalung Ridge 1 and Lal7 from Lalung Ridge2. Poorly preserved specimens from sample Lal53 and Lal54 from Lalung Cliff are tentatively assigned to this species.
Measurements. – No measurable specimen available.

***Ambites tenuis* Ware & Bucher, (this volume)**

Pl. 2: 11-12

v (this volume) *Ambites tenuis* nov. sp. Ware *et al.*, p. xxx, Pl. 9: 2-3.

Occurrence. – Samples Gul13 from Guling Village and Lal7 from Lalung Ridge2. Poorly preserved specimens from samples Lal53 from Lalung Cliff and Lal1 from Lalung Ridge 1 are tentatively assigned to this species.
Measurements. – No measurable specimen available.

***Ambites bojeseni* Ware & Bucher, (this volume)**

Pl. 3: 7; Pl. 4: 1-6; Pl. 5: 1; Fig. 20

v (this volume) *Ambites bojeseni* nov. sp. Ware *et al.*, p. xxx, Pl. 9: 11, Pl. 10: 1-3.

Occurrence. – Samples Mud6 from Mud Top Section, Mud27, Mud58a and Mud58.D3 from Mud Bottom Section, Til5 from Tilling, Gul27 from Guling River, Gul15 from Guling Village, and Lal13 from Lalung Ridge2.
Measurements. – see Fig. 20.
Discussion. – Compared to the Salt Range material, more abundant and better preserved specimens were found in Spiti, which allows the addition of the two following points to the description provided by Ware *et al.* (this volume). First, the slight allometry detected for the specimens from the Salt Range was in fact a sample bias. For specimens from Spiti, the relative umbilical size varies between 12 and 26 % for diameters above 25 mm (Fig. 20), without any clear trend toward greater evolution with size, except for large adult specimens with umbilical egression of the last half whorl. Second, at large size, the suture line tends to have more numerous indentations at the base of the lobes, and evolute variants have a suture line with considerably shallower lobes and shorter saddles.
This more abundant material also allows us to demonstrate that *Am. bojeseni* is generally more involute and compressed than *Am. lilangensis*. At a diameter of more than 25 mm, the means of the

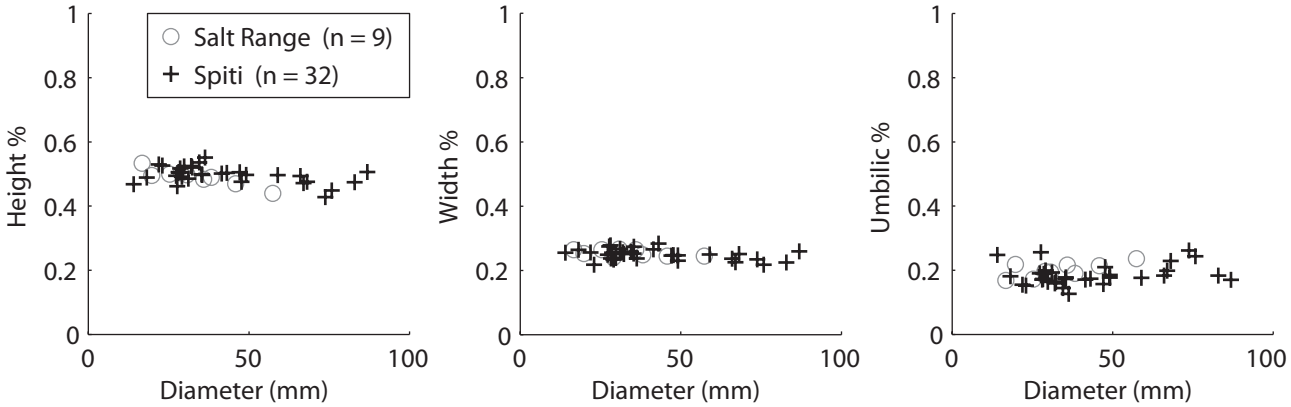

Fig. 20. Scatter diagrams of H/D, W/D, and U/D for *Ambites bojeseni* Ware & Bucher (this volume).

different parameters are as follow: for *Am. bojeseni*, x̄(U/D) = 18.6 %, x̄(W/D) = 24.9 %, and x̄(W/H) = 49.7 %, whereas for *Am. lilangensis*, x̄(U/D) = 20.1 %, x̄(W/D) = 26.2 %, and x̄(W/H) = 54.4 %.

***Ambites radiatus* (Brühwiler, Brayard, Bucher & Guodun, 2008)**

Pl. 5: 2-3

v 2008 *Pleurambites radiatus* nov. sp. Brühwiler *et al.*, p. 1168, Pl. 5: 1 (holotype), 2-3.
v (this volume) *Ambites radiatus* – Ware *et al.*, p. xxx, Pl. 9: 4-10.

Occurrence. – Sample Gul15 from Guling Village.
Measurements. – see Table 1.

Discussion. – This species is very rare in Spiti, only two incomplete small specimens were found in Guling.

***Ambites nyingmai* sp. nov.**

Pl. 5: 4-8; Fig. 21

Derivation of name. – Named after the Nyingma school of Buddhism, whose last few Buchen Lamas still live in the Pin Valley.
Holotype. – Specimen PIMUZ30867 (Pl. 5: 4).
Type locality. – Mud Bottom Section (section M05 of Krystyn *et al.* 2007), Himashal Pradesh, India.
Type horizon. – Sample Mud 58b, middle part of the shale interval at the base of the LSM, upper part of bed 8 of Krystyn *et al.* (2007a, b), *Ambites discus* beds.
Diagnosis. – Very evolute and compressed *Ambites* with

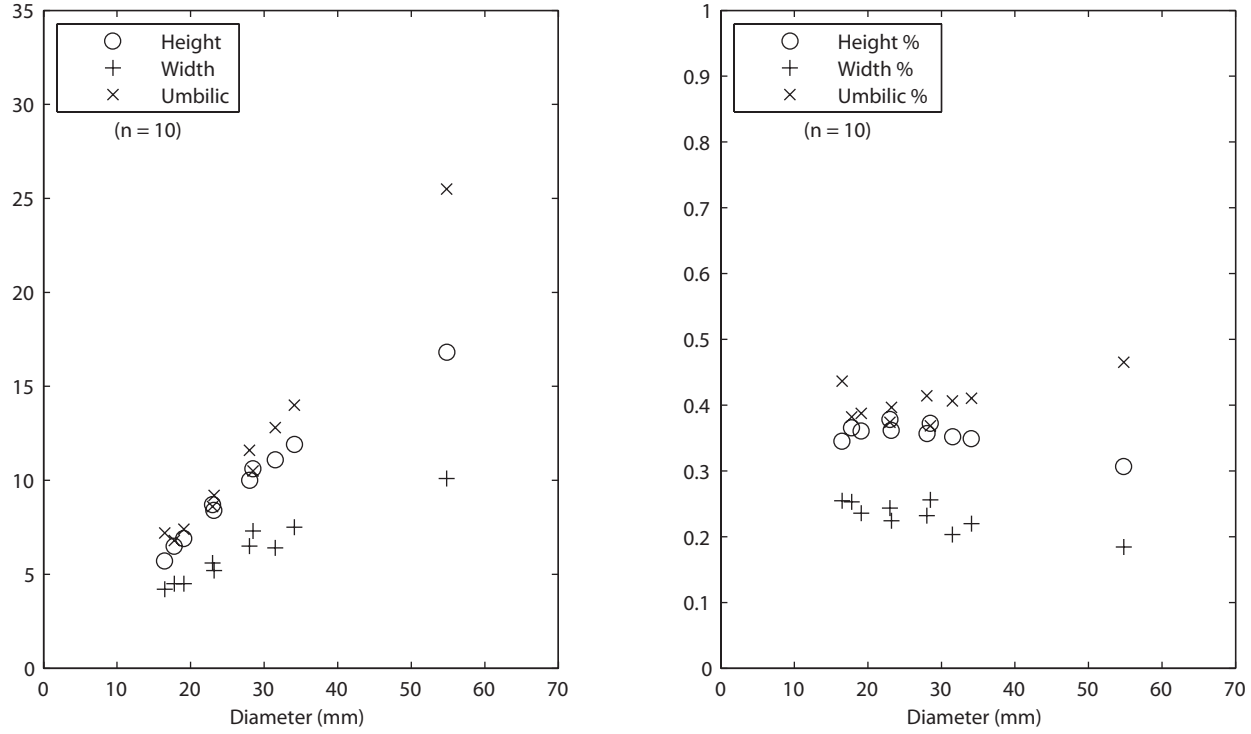

Fig. 21. Scatter diagram of H, W, and U, and of H/D, W/D, and U/D for *Ambites nyingmai* sp. nov.

either no or only faint ornamentation.
Occurrence. – Samples Mud58b and Mud58.D1 from Mud Bottom Section, Gul28 from Guling River, Gul16 from Guling Village, and Lal55, Lal56 and Lath6 from Lalung Cliff.
Description. – This species is characterised by its very evolute (for D > 25mm, U/D ≈ 42 %), compressed (for D > 25mm, W/D ≈ 22 % and W/H ≈ 63 %) and sub-platyconic shape, its flanks being slightly convex with maximal width at inner third. According to the graphs (fig. 21), the shell tends to become more evolute and compressed with growth, but more measurable specimens would be necessary to test this possible allometry. The bottleneck shaped venter is present but subdued, visible only on the outer shell of well-preserved specimens and absent on the internal mould. The umbilical wall is slightly oblique, poorly individualised and grading into a broadly rounded umbilical shoulder. Some specimens have low and broad radial folds on the flanks while others are nearly smooth, with weak folds parallel to growth lines. The suture line features very deep lobes and elongated saddles, the second lateral saddle being very broad whereas the third one is very small. The auxiliary series is very short with a few small indentations and no differentiated auxiliary lobe.
Measurements. – see fig. 21.
Discussion. – Adult specimens of this species closely resemble evolute variants of *Am. superior* (Waagen, 1895), from which they differ only by their much more evolute inner whorls. *Am. nyingmai* is otherwise very distinct from any other species of *Ambites*. It can also be mistaken with smooth evolute variants of *Gy. frequens*, but its bottleneck shaped venter, although poorly marked, and its more evolute inner whorls clearly differentiate it from this species. The Smithian flemingitid *Rohillites* Waterhouse, 1996 has a very close shell geometry but differs by its typically rursiradiate ribbing.

***Ambites subradiatus* Ware & Bucher, (this volume)**

Pl. 5: 11

v 2011 *Ambites* aff. *radiatus* – Ware *et al.*, p. 165-168, fig.7, 8b.
v (this volume) *Ambites subradiatus* nov. sp. Ware *et al.*, p. xxx, Pl. 10: 4-7.

Occurrence. – Samples Lal55, Lal56 and Lath6 from Lalung Cliff.
Measurements. – No measurable specimen available.

***Ambites* cf. *frechi* (Tozer, 1994)**

Pl. 5: 10

? 1994 *Pleurambites frechi* nov. gen. et sp. Tozer, p. 68, fig.14, Pl. 13: 1-3, 6.

Occurrence. – Samples Mud58b from Mud Bottom Section and Gul28 from Guling River.
Description. – The small complete phragmocone is a moderately evolute (U/D = 30.5 %), thick (W/D = 23.4 %, W/H = 55.6 %), and platyconic shell. Its flanks are very slightly convex with maximal width at inner third of the whorl section. The venter is tabulate with strongly prominent ventro-lateral shoulders. The umbilical wall is vertical and rather high, differentiated by a broadly rounded umbilical shoulder. It is characterised by strong, slightly convex blunt ribs, which fade towards the venter. The last preserved half whorl bears 11 ribs. The suture line has relatively deep lobes and elongated saddles, the second lateral saddle being the largest, slightly bent towards the umbilicus, whereas the third saddle is the smallest, with a rounded tip. The auxiliary series is rather short, with irregularly spaced denticules.
Measurements. – see Table 1.
Discussion. – Tozer (1994) created the genus *Pleurambites* for this ribbed species, but as already discussed in Ware *et al.* (this volume), the presence of ribs in a species is not sufficient to justify its separation from smooth forms by means of another genus. Therefore, *Pleurambites* is here synonymised with *Ambites*. Our specimens are slightly more involute and compressed than those of Tozer (1994). However, our description is here based on two small phragmocones only, one of them being strongly distorted and poorly preserved. We therefore cannot test whether this difference is due to the size difference and/or intraspecific variability, and thus leave them in open nomenclature.

***Ambites lilangensis* (Krafft, 1909)**

Pl. 5: 9; Pl. 6: 1-8; Figs. 22, 23.

1909 *Meekoceras lilangense* nov. sp. Krafft *in* Krafft & Diener, p. 23-25, Pl. 1: 1, 2 (lectotype), 3, 5-7.
non 1909 *Meekoceras lilangense* nov. sp. Krafft *in* Krafft & Diener, Pl.14: 1-2.
1909 *Meekoceras lingtiense* nov. sp. Krafft *in* Krafft & Diener, p. 25-26, Pl. 2: 1 (holotype).
1934 *Prionolobus lilangensis* – Spath, p. 101-102, Pl. 4: 4.
1967 Prionolobus sp. cf. *P. lilangense* – Tozer, p. 18, 73.
1970 *Prionolobus lilangense* – Tozer, Pl. 16: 6.
? 1976 *Prionolobus lilangensis* – Wang & He, p. 276, text-fig. 8b, Pl. 3: 4-5.
p? 1976 *Gyronites evolvens* – Wang & He, p. 273-274, text-fig. 7c, Pl. 3: 11-12.
p 1994 *Ambites fuliginatus* nov. sp. Tozer, p. 67, fig. 15a, Pl. 13: 5, 7, Pl. 14: 8 (holotype).
non p 1994 *Ambites fuliginatus* – Tozer, Pl. 13: 4.
1996 *Lilangia lilangensis* – Waterhouse, p. 36, 60-61,

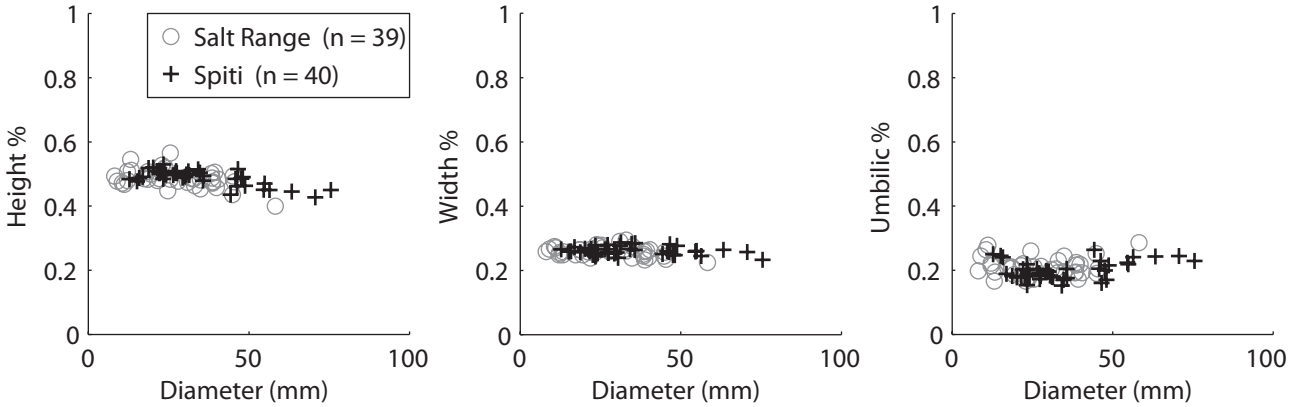

Fig. 22. Scatter diagrams of H/D, W/D, and U/D for *Ambites lilangensis* (Krafft, 1909).

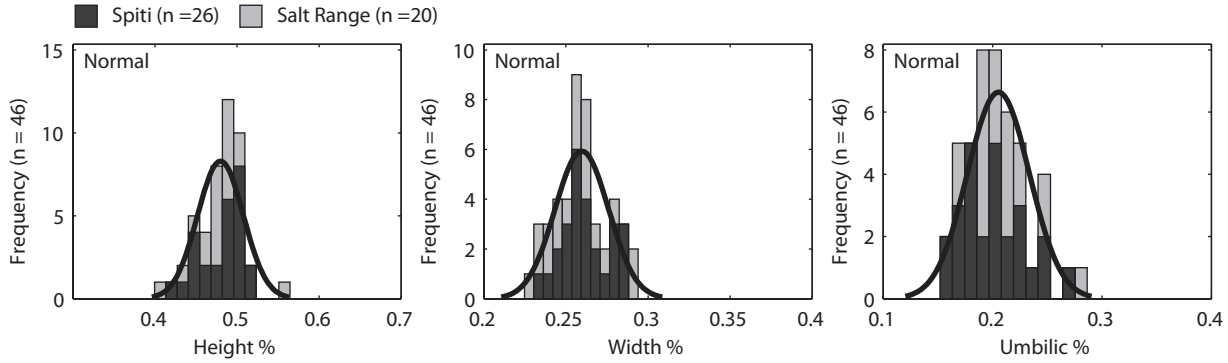

Fig. 23. Cumulative histograms of H/D, W/D, and U/D for *Ambites lilangensis* (Krafft, 1909). Because of growth allometries, specimens of less than 25 mm in diameters have been excluded from this analysis. The label "normal" on each histogram indicates that a Lilliefors test performed on the total population (Spiti plus Salt Range) does not allow rejecting the null hypothesis of normality at a confidence interval of 95 %.

text-fig. 7G, Pl. 5: 2-7,9-10, Pl. 6:1.
v 2011 *Ambites lilangensis* – Ware *et al.*, p. 164-165, figs. 4-5.
v (this volume) *Ambites lilangensis* – Ware *et al.*, p. xxx, Pl. 12: 2-5, Pl. 13: 1-2.

Emended diagnosis. – Rather involute (U/D ≈ 20 %) and thick (W/H ≈ 54 %, W/D ≈ 26 %) *Ambites* with a very slightly convex venter. Suture line with lobes generally having only a few deep indentations and a poorly differentiated auxiliary lobe.
Occurrence. – Samples Mud7, Mud17' and Mud20 from Mud Top Section, Mud28, Mud61, Mud203 and Mud205 from Mud Bottom Section, Til2 and Til6 from Tilling, Gul29 from Guling River, Gul17 from Guling Village and Lal57 from Lalung Cliff.
Description. – A rather complete description of this species has already been provided in Ware et al. (this volume) and is not repeated here. However, it was based only on incomplete specimens, and the better preserved specimens found in Spiti allow the addition of the following points. Its growth is only slightly allometric. Most sub-adult specimens (between 25 and 50 mm in diameter) have a relative umbilical diameter of less than 20 %, whereas all specimens of more than 50 mm in diameter have a relative umbilical diameter of more than 20 %, showing a slight umbilical egression on the adult body chamber. Instead of being perfectly flat like in other species of *Ambites*, the venter is often very slightly arched, some specimens having even a low blunt median ridge on the venter, imparting a very low roof shape. A few specimens do not have the bottlenecked venter typical of the genus. Most specimens have a more complex suture line than other *Ambites*, with less numerous but deeper indentations and a frequent auxiliary lobe. However, one specimen (Pl. 6: 7) has a simpler suture line, with more numerous and smaller indentations on the lobes, and a narrow ventral lobe with pointed branches. This illustrates the strong variability of the suture line.
Measurements. – see Figs. 22, 23.
Discussion. – Krafft (in Krafft & Diener, 1909) indicated that this species was present in five different layers within the "*Meekoceras* beds" of Lalung. However, as already discussed in Ware et al. (this volume), two of the specimens he illustrated were misidentified, and actually correspond to *Am. discus*, thus questioning the alleged long stratigraphic distribution of this species. Here, *Am. lilangensis* only occurs in one layer at each locality, inclusive of Lalung. As mentioned previously, *Am. lilangensis* and *Am. bojeseni* are very close to each other, but the former tends to be more evolute and depressed than the latter. This especially applies to complete adult specimens, the relative umbilical diameter of which is

always above 20 % for *Am. lilangensis*, whereas it is often (but not always) under 20 % for *Am. bojeseni*. Large and evolute variants of *Am. bojeseni* are very similar to adult specimens of *Am. lilangensis*, as the former differs only by its slightly thinner whorl section and venter. This underlines the importance of analysing large enough samples for a clear and consistent taxonomy for these smooth forms.

Family Paranoritidae Spath, 1930

Genus *Vavilovites* Tozer, 1971

Type species. – *Paranorites sverdrupi* Tozer, 1963.

***Vavilovites meridialis* sp. nov.**

Pl. 7: 1-7; Pl. 8: 1-2; Fig. 24

non 1897 *Meekoceras markhami* nov. sp. Diener, p. 75-77, Pl. 6: 4, 6.
1901 Meekoceras noetlingi nov. sp. Krafft *in* Griesbach, p. 30.
v *1901 Meekoceras noetlingi* – Noetling, p. 466.
v *1904 Meekoceras noetlingi* – Noetling, p. 546.
1909 *Meekoceras markhami* – Krafft & Diener, p.20-23, Pl. 11: 1-5, Pl. 12: 1-3, Pl. 13: 1-5, Pl. 15: 4-5.
v 2011 *Vavilovites* sp. indet. – Ware *et al.*, p. 176-177, fig. 19.
v 2012b *Paranorites* sp. indet. – Brühwiler *et al.*, p.137, 139, fig. 14AB-AE.
v (this volume) *Vavilovites* cf. *sverdrupi* – Ware *et al.*, p. xxx, Pl. 13: 10-13.

Derivation of name. – From the Latin "meridialis", from the South.
Holotype. – Specimen PIMUZ30883 (Pl. 7: 1).
Type locality. – Mud Bottom Section (section M05 of Krystyn *et al.* 2007a), Himashal Pradesh, India.
Type horizon. – Sample Mud 63, upper part of the shale interval at the base of the LSM, bed 9 of Krystyn *et al.* (2007a, b), *Vavilovites meridialis* beds.

Diagnosis. – *Vavilovites* with sharply tabulate venter on innermost whorls (at D < 3cm), becoming progressively arched to well rounded on outer whorls when reaching a diameter larger than ca. 70 mm.
Occurrence. – Samples Mud19' from Mud Top Section, Mud29, Mud60, Mud63 and Mud202 from Mud Bottom Section, Gul18 from Guling Village and Lal58 from Lalung Cliff.
Description. – Their large (mature specimens exceed 15 cm in diameter), moderately involute (adults with U/D ≈ 20%) discoidal shell shows a substantial change in whorl section during ontogeny. The inner whorls (up to a diameter of ca. 30 mm) are moderately involute (U/D ≈ 20%) and sub-platyconic, with a maximal width at inner third of the whorl section and a tabulate venter sometimes showing a slightly bottleneck shaped venter close to that of inner whorls of *Am. lilangensis*. The flanks carry some weak broad folds following the trajectory of growth lines. The next whorls (up to 10 cm) become more involute (U/D ≈ 14%). Their maximal width shifts progressively towards the umbilicus, giving the whorl section a more trapezoidal shape. The venter becomes broadly arched, and the ventral shoulders fade simultaneously. The ornamentation disappears completely. Adult specimens (D > 10 cm) become more evolute (U/D ≈ 20%) and their maximal width is at the inner fourth to inner fifth of the whorl height. Their flanks converge strongly towards the venter and sometimes show a slight concavity before reaching the perfectly rounded venter, giving the whorl section a sub-lanceolate shape. During the entire growth, the umbilical wall is vertical to slightly overhanging, with a gently rounded shoulder. The suture line is typical of Paranoritidae, with a vaguely differentiated auxiliary lobe and a broad flattened third lateral saddle.
Measurements. – see Fig. 24.
Discussion. – This species displays a large intraspecific variability, from thin involute variants to thick and more evolute variants, but this is difficult to evaluate because of ubiquitous *in vivo* encrusting bivalves. Every specimen of more than 2 cm in diameter has bivalves encrusting

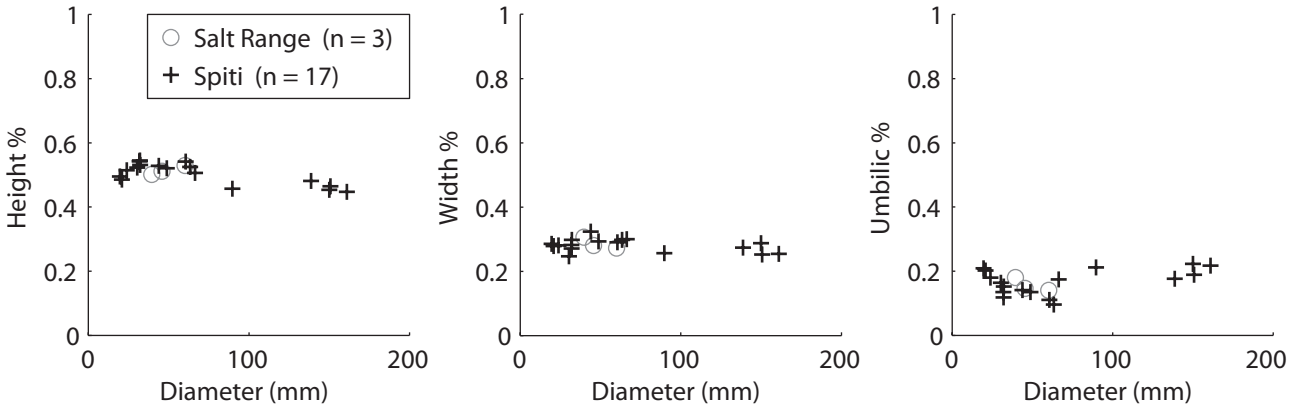

Fig. 24. Scatter diagram of H/D, W/D, and U/D for *Vavilovites meridialis* sp. nov.

both sides of the umbilicus, often inducing a deviation of the coiling and thus making measurements unsuitable for statistical analysis (on the graph, Fig. 24, only specimens without any obvious growth disturbance were included). The few large specimens (D > 10 cm) were all found to be crowded with hundreds of such epibionts on the whole surface of the shell, with exception of the last quarter of whorl of the body chamber.

This species clearly differs from *V. sverdrupi* by its more involute coiling and its rounded venter on adult whorls. It also resembles *V. subtriangularis* Vavilov (1976), which also has a rounded venter on the outer whorls, but has a thinner whorl section and less triangular whorl section with more convex flanks and a broader venter. The inner whorls of thin variants superficially resemble involute variants of *Kon. khoorensis* but clearly differ by their tabulate venter.

As explained by Diener in Krafft & Diener (1909), Krafft intended to create the species *Meekoceras noetlingi* for specimens belonging to the present species, and indeed used this denomination in several papers. He should have made the formal description in this monograph, but could not complete it. When Diener revised his notes, he considered it as identical to *Prop. Markhami*. Hence, the species *Me. noetlingi* was never formally described and remains a *nomen nudum*. The type specimens of *Prop. markhami* have a suture line typical of Proptychitidae with indentations on the sides of the lobes, whereas the specimens described in Krafft & Diener (1909) are strictly identical to ours. The specimens cited by Noetling (1901, 1904), curated at the University of Tübingen (Germany), are identical to the specimens described here. *Vavilovites* sp. indet., in Ware et al. (2011) corresponds to the inner whorls of thick variants. In Brühwiler et al. (2012), one specimen coming from a float block in Mud clearly corresponds to this species. It was then considered to be derived from the "*Parahedenstroemia* beds. It is also encrusted by numerous bivalves. Associated facies is also similar to that of our specimens from Mud, hence it must derive from the same bed as the specimens here under consideration. The few specimens from Pakistan described as *Vavilovites* cf. *sverdrupi* in Ware et al. (this volume) also correspond to inner whorls of the present species.

Genus *Koninckites* Waagen, 1895

Type species. – *Koninckites vetustus* Waagen, 1895.

***Koninckites vetustus* Waagen, 1895**

Pl.8: 3; Fig. 25

1895 *Koninckites vetustus* nov. gen. et sp. Waagen, p. 261-262, Pl. 27: 4 (lectotype), ?5.
1895 *Prionolobus rotundatus* nov. gen. et sp. Waagen, p. 310, Pl. 34: 1 (lectotype), 2, 3.
1905 *Prionolobus rotundatus* – Noetling, Pl. 23: 1.
1909 Meekoceras waageni nov. sp. Diener *in* Krafft & Diener , p. 16.
1909 *Meekoceras smithii* nov. sp. Krafft *in* Krafft & Diener, p. 39, Pl. 4: 1 (holotype).
1934 *Koninckites apertus* nov. sp. Koken *in* Spath, p. 154, Pl. 11: 1 (holotype).
? 1996 *Koninckites apertus* – Waterhouse, p. 46-48, Text-fig. 4H, Pl. 2: 9, 11, 13-15, Pl. 9: 7-12.
v 2010 *Prionolobus rotundatus* – Brühwiler *et al.*, p. 728, fig. 6,7.
v (this volume) *Koninckites vetustus* – Ware *et al.*, p. xxx, Pl. 14: 1-13; Pl. 15: 1-6; Pl. 16: 1-5; Pl. 17: 1.

Occurrence. – Samples Mud17 from Mud Top Section, Mud31 and Mud62 from Mud Bottom Section and Lal63 and Lath10 from Lalung Cliff.
Measurements. – see Fig. 25.

***Koninckites khoorensis* (Waagen, 1895)**

Pl. 8: 4-7; Pl. 9: 1-4; Fig. 26

1895 *Proptychites khoorensis* nov. gen. et sp. Waagen, p. 176-178, Pl. 20: 4 (holotype).

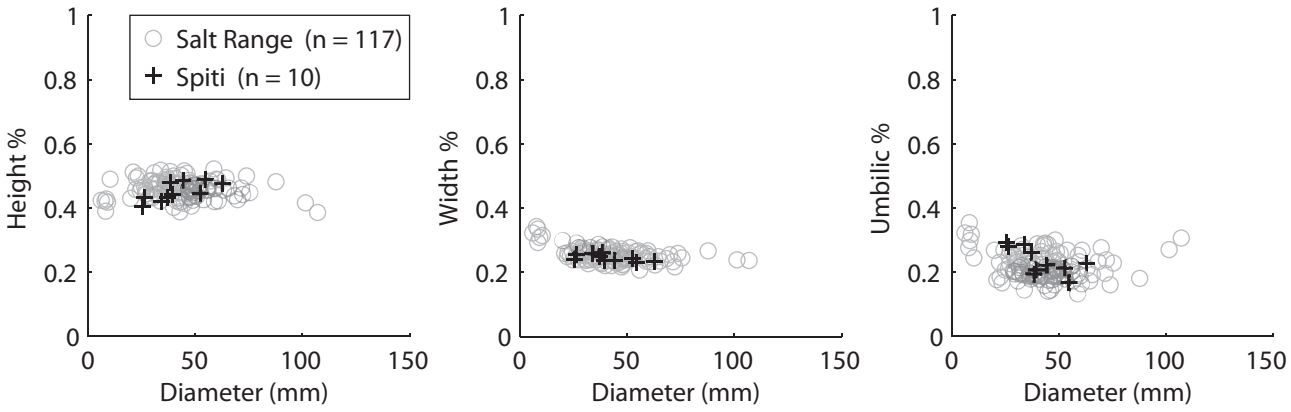

Fig. 25. Scatter diagram of H/D, W/D, and U/D for *Koninckites vetustus* Waagen, 1895.

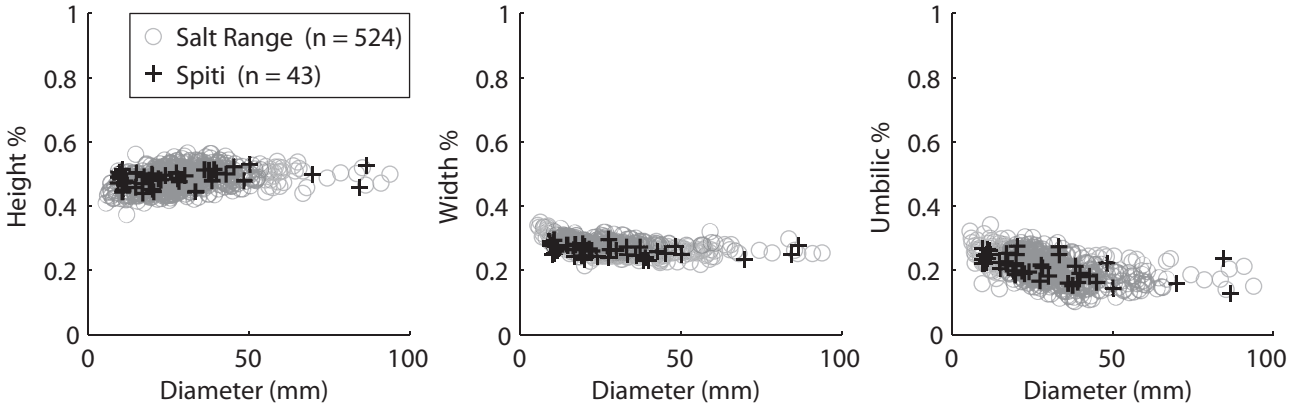

Fig. 26. Scatter diagram of H/D, W/D, and U/D for *Koninckites khoorensis* (Waagen, 1895).

1895 *Dinarites minutus* nov. sp. Waagen, p. 31-32, Pl. 7a: 1 (lectotype), 2.
1895 *Proptychites undatus* nov. gen. et sp. Waagen, p. 180-182, Pl. 24: 4 (holotype).
1895 *Meekoceras koninckianum* nov. gen. et sp. Waagen, p. 245-245, Pl. 26: 6 (holotype).
1895 *Koninckites ovalis* nov. gen. et sp. Waagen, p. 262-263, Pl. 28: 3 (lectotype), 4.
1905 *Aspidites declivis* – Noetling, Pl. 22: 8.
non 1905 *Prionolobus undatus* – Noetling, Pl. 25: 2.
1909 *Meekoceras tenuistriatum* nov. sp. Krafft *in* Krafft & Diener, p. 34, Pl. 4: 3 (holotype).
?p 1909 *Meekoceras varaha* – Diener *in* Krafft & Diener, p. 17, Pl. 2: 2.
v 1978 *Proptychites khoorensis* – Guex, Pl. 2: 3, 4, 6.
1996 *Prejuvenites angdawai* nov. gen. et sp. Waterhouse, p. 55-56, Text-fig. 7A, Pl. 3: 5-9, 10 (holotype), 11-13.
1996 *Proptychites chuluensis* nov. sp. Waterhouse, p. 68-70, Text-fig. 11E, Pl. 7: 7, 8 (holotype).
v 2008 *Proptychites* sp. indet. – Brühwiler *et al.*, p. 1164, Pl. 2: 3-5
v (this volume) *Koninckites khoorensis* – Ware *et al.*, p. xxx, Pl. 17: 2-13; Pl. 18: 1-18; Pl. 19: 1-5; Pl. 20: 1-5.

Occurrence. – Samples Mud8 and Mud19 from Mud Top Section, Mud30, Mud59 and Mud201 from Mud Bottom Section, Til1 from Tilling, Gul30 from Guling River, Gul19 from Guling Village and Lal59, Lal60, Lal61, Lal62, Lath8 and Lath9 from Lalung Cliff.
Measurements. – see Fig. 26.

Genus *Radioceras* Waterhouse, 1996

Type species. – *Meekoceras radiosum* Waagen, 1895.

***Radioceras truncatum* (Spath, 1934)**

Pl. 9: 5

1895 *Koninckites davidsonianus* nov. gen. Waagen, p. 272-273, Pl. 33: 4.
? 1897 *Meekoceras (Kingites) varaha* – Diener, p. 143-144, Pl. 6: 2, Pl. 7: 6.
1934 *Koninckites truncatus* nov. sp. Spath, p. 152-153, figs. 43c, 44 (holotype) [cop. *Koninckites davidsonianus* in Waagen 1895].
? 1996 *Radioceras truncatum* nov. gen. Waterhouse, p. 41, Text-fig. 4C, Pl. 2: 1, 2.
v 2010 *?Radioceras* cf. *kraffti* – Brühwiler *et al.*, p. 728-729, fig. 8-9.
v 2012a *Radioceras* cf. *kraffti* – Brühwiler *et al.*, p. 53, figs 31Q-T, 33A-U, 34A-Z.
v (this volume) *Radioceras truncatum* – Ware *et al.*, p. xxx, Pl. 21: 1-2.

Occurrence. – Samples Mud17 from Mud Top Section and Mud31 from Mud Bottom Section.
Measurements. – see figure 41 in Ware *et al.* (this volume).

Genus *Pashtunites* Ware & Bucher (this volume)

Type species. – *Koninckites kraffti* Spath, 1934.

***Pashtunites kraffti* (Spath, 1934)**

Pl. 9: 6

p 1909 *Meekoceras varaha* – Diener *in* Krafft & Diener, p. 17, Pl. 2: 4 (holotype of *Pa. kraffti* designated by Spath 1934).
non p 1909 *Meekoceras varaha* – Diener *in* Krafft & Diener, p. 17, Pl. 2: 2, 3, 5, 6.
1934 *Koninckites kraffti* nov. sp. Spath, p. 155-156, fig. 43c (holotype).
non v 2010 *?Radioceras* cf. *kraffti* – Brühwiler *et al.*, p. 728-729, fig. 8-9.
non v 2012a *Radioceras* cf. *kraffti* – Brühwiler *et al.*, p. 53, figs 31Q-T, 33A-U, 34A-Z.
v (this volume) *Pashtunites kraffti* nov. gen. Ware *et al.*, p. xxx, Pl. 21: 3-4.

Occurrence. – Sample Lal63 from Lalung Cliff.
Measurements. – No measurable specimen available.

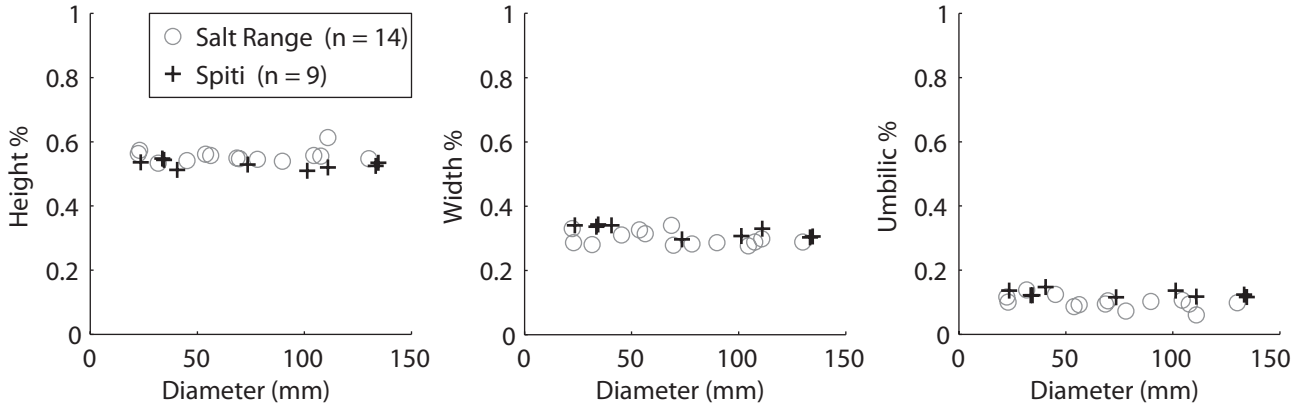

Fig. 27. Scatter diagram of H/D, W/D, and U/D for *Proptychites ammonoides* Waagen, 1895.

Family Proptychitidae Waagen, 1895

Genus *Proptychites* Waagen, 1895

Type species. – *Ceratites lawrencianus* de Koninck, 1863.

Proptychites lawrencianus (de Koninck, 1863) *sensu* Waagen, 1895

Pl. 10: 3

? 1863 *Ceratites lawrencianus* nov. sp. de Koninck, p. 14, Pl. 6: 3 (holotype).
1895 *Proptychites lawrencianus* nov. gen. Waagen, p. 168-170, Pl. 18: 1, Pl. 17: 2.
v 1978 *Proptychites ammonoides* – Guex, Pl. 8: 8.
v (this volume) *Proptychites lawrencianus* – Ware *et al.*, p. xxx, Pl. 22: 5, Pl. 23: 1-4.

Occurrence. – Sample Lal27, from a float block above Lalung Ridge 2.
Measurements. – No measurable specimen available.

Proptychites oldhamianus Waagen, 1895

Pl. 10: 1-2

1895 *Proptychites oldhamianus* nov. gen. et sp. Waagen, p. 166-167, Pl. 19: 3 (holotype).
1909 *Proptychites typicus* nov. sp. Krafft *in* Krafft & Diener, p. 77-79, Pl. 19: 4,5, Pl. 20: 6, Pl. 21: 2, 3 (lectotype), 4.
v (this volume) *Proptychites oldhamianus* – Ware *et al.*, p. xxx, Pl. 24: 2-4.

Occurrence. – Samples Mud51 and Mud52 from Mud Bottom Section, Gul23 from Guling River. Poorly preserved specimens from sample Mud16 from Mud Top Section, Gul24 from Guling River, Gul14 from Guling Village, Lal52 from Lalung Ridge2 and Lal2 from Lalung Ridge 1 are tentatively assigned to this species.
Measurements. – see Table 1.

Proptychites wargalensis Ware & Bucher (this volume)

Pl. 10: 4

v (this volume) *Proptychites wargalensis* nov. sp. Ware *et al.*, p. xxx, Pl. 24: 1.

Occurrence. – Samples Mud14 from Mud Top Section, Mud26 from Mud Bottom Section, GU6 from Guling Village. Poorly preserved specimens from sample Gul14 from Guling Village, Lal4 from Lalung Ridge 1 and Lal52 from Lalung Ridge 2 are tentatively assigned to this species.
Measurements. – No measurable specimen available.

Proptychites ammonoides Waagen, 1895

Pl. 10: 5-8; Pl. 11: 1; Fig. 27

1895 *Proptychites ammonoides* nov. gen. et sp. Waagen, p. 171-173, Pl. 17: 1 (lectotype), Pl. 19: 2.
1909 *Aspidites crassus* nov. sp. Krafft *in* Krafft & Diener, p. 58-59, Pl. 6: 4, Pl. 7: 1, Pl. 8: 1.
1909 *Koninckites haydeni* nov. sp. Krafft *in* Krafft & Diener, p. 68-70, Pl. 17: 1, 2, 3 (lectotype), 4- 6.
1909 *Koninckites alterammonoides* nov. sp. Krafft *in* Krafft & Diener, p. 70-72, Pl. 16: 1 (lectotype), 2.
? 1996 *Aspitella crassa* nov. gen. Waterhouse, p. 51, Text-fig. 41, Pl. 3: 2-4.
2009 *Proptychites alterammonoides* – Shigeta & Zakharov, p. 110-112, figs 98, 99.
v 2011 *Proptychites haydeni* – Ware *et al.*, p. 173-175, figs. 15-17.
v (this volume) *Proptychites lawrencianus* – Ware *et al.*, p. xxx, Pl. 24: 5; Pl. 25: 1-4, Pl. 26: 1.

Occurrence. – Samples Mud27, Mud58a, Mud58b and Mud58.D3 from Mud Bottom Section, Gul12, Gul15 and Gul16 from Guling Village, Lal54 and Lal55 from Lalung Cliff, Lal7 and Lal12 from Lalung Ridge2, and Lal1 from Lalung Ridge1. Poorly preserved specimens from sample Til3 from Tilling, Gul27 and Gul28 from Guling River,

Lal56 from Lalung Cliff and Lal13 from Lalung Ridge2 are tentatively assigned to this species.
Measurements. – see Fig. 27.

***Proptychites* cf. *pagei* Ware *et al.*, 2011**

Pl. 11: 2

v? 2011 *Proptychites pagei* nov. sp. Ware *et al.*, p. 175-176, fig. 18.
v (this volume) *Proptychites* cf. *pagei* – Ware *et al.*, p. xxx, Pl. 26: 2-3.

Occurrence. – Sample Til2 from Tilling and one poorly preserved specimen from sample Lal57 from Lalung Cliff tentatively assigned to this species.
Measurements. – No measurable specimen available.

Genus *Bukkenites* Tozer, 1994

Type species. – *Proptychites strigatus* Tozer, 1961.

***Bukkenites sakesarensis* Ware & Bucher (this volume)**

Pl. 11: 4-5

v (this volume) *Bukkenites sakesarensis* nov. sp. Ware *et al.*, p. xxx, Pl. 21: 12-13; Pl. 22: 1-4.

Occurrence. – Sample GU5/1 from Guling Village, and poorly preserved specimens from sample Lal6 from Lalung Ridge 1 tentatively assigned to this species.
Measurements. – No measurable specimen available.

Genus *Dunedinites* Tozer, 1963

Type species. – *Dunedinites pinguis* Tozer, 1963.

***Dunedinites* cf. *magnumbilicatus* (Kiparisova, 1961)**

Pl. 11: 3

? 1961 *Prosphingites magnumbilicatus* nov. sp. Kiparisova, p. 114, text-fig. 78, Pl. 25: 4.
? 2009 *Dunedinites magnumbilicatus* – Shigeta & Zakharov, p. 104, figs. 91, 92: 1-4.

Occurrence. – A single specimen from sample Mud52 from Mud, *Gyronites frequens* beds.
Description. – Cadiconic shell with a broadly rounded venter and a high vertical umbilical wall individualised by a narrowly rounded shoulder. No ornamentation visible. Suture line with deep and straight lobes and elongated saddles. Ventral lobe narrow. The three lateral saddles and two lateral lobes are nearly equally deep and narrow, the lobes bearing a few rather deep indentations at their base. Auxiliary series with one well individualised auxiliary lobe.
Measurements. – see Table 1.
Discussion. – This single specimen is too incomplete and poorly preserved for assignment at the species level. Its general shape is identical to the specimen of *Dunedinites magnumbilicatus* figured by Shigeta & Zakharov (2009), but it differs by its suture line with a clearly differentiated auxiliary lobe. It is also very close to the genus *Anotoceras* Hyatt, 1900, from which it differs by its broadly rounded venter and blunt umbilical shoulder. It should be noted here that the genus *Anotoceras* is of uncertain affinities. It has only been figured by Diener (1897), based only on a couple of specimens, the age of which is uncertain, as they come from the so-called "*Otoceras* beds" which in Diener's sense correspond both to the lower limestone member and the following Dienerian black shales. Its type species, *An. nala* (Diener, 1897), differs from our specimen only by its slightly tectiform venter and its sharp umbilical shoulder. These two features lead most previous authors to assign it to Otoceratidae in spite of its very simple suture line. Waterhouse (1994) created the family Anotoceratidae for this genus. These Griesbachian and Dienerian cadiconic ammonoids are very rare. Inclusive of our specimen, only 9 specimens are known and figured worldwide. Additional material with detailed stratigraphy would be necessary to decipher their affinity and establish any synonymy between *Anotoceras* and *Dunedinites*.

Family Mullericeratidae Ware, Jenks, Hautmann & Bucher, 2011

Genus *Mullericeras* Ware, Jenks, Hautmann & Bucher, 2011

Type species. – *Aspidites spitiensis* Krafft *in* Krafft & Diener, 1909.

***Mullericeras spitiense* (Krafft, 1909)**

Pl. 11: 6-8

1909 *Aspidites spitiensis* nov. sp. Krafft *in* Krafft & Diener, p. 54, Pl. 4: 4 (lectotype), 5, Pl. 16: 3- 8.
? 1996 *Clypeoceras spitiense* – Waterhouse, p. 50, text-fig. 4J, Pl. 2: 21-22.
non 2009 *Clypeoceras spitiense* – Shigeta & Zakharov, p. 125-126, fig. 113-114.
v 2010 *Mullericeras spitiense* gen. nov. Ware *et al.*, p. 171-172, figs. 11-12.
v (this volume) *Mullericeras spitiense* – Ware *et al.*, p. xxx, Pl. 27: 1-3.

Occurrence. – Samples Mud19' from Mud Top Section, Mud28, Mud29, Mud60, Mud63 and Mud202 from

Mud Bottom Section, Gul17 from Guling Village and one poorly preserved specimen from sample Lal57 from Lalung Cliff tentatively assigned to this species.
Measurements. – see Table 1.
Discussion. – A detailed, updated description of this species can be found in Ware *et al.* (2011).

***Mullericeras shigetai* Ware & Bucher, (this volume)**

Pl. 12: 1-2

?p 1994 *Ambites fuliginatus* – Tozer, Pl. 13: 4.
?p 1994 *Ambites ferruginus* – Tozer, Pl. 14: 1, 2, 5, 6.
? 2009 *Ambitoides fuliginatus* – Shigeta & Zakharov, p. 77-79, figs 63-64.
?v 2011 *Ussuridiscus* sp. indet. – Ware *et al.*, p. 169, fig. 8a.
v (this volume) *Mullericeras shigetai* nov. sp. Ware *et al.*, p. xxx, Pl. 27: 4-9.

Occurrence. – Samples Mud58b from Mud Bottom Section, Lal7 from Lalung Ridge2. Poorly preserved specimens from sample Gul16 from Guling Village are tentatively assigned to this species.
Measurements. – see Table 1.

***Mullericeras niazii* Ware & Bucher, (this volume)**

Pl. 12: 3-4; Fig. 28

v (this volume) *Mullericeras niazii* nov. sp. Ware *et al.*, p. xxx, Pl. 28: 5-7.

Occurrence. – Samples Mud28, Mud61 and Mud203 from Mud Bottom Section, Gul29 from Guling River, Gul17 from Guling Village. One poorly preserved specimen from sample Lal58 from Lalung Cliff is tentatively assigned to this species.
Measurements. – see Fig. 28.
Discussion. –The description provided in Ware *et al.* (this volume) was based on incomplete, rather small specimens (i.e. without adult body chamber). Here, some larger complete specimens were found, revealing that the maximal whorl width, which was already observed to shift from the inner third of the flanks in the juveniles to the middle of the flanks in sub-adults, shifts further on the external third of the flanks in large adult specimens. Our material otherwise agrees perfectly with the original description of this species.

Genus *Ussuridiscus* Shigeta & Zakharov, 2009

Type species. – *Meekoceras (Kingites) varaha* Diener, 1895.

***Ussuridiscus varaha* (Diener, 1895)**

Pl. 12: 5

1895 *Meekoceras (Kingites) varaha* nov. sp. Diener, p. 52, Pl. 1: 2 (lectotype).
non 1897 *Kingites varaha* – Diener, p. 143-144, Pl. 6: 2, Pl. 7: 6.
1905 *Meekoceras (Kingites) varaha* Noetling, Pl. 32: 5 [cop. Diener 1895].
non 1909 *Meekoceras varaha* – Krafft *in* Krafft & Diener, p. 17-20, Pl. 2: 2-6, Pl. 14: 7-8.
1968 *Koninckites varaha* – Zakharov, p. 91, text-fig. 20b, Pl. 17: 4-5.
2007 *Hubeitoceras* (?) *wangi* – Zakharov & Mu in Mu *et al.*, p. 871, figs 13.17-13.19, 15.2-15.5.
vp 2008 *"Koninckites"* cf. *timorense* – Brühwiler *et al.*, p. 1165-1166, Pl. 3. 1-4, Pl. 4: 1.
non vp 2008 *"Koninckites"* cf. *timorense* – Brühwiler *et al.*, Pl. 4: 2.
2009 *Ussuridiscus varaha* – Shigeta & Zakharov, p. 69-73, figs 50: 5-6, 55-57.
v (this volume) *Ussuridiscus varaha* – Ware *et al.*, p. xxx, Pl. 28: 8-11.

Occurrence. – Samples GU5/1 from Guling Village and one poorly preserved specimens from sample Mud25

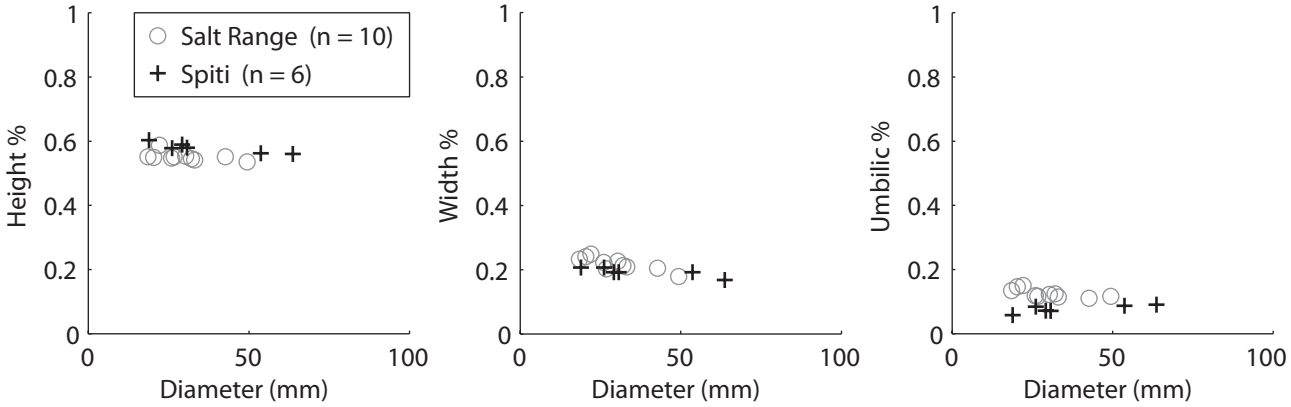

Fig. 28. Scatter diagram of H/D, W/D, and U/D for *Mullericeras niazii* Ware & Bucher (this volume).

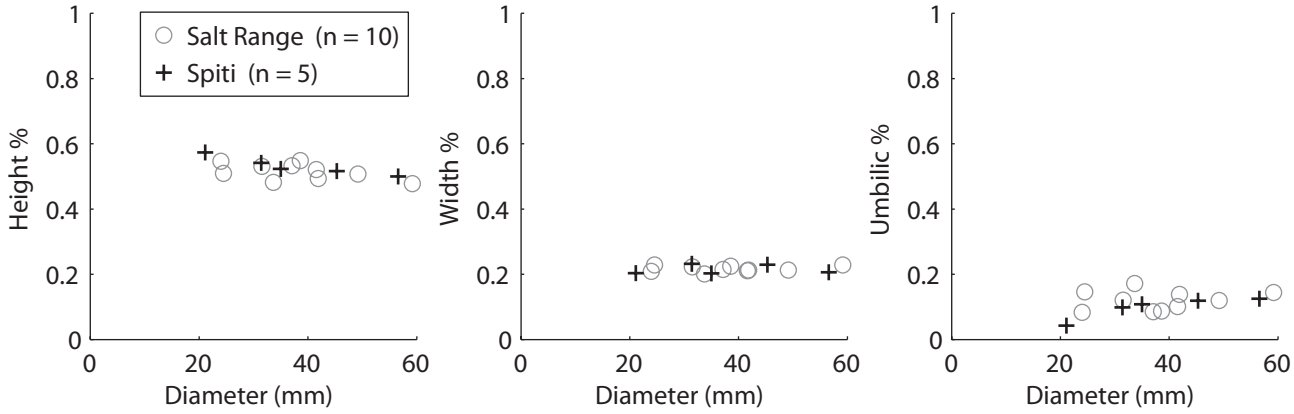

Fig. 29. Scatter diagram of H/D, W/D, and U/D for *Ussuridiscus ensanus* (Krafft, 1909).

from Mud Bottom Section tentatively assigned to this species.
Measurements. – No measurable specimen available.

***Ussuridiscus ensanus* (Krafft, 1909)**

Pl. 12: 6-8; Fig. 29

1909 *Aspidites ensanus* nov. sp. Krafft *in* Krafft & Diener, p. 56-57, Pl. 5: 3-4, 5(lectotype), 6-7, Pl. 6: 1, Pl. 14: 6.
p? 1909 *Meekoceras varaha* – Diener *in* Krafft & Diener, p. 17, Pl. 2: 3.
p? 1909 *Meekoceras hodgsoni* – Krafft *in* Krafft & Diener, p. 26-28, Pl. 30: 1.
1934 *Clypeoceras ensanum* – Spath, p. 160-161, Pl. 12: 3 [cop. Krafft 1909].
? 1996 *Clypeoceras ensanum* – Waterhouse, p. 49-50, Pl. 2: 16-20, Pl. 3:1.
v (this volume) *Ussuridiscus ensanus* – Ware *et al.*, p. xxx, Pl. 3: 1; Pl. 28: 12-14; Pl. 29: 1-5.

Occurrence. – Samples Mud4 and Mud5 from Mud Top Section, Mud26, Mud51 and Mud52 from Mud Bottom Section, Gul23 from Guling River, Gul13 from Guling Village, Lal67.1 and Lal67.2 from Lalung Cliff, Lal8 from Lalung Ridge 2, Lal2, Lal3 and Lal4 from Lalung Ridge 1. Poorly preserved specimens from sample Gul22 from Guling River, Gul14 from Guling Village, Lal10 from Lalung Ridge 2 and Lal5 from Lalung Ridge 1 are tentatively assigned to this species.
Measurements. – see Figs. 29.

***Ussuridiscus ornatus* Ware & Bucher (this volume)**

Pl. 12: 10

p 1897 *Koninckites vidharba* nov. sp. Diener, p. 139-141, Pl. 7: 8.
non 1897 *Koninckites vidharba* nov. sp. Diener, p. 139-141, Pl. 7: 9 (holotype).
1909 *Aspidites vidharba* – Krafft *in* Krafft & Diener, p. 63-64, Pl. 5: 1-2, Pl. 14: 14.
v (this volume) *Ussuridiscus ornatus* nov. sp. Ware *et al.*, p. xxx, Pl. 29: 6-7.

Occurrence. – Samples Mud14 from Mud Top Section and Gul24 from Guling River.
Measurements. – No measurable specimen available.

***Ussuridiscus ventriosus* Ware & Bucher, (this volume)**

Pl. 12: 9

v (this volume) *Ussuridiscus ventriosus* nov. sp. Ware *et al.*, p. xxx, fig. 49, Pl. 29: 10.

Occurrence. – Samples Mud53 from Mud Bottom Section. Poorly preserved specimens from sample Gul24 from Guling River are tentatively assigned to this species.
Measurements. – No measurable specimen available.

Family *incertae sedis*

Genus *Kingites* Waagen, 1895

Type species. – *Kingites lens* Waagen, 1895.

***Kingites davidsonianus* (de Koninck, 1863)**

Pl. 13: 1-3; Fig. 30

1863 *Ceratites davidsonianus* nov. sp. de Koninck, p. 13, Pl. 6: 2 (holotype).
1895 *Kingites lens* nov. gen. et sp. Waagen, p. 232-233, Pl. 26: 4 (holotype).
1895 *Kingites declivis* nov. gen. et sp. Waagen, p. 233-235, Pl. 26: 2 (holotype).
1934 *Koninckites davidsonianus* – Spath, p. 151-152, text-fig. 43a, Pl. 5: 2 (holotype).
1934 *Koninckites occlusus* nov. sp. Spath, p. 154-155, Pl. 5: 1 (holotype).
1934 *Kingites lens* – Spath, p. 157-158, fig. 45 [cop.

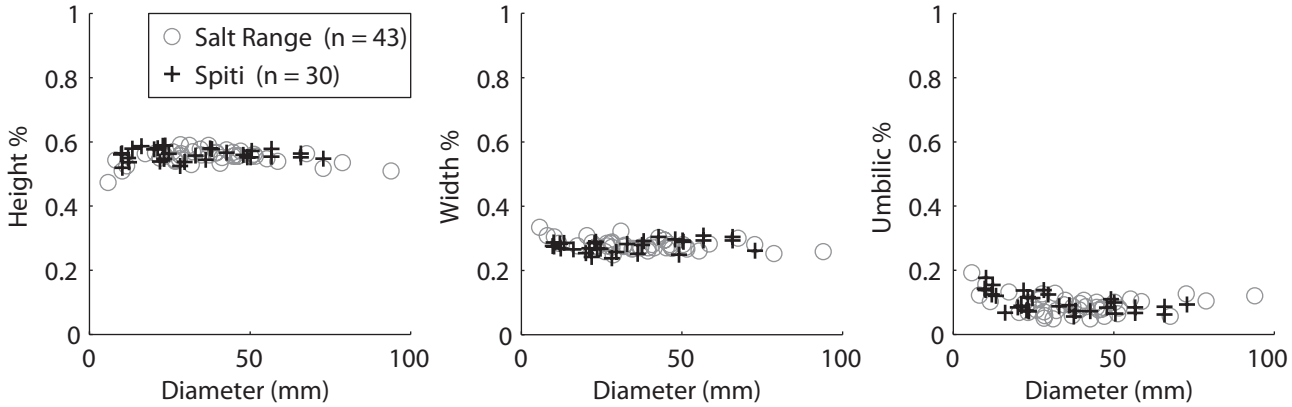

Fig. 30. Scatter diagram of H/D, W/D, and U/D for *Kingites davidsonianus* (de Koninck, 1863).

Waagen 1895].
? 1996 *Kingites lens* – Waterhouse, p. 43, text-fig. 4E, Pl. 2: 3.
1996 *Ceratites davidsonianus* – Waterhouse, p. 46, text-fig. 5 (holotype).
? 1996 *Aspitella crassa* – Waterhouse, p. 51, text-fig. 4I, Pl. 3: 2-4.
1996 *Kingites elegans* nov. sp. Waterhouse, p. 73-74, text-fig. 10D, Pl. 8: 4, 5, 9 (holotype), 6, 8, 10, 11.
v (this volume) *Kingites davidsonianus* – Ware *et al.*, p. xxx, Pl. 30: 1-7; Pl. 31: 1-2.

Occurrence. – Samples Mud19 from Mud Top Section, Mud30, Mud59 and Mud201 from Mud Bottom Section, Til1 from Tilling, Gul30 from Guling River and Lath9 from Lalung Cliff.
Measurements. – see Fig. 30.

***Kingites korni* Brühwiler, Ware, Bucher, Krystyn & Goudemand, 2010**

Pl. 13: 4

v 2010 *Kingites korni* nov. sp. Brühwiler *et al.*, p. 734, fig. 15 (holotype).
v 2010 *Kingites parkashi* nov. sp. Brühwiler *et al.*, p. 734, fig. 16 (holotype).
v 2012a ?*Kingites parkashi* – Brühwiler *et al.*, p. 53, fig. 36E-I.
v (this volume) *Kingites korni* – Ware *et al.*, p. xxx, Pl. 31: 3.

Occurrence. – Samples Mud31 from Mud Bottom Section and Lal63 from Lalung Cliff.
Measurements. – see Table 1.

Superfamily Sageceratacеae Hyatt, 1884
Family Hedenstroemiidae Hyatt, 1884
Genus *Pseudosageceras* Diener, 1895

Type species. – *Pseudosageceras* sp. indet. Diener, 1895.

***Pseudosageceras simplelobatum* Ware & Bucher (this volume)**

Pl. 13: 5; Fig. 31

1909 *Hedenstroemia lilangense* nov. sp. Krafft *in* Krafft & Diener, p. 151-152, Pl. 9: 1.
? 1985 *Pseudosageceras mulilobatum* – Pakistani-Japanese Research Group, Pl. 12: 5-7, Pl. 14: 3, 6.
? 1994 *Tellerites* sp. indet. – Tozer, p. 84, Pl. 20: 10.
1996 *Lilastroemia lilangensis* gen. et sp. nov. Waterhouse, p. 76-77.

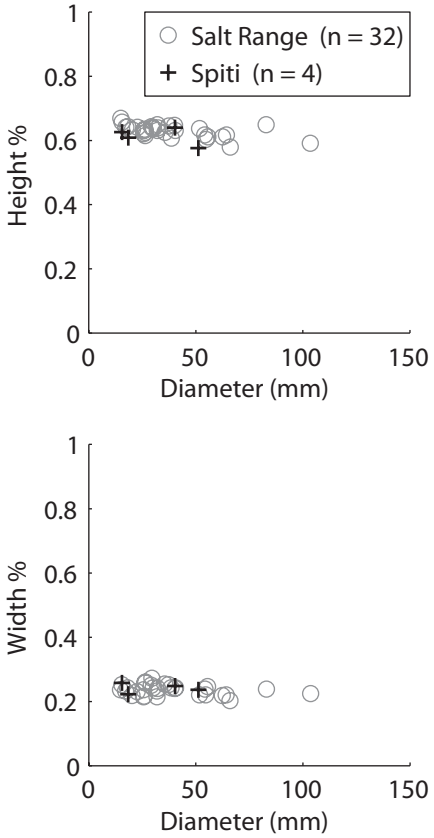

Fig. 31. Scatter diagram of H/D and W/D for *Pseudosageceras simplelobatum* Ware & Bucher (this volume).

non 1996 *Lilastroemia lilangensis* gen. nov. Waterhouse, Text-fig. 10E, Pl. 9: 13, 16, 17.
2010 *Clypites typicus* – Brühwiler *et al.*, p. 736-737, fig. 18.
v (this volume) *Pseudosageceras simplelobatum* nov. sp. Ware *et al.*, p. xxx, Pl. 32: 3-6; Pl. 33: 1-4.

Occurrence. – Samples Mud17 and Mud19 from Mud Top Section, Mud59 and Mud201 from Mud Bottom Section, Gul30 from Guling River and Lal61 from Lalung Cliff.
Measurements. – see Fig. 31.

Acknowledgements

O.N. Bhargava (Haryana, India) and T. Galfetti (Zürich) are acknowledged for their help in the field. James M. Neenan (Zürich) improved the English text. Claude Monnet (Lille) is thanked for providing his statistical analyses software. Nicolas Goudemand and Séverine Urdy (Zürich) are thanked for their help with Matlab. Mike Orchard from the Geological Survey of Canada (Vancouver) is thanked for providing access to the collections and archives of E.T. Tozer. Technical support for preparation and photography was provided by Markus Hebeisen and Rosemarie Roth (Zürich). Last but not least, Beli Parkash (Manali, India) is thanked for his assistance in the field. This work is a contribution to the Swiss National Science Foundation project 200020-135446 to HB. Additional field work was funded by the Swiss National Science Foundation project 200020-135075 to Winand Brinkmann. The publication costs were covered by the Swiss National Science Foundation. Earlier field work of L.K. was sponsored by the Austrian Academy of Sciences, National Committee for IGCP, within project 467 (Triassic Time).

References

Agassiz, L. 1847: Lettres sur quelques points d'organisation des animaux rayonnés. *Comptes Rendus de l'Académie des Sciences*, *25*, 677-682.

Arthaber, G.V. 1911: Die Trias von Albanien. *Beiträge zur Paläontologie und Geologie Österreich-Ungarns und des Orients 24*, 169-276.

Bengtson, P. 1988: Open nomenclature. *Palaeontology 31*, 223-227.

Bhargava, O. N., Krystyn, L., Balini, M., Lein, R. & Nicora, A. 2004: Revised Litho- and Sequence Stratigraphy of the Spiti Triassic. *Albertiana 30*, 21-39.

Brayard, A., Bucher, H., Escarguel, G., Fluteau, F., Bourquin, S. & Galfetti, T. 2006: The Early Triassic ammonoid recovery: Paleoclimatic significance of diversity gradients. *Palaeogeography, Palaeoclimatology, Palaeoecology 239*, 374-395.

Brühwiler, T., Brayard, A., Bucher, H. & Guodun, K. 2008: Griesbachian and Dienerian (Early Triassic) Ammonoid Faunas from Northwestern Guangxi and Southern Guizhou (South China). *Palaeontology 51*, 1151-1180.

Brühwiler, T., Ware, D., Bucher, H., Krystyn, L. & Goudemand, N. 2010: New Early Triassic ammonoid faunas from the Dienerian/Smithian boundary beds at the Induan/Olenekian GSSP candidate at Mud (Spiti, Northern India). *Journal of Asian Earth Sciences 39*, 724-739.

Brühwiler, T., Bucher, H., Ware, D., Schneebeli-Hermann, E., Hochuli, P.A., Roohi, G., Rehman, K. & Yaseen, A. 2012a: Smithian (Early Triassic) ammonoids from the Salt Range, Pakistan. *Special Papers in Palaeontology 88*, 1-114.

Brühwiler, T., Bucher, H. & Krystyn, L. 2012b: Middle and late Smithian (Early Triassic) ammonoids from Spiti, India. *Special Papers in Palaeontology 88*, 115-174.

Cuvier, G.L.C.F.D. An 6 [1797]: Tableau élémentaire de l'histoire naturelle des animaux, *14*, 710 pp. Baudouin, Paris.

Dagys, A. S. & Ermakova, S. 1996: Induan (Triassic) ammonoids from North-Eastern Asia. *Revue de Paléobiologie 15*, 401-447.

Diener, C. 1895: Triadische Cephalopodenfaunen der Ostsibirischen Küstenprovinz. *Mémoires du Comité Géologique St. Pétersbourg 14*, 1-59.

Diener, C. 1897: Part I: The Cephalopoda of the Lower Trias. *Palaeontologia Indica, Series 15*. *Himalayan fossils 2*, 1-181.

Griesbach, C.L. 1901: *General report on the work carried on by the Geological Survey of India for the period from the 1st April 1900 to the 31st March 1901*. Office of the Superintendent, Government Printing, Calcutta, India.

Guex, J. 1978: Le Trias inférieur des Salt Ranges (Pakistan): problèmes biochronologiques. *Eclogae Geologia Helvetica 71*, 105-141.

Guex, J. 1991: *Biochronological Correlations*. Springer, Berlin, 252 pp.

Hyatt, A. 1884: Genera of fossil cephalopods. *Proceedings of the Boston Society of Natural History 22*, 253-338.

Hyatt, A. 1900: Cephalopoda. *In* Zittel, K.A. (ed.): *Textbook of Palaeontology*, 502–592. Eastman, C. R., London.

Kiparisova, L.D. 1961: Paleontological fundamentals for the stratigraphy of Triassic deposits of Primorye region. 1. Cephalopod Mollusca. *Trudy Vsyesoyuzhogo Nauchno-isslyedovatyel'skogo Geologichyeskogo Instityta (VSEGEI). Novaya seriya 48*, 1-278 [In Russian].

de Koninck, L.G. 1863: Description of some fossils from India, discovered by Dr. A. Fleming, of Edinbourg. *The Quaterly Journal of the Geological Society of London 19*, 1-19.

Krafft, A.V. & Diener, C. 1909: Lower Triassic cephalopoda from Spiti, Malla Johar, and Byans. *Palaeontologia Indica 6*, 1-186.

Krystyn, L. & Orchard, M.J. 1996: Lowermost Triassic ammonoid and conodont biostratigraphy of Spiti, India. *Albertiana 17*, 10-21.

Krystyn, L., Balini, M. & Nicora, A. 2004: Lower and Middle Triassic stage and substage boundaries in Spiti. *Albertiana 30*, 40-53.

Krystyn, L., Bhargava, O.N. & Richoz, S. 2007a: A candidate GSSP for the base of the Olenekian Stage: Mud at Pin Valley; district Lahul & Spiti, Himachal Pradesh (Western Himalaya), India. *Albertiana 35*, 5-29.

Krystyn, L., Richoz, S. & Bhargava, O.N. 2007b: The Induan-Olenekian Boundary (IOB) in Mud – an update of the candidate GSSP section M04. *Albertiana 36*, 33-45.

Matthews, S.C. 1973: Notes on open nomenclature and synonymy lists. *Palaeontology 16*, 713-719.

Mu, L., Zakharov, Y.D., Li, W.-Z. & Shen, S.-Z. 2007: Early Induan (Early Triassic) cephalopods from the Daye Formation at Guiding, Guizhou Province, South China. *Journal of Paleontology 81*, 858-872.

Noetling, F. 1901: Beiträge zur Geologie der Salt Range, insbesondere der permischen und Triassischen Ablagerungen. *Neues Jahrbuch für Mineralogie, Geologie und Paläontologie, Beilage-band 14*, 369-471.

Noetling, F. 1904: Ueber das Alter der Otoceras-Schichten von Rimkin Paiar (Painkhanda) im Himalaya. *Neues Jahrbuch für Mineralogie, Geologie und Paläontologie, Beilage-band 18*, 528-555.

Noetling, F. 1905: Die asiatische Trias. *In* Frech, F. (ed): *Lethaea Geognostica, Das Mesozoicum*, 107-221. verlag der E. Schweizerbart'schen Verlagsbuchhandlung (E. Nägele), Stuttgart, Germany.

Pakistani-Japanese Research Group 1985: Permian and Triassic Systems in the Salt Range and Surghar Range, Pakistan. *In* Nakazawa, K. & Dickins, J.M. (eds): *The Tethys, her paleogeography and paleobiogeography from Paleozoic to Mesozoic*, 221-312. Tokai University Press, Tokyo.

Shigeta, S. & Zakharov, Y.D. 2009: Cephalopods. *In* Shigeta, Y., Zakharov, Y.D., Maeda, H. & Popov, A.M. (eds). *The Lower Triassic System in the Abrek bay area, South Primorye, Russia*, 44-140. National Museum of Nature and Science Monographs 38, Tokyo.

Spath, L.F. 1930: The Eotriassic Invertebrate Fauna of East Greenland. *Meddelelser om Grönland 83*, 1-90.

Spath, L.F. 1934: *Catalogue of the Fossil Cephalopoda in the British Museum (Natural History), part IV: The Ammonoidea of the Trias*, 521 pp. The Trustees of the British Museum, London.

Tozer, E.T. 1961: Triassic Stratigraphy and faunas, Queen Elizabeth Islands, Arctic Archipelago. *Memoir of the Geological Survey of Canada 316*, 1-116.

Tozer, E.T. 1963: Lower Triassic ammonoids from Tuchodi Lakes and Halfway River areas, northeastern British Columbia. *Bulletin of the Geological Survey of Canada 96*, 1-28.

Tozer, E.T. 1965: Lower Triassic stages and Ammonoid zones of Arctic Canada. *Paper of the Geological Survey of Canada 65-12*, 14 pp.

Tozer, E.T. 1967: A Standard for Triassic time. *Bulletin of the Geological Survey of Canada 156*, 1-103.

Tozer, E.T. 1970: Marine Triassic Faunas. *In* R. J. W. Douglas (ed): *Geology and Economic Minerals of Canada, 5 ed.*, 633-640. Geological Survey of Canada, Vancouver.

Tozer, E.T. 1971: Triassic time and ammonoids. *Canadian Journal of Earth Sciences 8*, 989-1031. Errata and addenda, p. 1611.

Tozer, E.T. 1994: Canadian Triassic Ammonoid Faunas. *Bulletin of the Geological Survey of Canada 467*, 1-663.

Vavilov 1976 (V. subtriangularis in Dagys & Ermakov 1996)

Waagen, W. 1895: Salt Ranges Fossils. vol. 2: Fossils from the Ceratites formation - Part I - Pisces, Ammonoidea. *Palaeontologia Indica 13*, 1-323.

Wang, Y.G. & He, G.X. 1976: Triassic ammonoids from the Mount Jolmo Lungma region. *In*: *A report of scientific expedition in the Mount Jolmo Lungma region (1966-1968)*, 223-502. Palaeontology, fascicule 3. Science Press, Beijing [In Chinese].

Ware, D., Jenks, J.F., Hautmann, M. & Bucher, H. 2011: Dienerian (Early Triassic) ammonoids from the Candelaria Hills (Nevada, USA) and their significance for palaeobiogeography and palaeoceanography. *Swiss Journal of Geoscience 104*, 161-181.

Ware, D. & Bucher, H. (this volume): Systematic palaeontology. *In* Ware, D., Bucher, H., Brühwiler, T., Schneebeli-Hermann, E., Hochuli, P.A., Roohi, G., Rehman, K. & Yaseen, A. (this volume): *Induan (Early Triassic) ammonoids from the Salt Range, Pakistan*. Fossil & Strata.

Ware, D., Bucher, H., Brühwiler, T., Schneebeli-Hermann, E., Hochuli, P.A., Roohi, G., Rehman, K. & Yaseen, A. (this volume): Griesbachian and Dienerian (Early Triassic) ammonoids from the Salt Range, Pakistan. *Fossil & Strata*.

Waterhouse, J.B. 1996: The Early and Middle Triassic ammonoid succession of the Himalayas in western and central Nepal. Part 2. Systematic studies of the Early Middle Scythian. *Palaeontographica A241*, 27-100.

Zakharov, Y.D. 1968: *Biostratigraphiya i Amonoidei Nizhnego Triasa Yuzhnogo Primorya (Lower Triassic biostratigraphy and Ammonoids of South Primorye)*, 175 pp. Nauka, Moskva [In Russian].

Plates

Plate 1

(All figures natural size unless otherwise indicated; asterisks indicate the position of the last septum)

1a-b: *Ghazalaites roohii* Ware & Bucher (this volume). PIMUZ30829.
Loc. Mud14, middle part of the Lower Limestone Member, Mud Top Section, *Gyronites plicosus* beds (early Dienerian).

2a-b: *Ghazalaites roohii* Ware & Bucher (this volume). PIMUZ30830.
Loc GU5/1, upper part of the Lower Limestone Member, Guling Village, *Gyronites dubius* beds (early Dienerian).

3a-c: *Ghazalaites roohii* Ware & Bucher (this volume). PIMUZ30831.
Loc. Mud52, top of the Lower Limestone Member, Mud Bottom Section, *Gyronites frequens* beds (early Dienerian). a-b) Lateral and ventral views. c) Suture line at H = 14.8 mm; × 1.5 (mirrored image).

4a-b: *Gyronites frequens* Waagen, 1895. PIMUZ30832.
Loc. Mud52, top of the Lower Limestone Member, Mud Bottom Section, *Gyronites frequens* beds (early Dienerian).

5a-b: *Gyronites frequens* Waagen, 1895. PIMUZ30833.
Loc. Mud52, top of the Lower Limestone Member, Mud Bottom Section, *Gyronites frequens* beds (early Dienerian).

6a-c: *Gyronites frequens* Waagen, 1895. PIMUZ30834.
Loc. Lal1, top of the Lower Limestone Member, Lalung Ridge 1, condensed bed with *Gyronites frequens* horizon (early Dienerian) and *Ambites atavus* horizon (middle Dienerian).

7a-c: *Gyronites dubius* (Krafft, 1909). PIMUZ30835.
Loc. Mud25, upper part of the Lower Limestone Member, Mud Bottom Section, *Gyronites dubius* beds (early Dienerian).

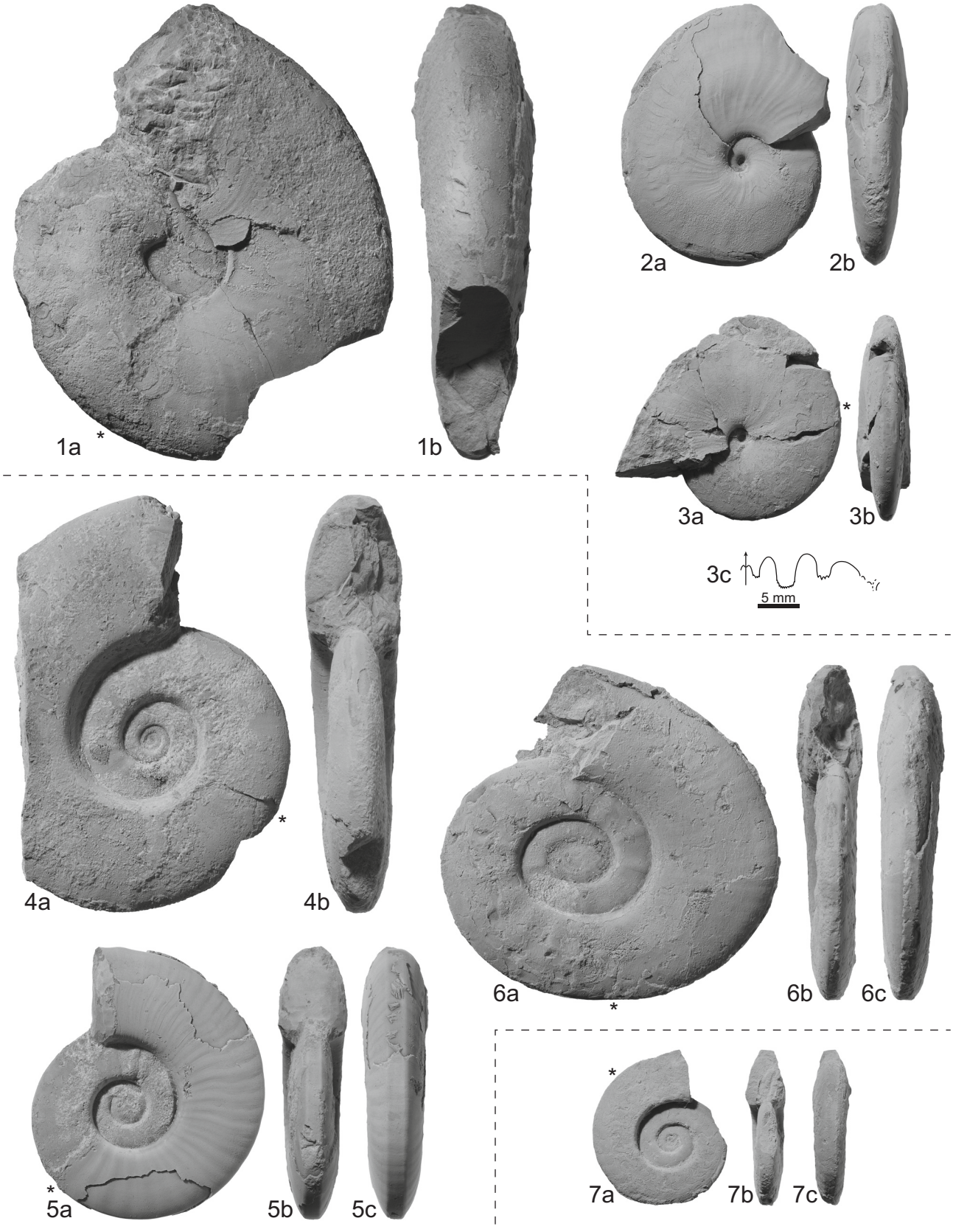
1a *
1b
2a
2b
3a *
3b
3c
5 mm
4a *
4b
6a *
6b
6c
5a *
5b
5c
7a *
7b
7c

Plate 2

(All figures natural size unless otherwise indicated; asterisks indicate the position of the last septum)

1a-c: *Gyronites plicosus* Waagen, 1895. PIMUZ30839.
Loc. Gul23, upper part of the Lower Limestone Member, Guling River, *Gyronites plicosus* beds (early Dienerian).

2a-b: *Gyronites plicosus* Waagen, 1895. PIMUZ30838.
Loc. Mud51, upper part of the Lower Limestone Member, Mud Bottom Section, *Gyronites plicosus* beds (early Dienerian).

3a-d: *Gyronites plicosus* Waagen, 1895. PIMUZ30840.
Loc. Mud15, upper part of the Lower Limestone Member, Mud Top Section, *Gyronites plicosus* beds (early Dienerian). a-c) Lateral, apertural and ventral views. d) Suture line at H = 8.9 mm; × 2 (mirrored image).

4a-c: *Gyronites sitala* (Diener, 1897). PIMUZ30841.
Loc. Mud3, middle part of the Lower Limestone Member, Mud Top Section, *Gyronites plicosus* beds (early Dienerian). Complete specimen.

5a-b: *Gyronites levilatus* n. sp. PIMUZ30842. Paratype.
Loc. Mud5, upper part of the Lower Limestone Member, Mud Top Section, *Gyronites plicosus* beds (early Dienerian).

6a-d: *Gyronites levilatus* n. sp. PIMUZ30843. Paratype.
Loc. Mud5, upper part of the Lower Limestone Member, Mud Top Section, *Gyronites plicosus* beds (early Dienerian). a-c) Lateral, apertural and ventral views. d) Suture line at H = 11.6 mm; × 2 (mirrored image).

7a-c: *Gyronites levilatus* n. sp. PIMUZ30844. Holotype.
Loc. Mud3, upper part of the Lower Limestone Member, Mud Top Section, *Gyronites plicosus* beds (early Dienerian).

8a-d: *Gyronites bullatus* n. sp. PIMUZ30846. Holotype.
Loc. Mud52, top of the Lower Limestone Member, Mud Bottom Section, *Gyronites frequens* beds (early Dienerian). a-c) Lateral, apertural and ventral views. d) Suture line at H = 4.1 mm; × 4 (mirrored image).

9a-b: *Gyronites bullatus* n. sp. PIMUZ30847. Paratype.
Loc. Mud52, top of the Lower Limestone Member, Mud Bottom Section, *Gyronites frequens* beds (early Dienerian); × 2.

10a-b: *Gyronites schwanderi* Ware & Bucher (this volume). PIMUZ30848.
Loc. Gul13, top of the Lower Limestone Member, Guling Village, condensed bed with *Gyronites frequens* horizon (early Dienerian) and *Ambites atavus* horizon (middle Dienerian).

11a-b: *Ambites tenuis* Ware & Bucher (this volume). PIMUZ30849.
Loc. Gul13, top of the Lower Limestone Member, Guling Village, condensed bed with *Gyronites frequens* horizon (early Dienerian) and *Ambites atavus* horizon (middle Dienerian).

12a-b: *Ambites tenuis* Ware & Bucher (this volume). PIMUZ30850.
Loc. Lal1, top of the Lower Limestone Member, Lalung Ridge 1, condensed bed with *Gyronites frequens* horizon (early Dienerian) and *Ambites atavus* horizon (middle Dienerian).

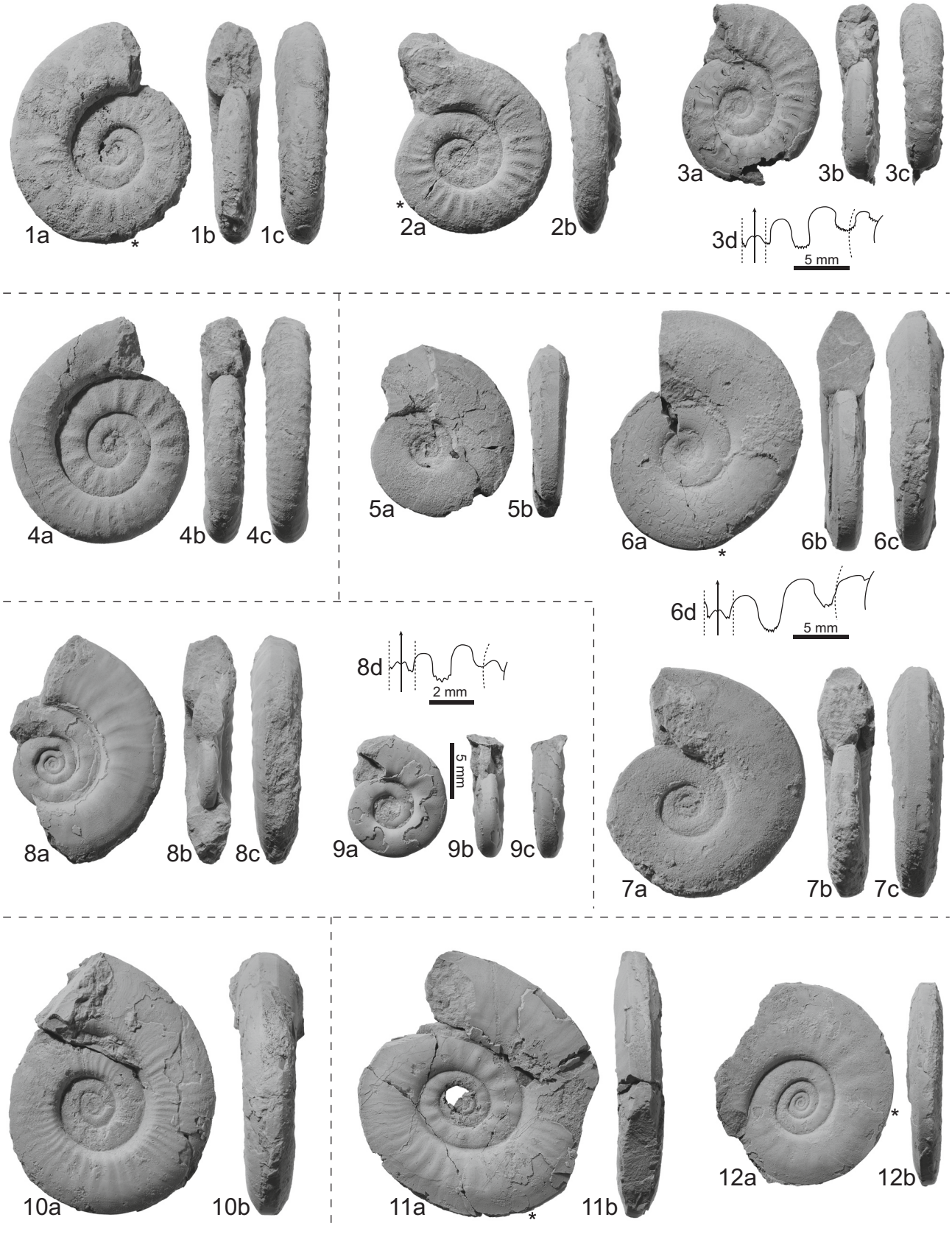
1a
*
1b
1c
2a
*
2b
3a
3b
3c
3d
5 mm
4a
4b
4c
5a
5b
6a
*
6b
6c
6d
5 mm
8a
8b
8c
8d
2 mm
9a
5 mm
9b
9c
7a
7b
7c
10a
10b
11a
*
11b
12a
*
12b

Plate 3

(All figures natural size unless otherwise indicated; asterisks asterisks indicate the position of the last septum)

1a-d: *Ambites discus* Waagen, 1895. PIMUZ30851.
Loc. Mud58b, base of the Limestone and Shale Member, Mud Bottom Section, *Ambites discus* beds (middle Dienerian). a-c) Lateral, apertural and ventral views. d) Suture line at H = 14.8 mm; × 1.5.

2a-c: *Ambites discus* Waagen, 1895. PIMUZ30852.
Loc. Mud58b, base of the Limestone and Shale Member, Mud Bottom Section, *Ambites discus* beds (middle Dienerian).

3a-b: *Ambites discus* Waagen, 1895. PIMUZ30853.
Loc. Lal55, base of the Limestone and Shale Member, Lalung Cliff, *Ambites discus* beds (middle Dienerian).

4a-b: *Ambites atavus* (Waagen, 1895). PIMUZ30855.
Loc. Lal7, base of the Limestone and Shale Member, Lalung Ridge 2, *Ambites atavus* beds (middle Dienerian).

5a-b: *Ambites atavus* (Waagen, 1895). PIMUZ30856.
Loc. Lal1, top of the Lower Limestone Member, Lalung Ridge 1, condensed bed with *Gyronites frequens* horizon (early Dienerian) and *Ambites atavus* horizon (middle Dienerian).

6a-b: *Ambites atavus* (Waagen, 1895). PIMUZ30857.
Loc. Gul12, base of the Limestone and Shale Member, Guling Village, *Ambites atavus* beds (middle Dienerian).

7a-c: *Ambites bojeseni* Ware & Bucher (this volume). PIMUZ30858.
Loc. Mud27, base of the Limestone and Shale Member, Mud Bottom Section, *Ambites bojeseni* beds (middle Dienerian). Complete specimen.

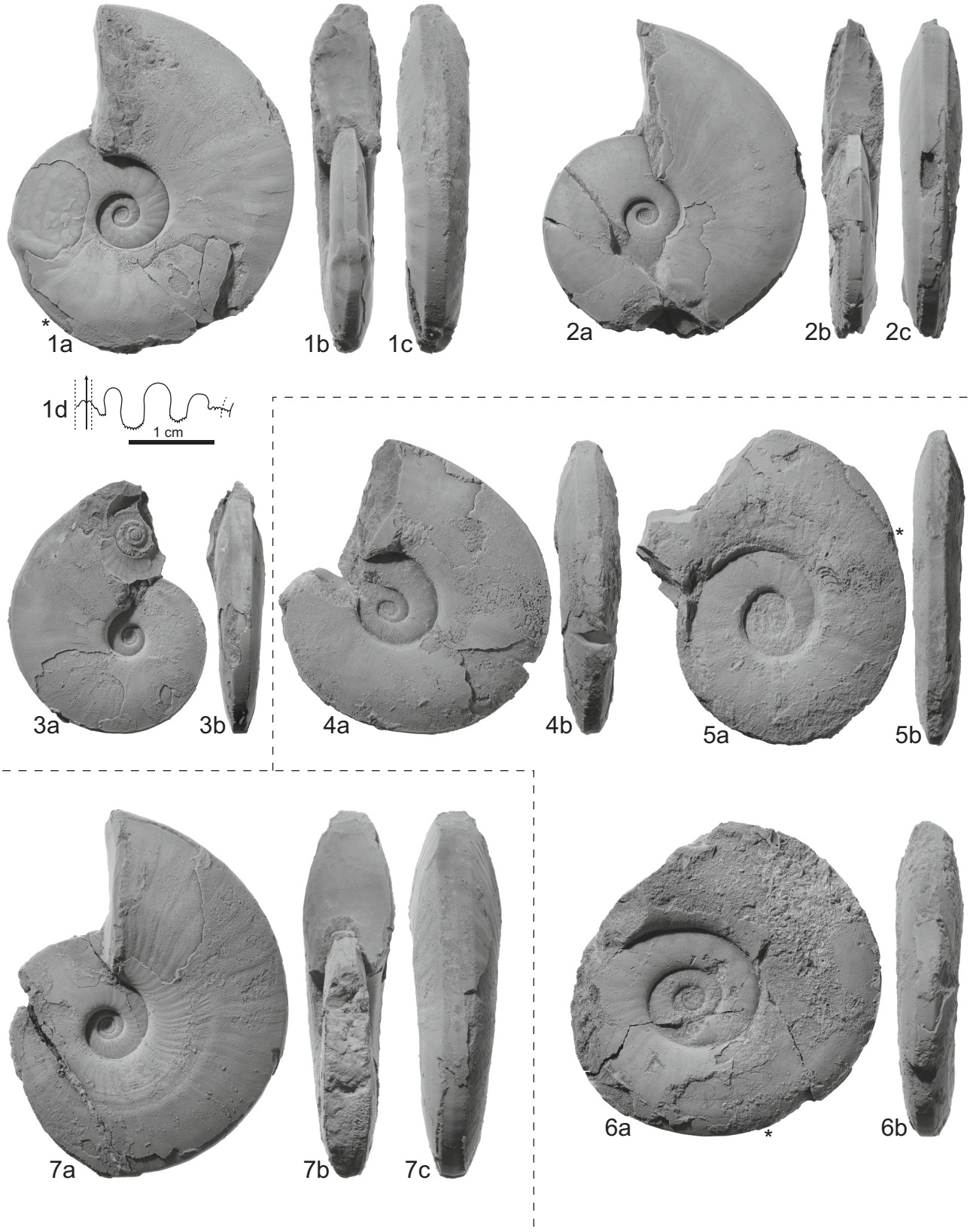
*
1a
1b
1c
2a
2b
2c
1d
1 cm
3a
3b
4a
4b
5a
*
5b
7a
7b
7c
6a
*
6b

Plate 4

(All figures natural size; asterisks indicate the position of the last septum)

1a-b: *Ambites bojeseni* Ware & Bucher (this volume). PIMUZ30859.
Loc. Gul15, base of the Limestone and Shale Member, Guling Village, *Ambites bojeseni* beds (middle Dienerian).

2a-c: *Ambites bojeseni* Ware & Bucher (this volume). PIMUZ30860.
Loc. Mud27, base of the Limestone and Shale Member, Mud Bottom Section, *Ambites bojeseni* beds (middle Dienerian). Specimen with a bivalve encrusting the umbilicus on both sides.

3a-b: *Ambites bojeseni* Ware & Bucher (this volume). PIMUZ30861.
Loc. Mud27, base of the Limestone and Shale Member, Mud Bottom Section, *Ambites bojeseni* beds (middle Dienerian).

4a-d: *Ambites bojeseni* Ware & Bucher (this volume). PIMUZ30862.
Loc. Mud27, base of the Limestone and Shale Member, Mud Bottom Section, *Ambites bojeseni* beds (middle Dienerian). Complete specimen. a-c) Lateral, apertural and ventral views. d) Suture line at H = 24.6 mm.

5a-c: *Ambites bojeseni* Ware & Bucher (this volume). PIMUZ30863.
Loc. Mud27, base of the Limestone and Shale Member, Mud Bottom Section, *Ambites bojeseni* beds (middle Dienerian). a-b) Lateral and ventral views. d) Suture line at H = 14.2 mm.

6: *Ambites bojeseni* Ware & Bucher (this volume). PIMUZ30864.
Loc. Gul15, base of the Limestone and Shale Member, Guling Village, *Ambites bojeseni* beds (middle Dienerian). Suture line at H = 23.5 mm (see also Pl. 5: 1).

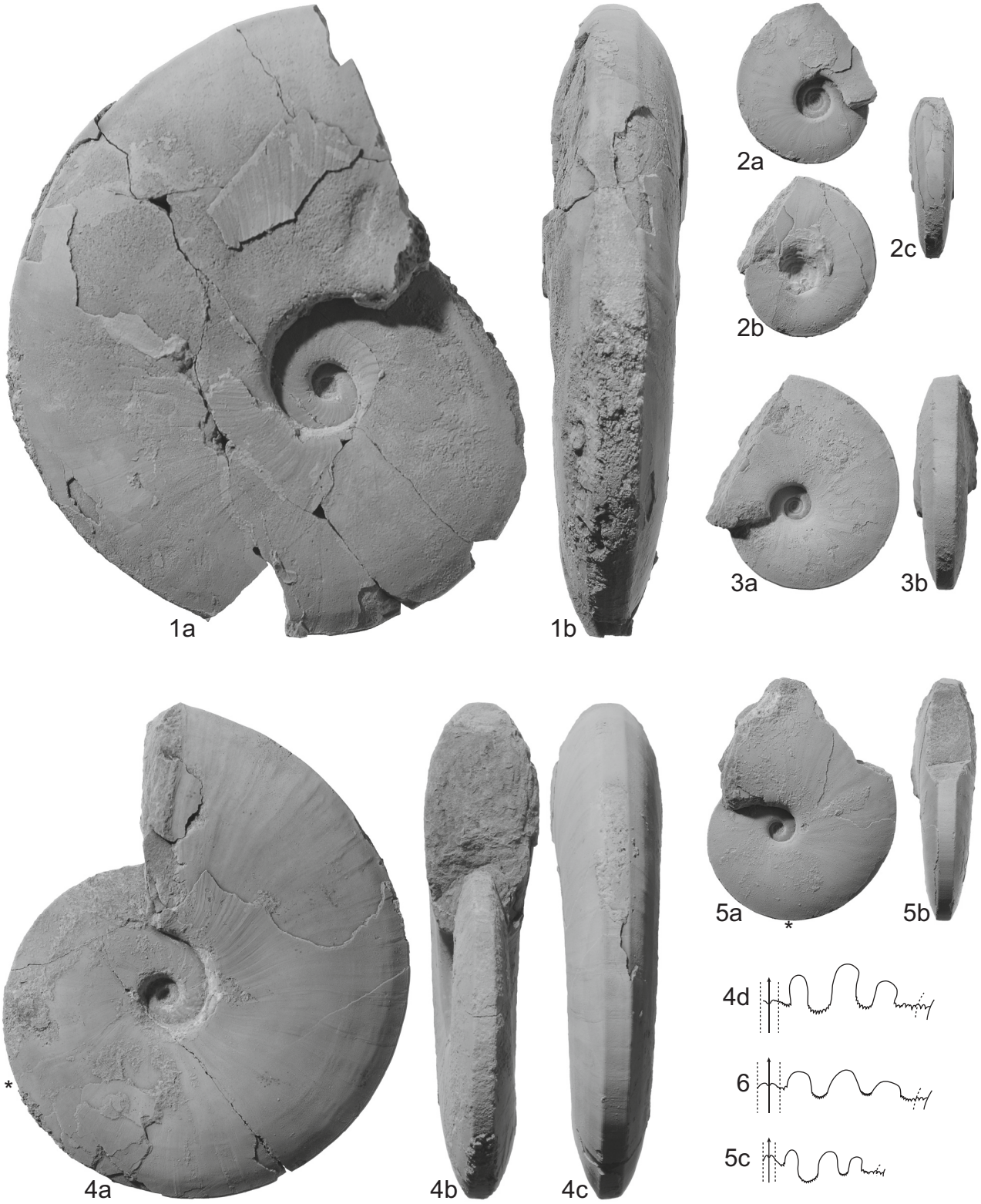
1a
1b
2a
2b
2c
3a
3b
4a
*
4b
4c
5a
*
5b
4d
6
5c

Plate 5

(All figures natural size unless otherwise indicated; asterisks indicate the position of the last septum)

1a-d: *Ambites bojeseni* Ware & Bucher (this volume). PIMUZ30864.
Loc. Gul15, base of the Limestone and Shale Member, Guling Village, *Ambites bojeseni* beds (middle Dienerian). Complete specimen with a bivalve encrusting the umbilicus on both sides. (see also Pl. 4: 6).

2a-b: *Ambites radiatus* (Brühwiler *et al.*, 2008). PIMUZ30865.
Loc. Gul15, base of the Limestone and Shale Member, Guling Village, *Ambites bojeseni* beds (middle Dienerian).

3a-c: *Ambites radiatus* (Brühwiler *et al.*, 2008). PIMUZ30866.
Loc. Gul15, base of the Limestone and Shale Member, Guling Village, *Ambites bojeseni* beds (middle Dienerian).

4a-d: *Ambites nyingmai* n. sp. PIMUZ30867. Holotype.
Loc. Mud58b, base of the Limestone and Shale Member, Mud Bottom Section, *Ambites discus* beds (middle Dienerian). a-c) Lateral, apertural and ventral views. d) Suture line at H = 11.8 mm; × 2.

5a-b: *Ambites nyingmai* n. sp. PIMUZ30868. Paratype.
Loc. Mud58b, base of the Limestone and Shale Member, Mud Bottom Section, *Ambites discus* beds (middle Dienerian).

6a-b: *Ambites nyingmai* n. sp. PIMUZ30869. Paratype.
Loc. Mud58b, base of the Limestone and Shale Member, Mud Bottom Section, *Ambites discus* beds (middle Dienerian).

7a-c: *Ambites nyingmai* n. sp. PIMUZ30870. Paratype.
Loc. Mud58b, base of the Limestone and Shale Member, Mud Bottom Section, *Ambites discus* beds (middle Dienerian).

8a-c: *Ambites nyingmai* n. sp. PIMUZ30871. Paratype.
Loc. Mud58b, base of the Limestone and Shale Member, Mud Bottom Section, *Ambites discus* beds (middle Dienerian).

9a-b: *Ambites lilangensis* (Krafft, 1909). PIMUZ30874.
Loc. Mud205, base of the Limestone and Shale Member, Mud Bottom Section, *Ambites lilangensis* beds (middle Dienerian).

10a-d: *Ambites* cf. *frechi* (Tozer, 1994). PIMUZ30872.
Loc. Mud58b, base of the Limestone and Shale Member, Mud Bottom Section, *Ambites discus* beds (middle Dienerian). a-c) Lateral, apertural and ventral views. d) Suture line at H = 10.7 mm; × 2 (mirrored image).

11a-b: *Ambites subradiatus* Ware & Bucher (this volume). PIMUZ30873.
Loc. Lal55, base of the Limestone and Shale Member, Lalung Cliff, *Ambites discus* beds (middle Dienerian).

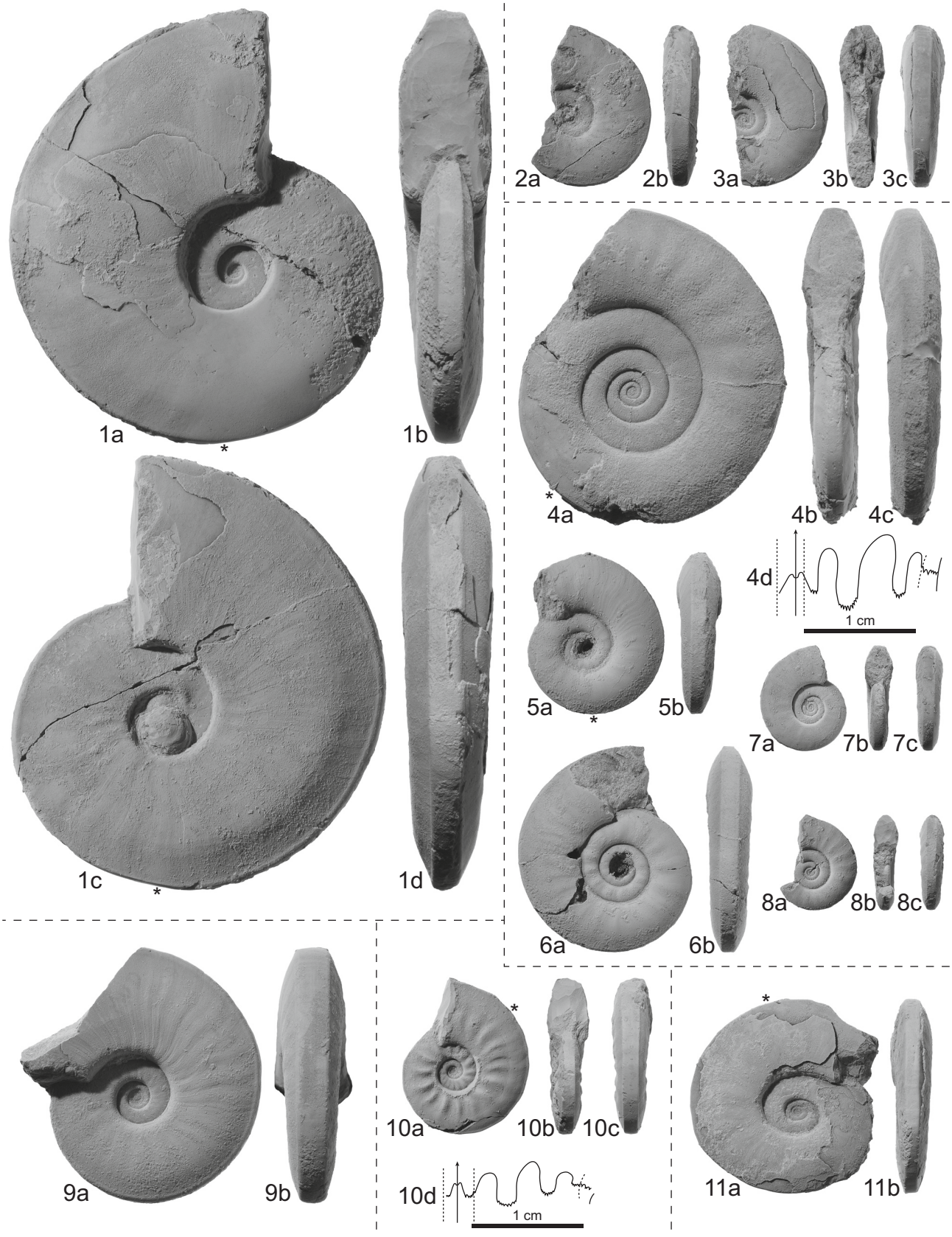
1a
*
1b
1c
*
1d
2a
2b
3a
3b
3c
*
4a
4b
4c
4d
1 cm
5a
*
5b
7a
7b
7c
6a
6b
8a
8b
8c
9a
9b
*
10a
10b
10c
10d
1 cm
*
11a
11b

Plate 6

(All figures natural size unless otherwise indicated; asterisks indicate the position of the last septum)

1a-d: *Ambites lilangensis* (Krafft, 1909). PIMUZ30875.
Loc. Mud28, base of the Limestone and Shale Member, Mud Bottom Section, *Ambites lilangensis* beds (middle Dienerian). Complete specimen with encrusting bivalves on both sides of the flanks which were prepared away on the left side.

2a-c: *Ambites lilangensis* (Krafft, 1909). PIMUZ30876.
Loc. Mud20, base of the Limestone and Shale Member, Mud Top Section, *Ambites lilangensis* beds (middle Dienerian). Complete specimen.

3a-c: *Ambites lilangensis* (Krafft, 1909). PIMUZ30877.
Loc. Mud61, base of the Limestone and Shale Member, Mud Bottom Section, *Ambites lilangensis* beds (middle Dienerian). Complete specimen.

4a-b: *Ambites lilangensis* (Krafft, 1909). PIMUZ30878.
Loc. Mud203, base of the Limestone and Shale Member, Mud Bottom Section, *Ambites lilangensis* beds (middle Dienerian). Complete specimen.

5a-c: *Ambites lilangensis* (Krafft, 1909). PIMUZ30879.
Loc. Mud28, base of the Limestone and Shale Member, Mud Bottom Section, *Ambites lilangensis* beds (middle Dienerian).

6a-d: *Ambites lilangensis* (Krafft, 1909). PIMUZ30880.
Loc. Mud61, base of the Limestone and Shale Member, Mud Bottom Section, *Ambites lilangensis* beds (middle Dienerian). Complete specimen with a bivalve encrusting the umbilicus. a-c) Lateral, apertural and ventral views. d) Suture line at H = 23.4 mm.

7: *Ambites lilangensis* (Krafft, 1909). PIMUZ30881.
Loc. Mud61, base of the Limestone and Shale Member, Mud Bottom Section, *Ambites lilangensis* beds (middle Dienerian). Suture line at H = 14.6 mm; × 1.5.

8a-c: *Ambites lilangensis* (Krafft, 1909). PIMUZ30882.
Loc. Mud28, base of the Limestone and Shale Member, Mud Bottom Section, *Ambites lilangensis* beds (middle Dienerian).

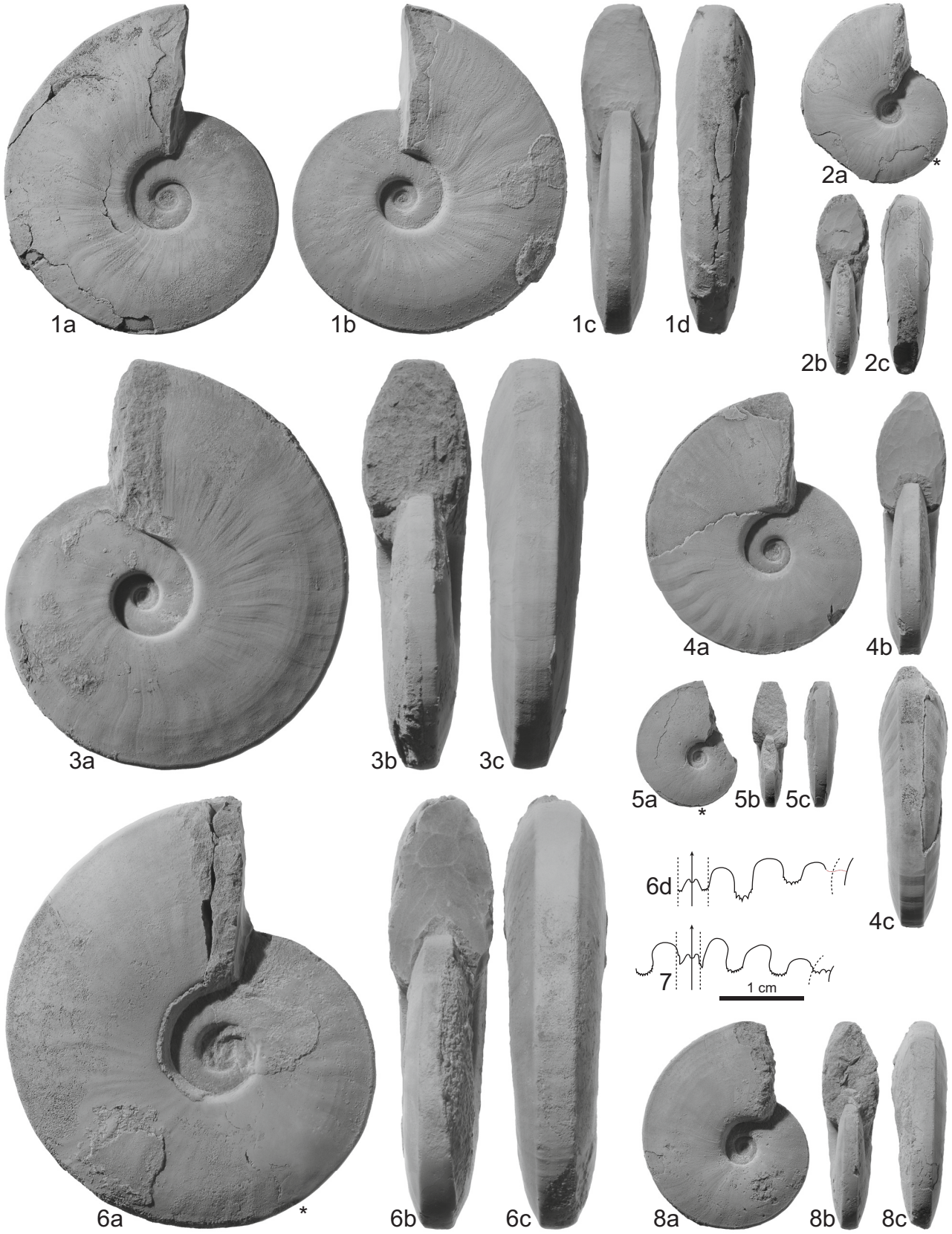
1a
1b
1c
1d
2a
*
2b
2c
3a
3b
3c
4a
4b
5a
*
5b
5c
4c
6d
7
1 cm
6a
*
6b
6c
8a
8b
8c

Plate 7

(All figures natural size unless otherwise indicated; asterisks indicate the position of the last septum)

1a-c: *Vavilovites meridialis* n. sp. PIMUZ30883. Holotype.
Loc. Mud63, base of the Limestone and Shale Member, Mud Bottom Section, *Vavilovites meridialis* beds (late Dienerian). Nearly complete specimen heavily encrusted by numerous bivalves on both sides, except the last third of the whorl. × 0.5.

2a-b: *Vavilovites meridialis* n. sp. PIMUZ30884. Paratype.
Loc. Mud19', base of the Limestone and Shale Member, Mud Top Section, *Vavilovites meridialis* beds (late Dienerian).

3a-c: *Vavilovites meridialis* n. sp. PIMUZ30885. Paratype.
Loc. Mud63, base of the Limestone and Shale Member, Mud Bottom Section, *Vavilovites meridialis* beds (late Dienerian). Specimen with a bivalve encrusting the umbilicus on both sides.

4a-b: *Vavilovites meridialis* n. sp. PIMUZ30886. Paratype.
Loc. Mud60, base of the Limestone and Shale Member, Mud Bottom Section, *Vavilovites meridialis* beds (late Dienerian).

5a-c: *Vavilovites meridialis* n. sp. PIMUZ30887. Paratype.
Loc. Mud60, base of the Limestone and Shale Member, Mud Bottom Section, *Vavilovites meridialis* beds (late Dienerian).

6a-c: *Vavilovites meridialis* n. sp. PIMUZ30888. Paratype.
Loc. Mud60, base of the Limestone and Shale Member, Mud Bottom Section, *Vavilovites meridialis* beds (late Dienerian). Nearly complete specimen with a bivalve encrusting the umbilicus on both sides.

7a-c: *Vavilovites meridialis* n. sp. PIMUZ30889. Paratype.
Loc. Mud63, base of the Limestone and Shale Member, Mud Bottom Section, *Vavilovites meridialis* beds (late Dienerian). Nearly complete specimen with a bivalve encrusting the umbilicus on both sides.

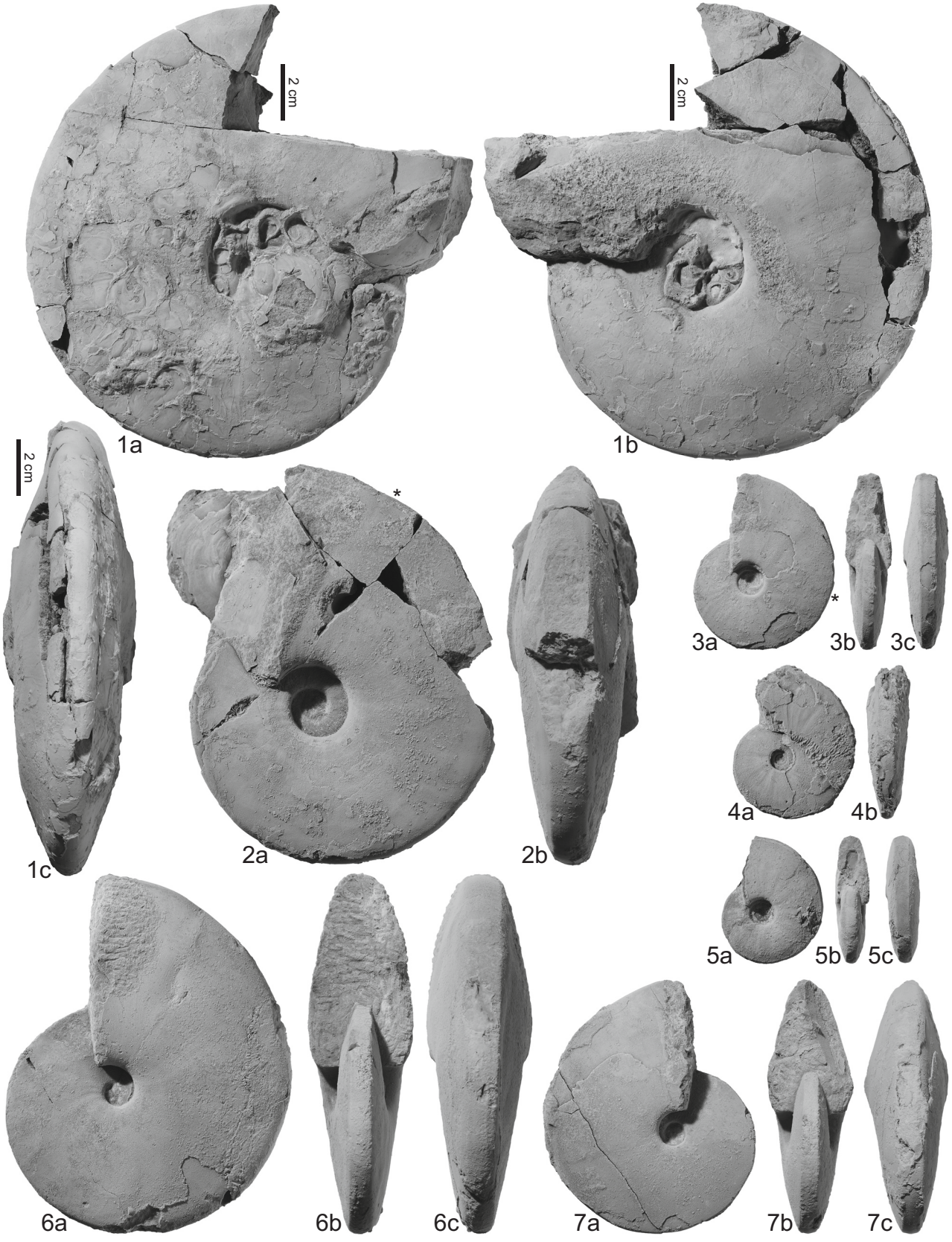
2 cm
1a
2 cm
1b
2 cm
1c
*
2a
2b
*
3a
3b
3c
4a
4b
5a
5b
5c
6a
6b
6c
7a
7b
7c

Plate 8

(All figures natural size unless otherwise indicated; asterisks indicate the position of the last septum)

1: *Vavilovites meridialis* n. sp. PIMUZ30890. Paratype.
Loc. Mud202, base of the Limestone and Shale Member, Mud Bottom Section, *Vavilovites meridialis* beds (late Dienerian). Nearly complete specimen with numerous encrusting bivalves prepared away on the left side to show the induced growth irregularity of the umbilicus. × 0.5.

2a-d: *Vavilovites meridialis* n. sp. PIMUZ30891. Paratype.
Loc. Gul18, base of the Limestone and Shale Member, Guling Village, *Vavilovites meridialis* beds (late Dienerian). a-c) Lateral, apertural and ventral views. d) Suture line at H = 25.1 mm.

3a-c: *Koninckites vetustus* Waagen, 1895. PIMUZ30892.
Loc. Lal63, base of the Limestone and Shale Member, Lalung Cliff, *Koninckites vetustus* beds (late Dienerian).

4a-c: *Koninckites khoorensis* (Waagen, 1895). PIMUZ30893.
Loc. Mud59, base of the Limestone and Shale Member, Mud Bottom Section, *Koninckites khoorensis* beds (late Dienerian). Complete specimen with a bivalve encrusting the umbilicus on both sides.

5a-c: *Koninckites khoorensis* (Waagen, 1895). PIMUZ30894.
Loc. Mud19, base of the Limestone and Shale Member, Mud Top Section, *Koninckites khoorensis* beds (late Dienerian).

6a-c: *Koninckites khoorensis* (Waagen, 1895). PIMUZ30895.
Loc. Mud201, base of the Limestone and Shale Member, Mud Bottom Section, *Koninckites khoorensis* beds (late Dienerian). Nearly complete specimen with a bivalve encrusting the umbilicus on both sides.

7a-c: *Koninckites khoorensis* (Waagen, 1895). PIMUZ30896.
Loc. Mud19, base of the Limestone and Shale Member, Mud Top Section, *Koninckites khoorensis* beds (late Dienerian). Complete specimen with a bivalve encrusting the umbilicus on both sides.

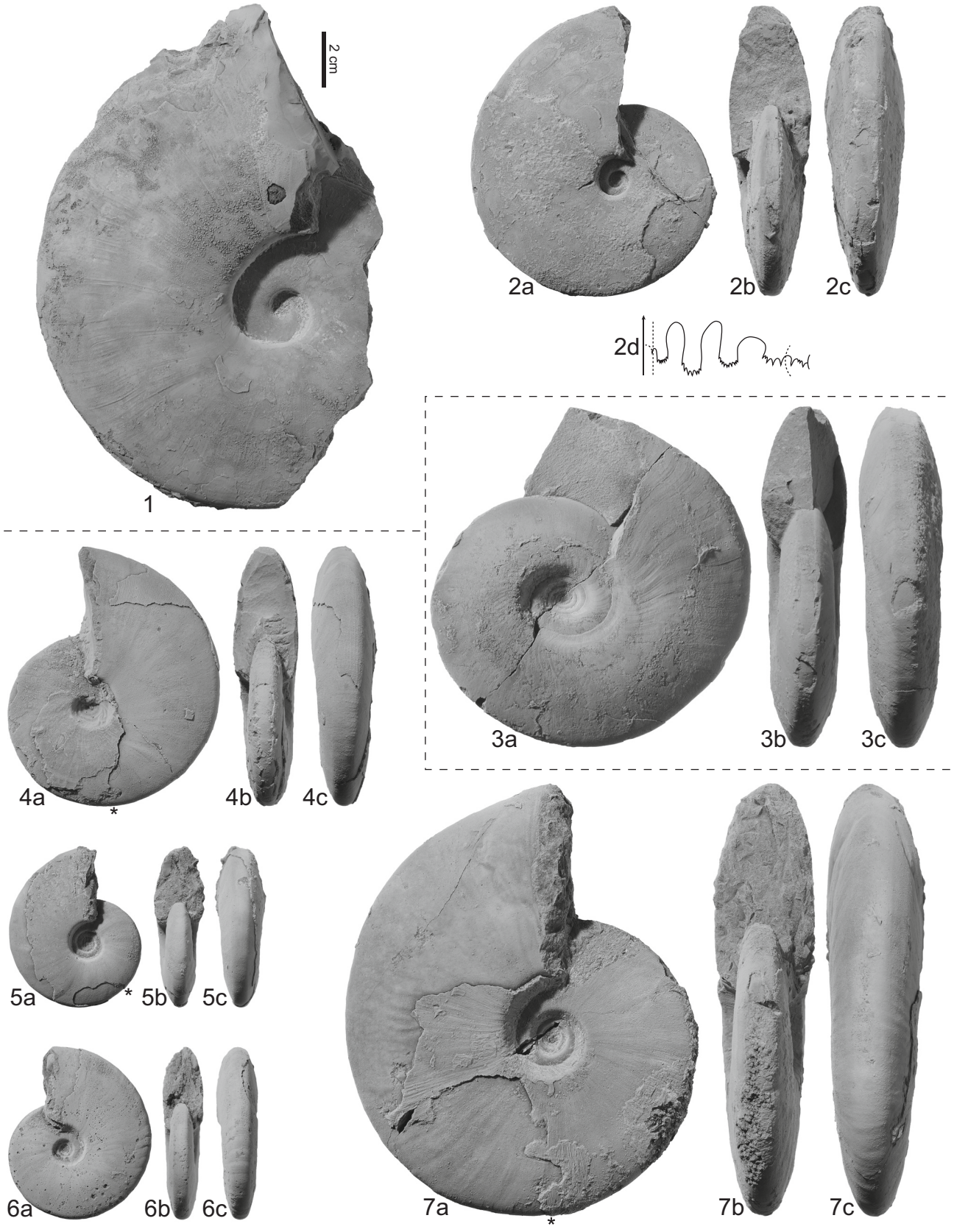
2 cm
1
2a
2b
2c
2d
3a
3b
3c
4a
*
4b
4c
5a
*
5b
5c
6a
6b
6c
7a
*
7b
7c

Plate 9

(All figures natural size unless otherwise indicated; asterisks indicate the position of the last septum)

1a-d: *Koninckites khoorensis* (Waagen, 1895). PIMUZ30897.
Loc. Mud59, base of the Limestone and Shale Member, Mud Bottom Section, *Koninckites khoorensis* beds (late Dienerian). a-c) Lateral, apertural and ventral views. d) Suture line at H = 25.7 mm (mirrored image).

2a-c: *Koninckites khoorensis* (Waagen, 1895). PIMUZ30898.
Loc. Mud19, base of the Limestone and Shale Member, Mud Top Section, *Koninckites khoorensis* beds (late Dienerian).

3a-c: *Koninckites khoorensis* (Waagen, 1895). PIMUZ30899.
Loc. Mud19, base of the Limestone and Shale Member, Mud Top Section, *Koninckites khoorensis* beds (late Dienerian). Nearly complete specimen. × 1.5.

4a-c: *Koninckites khoorensis* (Waagen, 1895). PIMUZ30900.
Loc. Mud19, base of the Limestone and Shale Member, Mud Top Section, *Koninckites khoorensis* beds (late Dienerian). × 1.5.

5a-b: *Radioceras truncatum* (Spath, 1934). PIMUZ30901.
Loc. Mud31, base of the Limestone and Shale Member, Mud Bottom Section, *Koninckites vetustus* beds (late Dienerian).

6a-c: *Pashtunites kraffti* (Spath 1934). PIMUZ30902.
Loc. Lal63, base of the Limestone and Shale Member, Lalung Cliff, *Koninckites vetustus* beds (late Dienerian).

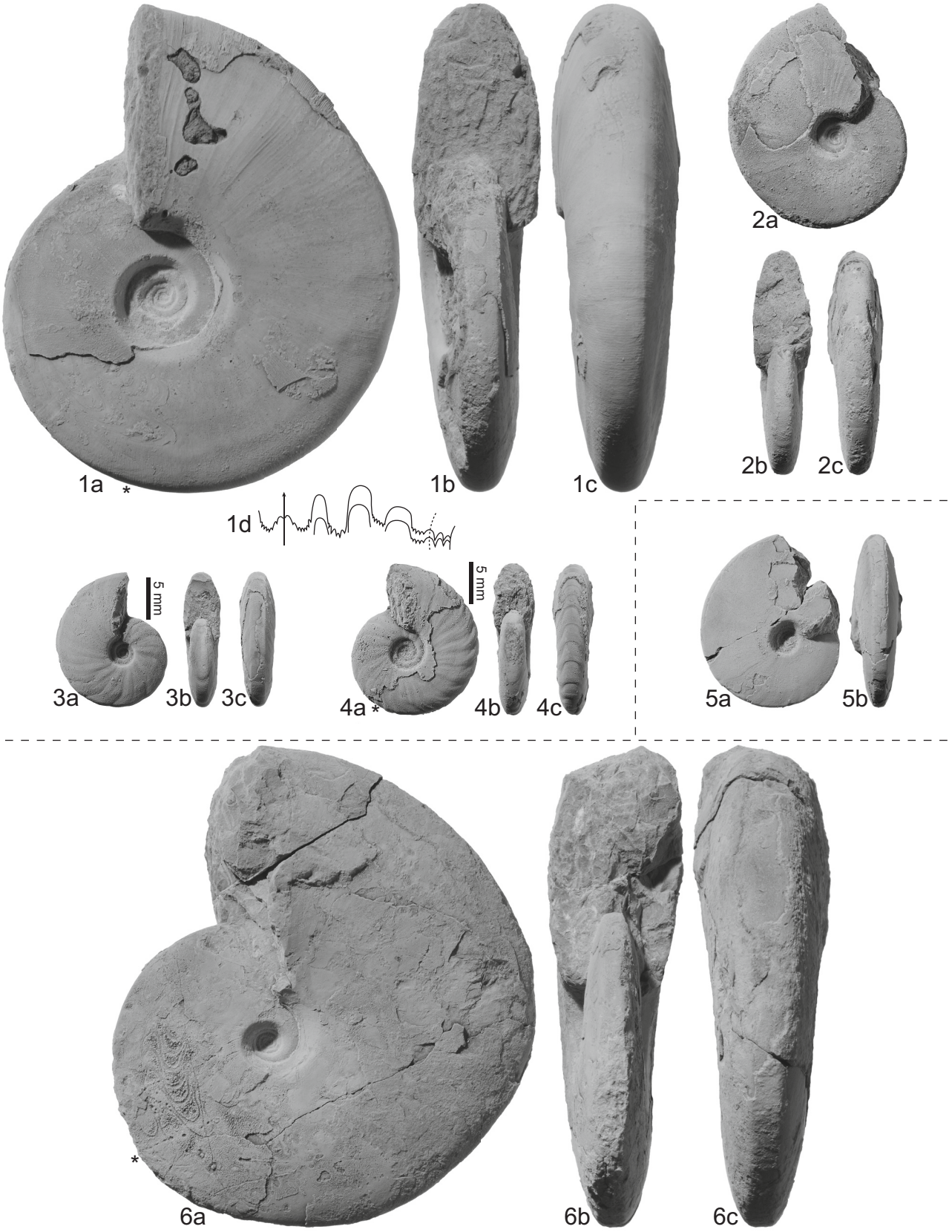
1a *
1b
1c
2a
2b
2c
1d
5 mm
3a
3b
3c
5 mm
4a *
4b
4c
5a
5b
*
6a
6b
6c

Plate 10

(All figures natural size unless otherwise indicated; asterisks indicate the position of the last septum)

1a-c: *Proptychites oldhamianus* Waagen, 1895. PIMUZ30903.
Loc. Mud52, top of the Lower Limestone Member, Mud Bottom Section, *Gyronites frequens* beds (early Dienerian). a-b) Lateral and ventral views. c) Suture line at H = 22.3 mm.

2a-c: *Proptychites oldhamianus* Waagen, 1895. PIMUZ30904.
Loc. Mud52, top of the Lower Limestone Member, Mud Bottom Section, *Gyronites frequens* beds (early Dienerian).

3a-b: *Proptychites lawrencianus* (de Koninck, 1863) *sensu* Waagen, 1895. PIMUZ30905.
Loc. Lal27, base of the Limestone and Shale Member, Lalung Ridge 2, from a floated block, precise stratigraphic position unknown (?middle Dienerian). × 0.5.

4a-b: *Proptychites wargalensis* Ware & Bucher (this volume). PIMUZ30906.
Loc. GU6, top of the Lower Limestone Member, Guling Village, *Gyronites plicosus* beds (early Dienerian).

5a-b: *Proptychites ammonoides* Waagen, 1895. PIMUZ30907.
Loc. Mud27, base of the Limestone and Shale Member, Mud Bottom Section, *Ambites bojeseni* beds (middle Dienerian).

6: *Proptychites ammonoides* Waagen, 1895. PIMUZ30908.
Loc. Mud58D3, base of the Limestone and Shale Member, Mud Bottom Section, *Ambites bojeseni* beds (middle Dienerian). Suture line at H = 30.2 mm.

7a-c: *Proptychites ammonoides* Waagen, 1895. PIMUZ30909.
Loc. Mud58a, base of the Limestone and Shale Member, Mud Bottom Section, *Ambites bojeseni* beds (middle Dienerian).

8a-d: *Proptychites ammonoides* Waagen, 1895. PIMUZ30910.
Loc. Mud58a, base of the Limestone and Shale Member, Mud Bottom Section, *Ambites bojeseni* beds (middle Dienerian). Specimen with bivalves encrusting the umbilicus removed to show the induced coiling irregularity. × 0.5.

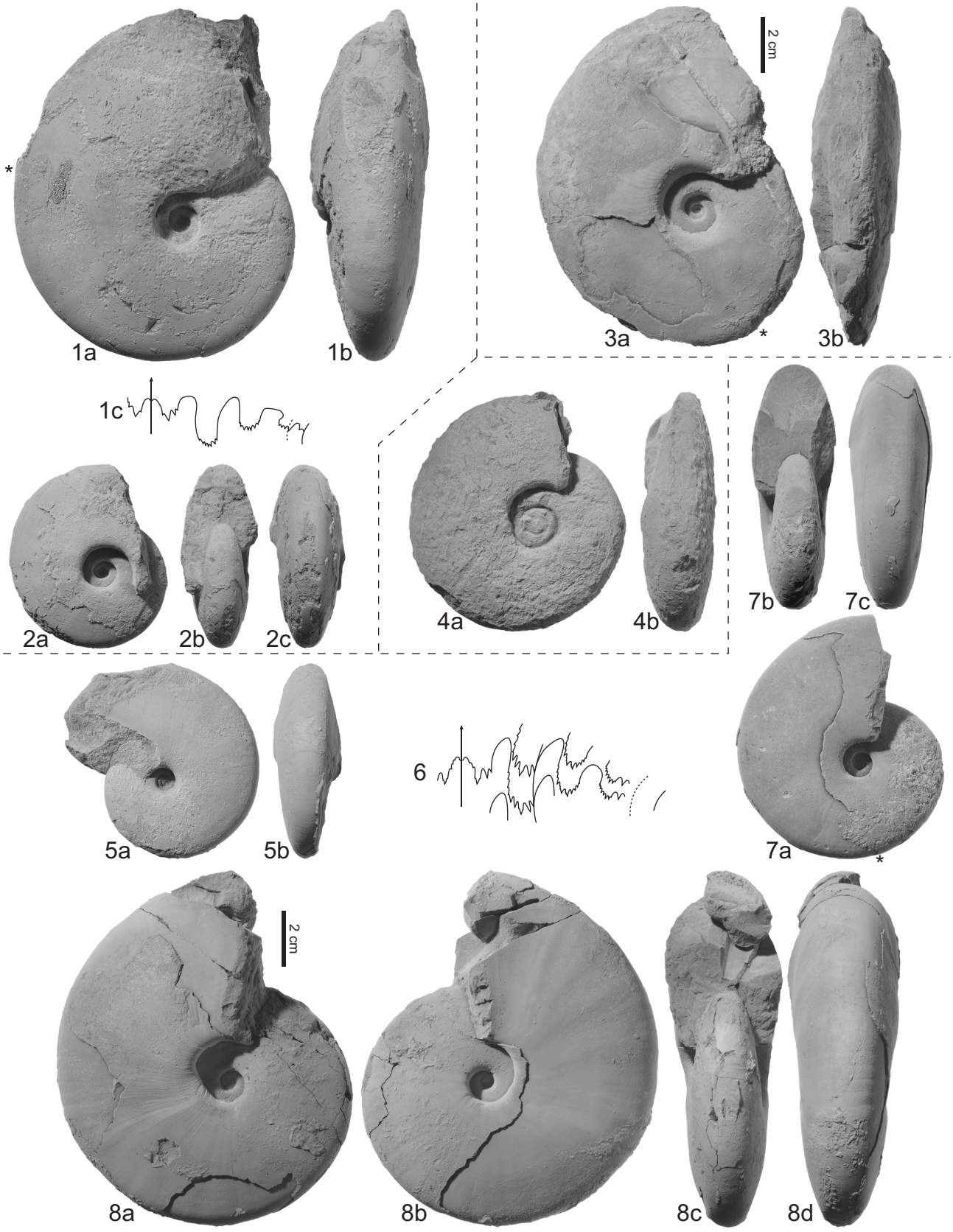
1a
1b
1c
2a
2b
2c
3a
3b
2 cm
4a
4b
5a
5b
6
7a
7b
7c
8a
8b
8c
8d
2 cm

Plate 11

(All figures natural size unless otherwise indicated; asterisks indicate the position of the last septum)

1a-c: *Proptychites ammonoides* Waagen, 1895. PIMUZ30911.
Loc. Mud58a, base of the Limestone and Shale Member, Mud Bottom Section, *Ambites bojeseni* beds (middle Dienerian). Complete specimen with bivalves encrusting the umbilicus and the flanks except on the last sixth of the whorl, without inducing any coiling irregularity. × 0.5.

2a-c: *Proptychites* cf. *pagei* Ware *et al*., 2011. PIMUZ30912.
Loc. Til2, base of the Limestone and Shale Member, Tilling, *Ambites lilangensis* beds (middle Dienerian). × 0.7.

3a-d: *Dunedinites* cf. *magnumbilicatus* (Kiparisova, 1961). PIMUZ30913.
Loc. Mud52, top of the Lower Limestone Member, Mud Bottom Section, *Gyronites frequens* beds (early Dienerian). a-c) Lateral, apertural and ventral views; × 2. d) Suture line at H = 6.2 mm; × 2.

4a-b: *Bukkenites sakesarensis* Ware & Bucher (this volume). PIMUZ30914.
Loc. GU5/1, middle part of the Lower Limestone Member, Guling Village, *Gyronites dubius* beds (early Dienerian).

5a-d: *Bukkenites sakesarensis* Ware & Bucher (this volume). PIMUZ30915.
Loc. GU5/1, middle part of the Lower Limestone Member, Guling Village, *Gyronites dubius* beds (early Dienerian). a-c) Lateral, apertural and ventral views. d) Suture line at H = 5.9 mm; × 3.

6a-c: *Mullericeras spitiense* (Krafft, 1909). PIMUZ30916.
Loc. Mud29, base of the Limestone and Shale Member, Mud Bottom Section, *Vavilovites meridialis* beds (late Dienerian). Complete specimen.

7a-c: *Mullericeras spitiense* (Krafft, 1909). PIMUZ30917.
Loc. Mud28, base of the Limestone and Shale Member, Mud Bottom Section, *Ambites lilangensis* beds (middle Dienerian). a-b) Lateral and ventral views. c) Suture line at H = 15.9 mm; × 1.5.

8: *Mullericeras spitiense* (Krafft, 1909). PIMUZ30918.
Loc. Mud60, base of the Limestone and Shale Member, Mud Bottom Section, *Vavilovites meridialis* beds (late Dienerian). Suture line at H = 17.9 mm; × 1.5 (mirrored image).

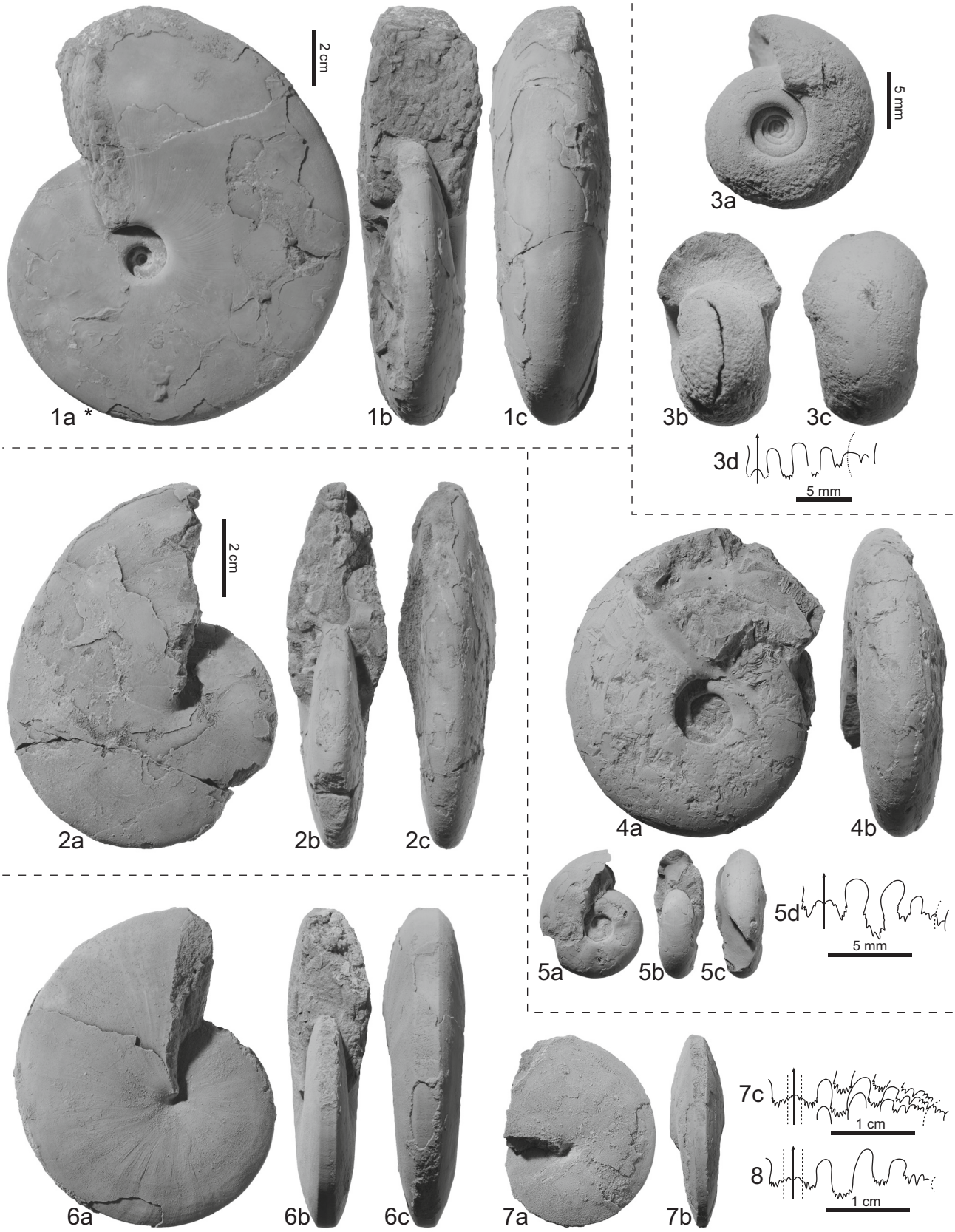
2 cm
1a *
1b
1c
5 mm
3a
3b
3c
3d
5 mm
2 cm
2a
2b
2c
4a
4b
5a
5b
5c
5d
5 mm
6a
6b
6c
7a
7b
7c
1 cm
8
1 cm

Plate 12

(All figures natural size unless otherwise indicated; asterisks indicate the position of the last septum)

1a-b: *Mullericeras shigetai* Ware & Bucher (this volume). PIMUZ30921.
Loc. Lal7, base of the Limestone and Shale Member, Lalung Ridge 2, *Ambites atavus* beds (middle Dienerian).

2a-c: *Mullericeras shigetai* Ware & Bucher (this volume). PIMUZ30922.
Loc. Lal7, base of the Limestone and Shale Member, Lalung Ridge 2, *Ambites atavus* beds (middle Dienerian).

3a-c: *Mullericeras niazii* Ware & Bucher (this volume). PIMUZ30923.
Loc. Mud28, base of the Limestone and Shale Member, Mud Bottom Section, *Ambites lilangensis* beds (middle Dienerian). Nearly complete specimen.

4a-c: *Mullericeras niazii* Ware & Bucher (this volume). PIMUZ30924.
Loc. Mud28, base of the Limestone and Shale Member, Mud Bottom Section, *Ambites lilangensis* beds (middle Dienerian).

5a-b: *Ussuridiscus varaha* (Diener, 1895). PIMUZ30925.
Loc. GU5/1, middle part of the Lower Limestone Member, Guling Village, *Gyronites dubius* beds (early Dienerian).

6a-b: *Ussuridiscus ensanus* (Krafft, 1909). PIMUZ30926.
Loc. Gul13, top of the Lower Limestone Member, Guling Village, condensed bed with *Gyronites frequens* horizon (early Dienerian) and *Ambites atavus* horizon (middle Dienerian).

7a-c: *Ussuridiscus ensanus* (Krafft, 1909). PIMUZ30927.
Loc. Mud52, top of the Lower Limestone Member, Mud Bottom Section, *Gyronites frequens* beds (early Dienerian). a-b) Lateral and ventral views. c) Suture line at H = 16.7 mm; × 1.5.

8a-b: *Ussuridiscus ensanus* (Krafft, 1909). PIMUZ30928.
Loc. Mud52, top of the Lower Limestone Member, Mud Bottom Section, *Gyronites frequens* beds (early Dienerian).

9a-b: *Ussuridiscus ventriosus* Ware & Bucher (this volume). PIMUZ30929.
Loc. Mud53, upper part of the Lower Limestone Member, Mud Bottom Section, *Gyronites plicosus* beds (early Dienerian).

10a-b: *Ussuridiscus ornatus* Ware & Bucher (this volume). PIMUZ30930.
Loc. Gul24, middle part of the Lower Limestone Member, Guling Village, *Gyronites plicosus* beds (early Dienerian).

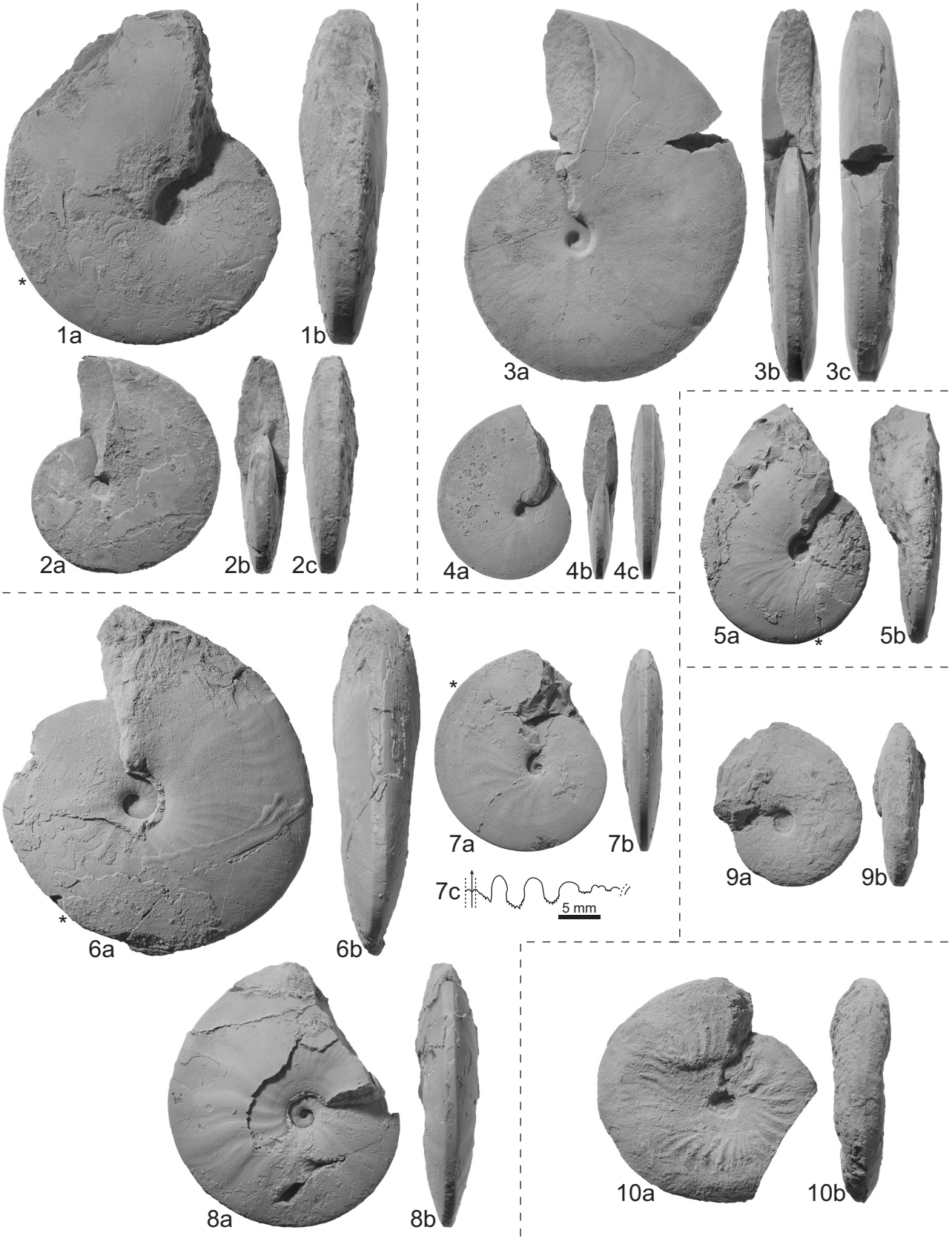
*
1a
1b
3a
3b
3c
2a
2b
2c
4a
4b
4c
5a
*
5b
*
6a
6b
*
7a
7b
7c
5 mm
9a
9b
8a
8b
10a
10b

Plate 13

(All figures natural size unless otherwise indicated; asterisks indicate the position of the last septum)

1a-d: *Kingites davidsonianus* (de Koninck, 1863). PIMUZ30931.
Loc. Mud59, base of the Limestone and Shale Member, Mud Bottom Section, *Koninckites khoorensis* beds (late Dienerian). Complete specimen. a-c) Lateral, apertural and ventral views. d) Suture line at H = 22.7 mm; × 1.5.

2a-b: *Kingites davidsonianus* (de Koninck, 1863). PIMUZ30932.
Loc. Mud19, base of the Limestone and Shale Member, Mud Top Section, *Koninckites khoorensis* beds (late Dienerian). Complete specimen.

3a-b: *Kingites davidsonianus* (de Koninck, 1863). PIMUZ30933.
Loc. Mud19, base of the Limestone and Shale Member, Mud Top Section, *Koninckites khoorensis* beds (late Dienerian).

4a-e: *Kingites korni* Brühwiler *et al.*, 2010a. PIMUZ27863. Holotype.
Loc. Mud31, base of the Limestone and Shale Member, Mud Bottom Section, *Koninckites vetustus* beds (late Dienerian). Complete specimen. a-d) Lateral (left and right), apertural and ventral views. e) Suture line at H = 21 mm; × 2 (mirrored image). Reproduced after Brühwiler *et al*. (2010a).

5a-d: *Pseudosageceras simplelobatum* Ware & Bucher (this volume). PIMUZ30934.
Loc. Mud19, base of the Limestone and Shale Member, Mud Top Section, *Koninckites khoorensis* beds (late Dienerian). a-c) Lateral, apertural and ventral views. d) Suture line at H = 23.7 mm; × 1.5 (mirrored image).

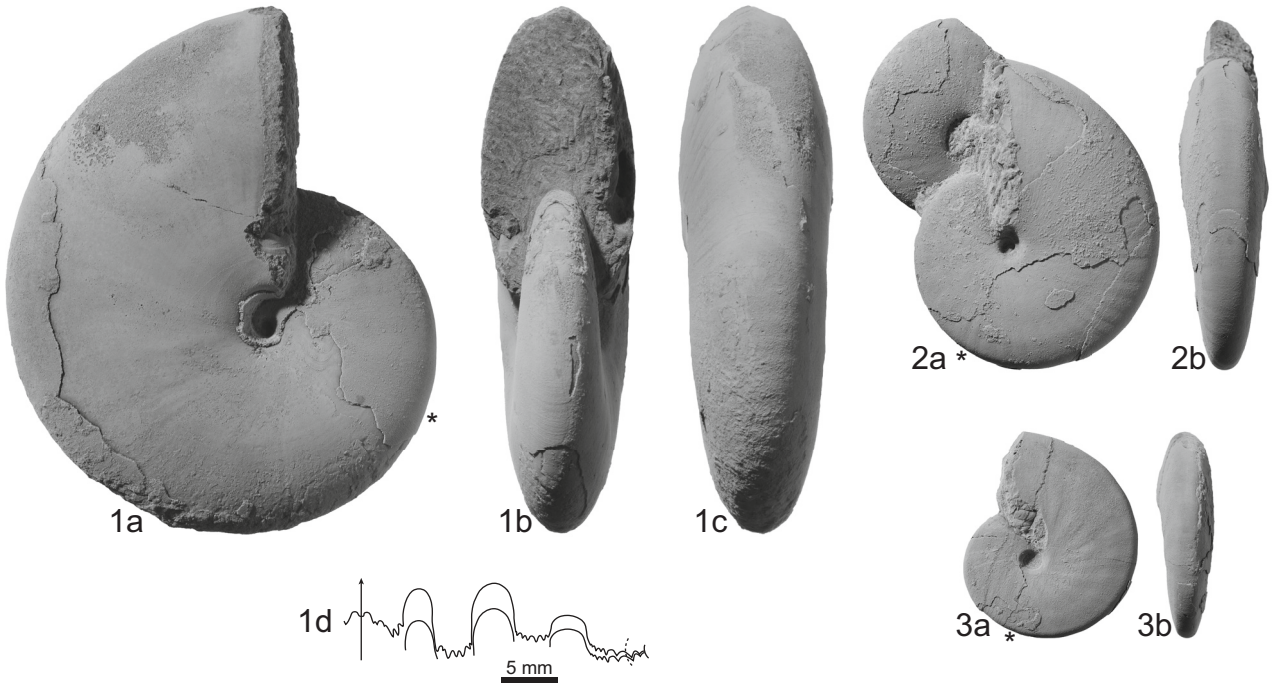
1a
*
1b
1c
1d
5 mm
2a *
2b
3a *
3b

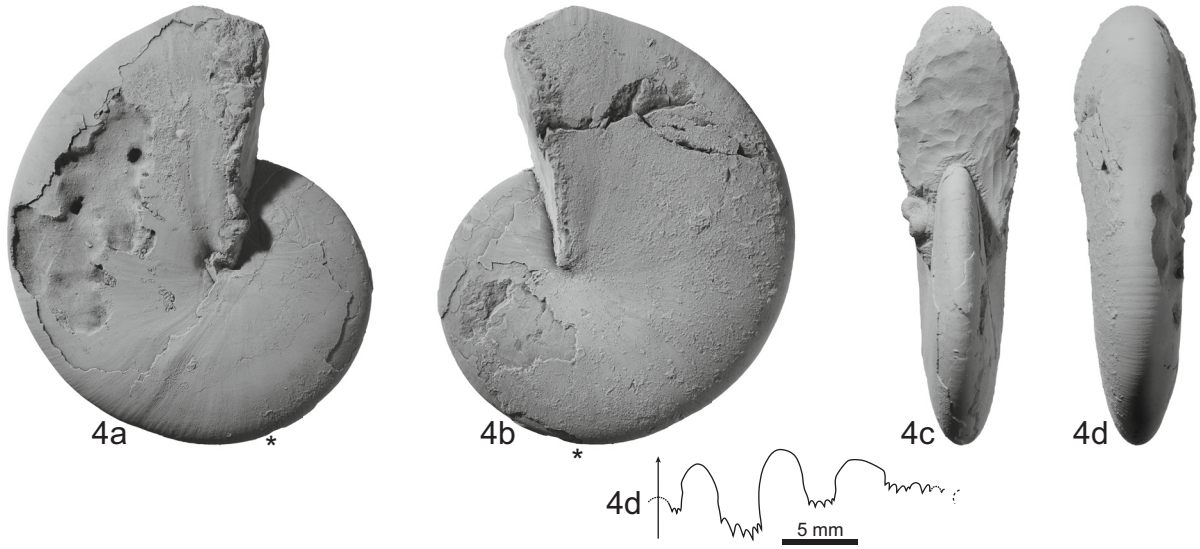
4a
*
4b
*
4c
4d
4d
5 mm

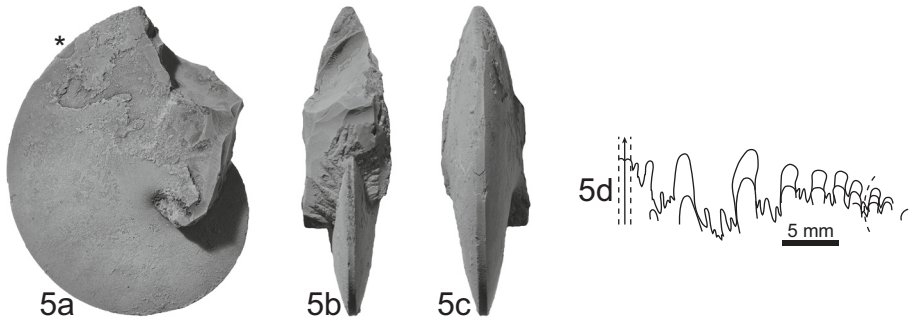
*
5a
5b
5c
5d
5 mm

CHAPTER 4

Dienerian (Early Triassic) ammonoids from Tulong area, South Tibet

Dienerian (Early Triassic) ammonoids from Tulong area, South Tibet

David Ware*, Thomas Brühwiler, Nicolas Goudemand & Hugo Bucher*
Paläontologisches Institut und Museum, Universität Zürich, Karl Schmid-Strasse 4, CH-8006 Zürich, Switzerland
* Corresponding authors. E-mail: david.ware@pim.uzh.ch. hugo.fr.bucher@pim.uzh.ch

Abstract

The Northern Indian Margin has long been recognized as a key area for Dienerian (Early Triassic) ammonoids and their biostratigraphy. Following extensive studies of rich Dienerian ammonoids from the Salt Range (Pakistan) and from Spiti (India) by Ware et al.(in press a & b), we first report here on the new occurrence of seven species of Dienerian ammonoids from only two layers at the base of the Tulong Formation from a new section East of the classic Tulong Triassic section (South Tibet). Biotratigraphically, these two beds correspond to three regional zones of the Salt Range. The oldest one corresponds to the *Gyronites frequens* regional zone of latest early Dienerian age. The second fauna is in a condensed layer including a mixture of the *Ambites discus* beds and to the *A. superior* beds of the Salt Range. This condensed layer is still entirely middle Dienerian in age. Occurrences of the same faunal associations in South Tibet, in the Salt Range and in Spiti pushes back in time the emergence of the Northern Indian Margin biogeographic domain from Smithian to Dienerian times. In a global paleobiogeographic view of the Early Triassic, the emergence of the northern Indian margin as biogeographic homogenous domain coincides with the onset of the latitudinal gradient of species richness in Dienerian times. The new occurrences described here represent a valuable addition for the construction of a high resolution and laterally reproducible Dienerian ammonoid biozonation and a further step towards higher resolution in time and space of the Early Triassic biotic recovery dynamics.

Keywords: Ammonoids; biostratigraphy; Dienerian; Early Triassic; South Tibet; Northern Indian Margin.

1. Introduction

After the end-Permian mass extinction, ammonoids were among the fastest marine clades to recover (Brayard et al. 2009). Recent works (Brayard et al 2006 & 2009, Brühwiler et al. 2010) indicate that ammonoid diversity started increasing within the Dienerian and first peaked during the middle Smithian. Detailed studies on Dienerian ammonoids mainly focus on the Boreal Realm (e.g. Tozer 1961, 1963, 1994 for British Columbia and Arctic Canada, and Popov 1961, Ermakova 1981 and Dagys and Ermakova 1996 for Siberia). Within the low palaeolatitude belt, only a few localities yielding well preserved material have been recently studied, (e.g. Shigeta and Zakharov 2009 in Primorye, Mu et al. 2007, Brühwiler et al. 2008 in Southern China and Ware et al. 2011 in Nevada) and more comprehensive successions such as the Nepalese one are obscured by extremely poor preservation (Waterhouse 1994, 1996a, 1996b). The best preserved, low palaeolatitude comprehensive successions of Dienerian ammonoids are situated on the Northern Indian Margin (NIM). With the exception of Guex (1978) who described a few Dienerian species from the Salt Range (Pakistan), the pioneer works of

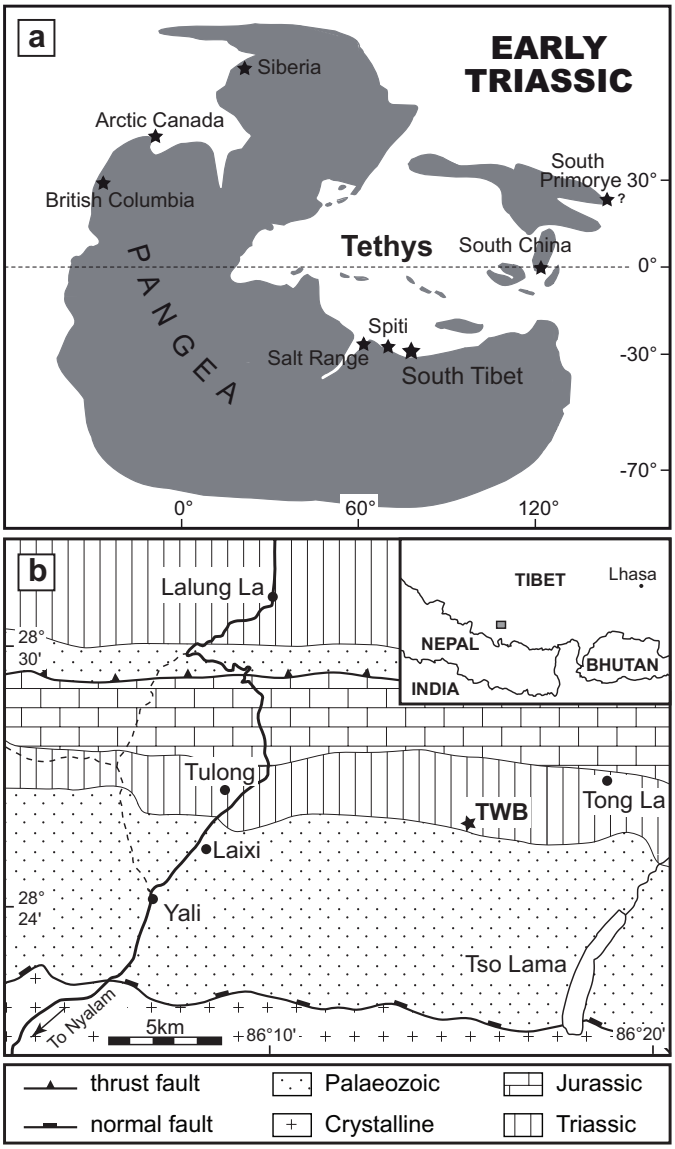

Fig. 1. (**a**) Simplified Early Triassic palaeogeography (modified after Brayard et al., 2006) and palaeoposition of South Tibet and other localities cited in the text. (**b**) Geological sketch map of the studied area and location of the studied section (TWB: Tong La West B section; modified from Brühwiler et al. 2009 and from Burg 1983).

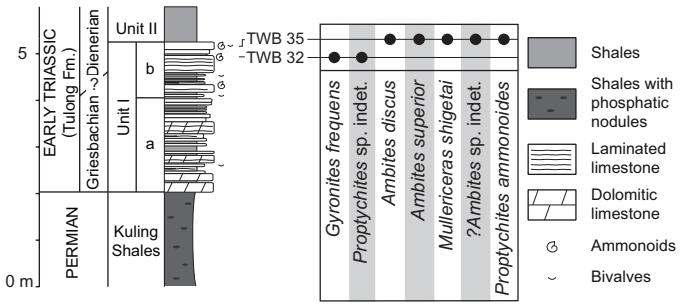

Fig. 2. Base of section TWB with stratigraphic position of ammonoids (modified after Brühwiler et al. 2009).

Waagen (1895) for the Salt Range and Diener (1895) and Krafft & Diener (1909) for north-western Indian Himalaya were lacking high resolution stratigraphic information as well as quantifications of intraspecific variation. This lack has now been filled by Ware et al (in press a & b), who extensively revised the taxonomy and biochronology of Dienerian ammonoids from the Salt Range and Spiti. They recognized twelve different maximal local horizons in the Salt Range, making the Dienerian sequence of this region the most resolved biostratigraphic record worldwide. Ten out of these twelve regional zones have also been recognised in Spiti. In order to assess the lateral reproducibility of these 12 biozones – a prerequisite for the definition of any robust biozonation at the palaeogeographic scale of the NIM – similar detailed studies must be conducted in other basins of the NIM. The present work focuses on the Dienerian ammonoid faunas from a new section (Brühwiler et al. 2009) located near the village of Tulong (South Tibet) and their correlation with the biostratigraphical scheme established in the Salt Range and Spiti.

Wang & He (1976) first reported Early Triassic ammonoids from Southern Tibet, but without precise stratigraphical occurrences and poor illustrations. Since then, several authors described the 'classic' section of Tulong and published other palaeontological information (e.g. Tian 1982, Rao & Zhang 1985, Liu 1992, Liu & Einsele 1994, Garzanti et al. 1998, Shen et al. 2006). Additional work by Brühwiler et al (2009) revealed that this 'classic' section (Tulong, Fig. 1b) was faulted and incomplete. They also discovered a new and much more complete section on strike, ca. 10 kilometres to the East (locality TWB, Fig. 1b). This TWB section, includes units I and II (Brühwiler et al., 2009), which have been removed by faulting in the classic Tulong section. The Smithian faunas of this area have recently been described in detail (Brühwiler et al., 2010). In the present paper, we describe two distinct Dienerian faunas collected from Unit I of the TWB section. We also discuss their biochronological and palaeogeographical significance.

2. Palaeogeographical and geological context

During Early Triassic times, the NIM was located on the southern side of the Tethys, at a palaeolatitude of about 30° S. The Tulong area was situated in a distal position of the passive NIM, at a palaeolongitude of about 80° W (fig. 1a).

In this area, Triassic rocks form an East-West trending belt of about 3 to 4 km in width. The Early Triassic is represented by the Tulong Formation, which consist of a mixed siliciclastic-carbonate sequence of about 100 meters thick. It rests unconformably on the Upper Permian Kuling shales, which typically contain black phosphatic diagenetic nodules. In the classic Spiti area, the Kuling shales yield ammonoid and brachiopod faunas of Wujianpingian age (e.g. Bucher et al. 1997). The Tulong Formation has been described in detail and subdivided into 6 units by Brühwiler et al. (2009). Its base is marked by an erosive surface. Unit I (fig. 2) consists of 3 m of carbonate rocks with intercalated thin shale layers. Its first part (subunit Ia) is composed of thin-bedded rusty dolomitic limestone which yielded some rare ammonoids too poorly preserved for identification and some typical Griesbachian conodonts (including *Hindeodus parvus*). The second part of unit I (subunit Ib) consists of light grey, thin-bedded shelly limestone. The base of subunit Ib is probably latest Griesbachian in age (occurrence of the conodont *Ng*. ? *discreta* in sample TWB25; Brühwiler *et al*., 2009). Its two uppermost layers yielded the typically Dienerian ammonoids described here. Their age is also confirmed by co-occurring conodonts (*Neospathodus dieneri* group). This unit is overlain by 50 to 100 m of dark green shales with rare carbonate lenses that did not yield any age-diagnostic fossils.

In comparison with the Salt Range and Spiti, the Dienerian ammonoids collected from Tulong are relatively poorly preserved. Their phragmocones are filled with coarse sparry calcite, which often destroys the septa and the suture lines. The body chamber of some specimens is partially filled with pyrite. Because of distortion, only estimates of the proportions of the shells are provided. Despite their poor preservation, most specimens can be clearly identified at the species level.

3. Systematic palaeontology

Systematic descriptions are based on the revised classification established by Ware et al. (in press a & b). As the specimens are distorted, no measurements are available, but to indicate at which size the suture lines have been drawn, the apparent whorl height (aH) is indicated in the figure captions. Also, proportions of the shell are estimated using the ratios of the umbilicus width with the diameter (U/D), of the whorl width with the diameter (W/D) and of the whorl width with the whorl height (W/H). All specimens are curated in the collections of the Palaeontological Institute and Museum of the University of Zurich, Switzerland (PIMUZ).

Class Cephalopoda Cuvier, 1797
Subclass Ammonoidea Agassiz, 1847
Order CERATITIDA Hyatt, 1884
Superfamily Meekocerataceae Waagen, 1895
Family Gyronitidae Waagen, 1895
Genus *Gyronites* Waagen, 1895
Type species. – *Gyronites frequens* Waagen, 1895

***Gyronites frequens* Waagen, 1895**
(Fig. 3)

1895 *Gyronites frequens* Waagen, p. 292-294, Pl. 38, Figs 1, 2 (lectotype), 3, 4; Pl. 40, Fig. 4.
1895 *Gyronites nangaensis* Waagen, p. 297-298, Pl. 37, Fig. 5 (holotype).
1895 *Lecanites psilogyrus* Waagen, p. 280-281, Pl. 39, Fig. 5 (holotype).
1895 *Lecanites undatus* Waagen, p. 281-282, Pl. 38, Figs. 1 (lectotype), 2.
1895 *Prionolobus compressus* Waagen, p. 313-315, Pl. 35, Fig. 3 (holotype).
1895 *Prionolobus plicatus* Waagen, p. 315-316, Pl. 35, Fig. 2 (holotype).
1895 *Prionolobus plicatilis* Waagen, p. 318-319, Pl. 36, Fig. 1 (holotype).
? 1909 *Xenodiscus lilangensis* Krafft *in* Krafft & Diener, p. 97-99, Pl. 25, Figs 6-10.
1909 Xenodiscus khoorensis Krafft *in* Krafft & Diener, p. 88.
1934 *Gyronites frequens* Waagen – Spath, p. 91-92, Fig. 19 [cop. Waagen 1895].
? 1976 *Gyronites psilogyrus* (Waagen) – Wang & He, p. 274, Fig. 7a, Pl. 1, Figs. 9-10.
? 1976 *Prionolobus plicatilis* Waagen – Wang & He, p. 275, Fig. 8a, Pl. 3, Figs. 13-15.
v 1978 *Gyronites frequens* Waagen – Guex, Pl. 1, Fig. 3.
v 1978 *Gyronites undatus* (Waagen) – Guex, Pl. 8, Fig. 3.
? 1996 *Gyronites frequens* Waagen – Waterhouse, p. 33-34, Text-fig. 4A, Pl. 1, Figs. 1-4.
? 1996 *Gyronites planissimus* Koken – Waterhouse, p. 34-35, Text-fig. 4A, Pl. 1, Figs. 5, 8
? 1996 *Gyronites spiralis* Waterhouse, p. 35-36, Text-fig. 4A, Pl. 1, Figs. 6, 7, 9, 10.
non v 2008 *Gyronites frequens* Waagen – Brühwiler et al., p. 1168, Pl. 5, Figs. 7, 8.
v (in press-a) *Gyronites frequens* Waagen – Ware et al., Pl. 3, Figs. 1-3; Pl. 4, Figs. 1-6.
v (in press-b) *Gyronites frequens* Waagen – Ware et al., Pl. 1, Figs. 4-6.

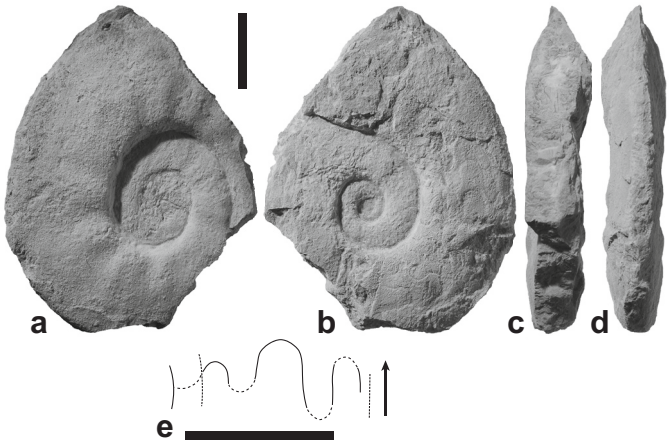

Fig. 3. *Gyronites frequens* Waagen, 1895. PIMUZ30955; incomplete phragmocone. (**e**) Suture line at aH = 13 mm. Scale bar: 1cm.

Material. – One specimen from sample TWB32.
Description. – Evolute (U/D estimated at about 35%), compressed (W/D estimated at about 20%, W/H at 50%) sub-platyconic shell with tabulate venter and angular ventro-lateral shoulders. Flanks slightly curved with maximum whorl thickness just above the umbilical wall. Umbilical wall sub-vertical, not well differentiated from the flanks. Ornamentation reduced to faint radial folds that disappear on the lower third of the flanks. Suture line ceratitic, typical of the genus *Gyronites*, with narrow, very finely indented lateral lobes, a very broad second lateral saddle and very narrow first and third lateral saddles.
Discussion. – This specimen clearly corresponds to a variant of *G. frequens* with low and broad folds, similar to *Lecanites undatus* and *Prionolobus plicatus* of Waagen (1895).

Genus *Ambites* Waagen, 1895
Type species. – *Ambites discus* Waagen, 1895

***Ambites discus* Waagen, 1895**
(Fig. 4)

1895 *Ambites discus* Waagen, p. 152-154, Pl. 21, Figs 4, 5 (lectotype).
1895 *Ambites magnumbilicatus* Waagen, p. 154-155, Pl. 21, Fig. 6 (holotype).
1895 *Koninckites impressus*, p. 263-265, Pl. 35, Fig. 6 (holotype).
1897 *Meekoceras hodgsoni* Diener, p. 133-135, Pl. 6, Fig. 1 (holotype).
? 1897 *Koninckites vidharba* Diener, p. 139-150, Pl. 7, Fig. 9 (holotype).
1905 *Ophiceras discus* (Waagen) – Noetling, Pl. 13: unnumbered text-fig. in footnote 2 (holotype).
non 1905 *Ophiceras discus* (Waagen) – Noetling, Pl. 13, Fig. 4.
p 1909 *Meekoceras lilangense* Krafft *in* Krafft & Diener, Pl. 14, Figs. 1, 2.
p 1909 *Meekoceras hodgsoni* Krafft *in* Krafft & Diener, p. 26-28, Pl. 2, Fig. 9 (holotype).
p? 1909 *Meekoceras hodgsoni* Krafft *in* Krafft & Diener, Pl. 3, Fig. 2.

non 1909 *Meekoceras hodgsoni* Krafft *in* Krafft & Diener, Pl. 30, Fig. 1.
1909 *Meekoceras* cf. *discus* (Waagen) – Krafft & Diener, p. 47-50, Pl. 6, Fig. 2.
1934 *Prionolobus impressus* (Waagen) – Spath, p. 100-101, Fig. 22 [cop. Waagen 1895].
1934 *Ambites discus* Waagen – Spath, p. 102-103, Fig. 23 [cop. Waagen 1895].
? 1976 *Prionolobus tulungensis* Wang & He, p. 277, Fig. 8d, Pl. 2, Figs 13-15 (holotype).
1985 *Prionolobus impressus* (Waagen) – Pakistani-Japanese Research group, Pl. 12, Fig. 1.
? 2007 *Prionolobus impressus* (Waagen) – Mu *et al.*, p. 869, Figs. 12.4, 13.1-13.3.
v (in press-a) *Ambites discus* Waagen – Ware et al., Pl. 6, Figs. 1-13; Pl. 7, Figs. 1-6.
v (in press-b) *Ambites discus* Waagen – Ware et al., Pl. 3, Figs. 1-3.

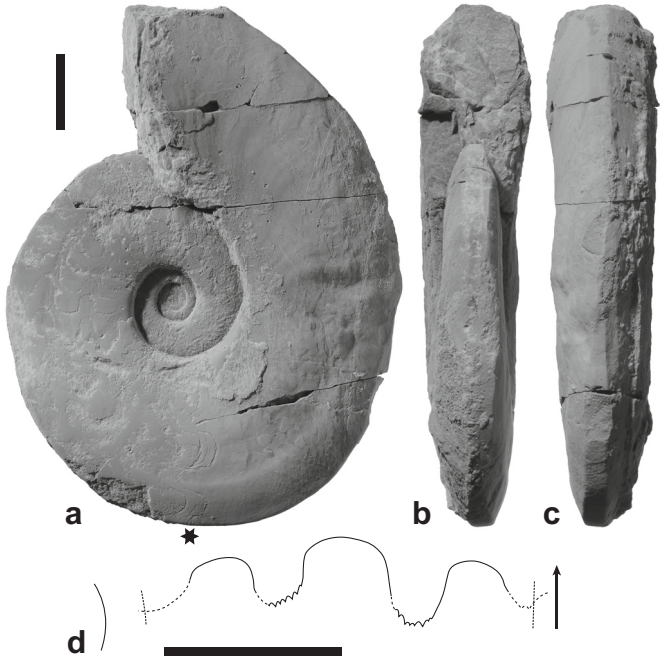

Fig. 4. *Ambites discus* Waagen, 1895. PIMUZ30956; nearly complete specimen. (**d**) Suture line at aH = 22.5 mm. Scale bar: 1cm. Asterisk indicates last septum.

Material. – 5 specimens from sample TWB35.
Description. – Platyconic shell with tabulate, bottleneck-shaped venter and angular ventro-lateral shoulders. Moderately broad umbilicus (U/D estimated at about 25%) with very low, indistinct umbilical wall. Flanks subdivided into three parts by two spiral folds bracketing the second lateral saddle, imparting the whorl section a flattened, sub-octagonal shape. External third of the flanks flat and converging towards the venter, middle part of the flanks flat and sub-parallel, and inner third of the flanks slightly convex, converging towards the umbilicus where they suddenly bend to form a low vertical umbilical wall. Weak sigmoidal folds visible on flanks. Suture line ceratitic with three lateral saddles separated by two finely denticulated lateral lobes, lateral lobes and saddles having approximately the same width. First lateral saddle rounded, second and third one flattened. Auxiliary series not exposed.
Discussion. – The best preserved specimen, figured here, is typical of this species. Additional specimens agree with material from the Salt Range and Spiti assigned to this species.

***Ambites superior* (Waagen, 1895)**
(Fig. 5)

1895 *Gyronites superior* Waagen, p. 294-295, Pl. 37, Fig. 6 (holotype).
? 1895 *Prionolobus ovalis* Waagen, p. 316-317, Pl. 35, Fig. 1 (holotype).
p? 1909 *Meekoceras disciforme* Krafft *in* Krafft & Diener, p. 45-47, Pl. 3, Figs. 5-6.
v (in press-a) *Ambites superior* (Waagen) – Ware et al., Pl. 10, Figs. 10-12; Pl. 11, Figs. 1-9; Pl. 12, Fig. 1.

Material. – Five specimens from sample TWB35.
Description. – Evolute, platyconic shell with tabulate bottleneck shaped venter. Involution varying from very evolute shells (see fig. 5-2, with U/D estimated to ca. 40%) to moderately evolute (see fig. 5-1, with U/D estimated at about 35%) platyconic shells. Very broad umbilicus with very short and vertical umbilical wall. Ornamentation characterized by two spiral folds and indistinct sigmoidal folds on flanks (similar to *A. discus*). Suture line ceratitic with narrow lateral lobes, a very wide second lateral saddle and narrow first and third lateral saddles, very similar to that of *Gyronites* but with stronger denticulation in the lobes.
Discussion. – Specimens assigned to this species clearly differ from *A. discus* by their more evolute coiling. This species is here reported for the first time outside the Salt Range, thus revealing its importance for correlations.

***?Ambites* sp. indet.**
(Fig. 6)

Material. – One specimens from sample TWB35.
Description. – Platyconic shell with tabulate venter, angular ventro-lateral shoulders and relatively thick whorl section. Umbilicus moderately broad with high umbilical wall and sharp shoulders. Ornamentation characterized by strong radial ribs. Suture line not preserved.
Discussion. – This poorly preserved fragment differs from the previously described species of *Ambites* by its thicker whorl section and its stronger ribbing. However its preservation is not sufficient for identification at the species level. Its general shape is close to that of

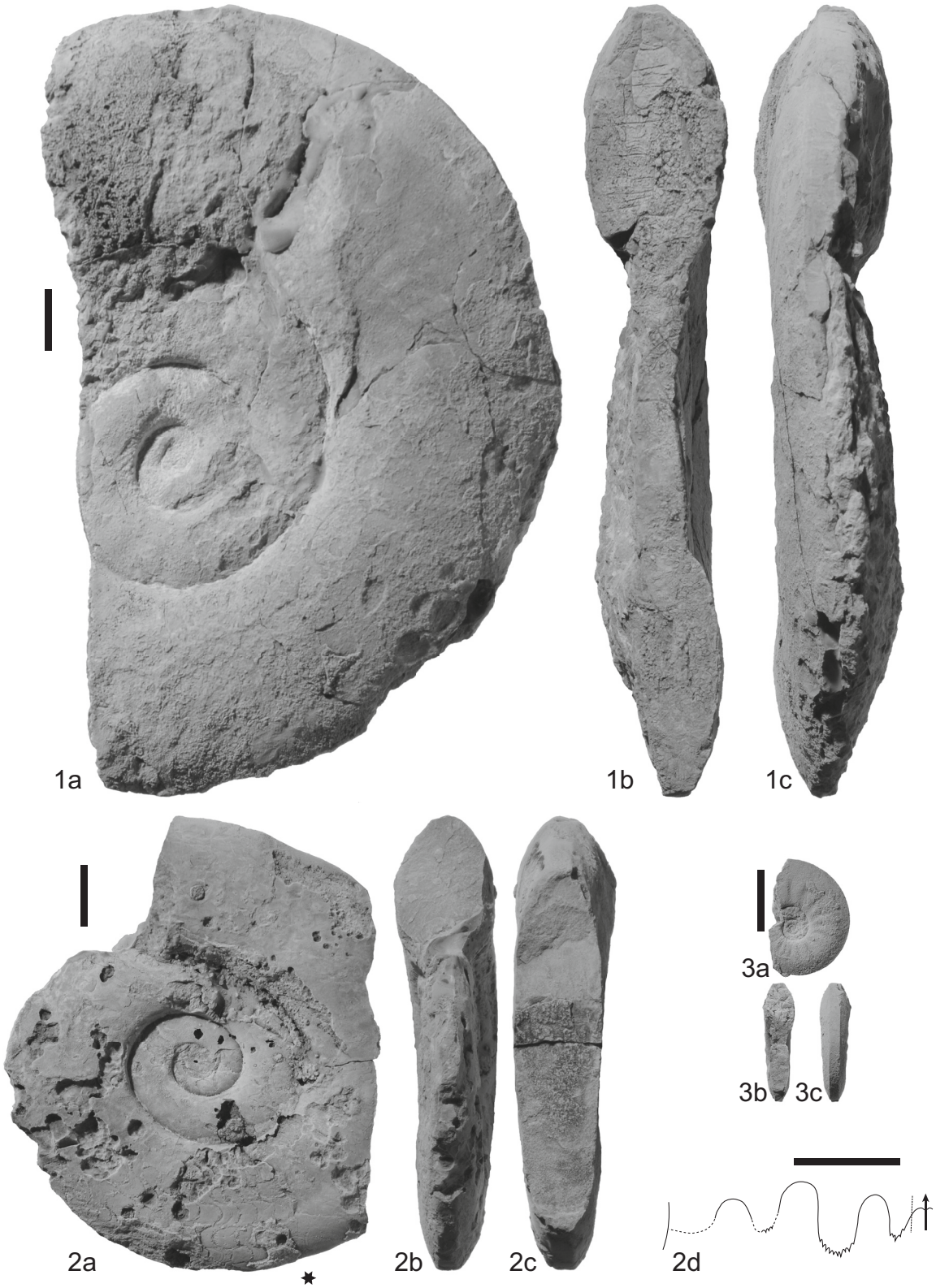

Fig. 5. *Ambites superior* (Waagen, 1895). (**1**) PIMUZ30958; suture lines not preserved. (**2**) PIMUZ30957; specimen with partly preserved body chamber. (**2d**) Suture line at aH = 22 mm. (**3**) PIMUZ30959; Juvenile, incomplete phragmocone. Scale bar: 1cm. Asterisk indicates last septum.

specimens ascribed by Tozer (1994) to his new genus *Pleurambites*. The later genus is here considered as a synonym of the genus *Ambites*, the strong ribbing being only the result of the thicker whorl section as expressed by Buckman's law of covariation (Westerman, 1966).

Family Mullericeratidae Ware, Jenks, Hautmann & Bucher, 2011

Genus *Mullericeras* Ware, Jenks, Hautmann & Bucher, 2011

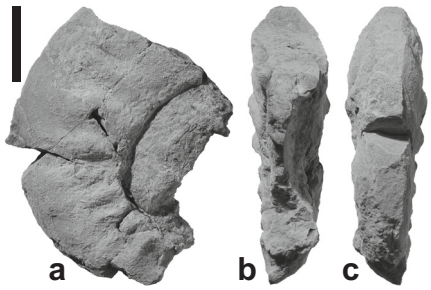

Fig. 6. ?*Ambites* sp. indet. PIMUZ30960. Scale bar: 1cm.

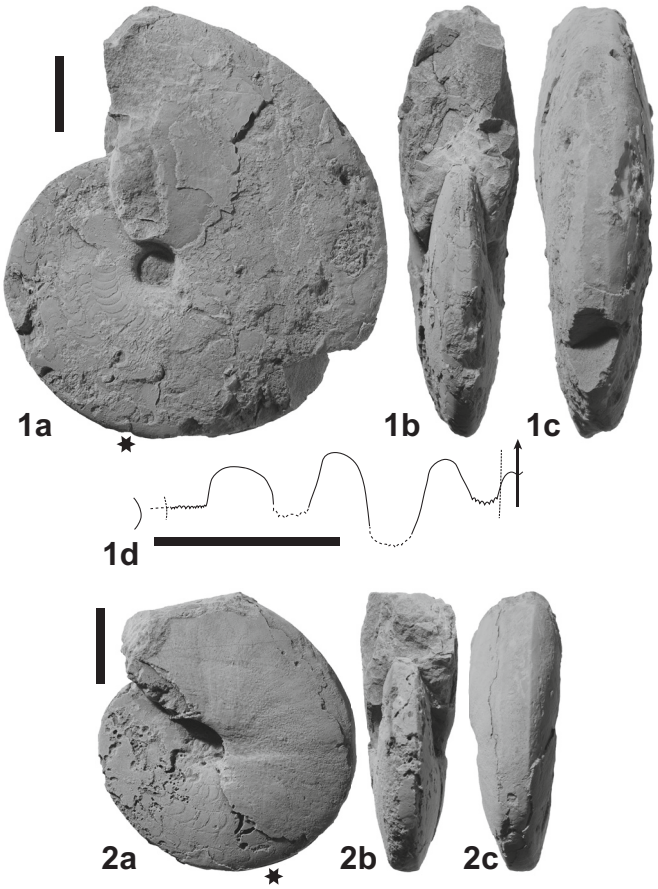

Fig. 7. *Mullericeras shigetai* Ware and Bucher (in press a). (**1**) PIMUZ30963; with partly preserved body chamber. (**1d**) Suture line at aH = 18.6 mm. (**2**) PIMUZ30964; nearly complete specimen. Scale bar: 1cm. Asterisks indicate last septum.

Type species. **–** *Mullericeras spitiensis* (Krafft, 1909)
***Mullericeras shigetai* Ware and Bucher (in press-a)**
(Fig. 7)

?p 1994 *Ambites fuliginatus* Tozer, Pl. 13, Fig. 4.
?p 1994 *Ambites ferruginus* Tozer, Pl. 14, Figs. 1, 2, 5, 6.
? 2009 *Ambitoides fuliginatus* Tozer – Shigeta & Zakharov, p. 77-79, Figs. 63-64.
?v 2011 *Ussuridiscus* sp. indet. – Ware et al., p. 169, Fig. 8a.
v (in press-a) *Mullericeras shigetai* Ware and Bucher *in* Ware et al., Pl. 27, Figs. 2 (holotype), 3-7.
v (in press-b) *Mullericeras shigetai* Ware and Bucher *in* Ware et al., Pl. 12, Figs. 1-2.

Material. **–** Seven specimens from sample TWB35.
Description. **–** Very involute (U/D estimated to ca. 10%) sub-platyconic shell with a tabulate venter and sharp ventro-lateral shoulders. Umbilicus narrow and deep, with vertical to slightly overhanging umbilical wall and sharp shoulders. No visible ornamentation. Suture line ceratitic with a very wide ventral lobe, relatively narrow and rounded first and second lateral lobes and saddles, the second lateral saddle being slightly bent towards the umbilicus. Third lateral saddle broadly arched and relatively elongated auxiliary series finely denticulated.
Discussion. – These specimens are strictly identical to *Mu. shigetai* described from the Salt Range and Spiti.

Family Proptychitidae Waagen, 1895
Genus *Proptychites* Waagen, 1895
Type species. – *Ceratites lawrencianus* de Koninck, 1863

***Proptychites ammonoides* Waagen, 1895**
(Fig. 8)

1895 *Proptychites ammonoides* Waagen, p. 171-173, Pl. 17, Fig. 1 (lectotype), Pl. 19, Fig. 2.
1909 *Aspidites crassus* Krafft *in* Krafft & Diener, p. 58-59, Pl. 6, Fig. 4, Pl. 7, Fig. 1, Pl. 8, Fig. 1.
1909 *Koninckites haydeni* Krafft *in* Krafft & Diener, p. 68-70, Pl. 17, Figs 1, 2, 3 (lectotype), 4- 6.
1909 *Koninckites alterammonoides* Krafft *in* Krafft & Diener, p. 70-72, Pl. 16, Figs. 1 (lectotype), 2.
? 1996 *Aspitella crassa* (Krafft) – Waterhouse, p. 51, Text-

Fig. 8. *Proptychites ammonoides* Waagen, 1895. PIMUZ30961; specimen with partly preserved body chamber. (**d**) Suture line at aH = 21.9 mm. Scale bar: 1cm. Asterisk indicates last septum.

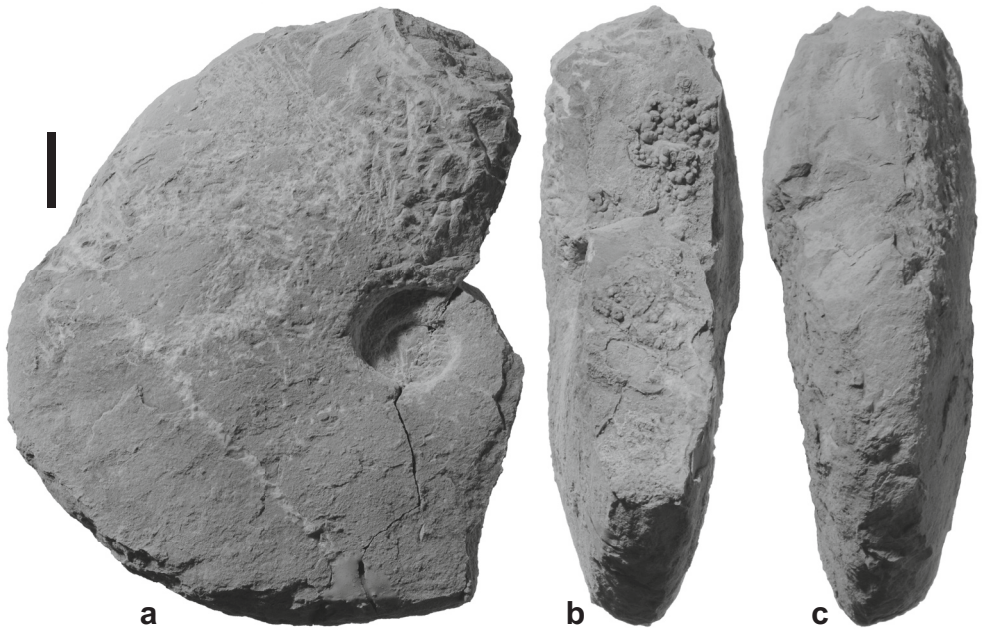

Fig. 9. *Proptychites* sp. indet. PIMUZ30962; suture lines not preserved. Scale bar: 1cm.

fig. 41, Pl. 3, Figs. 2-4.
2009 *Proptychites alterammonoides* (Krafft) – Shigeta & Zakharov, p. 110-112, Figs. 98, 99.
v 2011 *Proptychites haydeni* (Krafft) – Ware *et al.*, p. 173-175, Figs. 15-17.
v (in press-a) *Proptychites ammonoides* Waagen – Ware et al., Pl. 24, Fig. 5; Pl. 25, Figs. 1-4; Pl. 26, Fig. 1.
v (in press-b) *Proptychites ammonoides* Waagen – Ware et al., Pl. 10, Figs. 5-8; Pl. 11, Fig. 1.

Material. – Five specimens from sample TWB35.
Description. – Involute, relatively thick discoidal shell with rounded venter and no visible ventro-lateral shoulders. Umbilicus narrow and deep, with high vertical wall and rounded shoulders. Flanks convex with maximum whorl width at inner third of flank. No visible ornamentation. Suture line with elongated thin saddles slightly bent towards the umbilicus, broad and deeply indented lobes; auxiliary series not completely exposed but with an individualized auxiliary lobe.
Discussion. – The specimens from Tulong are generally of small size (between 5 and 8 cm) compared to the ones from the Salt Range. However, most of them are incomplete phragmocones, and one fragment of a much larger specimen has also been found. Their morphology is also identical to *Prop. ammonoides* described from the Salt Range and Spiti.

***Proptychites* sp. indet.**
(Fig. 9)

Material. – One specimen from sample TWB32.
Description. – Large, involute and thick shell with rounded venter and indistinct ventro-lateral shoulders. Umbilicus deep and narrow, with vertical wall and narrowly rounded shoulders. No visible ornamentation or suture line.
Discussion. – This specimen differs from *Proptychites ammonoides* by its slightly more open umbilicus and its thicker whorl section. Its general shape is in agreement with that of the genus *Proptychites*. However, the poor preservation prevents assignment at the species level.

4. Discussion.

As can be seen on figure 2, the two fossiliferous layers from Unit Ib in section TWB contain two very distinct faunal assemblages. Not surprisingly, these two faunas are identical to those from the Salt Range (Pakistan) and Spiti (India) recently revised by Ware et al. (in press a & b). *Gyronites frequens*, the only clearly identified species from sample TWB32, is the index species of the topmost horizon of the early Dienerian in the Salt Range and Spiti. The second fauna (sample TWB35) contains two species of *Ambites* (*A. discus* and *A. superior*), which are characteristic of two distinct and consecutive regional zones of middle Dienerian age in the Salt Range, (Ware et al., in press-a). Bed TWB35 is therefore interpreted as being condensed and it corresponds to a mixture of the *A. discus* beds and the *A. superior* beds of the Salt Range.

The *G. frequens* and the *A. discus* regional zones are also present in the Spiti District. Finding these two horizons in the Salt Range, the Spiti District and South Tibet demonstrates that they are laterally reproducible throughout the NIM and thus can be useful for defining laterally reproducible biozones for this province. Furthermore, it indicates that the NIM was a homogenous, well defined palaeobiogeographical domain during the Early and Middle Dienerian. The *A. superior* regional zone has however only been clearly identified in a single locality in the Salt Range. The presence of its characteristic species in South Tibet,

although in a condensed horizon, may indicate a regional significance for this horizon, but finding other non-condensed occurrences in the NIM would be necessary for this regional zone to qualify as a NIM-biozone.

Correlation of these two faunas outside the Northern Indian Margin is made difficult by the general scarcity of Dienerian faunas. Shigeta et al. (2009) described the genus *Gyronites* from Primorye and they considered it as upper Griesbachian in age (*Gyronites subdharmus* zone). Yet, *Gyronites* has never been found anywhere else, and its absence from the Canadian Arctic, where the Griesbachian and Dienerian stages have been formally defined by Tozer (1961) explains why it is considered as either Griesbachian or Dienerian depending on the authors. Tozer (1965) defined the base of the Dienerian by the appearance of Gyronitidae, a definition which we consider as valid. The genus *Ambites* has been found in Primorye (Shigeta et al. 2009), in the *Ambitoides fuliginatus* zone, and in British Columbia and Arctic Canada (Tozer 1994) in the *Proptychites candidus* zone. The genus *Ambites* is also known from the Candelaria Hills (Nevada, USA; Ware et al., 2011) and from South China (Brühwiler et al., 2008). This fauna has never been found in Siberia (e.g. Dagys & Ermakova 1996). The genus *Ambites* is characteristic of the middle Dienerian as defined by Ware et al. (in press-a), which was placed into the early Dienerian of the two-fold subdivision of Tozer (1965).

References

Brayard, A., Bucher, H., Escarguel, G., Fluteau, F., Bourquin, S. & Galfetti, T. 2006. The Early Triassic ammonoid recovery: Paleoclimatic significance of diversity gradients. Palaeogeography, Palaeoclimatology, Palaeoecology, 239, 374-395.

Brayard, A., Escarguel, G., Bucher, H., Monnet, C., Brühwiler, T., Goudemand, N., Galfetti, T. & Guex, J. 2009. Good Genes and Good Luck: Ammonoid Diversity and the End-Permian Mass Extinction. Science, 325, 1118-1121.

Brühwiler, T., Brayard, A., Bucher, H. & Guodun, K. 2008. Griesbachian and Dienerian (Early Triassic) Ammonoid Faunas from Northwestern Guangxi and Southern Guizhou (South China). Palaeontology 51 (5), 1151-1180.

Brühwiler, T., Goudemand, N., Galfetti, T., Bucher, H., Baud, A., Ware, D., Hermann, E., Hochuli, P.A. & Martini R. 2009. The Lower Triassic sedimentary and carbon isotope records from Tulong (South Tibet) and their significance for Tethyan palaeoceanography. Sedimentary Geology, 222, 314-332.

Brühwiler, T., Bucher, H. & Goudemand, N. 2010. Smithian (Early Triassic) ammonoids from Tulong, South Tibet. Geobios 43, 403-431.

Bucher, H., Nassichuk, W.W. & Spinosa, C. 1997. A new occurrence of the upper Permian ammonoid *Stacheoceras trimurti* Diener from the Himalayas; Himachal Pradesh, India.- Eclogae Geologicae Helveticae 90, 599-604.

Burg, J.P. 1983. Carte géologique du sud du Tibet / Ministère de la Géologie – Pékin (république populaire de Chine); Contours synth. par J.P. Burg. China. Ministry of Geology and Mineral Resources, Paris.

Dagys, A.S. & Ermakova, S. 1996. Induan (Triassic) ammonoids from North-Eastern Asia. Revue de Paléobiologie 15 (2), 401-447.

Diener, C. 1897. Part I. The Cephalopoda of the Lower Trias. Palaeontologia Indica, Series 15 (2), 181pp.

Ermakova, S.V. 1981. Ammonoids and biostratigraphy of the Lower Triassic of the Verkhoyansk Range. U.S.S.R. Academy of Sciences, Yakutsk Filial, Geological Institute, Nauka, Moscow, 138 pp. [in Russian].

Garzanti, E., Nicora, A. & Rettori, R. 1998. Permo-Triassic boundary and lower to middle Triassic in South Tibet. Journal of Asian Earth Sciences 16, 143–157.

Guex, J. 1978. Le Trias inférieur des Salt Ranges (Pakistan): problèmes biochronologiques. Eclogae Geologia Helvetica 71 (1), 105-141.

Krafft, A.V. & Diener, C. 1909. Lower Triassic cephalopoda from Spiti, Malla Johar, and Byans. Palaeontologia Indica, Series 15, 6 (1), 186 pp.

Liu, G. 1992. Permian to Eocene sediments and Indian passive margin evolution in the Tibetan Himalayas. Tübinger Geowissenschaftliche Arbeiten. Reihe A 13, 1–268.

Liu, G. & Einsele, G. 1994. Sedimentary history of the Tethyan basin in the Tibetan Himalayas. Geologische Rundschau 83, 32–61.

Mu, L., Zakharov, Y.D., Li, W.-Z. & Shen, S.-Z. 2007. Early Induan (Early Triassic) cephalopods from the Daye Formation at Guiding, Guizhou Province, South China. Journal of Paleontology 81 (5), 858-872.

Popov, Y.N. 1961. Triassic ammonoids of northeast USSR. Transactions, Scientific Research Institute for the Geology of the Arctic (NIIGA), v. 79, 179 pp. [in Russian].

Rao, R.B. & Zhang, Z.G. 1985. A discovery of Permo–Triassic transitional fauna in the Qomolangma Feng area: its implications for the Permo–Triassic boundary. Xizang Geology 1, 19–31.

Shen, S.-Z., Cao, C.-Q., Henderson, C.M., Wang, X.-D., Shi, G.R., Wang, Y. & Wang, W. 2006. End-Permian mass extinction pattern in the northern peri-Gondwanan region. Palaeoworld, 15, 3-30.

Shigeta, Y. & Zakharov, Y.D. 2009. Systematic paleontology: cephalopods, 44-140. In: Shigeta, Y., Zakharov, Y.D., Maeda, H. & Popov, A.M. (eds.) 2009. The Lower Triassic system in the Abrek Bay

area, South Primorye, Russia. National Museum of Nature and Science, Tokyo, 218pp.

Tian, C.R. 1982. Triassic conodonts in the Tulong section from Nyalam County, Xizang (Tibet), China. Contributions to Geology Qinghai-Xizang (Tibet) Plateau 8, 153–165.

Tozer, E.T. 1961. Triassic stratigraphy and faunas, Queen Elizabeth Islands, Arctic Archipelago. Geological Survey of Canada, Memoir 316, 116 pp.

Tozer, E.T. 1963. Lower Triassic ammonoids from Tuchodi Lakes and Halfway River areas, northeastern British Columbia. Geological Survey of Canada, bulletin 96, 1-28.

Tozer, E.T. 1994. Canadian Triassic Ammonoid Faunas. Bulletin of the Geological Survey of Canada, bulletin 467, 663 pp.

Waagen, W. 1895. Salt Ranges Fossils. vol. 2: Fossils from the Ceratites formation - Part I - Pisces, Ammonoidea. Palaeontologia Indica, Series 13, 323 pp.

Wang, Y.G. & He, G.X. 1976. Triassic ammonoids from the Mount Jolmo Lungma region. A report of scientific expedition in the Mount Jolmo Lungma region (1966-1968). Paleontology 3, 223–502 [in Chinese].

Ware, D., Jenks, J.F., Hautmann, M. & Bucher, H. 2011. Dienerian (Early Triassic) ammonoids from the Candelaria Hills (Nevada, USA) and their significance for palaeobiogeography and palaeoceanography. Swiss Journal of Geoscience 104, 161-181.

Ware, D., Bucher, H., Brühwiler, T., Schneebeli-Hermann, E., Hochuli, P.A., Roohi, G., ur-Rehman, K. & Yaseen, A. (in press-a). Induan (Early Triassic) ammonoids from the Salt Range, Pakistan. Fossil and Strata.

Ware, D., Bucher, H., Brühwiler, T. & Krystyn, L. (in press-b). Dienerian (Early Triassic) ammonoids from Spiti (Himashal Pradesh, India). Fossil and Strata.

Waterhouse, J.B. 1994. The Early and Middle Triassic ammonoid succession of the Himalayas in western and central Nepal. Part 1, stratigraphy, classification and Early Scythian ammonoid systematics. Palaeontographica, Abteilung A, 232, 1–83, pls 1–6.

Waterhouse, J.B. 1996a. The Early and Middle Triassic ammonoid succession of the Himalayas in western and central Nepal. Part 2, systematic studies of the early Middle Scythian. Palaeontographica Abteilung A, 241, 27–100, pls 1–12.

Waterhouse, J.B. 1996b. The Early and Middle Triassic ammonoid succession of the Himalayas in western and central Nepal, Part 3, late Middle Scythian ammonoids. Palaeontographica Abteilung A, 241, 101–167, pls 1–11.

Westerman, G.E.G. 1966: Covariation and taxonomy of the Jurassic ammonite *Sonninia adicra* (Waagen). Neues Jahrbuch für Mineralogie, Geologie und Paläontologie, Abhandlungen 124, 289–312.

CHAPTER 5

High-resolution biochronology and diversity dynamics of the Early Triassic ammonoid recovery: the Dienerian faunas of the Northern Indian Margin

High-resolution biochronology and diversity dynamics of the Early Triassic ammonoid recovery: the Dienerian faunas of the Northern Indian Margin

David Ware[a,*], Hugo Bucher[a,*], Arnaud Brayard[b], Elke Schneebeli-Hermann[a], Thomas Brühwiler[a]

[a] Paläontologisches Institut und Museum der Universität Zürich, Karl Schmid-Strasse 4, CH-8006 Zürich, Switzerland
[b] UMR CNRS 5561 Biogéosciences, Université de Bourgogne, 6 Bd. Gabriel, 21000 Dijon, France
* Corresponding authors. Tel.: +41 44 634 23 34; fax: +41 44 634 49 23.
E-mail addresses: david.ware@pim.uzh.ch (D. Ware), hugo.fr.bucher@pim.uzh.ch (H. Bucher).

Keywords: Early Triassic recovery – Dienerian – Ammonoids – Northern Indian Margin – Biochronology – Diversity

Abstract

Following the recent revision of the taxonomy and biostratigraphy of Dienerian ammonoids from the Salt Range (Pakistan) and from Spiti (Northern India), a new high resolution biozonation based on the Unitary Association (UA) method is constructed for the Dienerian of the Northern Indian Margin. It includes 12 UA-zones and leads to subdivide the Dienerian into three parts (early, middle and late). The corresponding diversity analyses, coupled with results previously obtained for the early Smithian of the same regions, highlight the four following phases: (1) a first modest peak of diversity in the early Dienerian; (2) a very low diversity persisting throughout the middle Dienerian; (3) a slow increase of diversity during the late Dienerian, and (4) a marked diversification in the early Smithian. Turnover rates are very high during this entire time interval, and the boundaries between early-middle and middle-late Dienerian are emphasized by complete renewals of the faunas. The low diversity values in the middle and early late Dienerian are concomitant with an anoxic event and coincide with warmer temperatures than those of the early Dienerian and early Smithian. This diversity pattern stands in strong contrast with the credo of a protracted or stepwise recovery following the end-Permian mass extinction. Together with the end-Smithian extinction, the middle and early late Dienerian diversity crises were both radical setbacks in the recovery of Early Triassic ammonoids. However, these two diversity crises do not necessarily imply identical environmental triggers that ultimately led to anoxic bottom waters on outer platforms in both cases.

1. Introduction

Modes and rates of biotic recovery following the end-Permian mass extinction are currently attracting a lot of efforts. Ammonoids have been documented to be one of the fastest clade to recover and even to largely overshoot their previous Permian record highs (Brayard et al., 2009). At the genus level, ammonoids show a low diversity in the Griesbachian, a slight increase during the Dienerian and an explosive radiation in the early Smithian (Brayard et al., 2009). Such a study provides the general outline of diversity trends, but is also influenced by uneven taxonomical practices across authors, relatively coarse time bins and the absence of consensus about some stage and sub-stage boundaries. More recently, a significant advance toward a refined diversity analysis (Brühwiler et al., 2010) hinged on a new, highly resolved biozonation of the Smithian from the Northern Indian Margin (NIM).

The NIM has long been recognised as a key area for the establishment of the Early Triassic time scale. The Salt Range (Pakistan) and Spiti District (Northern India; fig. 1) are especially notorious for their abundant and well preserved ammonoid faunas since the pioneer works of Waagen (1895) in the Salt Range and of Diener (1897) and Krafft & Diener (1909) in Spiti. However, until recently, no thorough and modern revisions of the taxonomy and biostratigraphy of the ammonoids of these two regions have been published. The understanding of most taxa described in these pioneering works is hampered by the small sample sizes and their at best approximate stratigraphic positions. Following the revision of the Smithian ammonoids from the Salt Range (Brühwiler et al. 2012a) and Spiti district (Brühwiler et al. 2012b), new abundant and well-preserved material allowed us to thoroughly revise the taxonomy and biostratigraphy of the Dienerian ammonoids from these two basins (Ware et al., in press-a & b). As for the Smithian, they represent the most complete and detailed Dienerian ammonoid records known worldwide, with 12 Dienerian local maximal horizons in the Salt Range and 10 in Spiti, compared to only 4 horizons in Canada (Tozer, 1994), 3 in Primorye (Shigeta et al., 2009) and 4 in Siberia (Dagys and Ermakova, 1996).

Here we present a new high-resolution zonation for the Dienerian of the NIM based on a synthetic biochronological analysis of the Salt Range and Spiti basins at the species level. This new biostratigraphic scheme is based on bed by bed extensive collections in order to produce a reliable taxonomy reflecting intraspecific vari-

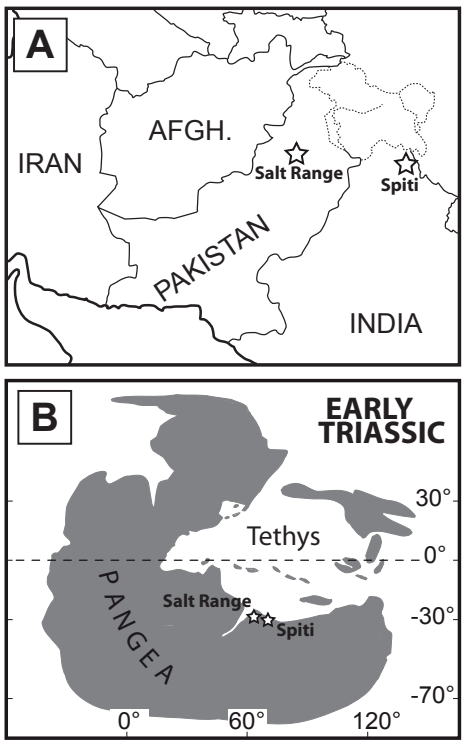

Fig. 1. [A] Situation of the Salt Range and Spiti; **[B]** simplified early Triassic palaeogeography (modified after Brayard et al., 2006) with the position of the Salt Range and Spiti.

ation as well as the best possible resolution in time. Correlation of the Dienerian ammonoid succession of the NIM with other regions will need additional, similarly detailed work. This succession of the NIM provides a robust reference scheme for Dienerian times and further correlations at larger geographical scales. The hitherto poorly know Dienerian faunas can now contribute to an improved understanding of the Early Triassic recovery. The new highly resolved biostratigraphic frame allows the analysis of the biodiversity dynamics of the Dienerian ammonoids from the NIM with unprecedented detail, and to compare it with palaeoenvironmental proxies obtained from the same sections.

2. Material and methods

The method used here is the same as in Brühwiler et al. (2010). Hence, only a short description is provided below. The reader is referred to Brühwiler et al. (2010) for further details. The new Dienerian biostratigraphic frame and ammonoid diversity data can thus be directly compared to the Smithian ones of Brühwiler et al. (2010, updated according to Brühwiler et al. 2012a and the new classification established in Ware et al., in press-a), thus significantly expanding downward the available high-resolution time window within the Early Triassic of the NIM.

2.1. Taxonomic data sets

In the Salt Range, Dienerian ammonoids were collected from four areas (Nammal, Chiddru, Amb and Wargal). Several sections were sampled in these four areas, and a composite section was constructed for each of them based on bed-by-bed correlations, an approach recommended by Guex (1991) for enhancing the completeness of the stratigraphic ranges of species. In Spiti, Dienerian ammonoids were collected from 8 sections distributed in three areas (Mud, Guling and Lalung). However, lateral lithological changes prevented constructing a composite section for each of these three areas.

The first step consists in a detailed revision and standardization of the ammonoid taxonomy, with special emphasis on intraspecific and ontogenetic variation. The results of this revision are presented in Ware et al. (in press-a and b). This led to an improved understanding of the taxonomy of Dienerian ammonoids, inclusive of above the specific level, where many genera were so far poorly defined. A grand total of 47 species were recognised. For the biochronological analysis, occurrences based on poorly preserved material or based on rare taxa found in only a single sample were removed from the initial dataset. For the Dienerian, five such species with unique occurrences were omitted and then re-inserted in the dataset after completion of the biozonation.

2.2. Unitary Association method

The biozonation presented here is based on the Unitary Associations (UA) method of Guex (1991). A general account of the advantages of this method is given in Brühwiler et al. (2010), and for the exhaustive description of the UA method the reader is referred to Guex (1991) and Monnet and Bucher (2002). The UA analysis was performed with the palaeontological data analysis software PAST (Hammer et al., 2001). This method has several crucial advantages. First, UAs are discrete (non-continuous) time bins consisting of unique and mutually exclusive assemblages of taxa, isolated from each other by intervals of separation, thus faithfully reflecting the discontinuous nature of the fossil record. These exclusive assemblages are maximal sets of co-occurring species and can accommodate any later modification of the data set without creating conflicting superpositional relationships such as is the case for all approaches based on the fluctuating positions of First Occurrences and Last Occurrences. Second, Escarguel and Bucher (2004) demonstrated that such zones based on the maximal association principle provide reliable counts of species richness, *whatever* the unknown duration of each UA-zone. The construction of UA-zones includes the following steps. First, an occurrence matrix for every section of

the Salt Range and Spiti is built (Appendix A – Table 1). Then, the regional UAs for the Salt Range and Spiti are computed separately using PAST. The regional zonations and species occurrences obtained (Appendix A – Table 2) are thus treated as a two sections dataset, which is again processed with PAST to obtain UAs at the NIM palaeogeographical level. Taxa with a single occurrence that were initially removed from the dataset are then dated and re-inserted into the zonation. Finally, UAs having a poor lateral reproducibility and/or which are based on very rare characteristic species are merged to construct the UA-zones sequence for the NIM (see discussion in Section 4.1).

2.3. Diversity dynamics

Analyses of diversity dynamics follow the same procedure as Brühwiler et al. (2010). Species richness corresponds to the number of species in a UA-zone, and originations and extinctions correspond to the number of species which appear and disappear between two successive zones. Origination rate is the number of originations divided by the species richness of the subsequent zone; extinction rate is the number of extinctions divided by the species richness of the previous zone. The turnover is the sum of originations and extinctions, and the turnover rate is the turnover divided by the total species richness of the two corresponding successive zones. A rarefaction analysis on the species richness was conducted using PAST to estimate the bias induced by sample size on species counts. This potential sampling bias was further investigated with incidence-based total richness estimators calculated with Estimates (Colwell, 2009). An additional analysis at the genus level was performed, including the generic richness and the corresponding originations, extinctions and turnovers. These results were completed with a poly-cohort analysis (Raup, 1978, 1986; Foote, 1988; Hartenberger, 1988). Finally, the respective contribution of each family to species richness (both in absolute and relative values) was computed.

2.4. Palaeoenvironmental proxies

The results of the biodiversity analysis are compared to various palaeoenvironmental proxies obtained from the same sections. These include palynofacies data from the Nammal section in the Salt Range, carbonate and organic carbon isotopes from Nammal, Chiddru and Amb in the Salt Range (Hermann et al., 2011, Schneebeli-Hermann et al. 2012), and oxygen isotopes from Nammal (Romano et al., 2013). Since these palaeoenvironmental proxies are obtained from the same sections from which ammonoid data are derived, it is possible to

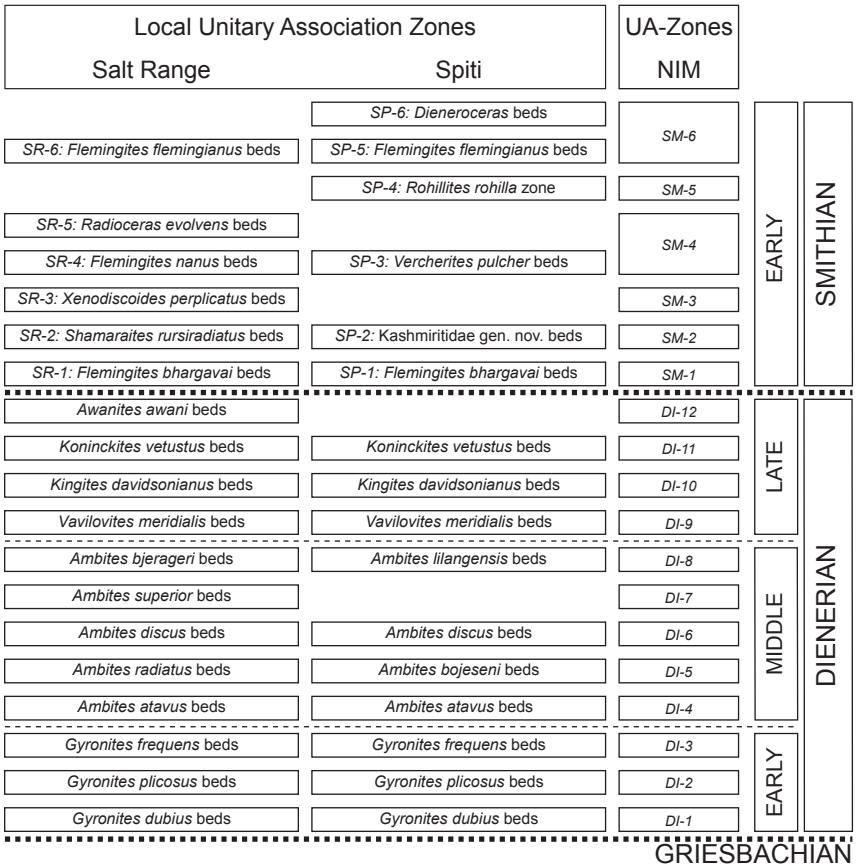

Fig. 2. Unitary Associations (UAs) of each basin and inter-basin UA-zonation.

calibrate them with our new biostratigraphic scheme by using the following piecewise approach. When a data point comes from a bed directly assigned to a UA-zone or is bracketed by beds belonging to the same UA-zone, this point is plotted in the middle of the UA-zone. When several data points are available within one UA-zone, they are plotted at equidistance, in stratigraphic order, within this UA-zone. When one or several data points come from an interval bracketed by two successive UA-zones, they were plotted at equidistance between these two UA-zones. Finally, when one or several data points are bracketed by beds containing faunas characteristic of two non-consecutive UA-zones (i.e. when one or several UA-zones are missing in the section where the data comes from), they were placed at equidistance between the two corresponding UA-zones.

3. Results

3.1. Biochronology

In the Salt Range, the procedure described above led to the recognition of 13 UAs within the Dienerian. However, two of these UAs (SR9 and SR10, see Appendix A – Table 2) are lumped together, because they are only differentiated by a very rare species (*Mullericeras spitiense*). Therefore, 12 UA-zones are recognized for the Dienerian of the Salt Range (fig. 2). These precisely correspond to the 12 empirical Dienerian ammonoid faunas previously established by Ware et al. (in press-a). For the Spiti region, 11 Dienerian UAs were detected. Again, two of them (SP2 and SP3, see Appendix A – Table 2) were lumped together, as the oldest UA differs from the subsequent one only by the presence of two very rare species (*Ussuridiscus ornatus* and *U. ventriosus*). The resulting 10 UA-zones also correspond to the empirical succession of 10 faunas recognized by Ware et al. (in press-b). These 10 UA-zones in Spiti are nearly identical to 10 out of the 12 UA-zones of the Salt Range, differing only by a few endemic species. Hence, 12 UA-zones are defined at the pooled level of the NIM. The resulting synthetic range chart shows the occurrences of the different species in these 12 UA-zones of the NIM (Fig. 3). Two of these (DI-7 and DI-12) occur only in one area (Nammal) of the Salt Range. Usually, such poorly laterally reproducible UA-zones are merged with one of the adjacent UA-zones. However, this option was rejected here as in both cases, the only taxa in common with the adjacent UA-zones are long ranging taxa. Thus, there was no objective way of deciding with which of the two neighbouring UA-zones these should be merged with. Until additional data become available, these two UA-zones only found in Nammal are kept as valid.

A new threefold subdivision of the Dienerian into early, middle and late Dienerian is proposed. The

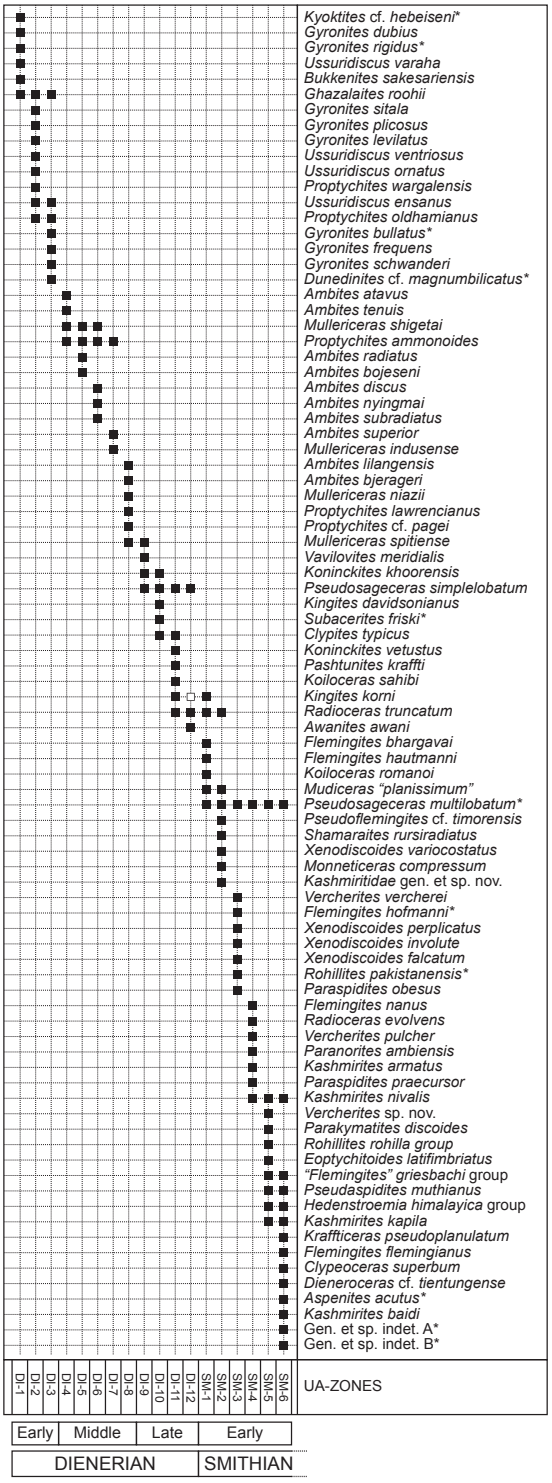

Fig. 3. Synthetic range chart with the distribution of Dienerian and early Smithian ammonoid species for the Northern Indian Margin. White squares indicate virtual occurrences. Species marked by an asterisk (*) were omitted in the dataset for the construction of the UAs (see text). They are dated and reincorporated into the range chart at the end of the processing.

early Dienerian is characterized by the co-occurrence of *Gyronites* and *Ussuridiscus* together with the youngest representative of ophiceratids (*Ghazalaites*). It includes the first three UA-zones (DI-1to DI-3). The middle Dienerian is characterized by the co-occurrence of *Ambites* and *Mullericeras*, and comprises five UA-zones (DI-4 to DI-8). The late Dienerian includes the oldest paranoritids (e.g. *Vavilovites*, *Koninckites*, *Awanites*) and hedenstroemiids (*Clypites* and *Pseudosageceras*) and is composed of four UA-zones (DI-9 to DI-12).

The early Smithian biozonation and synthetic range charts have been established by Brühwiler et al. (2010 & 2012a).These data are included in the present study and are used in the subsequent analyses.

3.2. Biodiversity dynamics

For the Dienerian, species richness (fig. 4) shows the same trends in both basins, which leads to a robust pattern at the pooled level of the NIM. A total of 43 species in the Salt Range and 37 species in Spiti were identified, representing 47 species for the Dienerian of the NIM. Species richness is generally rather low in the Dienerian, fluctuating between 3 and 8 species per zone in the Salt Range, between 2 and 9 in Spiti, and between 3 and 9 for the NIM. It reaches a distinctive first peak in the early Dienerian (DI-2) with 8 species in the Salt Range and 9 in Spiti and for the NIM. In the middle Dienerian species richness is stagnating at low values, with usually only 4 species per zone, with minor fluctuations (up to 6 in the latest middle Dienerian [DI-8] of the Salt Range). The lowest diversity is recorded in DI-7 with only 3 species. This zone is actually only known from Nammal in the Salt Range, which could lead to underestimate its diversity value. In the late Dienerian, a few minor differences can be seen between the Salt Range and Spiti. In the Salt Range, species richness increases from 4 to 7 species from DI-9 to DI-11. The low diversity in DI-12 is probably influenced by the fact that it has a unique occurrence (Nammal). In Spiti, only 2 species were found in DI-9, and the species richness then increases to reach 5 species in DI-11. The DI-9 zone is very well documented in Spiti, suggesting that this very low diversity is a genuine signal. The 2 additional species found to have their first occurrence in DI-9 in the Salt Range have their first occurrence later in DI-10 in Spiti, thus illustrating the diachronism of first occurrences between different basins. For the early Smithian, there are strong discrepancies between the Salt Range and Spiti. In the Salt Range, species richness peaks in SM-3 with 8 species, and then drops back to values similar to the late Dienerian, whereas in Spiti it stays low from SM-1 to SM-4 and peaks in SM-5 with 10 species. At the scale of the NIM, the following general trends can be recognised: 1/ a first minor diversity peak in the early Dienerian; 2/ a very low diversity in the middle Dienerian; 3/ a very slight in-

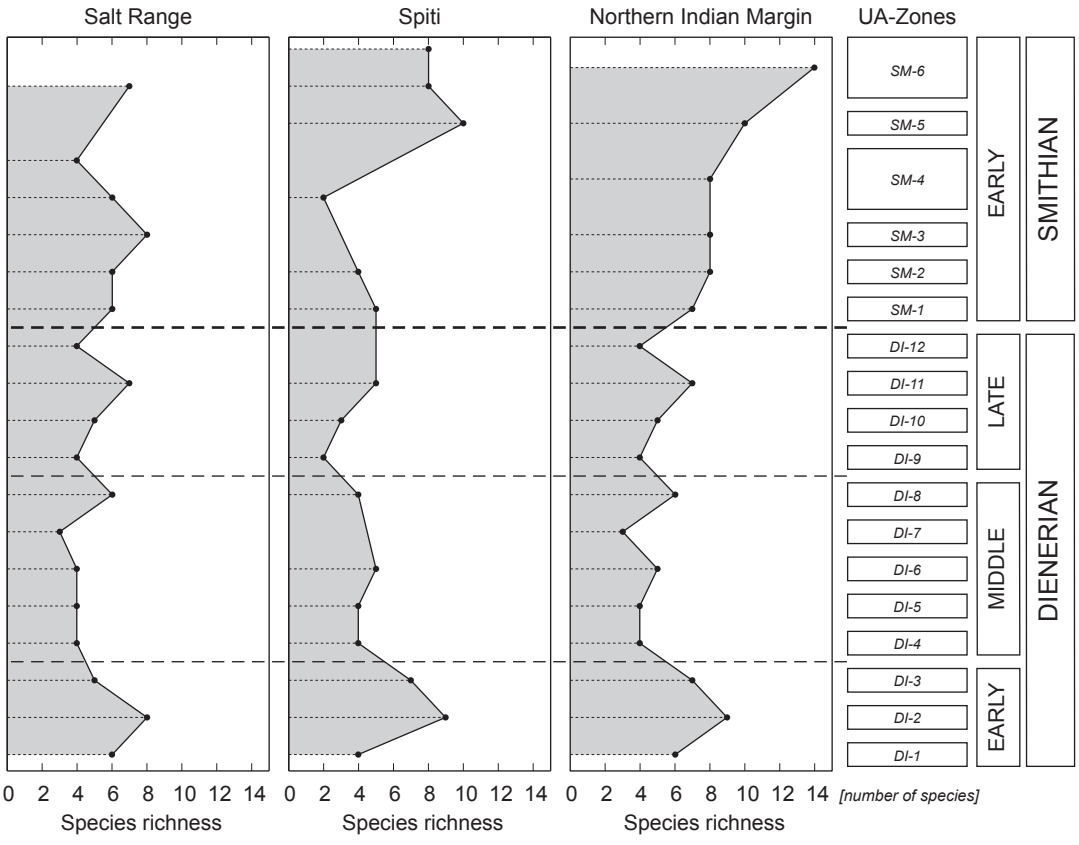

Fig. 4. Plots of ammonoid species richness for the Salt Range, Spiti and the Northern Indian Margin.

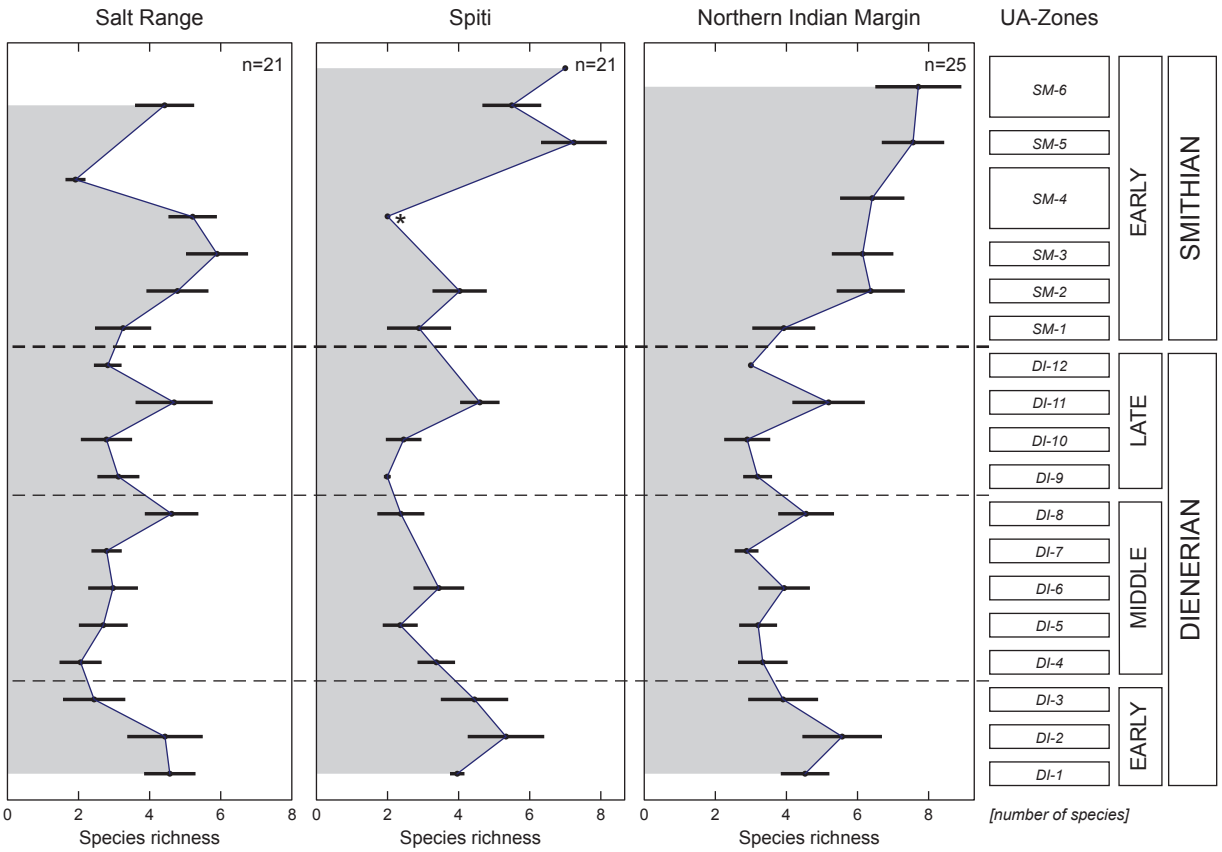

Fig. 5. Rarefied species richness curves and associated 95% confidence intervals. The curves for the Salt Range and Spiti have been rarefied to a sample size of *n* = 21; that of the Northern Indian Margin to a sample size of *n* = 25. The asterisk (*) marks a sample of very small size (6 specimens) that has not been included in the rarefaction analysis. Virtually present species (Fig. 4) are not included within this dataset.

crease in the late Dienerian; 4/ a rather high and stable diversity in the earliest early Smithian (SM-1 to SM-4); 5/ a sharp increase in diversity in the late early Smithian.

The rarefied diversity curves (fig. 5) closely match the species richness curves, indicating that there are no important sampling effort and/or preservation biases in our data. The only difference concerns the early Smithian at the pooled level of the NIM. Only a gradual increase in diversity is recorded there instead of a two-phased recovery as shown by the raw diversity data (with first a plateau followed by a sharp increase in diversity). The Chao2 and Jackknife2 indices (Appendix A-Table 3) are nearly identical to the species richness, giving further indication of absence of bias in our data. However, the Chao2 confidence intervals and Jackknife2 bootstrapped standard error are much more important in the early Smithian than in the Dienerian, indicating greater dissimilarities between the Salt Range and Spiti during the early Smithian than during the Dienerian. It should be noted that these two indices were calculated only for two basins, so data of similar age from other basins would be necessary to further test how these trends are laterally reproducible.

Originations and extinction rates (fig. 6) are very high during the whole studied interval, generally above 50% and sometimes reaching 100%. Extinctions exceed originations at the early-middle and middle-late Dienerian transitions. In the early Dienerian, both extinctions and originations are very high. Originations exceed extinctions between DI-1 and DI-2, while it is the opposite between DI-2 and DI-3. In the middle Dienerian, extinctions and originations are relatively well balanced and low, except around DI-7, a zone which could be affected by a sampling bias. In the late Dienerian, originations tend to slightly exceed extinctions, but both are rather low. The changes around DI-12 should not be taken into account as this zone is comparatively poorly documented. In the early Smithian, originations generally exceed extinctions, and the values are much higher.

Turnover rates (fig. 7) are always very high, above 60% and sometimes reaching 100%. The highest percentages are recorded at the early-middle and middle-late Dienerian transitions, and within the early Smithian. The lowest values occur within the middle and the late Dienerian.

Figure 8 shows the generic richness and the extinction, origination and turnover counts and rates at the generic level for the NIM. The generic richness follows the general trends recorded at the species level, except that the curve appears slightly smoothed out. The ge-

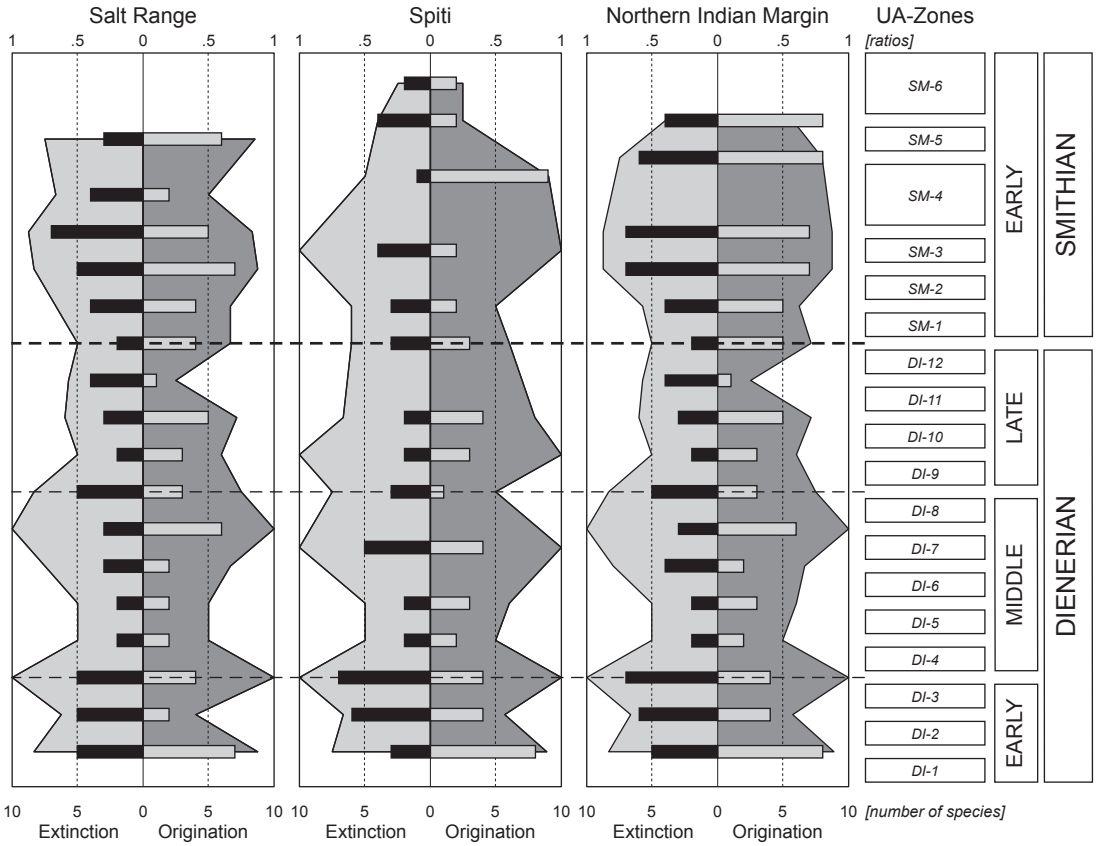

Fig. 6. Values (bars) and percentages (shaded areas) of ammonoid species origination and extinction throughout the Dienerian and early Smithian.

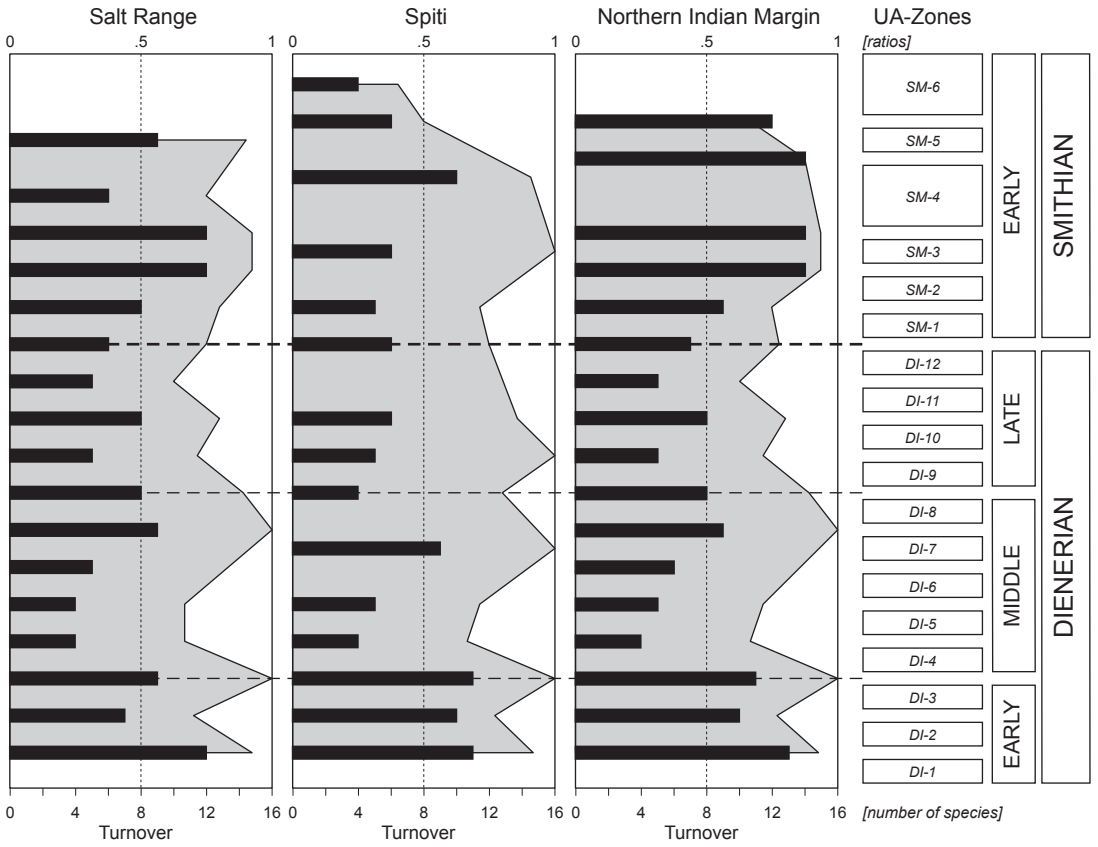

Fig. 7. Values (bars) and percentages (shaded areas) of turnover of ammonoid species throughout the Dienerian and early Smithian.

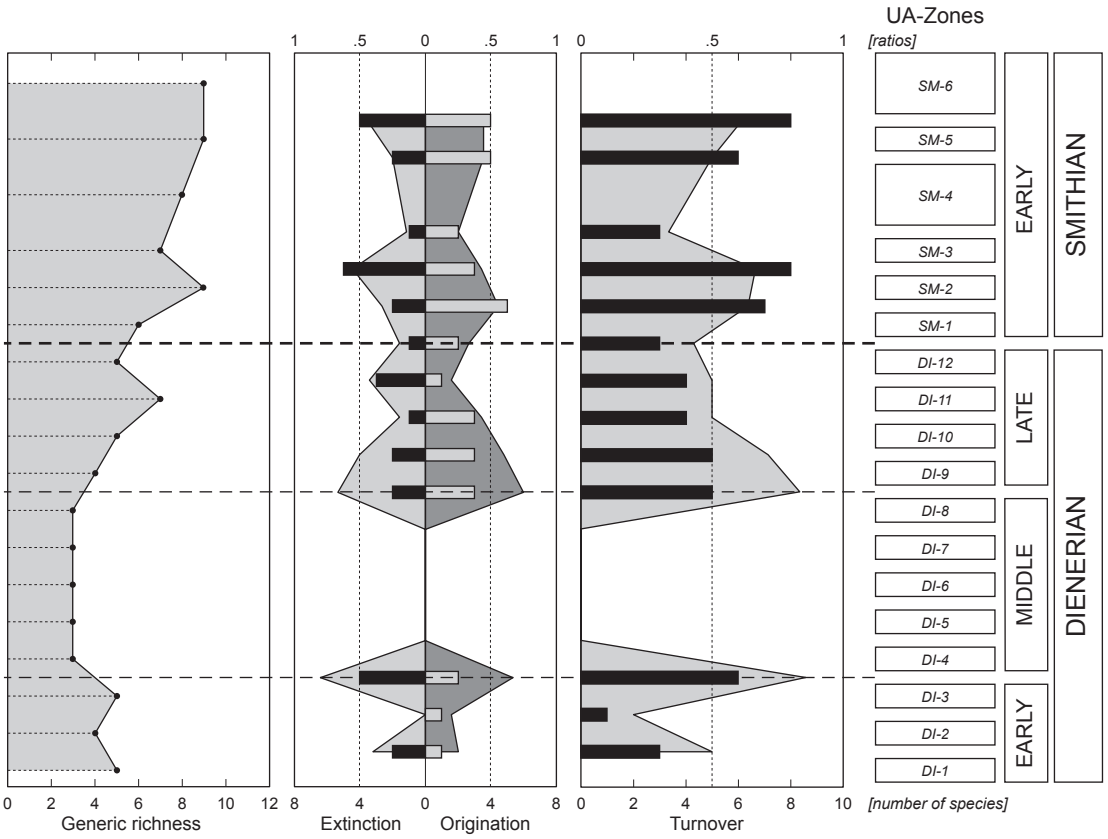

Fig. 8. Generic richness, origination, extinction and turnover throughout the Dienerian and early Smithian of the Northern Indian Margin.

neric richness is moderately high in the early Dienerian (4 to 5 genera), stagnates at low levels throughout the middle Dienerian with only 3 genera, and then starts increasing progressively in the late Dienerian before peaking in the late early Smithian with 9 genera. Origination, extinction and turnover rates at the genus level also follow the general trends observed at the species level, but with much lower values. They reach their highest values at the early-middle and middle-late Dienerian boundaries. They are very low in the early and late Dienerian, where originations usually exceed extinctions. In the middle Dienerian, they all drop down to zero, meaning that the same 3 genera occur throughout this interval and that the species richness fluctuations in this time interval are only the results of speciation events within these three lineages. In the early Smithian, their values become rather high (except between SM-3 and SM-4), and originations usually exceed extinctions.

Brayard et al.'s (2009) contour graph of the ammonoid poly-cohort matrix (PCM; fig. 9A) shows the high evolutionary rate of ammonoids during the Early Triassic compared with previous and subsequent times. The same analysis was performed on our regional dataset at the species level (fig. 9B), allowing us to zoom into the Dienerian and early Smithian part of the Early Triassic. Here too, the survivorship and prenascence contour lines are extremely contracted and mirroring each other, thus reflecting the very high turnover rates throughout the Dienerian (most species are confined to one single zone). The contour lines even fall to zero at the early-middle and middle-late Dienerian boundaries, meaning a complete replacement of the faunas between the three main subdivisions of the Dienerian. The three-fold subdivision of the Dienerian appears here again to be strongly supported. Moreover, it also reflects the four diversity phases previously discussed, with a first weak recovery in the early Dienerian, an extinction phase at the early-middle Dienerian boundary followed by a time interval of persistant low diversity, a renewal of the faunas at the middle-late Dienerian boundary followed by a slight diversification, followed by the early Smithian re-diversification, i.e. the accumulation of longer ranging species.

The graph showing the respective contributions of the different families in terms of species richness (fig. 10) gives some more insights about the diversity dynamics. The number of families stays rather low during the entire interval, with a maximum of seven families (plus two genera placed in incertae sedis) in the latest early Smithian. The early and middle Dienerian are dominated by Gyronitidae, which co-exist with Proptychitidae and Mullericeratidae. The early Dienerian differs from the middle Dienerian in including the last representatives of Ophiceratidae, whereas the middle Dienerian contains only the three other previously mentioned families. In the late Dienerian, Gyronitidae are replaced by

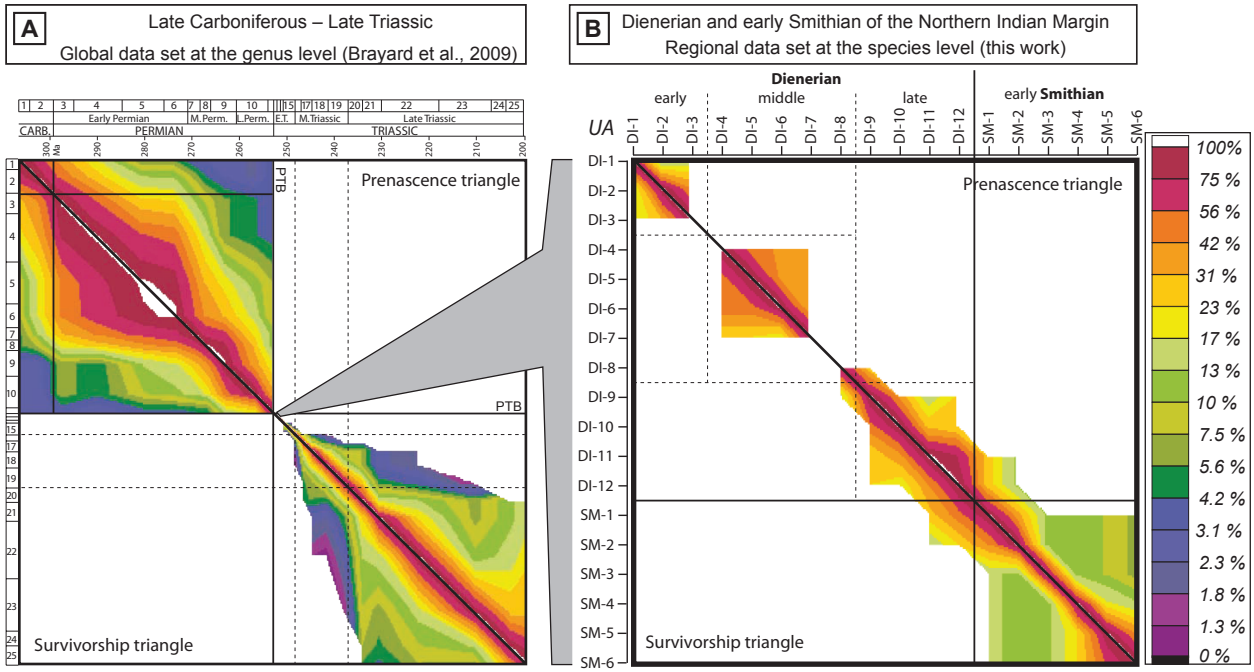

Fig. 9. [A] Brayard et al.'s (2009, modified) contour graph of the ammonoid poly-cohort matrix (PCM) for a global dataset at the genus level spanning the Late Carboniferous-Late Triassic time interval. Each column of the PCM records the prenascence (upper triangle) and survivorship (lower triangle) percentages of a target assemblage located on the diagonal "100% cell". Abbreviations: PTB, Permian-Triassic Boundary; 1, Kasimovian; 2, Gzhelian; 3, Asselian; 4, Sakmarian; 5, Artinskian; 6, Kungurian; 7, Roadian; 8, Wordian; 9, Capitanian; 10, Wuchiapingian; unlabelled successive intervals, Changhsingian, Griesbachian, Dienerian, Smithian; 15, Spathian; 16, Early Anisian; 17, Middle Anisian; 18, Late Anisian; 19, Ladinian; 20, Early Carnian; 21, Late Carnian; 22, Early Norian; 24, Late Norian; 25, Rhaetian. **[B]** Contour graph of the ammonoid PCM for the regional dataset at the species level for the Dienerian and early Smithian of the Northern Indian Margin.

Paranoritidae (which also dominate the faunas), while Mullericeratidae are replaced by Hedenstroemiidae. Proptychitidae disappear at the middle-late Dienerian boundary (unless the genus *Kingites,* here placed in Incertae Sedis, is included in proptychitids; see Ware et al., in press-a for details concerning the classification). In the early Smithian, several new families successively appear: Flemingitidae, Kashmiritidae, Aspenitidae and Dienoceratidae. The faunas are alternatively dominated by Paranoritidae and Flemingitidae. Interestingly, Proptychitidae first "reappear" in SM-2, "disappear" again in SM-3 and 4, and "reappear" again in SM-5.

4. Discussion

4.1. Biochronology

The new biochronological scheme proposed here for the Dienerian, with 12 UA-zones grouped into three subdivisions, strongly contrasts with all previously established Dienerian biozonation. For example, Tozer (1965, 1994), when erecting the Dienerian stage, recognised only 4 sub-zones, grouped into two zones. No conflicting stratigraphic relationships between taxa were found in our dataset, indicating the excellent quality of our taxonomic and biostratigraphic raw data. As a consequence, the zonation established here confirms the empirical scheme previously established by Ware et al. (in press-a, b).

The duration of each UA-zone can be estimated using the latest high-precision single zircon U-Pb ages obtained from South China. An age of 251.88 ± 0.031 Ma for the Permian-Triassic boundary has been recently proposed by Burgess et al. (2014). An age of 251.22 ± 0.2 Ma for the early Smithian *Kashmirites kapila* beds (corresponding here to SM-5 according to Brühwiler et al., 2010) is provided by Galfetti et al. (2007). A duration of ca. 0.66 My can thus be inferred for the time interval comprised between the Permian-Triassic boundary and SM-5. Krystyn et al. (2004) showed that the Griesbachian of Spiti can be subdivided into three ammonoid zones. Therefore, 19 zones have been identified in the NIM between the Permian-Triassic boundary and SM-5, which yields an average theoretical maximal duration of 34.7 ky per zone (including the intervals of separation between the UA-zones). This average duration is shorter than that obtained by Brühwiler et al. (2010) for the Smithian of the NIM, but considering the error embedded in the age of the *Kashmirites kapila* beds, it is within the same order of magnitude.

4.2. Diversity dynamics

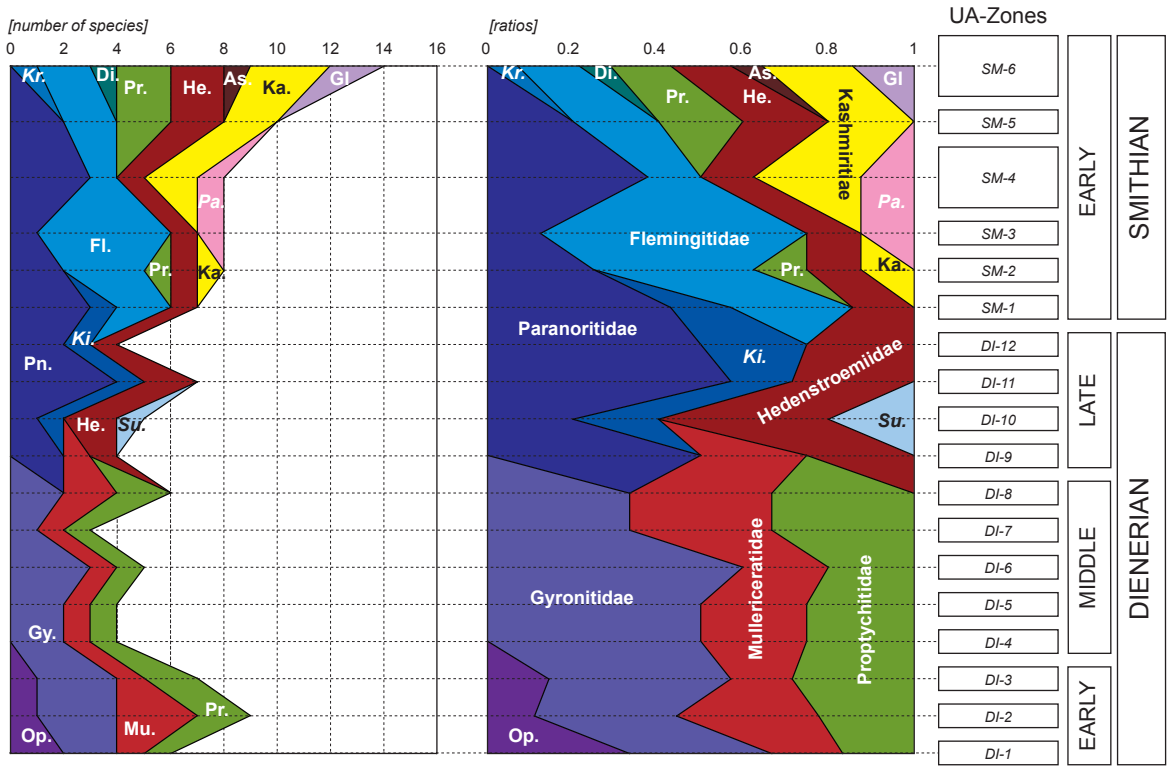

Fig. 10. Absolute and relative species richness for each Dienerian and early Smithian ammonoid family plotted against the UA-zonation of the Northern Indian Margin. Abbreviations for the families: As, Aspenitidae; Di, Dieneroceratidae; Fl, Flemingitidae; Gy, Gyronitidae; He, Hedenstroemiidae; Ka, Kashmiritidae; Mu, Mullericeratidae; Op, Ophiceratidae; Pn, Paranoritidae; Pr, Proptychitidae. Some genera could not be ascribed with certainty to a family, and are thus here shown at the same level as the families, with the following abbreviations: *Ki*, *Kingites*; *Kr*, *Krafftiсeras*; *Pa*, *Paraspidites*; *Su*, *Subacerites*; Gl, Gen. Indet.

The four following main phases in diversity patterns can be identified for Dienerian and early Smithian ammonoids from the NIM: 1/ a first small peak of recovery in the early Dienerian; 2/ an extinction followed by a very low diversity throughout the middle Dienerian; 3/ a slow increase in diversity in the late Dienerian; 4/ a much more rapid increase in diversity associated with the appearance of several new families in the early Smithian. These changes in diversity are associated with very high turnover rates, especially at the early-middle and middle-late Dienerian boundaries where entire faunas are replaced. Although the early Smithian shows comparably high turnover rates, it differs from the Dienerian in having a few longer lived species.

Three hypotheses can explain the temporary absence of Proptychitidae observed during the late Dienerian: 1/ an apparent absence due to sampling effort; 2/ a convergence problem between unrelated species; 3/ the local disappearance of this family in the NIM, followed by re-colonisation of this region from the global pool. As Proptychitidae are usually not very abundant, particularly in the early Smithian, the first hypothesis may be true for SM-3 and 4. It can however definitely be rejected for the late Dienerian as DI-10 and DI-11 yielded the most abundant material, representing more than a third (1504 out of a total of 4151 specimens) of all the ammonoids collected in this study. The second hypothesis is also unlikely, as Proptychitidae constitute a well-defined family, easily differentiated from other co-occurring families by the presence of indentations on the lobe sides (see Ware et al., in press-a for details). As a consequence, the absence of Proptychitidae in the late Dienerian is interpreted as a genuine signal which can only be explained by their survival in another province, and their reappearance in the early Smithian suggests a re-colonisation of the NIM by these forms.

Several palaeoenvironmental proxies (fig. 11) from the studied NIM sections provide some insights on possible causes of these diversity changes. Palynofacies analysis (Hermann et al., 2011) indicates three phases: 1/ a strong terrestrial influence in the early Dienerian (demonstrated by the high relative abundance of opaque phytoclasts) indicating a low sea level; 2/ dysoxic to anoxic conditions and higher sea level (indicated by high relative abundance of amorphous organic matter [AOM]) in the middle and late Dienerian and in the earliest Smithian; 3/ a return to normal oxic conditions and high sea level (indicated by high relative abundance of acritarchs and only minor contribution of AOM), for

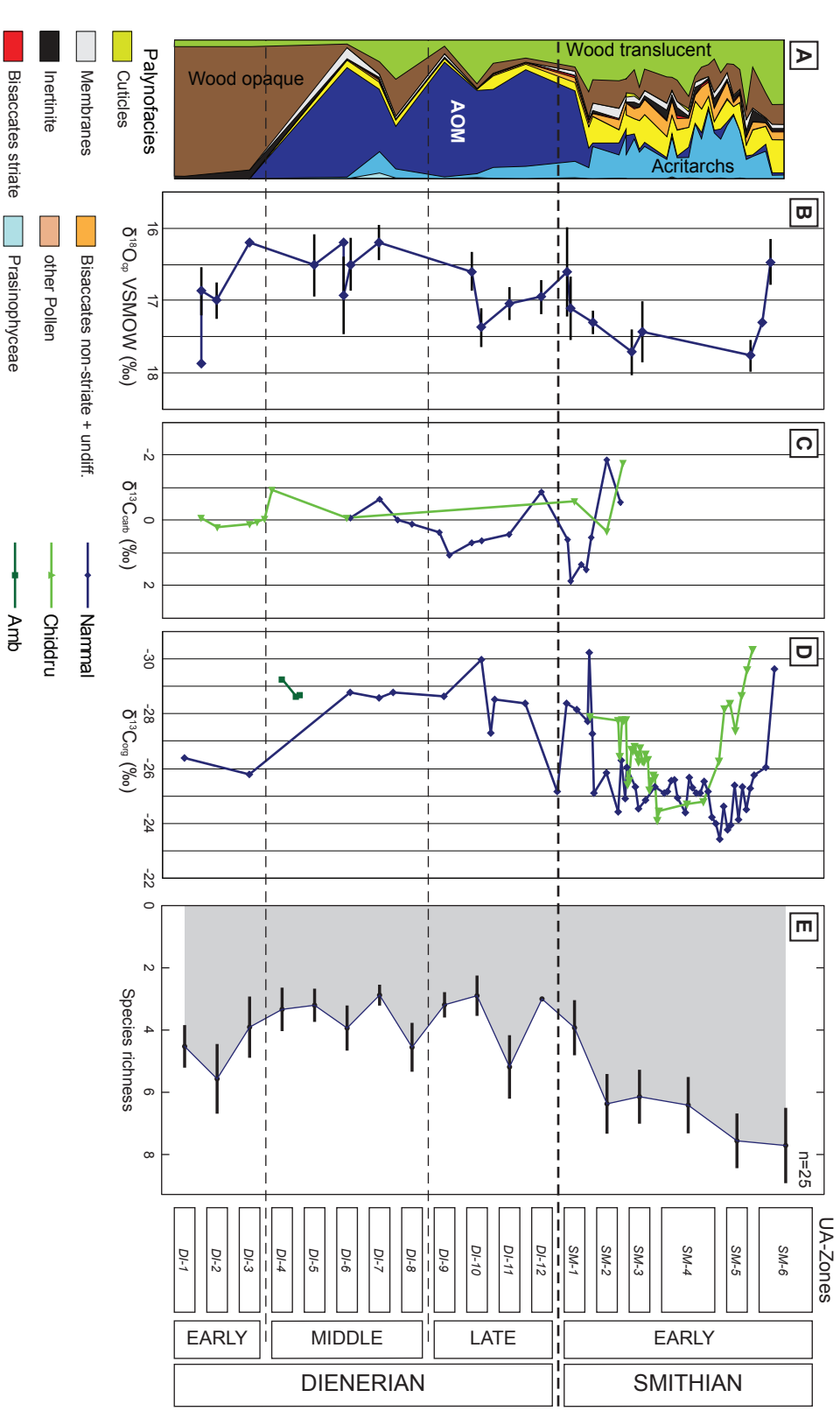

Fig. 11. Comparison of the biodiversity signal with palaeoenvironmental proxies: **[A]** Palynofacies of the section of Nammal Nala, modified after Hermann et al. (2011); AOM = Amorphous Organic Matter **[B]** Oxygen isotopes for the section of Nammal Nala, modified after Romano et al. (2013); **[C]** Carbonate carbon isotopes for Chiddru and Nammal (modified after Hermann et al., 2011), Amb (modified after Schneebeli-Hermann et al., 2012), and Mud and Lalung (this study); **[D]** Organic carbon isotopes for Chiddru and Nammal (modified after Hermann et al., 2011) and Amb (modified after Schneebeli-Hermann et al., 2012); **[E]** rarefied species richness curve and associated 95% confidences intervals for the Northern Indian Margin (see Fig. 5).

the rest of the early Smithian. Oxygen isotopes measured from biogenic phosphate (Romano et al., 2013) and organic carbon isotopes (Hermann et al. 2011) tend to track each other and also reveal three phases: 1/ moderately heavy values in the early Dienerian; 2/ very light values in the middle and late Dienerian, with lightest values in the middle Dienerian; 3/ heavy values in the early Smithian. The carbonate carbon isotope record from Nammal (after Hermann et al., 2011) shows rather constant values during most of the Dienerian. However, these data record a 3 ‰ positive excursion at the Dienerian-Smithian boundary.

The comparison of our diversity results with these palaeoenvironmental proxies clearly shows that early Dienerian and early Smithian ammonoids recovered within oxygenated and relatively cold waters. The

middle Dienerian diversity low is concomitant with an anoxic sediment-water interface and warmer sea water temperatures. Coupling with relative sea level changes in the Salt Range is not obvious as the entire Dienerian has been interpreted as a main transgressive phase and the early Smithian as a regressive phase (Hermann et al., 2011). Noteworthy, the middle Dienerian diversity minimum occurs during the transgression, thus largely pre-dating the high-sea level stand that coincides with the Dienerian-Smithian boundary. In Spiti, Early Triassic rocks are largely over-mature thus preventing environmental inferences from palynofacies and oxygen isotopes. However, the same trends in facies oxygenation and relative sea-level changes also emerge from sedimentological and taphonomical criteria in Spiti. There, rocks of middle and late Dienerian age consist of black shales containing early diagenetic, organic-rich limestone concretions yielding complete fishes (Ware et al., in press b), thus contrasting with the grey and bioturbated cliff-forming limestone of early Smithian age.

When brought into a larger palaeogeographical perspective, it appears that anoxic events throughout the Early Triassic are concentrated in two main episodes coinciding with the lowest relative diversity of ammonoids: a middle to late Dienerian event and a late Smithian event (Bucher et al., 2013). Evidence for the middle to late Dienerian anoxic episode is found in the following well-dated, ammonoid-bearing areas: Nevada (Ware et al., 2011), South China (Galfetti et al., 2008) and southern Tibet (Brühwiler et al., 2009). Dark shales of similar age are also recorded in Primorye (Shigeta et al., 2009) and anoxic shales of Dienerian age are described from British Columbia (Orchard and Zonnenveld, 2009). The present diversity results also highlight that at least at the scale of the NIM, the hypothesis of a progressive recovery of ammonoids (Brayard et al, 2006, 2009) from Griesbachian to Smithian times must be replaced by an uneven and highly dynamical recovery pattern with ups and downs.

5. Conclusions

The synthesis of the two recent works focusing on the taxonomical revision and detailed biostratigraphy of Dienerian ammonoids from the Salt Range (Ware et al., in press-a) and from Spiti (Ware et al., in press-b) allowed us to construct a new biostratigraphic scheme of unprecedented high resolution based on the Unitary Associations method. A total of 12 zones can be recognized in the Dienerian. On the basis of the turnover at the genus level, these zones are grouped into early, middle and late Dienerian. The U-Pb ages obtained in South China (Galfetti et al., 2007, Burgess et al., 2014) allow the calculation of a very short average maximal duration of 34.7 ky per ammonoid zone (inclusive of the separation intervals).

Based on this new zonation, ammonoid biodiversity dynamics for the Dienerian and early Smithian of the NIM show the following four phases: 1/ a moderately high diversity in the early Dienerian; 2/ a decline followed by a very low diversity throughout the middle Dienerian; 3/ a very slight increase in diversity in the late Dienerian; 4/ an important radiation in the early Smithian. Very high turnover rates are observed throughout the Dienerian, thus confirming the results obtained at a global scale and with a less well resolved time scale by Brayard et al. (2009). The very low diversity in the middle and late Dienerian is associated with an anoxic event and warm temperatures. This sequence of events is at variance with the general idea of a protracted and progressive recovery following the end-Permian mass extinction. It leads to propose a more realistic model consisting of alternating diversification and extinction phases related to unstable environmental conditions. An interesting and open forthcoming step is how the high-resolution ammonoid diversity dynamics of the Griesbachian compares to those of the Dienerian and the Smithian.

Acknowledgements – G. Roohi (Pakistan Museum of Natural History, Islamabad) and L. Krystyn (Insitut für Paläontologie, Wien, Austria) are thanked for field assistance. E. Maxwell (Staatliches Museum für Naturkunde, Stuttgart, Germany) improved the English text of this work. This work is supported by the Swiss National Foundation (project n°200020-135446 to H.B.).

References

Brayard, A., Bucher, H., Escarguel, G., Fluteau, F., Bourquin, S. & Galfetti, T. 2006: The Early Triassic ammonoid recovery: Paleoclimatic significance of diversity gradients. *Palaeogeography, Palaeoclimatology, Palaeoecology 239*, 374-395.

Brayard, A., Escarguel, G., Bucher, H., Monnet, C., Brühwiler, T., Goudemand, N., Galfetti T. & Guex, J. 2009: Good Genes and Good Luck: Ammonoid Diversity and the End-Permian Mass Extinction. *Science 325*, 1118-1121.

Brühwiler, T., Goudemand, N., Galfetti, T., Bucher, H., Baud, A., Ware, D., Hermann, E., Hochuli, P.A. & Martini, R. 2009: The Lower Triassic sedimentary and carbon isotope records from Tulong (South Tibet) and their significance for Tethyan palaeoceanography. *Sedimentary Geology 222*,314-332.

Brühwiler, T., Bucher, H., Brayard, A. & Goudemand, N. 2010: High-resolution biochronology and diversity dynamics of the Early Triassic ammonoid recovery: The Smithian faunas of the Northern Indian Margin. *Palaeogeography, Palaeoclimatology, Palaeoecology 297*, 491-501.

Brühwiler, T., Bucher, H., Ware, D., Schneebeli-Hermann, E., Hochuli, P.A., Roohi, G., Rehman, K. & Yaseen, A. 2012a: Smithian (Early Triassic) ammonoids from the Salt Range, Pakistan. *Special Papers in Palaeontology 88*, 1-114.

Brühwiler, T., Bucher, H. & Krystyn, L. 2012b: Middle and late Smithian (Early Triassic) ammonoids from Spiti, India. *Special Papers in Palaeontology 88*, 115-174.

Bucher, H., Hochuli, P.A., Goudemand, N., Schneebeli-Hermann E., Romano, C., Hautmann, M., Hofmann, R., Brayard, A., Vennemann, T., & Weissert, H. 2013: Some like it hot: The Smithian Diversification-Extinction Model (Keynote). *Geological Society of America Annual Meeting (Denver, 27-30 October), Paper No. 399-7*.

Burgess, S.D., Bowring, S., & Shen, S.-Z. 2014: High-precision timeline for Earth's most severe extinction. *Proceedings of the National Academy of Sciences of the United States of America 111*, 3316-3321

Colwell, R.K., 2009: Estimates: Statistical Estimation of Species Richness and Shared Species from Samples. Version 8.2. User's Guide and application published at: http://purl.oclc.org/estimates.

Dagys, A. S. & Ermakova, S. 1996: Induan (Triassic) ammonoids from North-Eastern Asia. *Revue de Paléobiologie 15*, 401-447.

Diener, C. 1897: Part I: The Cephalopoda of the Lower Trias. *Palaeontologia Indica, Series 15*. *Himalayan fossils 2*, 1-181.

Escarguel, G. & Bucher, H. 2004: Counting taxonomic richness from discrete biochronozones of unknown duration: a simulation. *Palaeogeography, Palaeoclimatology, Palaeoecology 202*, 181-208.

Foote, M., 1988: Survivorship analysis of Cambrian and Ordovician Trilobites. *Paleobiology 14*, 258-271.

Galfetti, T., Bucher, H., Ovtcharova, M., Schaltegger, U., Brayard, A., Brühwiler T., Goudemand, N., Weissert H., Hochuli, P., Cordey, F. & Guodon K. 2007: Timing of the Early Triassic carbon cycle perturbations inferred from new U-Pb ages and ammonoid biochronozones. *Earth and Planetary Science Letters 258*, 593-604.

Galfetti, T., Bucher, H., Martini, R., Hochuli, P.A., Weissert, H., Crasquin-Soleau, S., Brayard A., Goudemand, N., Brühwiler, T and Guodun, K. 2008: Evolution of Early Triassic outer platform paleoenvironments in the Nanpanjiang Basin (South China) and their significance for the biotic recovery. *Sedimentary Geology 204*, 36-60.

Guex, J. 1991: *Biochronological Correlations*, Springer, Berlin, 252 pp.

Hammer, Ø., Harper, D.A.T. & Ryan, P.D. 2001: PAST: Paleontological statistics software package for education and data analysis. *Palaeontologia Electronica 4 (1)*: 9pp.

Hartenberger, J.L., 1988: Taxonomic survivorship in fossil mammals during the Paleogene in Europe. *Comptes Rendus De L'Academie Des Sciences Serie II, 306*, 1197-1204.

Hermann, E., Hochuli, P.A., Méhay, S., Bucher, H., Brühwiler, T., Ware, D., Hautmann, M., Roohi, G., ur-Rehman, K. & Yaseen, A. 2011: Organic matter and palaeoenvironmental signals during the Early Triassic biotic recovery: The Salt Range and Surghar Range records. *Sedimentary Geology 234*, 19-41.

Krafft, A.V. & Diener, C. 1909: Lower Triassic cephalopoda from Spiti, Malla Johar, and Byans. *Palaeontologia Indica 6*, 1-186.

Krystyn, L., Balini, M. & Nicora, A. 2004: Lower and Middle Triassic stage and substage boundaries in Spiti. *Albertiana 30*, 40-53.

Monnet, C. & Bucher, H. 2002: Cenomanian (early Late Cretaceous) Ammonoid faunas of western Europe. Part 1: Biochronology (Unitary Associations) and diachronism of datums. *Eclogae geologicae Helvetiae 95*, 57-73.

Orchard, M.J. & Zonneveld, J.-P. 2009: The Lower Triassic Sulphur Mountain Formation in the Wapiti Lake area: lithostratigraphy, conodont biostratigraphy, and a new biozonation for the lower olenekian (Smithian). *Canadian Journal of Earth Sciences 46*, 757-790.

Raup, D.M., 1978: Cohort analysis of generic survivorship. *Paleobiology 4*, 1-15.

Raup, D.M., 1986: Biological extinction in earth history. *Science 231*, 1528-1533.

Romano, C., Goudemand, N., Vennemann, T.W., Ware, D., Schneebeli-Hermann, E., Hochuli, P.A., Brühwiler, T., Brinkmann, W. & Bucher, H. (2013): Climatic and biotic upheavals following the end-Permian mass extinction. *Nature geosciences 6*, 57-60.

Schneebeli-Hermann, E., Kürschner, W.M., Hochuli, P.A., Bucher, H., Ware, D., Goudemand, N. & Roohi, G. 2012: Palynofacies analysis of the Permian–Triassic transition in the Amb section (Salt Range, Pakistan): Implications for the anoxia on the South Tethyan Margin. *Journal of Asian Earth Sciences 60*, 225-234.

Shigeta, Y., Zakharov, Y.D., Maeda, H. & Popov, A.M. (eds). The Lower Triassic System in the Abrek bay area, South Primorye, Russia. *National Museum of Nature and Science Monographs 38, Tokyo*, 1-218.

Tozer, E.T. 1965: Lower Triassic stages and Ammonoid zones of Arctic Canada. *Paper of the Geological Survey of Canada 65-12*, 14 pp.

Tozer, E.T. 1994: Canadian Triassic Ammonoid Faunas. *Bulletin of the Geological Survey of Canada 467*, 1-663.

Waagen, W. 1895: Salt Ranges Fossils. vol. 2: Fossils from the Ceratites formation - Part I - Pisces, Ammonoidea. *Palaeontologia Indica 13*, 1-323.

Ware, D., Jenks, J.F., Hautmann, M. & Bucher, H. 2011: Dienerian (Early Triassic) ammonoids from the Candelaria Hills (Nevada, USA) and their significance for palaeobiogeography and palaeoceanography. *Swiss Journal of Geoscience 104*, 161-181.

Ware, D., Bucher, H., Brühwiler, T., Schneebeli-Hermann, E., Hochuli, P.A., Roohi, G., Rehman, K. & Yaseen, A. (in press-a): Griesbachian and Dienerian (Early Triassic) ammonoids from the Salt Range, Pakistan. *Fossil & Strata*.

Ware, D., Bucher, H., Brühwiler, T. & Krystyn, L. (in press-b): Dienerian (Early Triassic) ammonoids from the Spiti District, India. *Fossil & Strata*.

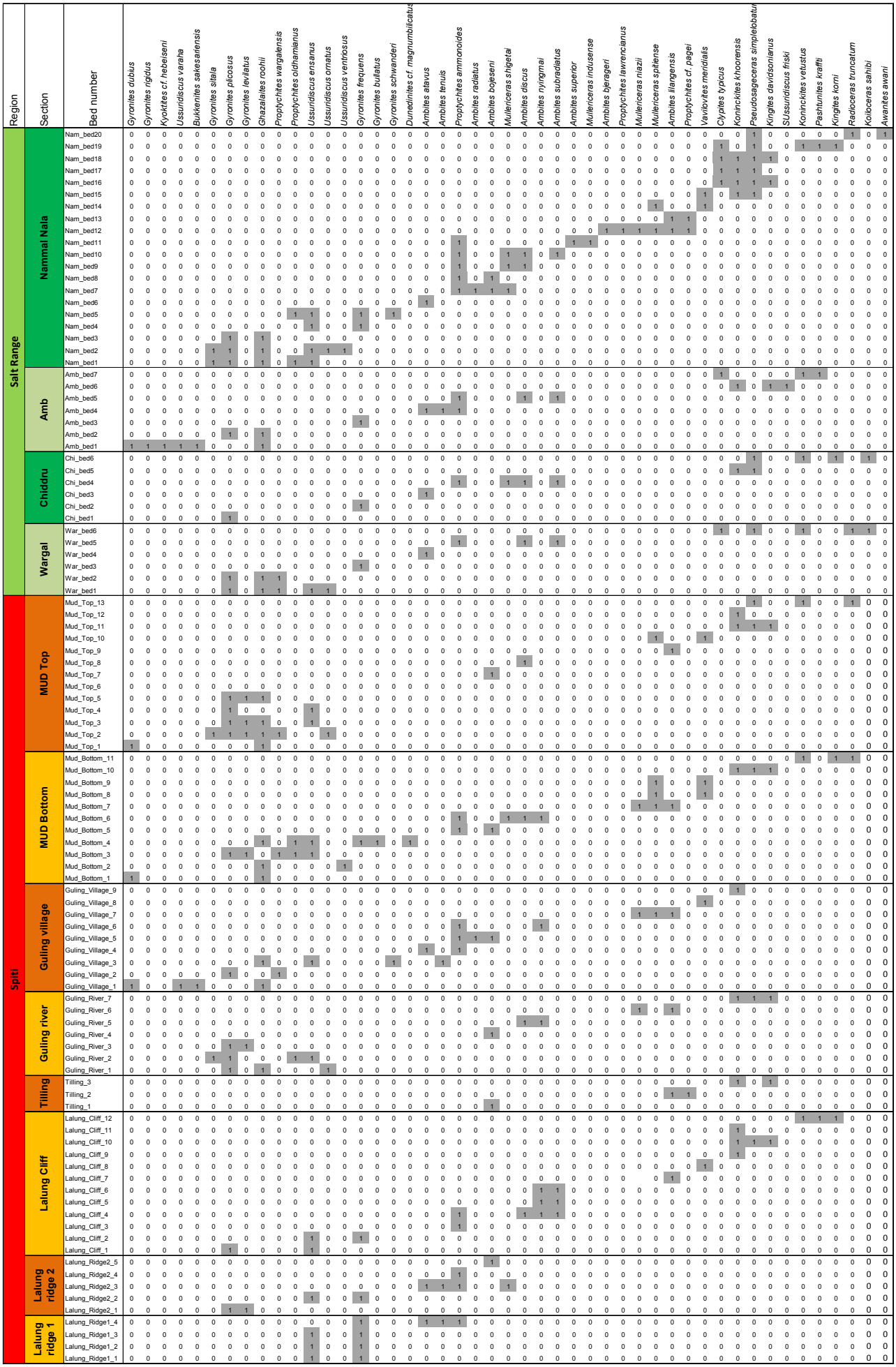

Appendix A, Table 1. Occurences of ammonoid species from the different sections in the Salt Range and Spiti.

Salt Range															Spiti											Region
SR-1	SR-2	SR-3	SR-4	SR-5	SR-6	SR-7	SR-8	SR-9	SR-10	SR-11	SR-12	SR-13	SP-1	SP-2	SP-3	SP-4	SP-5	SP-6	SP-7	SP-8	SP-9	SP-10	SP-11	Local UA-zones
1	0	0	0	0	0	0	0	0	0	0	0	0	1	0	0	0	0	0	0	0	0	0	0	*Gyronites dubius*
1	0	0	0	0	0	0	0	0	0	0	0	0	1	0	0	0	0	0	0	0	0	0	0	*Ussuridiscus varaha*
1	0	0	0	0	0	0	0	0	0	0	0	0	1	0	0	0	0	0	0	0	0	0	0	*Bukkenites sakesariensis*
1	1	0	0	0	0	0	0	0	0	0	0	0	1	1	1	1	0	0	0	0	0	0	0	*Ghazalaites roohii*
0	1	0	0	0	0	0	0	0	0	0	0	0	0	1	1	0	0	0	0	0	0	0	0	*Gyronites sitala*
0	1	0	0	0	0	0	0	0	0	0	0	0	0	1	1	0	0	0	0	0	0	0	0	*Gyronites plicosus*
0	0	0	0	0	0	0	0	0	0	0	0	0	0	1	1	0	0	0	0	0	0	0	0	*Gyronites levilatus*
0	1	0	0	0	0	0	0	0	0	0	0	0	0	1	1	0	0	0	0	0	0	0	0	*Proptychites wargalensis*
0	1	0	0	0	0	0	0	0	0	0	0	0	0	1	0	0	0	0	0	0	0	0	0	*Ussuridiscus ornatus*
0	1	0	0	0	0	0	0	0	0	0	0	0	0	1	0	0	0	0	0	0	0	0	0	*Ussuridiscus ventriosus*
0	1	1	0	0	0	0	0	0	0	0	0	0	0	0	1	1	0	0	0	0	0	0	0	*Proptychites oldhamianus*
0	1	1	0	0	0	0	0	0	0	0	0	0	0	0	1	1	0	0	0	0	0	0	0	*Ussuridiscus ensanus*
0	0	1	0	0	0	0	0	0	0	0	0	0	0	0	0	1	0	0	0	0	0	0	0	*Gyronites frequens*
0	0	1	0	0	0	0	0	0	0	0	0	0	0	0	0	1	0	0	0	0	0	0	0	*Gyronites schwanderi*
0	0	0	1	0	0	0	0	0	0	0	0	0	0	0	0	0	1	0	0	0	0	0	0	*Ambites atavus*
0	0	0	1	0	0	0	0	0	0	0	0	0	0	0	0	0	1	0	0	0	0	0	0	*Ambites tenuis*
0	0	0	1	1	1	1	0	0	0	0	0	0	0	0	0	0	1	1	1	0	0	0	0	*Proptychites ammonoides*
0	0	0	0	1	0	0	0	0	0	0	0	0	0	0	0	0	0	1	0	0	0	0	0	*Ambites radiatus*
0	0	0	0	1	0	0	0	0	0	0	0	0	0	0	0	0	0	1	0	0	0	0	0	*Ambites bojeseni*
0	0	0	0	1	1	0	0	0	0	0	0	0	0	0	0	0	1	1	1	0	0	0	0	*Mullericeras shigetai*
0	0	0	0	0	1	0	0	0	0	0	0	0	0	0	0	0	0	0	1	0	0	0	0	*Ambites discus*
0	0	0	0	0	1	0	0	0	0	0	0	0	0	0	0	0	0	0	1	0	0	0	0	*Ambites subradiatus*
0	0	0	0	0	0	0	0	0	0	0	0	0	0	0	0	0	0	0	1	0	0	0	0	*Ambites nyingmai*
0	0	0	0	0	0	1	0	0	0	0	0	0	0	0	0	0	0	0	0	0	0	0	0	*Ambites superior*
0	0	0	0	0	0	1	0	0	0	0	0	0	0	0	0	0	0	0	0	0	0	0	0	*Mullericeras indusense*
0	0	0	0	0	0	0	1	0	0	0	0	0	0	0	0	0	0	0	0	0	0	0	0	*Ambites bjerageri*
0	0	0	0	0	0	0	1	0	0	0	0	0	0	0	0	0	0	0	0	0	0	0	0	*Proptychites lawrencianus*
0	0	0	0	0	0	0	1	0	0	0	0	0	0	0	0	0	0	0	0	1	0	0	0	*Mullericeras niazii*
0	0	0	0	0	0	0	1	1	0	0	0	0	0	0	0	0	0	0	0	1	1	0	0	*Mullericeras spitiense*
0	0	0	0	0	0	0	1	0	0	0	0	0	0	0	0	0	0	0	0	1	0	0	0	*Ambites lilangensis*
0	0	0	0	0	0	0	1	0	0	0	0	0	0	0	0	0	0	0	0	1	0	0	0	*Proptychites cf. pagei*
0	0	0	0	0	0	0	0	1	1	0	0	0	0	0	0	0	0	0	0	0	1	0	0	*Vavilovites meridionalis*
0	0	0	0	0	0	0	0	0	0	1	1	0	0	0	0	0	0	0	0	0	0	0	0	*Clypites typicus*
0	0	0	0	0	0	0	0	0	1	1	0	0	0	0	0	0	0	0	0	0	0	1	0	*Koninckites khoorensis*
0	0	0	0	0	0	0	0	0	1	1	1	1	0	0	0	0	0	0	0	0	0	1	1	*Pseudosageceras simplelobatum*
0	0	0	0	0	0	0	0	0	0	1	0	0	0	0	0	0	0	0	0	0	0	1	0	*Kingites davidsonianus*
0	0	0	0	0	0	0	0	0	0	0	1	0	0	0	0	0	0	0	0	0	0	0	1	*Koninckites vetustus*
0	0	0	0	0	0	0	0	0	0	0	1	0	0	0	0	0	0	0	0	0	0	0	1	*Pashtunites kraffti*
0	0	0	0	0	0	0	0	0	0	0	1	0	0	0	0	0	0	0	0	0	0	0	1	*Kingites korni*
0	0	0	0	0	0	0	0	0	0	0	1	1	0	0	0	0	0	0	0	0	0	0	1	*Radioceras truncatum*
0	0	0	0	0	0	0	0	0	0	0	1	0	0	0	0	0	0	0	0	0	0	0	0	*Koiloceras sahibi*
0	0	0	0	0	0	0	0	0	0	0	0	1	0	0	0	0	0	0	0	0	0	0	0	*Awanites awani*

Appendix A, Table 2. Local Unitary Associations and corresponding occurences of ammonoid species from the Salt Range and Spiti.

UA-Zones	S_{obs}	Chao2 estimator			Jackknife2 estimator	
		Mean	Low. 95% CI	Upp. 95% CI	Mean	Boot. Std.Err.
S6	14	17.3	12.8	37.3	14.6	6.1
S4	8	9.3	7.0	22.9	8.3	3.9
S2	8	7.3	6.8	12.8	7.9	2.5
S1	6	5.5	5.5	8.0	5.9	1.0
Di11	7	6.5	6.5	9.0	7.0	1.3
Di10	5	4.5	4.6	7.2	5.1	1.2
Di9	4	3.8	3.7	6.5	4.2	1.1
Di8	6	5.7	5.7	8.3	6.3	1.1
Di6	5	4.7	4.7	7.3	4.9	0.7
Di5	4	3.7	3.7	5.9	3.9	0.6
Di4	4	3.8	3.8	6.1	4.0	0.6
Di3	7	6.5	6.5	9.0	7.0	1.3
Di2	9	8.8	8.8	12.6	9.0	0.6
Di1	6	5.5	5.4	8.0	5.8	1.2

Appendix A, Table 3. Chao2 and Jackknife2 estimators for Dienerian and early Smithian ammonoids from the NIM (S_{obs}: observed species richness). These indices could only be calculated for the zones present in both the Salt Range and Spiti.

Appendix 1

Co-authored publications linked to this dissertation

(Abstracts)

Vegetation history across the Permian-Triassic boundary in Pakistan (Amb section, Salt Range)

Schneebeli-Hermann, E., Kürschner, W.M., Bomfleur, B., Hochuli, P.A, Ware, D., Roohi, G. & Bucher, H.

Hypotheses about the Permian–Triassic floral turnover range from a catastrophic extinction of terrestrial plant communities to a gradual change in floral composition punctuated by intervals indicating dramatic changes in the plant communities. The shallow marine Permian–Triassic succession in the Amb Valley, Salt Range, Pakistan, yields palynological suites together with well-preserved cuticle fragments in a stratigraphically wellconstrained succession across the Permian–Triassic boundary. Palynology and cuticle analysis indicate a mixed Glossopteris–Dicroidium flora in the Late Permian. For the first time Dicroidium cuticles are documented from age-constrained Upper Permian deposits on the Indian subcontinent. Close to the Permian–Triassic boundary, several sporomorph taxa disappear. However, more than half of these taxa reappear in the overlying Smithian to Spathian succession. The major floral change occurs towards the Dienerian. Fromthe Permian–Triassic boundary up to the middle Dienerian a gradual increase of lycopod spore abundance and a decrease in pteridosperms and conifers are evident. Synchronously, the generic richness of sporomorphs decreases. The middle Dienerian assemblages resemble the previously described spore spikes observed at the end-Permian (Norway) and in the middle Smithian (Pakistan) and might reflect a similar ecological crisis.

Gondwana Research, 2014. DOI: 10.1016/j.gr.2013.11.007.

Climatic and biotic upheavals following the end-Permian mass extinction

Romano, C., Goudemand, N., Vennemann, T.W., Ware, D., Schneebeli-Hermann, E., Hochuli, P.A., Brühwiler, T., Brinkmann, W. & Bucher, H.

Recovery from the end-Permian mass extinction is frequently described as delayed, with complex ecological communities typically not found in the fossil record until the Middle Triassic epoch. However, the taxonomic diversity of a number of marine groups, ranging from ammonoids to benthic foraminifera, peaked rapidly in the Early Triassic. These variations in biodiversity occur amidst pronounced excursions in the carbon isotope record, which are compatible with episodes of massive CO2 outgassing from the Siberian Large Igneous Province. Here we present a high-resolution Early Triassic temperature record based on the oxygen isotope composition of pristine apatite from fossil conodonts. Our reconstruction shows that the beginning of the Smithian substage of the Early Triassicwas marked by a cooler climate, followed by an interval of warmth lasting until the Spathian substage boundary. Cooler conditions resumed in the Spathian. We find the greatest increases in taxonomic diversity during the cooler phases of the early Smithian and early Spathian. In contrast, a period of extreme warmth in the middle and late Smithian was associated with floral ecological change and high faunal taxonomic turnover in the ocean. We suggest that climate upheaval and carboncycle perturbations due to volcanic outgassing were important drivers of Early Triassic biotic recovery.

Nature Geoscience 6(1), 2013, p. 57-60.

Evidence for atmospheric carbon injection during end-Permian extinction

Schneebeli-Hermann, E., Kürschner, W.M., Hochuli, P.A., Ware, D., Weissert, H., Bernasconi, S.M., Roohi, G., Rehman, K. & Bucher, H.

The end-Permian mass extinction is marked by pronounced terrestrial ecosystem turnover and a severe loss of marine invertebrate biodiversity. This extinction event is accompanied by a prominent negative carbon-isotope excursion indicating massive changes in the global carbon cycle across the Permian-Triassic boundary. In this study, we present organic carbon-isotope data from land plant cuticles, fossil wood fragments, and bulk organic matter recovered from the Amb section in the Salt Range, Pakistan. We apply $\delta^{13}C$ data from cuticles as a proxy record for the carbon-isotope composition of atmospheric CO_2 across the Permian-Triassic boundary. The data show an ~5.5‰ negative excursion in terrestrial organic matter, reflecting the change in carbon-isotope composition of atmospheric CO_2. Our data demonstrate that these atmospheric changes coincide with biotic (mass extinction) and abiotic (carbonate carbon-isotope perturbation) changes in the marine realm, hence affecting the entire ocean-atmosphere system.

Geology, v. 41, 2013, p. 579-582.

Smithian (Early Triassic) ammonoids from the Salt Range

Brühwiler, T., Bucher, H., Ware, D., Hermann, E., Hochuli, P.A., Roohi, G., Rehman, K. & Yassen, A.

Intensive sampling of the Early Triassic successions at the Chiddru, Nammal and Zaluch localities in the Salt Range (Pakistan) has yielded abundant and well-preserved Smithian (Early Triassic) ammonoid faunas that are of prime importance for ammonoid taxonomy and biostratigraphy. The Salt Range is the type area of many Smithian taxa, and it has played a central role in the Early Triassic ammonoid zonation since the pioneer works of Waagen and Mojsisovics et al. in the late 19th century. Our data allow the construction of a highly-resolved ammonoid succession spanning the entire Smithian times. Boundary faunas with the older Dienerian and the younger Spathian are also well documented. The new biostratigraphical sequence comprises the following twelve distinct ammonoid faunas (in ascending order): the Flemingites bhargavai beds, the Shamaraites rursiradiatus beds, the Xenodiscoides perplicatus beds, the Flemingites nanus beds, the Radioceras evolvens beds, the Flemingites flemingianus beds, the Brayardites compressus beds, the Nammalites pilatoides beds, the Pseudoceltites multiplicatus beds, the Nyalamites angustecostatus beds, the Wasatchites distractus beds, and the Glyptophiceras sinuatum beds. Biostratigraphic correlations between Nammal and Chiddru reveal diachroneity of the lithological boundaries between the Lower Ceratite Limestone and the Ceratites Marls on one hand, and between the Ceratite Marls and the Ceratite Sandstone on the other. The faunal succession from the Salt Range correlates well with that of other Tethyan sequences such as Tulong (South Tibet), Spiti (India) and South China. Six new genera (Koiloceras, Monneticeras, Truempyceras, Punjabites, Hochuliites, Mianwaliites) and 13 new species (Koiloceras romanoi, Monneticeras compressum, Punjabites punjabiensis, Hochuliites retrocostatus, Mianwaliites multiradiatus, Paraspidites obesus, Flemingites hautmanni, F. hofmanni, F. planatus, Rohillites pakistanensis, Prionites nammalensis, Shamaraites rursiradiatus, Subinyoites punjabiensis) are described.

Special Papers in Palaeontology 88, 2012, p. 1-114.

Palynofacies analysis of the Permian-Triassic transition in the Amb section (Salt Range, Pakistan): implications for the anoxia on the South Tethyan Margin

Schneebeli-Hermann, E., Kürschner, W.M., Hochuli, P.A., Bucher, H., Ware, D., Goudemand, N. & Roohi, G.

The beginning of the Mesozoic, the Early Triassic, is characterized by several ecological perturbations following the end-Permian mass extinction. They are reflected in multiple C-isotope excursions coupled with climatic changes. Here we present palynological data from two accurately dated sections from the North Indian Margin (Pakistan and South Tibet). The climate of the Early Triassic was controlled by persistent monsoon circulation. The spore/pollen ratios, used as a proxy for humidity changes, indicate several significant climatic changes coinciding with C-isotope excursions. Comparison with published climate model simulations reveals that the climatic shifts were induced by orbital forcing and probably represent eccentricity cycles. Humidity peaks indicate an insolation forced shift of the intertropical convergence zone towards the North Indian Margin. Comparison with palynological data from Norway and other proxies reveal that the profound climatic change from humid to drier climate across the Smithian–Spathian boundary represents a global event, which affected southern and northern mid-latitudes and coincided with major ammonoid and conodont extinction events. This implies that increased greenhouse gas concentrations owing to recurring volcanic pulses increased the climate system sensitivity, resulting in climatic changes in distant parts of the world. Our data strongly support a link between C-isotope excursions, climatic changes and biotic responses.

Journal of Asian Earth Sciences 60, 2012, p. 225-234.

Climatic oscillations at the onset of the Mesozoic inferred from palynological records from the North Indian Margin

Hermann, E., Hochuli, P.A., Bucher, H., Brühwiler, T., Hautmann, M., Ware, D., Weissert, H., Roohi, G., Yaseen, A. & Rehman, K.

The beginning of the Mesozoic, the Early Triassic, is characterized by several ecological perturbations following the end-Permian mass extinction. They are reflected in multiple C-isotope excursions coupled with climatic changes. Here we present palynological data from two accurately dated sections from the North Indian Margin (Pakistan and South Tibet). The climate of the Early Triassic was controlled by persistent monsoon circulation. The spore/pollen ratios, used as a proxy for humidity changes, indicate several significant climatic changes coinciding with C-isotope excursions. Comparison with published climate model simulations reveals that the climatic shifts were induced by orbital forcing and probably represent eccentricity cycles. Humidity peaks indicate an insolation forced shift of the intertropical convergence zone towards the North Indian Margin. Comparison with palynological data from Norway and other proxies reveal that the profound climatic change from humid to drier climate across the Smithian–Spathian boundary represents a global event, which affected southern and northern mid-latitudes and coincided with major ammonoid and conodont extinction events. This implies that increased greenhouse gas concentrations owing to recurring volcanic pulses increased the climate system sensitivity, resulting in climatic changes in distant parts of the world. Our data strongly support a link between C-isotope excursions, climatic changes and biotic responses.

Journal of the Geological Society, London, Vol. 169, 2012, p. 227-237

Olenekian (Early Triassic) bivalves from the Salt Range and the Surghar Range, Pakistan

Wasmer, M., Hautmann, M., Hermann, E., Ware, D., Roohi, G., Rehman, K., Yassen, A. & Bucher, H.

Based on newly collected material from the uppermost Smithian and lower to middle Spathian (Olenekian, Lower Triassic) of the Salt Range and Surghar Range (Pakistan), 15 bivalve species belonging to 11 genera are described, including two new genera, *Eobuchia* and *Dimorphoconcha*, and one new species, *Palaeoneilo*? *fortistriata*. *Eobuchia* gen. nov. is placed in a new subfamily, the Eobuchiinae, which differs from the Buchiinae in having an almost planar and only moderately inclined or offset right anterior auricle. Inclination of the right anterior auricle is proposed as a synapomorphy of the revised suborder Monotidina, which includes the Buchiidae, Monotidae, Oxytomidae and, tentatively, the Dolponellidae. The Pseudomonotidae, Chaenocardiidae and Claraiidae are discussed as candidate ancestors of the Monotidina. *Dimorphoconcha* gen. nov., provisionally placed in the Limidae, is a morphologically unusual genus characterized by a globose shell centre and a strongly plicate fringe. *Permophorus costatus*, which was previously known exclusively from Permian strata, is reported from the Spathian of the Surghar Range. This record extends the range of *P. costatus* for at least 8 Myr and makes it the first reported Lazarus *species*, with an outage of more than 2 Myr after the end-Permian mass extinction. Ten of 15 species recognized in this study have not been reported from other regions, which may indicate increasing provincialism towards the end of the Early Triassic, or, alternatively, reflect the still insufficient knowledge of benthic faunas from the epoch that followed the greatest crisis in the history of life.

Palaeontology 55, 2012, p. 1043-1073.

Terrestrial ecosystems on North Gondwana in the aftermath of the end-Permian mass extinction

Hermann, E., Hochuli, P.A., Bucher, H., Brühwiler, T., Hautmann, M., Ware, D. & Roohi, G.

The impact of the end-Permian mass extinction on terrestrial ecosystems is still highly controversial. Here, new high-resolution palynological data from biostratigraphically well-dated Upper Permian to Middle Triassic successions of the Salt Range and Surghar Range (Pakistan) are presented. Our results reveal seven successive floral phases between the Late Permian and the Middle Triassic. At the onset of the Mesozoic, the flora is characterised by high abundances of lycopods associated with pteridosperms and conifers. This association prevails up to the middle Smithian and is followed by a prominent spore spike similar to the global spore spike reported from the Permian–Triassic boundary. Like that of the end-Permian, the middle Smithian spore spike is associated with a negative isotope excursion and is succeeded by a major marine faunal extinction event in the late Smithian. The recurrent patterns observed at the Permian–Triassic boundary and in the middle–upper Smithian suggest a common cause such as massive ejections of volcanic gases. The increasing abundance of conifers still associated with common lycopods in the Spathian suggests fading volcanically induced environmental perturbations and stabilisation of terrestrial ecosystems ca. 2.1My after the end-Permian event.

Gondwana Research 20, 2011, p. 630-637.

Organic matter and palaeoenvironmental signals in the Early Triassic of the Salt Range and Surghar Range

Hermann, E., Hochuli, P.A., Méhay, S., Bucher, H., Brühwiler, T., Hautmann, M., Ware, D., Roohi, G., Rehman, K. & Yaseen, A.

Latest Permian to the Middle Triassic mixed siliciclastic–carbonate shelf deposits of the northern Gondwana margin have been studied in four sections (Nammal, Chhidru, Chitta–Landu, and Narmia) in the Salt Range and Surghar Range of Pakistan. Sedimentological and palynofacies patterns combined with a high resolution ammonoid based age control have been used to assess environmental changes such as sea-level change, distance from the shore, and oxygenation conditions of the sections in the aftermath of the end-Permian mass extinction.The base and the top of the Early Triassic are marked by second order sequence boundaries (SRT1, SRT8). Within the Early Triassic two third order sequence boundaries could be delineated by means of palynofacies analysis and sedimentology, one near the Dienerian–Smithian (SRT2) and the second one near the Smithian–Spathian boundary (SRT5). The extinction event at the Smithian–Spathian boundary seems to be closely associated to the latter globally recorded sea-level low stand. Five additional sequences of undetermined order (SRT3, SRT 4, SRT5/1, SRT6, and SRT7) are reflected in the sedimentological record of the studied sections.The observed changes in the composition of the particulate organic matter (POM) indicate a general shallowing upward trend, which is modulated by smaller transgressive–regressive cycles supporting the sedimentologically defined sequences. The POM is mostly dominated by terrestrial phytoclasts and sporomorphs. The strongest marine signal is reflected by increased abundance of amorphous organic matter (AOM) in the lower part of the Ceratite Marls at Nammal (late Dienerian) and Chhidru (earliest Smithian) and the Lower Ceratite Limestone at Chitta–Landu (late Dienerian). AOM of marine origin is characteristic for deeper, distal basinal settings and is preferentially preserved under dysoxic and anoxic conditions, indicating reduced oxygen conditions during these intervals. Up-section transgressive events are reflected by increased numbers of acritarchs, reaching up to 50% of the POM. Well oxygenated conditions and low total organic carbon contents (TOC) continue up to the top of the Early Triassic (Mianwali Formation). The most pronounced terrestrial influx is expressed in the Middle Triassic.Organic carbon isotope data parallel the carbonate carbon isotope records from the Tethyan realm; therefore, they reflect real global changes in the carbon cycle independent of the OM composition. The biomarker study of the apolar hydrocarbons of three samples from the Nammal section indicates an enhanced bacterial productivity, especially in the Smithian and Spathian, reflected in high relative abundances of hopanes. POM, TOC data and redox sensitive biomarkers together with high resolution biostratigraphy demonstrate that well-oxygenated environmental conditions prevailed in the Early Triassic with the exception of the Dienerian to earliest Smithian interval. The POM assemblages of Late Permian to late Griesbachian age indicate well oxygenated conditions during this time interval. There is no evidence in support of an anoxic event in the late Griesbachian in these sections.

Sedimentary Geology 234, 2011, p. 19-41.

Palaeobiogeography and stratigraphy of advanced gnathostomian fishes (Chondrichthyes and Osteichthyes) in the Early Triassic and from selected Anisian localities (Report 1863-2009)

Brinkmann, W., Romano, C., Bucher, H., Ware, D. & Jenks, J.

Present paper gives an updated summary of research history on the Chondrichthyes and Osteichthyes of the Early Triassic (Griesbachian, Dienerian, Smithian, Spathian) and primarily of the early Anisian. Early Triassic and Anisian marine and freshwater ichthyofaunas are found on all continents except South America, and much more fish assemblages are known from the Northern than from the Southern Hemisphere. The Early Triassic and the Anisian are times of major importance for the phylogeny of the Chondrichthyes and Osteichthyes. After the end-Permian mass extinction the surviving groups of the cartilaginous and bony fishes recovered, and many new forms appeared in the Early Triassic. The neoselachians as well as close relatives of the teleosteans evolved, clades to which nearly all extant fishes belong. Present publication also provides a revised data base for the distribution of Early Triassic and early Anisian chondrichthyan and osteichthyan fishes in time and space on which future research on their paleobiodiversity shall be guided.

Zentralblatt für Geologie und Paläontologie. Teil II, 5/6, 2010, p. 765-812.

New Early Triassic ammonoid faunas from the Dienerian/Smithian boundary beds at the Induan/Olenekian GSSP candidate at Mud (Spiti, Northern India)

Brühwiler, T., Ware, D., Bucher, H., Krystyn, L. & Goudemand, N.

New collections at the Induan/Olenekian boundary GSSP candidate at Mud (Himachal Pradesh, Northern India) lead to the recognition of several well preserved ammonoid faunas that significantly improve the biostratigraphic resolution in the beds underlying the proposed GSSP level. In ascending order, the new biostratigraphical sequence comprises: the Ambites lilangense beds, the Fuchsites markhami beds, the Kingites lens beds, the Prionolobus rotundatus beds, the Flemingites bhargavai beds, the Kashmiritidae gen. nov. A beds and the Vercherites cf. pulchrum beds. The faunas from Bed 10, located about 1 m below the proposed GSSP level, contain certain ammonoids with typical early Smithian affinity (Flemingitidae, Kashmiritidae) and thus reflect the beginning of the early Smithian evolutionary radiation. Seen from an evolutionary point of view, the Dienerian/Smithian boundary can therefore be placed just below Bed 10. Ideally, the stage boundary should also be intercalibrated with other biological, chemical or physical proxies as additional tools for world-wide correlations. Four new species (Flemingites bhargavai, Kingites korni, ?Kingites parkashi and Xenodiscoides variocostatus) and two new genera (Mudiceras, Vercherites) are described.

Journal of Asian Earth Sciences 39, 2010, p. 724-739.

The Lower Triassic sedimentary and carbon isotope records from Tulong (South Tibet) and their significance for Tethyan palaeoceanography

Brühwiler, T., Goudemand, N., Galfetti, T., Bucher, H., Baud, A., Ware, D., Hermann, E., Hochuli, P.A. & Martini, R.

The Lower Triassic sedimentary and carbonate/organic carbon isotope records from the Tulong area (South Tibet) are documented in their integrality for the first time. New age control is provided by ammonoid and conodont biostratigraphy. The basal Triassic series consists of Griesbachian dolomitic limestones, similar to the Kathwai Member in the Salt Range (Pakistan) and to the Otoceras Beds in Spiti (India). The overlying thin-bedded limestones of Dienerian age strongly resemble the Lower Ceratite Limestone of the Salt Range. They are followed by a thick series of dark green, silty shales of Dienerian–early Smithian age without fauna that strikingly resemble the Ceratite Marls of the Salt Range. This interval is overlain by thin-bedded, light grey fossil-rich limestones of middle to late Smithian age, resembling the Upper Ceratite Limestone of the Salt Range. These are followed by a shale interval of early Spathian age that has no direct counterpart in other Tethyan sections. Carbonate production resumes during the late early and middle Spathian with the deposition of red, bioclastic nodular limestone ("Ammonitico Rosso" type facies). Apart from its colour this facies is similar to the one of the Niti Limestone in Spiti and of the Spathian nodular limestone in Guangxi (South China). As in other Tethyan localities such as Spiti, the early–middle Anisian part of the Tulong section is strongly condensed and is characterized by grey, thin-bedded limestones with phosphatized ammonoids. As for many other Tethyan localities the carbon isotope record from Tulong is characterized by a late Griesbachian–Dienerian positive δ13Ccarb excursion (2‰), and a very prominent positive excursion (5‰) at the Smithian–Spathian boundary, thus confirming the well-documented perturbations of the global carbon cycle following the Permian–Triassic mass extinction event.

Sedimentary Geology 222, 2009, p. 314-332

Appendix 2

List of conference abstracts

List of conference abstracts

- **As a first author:**

Ware, D., Bucher, H. & Schneebeli-Hermann, E. 2014: High-resolution biochronology and diversity dynamics of the Early Triassic ammonoid recovery: the Dienerian faunas of the Northern Indian Margin. *12th Swiss Geoscience Meeting*, Fribourg (21-22/11/2014).

Ware, D. & Bucher, H. 2014: High resolution biostratigraphy and biodiversity dynamics of Dienerian (Early Triassic) ammonoids from the Northern Indian Margin. *9th International Symposium, Cephalopods – Present and Past*, Zürich (04-14/09/2014).

Ware, D. & Bucher, H. 2013: High resolution biostratigraphy and biodiversity dynamics of Dienerian (Early Triassic) ammonoids from the Northern Indian Margin. *The Palaeontological Association 57th annual meeting*, Zürich (13-16/12/2013).

Ware, D., Goudemand, N., Bucher, H., Orchard, M.J., Schneebeli-Hermann, E., Hochuli, P.A., Brühwiler, T., Krystyn, L. & Roohi, G. 2012: Nammal Nala (Salt Range, Pakistan), a potential GSSP candidate for the Induan/Olenekian Boundary (Early Triassic). *34th IGC*, Brisbane, Australia (5-10/08/2012).

Ware, D., Bucher, H., Goudemand, N., Orchard, M.J., Hermann, E., . Hochuli, P.A., Brühwiler, T., Krystyn, L. & Roohi, G. 2011: Nammal Nala (Salt Range, Pakistan), a potential GSSP candidate for the Induan/Olenekian Boundary (Early Triassic): detailed biostratigraphy and comparison with other GSSP candidates. *9th Swiss Geoscience Meeting*, Zurich (11-13/11/2011).

Ware, D., Bucher, H, Goudemand, N., Orchard, M.J., Hermann, E., Hochuli, P.A., Brühwiler, T., Krystyn, L. & Roohi, G. 2011: The Induan/Olenekian Boundary: new data from the Spiti Valley (India) and the Salt Range (Pakistan). *21st Canadian Paleontology Conference, Special Session: Studies on the Triassic in Commemoration of Edward Timothy Tozer*. Vancouver, Canada (19-22/08/2011).

Ware, D., Bucher, H., Brühwiler, T. & Goudemand, N. 2010: Dienerian (Early Triassic) ammonoid successions of the Tethys: preliminary results from Pakistan and India. *8th Swiss Geoscience Meeting,* Fribourg (19-20/11/2010).

Ware, D., Bucher, H., Brühwiler, T. & Goudemand, N. 2010: Dienerian (Early Triassic) ammonoid successions of the Tethys: preliminary results from Pakistan and India. *8th International Symposium, Cephalopods – Present and Past*. Dijon, France (31/08-03/09/2010).

- **As a co-author:**

Meier, M., Bucher, H. & Ware, D. 2014: The diversity and phylogenetic bottleneck of ammonoids across the end-Permian mass extinction. *12th Swiss Geoscience Meeting*, Fribourg (21-22/11/2014).

Bucher, H., Meier, M. & Ware, D. 2014: The timing of cephalopod survival after the Permian-Triassic mass extinction. *9th International Symposium Cephalopods – Present and Past*, Universität Zürich (04-14/09/2014).

Goudemand, N., Coble, M., Romano, C., Ware D., Bucher, H. & Payne J. 2014: SHRIMP-RG measurements of U, Y and REE profiles on Early Triassic conodont elements from Nammal, Pakistan, and their implications for biotic recovery after the end-Permian mass extinction. *Geological Society of America Annual Meeting*, Vancouver, British Columbia (19-22/10/2014).

Goudemand, N., Orchard, M., Krystyn, L., Brühwiler, T., Ware, D., Brayard, A., Galfetti, T. & Bucher, H. 2011: New conodont data from Waili (South China) and Mud (northern India) and implications for the definition of the Induan-Olenekian Boundary. *XVII Internation Congress on the Carboniferous and Permian*, Perth, Australie (03-08/07/2011).

Hermann, E., Hochuli, P.A., Bucher, H., Brühwiler, T., Ware, D., Hautmann, M., Goudemand, N. & Roohi, G. 2011: End-Permian and mid-Early Triassic terrestrial ecosystem turnovers - a comparison. *European Geosciences Union General Assembly 2011*, Vienne, Autriche (03-08/04/2011).

Hermann, E., Kürschner, W., Hochuli, P.A., Goudemand, N., Ware, D., Bucher, H. & Roohi, G. 2011: Permian-Triassic paleoenvironment infreed from palynofacies data of Amb, Salt Range, Pakistan. *XVII Internation Congress on the Carboniferous and Permian*, Perth, Australie (03-08/07/2011).

Romano, C., Brinkmann, W., Goudemand, N., Vennemann, T., Ware, D., Hermann, E, Brühwiler, T. & Bucher, H. 2011: Recovery Patterns of Chondrichthyan and Osteichthyan Fishes after the end-Permian Mass Extinction. *9th Swiss Geoscience Meeting*, Zurich (11-13/11/2011).

Hermann, E., Hochuli, P. A., Bucher, H., Brühwiler, T., Ware, D., Hautmann, M., Weissert, H., Bernasconi, S.M., Roohi, G., Reman, K. & Yaseen, A. 2010: Climatic changes in the aftermath of the end Permian mass extinction - evidence from palynological records of Pakistan, *European Geoscience Union General Assembly 2011*, Vienne, Autriche (02-07/05/2010).

Brühwiler, T., Bucher, H., Goudemand, N., Ware, D. & Hermann, E. 2009: Smithian ammonoids (Early Triassic): explosive evolutionary radiation following the Permian/Triassic mass extinction. *7th Swiss Geoscience Meeting*, Neuchâtel (20-21/11/2009).

Bucher, H., Hochuli, P.A., Escarguel, G., Hautmann, M., Goudemand, N., Brühwiler, T., Brayard, A., Hermann, E., Galfetti, T. & Ware, D. 2008: The Early Triassic Biotic Recovery: a multiproxy approach. *Geological Society of America, Joint Annual Meeting*, Houston, USA (05-09/10/2008).

Goudemand, N., Orchard, M., Bucher, H., Brayard, A., Brühwiler, T., Galfetti, T., Hochuli, P.A., Hermann, E. & Ware, D. 2008: Smithian-Spathian Boundary: The Biggest Crisis in Triassic Conodont History. *Geological Society of America, Joint Annual Meeting*, Houston, USA (05-09/10/2008).

Goudemand, N., Orchard, M., Bucher, H., Brayard, A., Brühwiler, T., Galfetti, T., Hermann, E., Hochuli, P.A. & Ware, D. 2008: Smithian-Spathian boundary: The biggest crisis in Triassic conodont history. *6th Swiss Geoscience Meeting*, Lugano (21-23/11/2009). Price of the Swiss Commission of Palaeontology for the best talk.

Acknowledgements

I want first to thank my supervisor Prof. Dr. Hugo Bucher. He offered me the great opportunity to join the Early Triassic "task force" of the Palaeontological Institute and Museum (PIMUZ). His scientific advices and enthusiasm for Early Triassic ammonoids were the cornerstones of the success of this work.

I also gratefully acknowledge:

- Dr. Thomas Brühwiler, Dr. Elke Schneebeli-Hermann and Dr. Michael Hautmann for many interesting discussions, assistance during field work and collaboration;
- Dr. Nicolas Goudemand, Dr. Séverine Urdy (Zürich, formerly PIMUZ) and Dr. Carlo Romano (PIMUZ) for their support and stimulating discussions;
- James F. Jenks (Salt Lake City) for his guidance and help during fieldwork in Nevada, his fruitful collaboration and for improving the English text of a large part of this work;
- Dr. Christian Klug for his support and many interesting discussions concerning ammonoid palaeobiology and evolution;
- Dr. Claude Monnet (Université de Lille I, formerly PIMUZ) for providing his statistical analysis software and discussions over statistics and intraspecific variability;
- Prof. Dr. Leopold Krystyn (Vienna) for his guidance during field work in Spiti and for lending part of his collections;
- Dr. Arnaud Brayard (Université de Bourgogne, formerly PIMUZ) for his collaboration and discussions concerning Early Triassic ammonoid taxonomy;
- Dr. Thomas Galfetti (Zürich, formerly PIMUZ) and Lui Unterassner (Zürich) for their help during field work in Spiti;
- Markus Hebeisen (PIMUZ) for the extreme patience he showed when preparing the most delicate of my ammonoids and talking to me in his best German to improve my language skills;
- Rosie Roth (PIMUZ) for preparing a part of my material and for taking all ammonoid photographs;
- Julia Huber and Leonie Pauli (PIMUZ) for preparing a large part of my ammonoid collection;
- Jérôme Gapany (Zürich, formerly PIMUZ) for his guidance in the labyrinth of bibliography;
- Prof. Dr. Om Bhargava (Haryana) for his friendly guidance in the Spiti area;
- Ghazala Roohi (Islamabad) for her huge bureaucratic and logistic effort for enabling our field work in the Salt Range;
- Khalil Rehman and Aamir Yaseen (Islamabad) for their help during field work in the Salt Range;
- Dr. James Neenan (PIMUZ) and Dr. Erin Maxwell (Stuttgart) for improving the English text of a part of this work;
- Mike Orchard (Vancouver) for providing access to Tozer's collections and archives;
- Beli Parkash (Manali) for his guidance in Spiti and delicious food;
- The team of police men who protected us during the fieldwork in Pakistan.

And of course, this list will never be exhaustive, I need to thank all my other friends and colleagues from the PIMUZ, but also all my friends outside university and family for their constant support and many enjoyable moments.